

Algal community response to anthropogenic pollution and environmental change at Lake Baikal, Siberia, over recent centuries

Thesis submitted for the degree of

Doctor of Philosophy

University of Nottingham

Sarah Lily Roberts

School of Geography
University of Nottingham

October 2017

Abstract

Despite its large volume, Lake Baikal has been experiencing recent changes within its limnological and biological structure, as well as changes within lake water nutrient and dissolved organic carbon concentrations. The biological changes within Lake Baikal include alterations within the distribution and abundance of major phytoplankton and zooplankton groups. These limnological changes are likely to be from both climate warming and anthropogenic impact, particularly over the last few decades. Recent shoreline observations in the South and North regions of Lake Baikal have found large blooms of filamentous green algae, which has been associated with nutrient enrichment from surrounding settlements and growing tourism. This highlights the question as to whether the pelagic regions are similarly showing any signs of anthropogenic driven nutrient enrichment.

The aim of this thesis was to examine if pelagic Lake Baikal is showing any evidence of eutrophication and/or response to climate warming. The main themes of the research were to assess the modern-day limnological condition of Lake Baikal in the summer (August 2013) and winter (March 2013) months, and to examine Baikal's phytoplankton response to nutrient enrichment via the construction of mesocosm experiments. High-resolution limnological change was then reconstructed from sediment cores across the lake. Sites were chosen within pelagic regions, bays and shallow waters nearby river inflows, and palaeolimnological records were used to assess primary production changes and floristic changes over the last few centuries. This timespan enables both natural variability within the system to be explored, and more recent changes pre and post known human influence within the catchment area (c. 1950 AD). The main palaeolimnological techniques applied for primary production proxies were sedimentary algal pigments, stable isotope analysis of bulk organic carbon and diatom valve concentrations. Mercury analyses was also applied to water samples and sediment cores as a pilot study to explore toxic metal pollution at Lake Baikal, due to mining activity along the Selenga River, and examine historic levels of mercury contamination.

Both modern-day limnological surveys and palaeolimnological records seem to be showing increasing algal biomass (chlorophyll-*a* concentrations) over the last 60 years, with decreasing trends in diatom production (from diatoxanthin pigment concentrations and diatom valve concentrations) in the South basin. Spatial survey data represents a snap shot in Baikal's limnology in late summer (August 2013), and shows higher than expected concentrations of total phosphorus within the mixing layer, which fall within the meso-eutrophic range. Dissolved organic carbon concentrations seem to now be higher within Lake Baikal's waters,

and both nitrate and silicate concentrations appear to be similar to known previous concentrations at Lake Baikal. A pilot study of mercury concentrations within Lake Baikal waters and sediments, show no signs of mercury contamination from mining activity along the major river inflows, and atmospheric deposition. Experimental results show that within the pelagic regions of Lake Baikal, nitrogen, phosphorus and silicon are influencing algal communities, with Si addition stimulating diatom growth, nitrogen and phosphorus addition stimulating chlorophyte growth, although overall nutrient treatments did not increase chlorophyll-*a* yield. Interestingly, experimental findings also highlight the potential influence of picocyanobacteria populations on silicon cycling. Concentrations of sedimentary chlorophyll-*a* concentrations (plus its derivatives) rise prior to major industrial influence within the Baikal catchment region, and stable carbon isotope records show a positive correlation with chlorophyll-*a* concentrations in the South basin, Selenga and Maloe More sites. Total phosphorus concentrations could be a result of both anthropogenic nutrient pollution, entering into the lake via the Selenga River, and climate driven changes in lake stratification and nutrient utilisation by algae. Results from limnological surveys and palaeolimnological records are thus likely to be reflecting both recent anthropogenic impact and climate change (rising lake water temperatures, declining ice cover thickness and duration and increasing river inflow from permafrost thaw), within the pelagic regions, especially given that recent work provides evidence of toxic cyanobacterial and chlorophyte blooms within the shallow waters of Lake Baikal. For the Maloe More site, which is a bay off the Central basin, results show a rise in sedimentary chlorophyte pigments post 1950 AD, suggesting that this bay region of Lake Baikal is currently being affected more than deeper water sites, by human influence, showing signs of eutrophication due to a switch in algal community composition.

The wider research project

This PhD research was part of a wider research project at the University of Nottingham, funded by NERC, which used silicon isotopes ($\delta^{30}\text{Si}$) to examine recent environmental change and anthropogenic pollution at Lake Baikal. A modern-day $\delta^{30}\text{Si}$ from waters in August 2013 were collected to look at nutrient DSi utilisation of the spring bloom in Lake Baikal. The transfer of silicon isotopes into the sediment record was also examined (Panizzo et al. 2016). Production trends seen from pigment results presented in Chapter Five, support the trends seen in the vertical profiles of $\delta^{30}\text{Si}$ isotopes within Baikal's water column in August 2013 (Panizzo et al. submitted). Furthermore, sedimentary $\delta^{30}\text{Si}$ and pigment records (pigment data presented in Chapter Seven) provide methods of reconstructing changes in algal productivity from the photic zone, over the last 200 years and last 1000 years. These two timescales were chosen to examine impacts of recent 19th and 20th century catchment development and climate change on nutrient utilisation, and ascertain the response of Lake Baikal to longer term climatic changes, where the influence is through changes in snow/ice cover and nutrient supply to the photic zone.

Acknowledgements

I would like to thank my supervisors, Prof. Suzanne McGowan and Dr. George Swann at University of Nottingham and Prof. Anson Mackay at ECRC/UCL for their excellent advice, invaluable knowledge and continuous support throughout my PhD research. I've thoroughly enjoyed working alongside them, and very grateful for all the project meetings we've had, including those with all the Baikal team; George, Suzanne, Anson, Virginia and Jen, which were full of interesting discussions. Within the Baikal team, I am also grateful to Dr. Virginia Panizzo at University of Nottingham, for all her help, and I enjoyed working in the lab alongside her. I am extremely appreciative for all the assistance provided on the March and August 2013 fieldwork expeditions from colleagues mentioned above, as well as from scientists from the Institute of Earth's Crust, Irkutsk, and University of Zurich, namely Dr. Lena Vologina and Prof. Mike Sturm. Thanks also goes to many more people, including the Captain of the 'Geolog' research vessel and all the crew members, along with Alison Ball and Julia Lehman (two middle school teachers from Urban Promise Academy in Oakland who joined our expedition to help on-board the 'Geolog'). For my laboratory work, I would like to thank Teresa Needham, Graham Morris, Julie Swales and Ian Conway for their laboratory and fieldwork preparation assistance. For the stable isotope analysis and discussions on organic geochemistry at Lake Baikal I am very grateful to Prof. Melanie Leng at University of Nottingham and BGS for her invaluable knowledge, advice and time. I would also like to thank Chris Kendrick for running the carbon isotope samples and Dr. Chris Vane from BGS for his knowledge of Rock Eval analysis and for running the Baikal samples for Rock Eval analyses. Thanks also goes to Fengjuan Xiao at Loughborough University for running my DOC samples, Dr. Hangdong Yang and Prof. Neil Rose for mercury analysis and ^{210}Pb dating at UCL.

I am very grateful to Dr. Susanne Fietz, for her knowledge and datasets of pigments at Lake Baikal, Dr. Elena Vologina who generously provided me datasets on Baikal sediment core lithology, and Dr. David Jewson for his expert advice on Baikal phytoplankton. I would like to thank Savannah Worne, a PhD student at University of Nottingham who kindly gave me her undergraduate dissertation data on Baikal phytoplankton pigments at Maloe More, on the BAIK13-15 sediment core. Within the palaeo team at Nottingham and UCL, I am thankful to many PhD students and Post Doc's for making my time at Nottingham so enjoyable, and some of these include Mark Stevenson, Dr. Heather Moorhouse, Dr. Xu Chen, Rowan DeJardin, Nick Primmer, as well as Jen Adams and Lucia Lencioni at UCL. I would especially like to thank Dr. Heather Moorhouse for her knowledge and discussions on statistical analyses of

pigment datasets. Many thanks also go to my office colleagues, who I enjoyed sharing an office with; Joseph Bailey, Shaun Maskrey and Betsa De La Barreda. I am also very grateful to the Roberts family, for all your continuous support throughout. Many Thanks also goes to NERC, as this work was funded by a NERC PhD studentship (grant code: NE/Joo829X/1).

Table of Contents

Abstract.....	i
The wider research project	iii
Acknowledgements.....	iv
List of Abbreviations.....	xxiv
Grouping and location of sites	xxvi
Chapter One: Introduction	1
1.1 Anthropogenic impacts on ancient lakes	1
1.2 Algal community response to nutrient enrichment	4
1.3 Early signs of eutrophication at Lake Baikal	5
1.4 Anthropogenic climate change impacts on Lake Baikal	9
1.5 Research gap	12
1.5.1 Hypotheses and objectives	14
1.6 Using proxy records to investigate past primary production	17
1.6.1 Sedimentary pigments	17
1.6.2 Pigment diagenesis at Lake Baikal	24
1.6.3 Diatom assemblages	27
1.6.4 Geochemistry of organic matter	29
1.6.5 Rock Eval Pyrolysis	32
1.6.6 Applications of the $\delta^{13}\text{C}$ record	33
1.6.7 Carbon dynamics at Lake Baikal.....	35
1.7 Mercury as a pollution indicator.....	40
1.8 Nutrient enrichment experiments	41
1.9 Summary	42
Chapter Two: Site Description.....	43
2.1 Lake Baikal Basin	43
2.2 Climate controls in the regions.....	45
2.3 Limnology.....	46
2.4 Seasonal phytoplankton trends in Lake Baikal.....	48
2.5 Palaeolimnological and palaeoclimate records at Lake Baikal	49
2.6 Social and economic pressures at Lake Baikal.....	53
2.6.1 Pollution sources in and around Lake Baikal's watershed.....	56
2.6.2 Pollution sources in Lake Baikal's airshed	59
2.7 Summary	63
Chapter Three: Methodology	64
.....	64
3.1 Water samples	64
3.2 Nutrient enrichment experiments	66
3.3 Short cores.....	68
3.4 Core lithology and magnetic susceptibility.....	71
3.5 Sample processing	72
3.5.1 Nutrient and DOC analyses	72
3.5.2 Limnological parameters	73
3.5.3 Primary production measures using phytoplankton pigments	73
3.5.4 Chlorophyll-a spectrophotometric analysis.....	76
3.5.5 Diatom valve analyses	77
3.5.6 Geochemistry of organic matter	78

3.5.7 Rock Eval and n-alkanes analyses	78
3.5.8 Mercury analyses	79
3.5.9 Radiometric dating	79
3.6 Numerical analyses.....	81
3.6.1 Pigment measures and accumulation rates	81
3.6.2 Carbon mass accumulation rates	81
3.6.3 Comparison tests	82
3.6.4 Mann-Kendall analysis	83
3.6.5 Break point analysis	83
3.6.6 Temperature time-series data	84
Chapter Four: Limnology I – Seasonal sampling in South Basin	85
4.1 Under ice production.....	85
4.2 Nutrient limitation.....	87
4.3 Results	91
4.3.1 Comparison between winter and summer limnological parameters and nutrients	91
4.3.2 Comparison between under-ice, summer and past monitoring pigment composition	95
4.3.3 Nutrient enrichment experiments	100
4.4 Discussion	109
4.4.1 Seasonal measurements and comparison with previous studies	109
4.4.2 Impact of nutrient enrichment on Baikal’s pelagic phytoplankton	112
4.5 Summary	114
Chapter Five: Limnology II – Spatial and vertical summer limnological survey	116
5.1 Limnological surveys Lake Baikal	116
5.2 Vertical distribution of phytoplankton.....	120
5.3 Results	122
5.3.1 Lake-wide nutrient distributions	122
5.3.2 Mercury concentrations	134
5.3.3 Limnological parameters and chlorophyll-a measurements	136
5.3.4 Distribution of phytoplankton pigments.....	144
5.3.5 Correlations between phytoplankton pigments and physico-chemical variables	153
5.4 Discussion	155
5.4.1 Increased algal production in the mixing layer over the last decade	155
5.4.2 Depth distributions of algae across the lake and changes in lake functioning over the last decade	158
5.4.3 Spatial distribution of nutrients and comparisons with previous measurements	159
5.4.4 Correlations between phytoplankton pigment distribution and environmental variables	163
5.4.5 Spatial distribution mercury	164
5.5 Summary	165
Chapter Six: Recent palaeoproductivity in context within Longer-term variability	167
6.1 Longer-term reconstruction of environmental change at Lake Baikal	167
6.2 Past carbon records over the Holocene at Lake Baikal.....	171
6.3 Results	172
6.3.1 Core lithology (data produced by E. Vologina)	172

6.3.2 Comparing recent production changes with the longer term	182
6.3.3 Spatial comparison of short cores across Lake Baikal	189
6.3.4 Comparison with previous studies	199
6.4 Discussion	211
6.4.1 Recent production changes in context with longer term variability at Lake Baikal	211
6.5 Summary	214
Chapter Seven: Reconstructing palaeoproductivity over the last 200 years... 216	
7.1 Exploring limnological change over the last 200 years within the Baikal region	216
7.2 Results	219
7.2.1 Age models and Sedimentation rates	219
7.2.2 Investigating pigment preservation	222
7.2.3 Lake-wide spatial variability in surface sediment TOC, carbon isotopes, TOC/N ratios, pigments and diatom assemblages over the past 20 years	240
7.2.4 Temporal trends over the last 200 years.....	246
7.2.5 Carbon accumulation over the last two centuries	259
7.2.6 Carbon isotopic data over the last 200 years	260
7.2.7 Rock Eval data.....	261
7.2.8 Trends in algal production and climate.....	263
7.2.9 Pre and post- 1950 AD	267
7.2.10 Correlations between Chlas and $\delta^{13}C$	271
7.2.11 Pigments, $\delta^{13}C$ and regional annual temperatures	271
7.3 Discussion	277
7.3.1 Assessment of reliability of pigment records	277
7.3.2 Diatom assemblages and correction factors.....	280
7.3.3 Spatial differences in algal assemblage and production from surface sediments	281
7.3.4 Production trends over the last 200 years	284
7.3.5 Composition trends over the last 200 years.....	288
7.3.6 Linking production and floristic changes to anthropogenic pollution and/or climate response	289
7.4 Summary	292
Chapter Eight: Synthesis and future research at Lake Baikal	294
8.1 Site selection for environmental reconstruction at Lake Baikal	294
8.2 Is Lake Baikal eutrophying and showing anthropogenic impacts and/or responding to climatic changes?	295
8.3 How could Baikal's pelagic phytoplankton respond to nutrient enrichment? ..	299
8.4 Further work.....	299
8.5 End note	300
References	302
Appendix.....	363
Nutrients and DOC water profiles.....	363
Nutrient enrichment experiments datasets (results from day 0 and last day)	372
Mercury	376
^{210}Pb chronology profiles.....	377
Sedimentary diatom profiles.....	393

Figure 1: Ancient lakes across the globe. See Table 1 for name (Source: Mackay, 2013). Lake Baikal is shown as number 2.	2
Figure 2: Conceptual diagram of silicon accumulation in the sediment record (Schelske et al. 1983).	5
Figure 3: Coastal locations where <i>Spirogyra</i> blooms were observed (authors own map and survey data from Timoshkin et al. 2016).	7
Figure 4: Location of previously reported algal blooms of colonial cyanobacteria in littoral regions of Lake Baikal (modified from Wantanabe and Drucker, 1999).	8
Figure 5: (1) Annual air temperatures (current and 11-year running average) at Babushkin Station in southern Lake Baikal and (2) global temperature trends (Shimaraev and Domysheva, 2013).	10
Figure 6: Trends in ice cover duration and thickness over the last century in the South basin (modified from Todd and Mackay, 2003).	11
Figure 7: Chemical structures of chlorophyll-a and carotenoids; fucoxanthin (xanthophyll) and β -Carotene (carotene) (Reuss, 2005).	19
Figure 8: Chlorophyll-a degradation pathways to form chlorophyll-a transformation products (Schüller, 2014).	22
Figure 9: Conceptual diagram of pigment flux and degradation in the water column and sediments (modified from Reuss, 2005 and Leavitt, 1993).	23
Figure 10: $\delta^{13}\text{C}$ values for the major sources of carbon into lakes (Leng and Marshall, 2004).	30
Figure 11: $\delta^{13}\text{C}$ and TOC/N values of algae, C3 plants and C4 plants (Meyers and Lallier-Verges, 1999).	31
Figure 12: Rock Eval Van Krevelen-type diagram for sedimentary organic matter; shows the three types of organic matter and the oxidation pathway (Meyers and Lallier-Verges, 1999).	33
Figure 13: $\delta^{13}\text{C}$ and TOC/N values of phytoplankton, surface sediment, tributaries, soil catchment from Lake Baikal (Prokopenko et al. 1993) and land plants (C ₃ and C ₄) (Meyers and Lallier-Verges, 1999) (Source: Morley, 2005).	37
Figure 14: Annual mercury fluxes in Lake Baikal. Flux measurements taken in 1991, 1992 and 1993 (modified from Leermakers et al. 1996).	41
Figure 15: (a) Longitudinal profile of Lake Baikal, (b) Transverse profile of the South basin and (c) position of transect on Lake Baikal (modified from de Batist et al. 2002; Vologina and Sturm, 2009).	43
Figure 16: Lake Baikal and catchment (Brunello et al. 2004).	44
Figure 17: Lithological map of the Lake Baikal catchment (Heim et al. 2007).	45
Figure 18: Diagram of Lake Baikal's water column from the euphotic zone to the sediment surface.	46
Figure 19: Seasonal phytoplankton trends of the two dominant primary producers (diatoms and picocyanobacteria) at Lake Baikal (Moore et al., 2009).	49
Figure 20: Location of Lake Khall and Lake Kotokel on the coast of Lake Baikal.	51
Figure 21: Temperature reconstructions across the continents over the last 2000 years (PAGES 2k Consortium, 2013).	52
Figure 22: Location of Lake Mo-33b in Mongolia (modified from Tian et al. 2014).	54
Figure 23: Land cover map of Lake Baikal's catchment Area. Produced by S. Viridis (unpublished) (Data source: http://www.esa-landcover-cci.org).	55
Figure 24: Main settlements within Lake Baikal's watershed and along the outflow; the Angara River. Triangles represent settlement areas.	57

<i>Figure 25: Location of sampling stations in Mongolia for atmospheric aerosols (modified from Zhamsueva et al. 2012).</i>	60
<i>Figure 26: Global nitrogen deposition ($\text{kg N ha}^{-1} \text{ yr}^{-1}$) (Dentener et al. 2006 as cited in Galloway et al. 2008).</i>	62
<i>Figure 27: Global mercury deposition in 2010 (UNEP Global mercury Assessment, 2013).</i>	62
<i>Figure 28: Map showing the water sampling sites across Lake Baikal and in the catchment.</i>	65
<i>Figure 29: Nutrient enrichment experiment conducted underneath the ice at BAIK13-4 during the March 2013 field expedition. Mesocosm bags containing water samples from the DCM layer and nutrient treatments were suspended from string underneath the ice at 3 m water depth.</i>	66
<i>Figure 30: Sediment cores with green oasis at the top to remove excess water and allow for cores to be cut in half for lithology and magnetic susceptibility analyses.</i>	72
<i>Figure 31: Systematic diagram of the HPLC system (modified from Czaplicki, 2013).</i>	74
<i>Figure 32: A chromatogram of chlorophylls and carotenoids (modified from McGowan, 2013; Leavitt and Hodgson, 2001).</i>	75
<i>Figure 33: HPLC chromatogram output of eluting pigments (modified from McGowan, 2013; Leavitt and Hodgson, 2001); (1) Chl c, (2) fucoxanthin, (3) UV-absorbing compound, (4) alloxanthin, (5) diatoxanthin, (6) lutein-zeaxanthin, (7) canthaxanthin, (8) Chl b, (9) Chl a, (10) pheophytin b, (11) pheophytin a, (12) β-carotene.</i>	76
<i>Figure 34: Variability of TP concentrations in photic zone in March 2013 (green) and August 2013 (blue).</i>	93
<i>Figure 35: Variability of silicate concentrations in photic zone in March 2013 (green) and August 2013 (blue).</i>	93
<i>Figure 36: Variability of nitrate concentrations in photic zone in March 2013 (green) and August 2013 (blue).</i>	94
<i>Figure 37: Variability of DOC concentrations in photic zone in March 2013 (green) and August 2013 (blue).</i>	94
<i>Figure 38: Chlorophyll-a concentrations (nmol/L) down the water column in March 2013; Red line – YSI chlorophyll-a; blue line – spectrophotometric chlorophyll a; green line – HPLC chlorophyll-a.</i>	97
<i>Figure 39: Chlorophyll-a concentrations (nmol/L) down the water column in August 2013; Red line – YSI chlorophyll-a; blue line – spectrophotometric chlorophyll-a; green line – HPLC chlorophyll-a.</i>	98
<i>Figure 40: YSI chlorophyll-a concentrations ($\mu\text{g/L}$) in photic zone in March 2013 (green) and August 2013 (blue). No data for August 2013 BAIK13-5.</i>	99
<i>Figure 41: Photic zone March and August 2013 pigment concentrations (nmol/L) of zeaxanthin (dark blue), fucoxanthin (light blue) and lutein (dark green) in the South basin at BAIK13-1, BAIK13-4 and BAIK13-5.</i>	100
<i>Figure 42: March 2013 under ice experiment 1 (A) fucoxanthin (B) Zeaxanthin (C) Lutein (D) Chl-a on day 7. ANOVA results show significant differences between treatments. (Fucoxanthin concentrations in *C are significantly higher than *A and *B).</i>	103
<i>Figure 43: March 2013 experiment 2 carried out in the field laboratory and not under the ice (A) Fucoxanthin (B) Zeaxanthin (C) Lutein (D) Chl-a on day 6.</i>	

ANOVA results show significant differences between treatments. (Fucoxanthin concentrations in *B are significantly higher than *C).	105
Figure 44: August 2013 experiment (A) fucoxanthin (B).....	106
Figure 45: Growth rates for picocyanobacteria (inferred from zeaxanthin concentrations) chlorophytes (inferred from lutein concentrations) from the day 0 treatments until the final day of (A) March 2013 under ice experiment 1 (B) March 2013 experiment 2 (C) August 2013 experiment.	108
Figure 46: Spring chlorophyll-a concentrations in photic zone at Lake Baikal in March 2013 (this study) and from previous studies with chlorophyll-a measurements in March 2002 - 2003 (Fietz et al. 2005; Straskrabova et al. 2005; Hampton et al. 2008). These are spot sample measurement.	110
Figure 47: Trends in (A) <i>Aulacoseira baicalensis</i> (cells L ⁻¹) and (B) <i>Cyclotella baicalensis</i> (cells L ⁻¹) between 1950 - 2010 (modified from Silow et al. 2016).	111
Figure 48: Location of Bolshie Koty sampling station on the shore of the South basin, and previous water sampling sites from past limnological surveys between 1977 – 2003 by Hampton et al. 2008 (modified from Izmesteva et al. 2016).	116
Figure 49: (A) Average total phosphorus (µg/L), (B) silicate (mg/L) (C) nitrate (mg/L) and (D) DOC (mg/L) concentrations in the mixing layer across the three basins and major river inflows. Triangles show the location of settlements in the catchment. Shading represents the Baikal catchment region.	123
Figure 50: Mean mixing layer (ML) and mean deep water layer (DW) concentrations of total phosphorus and silicate concentrations.	126
Figure 51: Mean mixing layer (ML) and mean deep water layer (DW) concentrations of nitrate and dissolved organic carbon concentrations.	127
Figure 52: Mean mixing layer (ML) and mean deep water layer (DW) concentrations of major ion concentrations.	128
Figure 53: PCA of mean mixing layer nutrients, dissolved organic carbon and major ions.....	129
Figure 54: (A) TP concentrations from August 2013 and past measurements in 1995 and 2010 - 2012 (Liebzeit, 1992; Granina and Sigg, 1995; Sorokovikova et al. 2015) (µg/L); (B) DOC concentrations (mg/L) from August 2013 and past measurements from Yoshioka et al. 2002; 2007 from South, Central and North basin and river waters (Selenga, Barguzin, Vydrino and Mishika River).	133
Figure 55: Mercury concentrations (ng L ⁻¹) in pelagic lake sites in the South, Central and North basins and within the Selenga River.....	134
Figure 56: Down-core mercury concentrations at South basin (BAIK13-1C), Selenga (BAIK13-10A) and North basin (BAIK13-19B).....	135
Figure 57: (A) Average YSI Chlorophyll-a concentrations within the mixing layer and deep water layers. Red dotted line: Mean chlorophyll-a concentrations at DCM within the south basin, central basin, Maloe More and north basin from previous study in 2002 – 2003 (Fietz, 2005). (B) Limnological parameters (euphotic zone depth, mixing layer depth and deep chlorophyll maxima) at each water-sampling site across the three basins. Grey bars represent the light attenuation coefficient (K _d) values across the lake. DCM represents the water depths of the maximum chlorophyll concentrations down the water column.	138
Figure 58: YSI chlorophyll-a concentrations (µg/L) showing the DCM profiles in the South basin. Sites which do not exhibit a distinct DCM (BAIK13-1, BAIK13-4, BAIK13-5 and BAIK13-7) are still presented.	139

Figure 59: YSI chlorophyll-a concentrations ($\mu\text{g/L}$) showing the DCM profiles in the South basin. A site which does not exhibit a distinct DCM (BAIK13-10) is still presented.....	140
Figure 60: YSI chlorophyll-a concentrations ($\mu\text{g/L}$) showing the DCM profiles in the Central basin, Maloe More Bay (MM) and Chivsky Bay (CH) in the North basin.	141
Figure 61: YSI chlorophyll-a concentrations ($\mu\text{g/L}$) showing the DCM profiles in the North basin.	142
Figure 62: Mean phytoplankton pigment concentrations within the mixing layer; (A) zeaxanthin (cyanobacterial biomarker), (B) fucoxanthin (diatom and chrysophyte biomarker). South basin zeaxanthin concentrations are significantly different to the Central basin (black star).	146
Figure 63: Mean phytoplankton pigment concentrations within the mixing layer; (A) Peridinin (dinoflagellate biomarker) and (B) lutein (chlorophyte biomarker).	147
Figure 64: PCA of mean pigment concentrations in the mixing layer and each site.	148
Figure 65: Comparison between results from this study (2013) and past measures between 2001 – 2003 (Fietz et al. 2005) of (A) mean range of chlorophyll-a concentrations; (B) mean range of YSI chlorophyll-a concentrations at the deep chlorophyll maxima across the three basins.....	150
Figure 66: Comparison between results from this study (2013) and past measures between 2001 – 2003 (Fietz et al. 2005) of (A) deep chlorophyll maxima depth; (B) mixing layer depth across the three basins.	151
Figure 67: Comparison between results from this study (2013) and past measures between 2001 – 2003 (Fietz et al. 2005) of (A) fucoxanthin concentrations (nmol/L) and (B) zeaxanthin concentrations (nmol/L) across the three basins.	152
Figure 68: Comparison between results from this study (2013) and past measures between 2001 – 2003 (Fietz et al. 2005) of lutein concentrations (nmol/L) across the three basins.	153
Figure 69: Results from RDA between average mixing layer limnological variables (physical and chemical) and phytoplankton pigments using forward selection with Monte Carlo permutation tests. DOC is the only environmental variable which is significantly correlated with the algal pigments (p value = 0.02). (ODO – dissolved oxygen, ORP – redox potential, LAC – light attenuation coefficient).....	154
Figure 70: Regression correlation with 95% confidence regression lines between mixing layer DOC and zeaxanthin concentrations.	155
Figure 71: Lithology and magnetic susceptibility at BAIK13-1.	172
Figure 72: Lithology and magnetic susceptibility at BAIK13-4.	173
Figure 73: Lithology and magnetic susceptibility at BAIK13-7.	174
Figure 74: Lithology and magnetic susceptibility at BAIK13-10.....	175
Figure 75: Lithology and magnetic susceptibility at BAIK13-11.....	176
Figure 76: Lithology and magnetic susceptibility at BAIK13-14.....	177
Figure 77: Lithology and magnetic susceptibility at BAIK13-15B.....	178
Figure 78: Lithology and magnetic susceptibility at BAIK13-16.....	179
Figure 79: Lithology and magnetic susceptibility at BAIK13-18.....	180
Figure 80: Lithology and magnetic susceptibility at BAIK13-19.....	181

Figure 81: Chlas concentration (nmol g ⁻¹ OC) (green > 200 years and blue < 200 years). Turbidite sections are removed within the pigment record. (*BAIK13-7A and *BAIK13-18A show high levels of degradation).....	184
Figure 82: Total carotenoids concentration (nmol g ⁻¹ OC) (green > 200 years and blue < 200 years). Turbidite sections are removed from the pigment record. (*BAIK13-7A and *BAIK13-18A show high levels of degradation).....	185
Figure 83: δ ¹³ C values (green > 200 years and blue < 200 years) at sites in the South basin, Maloe More (MM) and North basin. Turbidite sections are removed within the δ ¹³ C record.....	188
Figure 84: TOC/N ratio (green > 200 years and blue < 200 years) at sites in the South basin, Maloe More (MM) and North basin. Turbidite sections are removed within the TOC/N record.	188
Figure 85: TOC content (green > 200 years and blue < 200 years) at sites in the South basin, Maloe More (MM) and North basin. Turbidite sections are removed within the TOC/N record.	189
Figure 86: Sediment cores collected in March 2013 and August 2013 in the South basin, Maloe More, Selenga and North basin. (*BAIK13-7 and *BAIK13-18 show high levels of degradation).	191
Figure 87: Pigment concentrations (nmol per g OM), pigment ratios, TOC %, δ ¹³ C, TOC/N ratio values and magnetic susceptibility values (10 ⁻⁶ SI un) in the entire BAIK13-1C sediment core. Grey shaded areas represent turbidite layers. Green line represents the sediment depth for the last 200 years from ²¹⁰ Pb dating. (T – turbidites).	192
Figure 88: Pigment concentrations (nmol per g OM), pigment ratios, TOC %, δ ¹³ C, TOC/N ratio values and magnetic susceptibility values (10 ⁻⁶ SI un) in the entire BAIK13-4F sediment core. Grey shaded areas represent turbidite layers. Green line represents the sediment depth for the last 200 years from ²¹⁰ Pb dating (T – turbidites).....	193
Figure 89: Pigment concentrations (nmol per g OM), pigment ratios, TOC %, δ ¹³ C, TOC/N ratio values and magnetic susceptibility values (10 ⁻⁶ SI un) in the entire BAIK13-7A sediment core. Grey shaded areas represent turbidite layers. Green line represents the sediment depth for the last 200 years from ²¹⁰ Pb dating. (T – turbidites).	193
Figure 90: Pigment concentrations (nmol per g OM), pigment ratios, TOC %, δ ¹³ C, TOC/N ratio values and magnetic susceptibility values (10 ⁻⁶ SI un) in the entire BAIK13-10A sediment core. Grey shaded areas represent turbidite layers. Green line represents the sediment depth for the last 200 years from ²¹⁰ Pb dating. (T – turbidites).	194
Figure 91: Pigment concentrations (nmol per g OM), pigment ratios, TOC %, δ ¹³ C, TOC/N ratio values and magnetic susceptibility values (10 ⁻⁶ SI un) in the entire BAIK13-11C sediment core. No turbidites in sediment core. Green line represents the sediment depth for the last 200 years from ²¹⁰ Pb dating.....	195
Figure 92: Pigment concentrations (nmol per g OM), pigment ratios, TOC %, δ ¹³ C, TOC/N ratio values and magnetic susceptibility values (10 ⁻⁶ SI un) in the entire BAIK13-14C sediment core. Grey shaded areas represent turbidite layers. Green line represents the sediment depth for the last 200 years from ²¹⁰ Pb dating. (T – turbidites).	195
Figure 93: Pigment concentrations (nmol per g OM), pigment ratios, TOC % and magnetic susceptibility values (10 ⁻⁶ SI un) in the entire BAIK13-15B sediment core. Grey shaded areas represent turbidite layers. (T – turbidites).....	196

Figure 94: Pigment concentrations (nmol per g OM), pigment ratios, TOC % and magnetic susceptibility values (10^{-6} SI un) in the entire BAIK13-16B sediment core. No turbidites in sediment core. Blue shaded area represents Pleistocene clays.	197
Figure 95: Pigment concentrations (nmol per g OM), pigment ratios, TOC %, $\delta^{13}\text{C}$, TOC/N ratio values and magnetic susceptibility values (10^{-6} SI un) in the entire BAIK13-18A sediment core. Grey shaded areas represent turbidite layers. Green line represents the sediment depth for the last 200 years from ^{210}Pb dating. (T – turbidites).	198
Figure 96: Pigment concentrations (nmol per g OM), pigment ratios, TOC %, $\delta^{13}\text{C}$, TOC/N ratio values and magnetic susceptibility values (10^{-6} SI un) in the entire BAIK13-19B sediment core. No turbidites in sediment core. Green line represents the sediment depth for the last 200 years from ^{210}Pb dating.	198
Figure 97: Diatoxanthin:canthaxanthin ratio. Red line represents sediment depth of last 200 years from ^{210}Pb dating chronologies.	199
Figure 98: $\delta^{13}\text{C}$, C/N % ratios, TOC % and CMAR values over the Holocene at the Vydrino site in the South basin (modified from Mackay et al. 2016).	200
Figure 99: Previous $\delta^{13}\text{C}$ records at Lake Baikal over the Holocene (from Ishiwatari et al. 2005; Watanabe et al. 2009; Mackay et al. 2016) (modified from Mackay et al. 2016).	201
Figure 100: Previous TOC % records at Lake Baikal over the Holocene (from Ishiwatari et al. 2005; Horiuchi et al. 2000; Watanabe et al. 2009; Mackay et al. 2016) (modified from Mackay et al. 2016).	201
Figure 101: $\delta^{13}\text{C}$ values from South basin, Selenga, Maloe More and North basin sediment cores.	202
Figure 102: TOC content from South basin, Selenga, Maloe More and North basin sediment cores.	202
Figure 103: TOC/N ratio from South basin, Selenga, Maloe More and North basin sediment cores.	203
Figure 104: Chlas concentrations in the North, Selenga and South basin sites over the Holocene (Fietz et al. 2007).	207
Figure 105: Fossil pigment concentrations ($\mu\text{mol g}^{-1}$ OC) from the Vydrino coring site in the South basin (Fietz et al. 2007).	207
Figure 106: Fossil pigment concentrations ($\mu\text{mol g}^{-1}$ OC) from the Continent Ridge coring site in the North basin (Fietz et al. 2007).	208
Figure 107: South basin sedimentary pigment profiles at Vydrino site (Fietz et al. 2007) and BAIK13-1C, BAIK13-4F and BAIK13-7A (this study: nmol g). Red line represents sediment depth of last 200 years from ^{210}Pb dating chronologies. Grey line represents horizon for radiocarbon dating. (*BAIK13-7A shows high levels of degradation).	209
Figure 108: Selenga sedimentary pigment profiles at Posolski site (Fietz et al. 2007) and BAIK13-10A and BAIK13-11C (this study: nmol g). Red line represents sediment depth of last 200 years from ^{210}Pb dating chronologies. Grey line represents horizon for radiocarbon dating.	210
Figure 109: North basin sedimentary pigment profiles at Continent Ridge site (Fietz et al. 2007) and BAIK13-18A and BAIK13-19B (this study: nmol g). Red line represents sediment depth of last 200 years from ^{210}Pb dating chronologies. Grey line represents horizon for radiocarbon dating. (*BAIK13-18A shows high levels of degradation).	210

Figure 120: Sedimentation rates for each ^{210}Pb dated sediment core in the South basin, Selenga, Maloe More and North basin.....	220
Figure 121: Age-depth models with polynomial line-fitting for each ^{210}Pb dated sediment core in the South basin, Selenga, Maloe More and North basin. The age units are years before 2013.	221
Figure 122: Comparison of Chlas concentration ($\text{nmol g}^{-1} \text{OC}$) between oxic (green) and anoxic (blue) layers in the sediment cores across the lake over the last 200 years. ANOVA results showed significant differences (as indicated by an asterisk).....	223
Figure 123: Comparison of Chlas AR ($\text{nmol pigment cm}^{-2} \text{yr}^{-1}$) between oxic (green) and anoxic (blue) layers in the sediment cores across the lake over the last 200 years. ANOVA results showed significant differences (as indicated by an asterisk).....	224
Figure 124: Comparison of CMAR ($\text{g C m}^{-2} \text{yr}^{-1}$) between oxic (green) and anoxic (blue) layers in the sediment cores across the lake over the last 200 years. ANOVA results showed significant differences (as indicated by an asterisk).	224
Figure 125: Comparison of chl-a:pheo-a pigment preservation ratio between oxic (green) and anoxic (blue) layers in the sediment cores across the lake over the last 200 years. T-test results show significant differences (as indicated by an asterisk).....	226
Figure 126: Chl-a: pheo-a pigment ratio in surface sediments (upper 2 cm) and water column depth at coring sites across the lake.	232
Figure 127: Chl-a:pheo-a pigment ratio and CMAR ($\text{g C m}^{-2} \text{yr}^{-1}$) plotted on a log scale at all the sites in the South basin, Selenga, Maloe More Bay and North basin.....	237
Figure 128: Mean Chla AR and SAR within oxic and anoxic sediments at all sites in the South basin, Selenga, Maloe More and North basin.....	239
Figure 129: TOC % in the surface (upper 2 cm) sediments (over the last 20 years) in the South, Selenga, Maloe More (MM) and North basin sites.	241
Figure 130: Biplot of surface sediment $\delta^{13}\text{C}$ and TOC/N ratio values over the last 20 years in the South (BAIK13-1C; BAIK13-4F; BAIK13-7A), Selenga (BAIK13-10A; BAIK13-11C), Maloe More (BAIK13-14C) and North basin (BAIK13-18A; BAIK13-19B) sites. TOC/N ratio values < 12 indicates predominately algal sources (Prokopenko et al. 1993).....	242
Figure 131: Chlorophyll-a and major carotenoid concentrations in the surface sediments over the last 20 years in the South, Selenga, Maloe More and North basin sites. (BAIK13-7A and BAIK13-18A pigment data removed).....	243
Figure 132: Main diatom species abundances in the surface sediments over the last 20 years in the South, Selenga, Maloe More and North basin sites.....	245
Figure 133: BAIK13-1C in the South basin. Chl-a and derivatives, carotenoids and organics (only major algal pigments) are shown. Dashed green line indicates onset of human influence in the Baikal region (Brunello et al. 2004). Grey shading represents recent sediments (Zone 1).....	248
Figure 134: BAIK13-4F in the South basin. Chl-a and derivatives, carotenoids, organics and diatoms (only major algal pigments and diatom species) are shown. Dashed green line indicates onset of human influence in the Baikal region (Brunello et al. 2004). Grey shading represents recent sediments (Zone 1).....	249
Figure 135: BAIK13-7A in the South basin. Chl-a and derivatives, carotenoids, organics, diatoms (only major algal pigments and diatom species) and	

<p><i>Spheroidal Carbonaceous Particles (SCP) are shown. SCP data from Prof. N. Rose. Diatom counts made by author are shown as white bars, and those made by Prof Anson Mackay are shown as black bars (as published in Mackay et al. 1998). Dashed green line indicates onset of human influence in the Baikal region (Brunello et al. 2004). Grey shading represents recent sediments (Zone 1).</i>.....</p>	251
<p><i>Figure 136: BAIK13-10A by the Selenga Delta. Chl-a and derivatives, carotenoids, organics, diatoms (only major algal pigments and diatom species) and mercury (Hg) Accumulation Rate (AR) are shown. Dashed green line indicates onset of human influence in the Baikal region (Brunello et al. 2004). Grey shading represents recent sediments (Zone 1).</i>.....</p>	252
<p><i>Figure 137: BAIK13-11C in the South basin, opposite the Selenga Delta. Chl-a and derivatives, carotenoids, organics, diatoms (only major algal pigments and diatom species) and Spheroidal Carbonaceous Particles (SCP) are shown. SCP data from Prof. N. Rose. Diatom counts made by author are shown as white bars, and those made by Prof Anson Mackay are shown as black bars (as published in Mackay et al. 1998). Dashed green line indicates onset of human influence in the Baikal region (Brunello et al. 2004). Grey shading represents recent sediments (Zone 1).</i>.....</p>	254
<p><i>Figure 138: BAIK13-14C in Maloe More Bay. Chl-a and derivatives, carotenoids, organics, diatoms (only major algal pigments and diatom species) are shown. Dashed green line indicates onset of human influence in the Baikal region (Brunello et al. 2004). Grey shading represents recent sediments (Zone 1)....</i></p>	255
<p><i>Figure 139: BAIK13-18A in the North basin. Chl-a and derivatives, carotenoids, organics, diatoms (only major algal pigments and diatom species) and Spheroidal Carbonaceous Particles (SCP) are shown. SCP data from Prof. N. Rose. Diatom counts made by author are shown as white bars, and those made by Prof Anson Mackay are shown as black bars (as published in Mackay et al. 1998). Dashed green line indicates onset of human influence in the Baikal region (Brunello et al. 2004). Grey shading represents recent sediments (Zone 1).</i>.....</p>	257
<p><i>Figure 140: BAIK13-19B in the North basin. Chl-a and derivatives, carotenoids, organics, diatoms (only major algal pigments and diatom species) and mercury (Hg) Accumulation Rate (AR) are shown. Dashed green line indicates onset of human influence in the Baikal region (Brunello et al., 2004). Exaggeration factor (x10) applied to Synedra abundances. Grey shading represents recent sediments (Zone 1).</i>.....</p>	258
<p><i>Figure 141: CMARs between 1840 – 2013 in the Selenga (red line), South basin (black line), Maloe More (blue line) and North basin (green and grey line).</i>..</p>	259
<p><i>Figure 142: $\delta^{13}\text{C}$ and TOC/N values over the last 200 years from sediment cores taken in the South basin (BAIK13-1C, BAIK13-4F, BAIK13-7A), North basin (BAIK13-18A, BAIK13-19B), Maloe More (BAIK13-14C) and Selenga (BAIK13-10A, BAIK13-11C). TOC/N ratio values < 12 indicates predominately algal sources (Prokopenko et al. 1993).</i>.....</p>	260
<p><i>Figure 143: HI and OI data grouped into significant zones down-core. Data is presented for sediment cores in the South basin (Baik13-1C), North basin (Baik13-19B) and Selenga (Baik13-10A). Note that the low resolution for this analysis is due to this being a pilot study.</i>.....</p>	261

Figure 144: Down-core HI, OI, HI/OI ratio values, $\delta^{13}\text{C}$ and TOC/N values for sediment cores taken in the (A) Selenga (BAIK13-10A), (B) South basin (BAIK13-1C) and (C) North basin (BAIK13-19B).....	262
Figure 145: Average annual temperature at Irkutsk, ice cover duration at Lystvyanka station in the South basin and PCA axis one scores on pigment datasets from sediment cores in the South, North, Maloe More (MM) and Selenga sites. Dashed line represents a significant zone within the pigment data.	263
Figure 146: PCA of pigments over the last 200 years at all sites in South basin, Selenga, Maloe More and North basin. Grey circles indicate North basin sites and black diamonds indicate South, Selenga and Maloe More sites. (Removed pigment data from BAIK13-7A and BAIK13-18A).	267
Figure 147: Chlas concentrations and $\delta^{13}\text{C}$ values (suess corrected) pre (green) and post (blue) 1950 AD across the lake. (*BAIK13-7A and *BAIK13-18A show high levels of degradation).	269
Figure 148: (A) Total carotenoids concentrations pre (green) and post (blue) 1950 across the lake. (B) Diatom valve concentrations (10^4 valves/g dry wt) pre (green) and post (blue) 1950 across the lake.	270
Figure 149: Regression correlations and p-values between average annual temperature at Irkutsk and Chlas concentrations in the South basin, Maloe More, Selenga and North basin. (BAIK13-7A pigment data removed from South basin correlation and BAIK13-18A pigment data removed from North basin correlation).	272
Figure 150: Regression correlations and p-values between average annual temperature at Irkutsk and $\delta^{13}\text{C}$ values in the South basin, Maloe More, Selenga and North basin.....	273
Figure 151: (A) Diatoxanthin:canthaxanthin pigment ratio, Irkutsk regional air temperature ($^{\circ}\text{C}$) and ice cover duration (days), (B) Diatom concentrations (10^4 valves/g dry wet), Irkutsk regional air temperature ($^{\circ}\text{C}$) and ice cover duration (days).	275
Figure 152: RDA analysis results of (A) BAIK13-11 in the South basin and (B) BAIK13-14 at Maloe More Bay, examining the influence of air temperature and tourist activity on down-core sedimentary algal pigments since c. 1950AD. Tourism is significantly (p value > 0.05) correlated with algal pigments in both BAIK13-11C and BAIK13-14, and temperature (p value > 0.05) in BAIK13-14C. Forward selection with Monte Carlo permutation tests were applied. 'Railway construction' refers to sediments post 1950 AD, 'Increased tourism' refers to sediments post 1990 AD and 'Temperature' refers to Irkutsk air temperatures.....	276
Figure 153: Water profiles of Silicate concentrations in the South basin sites. Light blue line represents March 2013 profiles and dark blue line represents August 2013 profiles.....	363
Figure 154: Water profiles of Silicate concentrations in the South basin/Selenga, Central Basin, Maloe More Bay and North basin/Chivsky Bay sites. Dark blue line represents August 2013 profiles.	364
Figure 155: Water profiles of Silicate concentrations in the North basin sites. Dark blue line represents August 2013 profiles.....	365
Figure 156: Water profiles of TP concentrations in the South basin sites. Light blue line represents March 2013 profiles and dark blue line represents August 2013 profiles.	366

Figure 157: Water profiles of TP concentrations in the South basin/Selenga, Central Basin, Maloe More Bay and North basin/Chivsky Bay sites. Dark blue line represents August 2013 profiles.	367
Figure 158: Water profiles of TP concentrations in the North basin sites. Dark blue line represents August 2013 profiles.	368
Figure 159: Water profiles of DOC concentrations in the South basin sites. Light blue line represents March 2013 profiles and dark blue line represents August 2013 profiles.....	369
Figure 160: Water profiles of DOC concentrations in the South basin/Selenga, Central Basin, Maloe More Bay and North basin/Chivsky Bay sites. Dark blue line represents August 2013 profiles.	370
Figure 161: Water profiles of DOC concentrations in the North basin sites. Dark blue line represents August 2013 profiles.....	371
Figure 162: Radiometric chronology of core BAIK13-1C taken from Baikal region, Russia, showing the CRS model ^{210}Pb dates and sedimentation rates. The solid line shows age while the dashed line indicates sedimentation rate.....	378
Figure 163: Radiometric chronology of core BAIK13-4F, showing the CRS model ^{210}Pb dates and sedimentation rates. The solid line shows age while the dashed line indicates sedimentation rate.....	380
Figure 164: Radiometric chronology of core BAIK13-7A taken from BPPM, showing the CRS model ^{210}Pb dates and sedimentation rates. The solid line shows age while the dashed line indicates sedimentation rate.....	382
Figure 165: Radiometric chronology of core BAIK13-10A taken from Selenga Delta region, showing the CRS model ^{210}Pb dates and sedimentation rates. The solid line shows age while the dashed line indicates sedimentation rate.....	384
Figure 166: Radiometric chronology of core BAIK13-11C, showing the CRS model ^{210}Pb dates and sedimentation rates. The solid line shows age while the dashed line indicates sedimentation rate.....	386
Figure 167: Radiometric chronology of core BAIK13-14C, showing the CRS model ^{210}Pb dates and sedimentation rates. The solid line shows age while the dashed line indicates sedimentation rate.....	388
Figure 168: Radiometric chronology of core BAIK13-18A, showing the CRS model ^{210}Pb dates and sedimentation rates. The solid line shows age while the dashed line indicates sedimentation rate.....	390
Figure 169: Radiometric chronology of core BAIK13-19B, showing the CRS model ^{210}Pb dates and sedimentation rates. The solid line shows age while the dashed line indicates sedimentation rate.....	392
Figure 170: Diatom profile for BAIK13-7A in the South basin. Most abundant species are shown (abundance > 2%), with total diatom concentrations and diatom dissolution index (DDI) down-core. Dashed green line indicates onset of human influence in the Baikal region (Brunello et al., 2004).	393
Figure 171: Diatom profile for BAIK13-11C in the South basin. Most abundant species are shown (abundance > 2%), with total diatom concentrations and diatom dissolution index (DDI) down-core. Dashed green line indicates onset of human influence in the Baikal region (Brunello et al., 2004).	393
Figure 172: Diatom profile for BAIK13-18A in the North basin. Most abundance species are shown (abundance > 2%), with total diatom concentrations and diatom dissolution index (DDI) down-core. Dashed green line indicates onset of human influence in the Baikal region (Brunello et al., 2004).	394

Table 1: Ancient lakes, defined as those which have experienced at least one full glacial cycle. Adapted from Herdendorf (1982) but updated from http://www.worldlakes.org/ (Source: Mackay, 2013).	3
Table 2: Algal pigments with their diagnostic algal groups and pigment stabilities (modified from Leavitt and Hodgson et al. 2001 and McGowan 2013). Bchl-a – bacterial chlorophylls. Stability is how resistant the pigment is to degradation, with 1 being the most stable and 4 being the least stable.	21
Table 3: Diatom correction factors (Battarbee et al. 2005). Preservation factors for five of Baikal’s major diatom species are calculated as the ratio of planktonic diatom taxa and sedimentary diatom accumulation rate. Correction factors are calculated from the estimates of the ratio of planktonic diatoms to diatoms preserved within the sedimentary record.	29
Table 4: $\delta^{13}\text{C}$ and TOC/N values at Lake Baikal (Prokopenko et al. 1993; Prokopenko and Williams, 2001; Morley, 2005).	36
Table 5: Processes affecting the TOC, TOC/N and $\delta^{13}\text{C}$ values of organic carbon at Lake Baikal (modified from Mackay et al. 2016).	39
Table 6: Nutrient treatments added to the mesocosms in March and August 2013.	68
Table 7: Sediment cores collected at the South basin, Selenga, Maloe More Bay (MM), Chivsky Bay (CH) and North basin coring stations in March 2013 and August 2013 University of Nottingham and Earth’s Crust Institute in Irkutsk.	69
Table 8: Location of the coring sites across Lake Baikal, core length and water depth of sites.	70
Table 9: Analyses carried out on the sediment cores.	70
Table 10: Solvent separation gradients modified from Chen et al. (2001).	75
Table 11: Light attenuation coefficient (LAC) values and photic zone depths for March 2013 and for August 2013 at the three transect sites in the South basin.	91
Table 12: March and August variables; conductivity, pH and dissolved oxygen (mean values in photic zone with standard deviation) as there is little variation down the water profile.	92
Table 13: Dominant pigment concentrations in March 2003 (Fietz, 2005) and March 2013 in the South basin.	100
Table 14: ANOVA results for March 2013 under-ice experiment 1 and Tukey test for assessing significant difference in pigment concentrations between treatments on day 7.	104
Table 15: ANOVA results for March 2013 experiment 2 in field laboratory and Tukey test for assessing significant difference in pigment concentrations between treatments on day 6.	104
Table 16: ANOVA results for August 2013 experiment and Tukey test for assessing significant difference in pigment concentrations between treatments on day 11.	107
Table 17: Results from normality, ANOVA, and KW tests performed on nutrient and DOC concentration datasets.	124
Table 18: P values presented from post-hoc tests for significant differences in nutrient concentrations between the South, Central and North basins.	124
Table 19: Average major ion concentrations within the mixing layer across the three basins and in the major river inflows.	125
Table 20: Comparisons of total phosphorus ($\mu\text{g/L}$), nitrate (mg/L) and sulphate (mg/L) from this study (2013) and past measurements from previous publications. TP data sources from Liebezeit, 1992; Granina and Sigg, 1995;	

Sorokovikova et al. 2015. Nitrate data sources from Zilov et al. 2012; Sorokovikova et al. 2012; 2015. Sulphate data sources from Falkner et al. 1991; Sorokovikova et al. 2015.	130
Table 21: Comparisons of silicate (mg/L) and DOC concentrations (mg/L) from this study (2013) and past measurements from previous publications. Silicate data sources from Jewson et al. 2010; Sorokovikova et al. 2012; Jewson and Granin, 2014. DOC data sources from Yoshioka et al. 2002; 2007.	131
Table 22: TP concentrations within surface waters across Lake Baikal and upper waters from tributaries between 1995 to 2009 (unpublished data from Prof. E. Silow).....	132
Table 23: DCM layer thickness within the South, Central and North basins sampled in August 2013.....	143
Table 24: Zeaxanthin and fucoxanthin pigment concentrations at the DCM layer in the South, Selenga, Central, Maloe More and North basin sites in August 2013.	143
Table 25: Results from normality tests, ANOVA, and KW tests performed on mixing layer pigment datasets.....	145
Table 26: P values presented from post hoc tests which indicate if there is any significant difference in concentrations between the South, Central and North basins.	145
Table 27: Mean concentrations mixing layer HPLC pigments (nmol/L) (fucoxanthin, lutein and zeaxanthin) and YSI chlorophyll-a (nmol/L) data in the South, Central and North basins.	145
Table 28: Mean and SD values of Chlas concentrations, Chlbs/Chlas, Diatox/Chlas, Cantha/Chlas over the last 200 years and in sediments > 200 years. Turbidite sections have been removed within the pigment records. (*BAIK13-7A and *BAIK13-18A show high levels of degradation).....	183
Table 29: Mean values of Chlas concentrations, Chlbs/Chlas, Diatox/Chlas, Cantha/Chlas over the last 200 years and in sediments > 200 years for the South basin, Selenga, Maloe More and North basin. Turbidite sections have been removed within the pigment records.	184
Table 30: Results from t-test to examine if Chlas concentrations are significantly different between the two intervals (> and < 200 years). (*BAIK13-7A and *BAIK13-18A show high levels of degradation).....	185
Table 31: Results from t-test to examine if total carotenoid concentrations are significantly different between the two intervals (> and < 200 years). (*BAIK13-7A and *BAIK13-18A show high levels of degradation).....	186
Table 32: Mean and SD values of $\delta^{13}\text{C}$, TOC content and TOC/N ratios over the last 200 years and in sediments > 200 years. Turbidite sections have been removed within the pigment records.	187
Table 33: Results from t-test to examine if TOC, TOC/N ratio and $\delta^{13}\text{C}$ values are significantly different between the two intervals (> and < 200 years).	189
Table 34: Previous ^{210}Pb derived sedimentation rates at Lake Baikal between c. 1930 – 1990 AD (Mackay et al. 1998).	217
Table 35: Results from t-test and p values for comparing Chlas concentrations (nmol g OC ⁻¹) between oxic and anoxic layers in the sediment cores across the lake over the last 200 years. Sites include South basin, South/Selenga, Central/MM (Maloe More Bay) and North basin.	225
Table 36: Results from t-test and p values for comparing Chlas AR values (nmol pigment g OC cm ⁻² yr ⁻¹) between oxic and anoxic layers in the sediment cores	

across the lake over the last 200 years. Sites include South basin, South/Selenga, Central/MM (Maloe More Bay) and North basin.	225
Table 37: Results from t-test and p values for comparing CMAR values ($\text{g C m}^{-2} \text{ yr}^{-1}$) between oxic and anoxic layers in the sediment cores across the lake over the last 200 years. Sites include South basin, South/Selenga, Central/MM (Maloe More Bay) and North basin.	225
Table 38: Results from t-test and p values for comparing chl-a:phco-a pigment preservation ratio between oxic and anoxic layers in the sediment cores across the lake over the last 200 years. Sites include South basin, South/Selenga, Central/MM (Maloe More Bay) and North basin.	227
Table 39: Correlations between CMAR/DMAR and Chlas concentration per organic content. Red = negative relationship. Sites include South basin, South/Selenga, Central/MM (Maloe More Bay) and North basin.	228
Table 40: Correlations between CMAR/DMAR and Chlas concentration per dry matter. Sites include South basin, South/Selenga, Central/MM (Maloe More Bay) and North basin.	229
Table 41: Correlations between CMAR/DMAR and Diatoxanthin concentrations. Red = negative relationship. Sites include South basin, South/Selenga, Central/MM (Maloe More Bay) and North basin.	230
Table 42: Correlations between CMAR/DMAR and Canthaxanthin concentrations. Red = negative relationship. Sites include South basin, South/Selenga, Central/MM (Maloe More Bay) and North basin.	231
Table 43: Regression correlation coefficients and significance values between the chl-a:phco-a pigment ratio and Chlas AR. Red = negative relationship. Sites include South basin, South/Selenga, Central/MM (Maloe More Bay) and North basin.	234
Table 44: Regression correlation coefficients and significance values between the chl-a:phco-a pigment ratio and CMAR. Red = negative relationship. Sites include South basin, South/Selenga, Central/MM (Maloe More Bay) and North basin.	235
Table 45: Regression correlation coefficients and significance values between the chl-a:phco-a pigment ratio and DMAR. Red = negative relationship. Sites include South basin, South/Selenga, Central/MM (Maloe More Bay) and North basin.	236
Table 46: Correlation coefficients and significance testing between Chlas, diatoxanthin and canthaxanthin pigment concentrations. BAIK13-18A in the North basin has not been included as no intact chlorophyll-a or diatoxanthin/canthaxanthin pigments were detected. Red = negative relationship. Sites include South basin, South/Selenga, Central/MM (Maloe More Bay) and North basin.	238
Table 47: Correlation coefficients and significance testing between diatoxanthin and canthaxanthin pigment concentrations. BAIK13-18A in the North basin has not been included as no intact diatoxanthin/canthaxanthin pigments were detected. Red = negative relationship. Sites include South basin, South/Selenga, Central/MM (Maloe More Bay) and North basin.	239
Table 48: Summary table of sediment cores to highlight which pigment records are suitable for interpretation. Grey indicates pigment records which can be interpreted.	240
Table 49: The upper cms which cover the last 20 years at each coring site and the age of the upper 1 cm at each coring site.	241

Table 50: P-values from ANOVA to test if there is a significant difference in pigment concentrations between regions (South basin, Selenga Shallows, Maloe More and North basin).....	243
Table 51: P-values from ANOVA to test if there is a significant difference in diatom species abundances between regions (South basin, Selenga Shallows, Maloe More (MM) and North basin).....	246
Table 52: MK trend test coefficients and p-values, and timing of break-point with p-value. BAIK13-4F is removed due to turbidite layer (* likely pigment degradation profiles).	265
Table 53: Regression coefficients and p-values for correlations between Chlas concentrations and $\delta^{13}\text{C}$ across the lake. Core data within the South basin and North basin have been merged.....	271
Table 54: Correlation coefficients and p-values for correlations between average annual temperature at Irkutsk and Chlas concentrations, $\delta^{13}\text{C}$, diatom concentrations, diatoxanthin: canthaxanthin pigment ratio and chl _b : chlas pigment ratio in the South basin, Selenga, Maloe More and North basin.	274
Table 55: Raw and corrected diatom abundances; average surface sediment abundances (0 – 2 cm); two cores in South basin; BAIK13-4F and BAIK13-7A. These cores have been selected as they have the highest abundances of <i>Synedra acus</i> var. <i>radians</i> , which is a lightly silicified diatom species.....	281
Table 56: Main pigment concentrations from each treatment (plus replicates) for nutrient enrichment experiment conducted underneath the South basin lake ice in March 2013.	372
Table 57: Nutrient concentrations from each treatment (plus replicates) for nutrient enrichment experiment conducted underneath the South basin lake ice in March 2013.	373
Table 58: Main pigment concentrations from each treatment (plus replicates) for nutrient enrichment experiment conducted in a laboratory kunk on the South basin lake shore in March 2013.	374
Table 59: Nutrient concentrations from each treatment (plus replicates) for nutrient enrichment experiment conducted in a laboratory kunk on the South basin lake shore in March 2013.	374
Table 60: Main pigment concentrations from each treatment (plus replicates) for nutrient enrichment experiment conducted in August 2013. Water was collected from BAIK13-12 and experimental in set-up in Maloe More Bay.	375
Table 61: Nutrient and DOC concentrations from each treatment (plus replicates) for nutrient enrichment experiment conducted in August 2013. Water was collected from BAIK13-12 and experimental in set-up in Maloe More Bay. (-) indicated no sample measured.	375
Table 62: Mercury (Hg) concentrations in the Baikal water samples.	376
Table 63: Mercury (Hg) concentrations in the sediments taken from Lake Baikal.	376
Table 64: ^{210}Pb chronology of core BAIK13-1C taken from Baikal region, Russia.	377
Table 65: ^{210}Pb concentrations for core BAIK13-1C taken from Baikal region, Russia.....	377
Table 66: ^{210}Pb chronology and sedimentation rates of core BAIK13-4F.	379
Table 67: ^{210}Pb concentrations for core BAIK13-4F.	379
Table 68: ^{210}Pb chronology of core BAIK13-7A taken from BPPM.	381
Table 69: ^{210}Pb concentrations for core BAIK13-7A.	381
Table 70: ^{210}Pb chronology of core BAIK13-10A.	383

<i>Table 71: ²¹⁰Pb concentrations for core BAIK13-10A.</i>	<i>383</i>
<i>Table 72: ²¹⁰Pb chronology of core BAIK13-11C.</i>	<i>385</i>
<i>Table 73: ²¹⁰Pb concentrations for core BAIK13-11C.</i>	<i>385</i>
<i>Table 74: ²¹⁰Pb chronology of core BAIK13-14C.</i>	<i>387</i>
<i>Table 75: ²¹⁰Pb concentrations for core BAIK13-14C.</i>	<i>387</i>
<i>Table 76: ²¹⁰Pb chronology and sedimentation rate of core BAIK13-18A.</i>	<i>389</i>
<i>Table 77: ²¹⁰Pb concentrations for core BAIK13-18A.</i>	<i>389</i>
<i>Table 78: ²¹⁰Pb chronology and sedimentation rates of core BAIK13-19B.</i>	<i>391</i>
<i>Table 79: ²¹⁰Pb concentrations for core BAIK13-19B.</i>	<i>391</i>

List of Abbreviations

AR	Accumulation rate
BPPM	Baikalsk Pulp and Paper Mill
BSi	Biogenic silica
Chl- <i>a</i>	Chlorophyll- <i>a</i>
Chlas	Chlorophyll- <i>a</i> plus its degradation products (Chlorophyllide, pheophorbide, pheophytin and pyropheophytin)
Chl- <i>b</i>	Chlorophyll- <i>b</i>
CMAR	Carbon mass accumulation rate
DCM	Deep chlorophyll maxima
DDI	Diatom dissolution index
DIC	Dissolved inorganic carbon
DOC	Dissolved organic carbon
DMAR	Dry mass accumulation rate
DSi	Dissolved silicate
DW	Deep water
Hg	Mercury
HI	Hydrogen index
HPLC	High performance liquid chromatography
LAC	Light attenuation coefficient
LIA	Little Ice Age
MCA	Medieval Climate Anomaly
MeHg	Methylmercury
ML	Mixing layer
MK	Mann-Kendall
MM	Maloe More
N	Nitrogen

OI	Oxygen index
OM	Organic matter
Pb	Lead
P	Phosphorus
PCA	Principal components analysis
RDA	Redundancy analysis
SAR	Sediment accumulation rate
SCE	Steryl chlorin esters
SCP	Spheroidal carbonaceous particle
Si	Silicon
TOC	Total organic carbon
TOC/N	Total organic carbon to nitrogen ratio
TP	Total phosphorus
UVR	Ultraviolet radiation

Grouping and location of sites

Table i: Location of Water Sampling and Coring Stations at Lake Baikal.

Location	Site	Basin	Sampling
1	BAIK13-1	South Basin	Water/Core
4	BAIK13-4	South Basin	Water/Core
5	BAIK13-5	South Basin	Water
7	BAIK13-7	South Basin	Water/Core
8	BAIK13-8	South Basin	Water
9	BAIK13-9	South Basin	Water
10	BAIK13-10	South Basin/Selenga	Water/Core
11	BAIK13-11	South Basin/Selenga	Water/Core
12	BAIK13-12	Central Basin	Water
13	BAIK13-13	Central Basin/Maloe More Bay	Water
14	BAIK13-14	Central Basin/Maloe More Bay	Water/Core
15	BAIK13-15	Central Basin/Maloe More Bay	Water/Core
16	BAIK13-16	North Basin/Chivsky Bay	Water/Core
17	BAIK13-17	North Basin	Water
18	BAIK13-18	North Basin	Water/Core
19	BAIK13-19	North Basin	Water/Core

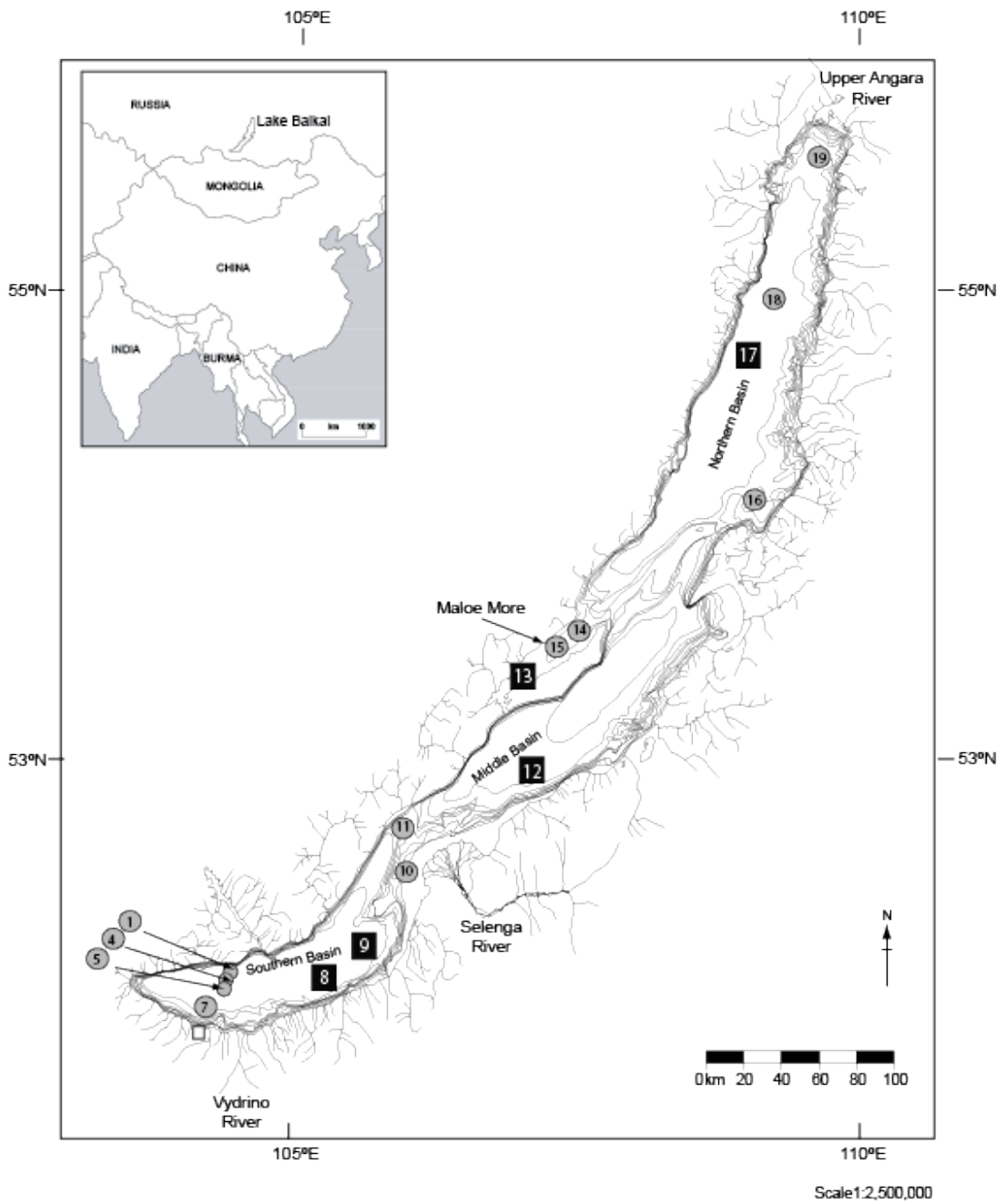


Figure i: Locations of Water Sampling (represented by both circle and squares) and Core Stations (represented by circles only) at Lake Baikal.

Chapter One: Introduction

1.1 Anthropogenic impacts on ancient lakes

High levels of endemism are found within all the worlds ancient lakes, and anthropogenic activity over the past century (agriculture, urban development, industrial development, anthropogenic climate change) has been resulting in alterations within nutrient concentrations, nutrient cycling, lake levels, water temperatures, thermal stratification and biological assemblages (Vander Zanden et al. 1999; O'Reilly et al. 2003; Micklin, 2007; Thackeray et al. 2013; Francis et al. 2014). For example, Lake Titicaca and the Aral Sea (Abbott et al. 1996; Cretaux et al. 2013) have experienced lower water levels and Lake Victoria has experienced drought, as well as recent anthropogenic pressures and increased nutrient pollution from urban growth (Abbott et al. 1996; Stager et al. 2003). Most of these rapid limnological and ecological changes have not been seen before in the lakes, occurring at unprecedented rates (Matzinger et al. 2007), and sites close to polluted river inflows in Lake Ohrid, Lake Victoria and Lake Biwa, exhibit shifts towards non-endemic species (Seehausen et al. 1997; Tsugeki et al. 2003; Matzinger, 2006; Matzinger et al. 2007; Lorenschat et al. 2014). These detected shifts towards non-endemic species and surface water blooms of cyanobacteria (Matzinger et al. 2007), are a result of eutrophication which is nutrient enrichment within lakes promoting growth of smaller and more competitive algae. Eutrophication will therefore have detrimental effects on the ecosystem of these ancient lakes, resulting in the loss of endemic species and water quality deterioration.

The research in this thesis focuses on the recent ecological changes occurring in Lake Baikal (*Figure 1; Table 1*), which is the oldest, deepest and most voluminous lake. Lake Baikal is a large UNESCO World Heritage site in southern central Siberia (Russia), located between 51° and 56° North, and 104° and 110° East. The lake formed over 25 million years ago on an active continental rift (Kozhov, 1963) (*Figure 1; Table 1*). It is more than 600 km long, 80 km wide, and the deepest point is 1640 m (Kozhov, 1963). Due to these dimensions, Lake Baikal has a water capacity of c. 23,600 km³, which is equivalent to all the Laurentian Great lakes together (Kozhova and Imesteva, 1998). Thus, Lake Baikal holds 20% of the worlds freshwater not locked up in ice-sheets, with photic zone depths up to 40 m (Kozhova and Izmet's'eva, 1998). Lake Baikal has never been glaciated due to its continental location (Grosswald and Kuhle, 1994), and has low extinction rates (Cristescu et al. 2010). This long-lived lake is an internationally important freshwater site, known for its great biodiversity, with 75% of its flora and fauna being endemic (Kozhova and Imesteva, 1998).



Figure 1: Ancient lakes across the globe. See Table 1 for name (Source: Mackay, 2013).
 Lake Baikal is shown as number 2.

Table 1: Ancient lakes, defined as those which have experienced at least one full glacial cycle. Adapted from Herdendorf (1982) but updated from <http://www.worldlakes.org/> (Source: Mackay, 2013).

Volume Rank	Name	Volume (km ³)	Latitude	Longitude	Origin	Country
1	Caspian	78,200	42°00'N	50°00'E	Tectonic	Azerbaijan Iran Kazakhstan Russian Federation Turkmenistan
2	Baikal	23,600	54°00'N	109°00'E	Tectonic	Russia
3	Tanganyika	19,000	6°00'S	29°30'E	Tectonic	Burundi Congo (Democratic Republic) Tanzania Zambia
4	Superior	12,100	47°30'N	88°00'W	Glacial	Canada USA
5	Malawi	7775	12°00'S	34°30'E	Tectonic	Malawi Mozambique Tanzania
6	Michigan	4,920	44°00'N	87°00'W	Glacial	Canada USA
7	Huron	3,540	45°00'N	81°15'W	Glacial	Canada USA
8	Victoria	2,760	01°00'S	33°00'E	Tectonic	Kenya Tanzania Uganda
9	Great Bear	2,292	66°00'N	121°00'W	Glacial	Canada
10	Great Slave	2,088	62°40'N	114°00'W	Glacial	Canada
11	Issyk-Kul	1,738	42°30'N	77°15'E	Tectonic	Kyrgyzstan
12	Ontario	1,640	43°30'N	77°45'W	Glacial	Canada USA
13	Titicaca	932	15°45'S	69°30'W	Tectonic	Bolivia Peru
14	Ladoga	908	61°00'N	31°30'E	Glacial	Russia
15	Hamouni Helmand	510	31°00'N	61°15'E	Tectonic	Afghanistan Iran
16	Erie	484	42°15'N	81°15'E	Glacial	Canada USA
17	Hovsgol	380	51°00'N	100°30'E	Tectonic	Mongolia
18	Winnipeg	371	52°30'N	97°45'W	Glacial	Canada
19	Kivu	333	2°13'S	29°10'W	Tectonic	Congo (Democratic Republic) Rwanda
20	Nipigon	320	49°50'N	88°31'W	Glacial	Canada

The high biodiversity at Lake Baikal is a result of evolutionary processes over millions of years, and due to the entire water column being oxygenated, allowing for the development of deep-water faunal communities (Shimaraev et al. 1994). Over 570 algal species have been identified in the lake, with nearly a third of these being endemic (Kozhova and Izmeteva, 1998; Popovskaya et al. 2006). Endemism is present at each level in the food web, with endemic diatoms, zooplankton, fish and the world's only freshwater seal.

Since mid 20th century, Lake Baikal's ecosystem and pristine waters have been threatened by anthropogenic pollution, largely in the form of industrial waste and untreated sewage from growing shoreline settlements and tourist resorts. The extent of anthropogenic activity within Baikal's catchment is discussed in detail in Chapter Two, along with the palaeolimnological studies which have examined the impact of hunter gatherer communities on Baikal's aquatic vegetation, and detected the onset of industrial activity since the 1950s. The extent of these potential impacts on Baikal's algal community composition remains largely unknown, and this research aims to examine the drivers of algal change through the application of experimental studies (Chapter Four), modern day sampling (Chapter Five) and historic trends (Chapter Six; Chapter Seven).

1.2 Algal community response to nutrient enrichment

As it is not known how Baikal algal groups might react to changes in nutrient concentrations, experimental studies are valuable tools to explore changes under controlled nutrient conditions. Eutrophication in lakes is the enrichment with nutrients (N, P and Si), which often results in the dominance of competitive non-motile algal groups, such as cyanobacteria (Schindler, 1971; Hecky and Kilham, 1988; Conley et al. 1993; Riedinger-Whitmore et al. 2005; Callieri, 2007, Heisler et al. 2008). Phosphorus loading from sewage, is one of the main causes of cyanobacterial blooms, along with warming of the surface waters and changes in the mixing regime, such as at Lake Erie, one of the Laurentian Great Lakes (Reavie et al. 2014b). Other factors such as temperature, light and pH may also affect the competitive ability of cyanobacteria. Silica is utilised by siliceous algae, such as diatoms, and nitrogen and phosphorus enrichment can result in lower dissolved silicate concentrations by promoting diatom blooms, leading to silicon limited diatom growth in some lakes (Conley et al. 1993). This is referred to as the silicon depletion hypothesis (Schleske and Stoermer, 1971; 1972), which has been observed in the Laurentian Great Lakes (Schelske et al. 1988).

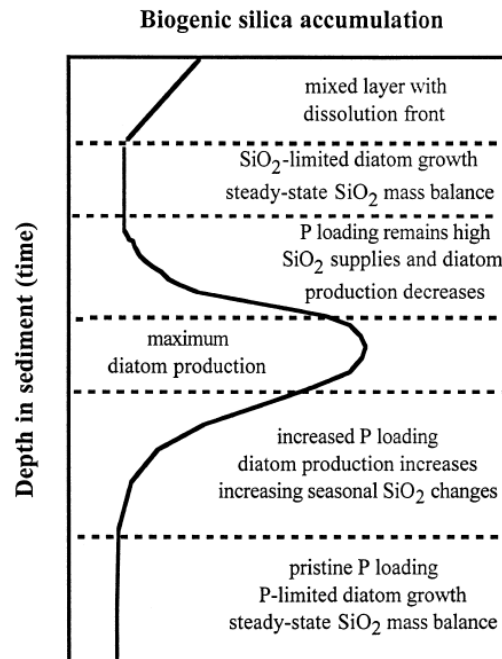


Figure 2: Conceptual diagram of silicon accumulation in the sediment record (Schelske et al. 1983).

The silicon depletion theory is applicable to deep lakes and associated with nitrogen and phosphorus enrichment, which cause an increase in diatom production (Schelske *et al.* 2006) (*Figure 2*). Some of the diatoms produced are sequestered within the sediments, or diatom dissolution occurs within the deep waters isolated from the photic zone. Once sequestered within sediments the silica is permanently removed from the water column, however within the water column, mixing of dissolved silica from the deep layers to the surface waters is a long-term process (Schelske *et al.* 1988). As the silicate supplies are depleted by diatom growth, the excess supply of phosphorus and nitrogen can then be utilised by chlorophytes and cyanobacteria (Officer and Ryther, 1980), potentially resulting in surface blooms of green filamentous and cyanobacteria algae. Therefore, long-term Si depletion is of concern in lakes which are undergoing nutrient enrichment, and could present a future concern for Lake Baikal if the pelagic waters are eutrophying from anthropogenic nutrient enrichment.

1.3 Early signs of eutrophication at Lake Baikal

The pelagic regions of Lake Baikal have not been recently examined for evidence of eutrophication, and previous studies have reported that the pelagic deep waters are not showing any evidence of cultural eutrophication from diatom assemblages (Mackay *et al.* 1998). This provides a gap for the research within this thesis, to examine the perceived threats

to water quality, which are discussed in detail in Chapter Two, on Lake Baikal. Recently published palaeolimnological work has found evidence of benthic eutrophication within the last 5 years, with the occurrence of *Spirogyra* blooms to water depths of 2–5 m, within the near-shore waters of Lake Baikal's North and South basins (Kravtsova et al. 2014; Timoshkin et al. 2015; 2016). *Spirogyra* blooms were by coastal settlements in Listvyanka in the South basin, Khuzhir in Maloe More Bay and Khakusy Bay in the North basin, which are popular tourist destinations and high concentrations of fecal indicator bacteria have been found (Timoshkin et al. 2016) (*Figure 3*). Diseases in endemic *Lubomirskiidae* sponges, which are water filters, were found across some of the North and South basin coastal regions, alongside the *Spirogyra* blooms (Timoshkin et al. 2015). The bioaccumulation of organochlorine contaminants within the endemic sponges has been suggested to be the cause of the mortality (Timoshkin et al. 2016), and nutrient enrichment from inputs of untreated waste water from shoreline settlements and tourist resorts has been suggested to be the cause of the large *Spirogyra* blooms (Kravtsova et al. 2014; Timoshkin et al. 2014; Timoshkin et al. 2016). Tourist activity is focussed around Baikal's bays, such as Listvyanka and Khuzhir, and these regions were visited by c. 300, 000 and c. 500, 000 tourists respectively in 2014 (Timoshkin et al. 2016). Prior to this recent work (Kravtsova et al. 2014; Timoshkin et al. 2015; 2016), palaeolimnological studies at Lake Baikal have found large blooms of colonial nitrogen-fixing cyanobacteria, mainly consisting of *Anabaena* and *Gloetrichia*, in Barguzin Bay, Chivyrkuy Bay and littoral regions of the North basin (Peshanaya Bay and Baikalskoe harbour), and within Listvyanka Bay in the South basin (Wantanabe and Drucker, 1999) (*Figure 4*). Blooms of *Microcystis* and *Aphanizomenon* have also been observed in Maloe More Bay, off the Central basin, and Chivyrkuy Bay in the North basin (Wantanabe and Drucker, 1999) (*Figure 4*). These algal species are seen in highly eutrophic temperate lakes, and within Lake Baikal they have been observed in littoral regions, such as bays into which large rivers flow, such as close to the Selenga and Barguzin River inflows (Wantanabe and Drucker, 1999) (*Figure 4*). Furthermore, previous studies have shown change in water quality via monitoring records in the Selenga River, with higher concentrations of phosphorus and sulphate concentrations since the mid 1900s, measured within the Selenga River waters (Sorokovikova et al. 2001; Sorokovikova et al. 2015a). Localised records of possible diatom response in shallow waters of the Selenga Delta also show changes in nutrient concentrations of the Selenga Shallows, with diatom assemblage changes to small increases in *Stephanodiscus minutulus* in the late 20th century, being indicative of nutrient enrichment (Mackay et al. 1998).

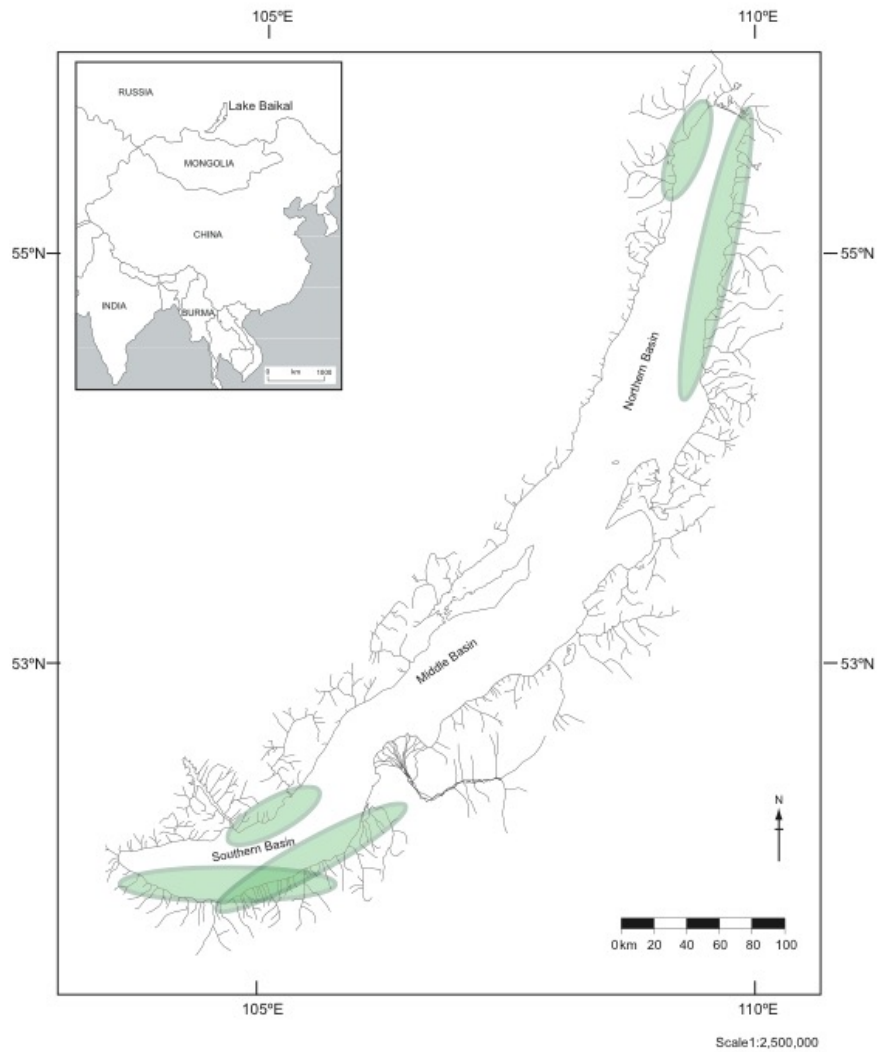


Figure 3: Coastal locations where *Spirogyra* blooms were observed (authors own map and survey data from Timoshkin et al. 2016).

Diatom studies carried out at Lake Baikal in 1987, 1991 and 1995 show increasing abundances of the cosmopolitan diatom species, *Nitzschia acicularis*, within the pelagic waters (Bondarenko, 1999). The highest proportional increase in *Nitzschia acicularis* abundance within phytoplankton samples were found at the shallow waters, near the rivers of the north and south basin (Bondarenko, 1999). *Nitzschia acicularis* are thought to be a eutrophic indicator, however the cause of their abundance increase at Lake Baikal has not been fully understood (Bondarenko, 1999). This species has no clear seasonal pattern at Lake Baikal, and is an opportunistic species, colonising niches rapidly due to their high growth rate and lightly silicified frustules, which means that they can grow in Si limited waters (Bondarenko, 1999; Morley, 2005).

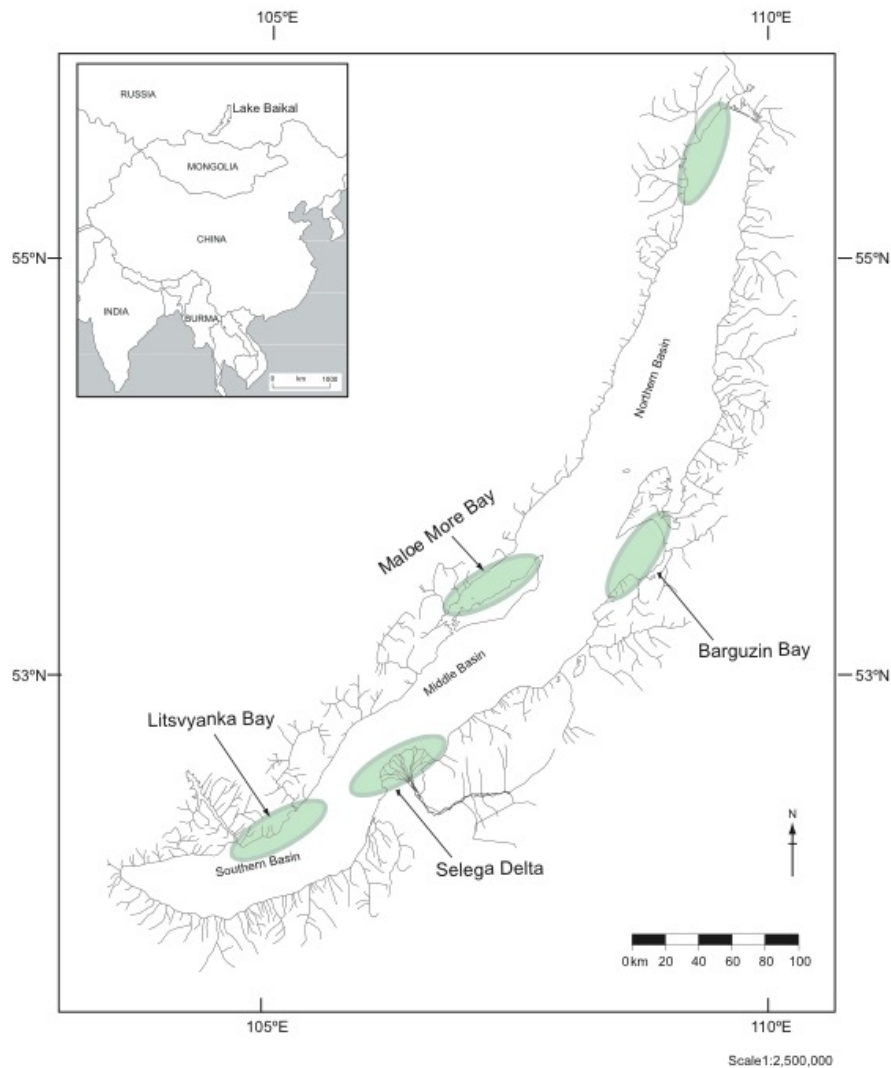


Figure 4: Location of previously reported algal blooms of colonial cyanobacteria in littoral regions of Lake Baikal (modified from Wantanabe and Drucker, 1999).

Diatom assemblages from surface sediments collected in the 1990s indicated water quality deterioration within the near-shore regions (Mackay et al. 1998). Small increases in *Synedra* diatom species (*Synedra acus* var. *acus* and *Synedra acus* var. *radians*) from abundances of < 2 % to c. 5 - 10 % were observed in sediments nearby the Baikal Pulp and Paper Mill (BPPM) in the South basin, and increases in *Stephanodiscus minutulus* from abundances < 5 % to abundances of c. 20 % were observed from sediments in the Selenga Shallows (Mackay et al. 1998). *Synedra acus* var. *acus*, *Synedra acus* var. *radians* and *Stephanodiscus minutulus* are all indicative of more nutrient-rich waters (Edlund et al. 1995). Increased abundances of non-endemic diatoms species, such as *Stephanodiscus meyerii*, *Synedra acus* and *Cyclostephanos dubius*, were also found within sediment cores from the South basin pelagic regions, with rising abundances post-1945 (Edlund et al. 1995). Although Edlund et al. (1995) suggests

diatom compositional changes to be a result of anthropogenic pollution (Edlund et al. 1995), other diatom studies (Flower et al. 1995; Mackay et al. 1998; Bangs et al. 2000) suggest that climate is the main control on the sedimentary diatom assemblage, and that diatoms do not provide early signs for pelagic eutrophication. Supporting this latter suggestion, there is evidence from chlorophyll-*a* concentrations and biological assemblages for lake warming affecting the algal biomass in Baikal's pelagic waters (Moore et al. 2009; Izmesteva et al. 2016). Observed increases in chlorophyll-*a* concentrations and changes in zooplankton community structure have occurred alongside rising surface water temperatures (Izmesteva et al. 2016). Furthermore, it is hypothesised that with lake warming, phytoplankton assemblages will occur, with a shift from a large endemic spring phytoplankton community to smaller cosmopolitan species e.g. *Synedra* and *Nitzschia*, due to changes within ice-cover dynamics and thermal stratification. Changes in lake water temperatures, thermal stratification and ice cover duration/thickness have already been observed at Lake Baikal (Todd and Mackay, 2003; Izmesteva et al. 2015).

1.4 Anthropogenic climate change impacts on Lake Baikal

Lake Baikal is responding strongly to recent climate warming, with rising surface summer water temperatures of 2.4°C over the last 60 years, declining ice cover duration by 16 days over the last century, and increasing summer plankton biomass lake-wide from 0.82 to 1.20 µg/L over the last c. 30 years (Hampton et al. 2008; Moore et al. 2009; Hampton et al. 2014; Izmesteva et al. 2015). Annual air temperature maps from Southern Siberia show that the Baikal region has experienced the largest increases globally in air temperatures over the past 50 years (Jones et al. 2012). Over the last 100 years, annual mean air temperatures at Lake Baikal have increased by > 1°C, which is greater than the global average rate (Shimaraev et al. 2002; Shimaraev and Domysheva, 2013) (*Figure 5*). Furthermore, winter air temperatures are increasing at a greater rate than summer air temperatures (Shimaraev et al. 2002; Shimaraev and Domysheva, 2013). The upper 25 m of the water column has warmed rapidly over the last 60 years, resulting in a stronger thermal gradient (Hampton et al. 2008; 2014). Increasing winter air temperatures have also caused declining ice-cover thickness and duration (Todd and Mackay, 2003) (*Figure 6*), with the ice-free season lengthening by 16 days in the southern basin over the last 130 years (Hampton et al. 2008). A stronger/longer thermal stratification, along with reduced seasonal ice-cover, has resulted in changes in the relative abundances and depth distributions of major phytoplankton groups and zooplankton species (Hampton et al. 2008; 2014; Silow et al. 2016). In lakes, including Lake Baikal, warming of lake waters have promoted the growth of species better adapted to reduced turbulent mixing, such as picocyanobacteria (Findlay et al. 2001; Bopp et al. 2005; Hampton et al. 2008).

Diatoms and total algal biomass (inferred from chlorophyll-*a* concentrations) have been found to respond to recent warming (Moore et al. 2009; Izmesteva et al. 2015; Silow et al. 2016). Chlorophyll-*a* concentrations have increased from 0.5 mg/L to 1.6 mg/L between 1980 and 2005 (Hampton et al. 2008; Moore et al. 2009; Izmesteva et al. 2015) and under ice diatoms (*Aulacoseria baicalensis*) have decreased from c. 5 to 3 cells L⁻¹ between 1950 to 2010 (Silow et al. 2016).

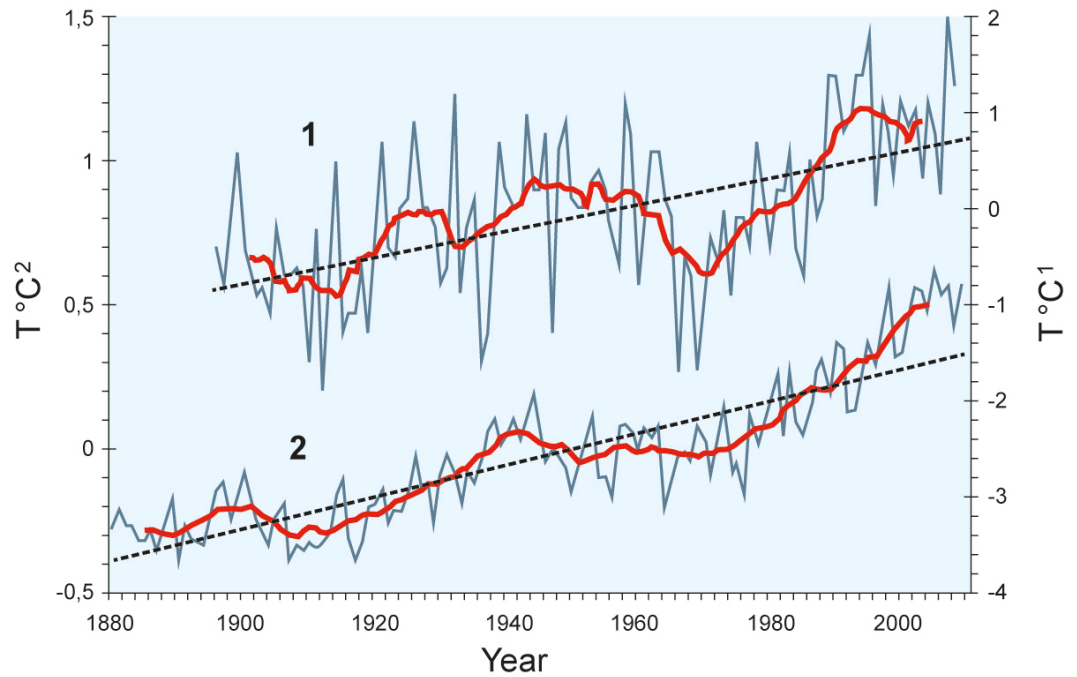


Figure 5: (1) Annual air temperatures (current and 11-year running average) at Babushkin Station in southern Lake Baikal and (2) global temperature trends (Shimaraev and Domysheva, 2013).

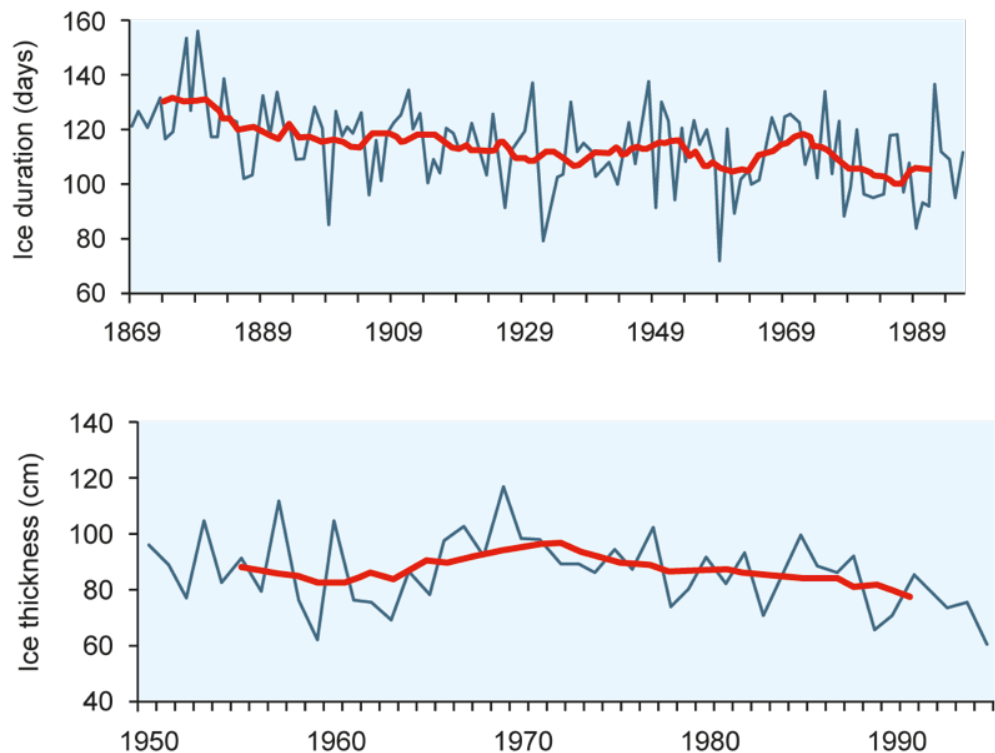


Figure 6: Trends in ice cover duration and thickness over the last century in the South basin (modified from Todd and Mackay, 2003).

Global climate change is affecting both the lake and its watershed (Yoshioka et al. 2002; Hampton et al. 2008; 2014; Moore et al. 2009; Izmesteva et al. 2015). Annual precipitation and snow depth has increased over the last 100 years within the Baikal region (Moore et al. 2009). Measurements of fluvial inflow into the lake show a rise of 300 m³ per second over the last 100 years (Shimaraev et al. 2002; Moore et al. 2009). Regional permafrost thaw and greater fluvial inputs are likely to result in higher levels of nutrients and dissolved organic carbon (DOC) concentrations entering Lake Baikal (Magnuson et al. 2000; Yoshioka et al. 2002; Hampton et al. 2008), influencing both the autotrophic algal and bacterial communities (Wrona et al. 2006). Coloured DOC can affect the light penetration and therefore the algal production, and it can also be a supply of nutrients, as microbial activity can break DOC down to release nutrients (Attermeyer et al. 2014). Increased frequency and severity of forest fires within Baikal's catchment will also release nutrients from ash (Moore et al. 2009).

Lake Baikal is divided into the South, Central and North basins, and previous limnological studies have found the South basin to be more productive than the Central and North basins (Kozhov, 1963; Kozhova and Izmesteva, 1998; Popovskaya, 2000; Fietz et al. 2005). In lakes generally, the productivity of a lake is closely linked to the availability of nutrients and light (Wetzel, 1983), and the supply of nutrients to the epilimnion is determined by both riverine

and hydrodynamical processes, namely upwelling, which is driven by temperature and wind stress, bringing colder nutrient rich deeper water to the surface. Wind, temperature, solar radiation and water transparency determine the mixing layer depth, and the depth of this layer in Lake Baikal has been increasing with climate warming (Hampton et al. 2014). Observed chlorophyll-*a* trends are coincident with the water temperature increases in the photic layer during stratification (Hampton et al. 2008; Moore et al. 2009; Izmesteva et al. 2011; 2015). However, with warming of surface waters to greater depths, a stronger thermal stratification may last for longer, and is predicted to result in a shift in the pelagic phytoplankton from cold-water diatoms e.g. *Aulacoseira baicalensis* to chlorophyte and cyanobacteria picoplankton (Hampton et al. 2008). Climatic-driven changes within the intensity of thermal stratification and physical mixing processes within similarly deep oligotrophic lakes, such as Lake Tahoe, have altered the diatom community structure, favouring the prevalence of small-sized planktonic diatom species (Winder et al. 2009). In deep temperate lakes, diatoms show strong seasonal patterns, largely blooming in the spring where mixing conditions and resource (nutrients and light) supply is optimal (Winder et al. 2009; Jewson et al. 2010; Jewson and Granin, 2014). Therefore, the occurrence of decreased mixing intensity and stronger/longer stratification periods with climatic warming are likely to alter Baikal's diatom abundance and community structure, and enhance the growth of algal groups better adapted to reduced turbulent mixing (Findlay et al. 2001; Bopp et al. 2005). Thus, examining Lake Baikal's current algal community composition and comparing modern-day records to historical trends prior to human impact in the region, is an essential starting point to understanding how Lake Baikal is responding to recent anthropogenic impacts and climate change.

1.5 Research gap

It is important to investigate whether lake Baikal is showing any signs of eutrophication within the pelagic regions, as the lake is an important freshwater reserve, with high evolutionary importance and a very long water residence period, which means lake recovery would take over 400 years to return to pristine conditions if the pelagic waters are eutrophic. We know that the littoral regions are showing signs of eutrophication, but not sure on the extent of this. Therefore, it is important to know the extent of eutrophication from human nutrient enrichment, and to know how algal communities are responding to climate change as the future global trends will continue to rise. Alongside assessing the extent of nutrient enrichment, if any, it is important to examine toxic metal pollution from mercury, due to the rising unregulated mining activity along the Selenga River in Baikal's catchment, which uses mercury to extract gold. Toxic elements deteriorate the water quality and bioaccumulate within the food chains, and mercury has already been found to biomagnify in trophic levels at

Lake Baikal (Ciesielki et al. 2016). However, it has not been widely measured within the waters, and unclear on the pelagic concentrations and river inflow concentrations. We know that the pelagic regions are showing signs of climate warming, with changes in algal biomass from chlorophyll concentrations, but not sure if this has resulted in floristic changes in the algal groups, and whether Baikal endemic diatoms and picoplankton have been replaced by green algae and more cosmopolitan species. We also do not know how climate change is affecting the carbon cycling, as Lake Baikal is an important carbon sink, and with warming temperatures melting permafrost and increased river inflow volumes will bring more carbon into the lake system. It is therefore important to get a measure of these and compare with historical records to help understand Baikal's carbon dynamics.

The response of Baikal's phytoplankton to changes in lake water nutrient concentrations remains unclear, and only a few nutrient enrichment experiments have been carried out at Lake Baikal in the summer months. Thus, there is a need to carry out experiments at Baikal to assess the influence of different nutrient concentrations on algal biomass composition in both winter and summer, to examine the response of the two main primary producers at Lake Baikal; diatoms and picocyanobacteria. These will be carried out in the especially vulnerable regions of Lake Baikal; Maloe More Bay, and in the South basin. There is also a need to explore both winter and summer biological production, nutrients and DOC concentrations in Lake Baikal, as anthropogenic climate change is affecting the thermal stratification and ice-cover periods, with shorter ice cover during the winter and stronger thermal stratification within the summer. The summer is the most productive season at Lake Baikal, except for large diatom blooms in spring during *Melosira* years, as picocyanobacteria largely dominate the waters during summer stratification. Blooms of picocyanobacteria (*Synechocystis limnetica*) generally develop within the pelagic waters during the summer, however Wantanabe and Drucker (1999) found picocyanobacteria blooms in Lake Baikal's surface waters during early spring and summers of 1992-1995, when the water is thermally stratified (Wantanabe and Drucker, 1999). The South basin has been most affected by lake warming over the last few decades, with declining ice cover thickness and duration (Todd and Mackay, 2003; Izmeteva et al. 2016), and therefore to understand the current conditions and algal production at Lake Baikal, it is important to consider the winter as well as the summer. Changes within the winter and summer limnology affect the under-ice primary production and the depth distribution of algal biomass in the water column in the summer. Under ice ecology at Lake Baikal has been examined by Jewson et al. (2009; 2010), however it is essential to collect modern-day samples of the phytoplankton, nutrient and DOC concentrations in the winter to explore the impact of anthropogenic climate change. This is also important as Baikal's endemics are cold-adapted,

and increasing water temperatures are hypothesised to alter the proportions of endemic and cosmopolitan species within the pelagic regions.

Palaeolimnology is an important tool to use at Lake Baikal, as sediment core analyses enable historic trends in primary production and anthropogenic pollution to be reconstructed. Geochemical biomarkers (pigments, $\delta^{13}\text{C}$) are known to be reliable proxies for reconstructing algal production using sedimentary records and both pigments and diatoms provide an insight into compositional change (Schelske and Hodell, 1995; Hodgson et al. 1998; Pienitz et al. 2000; Jones et al. 2011; McGowan et al. 2012; Schüller et al. 2013). Light-harvesting pigments, chlorophylls and carotenoids, are produced by all photosynthetic organisms and are essential for photoautotrophic production. Pigments are the most useful technique for primary production studies at Lake Baikal, as this method records non-siliceous algal groups which are not preserved within the fossil record, providing a holistic insight into all the major algal groups. The two dominant primary producers at Lake Baikal are diatoms (largely indicated by fucoxanthin biomarker in lake waters and diatoxanthin biomarker in sediment samples) and picocyanobacteria (indicated by zeaxanthin biomarker in lake waters and canthaxanthin biomarker in sediment samples) (Fietz, 2005).

1.5.1 Hypotheses and objectives

The hypotheses which the research presented in this thesis will test are the following:

- 1) The development of the South catchment and Maloe More Bay since the 1950s (Brunello et al. 2004) has led to significant inputs of excess nutrients into the South basin and Maloe More Bay in Lake Baikal. These nutrient level changes, along with climatically driven changes in water temperatures (Hampton et al. 2008; 2014) and ice-cover (Todd and Mackay, 2003), have increased algal biomass to levels that are unprecedented over the last 1000 years and floristic change. The algal community shift will be towards higher abundance of chlorophyte pigments with excess nutrient concentrations over the last few decades.
- 2) In the North catchment, the lack of development (Brunello et al. 2004) and nutrient loading into the North basin have minimised any ecological disturbance in this area of the lake over the last 60 years. Thus, there is no evidence of pelagic

eutrophication in the North basin, with no algal community shifts to more nutrient rich diatom species or higher abundances of chlorophyte pigments.

- 3) There is evidence of climate change impacts within the pelagic regions of Lake Baikal (Izmesteva et al. 2016), with the South basin responding more than the North basin, with rising chlorophyll-*a* concentrations, and a higher magnitude of change in the South basin compared to the North basin.
- 4) Lake Baikal phytoplankton will be limited by P, with diatoms being limited to both P and Si. This will be tested within nutrient enrichment experiments and will show higher chlorophyll-*a* and diatom concentrations respectively.

These hypotheses will be tested using pigment biomarkers, to provide information on algal groups in Lake Baikal, along with using $\delta^{13}\text{C}$ isotopes and diatom assemblages to further examine algal production and diatom community change respectively. Short-term nutrient enrichment experiments will be used to test the hypothesis of algal response to nutrient inputs.

Objective 1: Modern day limnological survey across Lake Baikal (hypotheses one and two)

Contemporary water sampling was undertaken in August 2013 across Lake Baikal and its catchment, to examine spatial and vertical analysis of nutrients (nitrate, total phosphorus and silicate) and algal groups, both across Lake Baikal, through the water column and in the major river inflows. Summer surveys were complemented by additional sampling during March 2013, to capture winter limnology at Lake Baikal, and assess the status of limnological conditions in Spring and Summer (Chapter Four and Chapter Five). Water samples will be analysed for phytoplankton pigments, nutrients, major ions and DOC concentrations. This will investigate the modern-day pigment record and their link to environmental conditions. Multivariate analyses (e.g. redundancy analysis) will be used to link environmental variables with phytoplankton pigment assemblages and elucidate the important factors driving variability in phytoplankton community composition.

Objective 2: Nutrient enrichment experiments (hypothesis four)

The effects of nutrient enrichment on Baikal phytoplankton was tested via the construction of controlled nutrient enrichment experiments. These short-term bioassays were set up in March

2013 and August 2013, to examine algal response to the addition of N+P and N+P+Si treatments (Chapter Four).

Objective 3: Reconstruct the impact of anthropogenic changes since c. 1950 A.D.

(hypotheses one and two)

To investigate the impact of anthropogenic changes on the lake's ecosystem and algal community composition, down-core proxy measurements were made from sediment cores across Lake Baikal over the last 200 years. ²¹⁰Pb dated sediments from pelagic South basin, littoral bay regions, river influenced sites and pelagic North basin were used to examine historic trends in primary production along a nutrient enrichment gradient, with "pristine" sites in the North and human influence sites at Maloe More Bay, Selenga River Delta and in the South basin (*Figure 29*) (Chapter Seven). The focus of this work will be on using algal pigments as a measure for the response of algal groups and obtain a fully holistic insight as to the impact of natural and anthropogenic changes on the lake. Existing work has highlighted the potential in using photosynthetic pigments to document changes in non-siliceous algal groups with studies showing the occurrence of individual pigments in Lake Baikal's water column and their flux into the sediment record. Pigment records will be complemented by organic $\delta^{13}\text{C}$, which is a technique that has been widely used in Lake Baikal to constrain changes in whole-lake productivity, with organic C/N ratios used to verify that the signal is derived from aquatic rather than terrestrial sources. Published diatom taxonomy, as well as heavy metal pollutants (mercury) and spheroidal carbonaceous particles (SCP) will further help to constrain the nature of environmental/anthropogenic changes through this interval.

Objective 4: Examine the impact of natural climatic changes prior to human impact

(hypothesis three)

To understand the impact of natural, climatically driven, variability, the same sediment cores will be examined back to cover the past c. 1,000 years. This period covers two major climatic events, the LIA and MCA, which likely impacted the ecosystem through changes to snow/ice-cover and lake stratification. Using the same proxies as used in Objective 3, samples will be analysed to provide an indication of the impact of natural climatic driven variability on algal community composition.

1.6 Using proxy records to investigate past primary production

1.6.1 Sedimentary pigments

Autotrophic algae, which are photosynthesising organisms, produce pigments (both carotenoids and chlorophylls), and these pigments can be specific to certain algal groups (Jeffrey et al. 1997). Pigments can be used as biomarkers for algae to assess modern-day composition within lake waters and to reconstruct past algal communities and ecological conditions from sedimentary algal assemblages (Bianchi and Canuel, 2011; Reuss et al. 2005; Villanueva and Hastings, 2000; Schuller et al. 2014). Algal pigments are a valuable tool for palaeolimnological studies, as not all algae leave morphological remains. Examples include diatoms, which are comprised of siliceous structures, and are preserved within the sedimentary record. Thus, algal biomarkers can be used to infer changes in both siliceous and non-siliceous algal groups. Sedimentary algal pigments can be used to reconstruct past phytoplankton communities and biomass, giving an insight into the whole-lake primary production, across multiple algal groups. This is important at Lake Baikal, as picocyanobacteria are a main group of primary producers. Palaeolimnological studies have applied algal pigments to document changes in water column primary production (Guilizzoni et al. 1983), phytoplankton community composition (Bianchi et al. 2000), and water clarity/light penetration (Leavitt et al. 1997) in aquatic ecosystems (Leavitt and Hodgson, 2001). Algal pigments have therefore been used to assess the impact of cultural eutrophication (increased nutrient load), acidification, climate change (increased water temperatures and changing ice-cover dynamics), and ecosystem shifts (changes in zooplankton grazing pressures) in freshwater lakes (Leavitt et al. 1999; Leavitt and Hodgson, 2001; Kowalewska, 2005; Reuss, 2005; McGowan et al. 2012). Out of these applications, the most extensive sediment pigment analyses have been studies investigating nutrient enrichment (Marchetto et al. 2004; Bonilla et al. 2005; Kowalewska, 2005; Reuss, 2005; Savage et al. 2010; Zhao et al. 2012). At Lake Baikal, algal pigments preserved in the deep basin sediments present only a small proportion of the original algal pigment standing stock in the water column. Although despite a small fraction of the standing stock being preserved (Leavitt and Hodgson, 2001), the algal pigment record can provide an insight into relative changes in algal production and within algal groups.

There are several methods for analysing phytoplankton pigments in water samples, and these include HPLC-based pigment analyses, spectrophotometric and fluorometric methods, measuring algal biomass in the laboratory and in situ. In water samples, pigment analyses have been used to determine phytoplankton community structure, and provide information on primary production, trophic state and water quality. High-performance liquid chromatography

(HPLC) phytoplankton pigments have been found to be in good agreement with standing crop algal group estimates from taxonomic phytoplankton analyses within the photic zone of deep temperate and alpine lakes, and marine waters (Andersen et al. 1996; Buchaca et al. 2005; Greisberger and Teubner, 2007). This agreement in HPLC inferred algal group assemblage and phytoplankton analyses is not the case below the photic zone (Andersen et al. 1996; Buchaca et al. 2005). Overall, HPLC pigment analysis is considered to sometimes be more representative of algal biomass and community composition than microscopic phytoplankton counts alone (Millie et al. 1993; Roy et al. 1996; Muylaert et al. 2006). This is as, for example, small picocyanobacterial cells group together, making accurate counts difficult. HPLC pigment analysis enables samples to be processed quickly, generally allowing for faster high resolution measurements of total algal (chlorophyll-*a* concentrations) down the water column, than from phytoplankton counts alone. However, specifically, HPLC pigment analysis gives individual pigments, unlike spectrophotometric analysis which combines chlorophyll degradation products with chlorophylls, and does not measure individual carotenoids (carotenes and xanthophylls). Spectrophotometry measures chlorophyll based on its known optical properties, scanning between 600 to 700 nm wavelengths (see *Chlorophyll-a spectrophotometric analysis* section). Fluorometric analysis measures chlorophyll (with its degradation products) and can also separately measure carotenoid concentrations from picocyanobacteria.

Palaeolimnological studies allow any recent ecological changes to be put into context with long-term variability to assess the lake conditions prior to major human influence and during past climatic changes. Algal pigments can be quantitatively analysed in lake waters and sediments using reversed-phase High Performance Liquid Chromatography (HPLC) techniques (Chen et al. 2001; McGowan et al. 2012). Individual pigments and their degradation products can be biomarkers of algal groups, and thus used to infer the algal community composition. Algal pigment studies previously carried out at Lake Baikal highlight the use of fossil pigment biomarkers to trace changes in algal production during the Holocene (Fietz, 2005; Fietz et al. 2007), and over Pleistocene timescales (Soma et al. 2001; 2007). Furthermore, contemporary Baikal pigment studies have investigated spatial, vertical and seasonal variation in phytoplankton assemblages (Fietz and Nicklisch, 2004; Fietz, 2005; Fietz et al. 2005). However high-resolution studies of Baikal algal community response to nutrient enrichment over the last 150 years remains an important scientific gap to research.

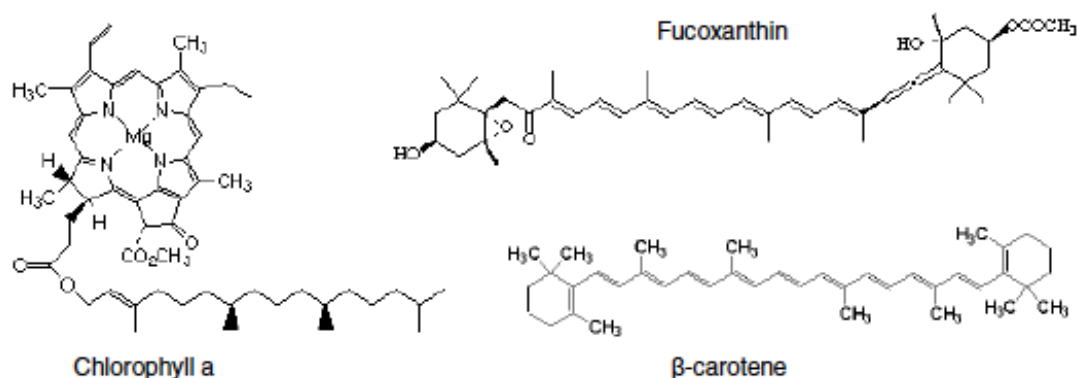


Figure 7: Chemical structures of chlorophyll-*a* and carotenoids; fucoxanthin (xanthophyll) and β -Carotene (carotene) (Reuss, 2005).

Pigments are bound in pigment-protein complexes, and the major pigment groups include chlorophylls, carotenoids and ultraviolet radiation (UVR) absorbing pigments. Chlorophylls are magnesium coordination complexes of four cyclic tetrapyrroles, with a fifth isocyclic ring, known as a phorbium (McGowan, 2013) (Figure 7). There are four major groups of chlorophylls, which are Chl-*a*, Chl-*b*, Chl-*c* and bacteriochlorophylls, with the latter being produced only by photosynthesising bacteria (McGowan, 2013). Carotenoids are comprised of a long aliphatic polyene chain of isoprene units with double bonds, and different carotenoids are formed by the modification of the end groups (McGowan, 2013). The two groups of carotenoids are carotenes, such as β -carotene, which are hydrocarbons, and xanthophylls, such as fucoxanthin, which are oxygenated derivatives of carotenes (Figure 7).

Pigments are labile organic compounds, being degraded by chemical, photochemical and biological processes, however pigment stability is not the same across all the chlorophylls and carotenoids (Table 2). The most stable carotenoids include alloxanthin (cryptophyte), lutein (chlorophyte), zeaxanthin (many cyanobacteria), canthaxanthin (colonial cyanobacterial) and β -carotene (found in most algae) (Leavitt and Hodgson et al. 2001; McGowan, 2013). The least stable carotenoids include peridinin (dinoflagellate biomarker), neoxanthin (chlorophyte biomarker) and violaxanthin (chlorophyte biomarker) (Leavitt and Hodgson et al. 2001; McGowan, 2013). Within the chlorophyll-*a* derivatives, the most resistant degradation product is pheophytin-*a* and the least stable chlorophyll pigment is Chl-*c* (dinoflagellate, diatoms and chrysophytes biomarker pigment) (Leavitt and Hodgson et al. 2001; McGowan, 2013).

In general, chlorophylls contain nitrogen and are more prone to oxidative degradation than carotenoids, forming coloured breakdown products (Reuss, 2005). These tetrapyrrole derivatives of chlorophyll-*a* include chlorophyllide-*a*, pheophorbide-*a*, pheophytin-*a*, pyropheophytin-*a* and pyropheophorbide-*a* and the derivatives of Chl-*b* include pheophorbide-*b* and pheophytin-*b* (Figure 8). Chlorophyll-*a* undergoes three primary early diagenetic reactions; demetallation (phaeophytins), loss of the COOCH₃ group (pyro derivatives), and loss of the phytol chain (phaeophorbides and chlorophyllones) (Villanueva and Hastings, 2000). Chlorophyllide-*a* is formed by chlorophyllase, which is the removal of the phytol side-chain by enzyme activity. Pheophorbide-*a* is product of herbivorous grazing (Welschmeyer and Lorenzen, 1985a) from the loss of Mg⁺⁺ from chlorophyllide-*a*, or the loss of the phytol side-chain from pheophytin-*a*. Pheophytin-*a* forms from the loss of Mg⁺⁺ from the haem ring of chlorophyll-*a*, due to bacterial decay, metazoan grazing or cell lysis (Daley and Brown, 1973). Furthermore, pyropheophytin-*a* and pyropheophorbide-*a* are formed from zooplankton grazing, with the removal of the methylcarboxylate group (-COOCH₃) (Bianchi, 2007). Another chlorophyll-*a* derivative is steryl chlorin ester (SCE), formed from bacterial activity and zooplankton grazing (King and Repeta, 1994; Harradine et al. 1996; Talbot et al. 1999b; Soma et al. 2005). However, SCEs are difficult to detect with standard HPLC methods, which do not use mass spectroscopy. These are formed through the esterification of the pyropheophorbide-*a* or pyro-pheophytin-*a* with sterols (Soma et al. 2005).

In contrast to the chlorophylls, carotenoids degrade directly to produce colourless compounds, which are undetectable by spectrophotometric techniques (Moss, 1978; McGowan, 2013). As an exception to most colourless carotenoid degradation products, carotenoid chlorin esters, for example fucoxanthinol pheophorbide esters, are derivatives of carotenoids (McGowan, 2013). There are differences in the resistance of carotenoids to degradation, such as β -carotene, which is more stable than xanthophylls. The lower stability is due to the presence of oxygen and the 5,6-epoxy group in some xanthophylls, such as fucoxanthin and peridinin, which are very susceptible to microbial decay (Porra et al. 1997).

Pigment degradation and preservation processes have been studied within the water column via sediment traps and grazing experiments (Fietz, 2005; Schüller, 2014), and analysing surface sediments. Studies have found a bias in the pigments preserved due to degradation. This bias is a result of rapid degradation of pigments as they sink from the photic zone, with 90% of the standing stock being lost in the water column, and degradation also occurs during burial within the sediments (Furlong and Carpenter, 1988; Hurley and Armstrong, 1990; 1991). Zooplankton grazing can modify pigments into degradation products and transfer pigments to the lake sediments via faeces (Leavitt, 1993). Algal pigments within the water

column, exposed to light and oxygen, can also degrade as they sink down to the sediments, which can take weeks/months (Leavitt et al. 1993; Cuddington and Leavitt, 1999) (Figure 9).

Table 2: Algal pigments with their diagnostic algal groups and pigment stabilities (modified from Leavitt and Hodgson et al. 2001 and McGowan 2013). Bchl-a – bacterial chlorophylls. Stability is how resistant the pigment is to degradation, with 1 being the most stable and 4 being the least stable.

Pigment	Affinity	Stability
Chl- <i>a</i>	All photosynthetic algae, higher plants	3
Chl- <i>b</i>	Green algae, euglenophytes, higher plants	2
Chl- <i>c</i>	Dinoflagellates, diatoms, chrysophytes	4
Bchl- <i>a</i> and <i>b</i>	Purple sulfur and nonsulfur bacteria	(-)
Bchl- <i>c</i> , <i>d</i> and <i>e</i>	Green sulfur bacteria	(-)
Pheophytin- <i>a</i>	Chl <i>a</i> derivative	1
Pheophytin- <i>b</i>	Chl <i>b</i> derivative	2
Pheophorbide- <i>a</i>	Grazing, senescent diatoms	3
Pyro-pheo pigments	Derivatives of <i>a</i> and <i>b</i> phorbins	2
Steryl chlorin esters	Chlorophyll derivatives from grazing	(-)
β-Carotene	Most algae and plants	1
Alloxanthin	Cryptophytes	1
Fucoxanthin	Diatoms, chrysophytes, dinoflagellates	2
Diadinoxanthin	Diatoms, dinoflagellates, chrysophytes	3
Diatoxanthin	Diatoms, dinoflagellates, chrysophytes	2
Peridinin	Dinoflagellates	4
Canthaxanthin	Colonial cyanobacteria	1
Zeaxanthin	Cyanobacteria	1
Lutein	Green algae, euglenophytes, higher plants	1
Neoxanthin	Green algae, euglenophytes, higher plants	4
Violaxanthin	Green algae, euglenophytes, higher plants	4

The sinking rate of algal pigments influences the pigment composition preserved within the sediments, with the composition of biomarkers favouring fast-sinking algal pigments (Reuss, 2005). The mechanisms which promote fast sinking algal pigments down the water column are the aggregation of algal cells from algal blooms (Kiorboe et al. 1994) and faecal pellets from zooplankton grazing, which remove pigments from degradation in the water column (Leavitt, 1993). Along with photo-oxidation, microbial activity degrades algal pigments, and thus the water column is where most pigment degradation occurs (Leavitt et al. 1993; Cuddington and Leavitt, 1999; Bianchi, 2007). Once algal pigments reach the sediments, degradation can occur via oxidation and microbial activity (Leavitt, 1993). Pigment degradation within the surface sediments is particularly prevalent in lakes with oxic bottom waters, such as Lake Baikal, where oxidised layers in the sediment core can extend over the top 20 cm (Vologina et al. 2010).

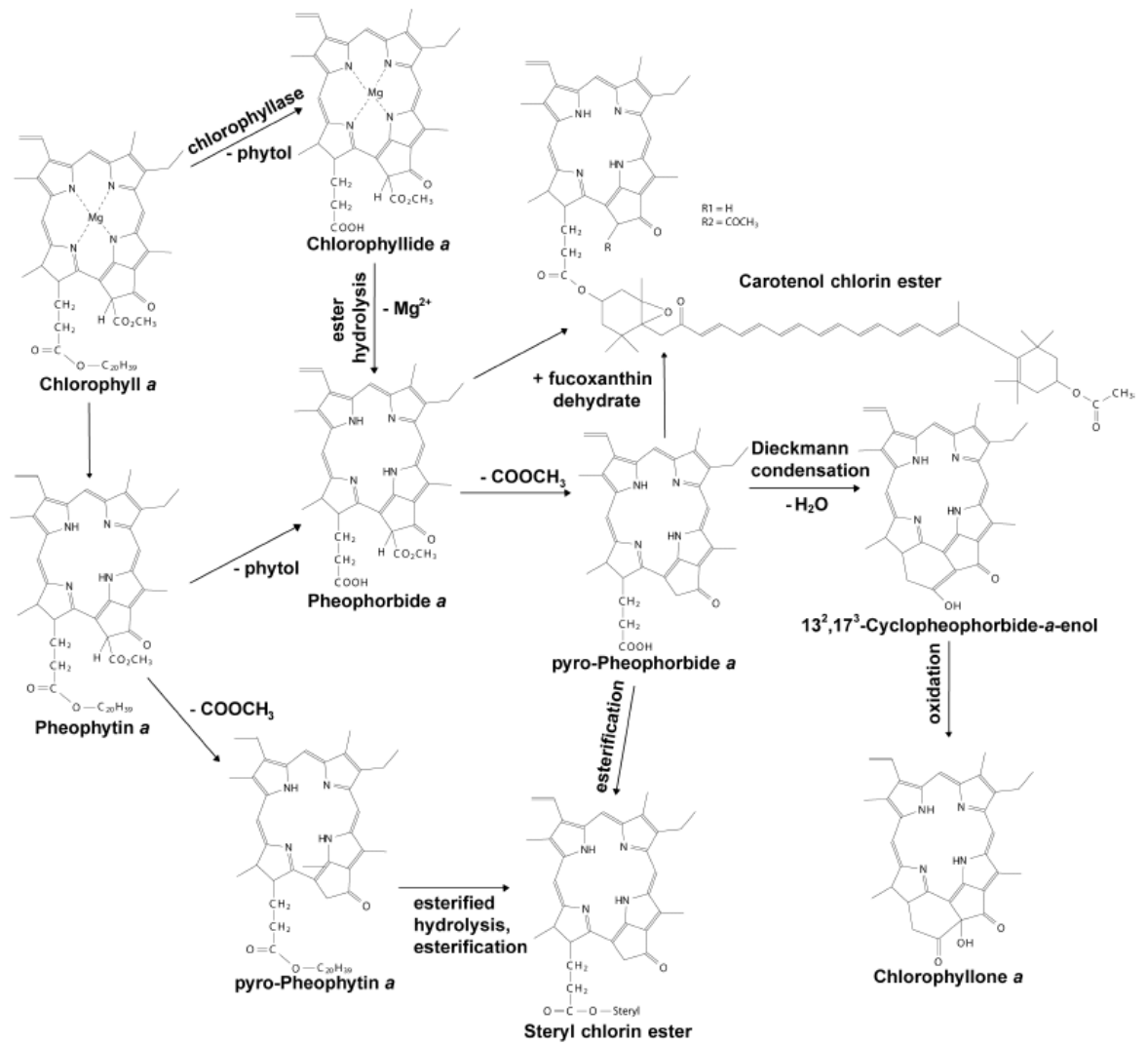


Figure 8: Chlorophyll-a degradation pathways to form chlorophyll-a transformation products (Schüller, 2014).

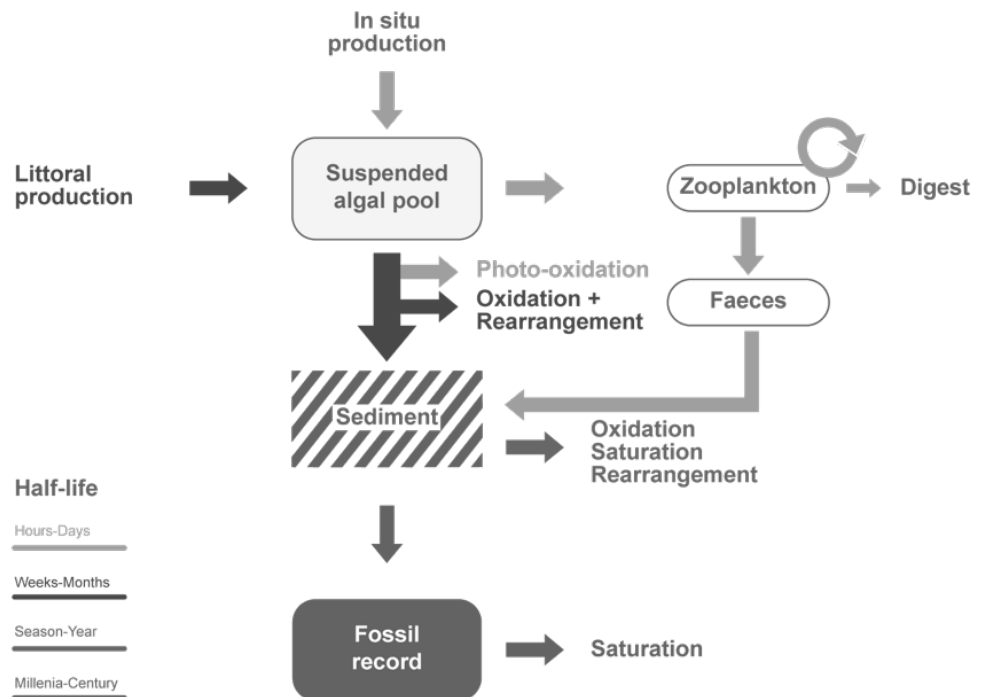


Figure 9: Conceptual diagram of pigment flux and degradation in the water column and sediments (modified from Reuss, 2005 and Leavitt, 1993).

Algal pigments have been analysed in the lake waters at Lake Baikal in the summer and spring (Fietz, 2005; Fietz et al. 2005) and within the lake sediments (Soma et al. 1996; Airs et al. 2000; Fietz et al. 2007; Tani et al. 2009). Despite the large water depths in the pelagic basins (> 800 m) and the oxygenated bottom waters, algal pigments have been detected within the sediments and used to infer past climatic conditions via production changes (Fietz *et al.* 2007). Chlas, which consist of chlorophyll-*a* and its derivatives, have been used as a production proxy at Lake Baikal (Fietz, 2005). Chlas is used as a measure of algal production in Lake Baikal's sedimentary record, as intact chlorophyll-*a* concentrations tend to be either minimal or below detection limits due to the exposure of algal pigments excessive levels of oxygen, light, microbial and grazing activity within the water column and surface sediments. This extent of degradation results in predominantly the preservation of chlorophyll-*a* derivatives, which can be used as a measure of relative total algal abundance when combined with intact chlorophyll-*a* measurements. Certain stable carotenoids have been found preserved in Lake Baikal's sediments and used to reconstruct past contributions of diatoms, chrysophytes, picocyanobacteria, chlorophytes and cryptophytes within the total algal assemblages (Soma et al. 1996; Fietz, 2005; Fietz et al. 2005). Other studies at Lake Baikal have focussed on chlorophyll-*a* derivatives, namely steryl chlorin esters (SCE), to reconstruct past phytoplankton biomass over the last 4.5 Ma years (Soma et al. 1996; Airs et al. 2000; Tani et

al. 2002; 2009). Lipids of *n*-alkanes, fatty acids and sterols have also been used as another tool to reconstruct biological production at Lake Baikal (Russell and Rosell-Melé, 2005). Perylene has been detected at Lake Baikal (Soma *et al.* 1996; Fietz, 2005). Perylene is suggested to have derived from phytoplankton in anoxic conditions (Aizenshtat, 1973; Laflamme and Hites, 1978). Perylene is used as an indicator of depositional conditions, tracking changes in redox conditions (Silliman *et al.* 1998).

Algal pigments are highly degradable, and oxygen availability plays a major role in controlling pigment deterioration alongside temperature, light and grazing by zooplankton (Sun *et al.* 1993; Bianchi *et al.* 2000). Deep-water ventilation in Lake Baikal maintains high oxygen concentrations throughout the water column and at the bottom sediment layer (Weiss *et al.* 1991; Callender *et al.* 1997b). Furthermore, it has been suggested that the top 2 - 20 cm of the surface sediments are oxic (Vologina *et al.* 2000; Müller *et al.* 2005). Thus, within oxic environments, there is faster degradation of algal pigments, and only resistant pigments which avoid deterioration to colourless end-products can be preserved within sediments, and analysed to reconstruct past phytoplankton biomass and composition (Leavitt, 1993; Steenbergen *et al.* 1994). As a result, previous Baikal photosynthetic pigment profiles consist largely of chlorophyll derivatives, such as pheopigments and Steryl Chlorin Esters (SCE) (Soma *et al.* 1996; Airs *et al.* 2000; Tani *et al.* 2009).

1.6.2 Pigment diagenesis at Lake Baikal

There are different controls on pigment degradation in lakes, with the presence of light, temperature and oxygen promoting pigment diagenesis. In Lake Baikal waters, pigment degradation is largely from oxic waters, light penetration to water depths of c. 40m and zooplankton grazing. Taking all these into consideration, grazing is likely to contribute the most to pigment degradation at Lake Baikal, due to extensive decomposition of organic material due to grazing during sinking down the water column. Those pigments which reach the lake sediments are then largely affected by the oxic bottom waters and surface sediments and bacterial activity. Pigment preservation measures have been assessed within Chapter Seven to examine whether phytoplankton pigments provide a reliable proxy for reconstructing past production. Fietz (2005) has previously explored pigment degradation, and found that chlorophylls and certain carotenoids are good indicators of primary production below the upper oxidised layers of sediment cores from Lake Baikal with the application of correction values from sediment trap studies to account for pigment degradation. Algal pigments are highly degradable, and oxygen availability plays a major role in controlling pigment deterioration alongside temperature, light and grazing (Sun *et al.* 1993; Bianchi *et al.* 2000).

Deep-water ventilation in Lake Baikal maintains high oxygen concentrations throughout the water column and at the bottom sediment layer (Weiss et al. 1991; Hohmann et al. 1997; Callender et al. 1997; Ravens et al. 2000). Most degradation takes place in the water column, and the photic zone in Lake Baikal extends over c. 20 – 40 m across the lake (Fietz, 2005). Within the water column, degradation models applied at Lake Baikal show that chlorophyll-*a* flux decreased from c. 300 $\mu\text{mol m}^{-2}$ to < 100 $\mu\text{mol m}^{-2}$ below 250 m, where it remained relatively stable (Fietz et al. 2005). Differential degradation has been observed between the South and North basins, with more degradation in the water column in the South basin (Fietz, 2005). Studies of pigment and lipid biomarker fluxes down the water column in the South basin of Lake Baikal also shows that over 90% of chlorophyll and its degradation products, and lipid biomarkers, are lost prior to permanent burial in the sediments (Fietz et al. 2005; Russell and Rosell-Mele, 2005).

The high levels of oxygen within Baikal's bottom waters provide an unstable environment for pigment preservation. It has been suggested that the top 2 cm of surface sediments are oxic, and at sites with low sedimentation rates of organic carbon the top 5 cm of the surface sediments are oxic (Müller et al. 2005; Maerki et al. 2006). Furthermore, up to 30 cm of some sediment cores at Lake Baikal have been found to be oxic (Granina et al. 2000; Vologina et al. 2000; Müller et al. 2005). At the Academician Ridge region, more than 60 cm of the sediment core was oxidised (Vologina et al. 2000; 2003). In contrast, at sites with high production, such as the Selenga Delta, oxygen penetration has been found to only extend over the top 5 mm of the sediment core (Vologina et al. 2000). Oxygen penetration within Baikal's sediments is greater at sites with lower sedimentation rates, and organic material within pelagic deep basins can be exposed to oxic conditions for years, and even decades, given a mean annual sedimentation rate between c. 0.02 - 0.65 mm yr^{-1} (Vologina et al. 2003; Sturm et al. 2016). Thus, unlike most other deep lakes, fossil pigments remain within oxic conditions for several decades at Lake Baikal. Burial efficiency is the amount of organic carbon lost after deposition, and this has been assessed using oxygen profiles to examine the oxygen exposure time for pigments (Maerki et al. 2006). Oxygen profiles from pelagic South and North basin of Lake Baikal suggest low burial efficiencies of 16 % and 3 % of original organic carbon being preserved respectively (Maerki et al. 2006). Oxidised layers within Baikal's sediment cores can be identified (Vologina et al. 2003; 2010) by the formation of layers of iron (Fe) and manganese (Mn) oxide crusts that represents the transition between oxic and anoxic sediments, indicating the redox boundary (Deike et al. 1997; Müller et al. 2002; Vologina et al. 2003; Granina et al. 2004; Och et al. 2014; Torres et al. 2014). Within oxic environments, there is faster degradation of algal pigments, and only resistant pigments which avoid deterioration to colourless end-products are preserved within sediments (Leavitt, 1993;

Steenbergen et al. 1994). As a result, previous Baikal photosynthetic pigment profiles consist largely of chlorophyll derivatives, such as pheopigments and Steryl Chlorin Esters (SCE) (Soma et al. 1996; Airs et al. 2000; Tani et al. 2009). However, SCEs cannot be detected on a HPLC alone, and have not been measured within Chapter Seven. Chapter Seven examines the difference in pigment preservation between the oxic and anoxic sediment layers, to assess how much of an influence oxic layers have on the pigment signal down-core and if their presence significantly affects the reliability of reconstructing past production.

Stable chloropigments (pheophytin-*b*, pheophytin-*a*, pyropheophytin-*a*), stable sedimentary carotenoids have been detected in deep Baikal sediment samples, which include; diatoxanthin, alloxanthin, lutein, canthaxanthin and β -carotene (Soma et al. 1996; Fietz, 2005; Fietz et al. 2007). In contrast xanthophylls with epoxide groups, such as fucoxanthin, were not detectable in the Baikal sediments (Soma et al. 1996; Fietz, 2005; Fietz et al. 2007). Unstable pigments from large diatoms, such as fucoxanthin and chlorophyll-*c*, have a very fast sinking rate of 60 – 100 m d⁻¹ (Ryves et al. 2003), which means that these pigments do not undergo as much modification from light induced degradation processes compared to pigments from smaller algae, such as chlorophyta and cyanobacterial picoplankton (Fietz, 2005). Furthermore, selective grazing is an important factor in pigment preservation, as large diatoms suffer less from zooplankton grazing compared to picoplankton (Hurley and Armstrong, 1990). The grazer size influences the rate of pigment degradation, as faecal pellets of mesozooplankton, such as cladocerans have higher sinking rates than those of microzooplankton, such as protozoa (Welschmeyer and Lorenzen, 1985a). The major zooplankton groups at Lake Baikal are cladocerans, rotifers and copepods (Hampton et al. 2014).

Pigment transformation is also dependent on gut passage time, as both micro and mesozooplankton can degrade pigments into fluorescent degradation or colourless products (Klein et al. 1986; Burkill et al. 1987; Barlow et al. 1988; Head and Harris, 1992). Carotenoids are generally more stable than chlorophylls in the presence of light, oxygen (Leavitt and Findlay, 1994) and grazers (Strom et al. 1998). However, in Baikal's oxic sediments the carotenoids were found to be more susceptible to decomposition compared to chlorophylls (Soma et al. 2001a), with fucoxanthin being the most susceptible to decomposition and zeaxanthin being the most stable carotenoid pigment (Leavitt and Findlay, 1994). Similar problems are known from diatom valve analyses, where Battarbee et al. (2005) reports that differential dissolution of diatom species occurs mainly at the water to sediment interface. However, these parent pigment decay products have been proven by many studies to be good indicators of past and present phytoplankton biomass (Leavitt and Hodgson, 2001; Chen et al. 2003a; 2003b; Fietz, 2005; Reuss et al. 2005).

The noted differences in pigment preservation found between the South and North basin (Fietz, 2005) are likely to be due to variances in mixing water column depth, ice cover, temperature (Shimaraev et al. 1994) and productivity (Kozhov, 1963; Kozhova and Izmeteva, 1998), with chlorophyll-*a* fluxes being reported to be highest within the South basin sediment traps and surface sediments, while the TOC was distributed evenly (Soma et al. 1996; Fietz, 2005). Correlation between surface sediment pigments and pigments within the standing crop have been made at Lake Baikal and show that surface sediments were mainly comprised of chlorophyll derivative pigments, due to diagenetic processes, unlike within the water column which has higher concentrations of intact chlorophyll-*a* (Fietz, 2005). Sediment trap studies at Lake Baikal show that the largest proportion of degradation occurred within the upper 250 m of the water column before settlement into the traps, with an exponential rise in chlorophyll-*a* degradation products (pheophytin-*a*) from c. 2.5 to 6 $\mu\text{mol g}^{-1}$ in the upper 250 m (Fietz, 2005). Extensive degradation occurred at the sediment surface before permanent burial, with much lower concentrations in the oxidised core top than even in the deepest sediment traps at c. 1400 m in the South basin, due to anoxic conditions in the sediment traps (Fietz, 2005). The main pigments detected within the settling material over the 16 months of deployment in 2001 – 2003 were from heavy non-edible diatoms, which accounted for 87% of the chlorophyll-*a*, whereas small light edible phytoplankton, such as picocyanobacteria, was strongly degraded and zeaxanthin only contributed to 2% of the chlorophyll-*a* (Fietz *et al.* 2005). These findings are similar to sediment traps studies in deep basin fjords in New Zealand (Schüller and Savage, 2011; Schüller *et al.* 2014).

1.6.3 *Diatom assemblages*

Sedimentary diatoms provide a good biological tool to use at Baikal to investigate climate and water quality changes, over the last 1000 years (Edlund *et al.* 1995; Flower *et al.* 1995; Mackay *et al.* 1998; Bangs *et al.* 2000; Mackay *et al.* 2003; Mackay *et al.* 2005) and longer time scales covering the Pleistocene and Pliocene (Grachev *et al.* 1998; Morley *et al.* 2005; Rioual *et al.* 2005). Changes in diatom assemblages have been seen with climate variability, with shifts in the abundances of the major endemic diatom species; with relative abundance increases in *Aulacoseira baicalensis* and relative abundance decreases in *Cyclotella minuta* since the cooler climatic conditions in the Little Ice Age (LIA) (Edlund *et al.* 1995; Mackay, 2007). Despite diatoms providing a useful proxy for past production, diatom dissolution can affect the reliability of interpretations from the fossil diatom assemblages in the sediments. Ryves *et al.* (2003) found that only 1% of diatom valves are preserved in the sediments at Lake Baikal, similar to within marine sediments, due to dissolution. Microbioturbation and bacterial

activity also promotes dissolution within the surface sediments, and zooplankton grazing can increase the susceptibility of diatom valves to dissolution due to fragmentation (Mackay, 2007). An example of a diatom species which is highly susceptible to dissolution in Lake Baikal is *Nitzschia acicularis*. *Nitzschia acicularis* is tolerant of pollution and only observed in the pelagic lake waters, as it is not preserved within the sediments of deep basins (Mackay et al. 1998).

Sediment trap studies at Lake Baikal show differential dissolution across the diatom taxa (Ryves et al. 2003). This differential dissolution is assessed via the comparison between phytoplankton assemblages within the water column and assemblages within the trap material (Ryves et al. 2003). Dissolution was found to affect all the diatom species at Lake Baikal, however heavily silicified species, such as *Aulacoseria baicalensis*, were most resistant to dissolution and lightly silicified species, such as *Synedra* species and small centrics (e.g. *Stephanodiscus meyerii* species) were more prone to dissolution (Ryves et al. 2003). Dissolution can bias the inferences made from the diatom assemblages preserved in the sediments. Thus, to account for diatom dissolution at Lake Baikal, diatom dissolution indices (Ryves et al. 2001; 2009) and species-specific correction factors have previously been applied to the sedimentary diatom data (*Table 3*) (Battarbee et al. 2005). These consider the differential dissolution of diatom species and allow the composition of source diatom populations to be reconstructed. Sample dissolution indices, which are developed by using a simple pristine/dissolved classification, allow the diatom preservation to be quantified (Ryves et al. 2009). These have been applied to palaeoclimate diatom studies at Lake Baikal (Mackay et al. 1998; Morley, 2005; Rioual et al. 2005). Correction factors for the main taxa have been calculated from the estimates of the ratio of diatoms produced in the water column to diatoms preserved in the sediment (*Table 3*) (Battarbee et al. 2005). The application of these dissolution-based correction factors, to adjust the diatom species abundances, have been found to improve the palaeoclimatic reconstructions at Lake Baikal (Battarbee et al. 2005; Mackay et al. 2005; Mackay, 2007).

Table 3: Diatom correction factors (Battarbee et al. 2005). Preservation factors for five of Baikal's major diatom species are calculated as the ratio of planktonic diatom taxa and sedimentary diatom accumulation rate. Correction factors are calculated from the estimates of the ratio of planktonic diatoms to diatoms preserved within the sedimentary record.

	<i>Aulacoseira skvortzowii</i>	<i>Aulacoseira baicalensis</i>	<i>Cyclotella minuta/ornata</i>	<i>Stephanodiscus meyerii</i>	<i>Synedra acus</i>
Correction factor	142.78	36.16	10.84	354.6	679.34
Preservation factor	0.007	0.027	0.092	0.003	0.001

1.6.4 Geochemistry of organic matter

Organic matter (OM) is comprised of a mixture of lipids, carbohydrates and proteins, as well as other constituents produced by organisms living both within the lake and in the catchment (Meyers, 2003). Carbon has two stable isotopes; ^{12}C and ^{13}C , and the fractionation between these two is expressed as $\delta^{13}\text{C}$. If the $\delta^{13}\text{C}$ of total organic matter is controlled by algal growth rates, then it can be used as a primary production proxy (Brenner et al. 1999; Wang et al. 2009; Torres et al. 2012). The $\delta^{13}\text{C}$ of OM is governed mainly by the $\delta^{13}\text{C}$ composition of dissolved inorganic carbon (DIC), which is comprised of dissolved carbon dioxide, bicarbonate and carbonate (Marchitto, 2007). DIC is utilised by primary producers, and the $\delta^{13}\text{C}$ of organic carbon is also governed by the isotope fractionation of DIC during carbon fixation (Kluijver et al. 2014). If primary production is controlling the $\delta^{13}\text{C}$ signal, then an increase in production leads to an increase in the $\delta^{13}\text{C}$ values. The basis of using carbon isotopes, is that the $\delta^{13}\text{C}$ of organic carbon produced photosynthetically responds to the rate of primary productivity in the water column (Schelske and Hodell, 1991; Meyers, 2003), as algae preferentially utilise the lighter carbon isotope (^{12}C) rather than the heavier (^{13}C), creating lake waters with DIC more enriched in the heavier carbon isotope (^{13}C). It is assumed that the carbon isotopic ratio ($^{13}\text{C}/^{12}\text{C}$) is enriched (increases) or depleted (decreases) with increases or decreases in primary production. Several other processes affect the carbon isotopic composition of algal derived organic matter at Lake Baikal (Figure 10).

These include algal composition and abundance, concentration of atmospheric carbon dioxide, lake-water pH, temperature, nutrient limitation, algal growth rates and lake residence time (Laws et al. 1995). The $\delta^{13}\text{C}$ values are also influenced by the contribution of microbial biomass (Teranes and Bernasconi 2005; Kluijver et al. 2014), and thus any increases or decreases in the $\delta^{13}\text{C}$ values cannot be solely attributed to a single carbon source (i.e. solely phytoplankton or terrestrial).

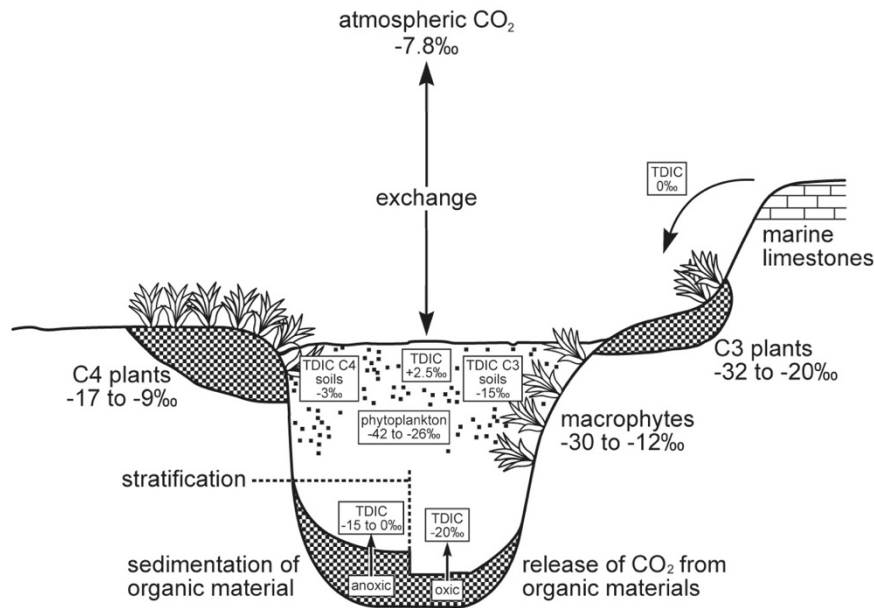


Figure 10: $\delta^{13}\text{C}$ values for the major sources of carbon into lakes (Leng and Marshall, 2004).

The approach of using $\delta^{13}\text{C}$ to reconstruct past production assumes that there are no other controls on the carbon isotopic composition of sediments. A major caveat to this is that carbon is derived from both terrigenous and aquatic sources, which will have different isotopic signatures, and therefore a mixture of carbon material complicates the interpretation (Wei et al. 2010). The fractionation from dissolved CO_2 to organic material with lake water can depend on both CO_2 concentration and temperature, for example low $\delta^{13}\text{C}$ values can be due to increased atmospheric CO_2 concentrations (Wolfe et al. 1999). The concentration of dissolved CO_2 for photosynthesis within lake waters affects the $\delta^{13}\text{C}$ signal of lake OM, as for example, with low dissolved CO_2 concentrations algae begin to utilise HCO_3^- as their carbon source, which can result in higher (more positive) $\delta^{13}\text{C}$ values which are closer to the $\delta^{13}\text{C}$ values found within C_4 plants (Meyers and Lallier-Verges 1999). The $\delta^{13}\text{C}$ of lake water total dissolved inorganic carbon (TDIC) is influenced by the inflow of ground waters, which have isotopically lower $\delta^{13}\text{C}$ values due to the interactions with rocks and soils, especially in limestone areas (Meyers and Lallier-Verges 1999). Closed basin lakes with a long residence time have a greater exchange between surface water and atmospheric carbon dioxide concentrations as well as progressive removal of $\delta^{12}\text{C}$ by photosynthesis, as compared to open basin lakes with a short residence time (Morley, 2005). In Lake Baikal, a variety of factors will influence the $\delta^{13}\text{C}$ values, as discussed in the 1.6.7 *Carbon dynamics at Lake Baikal* section. One of the main factors to consider, which is important for algal pigments (as discussed in the 1.6.2 *Pigment diagenesis at Lake Baikal* section), is the presence of

oxygenated bottom waters at Lake Baikal. Oxic layers within the sediments will affect the $\delta^{13}\text{C}$ values, as oxidation of sedimentary organic matter results in the relative depletion of ^{13}C in the TDIC reservoir (Lamb et al. 2002).

The carbon isotope composition of bulk organic material can provide information on carbon sources (Meyers and Lallier-Verges 1999), as higher plants, such as trees, utilise the C_3 Calvin pathway of incorporating organic matter. This cycle preferentially removes $\delta^{12}\text{C}$ with an average discrimination of -20 ‰ (O’Leary, 1988). Plants such as arid grasses use the C_4 Hatch-Slack pathway, which discriminates at -4 to -20 ‰ (Meyers and Lallier-Verges, 1999). Therefore, C_4 plants have a higher $\delta^{13}\text{C}$ value than C_3 plants (*Figure 11*).

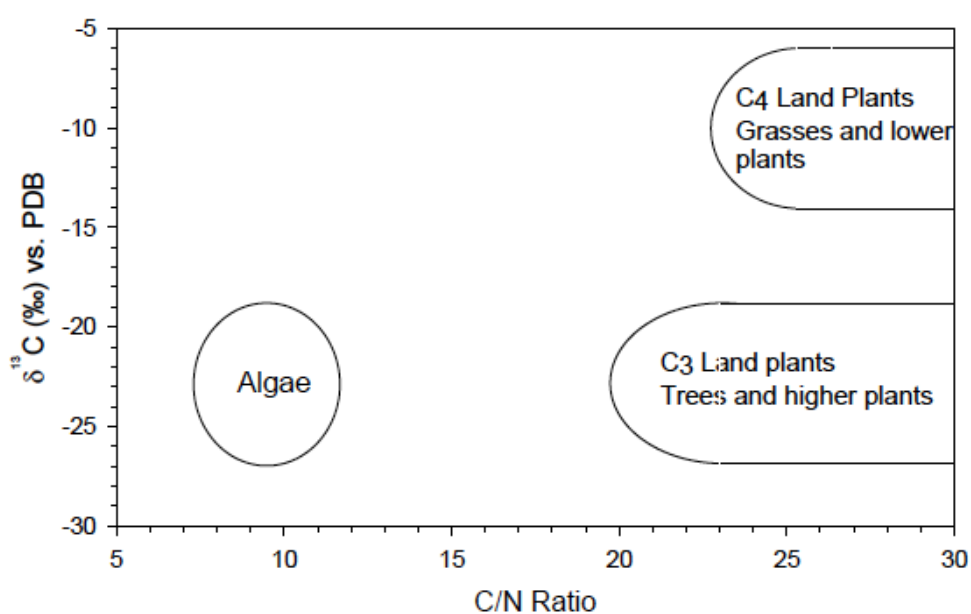


Figure 11: $\delta^{13}\text{C}$ and TOC/N values of algae, C_3 plants and C_4 plants (Meyers and Lallier-Verges, 1999).

The total amount of autochthonous and allochthonous OM preserved within the sedimentary record may only represent a small fraction of that originally produced, due to oxidation during settling prior to its incorporation into the sediment. Despite this, bulk organic carbon still provides important sources of information from $\delta^{13}\text{C}$ isotopes, even if a large proportion of organic carbon is removed via degradation (Meyers and Eadie, 1993; Meyers et al. 1995; Hodell and Schelske, 1998). Lehmann et al. (2002) found that from both oxic and anoxic incubation experiments, that the $\delta^{13}\text{C}$ of bulk OM decreased by 1.6 ‰, due to bacterial degradation in the water column and early diagenesis in the sediments. The TOC/N ratio can be affected by diagenesis by the preferential degradation of high-N compounds, resulting in higher TOC/N values (Fenchel et al. 1998). Considering degradation, isotopic composition of bulk organic matter can sometimes be used to determine the source of organic material (Lamb

et al. 2004), although lacustrine algae have a similar range of $\delta^{13}\text{C}$ values to most C_3 terrestrial plants (*Figure 11*). The TOC/N ratio of OM is used to distinguish algal derived carbon from vascular and non-vascular plant compositions, as the TOC/N ratio values are generally < 10 in aquatic plants (Talbot and Johannessen 1992). This is as algae are protein rich and relatively high in nitrogen, and will generate a low TOC/N ratio while lignin and cellulose rich higher plants such as trees will generate higher TOC/N ratios (Meyers, 1994). Therefore TOC/N ratios are important to determine whether the $\delta^{13}\text{C}$ signal is aquatic and not terrestrial. Previous work reports that TOC/N values of Baikal's bulk sediments range between 9 to 12 (Prokopenko et al. 1993), which suggests negligible influence from terrestrial input and a predominate carbon source from algal production. To further examine the carbon source, alongside TOC/N ratios, rock eval (Meyers and Teranes, 2001) and *n*-alkanes analyses (Brincat et al. 2000) can be applied to help interpret lacustrine and terrestrial carbon sources.

1.6.5 Rock Eval Pyrolysis

Rock Eval pyrolysis can be used to further identify and characterise the potential carbon source. The most useful derived measurements from Rock Eval pyrolysis for lake studies are the Hydrogen Index (HI) and the Oxygen Index (OI), which are thought to reflect the origin of sedimentary OM (Meyers and Teranes, 2001) and compliment TOC/N data. The HI indicates algal content of the bulk sediments and the OI is used as a measure of oxidation (Meyers and Teranes, 2001). Three main types of OM (Types I, II and III) are distinguished using a van Krevelen-type HI-OI diagram, but these types are also controlled by the degree of oxidation and alteration during thermal maturation (Talbot and Livingstone 1989) (*Figure 12*). Type I sediments arise from material that is rich in hydrocarbon from microbial biomass or waxy land plants, Type II from algal OM and Type III from woody plant material (Meyers and Teranes, 2001).

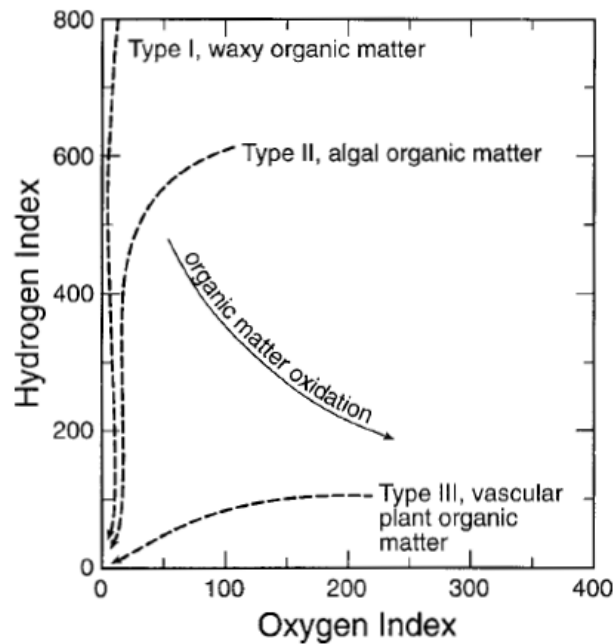


Figure 12: Rock Eval Van Krevelen-type diagram for sedimentary organic matter; shows the three types of organic matter and the oxidation pathway (Meyers and Lallier-Verges, 1999).

In sediments, a range of HI values between 200 – 300 mg hydrocarbons (HC)/g/ TOC is generally used to infer algal derived organic matter in marine and lake systems, and a threshold of 100 mg HC/g/ TOC is used to characterise the shift to mainly terrigenous organic material (Stein and Fahl 2004; Stein and Macdonald 2004; Hare et al. 2014). However, some terrestrial material, such as lipid-rich leaf waxes, have similar HI and OI values to algal derived carbon, and there is differentiation between these is achieved via C/N ratios and lipid biomarker data (Luniger and Schwark, 2002). Generally, variations within the HI values of lake sediments are caused by several processes (Talbot and Livingstone 1989; Meyers and Lallier-Verges, 1999). Very low HI values can be a result of terrigenous-derived woody organic matter and/or bacterial degradation and oxidation (Tissot and Welte 1984; Hunt 1995). A decrease within the HI values could be due to reworking of organic matter during transportation through the water column, oxidation, and microbial degradation (Luniger and Schwark, 2002).

1.6.6 Applications of the $\delta^{13}\text{C}$ record

The $\delta^{13}\text{C}$ record can be used to track changes in climatically driven catchment vegetation changes, changes in algal production from climate and/or cultural eutrophication, and changes in the carbon cycle of the lake. Carbon isotopes ($\delta^{13}\text{C}$) from sedimented total organic carbon

in lake sediments have been used as a proxy for recent aquatic production over the last century (Meyers, 1994; Schelske and Hodell, 1991; Schelske and Hodell, 1995; Hodell and Schelske, 1998; Lu et al. 2010; O'Beirne et al. 2015), in response of lakes to historic anthropogenic activities, such as nutrient loading. Positive shifts in $\delta^{13}\text{C}$ values related to increased productivity have been found by Mackenzie (1985), Schelske and Hodell (1991), Meyers and Ishiwatari (1993), Schelske and Hodell (1995), Wolfe et al. (1999) and Prokopenko et al. (1999). $\delta^{13}\text{C}$ records have been used in the lower Laurentian Great Lakes for this purpose, particularly Lake Erie and Lake Michigan, in the United States and Canada (Schelske and Hodell, 1991; 1995; Lu et al. 2010; O'Beirne et al. 2015). These lakes have a history of anthropogenic phosphorus enrichment from industry and agriculture, being severely impacted by eutrophication in the 20th century (Charlton et al. 1993; Charlton and Milne, 2005 as cited in Ostrom et al. 2005; Michalak et al. 2013; Rucinski et al. 2014). Lake Erie was well known as an example of a eutrophic ecosystem (Stoermer et al. 1985a as cited in Reavie and Allinger, 2011; Barbiero et al. 2002; Ostrom et al. 2005; Allinger and Reavie 2013; Steffan et al. 2014). The application of $\delta^{13}\text{C}$ at these Great Laurentian Lakes found increases in lacustrine production (an increase in $\delta^{13}\text{C}$) with historic changes in anthropogenic phosphorus loading during the development of the watershed, and subsequent decreases in $\delta^{13}\text{C}$ were related to the implementation of phosphorus abatement programs in the mid 1970s (O'Beirne et al. 2015). Along with using $\delta^{13}\text{C}$ as a primary production measure, Biogenic Silica (BSi) content of sediments can be used as an estimate of siliceous microfossil abundance. BSi records at Lake Superior also show evidence of a low-level eutrophication at the time of European habitation and watershed development in the late 1800's (Schelske et al. 2006). In contrast to the lower Great Lakes, Lake Superior has been less subjected to anthropogenic pressures (Allan et al. 2013; Rucinski et al. 2014), being classified as a deep cold oligotrophic lake (Dobiesz *et al.* 2010), comparable to Lake Baikal although it is shallower than Baikal, by c. 800 m in the deepest part. This is relevant to Lake Baikal, as Lake Superior is a similarly large and deep oligotrophic lake which is experiencing rising lake water temperatures (Austen and Colman, 2008) and climatic driven changes within its pelagic diatom assemblages, with increases in *Cyclotella comensis* in surface sediments (Reavie et al. 2014).

Past changes in carbon in Lake Baikal and environmental conditions over longer time scales have been investigated using $\delta^{13}\text{C}_{\text{TOC}}$ (Meyers and Lallier-Verges, 1999; Meyers, 2003; Lücke and Brauer, 2004; Wantanabe et al. 2004; Swann et al. 2005; Wei et al. 2010; Prokopenko and Williams, 2001; Mackay et al. 2016). At Lake Baikal, carbon dynamics over the Holocene have been investigated using bulk sediment $\delta^{13}\text{C}_{\text{TOC}}$, and the record shows the influence of glacial and interglacial climates on $\delta^{13}\text{C}_{\text{TOC}}$ values (Mackay et al. 2016). The $\delta^{13}\text{C}_{\text{TOC}}$ record at Lake Baikal has also been used to investigate past climatic conditions, inferred from algal

production changes, over the last c. 20,000 years (Prokopenko and Williams, 2001; Morley, 2005) and last 75,000 years (Prokopenko et al. 2001). This highlights the use of $\delta^{13}\text{C}_{\text{TOC}}$ as a proxy for algal production at Lake Baikal, supporting its application to sediments presented within this thesis, to reconstruct primary production changes over the last 200 years (Chapter Seven) and longer term within the last millennium (Chapter Six). Prokopenko et al. (1993; 2001) suggests that at Lake Baikal the $\delta^{13}\text{C}$ signal of bulk sediments is derived from algal growth and can therefore be used as a production proxy.

1.6.7 Carbon dynamics at Lake Baikal

Large freshwater lakes, such as Lake Baikal, have an influence on the global carbon cycle, removing carbon from the atmosphere and storing it within the sediments (Alin and Johnson, 2007). However, the carbon burial efficiency at Lake Baikal is reduced by the oxygenated bottom waters (Sobek *et al.* 2009). Degradation in Baikal's surface-water interface (Weiss *et al.* 1991), leads to lower values of TOC within the sediment record. A large proportion of particulate organic carbon (c. 30%) is suggested to be mineralised within the water column (Müller *et al.* 2005), and thus TOC values within Lake Baikal's sediments are below 3 % in the pelagic deep basins, due to mineralisation and the exposure of surface sediments to oxygen for decades (Maerki *et al.* 2006). Despite the extent of TOC dissolution, the measurement of organic carbon can still be used to examine relative changes in algal production at Lake Baikal (Mackay *et al.* 2016).

Pelagic phytoplankton are the main carbon source at Lake Baikal, and due to the enormous size of the lake only a small proportion of organic material contributing to the dissolved carbon pool is sourced from terrigenous organic matter (Prokopenko and William, 2003). These terrigenous sources of carbon in Lake Baikal include DOC from vegetation succession and soil leaching (Hanson *et al.* 2004; Cole *et al.* 2007). Carbon isotopic analyses on Baikal's pelagic food web further support that pelagic phytoplankton produce most the organic carbon (Yoshii *et al.* 1999). The pelagic food web structure at Lake Baikal only consists of five major trophic levels (phytoplankton, mesozooplankton, macrozooplankton, fish and seal), and $\delta^{13}\text{C}$ values can be used to estimate dietary composition of each level (Yoshii *et al.* 1999). The carbon isotope data shows that $\delta^{13}\text{C}$ increases further up the trophic level as the food source becomes more $\delta^{13}\text{C}$ -enriched (Yoshii *et al.* 1999).

Table 4: $\delta^{13}\text{C}$ and TOC/N values at Lake Baikal (Prokopenko et al. 1993; Prokopenko and Williams, 2001; Morley, 2005).

	$\delta^{13}\text{C}$	TOC/N
Composition of modern spring phytoplankton (1994):		
Phytoplankton (pelagic north basin)	-32.3	6.4
Phytoplankton (pelagic south basin)	-31.1	7.5
Phytoplankton (pelagic central basin and selenga delta)	-29.7	6.9
Zooplankton	-31 to -25	4.5 to 7
Surface sediment	-27.4	13
Soil organic matter/ watershed	-23.4	20
Selenga River Channel	-23.2 to -26.3	5.5 to 12.9

Modern day isotopic $\delta^{13}\text{C}$ values of pelagic phytoplankton and zooplankton at Lake Baikal are -29.7 to -32.3 ‰ and -25 to -31 ‰ respectively, and TOC/N ratio values of 6.4 to 7.5 and 4.5 to 7 respectively (Table 4) (Prokopenko and Williams, 2001). The $\delta^{13}\text{C}$ values of Baikal's phytoplankton are generally lower than surface sediment $\delta^{13}\text{C}$ values, with average surface sediment $\delta^{13}\text{C}$ values of -27.4 ‰, ranging between -24 and -33 ‰ as surface sediments contain terrestrial material (Prokopenko et al. 1993; Morley, 2005). The Selenga River Channel has $\delta^{13}\text{C}$ values between -23.3 ‰ and -26.3 ‰ within its sediments (Morley, 2005), and soils in the watershed have a $\delta^{13}\text{C}$ value of c. -23.4 ‰ (Prokopenko et al. 1993). The TOC/N ratio values are highest in the catchment soils (c. 20) (Prokopenko et al. 1993) and Selenga River Channel (between 5.5 to 12.5) (Morley, 2005), being lowest in the surface sediments (largely ranging between 7 –13) (Prokopenko et al. 1993; Morley, 2005) and modern day phytoplankton (6.4 – 7.5) (Prokopenko and Williams, 2001) (Figure 13). $\delta^{13}\text{C}$ values have been obtained for specific algal and zooplankton species at Lake Baikal (Yoshii et al. 1999). *Aulacoseira baicalensis* diatom species have the most positive $\delta^{13}\text{C}$ values at Maloe More (-17.7 ‰) and the least positive $\delta^{13}\text{C}$ values in the Central basin and at Barguzin Bay (-28.6 – 29.6 ‰) (Yoshii et al. 1999). The two dominant zooplankton species, *Epischura baicalensis* and *Cyclops kolensis*, have a range in $\delta^{13}\text{C}$ values between -22.8 ‰ to -29.9 ‰ and -25.9 ‰ to 26.5 ‰ respectively, across the lake (Yoshii et al. 1999).

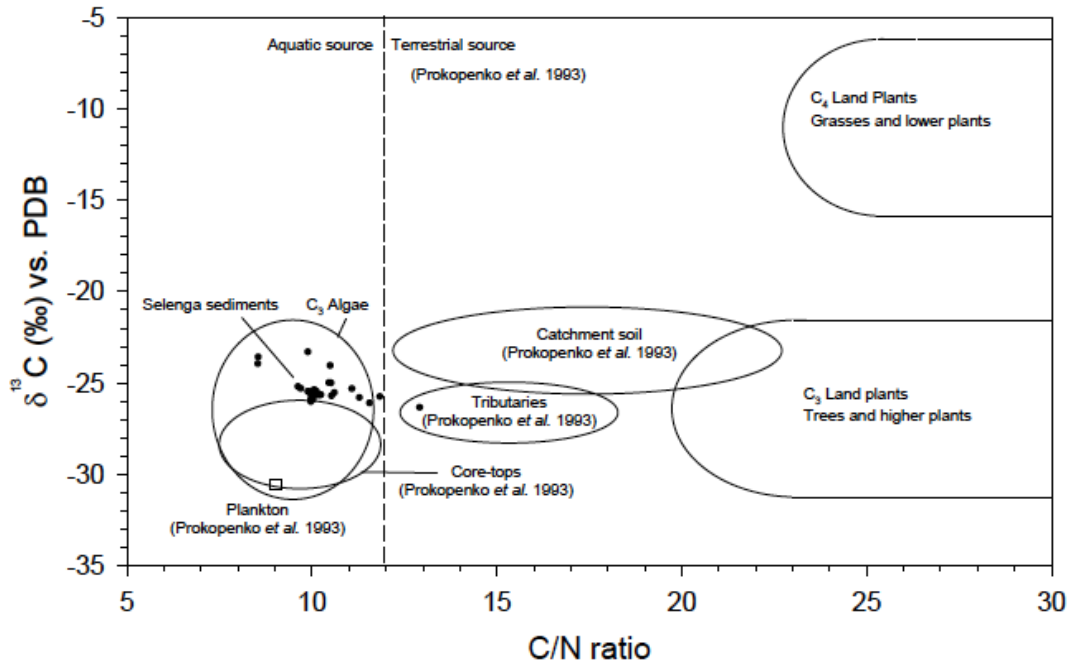


Figure 13: $\delta^{13}\text{C}$ and TOC/N values of phytoplankton, surface sediment, tributaries, soil catchment from Lake Baikal (Prokopenko et al. 1993) and land plants (C_3 and C_4) (Meyers and Lallier-Verges, 1999) (Source: Morley, 2005).

The catchment area of Lake Baikal is mainly comprised of C_3 plants, with very little contribution of organic matter from C_4 plants (Prokopenko and Williams, 2001; Morley, 2005). However, despite minor influence of terrestrial input on the deep basins organic matter as inferred from TOC/N values below 12, the $\delta^{13}\text{C}$ signal within Baikal's bulk sediments can be influenced by factors other than primary production. These include degradation, diatom abundance, near-shore productivity due to the influence of macrophytes, catchment DOM and terrestrial input from mature soils (Table 5). An increase in catchment DOM results in higher $\delta^{13}\text{C}$ values, whereas lower $\delta^{13}\text{C}$ values are a result of increased diatom abundance and increased terrestrial input (Table 5). However terrestrial input has minimal influence on pelagic bulk sediment carbon isotopic values due to the large size of lake Baikal, with sites presented in this thesis being > 5 km from the shoreline. Ice cover does not affect the $\delta^{13}\text{C}$ values, and it is unknown whether ice cover affects the TOC/N ratio values. Furthermore, gas hydrates, which are unique to Lake Baikal, are localised in the Central and South basin near the Selenga Delta, and do not influence all the lake. Gas hydrates are very unlikely to be a factor controlling TOC content, TOC/N ratio or $\delta^{13}\text{C}$ values (Mackay et al. 2016). Thus, alongside algal productivity being the most likely influence on the $\delta^{13}\text{C}$ values, the algal composition (i.e diatom or picocyanobacteria dominated) will have an impact on the $\delta^{13}\text{C}$

values, as higher diatom abundance will result in lower $\delta^{13}\text{C}$ values and higher picocyanobacteria abundance will result in higher $\delta^{13}\text{C}$ values.

The possible drivers of an increase in TOC content and decrease in TOC/N ratio values of sediments could be a result of increased diatom abundance, increased picocyanobacterial abundance and increased pelagic productivity (*Table 5*) (Mackay et al. 2016). An increase in terrestrial input from mature soils would also result in higher TOC content, although the TOC/N ratios would increase, indicating terrestrial organic material (*Table 5*). There are problems with using $\delta^{13}\text{C}$ values and TOC/N ratios from lake sediments, as microbial reworking can alter the isotopic content, and bulk organic matter represents a mixture of carbon making it difficult to identify the carbon source. To further understand the carbon dynamics and the $\delta^{13}\text{C}$ signal, individual biomarkers have been analysed for their carbon isotopic composition within Lake Baikal's sediments (Russell and Russell-Mele, 2005). These biomarkers include major lipid classes of *n*-alkanes, fatty acids and sterols (Russell and Russell-Mele, 2005). Lipid biomarker analyses on Baikal's bulk sediments further support that within the deep pelagic basins, algal input dominates the organic carbon content, with some contribution from terrestrial plants from the surrounding environment (Russell and Russell-Mele, 2005).

Table 5: Processes affecting the TOC, TOC/N and $\delta^{13}\text{C}$ values of organic carbon at Lake Baikal (modified from Mackay *et al.* 2016).

Process	TOC	TOC/N	$\delta^{13}\text{C}$
Increased diatom abundance	Increase	Decrease	Decrease ¹
Increased picoplankton abundance	Increase	Decrease	Unknown ⁴
Increased pelagic productivity	Increase	Decrease	No change ²
Increase in near-shore productivity	Decrease	Unknown	Increase ³
Increased gas hydrate release ¹⁰	No change	No change	No change
Increased atmospheric $p\text{CO}_2$ ⁸	No change	No change	No change
Increased ice cover ⁹	Decrease	Unknown	No change
Catchment DOM	No change	Increase	Increase ⁶
Increased terrestrial input from mature soils	Increase	Increase	Decrease ⁵
Increased C_4 terrestrial input ⁷	NA	NA	NA

- 1:** Diatoms are the main primary producer during spring and autumn, and pelagic diatoms range between -28 ‰ to -35 ‰ (mean -29 ‰). Over 90% of organic matter in Lake Baikal is derived from phytoplankton.
- 2:** Within the pelagic regions of Lake Baikal no isotopic discrimination takes place due to the size the HCO_3 pool (Yoshii *et al.*, 1999).
- 3:** Aquatic macrophytes in littoral regions of Lake Baikal have higher $\delta^{13}\text{C}$ values between -5 ‰ to -18 ‰ and benthic algae have higher $\delta^{13}\text{C}$ values than pelagic algae, ranging between -5 ‰ to -11 ‰ (mean -9 ‰) (Kiyashko *et al.*, 1998; Yoshii, 1999; Yoshii *et al.*, 1999).
- 4:** Little research has examined C fractionation in picoplankton, although higher $\delta^{13}\text{C}$ values than diatoms have been suggested, ranging between -22 ‰ to -30 ‰ (Sakata *et al.*, 1997).
- 5:** Developed soils results in an increase in ^{13}C -depleted respired CO_2 (Hammarlund, 1992; Ruess *et al.*, 2010).
- 6:** Dissolved organic matter from catchment rivers has $\delta^{13}\text{C}$ values of -26 ‰ to -27 ‰ (Yoshioka *et al.*, 2002).
- 7:** Isotopic analyses of long-chain n -alkanes did not detect any C_4 plants within Baikals watershed during the late Quaternary (Brincat *et al.*, 2000).
- 8:** Higher atmospheric CO_2 concentrations during the Holocene resulted in lower $\delta^{13}\text{C}$ values of organic matter (Prokopenko *et al.*, 1999), although no relationship between Holocene CO_2 concentrations and $\delta^{13}\text{C}$ values was found by Mackay *et al.* (inpress).
- 9:** Diatom production as inferred from biogenic silica is lower than during glacial periods than interglacial periods (Mackay, 2007). However due to low under ice primary production and higher CO_2 solubility in colder waters, isotopic discrimination is not considered to be important (Watanabe *et al.*, 2004).
- 10:** Sedimentary methane hydrates which are unique to Lake Baikal (Granin and Granina, 2002) are suggested to not have a large influence on $\delta^{13}\text{C}$ values. This is as only 10s of megagrams of methane have been measured at Lake Baikal (Schmid *et al.*, 2007), and teragrams of methane would need to be emitted to result in a decrease in $\delta^{13}\text{C}$ values as suggested by Prokopenko and Williams (2004).

1.7 Mercury as a pollution indicator

Mercury (Hg) is produced by both natural and anthropogenic sources, however technogenic mercury concentrations have risen alongside industrial development. Mercury is a potentially toxic trace element, and anthropogenic sources include industrial, agricultural and mining activity within Baikal's catchment area. Mercury is then transported into Baikal's pelagic waters via river inflows. Mercury has been used within agricultural pesticides and to extract gold (Koval et al. 2000). The main anthropogenic mercury sources of technogenic contamination are in the Irkutsk-Cheremkhova industrial zone, from thermal energy and power plants (Koval et al. 1999), and the Selenga River (Koval et al. 2000). Riverine inputs, particularly from the Selenga River, are an important source of mercury into Lake Baikal, due to mining activity within Northern Mongolia and the cities of Ulan Ude and Selenginsk (*Figure 28*). Bioaccumulation of potentially toxic elements have been found within the benthic and pelagic food chain of Lake Baikal (Watanabe et al. 1998; Perrot et al. 2010; Ciesielski et al. 2016). Mercury has been measured in water from riverine and pelagic sites at Lake Baikal, and within plankton, zooplankton, fish and the livers of Baikal seals (Koval et al. 1999; Ciesielski et al. 2016). Biomagnification of mercury has been found at Lake Baikal, which is when mercury is transported along the food chain and concentrations rise at each higher trophic level (Ciesielski et al. 2016). Biomagnification can therefore result in severe toxicological effects in aquatic top predators (Watanabe et al. 1998).

Fluxes of mercury (Hg) and methylmercury (MeHg) into Lake Baikal from water, atmosphere, biota and sediments has been previously investigated from surveys carried out in September 1990, June 1992 and March 1993 (*Figure 14*) (Leermakers et al. 1996). Higher concentrations of mercury were found in the wet deposition (119 ng/g), compared to the dry deposition (54.6 ng/g) and river inflows (59.4 ng/g) (Leermakers et al. 1996). Atmospheric deposition of mercury at Lake Baikal is therefore a major source, and sources of atmospherically derived mercury are further discussed in Chapter Two. Previous sedimentary mercury analyses have found the Central basin to have higher Hg concentrations in surface and down core sediments over the last c. 250 years (range between 40 – 70 ng/g) than cores taken in the South basin and Selenga Shallows in Lake Baikal (range between 10 – 40 ng/g) (Leermakers et al. 1996).

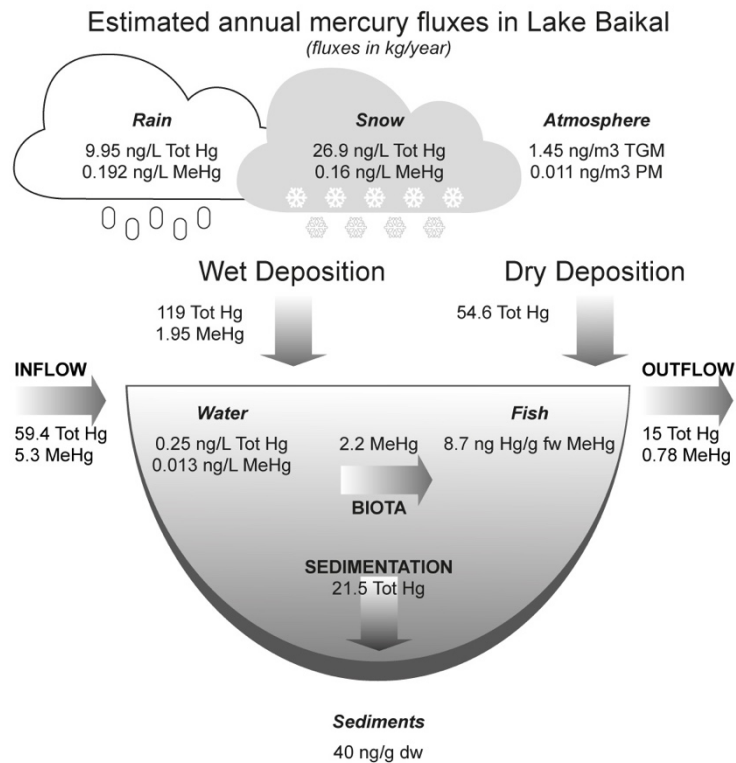


Figure 14: Annual mercury fluxes in Lake Baikal. Flux measurements taken in 1991, 1992 and 1993 (modified from Leermakers et al. 1996).

1.8 Nutrient enrichment experiments

Experimental studies report useful methods to further understand the role of nutrients on algal communities (Schindler, 1977; Elser and Kimmel, 1986; Hecky and Kilham, 1988; Sterner et al. 2004). Nutrient enrichment experiments have been extensively applied to both freshwater and marine systems, via small-scale in situ mesocosm approaches (Oviatt et al. 1986; Schelske et al. 1986; Elser et al. 1990; Cottingham et al. 1997; Graneli et al. 1999; Camacho et al. 2003; Gilpin et al. 2004; Gobler et al. 2006; Marcarelli et al. 2006; Veraart, 2008; Felisberto et al. 2011) and whole-lake fertilisation (Carpenter et al. 2001; Vadebancoeur et al. 2001; Vadebancoeur et al. 2003), such as in the Experimental Lakes Area (ELA) in Canada (Schindler, 1974; Schindler and Fee, 2011). These experiments are conducted to determine nutrient limitation of phytoplankton, i.e. which nutrients are controlling algal biomass. The ELA studies found phosphorus to be the main limiting nutrient (Schindler et al. 2008; Wang and Wang, 2009; Paterson et al. 2011; Schindler, 2012). However other studies suggest that biological fixation of atmospheric nitrogen is not sufficient to meet algal demands for nitrogen

and maintain phosphorus limitation of lake production, supplying less than 10% of the nitrogen needs of primary producers in eutrophic lakes (Howarth et al. 1998 as cited in Patoine and Leavitt, 2008; Patoine and Leavitt, 2008). Thus, many nutrient enrichment studies highlight the importance of both nitrogen and phosphorus as limiting nutrients on lake production (Leavitt et al. 2006; Conley et al. 2009; Paerl, 2009; Paerl et al. 2011; 2014; Scott and McCarthy, 2011). Although phosphorus and nitrogen are commonly the focus of eutrophication, studies have also highlighted the importance of silica on diatom production (Hamilton, 1969; Kilham, 1971; Officer and Ryther, 1980; Hecky and Kilham, 1988), and marine studies have found silicon accumulation within picocyanobacterial cells (Baines et al. 2012).

1.9 Summary

Overall Lake Baikal is under threat from anthropogenic activity within the catchment, which is discussed further in Chapter Two, with the sources of pollution, both from the river inflows and atmospheric deposition. Recent work has shown evidence of signs of eutrophication within the littoral regions of Lake Baikal, and there is no current published research which has considered the current limnological state of Baikal's pelagic waters. Lake Baikal's limnological structure is also under pressure from rising regional temperatures, which are the shortening of the ice cover season, and deepening of the thermocline depth. Baikal's limnology is further discussed in Chapter Two. Algal pigments are a well-known technique to consider all the algal groups, and despite their high lability especially within a lake such as Baikal, they have previously been shown to provide reliable primary production proxies, and this thesis provides an opportunity to test the application of this technique over more recent timescales, the last couple of centuries. Carbon isotopes will also be important, to see if they agree with the production trends from the pigments. The mercury analyses, although it is a pilot study, is an important aspect to this project, to enable understanding into the human impact on Baikal's waters and extent of industrial pollution. Furthermore, the nutrient enrichments provide a key way to looking at how Baikal's algal community might respond to excessive nutrient enrichment, double the previously published levels during a 'pristine' state.

Chapter Two: Site Description

As discussed in Chapter One, Lake Baikal is a large ancient tectonic lake which is under pressure from anthropogenic activity and climate change. Anthropogenic activity largely began within Baikal's catchment since the 1950s, and regional air temperatures have increased by c. 1.2°C over the last 60 years (Shimaraev and Domysheva, 2013). Previous studies have shown how Lake Baikal is responding to climatic changes (Hampton et al. 2008; Moore et al. 2009; Izmesteva et al. 2015; Silow et al. 2016), and signs of eutrophication have been found within the littoral regions (Timoshkin et al. 2016). This study aims to explore the response of pelagic Lake Baikal to anthropogenic nutrient enrichment and/or climate change. Contemporary and historic limnological conditions will be examined at Lake Baikal, to investigate if there is pelagic eutrophication or changes related to lake warming. Palaeolimnological changes over the last 200 years will enable primary production pre and post anthropogenic influence (c. 1950 AD) to be examined, and longer term records will enable recent primary production changes to be put into context with natural variability.

2.1 Lake Baikal Basin

Lake Baikal is located on an active rift zone, and can be divided into three main basins; the North basin is separated from the Central basin by the Academician Ridge, which is an underwater mountain range. The Central basin is separated from the South basin by the Buguldeika Ridge and the more than 20 km wide Selenga River Delta (*Figure 15*).

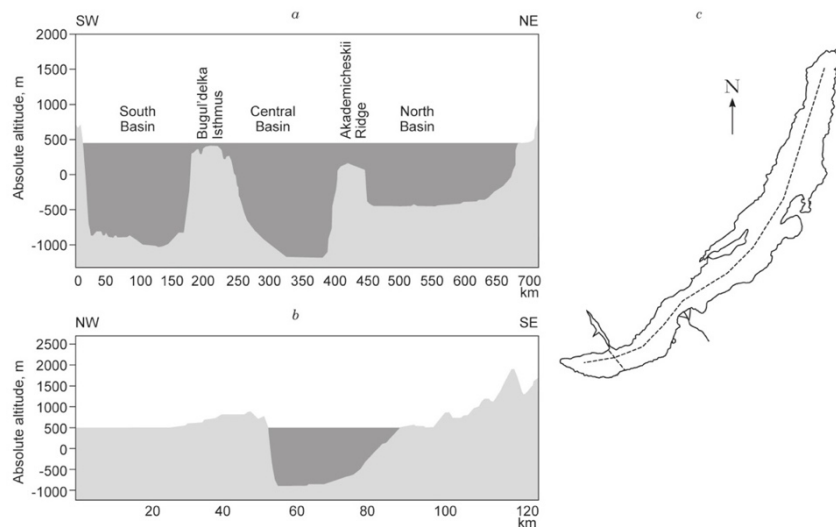


Figure 15: (a) Longitudinal profile of Lake Baikal, (b) Transverse profile of the South basin and (c) position of transect on Lake Baikal (modified from de Batist et al. 2002; Vologina and Sturm, 2009).

The delta regions of the lake; Selenga, Upper Angara and Barguzin rivers are up to several kilometres wide (Figure 16). Thus, the geomorphology at the bottom of the basins is full of undulating ridges and large turbidite deposits, which are discussed further in Chapter Six, and are a result of mass movement on the tectonic rift boundary. In total 365 inflowing rivers feed the lake and there is only one outflow, the Angara River in the South basin. The three largest tributaries which flow into Lake Baikal are the Selenga, Barguzin and Upper Angara (Callender and Granina, 1997), with the Selenga being the largest of the three (Figure 16). These rivers contribute to over 92% of the riverine inputs, bringing nutrient-rich waters into the delta regions (Genkai-Kato et al. 2002). Therefore, Baikal's catchment area is 560,000 km², spanning both southeast Siberia and northern Mongolia (Kozhov, 1963) (Figure 16).



Figure 16: Lake Baikal and catchment (Brunello et al. 2004).

The overall mean water residence time for Lake Baikal is over 300 years (Brunello et al. 2004) and the water residence time differs for each basin, being lower in the South basin and highest in the North basin. The catchment area is forested predominately by Scots pine (*Pinus sylvestris*) and Siberian larch (*Larix sibirica*). The geological structure of Lake Baikal's

catchment is made up of formations which differ in age and composition. The main rock types are granite and other igneous rocks, and the lithology of the lake catchment is largely comprised of Archaean and Proterozoic rocks (Heim et al. 2007) (*Figure 17*). At the edge of Lake Baikal there are quaternary lake, river and glacial formations (Heim et al. 2007) (*Figure 17*).

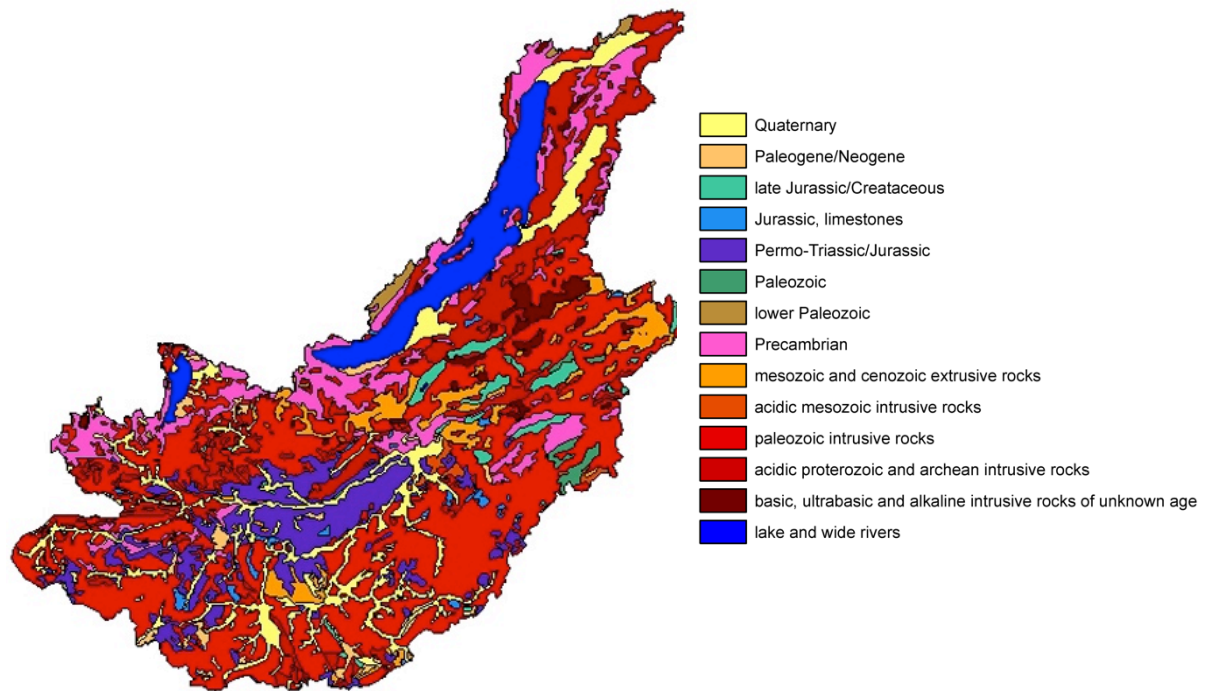


Figure 17: Lithological map of the Lake Baikal catchment (Heim et al. 2007).

Permafrost is extensive within the Baikal catchment region, especially around the Selenga River basin. Continuous and discontinuous permafrost dominate c. 30% of the east and west sections of the Selenga River basin, and sporadic and isolated permafrost dominate the south sections (Sharku, 1998; Törnqvist et al. 2014 as cited in Mackay et al. 2016). Permafrost is degrading within the Baikal region due to warming, human impact and increased wildfires (Sharku 1998; Romanovsky et al. 2010; Zhao et al. 2010; Törnqvist et al. 2014).

2.2 Climate controls in the regions

The climate within the region is arid and continental, as the Primorsky Mountain Range (1000 – 1500 m a.s.l) on the western coast of Lake Baikal blocks moisture carried by the Atlantic Westerlies (Gustokashina and Bufal, 2003; Bezrukova et al. 2013). Mean January and July temperatures within the Baikal region are c. -19.7°C and 15.4°C respectively (Galaziy, 1993;

Bufal et al. 2005; Bezrukova et al. 2013). The summers within this continental region are short, warm and wet and the winters are long, dry and cold (Mackay et al. 2016). The timing of ice cover formation and break-up at Lake Baikal is driven by large-scale atmospheric circulation patterns, which include the North Atlantic Oscillation (NAO), Arctic Oscillation (AO) and the Siberian High (Livingston, 1999; Todd and Mackay, 2003). The position and intensity of the Siberian high, which is a cold anticyclone that forms over eastern Siberia in winter, dominates the climate, along with the jet streams, and both the summer and winter monsoons (Mackay et al. 2003). In the winter, the Siberian high-pressure system brings cold Arctic air into the region from the Kara Sea to central Asia (Gong and Ho, 2002 as cited in Mackay et al. 2016), which influences the intensity of the East Asian Winter Monsoon (EAWM) (Wu and Wang, 2002 as cited in Mackay et al. 2016). In spring the Siberian high-pressure decreases and the air masses move towards Europe. The weakening of the Siberian high pressure is variable within the Baikal region, and this affects the timing of the ice-off period and spring bloom development. In the summer months, the Asiatic Low moves towards the Baikal region, bringing moisture from the Indian Ocean.

2.3 Limnology

Three different zones occur in the water column of Lake Baikal; the euphotic zone which extends between 4 and 50 m water depths, the aphotic zone, which is mixed by convective cooling down to 200 m during autumn and down to 300 m by warming in the spring, and the permanently stratified aphotic zone, which is the oxic deep water zone from approximately 300 m to the bottom waters (Fietz et al. in prep) (*Figure 18*).

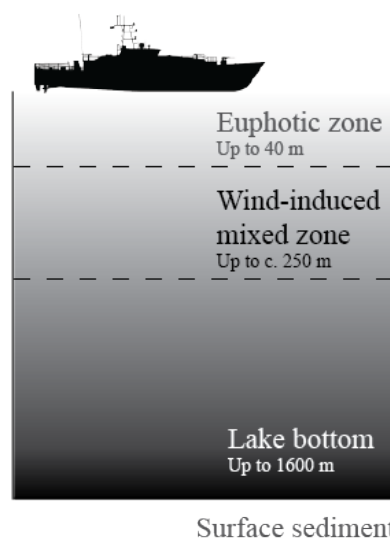


Figure 18: Diagram of Lake Baikal's water column from the euphotic zone to the sediment surface.

The water masses below the mixing layer are homothermal (c. 4°C; Granin et al. 1991; Shimaraev et al. 1994), and Lake Baikal has permanent high oxygen content within its deep waters, throughout the water body (Fietz et al. in prep). This is due to deep-water ventilation and turbulent diffusion from weak stratification of the water masses (Weiss et al. 1991; Shimaraev et al. 1993; 1994; Hohmann et al. 1997; Dobretsov et al. 2000; Wüest et al. 2005). Deep-water ventilations occur regularly (Weiss et al. 1991; Shimaraev et al. 1994; Wüest et al. 2005), and the two mechanisms suggested to be driving this deep-water ventilation are thermal instability (Weiss et al. 1991) and cabbeling (Shimaraev et al. 1993; 1994). Cabbeling, is the sinking of denser water as the warmer littoral waters mix with the colder pelagic waters, and this occurs at thermal bars within the lake (Shimaraev et al. 1993; 1994). Thermal bars form close to the coastal regions in Lake Baikal in the spring due to faster warming of shallow waters, compared to deeper pelagic waters (Likhoshway et al. 1996). Thermal instability involves the relationship between temperature and pressure, with plumes of colder water sinking from the upper zone (0 – 250 m) to displace the deeper permanently stratified waters in spring (Shimaraev and Granin, 1991; Ravens et al. 2000). During spring, the surface waters (c. 4°C) are above colder waters and the boundary between the upper waters and the deeper waters is known as the mesothermal temperature maximum (MTM), where $T = T_{md}$ (temperature at maximum density), with temperature decreasing at a rate of $0.021^{\circ}\text{C bar}^{-1}$ with depth due to increasing pressure (Chen and Millero, 1986 as cited in Morley, 2005). Free convection does not occur between upper and lower waters, as the water at the boundary is at maximum density (Shimaraev et al. 1994). Convection only occurs when the boundary between these two zones is deepened, by wind stress or salinity, forming a plume as the temperature of the upper waters become closer to the T_{md} (Weiss et al. 1991). This theory is disputed by Hohmann et al. (1997), as it is unclear as to how the upper waters can cross the MTM. Instead Hohmann et al. (1997) suggests that plumes of colder denser water occur in areas where water masses of differing temperatures and salinity meet horizontally, such as where the Selenga River waters meet the colder North Basin waters at the Academician Ridge. Therefore, both low primary productivity and efficient deep-water mixing of Lake Baikal ensures permanently oxygenated bottom waters with a high oxygen penetration depth in the sediments (Weiss et al. 1991; Vologina et al. 2003).

Lake Baikal is a dimictic temperate lake, circulating twice a year in the spring and autumn, and its waters stratify in the summer months, with mixing depths of c. 20 m (Wetzel, 2001). Stratification develops during the summer as solar radiation heats surface waters faster than the water-mixing rate, resulting in an upper warm layer (epilimnion) and lower cooler layer (hypolimnion) either side of the metalimnion (Morley, 2005). In the autumn, a net heat loss causes the epilimnion to become cooler and denser. Autumn turnover is formed from the

sinking water from the epilimnion, which results in the metalimnion deepening, until the entire water column circulates, and this temperature loss continues until the water is 4°C or less. During winter ice development, an inverse stratification forms as cold, less dense water lies above warmer denser water at c. 4°C. Then during ice break-up in spring, the lake overturns and becomes isothermal, which allows for direct summer stratification to develop (Morley, 2005). However, even during homothermy, due to the size of Lake Baikal, convective currents and the wind-induced overturn is limited to the upper 250 – 300 m, forming two layers; the upper 250 m where mixing occurs and the lower zone from 250 m where the water is permanently stratified (Shimaraev 1977; Shimaraev and Granin 1991; Ravens et al. 2001). Water renewal occurs twice a year for the upper layers of the water column, and it takes a mean of 8 years for complete deep-water renewal (Weiss et al. 1991). Below 300 m, deep-water renewal differs between basins, taking c. 11.2, 10.4 and 6.2 years in the South, Central and North basins respectively, before the deep water returns to the surface (Weiss et al. 1991; Peeters et al. 1997). Due to the size of Lake Baikal, spanning several latitudes, the South and North basins have different ice-off timings and length of summer stratification. The lake freezes earlier in the north basin (December) than the South basin (January), and ice-off begins earlier in the South basin (March) than in the North basin (April). Therefore, the South basin becomes ice-free and stratifies in the summer months before the North basin, having a longer growing season.

2.4 Seasonal phytoplankton trends in Lake Baikal

Diatoms are one of the main primary producers and in the spring, they bloom underneath the ice, with planktonic species growing within the water column (Jewson et al. 2009) (*Figure 19*). During the summer, non-siliceous autotrophic picoplankton account for up to 90% of the total primary production and then in the autumn diatom populations are re-established in the water column, with blooms of *Cyclotella minuta* (Back et al. 1991; Popovskaya et al. 2004) (*Figure 19*). The dominant Baikal diatom species vary from year to year, with *Melosira* years (which are now known as blooms of *Aulacoseira baicalensis*) and *Synedra acus* years (Antipova, 1963; Votintsev et al. 1975; Popovskaya, 2000 as cited in Sorokovikova et al. 2012). The occurrence of *Melosira* (*Aulacoseira baicalensis*) ‘high productive’ years are a natural phenomenon on Lake Baikal, occurring every 3 – 4 years, at least in the South basin during spring and can have up to 10 times greater algal biomass compared to non-*Melosira* years (Bondarenko and Evstafev, 2006). Pre-*Melosira* years are often marked by high abundances of *Cyclotella minuta*, and *Melosira* years are often followed by *Synedra* years (Rychkov et al. 1989 as cited by Morley, 2005). These large under-ice blooms of *Aulacoseira baicalensis* have been suggested to be meteorologically driven (Shimaraev, 1971 as cited in

Katz et al. 2015) and astronomically driven by solar activity (Bondarenko and Evstafev, 2006). Katz et al. (2015) found that the peak abundance of *Aulacoseira baicalensis* shifted by 1.6 months later across a 50-year time series, corresponding with the delay in ice-on timing that has been associated with climate change. Kozhov (1955, 1963) as cited in Katz et al. 2015 found that there is no evidence for nutrient controls of *Aulacoseira* blooms but suggests that water temperatures in the months leading up to ice cover might create favourable conditions for blooms if they promoted retention of a large “seed bank” of *Aulacoseira* cells in the photic zone. In addition to autumn water temperatures, light availability through the ice cover plays a major role in the formation of large *Aulacoseira* blooms (Kozhova, 1961; Jewson et al. 2009).

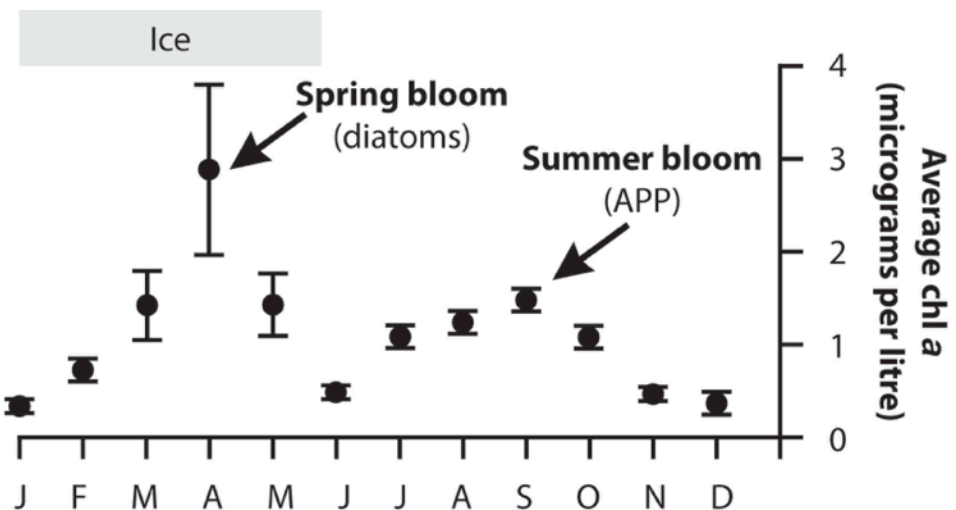


Figure 19: Seasonal phytoplankton trends of the two dominant primary producers (diatoms and picocyanobacteria) at Lake Baikal (Moore et al., 2009).

2.5 Palaeolimnological and palaeoclimate records at Lake Baikal

Regional climate reconstructions have previously been conducted using palynological records and geochemical data from lakes on the shore of Lake Baikal, namely Lake Kotokel and Lake Khall (Figure 20) (Tarasov et al. 2009; Mackay et al. 2013b). Lake Kotokel is located on the eastern coast of Lake Baikal (Tarasov et al. 2009), and Lake Khall is a small shallow lake located to the south of Ol’khon Island, on the west coast of Lake Baikal (Figure 20) (Mackay et al. 2013b). These records show similar climatic trends to regional climate modelling (White and Bush, 2010), showing declining atmospheric precipitation and increase in continentality over the mid to late Holocene. This decrease in precipitation occurred alongside a change in

seasonality, with the strengthening of Westerlies within the region resulting in greater winter snow accumulation. Higher winter snow accumulation, along with drier summers, favoured the spread of drought resistant Scots pine (*Pinus sylvestris*) (Tarasov et al. 2009; White and Bush, 2010; Mackay et al. 2013b). Furthermore, the Lake Khall geochemical record shows a period of relative stability which coincides with the Medieval Climate Anomaly (MCA), and cool, moist conditions which coincide with the timing of the LIA (Mackay et al. 2013b).

Diatom production proxies such as BSi have been used to reconstruct diatom response to long-term climatic changes and biogenic silica concentrations have been directly linked to insolation forcing (Qui et al. 1993; Colman et al. 1995; Williams et al. 1997; 2001; Kashiwaya et al. 1999; Karabanov et al. 2000; Prokopenko et al. 2001). This highlights the use of algal production proxies at Lake Baikal in reconstructing past climates. Biogenic silica records have shown changes in climate inferred from diatom production over the Holocene (Qui et al. 1993), the MIS 3 and early MIS 2 (Swann and Mackay, 2006), over the last 250 ka years (Colman et al. 1995) and 5 Ma years (Williams et al. 1997). Diatom assemblages (Morley, 2005; Mackay et al. 1998; 2003), carbon isotopes (Prokopenko and William, 2001) and phytoplankton pigments (Fietz et al. 2007) have also been used to examine limnological change at Lake Baikal in relation to climate, and pollen records have been used to examine past vegetation histories (Demske et al. 2005; Bezrukova et al. 2003). These records show changes towards higher Chlas (Fietz et al. 2007) and diatom valve concentrations (Morley, 2005), greater forest vegetation within Baikal's catchment (Demske et al. 2005), and lower $\delta^{13}\text{C}$ values (as discussed in Chapter Six) (Prokopenko and William, 2001), during warm climatic conditions, in comparison to glacial periods.

Both diatom and biogenic silica records report changes in primary production in relation to variations within Milankovitch orbital parameters (precession, obliquity and eccentricity) (Colman et al. 1995; Williams et al. 1997). Diatom assemblage records provide information on past climates over the last 2.5 Ma years, showing diatom extinctions related to transitions to glacial periods, and speciation within the interglacial periods (Julius et al. 1997; Grachev et al. 1998; Khursevich et al. 2001). Diatom assemblage changes within a sediment core from the Vydrino Shoulder in the South basin also shows similarities between diatom shifts and North Atlantic climate events recorded in the GISP2 ice core, during the late glacial-Holocene transition, suggesting teleconnections between Central Asia and the North Atlantic (Morley, 2005). In addition to algal production records, regional vegetation history from long sediment records at Lake Baikal span over the Holocene (Bezrukova et al. 2003) and Quaternary period (Müller et al. 2001; Demske et al. 2002). Palaeolimnological records from fossil pigments and diatoms at Lake Baikal show that the last interglacial (Eemian, MIS 5e) in central Asia lasted

c. 10.5 ka years (Rioual and Mackay 2005; Fietz *et al.* 2007), and the short-lived mid-Eemian cooling event detected within the last interglacial matches up with the North Atlantic records (Karabanov *et al.* 2000). Furthermore, the timing of the glacial periods as inferred from zero values of biogenic silica concentrations, match the glacial periods within the marine $\delta^{18}\text{O}$ profile (Colman *et al.* 1999). Diatom production records show millennial-scale variability during the Holocene, linked to Northern Hemisphere cooling, with the occurrence of ice-rafting (Heinrich) events, Dansgaard-Oeschger Events and Bond Cycles at Baikal (Prokopenko *et al.* 2001). An oxygen isotope record of diatom silica from Lake Baikal also provides evidence for Holocene cooling events (Mackay *et al.* 2011). These cooling events have been suggested to be related to variations within solar radiation and melt-water outburst event from the Laurentide ice sheet (Mackay *et al.* 2011).

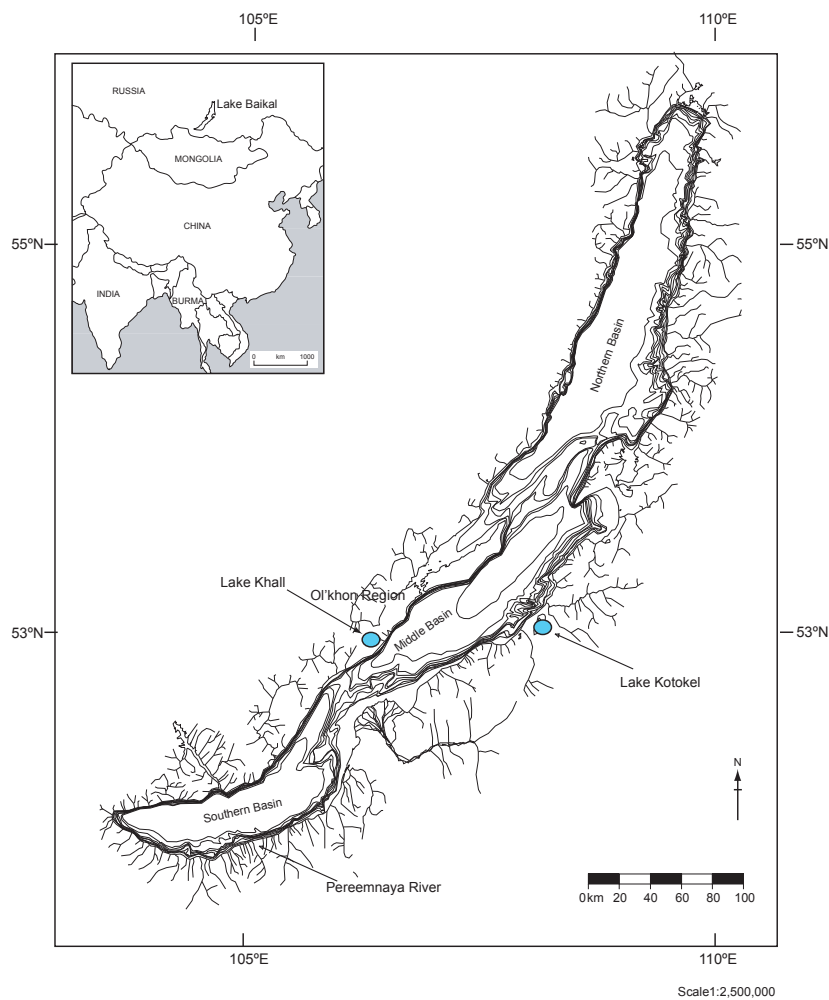


Figure 20: Location of Lake Khall and Lake Kotokel on the coast of Lake Baikal.

Across the Northern Hemisphere, short-term climate events within the late Holocene have been detected from sediment records, which are referred to as the Little Ice Age (LIA) and the

Medieval Climate Anomaly (MCA) (Campbell et al. 1998; Jones and Mann, 2004 as cited in Mackay 2007). Palaeoclimate records show clear regional fluctuations which correspond with the LIA and MCA periods (Nesje et al. 2005 as cited in Mackay, 2007), and mid to high-latitude continental regions, such as Lake Baikal, experienced lower temperatures during the LIA period compared to similar regions close to the North Atlantic (Bradley, 2003 as cited in Mackay, 2007). Therefore, this cooling during the LIA period impacted Baikal’s ecosystem (Mackay et al. 1998). Regional temperatures over the last 1000 years within Asia have been reconstructed using tree ring reconstructions, and climatic changes do not fully match up in timing and magnitude with climatic changes observed (D’Arrigo et al. 2000; Cook et al. 2013). For example, the transition to colder climatic conditions during the LIA occurred earlier in the Arctic, Europe and Asia than in North America or the Southern Hemisphere regions (PAGES 2k Consortium, 2013) (*Figure 21*). Regional climatic changes within the Baikal region in the late Holocene may not necessary match up in timing and magnitude with observed short-lived climatic events, such as the LIA, in the North Atlantic.

Pollen records show changes in regional vegetation assemblages in response to these climatic changes over the last millennium at Lake Baikal, with increasing abundance of fir (*Abies*) in the mid-taiga forest mountain, suggesting higher winter temperatures and precipitation with intensification of winter cyclonic activity during the MCA (Bezrukova *et al.* 2006). The MCA was then followed by an expansion of scrub pine (*Pinus*), spruce (*Picea*), and larch (*Larix*) with cooler climatic conditions in the LIA (Bezrukova et al. 2006).

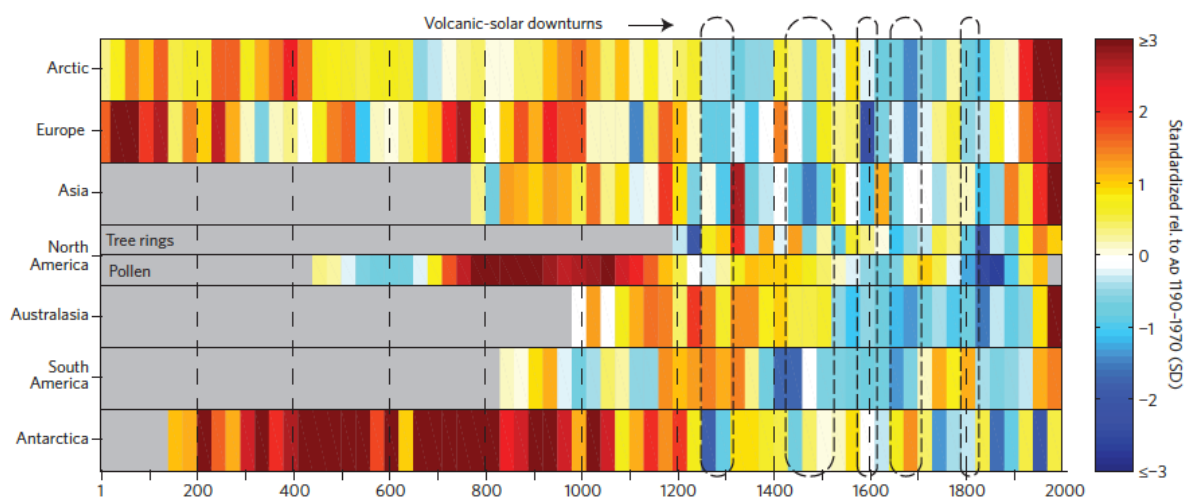


Figure 21: Temperature reconstructions across the continents over the last 2000 years (PAGES 2k Consortium, 2013).

A previous palaeolimnological study at Lake Baikal detected sedimentary diatom assemblage changes at the timings of the MCA and LIA (Mackay et al. 2005). Past diatom assemblages

have also been used to infer snow cover over the last 1000 years, and during the LIA the diatom assemblages suggest increased snow cover, which is likely to be a result of increased intensity of the Siberian High and weakening of the North Atlantic Oscillation within the region (Mackay et al. 2005). The onset of the LIA at Lake Baikal is shown by changes within the abundances of spring blooming and autumnal blooming diatoms, namely *Aulacoseira baicalensis* and *Cyclotella minuta*, and not by total diatom concentrations (Mackay et al. 1998). It is suggested that continuous snow cover on Lake Baikal and a prolonged cooler climate during the LIA resulted in conditions which promoted the growth of *Cyclotella minuta* over under-ice blooms of *Aulacoseira baicalensis* (Mackay et al. 2011). However, a climate reconstruction study from the $\delta^{18}\text{O}$ isotopic composition of diatom silica at Lake Baikal does not provide evidence for the LIA in the late Holocene (Mackay et al. 2011). This has been suggested to be due to the LIA being a short climatic event of low magnitude, in comparison to late glacial climatic changes, which have been detected via diatom assemblage changes (Mackay et al. 2011). Therefore, photosynthetic pigments are vital to use at Lake Baikal to examine climatic changes over the last 1000 years, as they provide a complete picture of past algal production and of other algal groups, and not just diatoms as inferred from biogenic silica records.

2.6 Social and economic pressures at Lake Baikal

The Baikal region has a long history of hunter-gatherers and pastoralists from at least 8800 cal. yrs BP (Bezrukova et al. 2006; Nomokonova et al. 2010; Mackay et al. 2013), and since the late Holocene pastoralists dominated the Ol'khon region (Nomokonova et al. 2010). Despite the long history of prehistoric populations around Lake Baikal, human impact on vegetation was local and not intensive enough to affect the regional vegetation development (Tarasov et al. 2007). Therefore, before the 1950s there is no evidence of anthropogenic activity within the lake sediment pollen and charcoal records (Demske et al. 2005; Tarasov et al. 2007). Lake Mo-33b is a small shallow lake, located in the Selenga River watershed in the southern part of the Bulgan Province, in central Mongolia (*Figure 22*), and sedimentary pollen analysis has been carried out to examine vegetation change (Tian et al. 2014). Low economic activity, such as forest clearing for pastures, forest fires, agriculture occurred prior to 1950 (Kozhova and Silow, 1998), and pollen records from Lake Mo-33b show that agricultural activities largely began in the 1980's (Tian *et al.* 2014), with increased regional farming resulting in higher abundances of *Pediastrum* spp. within Lake Mo-33B (Tian et al. 2014).



Figure 22: Location of Lake Mo-33b in Mongolia (modified from Tian et al. 2014).

Pediastrum spp is Chlorophyceae green algae, and has been suggested to be indicative of nitrogen-rich waters (Mackay et al. 2013). The appearance of *Pediastrum* spp. within the palynological record from Lake Khall has been observed since c. 1845 AD (Mackay et al. 2013). The rise in *Pediastrum* spp. at Lake Khall largely occurred over the last c. 100 years, with increases more than 3-fold in abundance over the last c. 50 years (Mackay et al. 2013). The appearance of *Pediastrum* spp. at c. 1845 AD coincides with the intensification of animal husbandry within the Lake Baikal region and the influx of Russian settlers (Tarasov et al. 2007). Following this, tree-felling by local populations occurred, although this is not observed within the palynological record (Sizykh, 2007; Mackay et al. 2013). Despite observed changes within aquatic plant assemblages in the mid 19th century, major human impact has only been the major driver of larger scale regional vegetation changes over the last 60 years, with crop cultivation and herding explaining a greater proportion of variance within the pollen record than climate (Tarasov et al. 2007; Tian et al. 2014). The increase in *Pediastrum* spp. within the palynological record from Lake Khall (Mackay et al. 2013b) and within Lake Mo-33b also highlights a recent phase of human impact within the Lake Baikal region, over the last c. 50 years.

Vegetation land cover data from 2000 to 2010 was collected from <http://www.esa-landcover-cci.org> (by S. Virdis), and reductions in forest cover, increases in cropland, and increases bare and shrub land have been observed (S. Virdis per comms). The predominant land cover changes observed over the last decade within Lake Baikal's catchment have been increases

within the area of cropland (increase by 40,000 ha), deciduous shrubland (30,000 ha) and grassland (35,000 ha), and decreases within regional forest cover (15,000 ha, 1,700 ha and 6,000 ha in needle-leaved evergreen tree cover, broadleaved deciduous tree cover and needle-leaved deciduous tree cover respectively) within the southern catchment area (Figure 23).

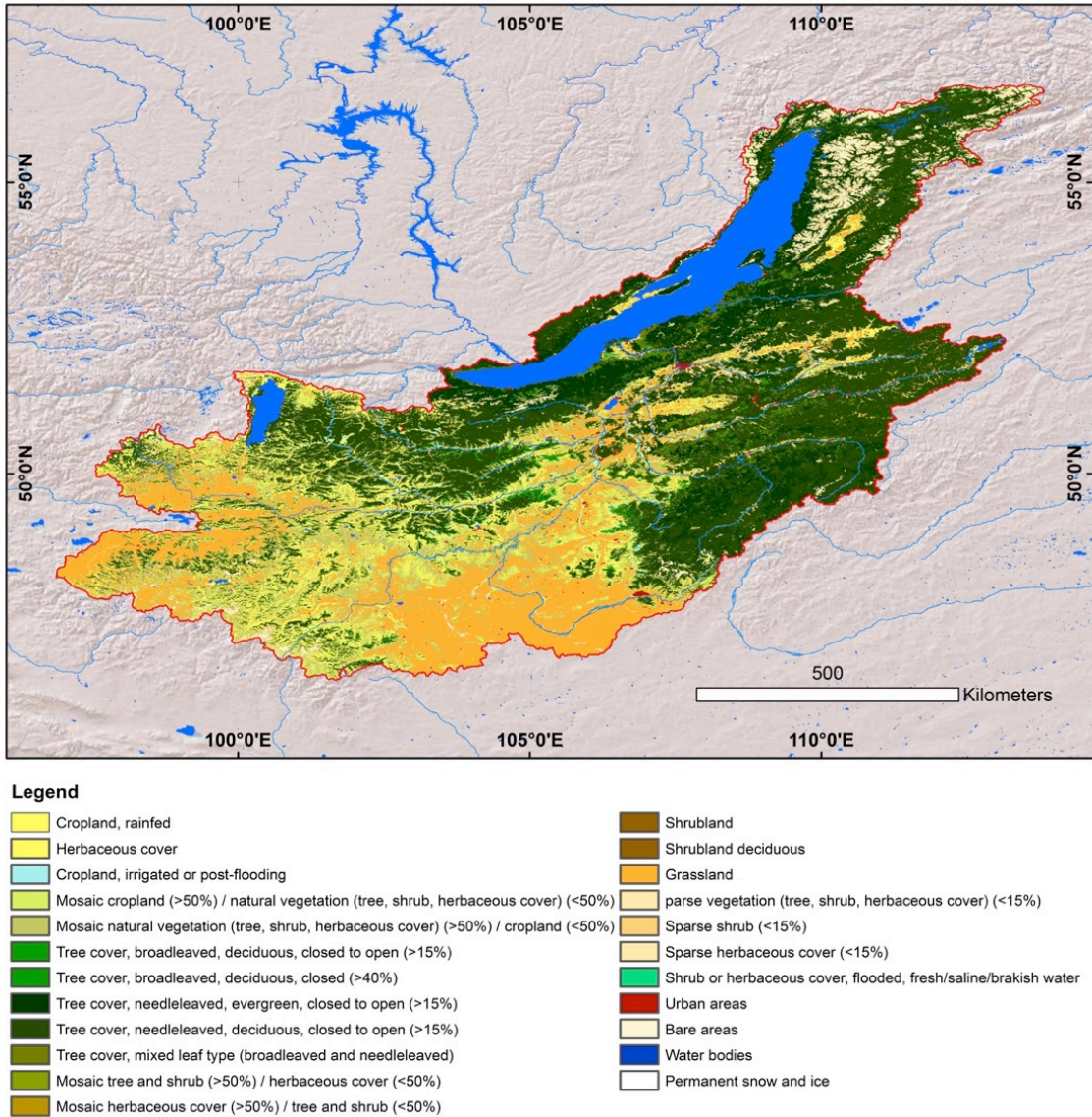


Figure 23: Land cover map of Lake Baikal's catchment Area. Produced by S. Virdis (unpublished) (Data source: <http://www.esa-landcover-cci.org>).

2.6.1 Pollution sources in and around Lake Baikal's watershed

Since the 1950s, pollution sources have become of national and international concern, from industry, mining, urban growth and tourism (Brunello et al. 2004). There are several large cities and industrial centres around Lake Baikal, including Irkutsk, Angarsk, Chermkovo and Usolye-Sibirskoye (*Figure 24*) (Van de Vel et al. 2010). Human population within the lake's basin is relatively sparse, and reaches over one million within all the cities combined (Van de Vel et al. 2010). One of the main cities, Irkutsk, which is not within the catchment but along the Angara River, has a population of c. 640,500 (McConnell et al. 1996; Russian Federal State Statistics Service, 2011). Another main city is Ulan-Ude, which is in Baikal's watershed along the Selenga River and has a population of c. 400,000 (McConnell et al. 1996). The population of Ulan Ude has increased from c. 21,000 in 1923 to c. 250,000 in 1970 and c. 400,000 in 2010 (McConnell et al. 1996; Russian Federal State Statistics Service, 2011). The current population of c. 640,500 in Irkutsk has been relatively stable over last few decades (McConnell et al. 1996; Russian Federal State Statistics Service, 2011). Angarsk has a smaller population today, of 23,000, and Severobaykalsk in the north, was founded in the early 1970's has a population of c. 25,000 (Russian Federal State Statistics Service, 2011).

Increasing pressures from shoreline settlements and tourism within Baikal's catchment have been observed and are causing greater loading of phosphorus and nitrogen into the littoral regions of the lake (Ciesielki et al. 2006), due to outdated sewage-treatment plants in coastal cities (Timoshkin et al. 2016). As discussed previously in this thesis, there is now evidence of eutrophication in Baikal's coastal waters, with algal blooms of *Spirogyra* found in 2013 along the northwest coast near the town of Severobaikalsk (Timoshkin et al. 2016). It is unknown if there have been any changes in nutrient concentrations within the pelagic regions, and what impact changes in lake water nutrient concentrations would have on Baikal's pelagic phytoplankton (Mackay et al. 2006; Moore et al. 2009). Previous limnological surveys show higher phosphorus concentrations within the Selenga River waters (Sorokovikova et al. 2015) than previous measurements in the 1960s -1980s (Votinstev et al. 1965; Tarasova and Mescheryakova, 1992; Sorokovikova and Avdeev, 1992; Sorokovikova et al. 1995). Primary production in the Selenga River has risen four-fold between 1961 and 1990 (Sorokovikova and Avdeev, 1992), alongside gradual increases in phosphorus concentrations (Tarasova and Mescheryakova, 1992; Sorokovikova et al. 2001). An increase in the sulphate concentrations from atmospheric precipitation and wastewater discharges over the last 60 years in the Selenga River waters and small tributaries flowing into the South basin have been recently reported,

highlighting the deterioration of water quality from pollution (Sorokovikova et al. 2015a; 2015b).

Over the last 10 years, urban areas within Baikal's catchment area have increased by c. 15,000 hectares (S. Viridis per comms). The main industries are energy, logging, oil and fuels, chemicals and hydro-electricity, and the major industrial centres, Ulan-Ude, Angarsk, Shelekhov, and Baikalsk, are located within 0-100 km of the lake (McConnell et al. 1996; Van de Vel et al. 2010). Irkutsk is another major industrial centre on the outflow from the Angara River, which is not located within the watershed, but is a potential source of atmospheric pollutants into Lake Baikal.

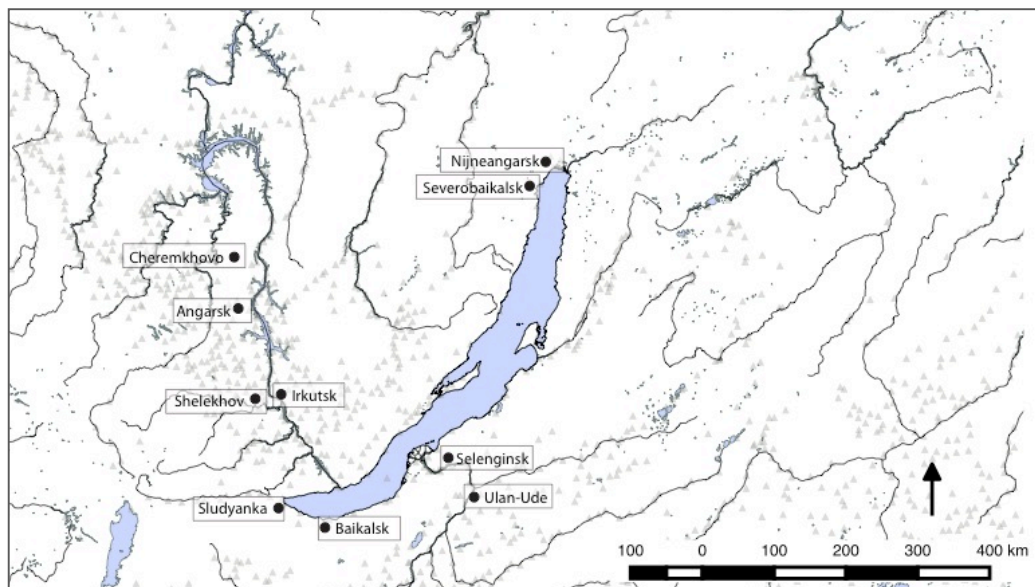


Figure 24: Main settlements within Lake Baikal's watershed and along the outflow; the Angara River. Triangles represent settlement areas.

Industrial development began in the 1950s, with point source pollution from pulp and paper mills and power stations situated around the lake, mainly in Irkutsk, Angarsk, Baikalsk and Selenginsk (Brunello et al. 2004) (Figure 24). In contrast, there are only a few industrial regions in the watershed of the North Basin, which include Severobaikalsk and Nijneangarsk (Rose et al. 1998). Point source pollution in the north includes effluents from partially treated sewage, which enters the lake at Severobaikalsk (Rose et al. 1998). Along with sewage, factory waste products enter the South basin, both directly and from rivers, especially the Selenga River (Rose et al. 1998). The two pulp and paper mills in the region were constructed on the South basin shore in Baikalsk, and along the Selenga River, in Selenginsk (Lindström-Seppä et al. 1998; Stepanova et al. 2000). The Baikalsk Pulp and Paper Mill (BPPM) (Figure 24), located in Baikalsk on the South Basin shoreline, was the major polluter of the lake, due

to its emissions and release of wastewaters directly into the lake, which had high levels of sulphates, chlorides, and organic compounds (Lindström-Seppä et al. 1998; Brunello et al. 2004; Kotelevtsev et al. 2000). The BPPM produced over 50,000 cubic meters of water pollution and 20,000 tons of air pollution annually (Brunello et al. 2004), and it has been shown that the Baikalsk mill caused enhanced levels of persistent organic chlorines in the southern basin, particularly in the 1960s to 1970s (Maatela et al. 1990; Oyuna et al. 2003). Emissions of methanethiol were also released from the BPPM (Toda et al. 2010) and are currently being released from the pulp mill in Selenginsk.

Bioaccumulation of organic chlorine compounds and chemical elements within the food web has been detected within the livers of Baikal seal, plankton, zoobenthos and fish (Watanabe et al. 1998; Ciesielski et al. 2006; Imaeda et al. 2009; Isobe et al. 2009; Iwata et al. 1995; Nakata et al. 1995; Imaeda et al. 2009; Hirakawa et al. 2011), and levels of dioxin and dibenzofuran (PCDD/Fs) within Baikal's freshwater seals have been reported to be high, being similar to the levels detected within the Baltic Sea seals (Tarasova et al. 1997). The outbreak of the morbilivirus in the late 1980s, which resulted in high mortality rates within the Baikal seal population, has been associated with this increasing organochlorine pollution from the BPPM, as organic chlorine compounds caused immunosuppression (Galazii, 1991; Grachev et al. 1989; Nakata et al. 1995; Nakata et al. 1997). Thus, due to the emissions of pollutants, effluent wastewater discharges and ground water contamination, the BPPM was officially closed in 2013 for the protection of Lake Baikal (Environmental Monitoring of Lake Baikal website, 2015).

Industrial activity within the Baikal region was greatest during the 1990s, and then the level of pollution decreased due to a fall in economic activity and the inclusion of Baikal on the UNESCO World Heritage list in 1996 (Brunello et al. 2004). Tourism started to increase in the 1990s, along with navigation activity. Increasing tourism around the shore of bays, such as Litsvyanka and Maloe More, is a growing environmental threat to Lake Baikal, as tourist resorts and boats release waste directly into the lake (Kravtsova et al. 2014; Timoshkin et al. 2016). The spread of *Elodea canadensis*, an alien species of submerged macrophyte, which was found in the bays, along shorelines and within pelagic regions of the lake, in the 1970s, has been linked to navigational activity (Kozhova and Pautova, 1985 as cited in Kravtsova et al. 2010; Kozhova and Izhboldina, 1992). Another pollutant; microplastics (< 5 mm in size) from household plastics could also disrupt Baikal's aquatic foodweb, and these have been a growing concern for the Laurentian Great Lakes (Eriksen et al. 2013; Driedger et al. 2015). Microplastics have been found in high concentrations in Lake Hovsgol (Free et al. 2014), next

to Lake Baikal, where the level of pollution is suggested to be higher than at the Great Lakes. However, microplastic pollution has not yet been reported in Lake Baikal

Along with industrial enterprises, mining activity within the Baikal catchment has increased substantially over the last decade (Brunello et al. 2004). Gold mines are largely in operation in the northeastern Mongolian region, releasing pollutants into the Selenga River (Stubblefield et al. 2005; Chalov et al. 2012; Thorslund et al. 2012). Over the last 10 years many of the sub-basins of the Selenga River have been used for mining gold, silver and coal (Chalov et al. 2012). In 2011, there were 204 small-scale gold mining companies operating in Northern Mongolia along the Selenga River (Batimaa et al. 2011), and the Zaamar Goldfield has been reported as a major source of heavy metals (Thorslund et al. 2012) (*Figure 25*). Mining activity within the region uses mercury to extract the gold (Thorslund et al. 2012), which is then transported into Lake Baikal via river waters. The Selenga River has been suggested to be already very polluted, with elevated levels of heavy metals and suspended sediment transport (Thorslund et al. 2012). Lake Baikal's watershed has a significant risk of mercury pollution due to a large technogenic mercury placer for gold mining in the Boroo River, a tributary of the Selenga-Orkhon river (Tumenbayar et al. 2000). High levels of pollutants (Al, Fe, Cu, As, Mo and Hg) from mining have been reported in several Mongolian rivers, including the Tuul River near the Ulan Bator and Zaamar Goldfield (Lee et al. 2006; Bayamba and Todo, 2011; Thorslund et al. 2012; Chalov et al. 2014) (*Figure 25*). However, mercury is not used in the extraction process in the Zaamar mines (Lee et al. 2006; Thorslund et al. 2012). Thus, current levels of metals in Baikal are greatest in the southern basin, due to the inflowing Selenga River waters (Jambers and VanGrieken, 1997). Tributaries are the major source of pollution at present, accounting for over 80% of the total pollution into the lake (per comms E.A. Silow). Industrial, mining and domestic effluents from riverine inputs have not been observed to be affecting Baikal's pelagic water quality, however atmospheric pollutants can be carried over larger distances and have therefore be found in remote regions of the lake (Rose et al. 1998).

2.6.2 Pollution sources in Lake Baikal's airshed

Contamination of Lake Baikal by air pollution has been recognised as a problem since the early 1990s (Kokorin and Politov, 1991; Rose et al. 1998; Cofala et al. 2005; Van de Vel et al. 2010), however local air quality data is sparse (Van de Vel et al. 2010). Industrial emissions from factories around Lake Baikal have been increasing (Stewart, 1990; Obolkin et al. 2010). The largest coal power plants within the region are situated in Irkutsk and Angarsk, close to the south basin shore, and emit plumes of sulphur dioxide and nitrogen oxide gases into the

atmosphere (c. 130 and 80 thousand tons per year respectively) (Obolkin et al. 2013). The anthropogenic sulphur dioxide and nitrogen oxide gases are then deposited in the lake at high concentrations, as the atmospheric jet flows constrain transformation and dissipation of the plume gases (Obolkin et al. 2013). During the winter months, atmospheric contaminants accumulate in the ice, and are deposited into the lake during ice-off (Obolkin et al. 2014). Pollutants indicative of fossil fuel combustion, spheroidal carbonaceous particles (SCPs) in sediments, have increased over the last 50 years; increases were greatest in the southern basin at sites nearest to Irkutsk (Rose et al. 1998), although small increases were evident in the North basin too (Rose et al. 1998).



Figure 25: Location of sampling stations in Mongolia for atmospheric aerosols (modified from Zhamsueva et al. 2012).

Industries in the Irkutsk region release fly-ash, sulphates and metals into the atmosphere, and the SCP records indicate that the industry within the region started in the 1950s (Rose et al. 1998). The largest sources of sulphur dioxide and particulates are from Angarsk (c. 250,000 tonnes yr⁻¹ of sulphur dioxide and particulates combined), situated along the Angara River, followed by Irkutsk and Bratsk (Rose et al. 1998). There are smaller industries within the South basin at Shelekhov, Usolye-Sibirskoe, Cheremkhovo, Sludyanka, Ulan-Ude and Kamensk (Rose et al. 1998). In total, there are 16 industrial regions around the South basin, with four of these being situated along the Selenga River, such as Ulan-Ude and Gusinozersk (Rose et al. 1998). In contrast to the South basin, there are only two small industrial regions on the North basin shore (Severobaikalsk and Nijneangarsk), emitting less than 50,000 tonnes yr⁻¹ of sulphur dioxide and particulates combined (Rose et al. 1998). Emissions from power stations, industry and transport from industrial cities (Ulan Bator and Sükhbaatar) in Mongolia

(*Figure 25*) have been measured (Zhamsueva et al. 2012). Measurements of atmospheric aerosols consisting of sulphate ions, nitrate ions and ammonium ions were taken in 2005 – 2010 at Sainshand station in the Gobi Desert, Ulan Bator, Sükhbaatar and Baruun-Urt (*Figure 25*). These emissions have resulted in acidification and eutrophication of soils and water at these sampling station locations in Mongolia (*Figure 25*).

The sedimentary SCP records show high concentrations of contaminants within both the south and northern part of the lake (Rose et al. 1998), the heavy metal record suggest an increase in lead (Pb) concentrations in the 1950s and 1960s in the South basin which are a result of pollution and not natural variation, with no anthropogenic Pb enrichment in the Central and North basins (Boyle et al. 1998). This suggests that long-distance Pb pollution is minimal and any atmospheric signal may have been lost in the background noise in the Central and North basins, and that Pb pollution from industrial sources has only occurred in the South basin. This is also shown by the high SCP concentrations detected within this south basin region. However, this work is c. 20 years old, and recent changes in SCP and Pb enrichment, from industrial activity within the region remain unknown. Higher concentrations of industrial sulphur oxides and particulates have been found in the South basin, in comparison to Central and North basin concentrations, although the industries in Irkutsk Oblast and the Selenga have an impact on the atmosphere over the entire lake (Malderen et al. 1996; Rose et al. 1998). Plumes of sulphur and nitrogen oxides from large coal power plants on the southern shore of Lake Baikal have been found to have caused acidification of the Pereemnaya River waters (*Figure 20*), a small tributary feeding into the South basin (Obolkin et al. 2016). These emissions are sourced from the Irkutsk Oblast, one of the developed industrial centres in East Siberia, which release over 100,000 tonnes of sulphur dioxide and c. 60,000 – 80,000 tonnes of nitrogen oxides annually (Obolkin et al. 2016). The Pereemnaya River is c. 100 – 150 km from the Irkutsk Oblast emission source, and prevailing north-west winds transport these emissions towards the lake. Concentrations of sulphate and nitrate ions have been found to be 2 – 3 times higher than in pelagic Lake Baikal (Obolkin et al. 2016). Higher sulphate and nitrate ions have resulted in changes in the chemistry and acidification of the Pereemnaya River waters, causing lower pH levels of c. 6.8 in comparison to values with the lake and other tributaries (pH of c. 7.8) (Obolkin et al. 2016).

Nitrogen and mercury are also atmospherically deposited into Lake Baikal, and the major sources nearby are from India, China and Japan, with $> 5 \text{ kg N ha}^{-1}\text{yr}^{-1}$ of nitrogen emissions (Phoenix et al. 2006) and $> 100 \text{ g/km}^2$ of mercury emissions (UNEP Global mercury Assessment, 2013), in the mid-1990s and 2010 respectively (*Figure 26*; *Figure 27*). Total atmospheric reactive N has more than doubled since the 1900s due to anthropogenic activities

including intensive agricultural practices, increased fossil fuel combustion and rising vehicle use (Galloway et al. 2008).

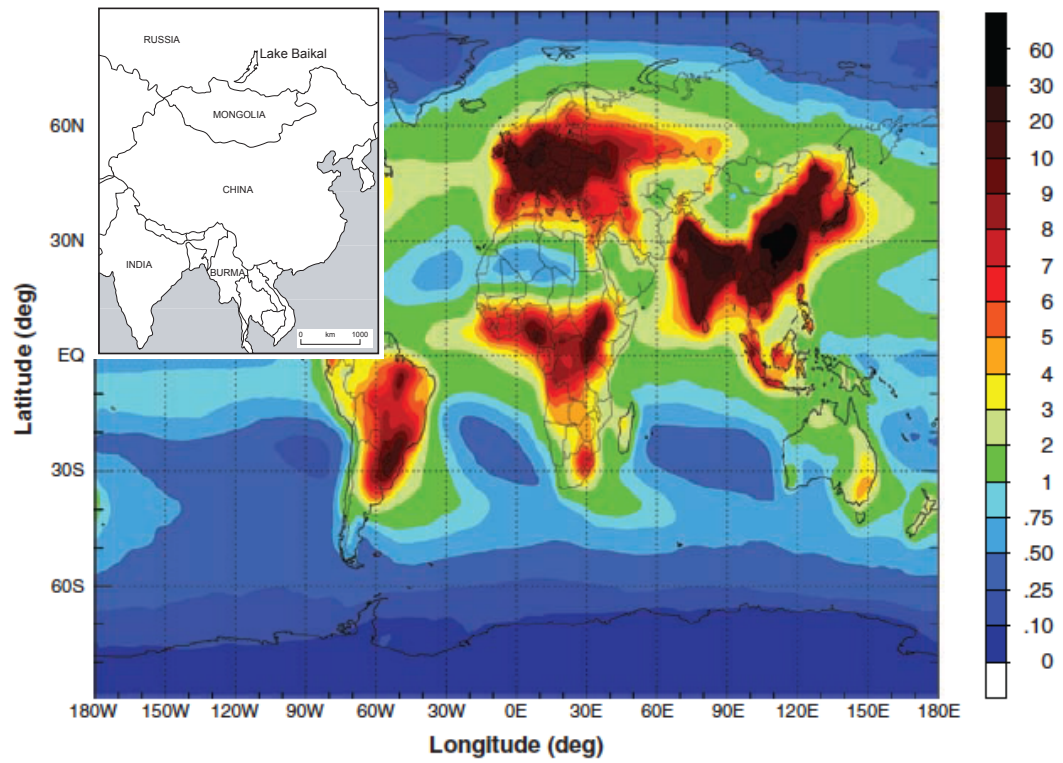


Figure 26: Global nitrogen deposition ($\text{kg N ha}^{-1} \text{yr}^{-1}$) (Dentener et al. 2006 as cited in Galloway et al. 2008).

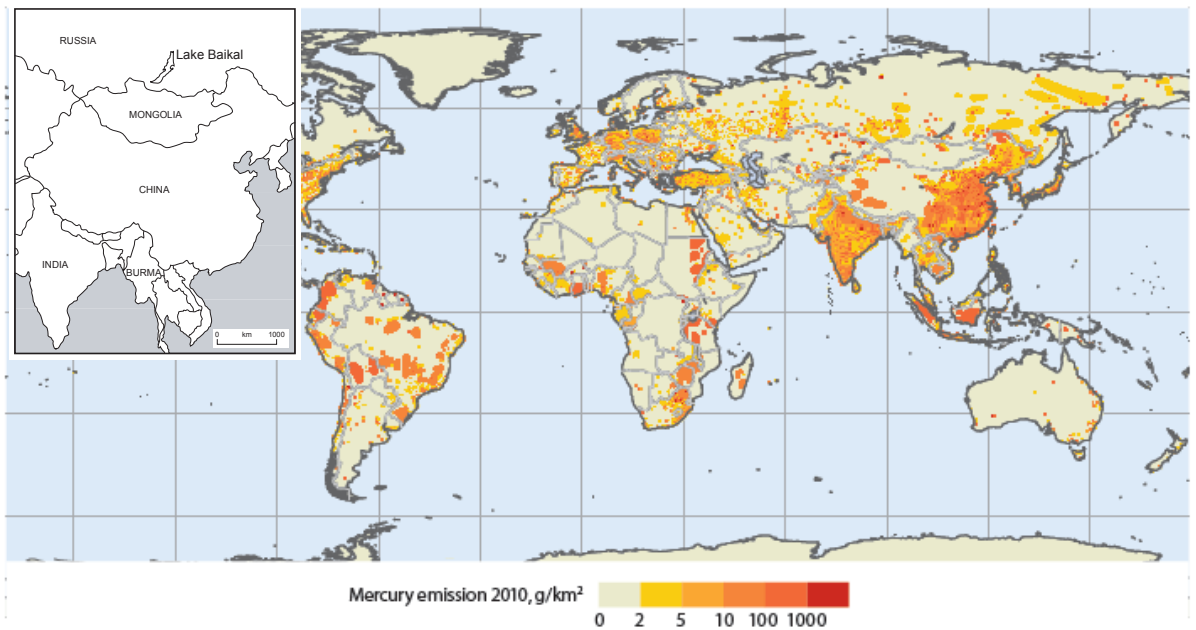


Figure 27: Global mercury deposition in 2010 (UNEP Global mercury Assessment, 2013).

Efforts have been taken to minimise environmental pollution at Lake Baikal, and numerous environmental laws have been created to control logging, to protect spawning grounds of the endemic omul, to convert the Selenginsk paper and pulp mill to a closed cycle water system and to shut down the BPPM (Mackay *et al.* 1998; Environmental Monitoring of Lake Baikal website, 2015). Protected areas and national parks have been set up through the Baikal catchment during the 1970s and 1980s (Environmental Monitoring of Lake Baikal website, 2015). Water levels at Lake Baikal have also been impacted by the construction of hydroelectric power stations and dams. There have been four dams constructed on the Angara River since the 1950s for hydroelectric power (the Irkutsk dam, Bratsk dam, Ust-Ilisk dam and Boguchany dam), and the Irkutsk dam increased the water levels in Lake Baikal by more than a metre (Jagus *et al.* 2015). Prior to the construction of the Irkutsk reservoir, the water level of Lake Baikal was controlled by atmospheric pressure and wind (Jagus *et al.* 2015). The rise in water level impacted the lakes ecosystems, causing flooding and disrupting the Selenga delta's ecosystem, and spawning grounds of the Baikal omul fish (Jagus *et al.* 2015). However, currently there are growing threats from lower water levels due to activities by the dam on coastal communities, and the threat of the construction of the Shuren dam, and possibly others, upstream on the Selenga in northern Mongolia (Mackay, 2015).

2.7 Summary

Lake Baikal is a superlative lake, which is undergoing threats from environmental change and anthropogenic pollution. Most of the pollutants (c. 83%) are brought into Lake Baikal via rivers, namely the Selenga River, which contributes to over 50% of river inflow into the lake (Silow, 2013; 2014). The remainder of the pollutants are brought in from the atmosphere (15%), with the Baikal Pulp and Paper Mill (BPPM) contributing to < 1% when it was operating between 1961 to 2013 (Silow, 2013; 2014). Economic activities within the Baikal region began post 1950, with the construction of power stations and pulp and paper mills, log rafting, intensive use of mineral fertilisers and the development of transportation, including the Baikal-Amur railroad (Silow, 2013; 2014). Both tourist and population numbers are vague within the Baikal region, with no clear historic record, but post 1950, there has been population growth in shoreline settlements and mass tourism, since the construction of the railroad (Silow, 2013; 2014). Tourism has been a growing phenomenon within the region since Lake Baikal was listed as a world heritage site in 1996, largely attracting tourists to the shoreline region during the summer season. Thus, within this thesis, sampling and coring sites have been chosen across Lake Baikal (Chapter Three) to examine whether there are any signs of pollution within the pelagic regions, given that algal blooms from human influence have already been seen within the shoreline region (Timoshkin *et al.* 2016).

Chapter Three: Methodology

3.1 Water samples

Fieldwork was carried out in March 2013 and August 2013. Water surveys in the South basin were conducted in spring, to examine under-ice ecology. Sites along a transect in the South basin (BAIK13-1, BAIK13-4 and BAIK13-5) (*Figure 28*) were sampled in both seasons, in winter before ice-thaw and during the summer stratification period. Water sampling sites across Lake Baikal, in the South basin, Central basin, North basin, Maloe More Bay, Selenga Shallows and Chivsky Bay were surveyed in August 2013, alongside catchment river inflow sites (*Figure 28*). In March 2013 and August 2013, samples were collected with a Van Dorn sampler from depths of 1, 3, 5, 10, 20, 30, 100, 180 m for analysis of algal pigments, nutrients and dissolved organic carbon. Approximately 4 L of water was collected at each water depth and filtered through a zooplankton mesh. sampling down the water column took place at 3 sites (BAIK13-1, BAIK13-4 and BAIK13-5) in March 2013 in the South basin, and 15 sites in August 2013 across the three basins (*Figure 28*). Water samples were accompanied by measurements of pH, redox potential, dissolved oxygen, conductivity, temperature and chlorophyll-*a* logged every 3 seconds using a YSI EXO2 sonde. Light intensity was measured every 1 m to a maximum depth of 70 m using Licor (Brand) light meter. Multiple chlorophyll-*a* measurements (HPLC, spectrophotometric and fluorescence) were obtained as an estimate of phytoplankton biomass and the three techniques have been compared. Spectrophotometric methods of chlorophyll-*a* analysis involves the measurement of chlorophyll-*a* samples at four different wavelengths (See 3.5.4 *Chlorophyll-a spectrophotometric analysis* section). Water samples for mercury analyses were collected in August 2013 from 2 sites along the Selenga River, 5 sites within the Selenga Delta, and 5 sites within the pelagic lakes waters. Spot samples from three main inflowing rivers (Selenga, Barguzin and Upper Angara) were also collected along with water samples from several smaller tributaries entering the South basin (Vydrino, Mishika, Snezhnaya, Khara-Murin and Solzan Rivers), for nutrients and dissolved organic carbon analyses.

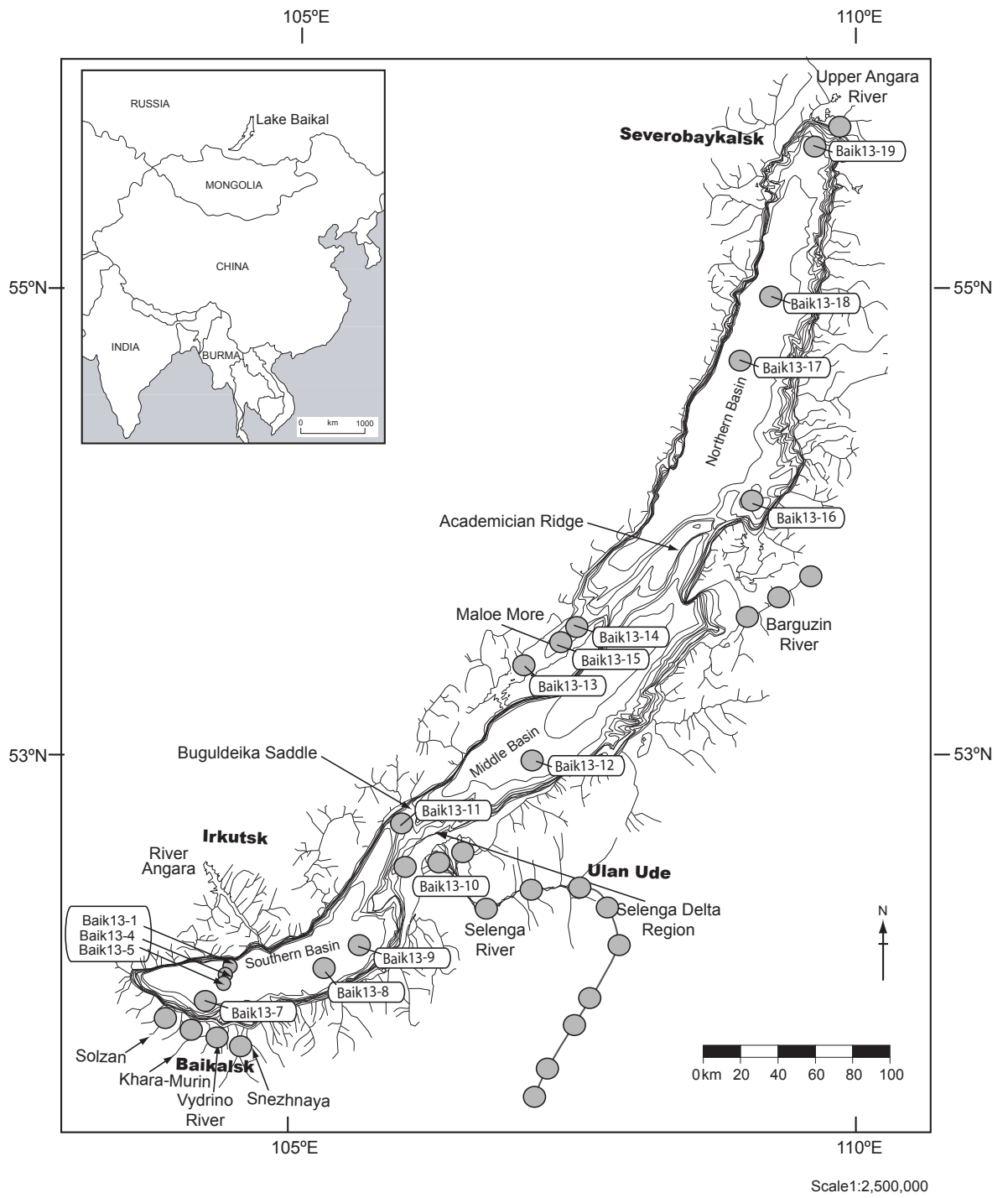


Figure 28: Map showing the water sampling sites across Lake Baikal and in the catchment.

3.2 Nutrient enrichment experiments

Previous work at Lake Baikal shows that depending on the environment, some diatom species are silicon limited (Jewson and Granin, 2014), but it is unclear how nutrient availability (nitrogen, phosphorus and silicon) impacts other major algal groups; chlorophytes and picocyanobacteria at Lake Baikal. Studies suggest nutrient enrichment is occurring in the coastal regions from settlements as inferred from the *Spirogyra* blooms (Kravtsova et al. 2014; Timoshkin et al. 2016), although nutrient concentrations have not been measured. Therefore, it is unknown how benthic and pelagic phytoplankton at Lake Baikal respond to nutrient enrichment (N, P, Si). Short-term nutrient enrichment experiments were conducted as a pilot study for this thesis, to examine the bottom-up factors that limit Baikal phytoplankton, which include nutrients. Temperature was not applied as a treatment within these experiments, as the experiments are solely focussing on algal response to nutrient enrichment. As the temperature was not monitored however, this may have had a slight influence on the algal communities during the experimental periods (6 – 11 days). Results from nutrient enrichment experiments are presented in Chapter Four, where the natural nutrient supply has been doubled within the nutrient experiments. These experiments have been conducted in the spring (*Figure 29*) and summer to examine whether nutrient limitation differs between seasons. The water collected for these experiments was sourced from the South and Central basins, which are assumed to be relatively similar as both are influenced by Selenga River inflows.



Figure 29: Nutrient enrichment experiment conducted underneath the ice at BAIK13-4 during the March 2013 field expedition. Mesocosm bags containing water samples from the DCM layer and nutrient treatments were suspended from string underneath the ice at 3 m water depth.

Water samples were collected in March 2013 from the South basin (at BAIK13-4) at 3 m water depth (as high chlorophyll-*a* concentration was found at this depth). Water samples were

also collected from the Central basin (at BAIK13-12) in August 2013 from the deep chlorophyll maxima (DCM) layer at 35 m water depth, for algal pigment, nutrients and dissolved organic carbon analyses. This is as the DCM represents the position of peak algal production within the water column. Mesocosms (plastic bags) were set-up in triplicate, with three treatments: nitrogen plus phosphorus (N+P), nitrogen plus phosphorus plus silicon (N+P+Si); plus, a control treatment. Each mesocosm was filled with c. 2 L of lake water, which had been previously filtered through a zooplankton mesh to remove grazers. These mesocosms were closed, consisting of plastic bags suspended from string underneath the ice at 3 m water depth (at BAIK13-4 in the South basin) for the under-ice experiment in March 2013. Ice was removed regularly from the water surface to allow sunlight penetration through the ice to the mesocosms in the water column. The second experiment in March 2013 was carried out by hanging the mesocosms within the field laboratory. In August 2013, mesocosms were placed within littoral waters of Maloe More. The bags were attached with string from the shoreline and extended to distances of 6 m from the shore, and were at water depths of c. 90 cm. Phosphorus (potassium dihydrogen phosphate) and nitrogen (potassium nitrate) were added to each 2 L N+P and N+P+Si mesocosm, to obtain a concentration of 100 µg/L and 1.25 mg/L respectively, which is more than four-fold higher than the phosphorus and nitrogen concentrations of Baikal's waters (*Table 6*). Silicon (metasilicate Na₂SiO₃) was added to each 2 L NPSi mesocosm, for a concentration of 6 mg/L (*Table 6*).

Water samples were collected for analyses on day 0 after the nutrient treatments were applied, and the last day of the experiment being after 7 days (for the March 2013 under ice experiment), 6 days (for the March 2013 field laboratory experiment), and 11 days (for the August 2013 experiment). Water samples were measured for TP, N, Si, major ions, DOC and pigment concentrations. 30mL water samples were also collected for phytoplankton cell analyses and preserved with Lugol's Iodine solution. Phytoplankton cell counts were not carried out during this project, and represent a potential future opportunity to examine phytoplankton cell counts alongside pigment inferred phytoplankton compositions. Growth rates were examined for picocyanobacteria, chlorophytes and diatoms by calculating the rate of change in pigment concentrations (zeaxanthin, lutein and fucoxanthin respectively) from day 0 of the treatment until the final day.

Table 6: Nutrient treatments added to the mesocosms in March and August 2013.

Nutrient	Estimated concentration in Baikal waters	Total concentration in mesocosm
Total Phosphorus ($\mu\text{g/L}$)	25	100
Silicate (mg/L)	1.5	6
Nitrate (mg/L)	0.3	1.2

3.3 Short cores

Short cores (< 65 cm) were collected using a UWITEC corer in March and August 2013 from a total of 10 coring stations in the South and North basins, Selenga Delta and Maloe More Bay, which is an isolated bay off the Central basin (*Figure 28; Table 8*). Maloe More Bay was chosen, as it is a tourist destination and away from any major river inflows. Sites nearby the BPPM and Selenga Delta in the South basin and within Maloe More are considered as “vulnerable” areas of Lake Baikal to nutrient enrichment from social and economic development in the watershed. Sites within the pelagic North basin are considered to have experienced no anthropogenic nutrient enrichment, but will have experienced climate driven changes.

Multiple cores were collected at each coring station, to allow for pigment, $\delta^{13}\text{C}$ and ^{210}Pb analyses to be carried out at the University of Nottingham on one of the sediment cores, and detailed sediment lithology to be carried out by E. Vologina at the Earth’s Crust Institute in Irkutsk (*Table 7*). Cores at each coring station were taken next to one another and the coordinates of their location are displayed in *Table 7*. As detailed sediment lithology was carried out on cores separate to pigment and $\delta^{13}\text{C}$ analyses, their location does need to be taken into consideration. Despite slight differences in location however, any turbidites detected in one sediment core is highly likely to affect a nearby sediment core, as turbidites cover several meters to several kilometres across Lake Baikal’s basin.

Table 7: Sediment cores collected at the South basin, Selenga, Maloe More Bay (MM), Chivsky Bay (CH) and North basin coring stations in March 2013 and August 2013 University of Nottingham and Earth's Crust Institute in Irkutsk.

Core	Basin	N	E	Date	Location of analyses
BAIK13-1C	South	51°46'04.2"	104°24'58.6"	Mar 13	UoN
BAIK13-1A	South	51°46'04.4"	104°24'58.7"	Mar 13	EC Institute
BAIK13-4F	South	51°41'33.8"	104°18'00.1"	Mar 13	UoN
BAIK13-4C	South	51°41'33.8"	104°18'00.1"	Mar 13	EC Institute
BAIK13-7A	South	51°34'06"	104°31'43"	Aug 13	UoN
BAIK13-7B	South	51°34'06"	104°31'43"	Aug 13	EC Institute
BAIK13-10A	South/Selenga	52°11'07"	106°05'38"	Aug 13	UoN
BAIK13-10B	South/Selenga	52°11'07"	106°05'38"	Aug 13	EC Institute
BAIK13-11C	South/Selenga	52°27'00"	106°07'32"	Aug 13	UoN
BAIK13-11A	South/Selenga	52°27'00"	106°07'32"	Aug 13	EC Institute
BAIK13-14C	Central/MM	53°21'03"	107°29'88"	Aug 13	UoN
BAIK13-14B	Central/MM	53°21'03"	107°29'88"	Aug 13	EC Institute
BAIK13-15A	Central/MM	53°23'27"	107°35'34"	Aug 13	UoN
BAIK13-15B	Central/MM	53°23'27"	107°35'34"	Aug 13	EC Institute
BAIK13-16B	North/CH	53°52'26"	109°09'49"	Aug 13	UoN
BAIK13-16A	North/CH	53°52'26"	109°09'49"	Aug 13	EC Institute
BAIK13-18A	North	54°47'31.4"	109°14'15.3"	Aug 13	UoN
BAIK13-18C	North	54°47'22.3"	109°14'27.0"	Aug 13	EC Institute
BAIK13-19B	North	55°38'54.9"	109°46'54.6"	Aug 13	UoN
BAIK13-19A	North	55°38'57.8"	109°46'57.7"	Aug 13	EC Institute

All coring stations were > 5 km from the shore, and some of the coring sites coincided with former locations of cores taken at Baikal (Mackay et al. 1998). These include BAIK13-7, which was cored at the same location as the previous core BAIK38 (Mackay *et al.* 1998), and BAIK13-10 which was cored at the same location as the previous core BAIK17 (Mackay et al. 1998). BAIK13-11 was cored at the same location as the previous core BAIK19 (Mackay et al. 1998) and BAIK13-18 was cored at the same location as the previous BAIK29 (Mackay et al. 1998). Cores were taken in the same location as those in Mackay et al. 1998 to extend the published diatom record, by analysing the top 2 cm of the sediment cores. Cores were extruded and sliced in the field in 0.25 cm - 0.5 cm thick sections, to reconstruct change at high-resolution, particularly over the last 200 years. The top water-sediment interface interval of the sediment cores was split into three samples and samples were frozen at -25°C. Sediment samples were analysed for algal pigments, diatom assemblages, total organic carbon (TOC), $\delta^{13}\text{C}$, total organic carbon to nitrogen atomic ratios (TOC/N), ^{210}Pb dating, mercury and Rock Eval measurements (*Table 9*).

Table 8: Location of the coring sites across Lake Baikal, core length and water depth of sites.

Site	Location	North	East	Core length (cm)	Water depth (m)
BAIK13-1	South basin	51°46'04.2"	104°24'58.6"	22.7	1360
BAIK13-4		51°41'33.8"	104°18'00.1"	20.5	1350
BAIK13-7		51°34'06"	104°31'43"	47.5	1080
BAIK13-10	South basin/Selenga	52°11'07"	106°05'38"	53.5	66
BAIK13-11	South basin/Selenga	52°27'00"	106°07'32"	64.0	345
BAIK13-14	Maloe More	53°21.033	107°29.885'	29.0	200
BAIK13-15	Maloe More	53°23.270	107°35.346'	29.5	220
BAIK13-16	Chivsky Bay/North basin	53°52'26"	109°09'49"	59.0	650
BAIK13-18	North basin	54°47'31.4"	109°14'15.3"	57.5	890
BAIK13-19		55°38'57.8"	109°46'57.7"	64.9	460

Table 9: Analyses carried out on the sediment cores.

Site	Sedimentary pigments	Diatoms	TOC, $\delta^{13}\text{C}$ and TOC/N	^{210}Pb dating	Mercury	Rock Eval
BAIK13-1	x		x	x	x	x
BAIK13-4	x	x	x	x		
BAIK13-7	x	x	x	x		
BAIK13-10	x	x	x	x	x	x
Selenga River						x
BAIK13-11	x	x	x	x		
BAIK13-14	x	x	x	x		
BAIK13-15	x	x				
BAIK13-16	x		x			
BAIK13-18	x	x	x	x		
BAIK13-19	x	x	x	x	x	x

3.4 Core lithology and magnetic susceptibility

Sediment lithology and magnetic susceptibility of short cores taken at the same coring stations (*Table 8*) were analysed at the Earth's Crust Institute in Irkutsk by E. Vologina. Garden 'oasis' was applied to the tops of the core, to remove excess water and form a solid seal (*Figure 30*). Surface sediments of these cores were not disturbed with the addition of garden 'oasis'. The cores were cut in half without further material being lost, and measured for sedimentary structures, including oxidised layers, and sediment composition (biogenic-terrigenous sediments, turbidite, sandy sediment, diatoms, clay, silt, sand, plant remains) (Vologina et al. 2010). Oxidised layers were detected by the presence of Fe and Mn oxide deposits, which form at the oxic-anoxic interface (Müller et al. 2002, Och et al. 2012). The ultimate cause for the accumulation of Fe/Mn oxides is unknown (Torres et al. 2014), although some proposed mechanisms include changes in sedimentation rates, carbon organic accumulation rates, porosity and O₂ supply to the sediment (Torres et al. 2014). Fe and Mn oxide layers form underneath the depth of maximum O₂ penetration, and have been found in the reducing sediments at Lake Baikal, below the upper surface Fe/Mn oxide layer (Torres et al. 2014). As sediment accumulates, the buried Fe/Mn layer dissolves due to anaerobic oxidation of CH₄ by sulphate and/or Fe oxides in the deeper sediment, and the formation of the upper Fe/Mn oxide layer by the flux of O₂ from the water column into the sediment (Torres et al. 2014). However, some Fe/Mn layers are preserved in the sediment, and the mechanism behind this remains unknown, as potential reductants (Mn, Fe, TOC and CH₄) are abundant. The detected oxidised layers within sediment cores presented in Chapter Seven represent periods of longer exposure to oxic conditions. Pigment data collected within these identified oxidised layers have not, however, been excluded from core analyses, due to findings presented in Chapter Seven. These findings were that pigment preservation, as indicated from Chl_as concentrations, within sediment layers identified as 'oxic' was not substantially less than pigment preservation with anoxic sediment layers.

Alongside detecting oxidised layers, smear slides of the biogenic-terrigenous sediments were taken to analyse fossil diatoms and grain size composition under a light microscope at magnification x 100 (Vologina et al. 2010). Magnetic susceptibility of sediments was measured at intervals of 1 cm using a Bartington-point sensor (SI-units), which measured the degree of magnetisation of the sediments (Searle, 2008; Vologina et al. 2010).



Figure 30: Sediment cores with green oasis at the top to remove excess water and allow for cores to be cut in half for lithology and magnetic susceptibility analyses.

3.5 Sample processing

3.5.1 Nutrient and DOC analyses

In the field the 25 mL water samples were preserved with 1.5 mL 278:722 H₂SO₄, and stored at 4°C prior to TP analyses. Total phosphorus (TP) analyses were performed on unfiltered water samples following persulphate digestion using the molybdate blue method (Mackereth et al. 1978). Silicate (SiO₄) analyses were performed on filtered (0.45 µm) water samples, using the molybdate yellow reactive method (Eaton et al. 1995). Nitrate (NO₃-N) and major ion concentrations were determined from filtered (0.45 µm) water samples, using a Metrohm Basic 792 ion chromatography system (Metrosep A Supp 4-250 column, with 1 mmol sodium bicarbonate and 3.2 mmol of sodium carbonate eluent at 1.0 mL min⁻¹). The major ions analysed were sodium (Na⁺), potassium (K⁺), magnesium (Mg²⁺), calcium (Ca²⁺), chloride (Cl⁻), nitrate (NO₃-N) and sulphate (SO₄²⁻). Filtered 30 mL samples for dissolved organic carbon (DOC) analysis were acidified in the field with 0.24 mL 25% H₂SO₄, and analysed at Loughborough University using a Shimadzu TOC-5000 analyzer.

3.5.2 Limnological parameters

Light attenuation coefficients (K_d , unit: m^{-1}) were calculated at each water-sampling site from the irradiance versus depth relationship, which was constrained to log-linear. Euphotic zone depths were determined from the regression between log transformed % of surface light through the water column and depth, to identify the depth at which 1% of the surface light penetrated (y intercept) (Saros et al. 2005). The deep chlorophyll maximum (DCM) was defined as the water depth where chlorophyll-*a* concentrations were the highest in the YSI sonde dataset. The thickness of the whole DCM layer for each site was determined from values greater than 90% of the total chlorophyll-*a* average within the water profile. The depth of the mixed layer was established from the YSI sonde temperature profiles, using the rLakeAnalyzer version 1.4 package in R to calculate the top and bottom depths of the metalimnion (Winslow et al. 2014). A depth correction was applied to the YSI sonde dataset to consider drift whilst sampling down the water column. This was generally applied below 50 m in the water column.

3.5.3 Primary production measures using phytoplankton pigments

Algal pigments are used to examine modern-day and historic algal community composition and biomass. All photosynthetic algae produce carotenoids and chlorophylls, and certain pigments are diagnostic for some algal groups. Algal pigment biomarkers were used within this thesis to assess algal biomass and community composition, using reverse-phase high-performance liquid chromatography (HPLC), in the School of Geography, Nottingham, UK. This analytical technique isolated and separated the algal pigments, due to their different polarities. A modified method (Chen et al. 2001) was used to separate the carotenoids, chlorophylls and their derivatives from the pigments samples, and separation methods used are detailed in McGowan et al. (2012). During HPLC analyses, pigment samples travel through a column (*Figure 31*), at high pressure, and those which are polar (more water soluble) elute from the column earlier than those which are more lipid soluble (Leavitt and Hodgson, 2001; McGowan, 2013). Therefore, the retention time is the amount of time the pigment is retained on the column, and pigments elute in a certain order from the column (McGowan, 2013) (*Figure 32*; *Figure 33*). Then a photodiode array (PDA) spectrophotometer scans the pigment at multiple UV and visible wavelengths (300 – 750 nm) to produce an absorbance spectrum (McGowan, 2013) (*Figure 31*).

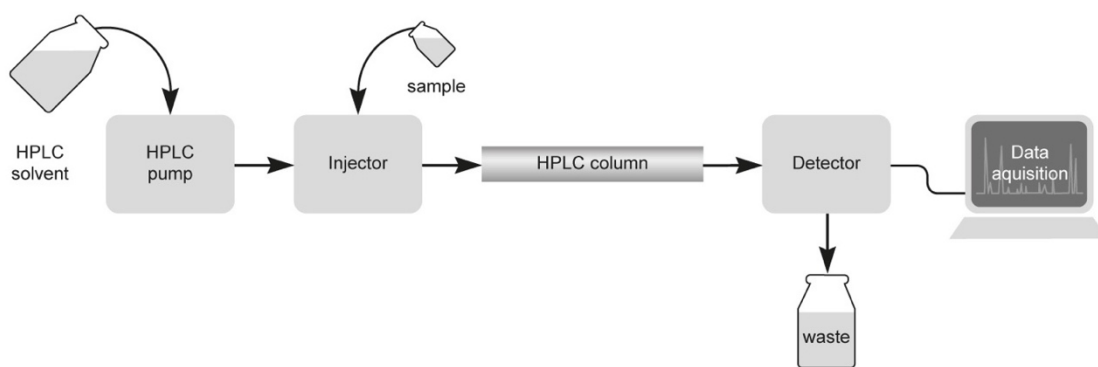


Figure 31: Systematic diagram of the HPLC system (modified from Czaplicki, 2013).

Water samples were filtered (a known amount of water was filtered between 1 – 3 L), through a GFF (0.45µm pore size) filter paper, and the filter papers were folded and wrapped in tin foil, and then stored frozen until HPLC pigment and spectrophotometric Chl-*a* analyses was carried out on the filter paper samples.

Frozen sub-samples of sediment core intervals were freeze-dried a few days prior to HPLC analyses, and stored in the cold and dark. Filtered water samples and c. 5 g of freeze-dried sediment were extracted overnight in an acetone, methanol and water mixture (80:15:5 by volume), stored at -20°C. The supernatant was then decanted, with three successive solvent washes, and filtered using a 0.22 µm PTFE syringe filter. Samples were dried under nitrogen gas and then stored in the freezer, until being re-dissolved in injection solution (70:25:5 acetone: ion-pairing reagent stock solution: methanol) and injected into the HPLC unit (Agilent 1200 series).

Each pigment sample had a 52-minute run, and within the batch of samples and first and last samples were calibration ‘green’ standards, which is a pigment extract from grass as it contains chlorophyll-*a* and its derivatives, chlorophyll-*b* and carotenoid pigments (lutein and β-carotene), to provide standard pigment retention times. The solvents used for the chosen method (Chen et al. 2001) were solvent A (80:20 methanol: ammonium acetate), solvent B (90:10 acetonitrile: de-ionised water), and solvent C (ethyl acetate) (Table 10). These solvents were de-gassed for 5 minutes using a sonicator prior to the sample analyses, and pigments were separated at a flow rate of 1 ml min⁻¹.

Table 10: Solvent separation gradients modified from Chen et al. (2001).

Time (mins)	Solvent A (%)	Solvent B (%)	Solvent C (%)	Flow (mL/min ⁻¹)
0	100	0	0	1
4	0	100	0	1
38	0	25	75	1
39	0	25	75	1
43	100	0	0	1
52	100	0	0	1

Pigments were identified and quantified from the chromatograms by comparing retention times and spectral characteristics with calibration standards (DHI Denmark) (Figure 32; Figure 33). Pigment concentrations were expressed as nmol, and sedimentary pigment concentrations were calculated relative with TOC %. Pigment concentrations are corrected with organic carbon content, as a method to further correct the pigment record from the influence of minerogenic material and pigment degradation from mineralisation of bulk organic content (McGowan, 2013). A TOC % correction is applied to the Lake Baikal pigment records in this thesis, although this correction may not account fully for pigment degradation, due to the large water column depths, high light penetration levels and oxic conditions within the bottom waters and surface sediments.

Equation below for pigment concentration calculation:

$$\text{Pigment conc} = \frac{[\text{Peak area} / \text{Calibration slope}] \times [\text{Total volume} (\mu\text{L}) / \text{Injection volume} (\mu\text{L})]}{(\text{nmol g}^{-1} \text{ OC}) \quad \text{Extraction weight (g)} \times [\% \text{ organic}]}$$

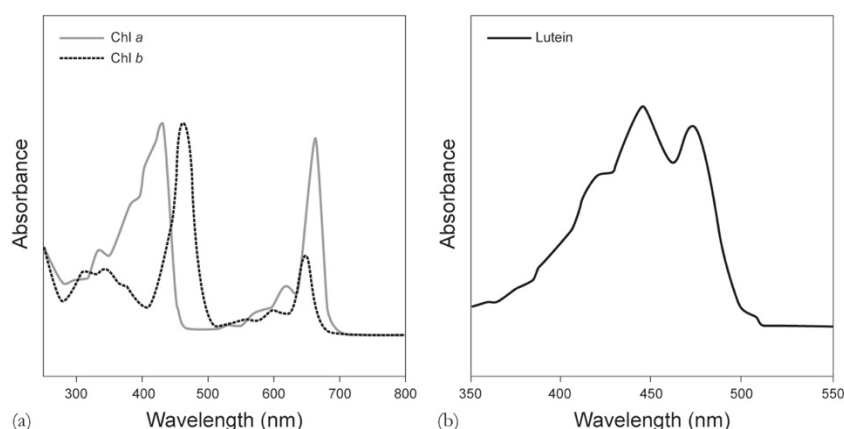


Figure 32: A chromatogram of chlorophylls and carotenoids (modified from McGowan, 2013; Leavitt and Hodgson, 2001).

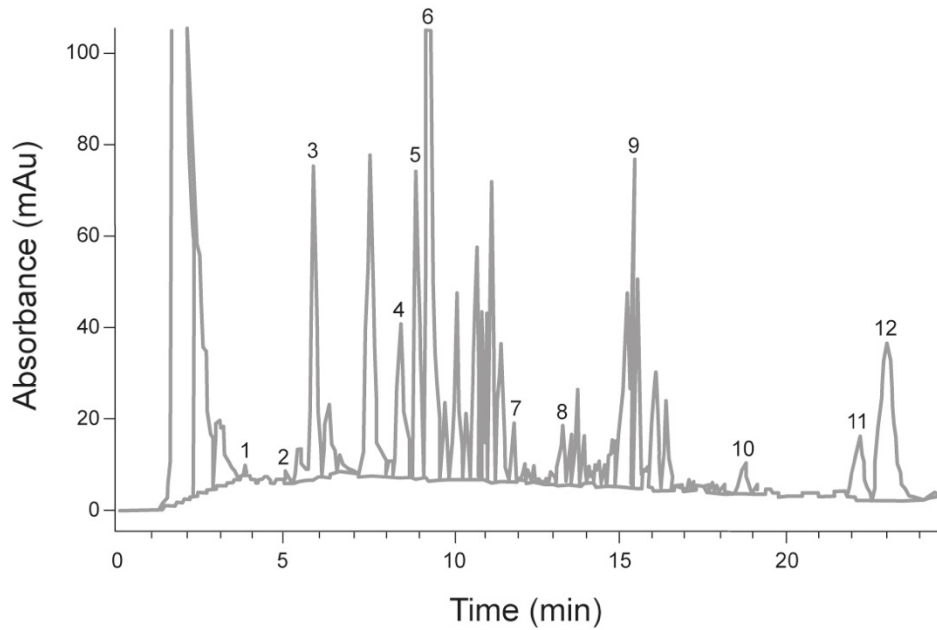


Figure 33: HPLC chromatogram output of eluting pigments (modified from McGowan, 2013; Leavitt and Hodgson, 2001); (1) Chl *c*, (2) fucoxanthin, (3) UV-absorbing compound, (4) alloxanthin, (5) diatoxanthin, (6) lutein-zeaxanthin, (7) canthaxanthin, (8) Chl *b*, (9) Chl *a*, (10) pheophytin *b*, (11) pheophytin *a*, (12) β -carotene.

3.5.4 Chlorophyll-*a* spectrophotometric analysis

In addition to YSI sonde chlorophyll-*a* and HPLC chlorophyll-*a* measurements, total algae (measured as chlorophyll-*a*) was estimated by filtering known quantities of lake water through 47 mm Whatman (0.45 μ m) GF/F glass-fibre filter papers, and wrapping the filter paper immediately in labelled foil. The filter paper was stored frozen and then cut into strips, placed into a glass vial and c. 5 mL of extraction solvent (80 % acetone, 15 % methanol and 5 % nanopure deionised water) was added. Samples were stored at 4°C for 12 hours, then the solvent was decanted into centrifuge tubes and centrifuged at 700g for 10 minutes. Samples were then analysed using a spectrophotometer, which was blanked using extraction solvent and multiple wavelengths were measured for each sample (750, 665, 645, 630, 480, 430 and 410 nm), to obtain measurements for chlorophyll-*a*.

Chlorophyll *a* was then calculated manually as shown by the equation below:

$$\text{Chl-}a \text{ (}\mu\text{L)} = (11.85(A_{665} - A_{750}) - 1.54 (A_{645} - A_{750}) - 0.08 (A_{630} - A_{750})) \times E/V$$

E = Volume of the extraction solvent (mL)

V = Volume of water filtered (L)

3.5.5 Diatom valve analyses

Sedimentary diatom valve analysis techniques are applied to examine modern-day diatom assemblage composition and historical trends from diatom compositional changes down-core. Surface sediment samples (upper 2 cm) were analysed for diatoms, and no chemical pretreatments, such as HCl or H₂O₂, were used. The top 2 cm of the sediment cores were analysed for diatoms as this covers c. at least the last 20 years, which enables the published diatom records (Mackay *et al.* 1998) to be built upon.

The methodology followed previous protocols for diatom analysis on Lake Baikal sediment samples (Mackay *et al.* 1998), as Flower (1993) suggested that chemical pretreatments on Baikal diatom samples affected the frustule preservation, especially of lightly silicified diatom species. Approximately 0.1 – 0.3 g of wet sediment per samples was put into a plastic centrifuge tube, weighed and then washed three times in distilled water. To calculate diatom concentrations, a known weight of divinylbenzene microspheres (approximately 1 – 2 g) was then added to the cleaned samples (Battarbee and Kneen, 1982). Subsamples of the suspensions were diluted and settled out onto coverslips until dry. The cover slips were fixed onto slides by heating with Naphrax on a hotplate at 130°C. A total of 300 valves were counted at x1000 magnification by using an oil immersion lens and phase contrast under a light microscope. Diatom dissolution was measured by categorising large endemic diatom species; *Aulacoseira baicalensis* (Meyer) Simonsen, *Cyclotella baicalensis*, *Cyclotella ornata* and *Cyclotella minuta* (Skv.) Antipova, into three stages of valve preservation. The diatom species were chosen as they made up over 60% of the diatom assemblage. A diatom dissolution index (DDI) (Flower and Likhoshway, 1993) was then calculated using the equation below (Mackay *et al.* 1998):

$$\text{DDI} = \left(\sum_{i=1}^n x_{1i} \right) / \left(\sum_{i=1}^n x_{1i} + \sum_{i=1}^n x_{2i} \right)$$

n = Number of taxa

x_{1i} = Number of valves in preservation stage 1 (pristine)

x_{2i} = Number of valves in preservation stage 2 and above

If all the *Aulacoseira baicalensis* and *Cyclotella minuta/ornata/baicalensis* valves are affected by dissolution then DDI=0, but if the valves are pristine then the DDI=1. Indices have been combined to express the index as dissolution per sample.

Correction factors were applied to the main diatom taxa (*Aulacoseira skvortzowii*, *Aulacoseira baicalensis*, *Cyclotella minuta/ornata*, *Stephanodiscus meyerii*, *Synedra acus*) in this thesis, which make up > 80 % of the diatom assemblage (Table 3) (Battarbee et al. 2005).

3.5.6 Geochemistry of organic matter

$\delta^{13}\text{C}$ values and TOC/N % ratios were measured at the same sampling intervals as the algal pigment samples. Sample preparation was carried out in the laboratories at the University of Nottingham, UK, and sample analysis was carried out at in the organic geochemistry facility at the British Geological Survey (BGS). Sediment sub-samples were treated overnight with 5% HCL to remove carbonate, rinsed in deionised water and dried at 40°C. Dried samples were then ground into a fine powder, homogenised and weighed into a tin capsule for combustion using a Costech ECS4010 elemental analyser. Samples were then analysed using a VG Optima dual inlet mass spectrometer. Carbon stable isotope ratios were expressed per mil (‰) and calculated relative to known international standards of Vienna Pee Belemnite (VPDB) for $\delta^{13}\text{C}$. To account for the change in $\delta^{13}\text{C}$ of atmospheric carbon dioxide from anthropogenic fossil fuel burning over the past two centuries, a Suess effect correction was applied to the bulk carbon values, using the equation from Verburg (2007). Typical analytical errors at the laboratory were < 0.2‰ for $\delta^{13}\text{C}$. The suess effect calculation was applied to the sediment samples dating back to c. 1850 AD, using ^{210}Pb chronologies.

Equation for Suess corrections (Verburg, 2007):

Suess effect correction =

$$(7.77 \times 10^{-16} \times Y^6) - (1.22 \times 10^{-11} \times Y^5) + (7.16 \times 10^{-8} \times Y^4) - (2.11 \times 10^{-4} \times Y^3) + (3.33 \times 10^{-1} \times Y^2) - 273.72 \times Y + 91703.26$$

Y –Year

3.5.7 Rock Eval and n-alkanes analyses

Rock Eval analyses were carried out to help interpret the TOC/N ratios which indicate mixed sources of carbon, and to further identify the main carbon source from the hydrogen index, which is a measure of the amount of algal material. The oxygen index from Rock Eval analyses provides a degradation measure. For Rock Eval analysis, approximately 60 mg of sediment was used, and samples were outsourced to the organic geochemistry facility at the British Geological Survey (BGS) for preparation and analysis. Samples were heated up to 300 – 650 °C in an inert atmosphere of N_2 , and the residual carbon was oxidised from 300 – 850°C. Hydrocarbons were measured via a flame ionisation detector as they were released during the

two-stage pyrolysis, and CO and CO₂ levels were monitored during thermal cracking of the bound organic matter. Rock Eval analyses produces 13 acquisition parameters (Lacey et al. 2014), which are determined by integrating the amounts of OM, CO and CO₂, such as SI (hydrocarbons previously generated) and S2 (hydrocarbons generated through cracking of bound organic matter). Hydrogen Index (HI) ($S2 * 100/TOC$) and Oxygen Index (OI) ($S3 * 100/TOC$) values were calculated.

3.5.8 Mercury analyses

Mercury analyses were conducted as pilot work, on both water samples and sediment cores, to obtain modern-day concentrations and historic trends down cores to assess mercury contamination at Lake Baikal. Water samples and freeze-dried sediment samples were outsourced to the Environmental Radiometric Facility at University College London, UK (UCL). Mercury analyses on sediment samples followed procedures in Yang et al. (2010), and freeze-dried samples were digested with 8 mL aqua regia at 100°C on a hotplate for 2 hours in rigorously acid-leached 50 mL polypropylene digestion tubes. Standard reference material and sample blanks were digested with every 20 samples. Digested samples were analysed for mercury using cold vapour-atomic fluorescence spectrometry (CV-AFS).

In the field, water samples for mercury analyses (120 mL) were acidified with 1.25 mL HCL and stored at 4°C prior to analyses. For water sample analyses, 45 mL of water samples were added with 0.25 mL concentrated HCL (Romil, pure grade), 0.25 mL 0.1N BrO₃⁻/Br⁻ (purified) and sealed for 30 minutes, then added with 15 µg/L 12% NH₂OH-HCL, and the samples were diluted to 50 mL. The prepared water samples were analysed for mercury using gold trap CV-AFS (Kopp *et al.* 1972). For water sample mercury concentrations, less than 4 ng L⁻¹, the measurement errors are +/- 0.4 ng L⁻¹.

3.5.9 Radiometric dating

The radionuclide ²¹⁰Pb has a half-life of 22.3 years, and this is produced by both the atmosphere and in the earth, occurring naturally as a product of the ²³⁸U decay series. ²¹⁰Pb is a widely used natural radioactive isotope to date recent sediments over the last 150 years, as unsupported ²¹⁰Pb is largely derived from atmospheric fallout. ¹³⁷Cs (half-life of 30 years) and ²⁴¹Am are artificially produced radionuclides, which are derived from nuclear weapons testing and nuclear reactor accidents and are deposited into the lake sediments via atmospheric fall-out. Therefore, ¹³⁷Cs and ²⁴¹Am can act as marker horizons within the recent sediment record and provide calibration of the ²¹⁰Pb chronology. ¹³⁷Cs is a global peak concentration found in all sediments, being deposited in 1964 AD, due to nuclear bomb testing (Appleby, 2001). ²¹⁰Pb

is produced in the decay series of ^{238}U (Uranium), which includes daughter elements of radium (^{226}Ra), radon (^{222}Rn), lead (^{210}Pb) bismuth (^{210}Bi) and stable isotope of lead (^{206}Pb) (Appleby, 2001). In soils, ^{226}Ra which is a product from ^{238}U and has a half-life of 1602 years, decays to an inert gas ^{222}Rn in 3.8 days, releasing ^{222}Rn into the atmosphere (Handong and Appleby, 2016). ^{222}Rn in the atmosphere then decays to release four daughter products, one being unsupported ^{210}Pb , which attach to airborne particles and are deposited into lake systems via wet deposition or dry deposition (Handong and Appleby, 2016). This fall out ^{210}Pb accumulation (atmospherically derived) is called unsupported ^{210}Pb . In contrast to unsupported ^{210}Pb , supported ^{210}Pb is a product of in-situ decay of ^{226}Ra (Noller, 2000). Supported ^{210}Pb is measured using gamma spectrometry, measuring the ^{226}Ra activity, and unsupported ^{210}Pb is calculated by subtracting supported ^{210}Pb from the total ^{210}Pb activity (Appleby, 2008).

All short cores, except BAIK13-16 and BAIK13-15 were ^{210}Pb dated. BAIK13-16 was not dated as the sediments within this short core contained late Pleistocene clays, and BAIK13-15 was not ^{210}Pb dated due to financial limitations. Wet density and dry weight measurements were obtained for ^{210}Pb dating samples. Wet density was measured using a 2cm^3 capacity brass phial, and dry weights were obtained by weighing samples prior to and after freeze drying for the calculation of dry mass accumulation rates (DMAR). Subsamples of wet sediment were freeze-dried to determine dry-mass accumulation rates (DMAR), and dried sediment samples were analysed for ^{210}Pb , ^{226}Ra , ^{137}Cs and ^{241}Am by non-destructive direct gamma spectrometry (Appleby *et al.* 1986). This was done at the Environmental Radiometric Facility at University College London, UK (UCL), using ORTEC HPGe GWL series well-type coaxial low background intrinsic germanium detector. All cores analysed contained good records of ^{210}Pb in recent sediments. Dates were calculated by using both the CRS (constant rate of supply) ^{210}Pb dating model and these dates agreed with the ^{137}Cs record (Appleby and Oldfield, 1978). The CRS model is applied as in recent years climatic and anthropogenic activity has altered the flux of unsupported ^{210}Pb into lake sediments, due to erosion and sedimentation (Appleby, 2001). The CRS model assumes uniform atmospheric ^{210}Pb flux, and non-uniform sedimentation (Appleby and Oldfield, 1978). Stable sedimentation rates after 1940 have been used to extend the chronologies over the last 200 years by constructing an age-depth model for each ^{210}Pb dated sediment core. Previous work shows that this is the best technique, due to the large errors that arise from radiocarbon dating recent sediments at Lake Baikal, although a caveat to this approach is that chronologies beyond the ^{210}Pb dating limit are tentative.

3.6 Numerical analyses

3.6.1 Pigment measures and accumulation rates

From the ^{210}Pb chronologies, sedimentation rates (cm/year), total organic carbon flux (g OC/cm² yr⁻¹), dry mass flux (g DW/cm² yr⁻¹), pigment flux (both g pigment per OC cm² yr⁻¹ and g pigment dry weight cm² yr⁻¹) and mercury flux (ng cm² yr⁻¹) were calculated. Pigment preservation condition was calculated by the ratio of chl-*a* to total pheo-*a* pigments (pheophorbide-*a*, pheophytin-*a*, pyropheophytin-*a*) (Leavitt and Hodgson, 2001). The UV radiation (UVR), also referred to as a water clarity index, was calculated for the sites which had UVR absorbing compound in the core sediments. Historic changes in algal exposure to UVR were measured as changes in the ratio of UVR-absorbing compound to the sum of four abundant carotenoids (alloxanthin, diatoxanthin, lutein and zeaxanthin) and multiplying by 100 (Leavitt et al. 1997). The ratio of carotenoids (fucoxanthin, alloxanthin, diatoxanthin, lutein, zeaxanthin and canthaxanthin) to Chl_{as}, which include chlorophyll-*a* and its derivatives (pheophorbide-*a*, pheophytin-*a*, pyropheophytin-*a*) were calculated to explore the contribution of certain algal groups to total algal biomass, and measured as concentrations (nmol of pigment per g of OC). The ratios of fucoxanthin to zeaxanthin and diatoxanthin to canthaxanthin were calculated to explore the abundances of diatom pigments in relation to cyanobacterial pigments. The ratio of chl-*b* to chl_{as} were calculated to explore the abundance of chlorophyte pigments in relation to total algae. Pigment ratios can also be used to assess preservation conditions, as the chlorophyll-*a*: total pheo-*a* pigment ratio can be used to indicate the concentrations of intact chlorophyll-*a* in relation to chlorophyll-*a* derivatives (Leavitt and Hodgson, 2001; Fietz, 2005).

3.6.2 Carbon mass accumulation rates

To estimate organic carbon burial at Lake Baikal, carbon mass accumulation rates (CMAR; g C m⁻² yr⁻¹) were calculated (Meyers & Teranes, 2001), using %TOC measurements and sedimentation rates. CMARs were calculated for the past c. 150 years, from sediment cores across Lake Baikal (*Table 8*). Raw CMAR values have been presented in Chapter Seven, and have not been corrected for sediment focussing. Previous studies which have used lake sediment cores from central, deep locations have applied correction factors, to account for sediment focussing (Anderson et al. 2013; Heathcote et al. 2015). This is as sediment focussing can result in carbon burial rates being higher than expected. Whilst other studies, where lake sediment cores were not located within deep regions of the lake (Mackay et al. 2016) or carbon content in sediments is very low (TOC < 2%) (Dong et al. 2012), correction factors have not been applied to carbon burial. Within this thesis, the sediment cores from

BAIK13-7A and BAIK13-11C (*Figure 28*), located on Vydrino Shoulder and Buguldeika Ridge respectively, are not subject to sediment focussing as these are inter-basin highs, and hence correction factors are not needed. For sites, however, which are located within deep basins (BAIK13-1C, BAIK13-4F and BAIK13-18A), Maloe More Bay (BAIK13-14C) and nearby delta regions (BAIK13-10A and BAIK13-19B), sediment focussing needs to be considered when interpreting results in Chapter Seven.

3.6.3 Comparison tests

Nutrient and DOC concentrations within the mixing layer have been compared between the South basin, Central basin and North basin sites. For limnological survey comparisons, Selenga sites are situated in the South basin and Maloe More sites have been included within the Central basin groups. Around 40% of the Selenga River waters feeds into the South basin, and Maloe More is a bay next to the Central basin (*Figure 28*). Statistical analyses were carried out to test lake-wide trends in phytoplankton pigment, nutrients and DOC concentrations. A Shapiro-Wilks normality test was applied to the log-transformed pigment datasets from the lake waters, and the nutrients and DOC data, using R. A non-parametric Kruskal Wallis test was applied with a post hoc test (Nemenyi test with a chi square tie correction method) to data with p value < 0.05 from the normality test, and an ANOVA and Tukey post hoc test was applied to datasets with $p > 0.05$ in the R package for basin comparison. Either a Kruskal Wallis or ANOVA test were performed on the datasets to examine whether the mean pigment, nutrient and DOC concentrations within the mixing layer in the pelagic south basin, Selenga Delta, Maloe More and pelagic north basin are significantly different from one another.

Normality assumptions were tested for nutrient enrichment pigment data (zeaxanthin, fucoxanthin, lutein and Chl-*a* concentrations) with Shapiro Wilks test and significant differences between means were assessed using the R package. As p value were > 0.05 , one-way ANOVA and Tukey HSD were performed on the nutrient enrichment pigment datasets, and the three treatments were control, N+P and N+P+Si.

For comparing oxic and anoxic sediments in the sediment cores, sedimentary primary production measurements pre and post 1950 AD, a paired t-test was performed on datasets using the R package. Pearson correlation coefficient analyses were carried out to explore relationships between the datasets and tested for significance ($p < 0.01$).

Ordinations using the CANOCO version 4.5 software package were performed on the datasets from the lake waters. Detrended correspondence analysis (DCA) were first applied and if the

gradient length of the first DCA axis is less than 2, then principal components analysis (PCA) ordination was applied. Pigment data were log-transformed prior to PCA analyses, and PCA axis one scores were obtained from standardised pigment data using the R package. PCA axis one scores were obtained from sedimentary pigment data, to assess floristic changes down-core. Redundancy analysis (RDA) was carried out on the average pigment concentrations within the mixing layer and environmental variables, to examine if any of the variables are correlated with the phytoplankton pigment distributions across the three basins. Pigment and environmental variable data (nitrate and sulphate concentrations) was log-transformed, and forward selection of environmental variables was carried out with Monte Carlo permutation tests, with 499 permutations, and variables were tested for significance using p-value < 0.05. Variables with p value < 0.05 are assumed to have an influence on the spatial distribution of phytoplankton pigments within the mixing layer.

Zonation was carried out on the square root transformed pigment stratigraphic profiles using CONISS and b-stick analyses to test the significance of the zones using *rioja* within R. The zonation method applied was CONISS, which performs stratigraphically constrained cluster analysis by the method of incremental sum of squares (Grimm, 1987).

3.6.4 Mann-Kendall analysis

To examine the algal trends over the last 200 years, Mann-Kendall analyses was carried out on the stable carotenoids (alloxanthin, diatoxanthin, lutein, zeaxanthin and β -carotene) and chlorophyll-*a* and chlorophyll-*b*. Mann-Kendall (MK) is a non-parametric statistical method to assess whether there is a monotonic increasing or decreasing trends in the data over time, and to quantify any trends (Taranu et al. 2015). The analysis uses the Kendall rank correlation, and the *Kendall* library in the R package was used to perform these analyses (McLeod, 2011). The MK correlation coefficient score varies between +1 and -1, with positive values suggesting an increasing trend in the dataset and negative values suggesting a decreasing trend. The MK trend test was used to explore whether the concentration of the most resistant carotenoids and chlorophyll-*a*, as well as the $\delta^{13}\text{C}$ values, increased or decreased, or remained similar over the last 200 years.

3.6.5 Break point analysis

Break point analyses were carried out on the stable carotenoids (alloxanthin, diatoxanthin, lutein, zeaxanthin and β -carotene) and chlorophyll-*a* and chlorophyll-*b* to examine the timing of significant changes within the pigment datasets. To determine, if there is a breakpoint, where it lies in datasets which have a significant increasing or decreasing trend from the MK

analyses, a two-segment, piecewise linear regression model was applied. The model determines a sharp change in the directionality of the dataset by fitting two linear regression models, joined at a breakpoint (Toms and Lesperance, 2003). This was performed in the *R* package using the *segmented* library (Muggeo, 2008). The formula `confint` was also applied to determine the 95% CI in the breakpoint. Breakpoint analysis was applied to the most resistant carotenoids and chlorophyll-*a*, as well as $\delta^{13}\text{C}$, to estimate the timing of significantly increasing or decreasing trends. This is different to zonation, as breakpoint analyses use a single variable whereas zonation uses a range of variables.

3.6.6 Temperature time-series data

Annual temperature data from 1820 - 2015 were sourced from the KNMI Climate Explorer database (<http://climexp.knmi.nl/>) from Irkutsk climate station in the South basin of Lake Baikal. Moving averages were applied to the temperature datasets for each site down-core. Three different weightings were applied down-core, depending on the age model errors with smoothing windows over the data of 5, 11 and 21 years.

Chapter Four: Limnology I – Seasonal sampling in South Basin

The aims to be addressed within this chapter are to examine the limnological conditions in spring in the South basin of Lake Baikal, and to compare measurements of algal production (chlorophyll-*a* concentrations) and nutrients to previous measurements at Lake Baikal (Fietz, 2005; Straskrabova et al. 2005; Hampton et al. 2008). An additional aim is to explore the impact of changing nutrient concentrations on Baikal's pelagic phytoplankton by conducting nutrient enrichment experiments. These experiments will assess if additions of nitrogen, phosphorus and silicon result in higher algal biomass and a change in Baikal's algal community composition within the mesocosms. Nutrient enrichment experiments will assess nutrient limitation of major algal groups within Baikal's waters in both summer (August 2013) and spring (March 2013).

4.1 Under ice production

Spring and summer have traditionally been considered as the most ecologically significant growing period in temperate seasonally ice-covered lakes, and as a result limnological studies have largely focussed on understanding summer rather than winter lake functioning (Salonen et al. 2009; Hampton et al. 2015). To fully understand the drivers, including nutrient availability and light limitation, of a lake ecosystem, limnological studies must consider seasonal dynamics in algal production and composition. In temperate lakes, such as Lake Baikal, the conditions for phytoplankton development in winter differ greatly from those in the summer (Babanazarova et al. 2013). In the winter a thin convective layer occurs under the ice, where temperatures are below 0.5 °C to depths of 25 m, and then temperature increases to 4 °C from 250 m onwards (Fietz, 2005). This is a period of inverse stratification, and mixing is restricted to the shallow layer under the ice (Fietz, 2005). Late spring is dominated by diatoms, which grow at the end of the ice-covered season as snow and ice cover decrease and in the summer picoplankton dominate at Lake Baikal (Belykh and Sorokovikova, 2003). Winter limnology is important, especially at Lake Baikal, as it is ice-covered for almost half of the year (January – May) with weak summer stratification occurring for 6 – 8 weeks in August to September (Hampton et al. 2014). Light, temperature, pH and oxygen all change under ice and affect the algal assemblage and water chemistry (Jewson et al. 2009). Baikal's ice provides a vast habitat for algal cells to grow, and high levels of photosynthesis can occur at low light penetration levels, even at values as low as 2 % of the surface values (Hampton et al. 2015). Many of Baikal's endemic diatoms, bloom underneath the ice in spring. Generally,

winter algal biomass is less than during the summer (Bertilsson et al. 2013), however this is not always the case at Lake Baikal, because these diatom species may form large blooms every 3 - 4 years in spring as the ice breaks up, known as *Melosira* years, which result in winter production exceeding summer production. The timing of these large under ice blooms are changing due to lake warming (Katz et al. 2015), and shortened ice cover duration could limit or even prevent them (Moore et al. 2009). There is bacterial activity underneath the ice in Baikal (Melnik et al. 2008), and a shorter ice cover duration has been suggested to result in increased heterotrophic bacterial production (Straskrabova et al. 2005). With reduced seasonal ice cover, bacterial activity could contribute to up to 20 – 40 % of daily production in the summer mixing layer waters (Straskrabova et al. 2005). Biological activity also occurs within the ice, with diatoms, chrysophytes, ciliates and rotifers being detected living (Obolkina et al. 2000; Bondarenko et al. 2012), along with bacteria, viruses and contaminants (Melnik et al. 2008; Hampton et al. 2015). Seasonal phytoplankton primary production has been measured in the South basin of Lake Baikal between March – October in 1999 and 2000 by Yoshida et al. (2003), using in situ ^{13}C bicarbonate incubations, and results show primary production values of $79 \text{ mg Cm}^{-2} \text{ day}^{-1}$ in March, and $424 \text{ mg Cm}^{-2} \text{ day}^{-1}$ in August (Yoshida et al. 2003).

The ice also acts as a “second bottom” at Lake Baikal, allowing productivity to span the whole lake surface, which can result in greater algal production in the winter months compared to the summer (Kozhova and Izmesteva, 1998; Timoshkin, 2001; Hampton et al. 2008; Hampton et al. 2015). Large endemic diatoms which can be ice attached, namely *Aulacoseira baicalensis*, dominate the lake waters under the ice, and are kept in suspension within the water column via convective mixing. *Aulacoseira baicalensis* have a thermal optimum of 2 – 3 °C, and as they are unable to grow within waters > 8 °C (Richardson et al. 2000), they produce resting cells, which sink and then re-establish the populations in the spring. The depth of snow cover has been found to influence the growth of *Aulacoseira baicalensis*, and their development occurs when there is little (< 10 cm) or no snow on the ice (Jewson et al. 2009). Mackay et al. (2005) however shows a correlation between low snow cover and low *Aulacoseira baicalensis* abundances within the Central basin sediments only. This has been suggested to be a result of photoinhibition from greater frequency of clear ice in the Central basin, compared to the South and North basins (Mackay et al. 2006). To examine modern day limnological conditions (including water transparency and nutrient concentrations), algal production, and the influence of climate change, both summer and winter limnology need to be studied and compared with previous surveys to examine production changes. This is as shorter ice cover duration will reduce under ice diatom production and increase heterotrophic bacterial production (Straskrabova et al. 2005; Moore et al. 2009), and greater summer thermal

stratification and warmer lake temperatures will influence depth distributions and composition of algal assemblages (Hampton et al. 2015).

4.2 Nutrient limitation

Nutrient limitation of primary production occurs when access to nutrients (nitrogen and/or phosphorus and/or silicon) becomes unbalanced in relation to the phytoplankton growth demands (Rast and Thornton, 2005). In oligotrophic lakes, algal growth is usually controlled by nutrient (N, P, Si) availability (Bonella et al. 2005; Hogan et al. 2014; Whiteford et al. in press), and thus phytoplankton populations in Lake Baikal will be controlled by nutrient availability. The most common approach to assessing nutrient limitation of phytoplankton growth is by deploying nutrient enrichment experiments. Experimental nutrient enrichment bioassays determine nutrient limitation by measuring the response of phytoplankton to manipulated nutrient concentrations (Elser et al. 1990; Levine and Whalen, 2001; McMaster and Schindler, 2005; Symons et al. 2012). Alternatively, nutrient limitation can be assessed via either correlations between in situ chlorophyll-*a* and nutrient concentrations (McMaster and Schindler, 2005), or by comparing nutrient availability in the water column with the Redfield (1958) ratio (N:P of 16:1 by mass) (Beardall et al. 2001). Nutrient limitation can differ amongst the algal groups in oligotrophic lakes, for example O'Brien et al. (1992) found N+P to result in higher abundances of chrysophytes and chlorophytes, and not diatoms or cyanobacteria. Experimental studies have also found N+P to control chlorophyte populations (Whalen and Cornwell, 1985; Levine and Whalen, 2001; Lewis and Wurtsbaugh, 2008). Algal-wide community response has also been reported, with N+P treatments stimulating the growth of all algal groups (diatoms, chlorophytes and cyanobacteria) (Whiteford et al. in press). Seasonal variation is an important factor to consider when investigating nutrient limitation of phytoplankton (Levine and Whalen, 2001), and few studies have investigated nutrient limitation in both ice on and ice off seasons at Lake Baikal. Jewson et al. (2008) investigated nutrient limitation of *Aulacoseira skvortzowii*, and culture experiments found a link between sporulation, which is the formation of dormant cells, and low phosphate concentrations (< 15 – 20 µg/L), whereas only 15% of these cells sporulated when nitrate was limiting (Jewson et al. 2008). *Aulacoseira baicalensis* require large amounts of silica, and Jewson et al. (2010) found silicon becomes limiting during *Melosira* years at Lake Baikal. The recent finding of anthropogenic nutrient enrichment in the coastal region (Timoshkin et al. 2016), highlights the need to examine the impact of changing nutrient concentrations on Baikal's phytoplankton assemblages in the pelagic zones. Previous work by Jewson et al. (2015) has investigated seasonal change of three main diatom species at Lake Baikal (*Cyclotella minuta*, *Cyclotella baicalensis* and *Aulacoseira baicalensis*) and nutrient

concentrations (phosphate, silicate and nitrate) during 1999 and 2000. The study found a decline in nutrient concentrations in the summer months (July, August, September) coinciding with higher temperatures ($> 10^{\circ}\text{C}$) and higher abundances of *Aulacoseira baicalensis*. In contrast, seasonal abundances of *Cyclotella minuta* and *Cyclotella baicalensis* do not coincide with seasonal nutrient concentration and temperature changes (Jewson et al. 2015). To explore nutrient limitation, this chapter presents data from nutrient enrichment experiments conducted at Lake Baikal in both March 2013 and August 2013. Winter experiments were conducted in the pelagic South basin, and the summer experiment used water from the pelagic Central basin. These sites were chosen as the South and Central basins are both influenced by the Selenga River. Water from the Central basin was collected during the August 2013 expedition, instead of from the South basin, as nutrient enrichment experiments were set up on the shoreline of Maloe More Bay, off the Central basin. Thus, transporting collected water samples from the Central basin would allow for a smaller storage time on the research vessel, in comparison to transporting samples from the South basin to Maloe More Bay.

Nutrient enrichment studies at Lake Baikal have differed in their results in terms of limiting nutrients (Weiss et al. 1991; Watanabe and Drucker, 1999; Goldman et al. 1996; Genkai-Kato et al. 2002; Satoh et al. 2006). One of the first enrichment studies at Lake Baikal in Summer 1992 was conducted by Watanabe and Drucker (1999), using surface waters from the South basin, and found nitrate limitation. This agrees with Weiss et al. (1991) who suggested nitrogen to be the most limiting nutrient, whereas Goldman et al. (1996) reported co-limitation by both nitrogen and phosphorus in July 1990. A nutrient enrichment study, carried out in August 2002 in the South and Central basins, also found that phosphate and phosphate plus nitrate treatments stimulated phytoplankton growth, and therefore reported phosphorus limitation (Satoh et al. 2006). However, in contrast to these findings, Genkai-Kato et al. (2002) report that Baikal's phytoplankton were not deficient in either nitrogen or phosphorus. Similarly, Verkhovzina et al. (2000) reports that the limiting factors on Baikal's phytoplankton are not nutrients, but hydrodynamics. Verkhovzina et al. (2000) argues that it is the turbulent mixing of water which determines the dynamics of the phytoplankton biomass, by bringing nutrient rich deep water to the surface. Verkhovzina et al. (2000) states that Lake Baikal should not become phosphorus limited, as during *Melosira* blooms nitrogen in the surface layer declines but phosphorus is never fully depleted (Votyntsev et al. 1975). It is suggested that phytoplankton biomass should therefore be proportional to the nitrate concentrations (Verkhovzina et al. 2000). Snow cover thickness during ice periods have instead been suggested to be affecting the interannual variation in phytoplankton by altering the light intensity below the ice (Verkhovzina et al. 2000). The most recent nutrient enrichment study at Lake Baikal in August 2013 (O'Donnell et al. 2017) supports the argument above, as no nutrient limitation

of Baikal phytoplankton in pelagic waters were found after a 6-day experiment. The nutrient concentrations applied in O'Donnell et al. (2017) were 10x the natural concentrations of Lake Baikal surface waters published by Kozhova and Izmet'eva (1998). Instead, O'Donnell et al. (2017) reports that nutrient limitation is dependent on location, as results show co-limitation by N and P of phytoplankton in Proval Bay, which is close to the Selenga Delta, due to an increase in chlorophyll-*a* fluorescence by 70% on average.

Prior to O'Donnell et al. (2017), silicon limitation has not previously been examined within Lake Baikal's waters. Si addition was not found by O'Donnell et al. (2017) to result in any positive response in chlorophyll-*a* fluorescence, unlike the N+P treatments. The experiments presented in this chapter, conducted in March 2013 and August 2013 were not extensive, but provide data from pilot studies on nitrogen, phosphorus and silicon enrichment. Although silicon, nitrogen and phosphorus availability drives diatom growth, previous marine nutrient enrichment experiments have mainly examined nitrogen and phosphorus and not the effects of silicon (Lagus et al. 2004; Felisberto et al. 2011; Trommer et al. 2013). Silicon is different from N and P, which are regenerated by biological activity, as silicon recycling depends on the dissolution rate of siliceous organisms, the sinking rate and the mixing depth (Kristiansen and Hoell 2002). Thus, the internal cycle of silica in large lakes is mainly controlled by silica uptake from diatom production and dissolution of diatoms in the water column or sediments. Large diatom blooms from nitrogen and phosphorus addition, deplete the dissolved silicate in the water column, limiting diatom biomass (Schleske and Stoermer, 1971; 1972). Higher diatom production also leads to greater accumulation of biogenic silica in the sediments, which reduces the water column DSi reservoir. This is known as the Schelske-Stoermer silica depletion hypothesis, as discussed in Chapter One, which was developed from studies on the North American Great Lakes, namely Lake Superior and Lake Michigan (Schelske and Stoermer, 1971; 1972). Changes in the silica cycle from phosphorus eutrophication have been observed within the North American Laurentian Great Lakes, as the silica reservoir in Lake Michigan was depleted by the late 1960s to the extent that silica concentrations become limiting for epilimnetic diatom production (Schelske and Stoermer, 1972; Schelske, 1985). Schleske and Stoermer (1971; 1972) hypothesised that the limitation of diatom growth by reduced dissolved silicon (DSi) concentrations would impact the phytoplankton community, resulting in the dominance of chlorophytes and cyanobacteria. This DSi depletion has also been observed in the Baltic Sea (Wulff et al. 1990; Conley et al. 1993; Wasmund et al. 1998; Humborg et al. 2000).

Reduction of water column silicate occurs in many freshwater and marine systems throughout the world in response to nitrogen and phosphorus, and examples of increased N:Si and P:Si

ratios and reduced abundance of diatoms have also been reported from studies in the Mississippi River (Turner and Rabalais, 1994) and the Black Sea (Humborg et al. 1997). Studies over the last decade have similarly found DSi depletion to occur at sites of eutrophication (Muylaert et al. 2009). However, Conley et al. (1993) reviewed the effects of eutrophication on the biogeochemical cycle of Si, and has questioned the silica depletion hypothesis, as only a small fraction of diatoms produced in the water column were preserved in the sediments (Conway et al. 1977; Parker and Edgington, 1976). The argument is that not a large amount of silicon is lost to the sediments but recycled for diatom growth. The hypothesis has therefore been questioned due to the lack of permanent sedimentation of diatoms. Seasonal DSi depletion is also questioned by Conley et al. (1993), as there is a difference between annual DSi cycle which includes depletion (such as when spring bloom is terminated by the depletion of DSi) and long-term historical depletion of water column DSi (burial in the sediments). Schleske (1985) however states that even though most diatom production is recycled on an annual basis, it only takes a small percentage of diatom production to be lost in long-residence time systems, like Lake Baikal, for it to have a major effect on the biogeochemical cycle within the water column. This is due to the accumulation of biogenic silica in sediments and the bottom waters, and exchange of waters below 200 m in Lake Baikal takes c. 8 years (Weiss et al. 1991). Palaeolimnological studies have used BSi as a proxy for silicon depletion, such as in Lake Victoria (Verschuren et al. 2002), Lake Ontario (McFadden et al. 2004) and other lakes (Johnson et al. 2002; Bradbury et al. 2004 as cited in Schleske et al. 2006). Studies show a decrease in biogenic silica between 1995 – 2001 at Lake Baikal in the South basin with regional warming and increasing algal production (Shimaraev and Domysheva, 2013). Over Pleistocene timescales, variations in silica content on glacial –interglacial timescales at Lake Baikal has been linked to climate (Qui et al. 1993; Colman et al. 1995; William et al. 1997; Kashiwaya et al. 1999; Karabanov et al. 2000; Prokopenko et al. 2001), with higher silicon utilisation, as inferred from diatom production, and accumulation within the sediments at warming peaks. Shimaraev and Domysheva (2013) also state that the modern Baikal diatom production cannot be silicon limited due to the river input of silicon and vertical water exchange mixing the large silica reserve in the waters from diatom dissolution.

With the link between silicon and diatoms, N+P+Si treatments have been included alongside N+P treatments in the experiments carried out in March 2013 and August 2013, as presented in this chapter. Nutrients and phytoplankton pigments have been measured within each treatment, at the start and the end of the experiment, and phytoplankton samples were additionally collected. Phytoplankton cells were not counted within this pilot study, however do provide a future opportunity to validate the pigment data.

4.3 Results

4.3.1 Comparison between winter and summer limnological parameters and nutrients

The results presented in this chapter are from sampling sites BAIK13-1, BAIK13-4 and BAIK13-5 in the South basin of Lake Baikal, from surveys conducted in both March 2013 and August 2013. All the August 2013 spatial survey dataset is presented in Chapter Five as these other sites do not have corresponding March 2013 data.

Light attenuation coefficient values ranged between 0.14 to 0.17 m⁻¹ in March 2013 and 0.17 m⁻¹ in August 2013 (*Table 11*). In March 2013, photic zone depths range between 15.4 – 21.4 m (*Table 11*). In comparison to summer values, photic zone depths were larger (23.5 – 24.6 m) than in March 2013.

Table 11: Light attenuation coefficient (LAC) values and photic zone depths for March 2013 and for August 2013 at the three transect sites in the South basin.

Site	March 2013		August 2013	
	Light Attenuation Coefficient (m ⁻¹)	Photic zone depth (m)	Light Attenuation Coefficient (m ⁻¹)	Photic zone depth (m)
BAK13-1	0.17	19.9	0.17	23.5
BAIK13-4	0.14	21.4	0.17	24.6
BAIK13-5	0.15	15.4	(-)	(-)

Average temperatures within the photic zone in March 2013 were between 0.05 – 0.16 °C and in August 2013 they were between 5.87 – 6.39 °C (*Table 12*). Conductivity was slightly higher in March 2013 than August 2013, with average measurements of 0.10 and 0.07 µS/cm⁻¹ respectively. pH was slightly higher in August 2013 than March 2013, with average measurements of 8.5 and 7.9 – 8.1. Mean TP concentrations were higher in the photic zone in March than August (*Figure 34*), with mean values between c. 15 – 20 µg/L in August and 18 – 24 µg/L in March. The largest variability within the photic zone in TP concentrations is within one of the South basin sites (BAIK13-5) in August 2013, between 1 – 28 µg/L within the photic zone. Mean silicate concentrations were higher and more variable in the photic zone in March than August (*Figure 35*), with mean values between c. 0.4 – 0.6 mg/L in August and c. 0.7 – 0.8 mg/L in March. Mean DOC concentrations were higher in August than March (*Figure 37*), ranging between c. 2.2 – 2.3 mg/L in August and c. 1.7 – 1.8 mg/L in March. The

variability in DOC concentrations is similar, except for in one of the South basin sites in March. Nitrate concentrations were slightly lower in August than March, with mean values between c. 0.022 – 0.025 mg/L in August and c. 0.026 – 0.029 mg/L in March (*Figure 36*). The largest variation in nitrate values within the photic zone occurs in March, at sites BAIK13-1 and BAIK13-5 in the South basin.

Table 12: March and August variables; conductivity, pH and dissolved oxygen (mean values in photic zone with standard deviation) as there is little variation down the water profile.

	Water temperature °C		Conductivity $\mu\text{S}/\text{cm}^{-1}$		pH		Dissolved Oxygen %	
	Average	SD	Average	SD	Average	SD	Average	SD
March (2013) photic zone measurements								
BAIK13-1	0.16	0.11	109.9	23.9	8.2	0.1	100.5	2.6
BAIK13-4	0.06	0.06	101.4	25.2	8.0	0.0	89.7	3.0
BAIK13-5	0.05	0.06	124.0	2.9	8.0	0.0	102.4	2.0
	Water temperature °C		Conductivity $\mu\text{S}/\text{cm}^{-1}$		pH		Dissolved Oxygen mg/L	
	Average	SD	Average	SD	Average	SD	Average	SD
August (2013) photic zone measurements								
BAIK13-1	5.87	2.21	75.8	4.8	8.5	0.3	13.4	0.6
BAIK13-4	6.40	3.76	77.0	8.5	8.6	0.3	13.7	1.1
BAIK13-5	(-)	(-)	(-)	(-)	(-)	(-)	(-)	(-)

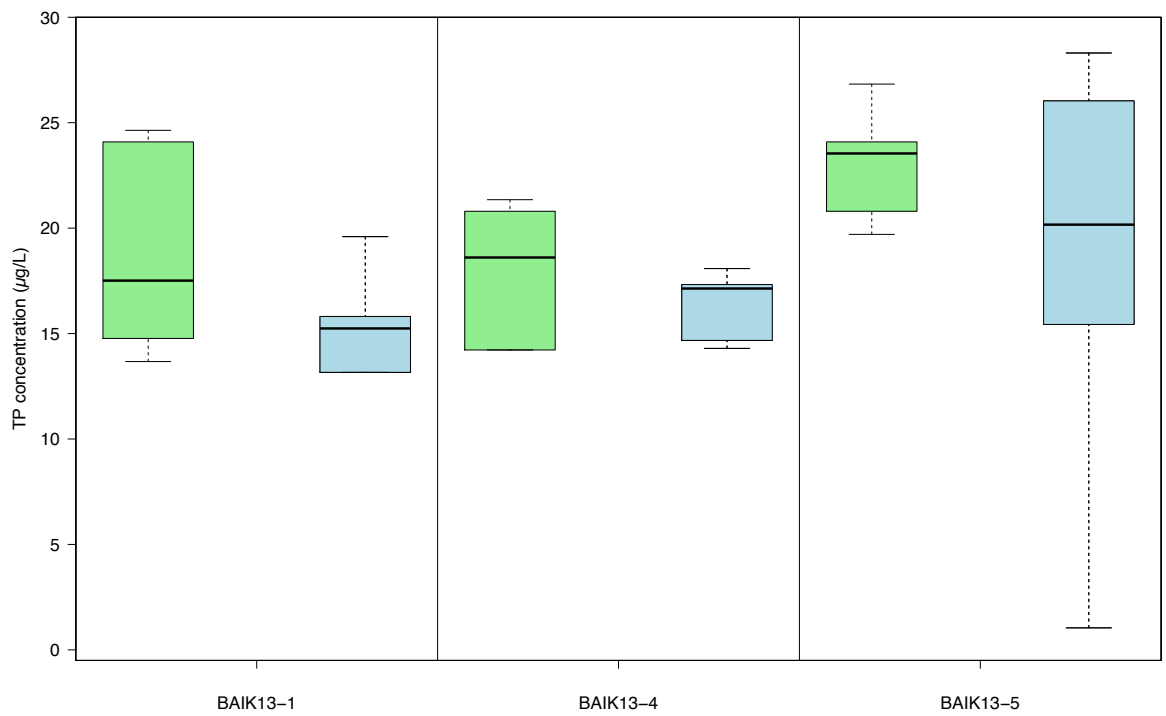


Figure 34: Variability of TP concentrations in photic zone in March 2013 (green) and August 2013 (blue).

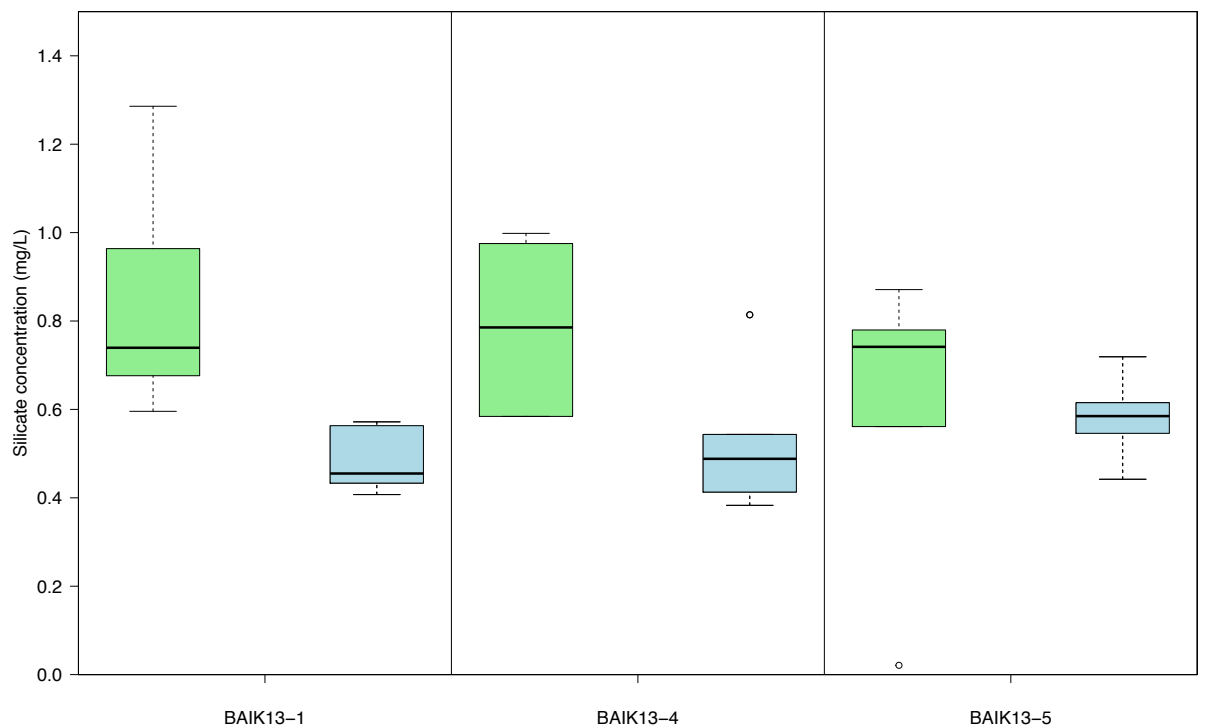


Figure 35: Variability of silicate concentrations in photic zone in March 2013 (green) and August 2013 (blue).

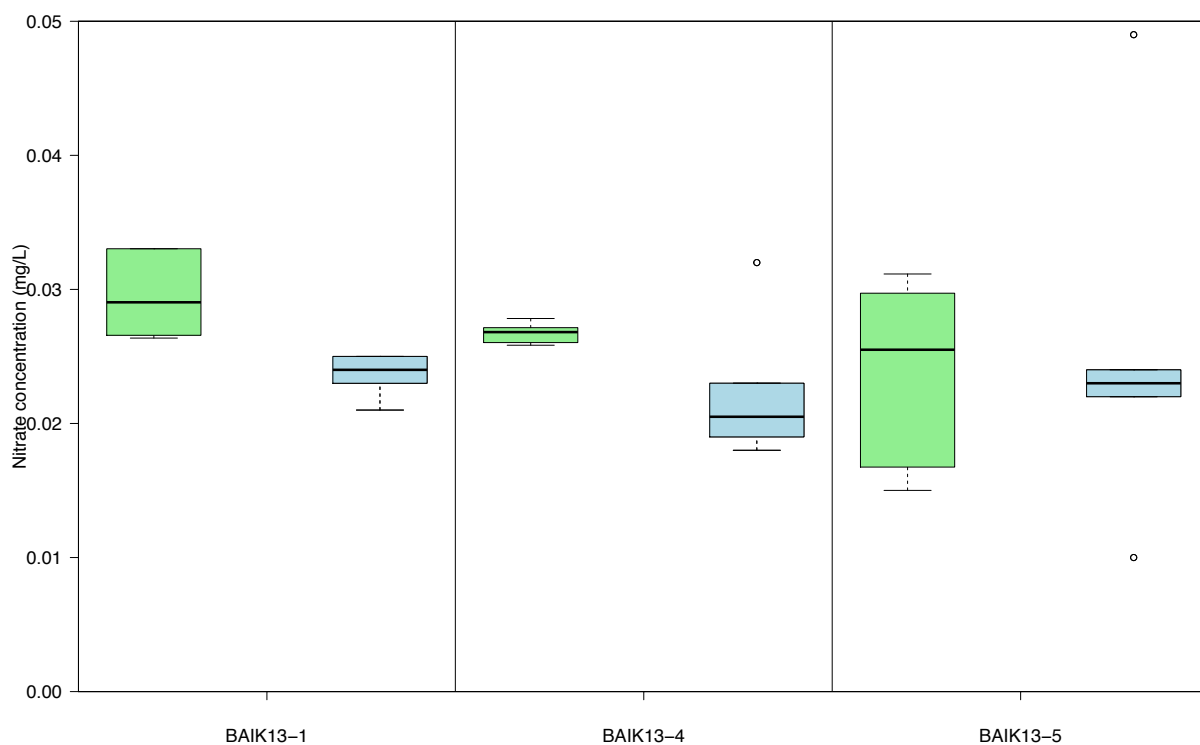


Figure 36: Variability of nitrate concentrations in photic zone in March 2013 (green) and August 2013 (blue).

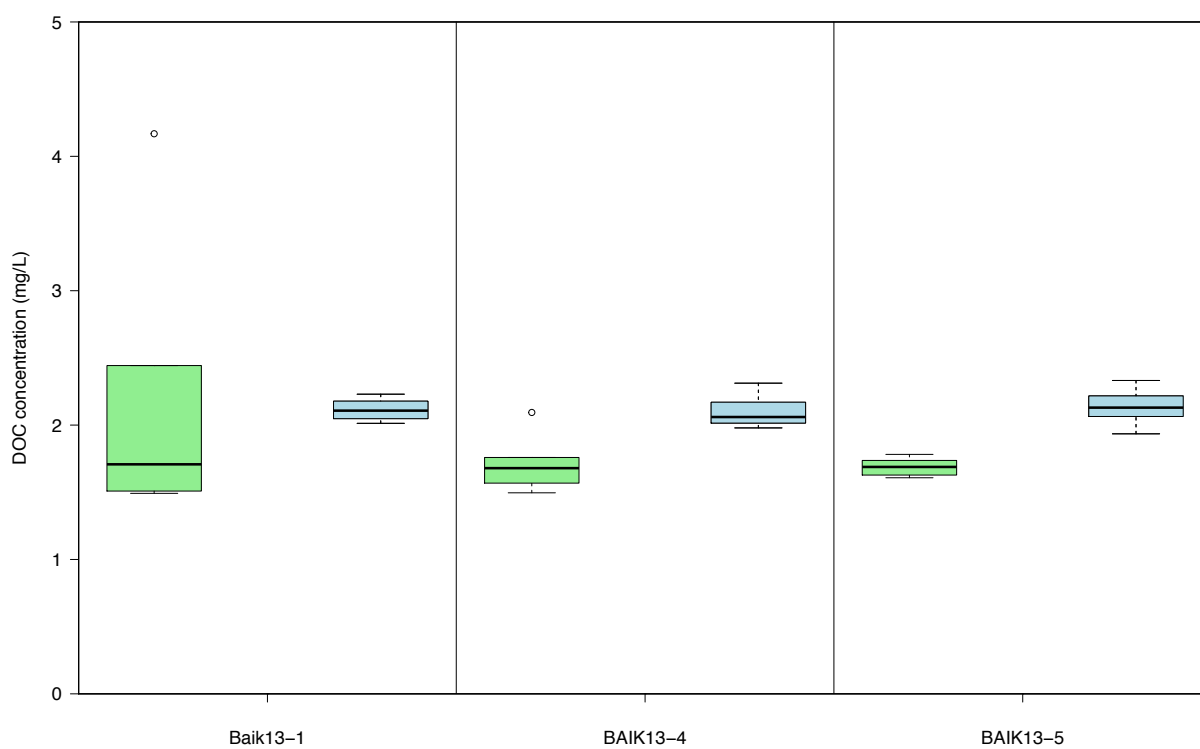


Figure 37: Variability of DOC concentrations in photic zone in March 2013 (green) and August 2013 (blue).

4.3.2 Comparison between under-ice, summer and past monitoring pigment composition

In March 2013 chlorophyll-*a* concentrations from the YSI, spectrophotometric and HPLC measures are all relatively similar, showing the same trends in chlorophyll-*a* concentrations within the photic zone (*Figure 38*). Chlorophyll-*a* concentrations in the upper 30 m at BAIK13-1 range between 0.1 – 1.2 nmol/L (*Figure 38*). Lower concentrations were observed at BAIK13-4 and BAIK13-5, between 0.1 – 0.3 and 0.1 – 0.2 nmol/L respectively (*Figure 38*). These sites also show homogenous values down the water profile in the photic zone, whereas at BAIK13-1 higher chlorophyll-*a* concentrations are observed in the upper 10 m (*Figure 38*). For the March results, any of these chlorophyll-*a* measures can be used, but YSI chlorophyll *a* is chosen as it provides continuous values in the photic zone rather than just spot samples at water depth intervals.

In August, the YSI and spectrophotometric chlorophyll-*a* concentrations were significantly (p value < 0.005) higher than the HPLC chlorophyll-*a* values in the photic zone (upper c. 40 m) (*Figure 39*). YSI chlorophyll-*a* concentrations were always higher (YSI $>$ Spectrophotometric $>$ HPLC) (*Figure 39*). The chlorophyll-*a* concentrations at these three South basin sites are relatively similar from the YSI and spectrophotometric values, and show similar trends down the water column (*Figure 39*). In contrast the HPLC chlorophyll-*a* values were significantly (p value < 0.005) lower (*Figure 39*). YSI chlorophyll-*a* concentrations have therefore been chosen to compare with March values, as these provide continuous values down the water column. These YSI chlorophyll-*a* values have also been chosen to present the summer chlorophyll-*a* concentrations in Chapter Five.

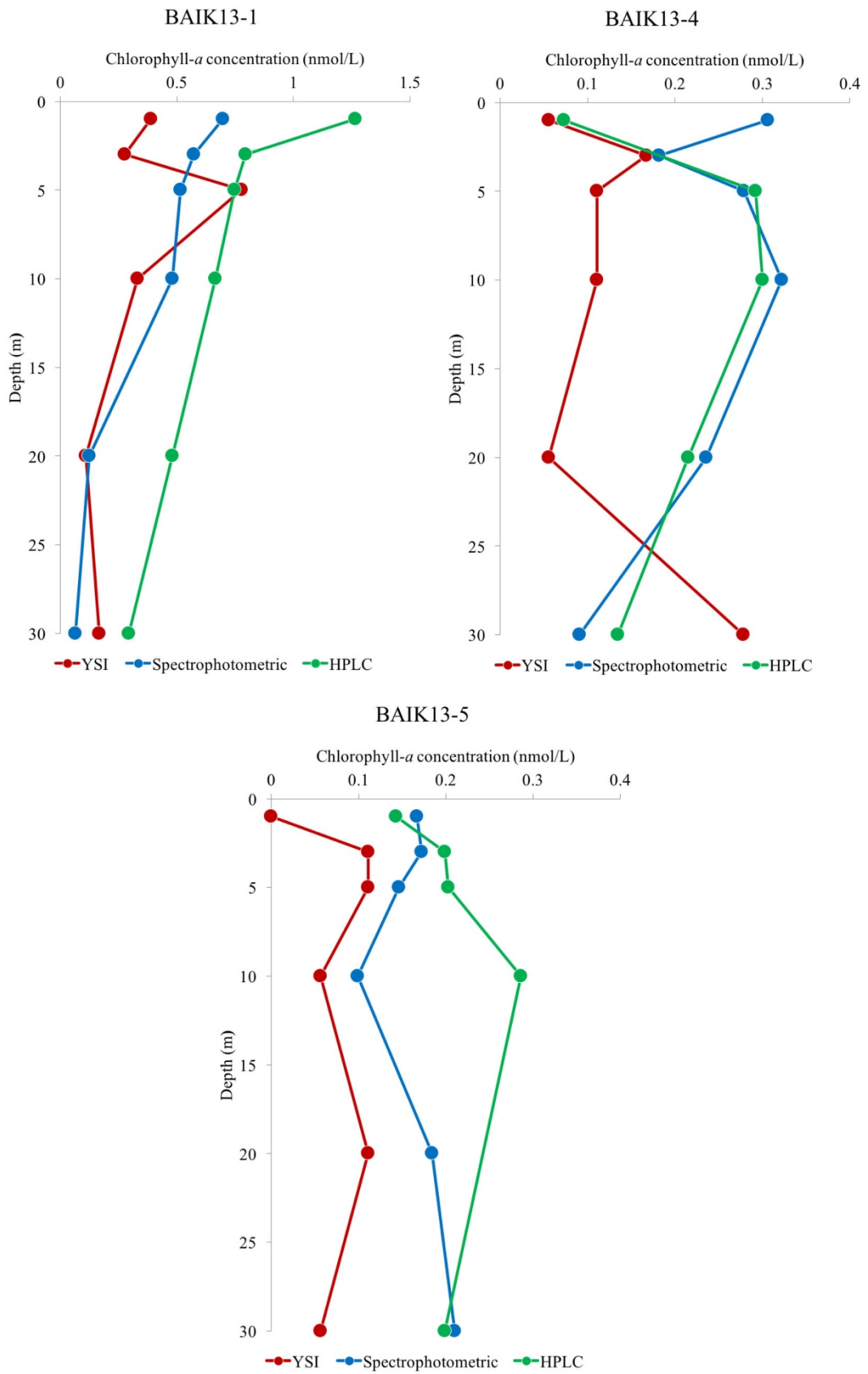


Figure 38: Chlorophyll-a concentrations (nmol/L) down the water column in March 2013; Red line – YSI chlorophyll-a; blue line – spectrophotometric chlorophyll a; green line – HPLC chlorophyll-a.

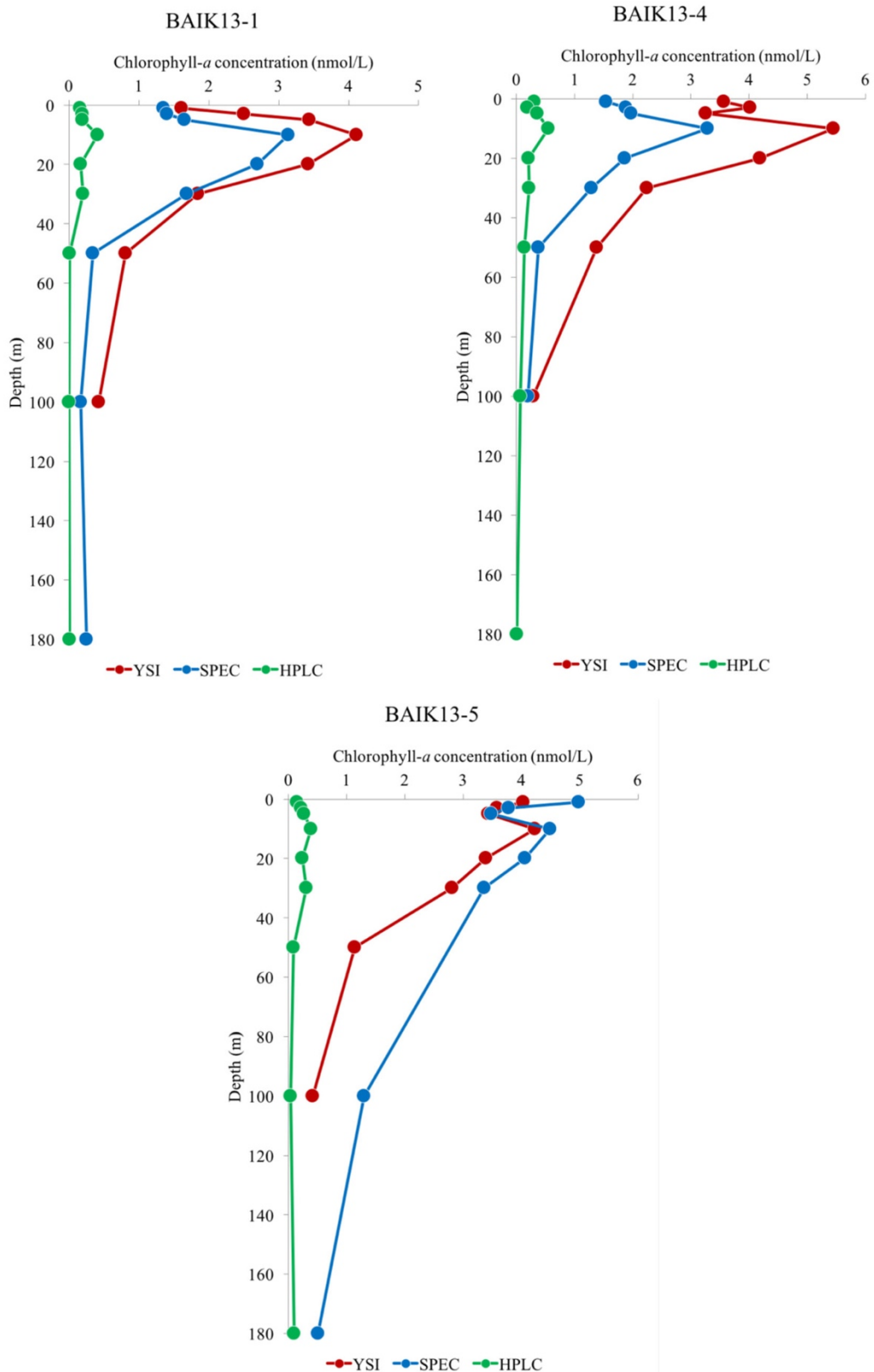
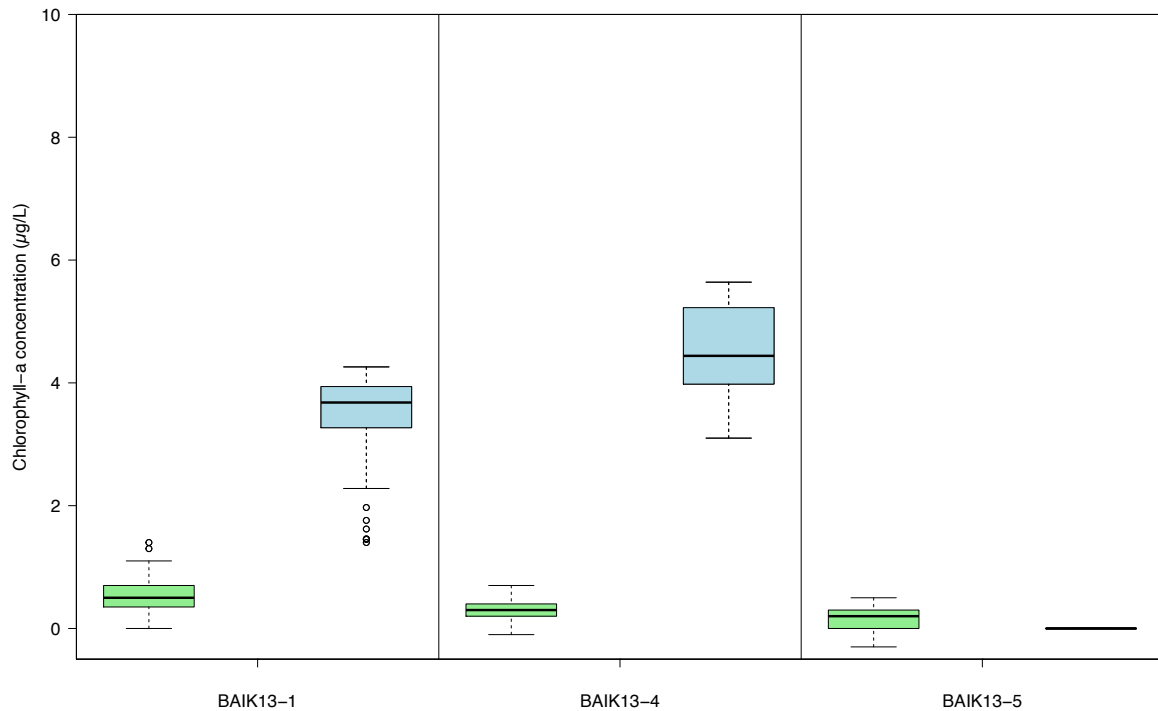


Figure 39: Chlorophyll-*a* concentrations (nmol/L) down the water column in August 2013; Red line – YSI chlorophyll-*a*; blue line – spectrophotometric chlorophyll-*a*; green line – HPLC chlorophyll-*a*.

YSI chlorophyll-*a* concentrations are higher in August 2013 than March 2013, with mean values between c. 3 – 5 µg/L in August and 0.1 – 0.5 µg/L in March (*Figure 40*). August has a larger variability within the photic zone compared to March, although the minimum values are still higher than the maximum values in March.



*Figure 40: YSI chlorophyll-*a* concentrations (µg/L) in photic zone in March 2013 (green) and August 2013 (blue). No data for August 2013 BAIK13-5.*

Under ice chlorophyll-*a* measurements taken in the South basin in March 2001, 2002 and 2003 at five depths in the photic zone (Straskrabova *et al.* 2005) were 1.3 µg/L (1.5 nmol/L), 1.6 µg/L (1.8 nmol/L) and 3.8 µg/L (4.3 nmol/L) respectively. Similarly, mean chlorophyll-*a* concentrations from Hampton *et al.* (2008) for March between 1979 – 2003 were c. 1.5 µg/L with a range between c. 1 – 2 µg/L. Mean chlorophyll-*a* concentrations from December – February between 1979 – 2003 were < 0.5 µg/L, which shows minimal levels of production, similar to values observed in March 2013. In line with this, Fietz (2005) measured under ice chlorophyll-*a* in March 2001 – 2003 to be 0.7 – 2.0 nmol/L, which is slightly higher than chlorophyll-*a* measurements in March 2013. Zeaxanthin, fucoxanthin and lutein concentrations in March 2013 are similar across the three sites, and range between 0.01 – 0.04 nmol/L, 0.03 – 0.12 nmol/L and 0.01 – 0.11 nmol/L respectively (*Figure 41*). March 2013 zeaxanthin and fucoxanthin concentrations are significantly lower than August 2013, whereas

lutein concentrations are similar between seasons. Fucoxanthin and zeaxanthin concentrations in March 2013 are lower than in March 2003, and lutein concentrations are similar between March 2003 and 2013 (Fietz, 2005) (Table 13).

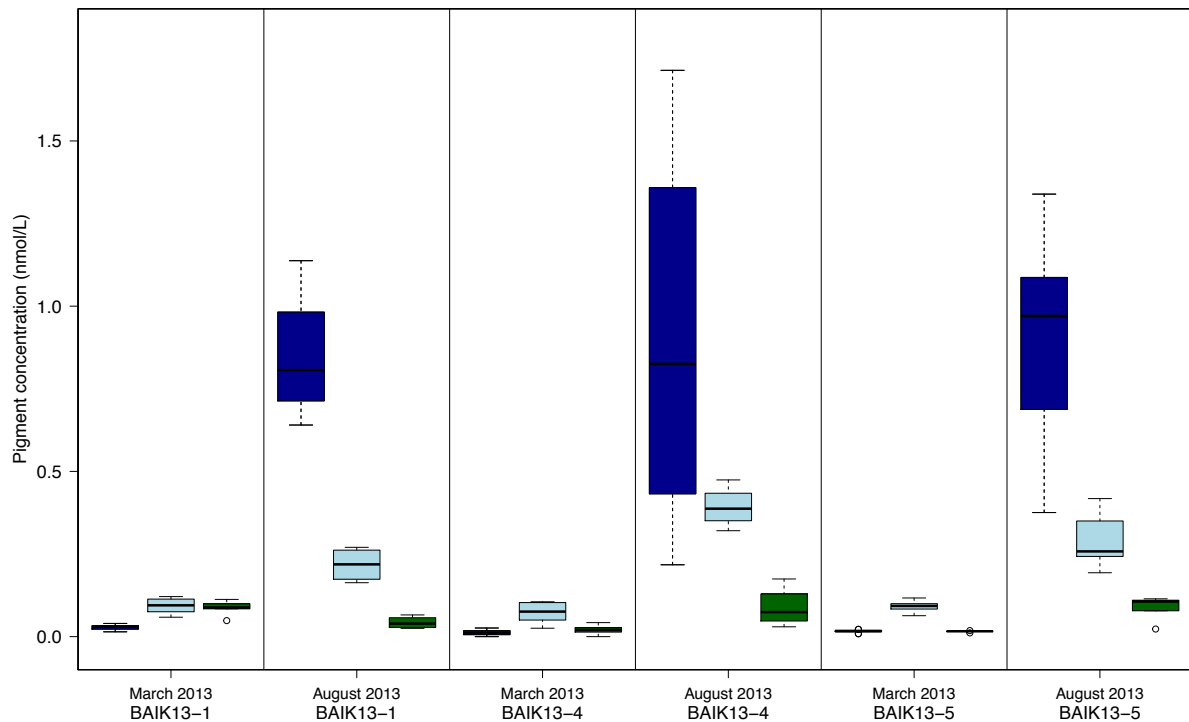


Figure 41: Photic zone March and August 2013 pigment concentrations (nmol/L) of zeaxanthin (dark blue), fucoxanthin (light blue) and lutein (dark green) in the South basin at BAIK13-1, BAIK13-4 and BAIK13-5.

Table 13: Dominant pigment concentrations in March 2003 (Fietz, 2005) and March 2013 in the South basin.

	March 2003 (Fietz 2005)	March 2013 (this study)
Zeaxanthin (nmol/L)	c. 0.1	0.01 - 0.04
Fucoxanthin (nmol/L)	c. 0.2 - 0.7	0.03 - 0.12
Lutein (nmol/L)	c. 0.02	0.01 - 0.11

4.3.3 Nutrient enrichment experiments

Nutrient enrichment experiments were conducted in both winter and summer, to assess algal community response to nutrient inputs. On the first day of the experiment, pigment data show that water samples collected in March 2013 from the South basin (at BAIK13-1), for the

mesocosms, were largely comprised of diatoms (*Table 56; Table 58 in Appendix*). By the end of the experiments (Day 7), however, the dominant algal group switched to chlorophytes, as inferred from higher lutein concentrations (*Table 56 in Appendix*), in all mesocosm treatments (Control, N+P and N+P+Si) which were suspended underneath the ice. Within the second March 2013 experiment, diatoms dominate the algal assemblage on day 0 of the experiment within the offshore laboratory, and by the end of the experiment (Day 6) there was a switch to higher concentrations of picoplankton, rather than chlorophytes in all treatments (Control, N+P and N+P+Si).

ANOVA results show that in the March 2013 under ice experiment and the second March 2013 experiment, pigment concentrations (zeaxanthin, lutein and Chl-*a*) were not significantly different between the control and treatments on day 7 and day 6 respectively (*Table 14*). Nutrient enrichment did not significantly increase chlorophyll-*a* concentrations in the March 2013 under ice experiment 1 (*Figure 42*). Nitrogen and phosphorus addition resulted in higher mean concentrations of zeaxanthin (mean = 0.06 nmol/L; *p* values = 0.83) compared to the control (mean = 0.04 nmol/L). Lutein (mean = 0.11 nmol/L) concentrations were not higher than control values (0.03 and 0.12 nmol/L respectively). Fucoxanthin concentrations were significantly higher in the N+P+Si treatment compared to the N+P treatment (*p* value = 0.03) and control (*p* value = 0.02). The addition of nitrogen, phosphorus and silicon resulted in higher mean concentrations of fucoxanthin (mean = 0.04 nmol/L) compared to the control (mean = 0.03 nmol/L). In the March 2013 experiment 2, nutrient enrichment did not significantly increase chlorophyll-*a* in the laboratory (Control mean = 0.08 nmol/L; N+P = 0.13 nmol/L; N+P+Si = 0.06 nmol/L) (*Figure 39*). Nitrogen and phosphorus addition resulted in higher mean concentrations of fucoxanthin (0.02 nmol/L), zeaxanthin (0.08 nmol/L) and lutein (0.05 nmol/L), compared to within the control (0.004, 0.03, 0.02 nmol/L respectively). The addition of nitrogen, phosphorus and silicon resulted in higher mean concentrations of zeaxanthin (mean = 0.15 nmol/L) compared to the control (mean = 0.03 nmol/L).

Within the August 2013 nutrient enrichment experiment, diatoms were also seen to be the dominate algal group within the water samples collected on Day 0 (*Table 60 in Appendix*). Water samples were collected from BAIK13-12 in the Central Basin, at the deep chlorophyll maxima (DCM) (c. 20m), and captured algal populations from the late *Melosira* bloom. By the end of the experiment (Day 11), diatoms remained in high concentration in the Control and N+P treatments, however picoplankton concentrations increased, to be slightly higher than diatom concentrations in the N+P+Si treatments (*Table 60 see Appendix*).

On day 11 of the August 2013 experiment, zeaxanthin concentrations were significantly higher between Control – N+P+Si and N+P – N+P+Si (p value = 0.02 and 0.03 respectively), and lutein concentrations were significantly different between all three treatments (p value < 0.01) (*Table 16*). Nutrient enrichment did not significantly increase chlorophyll-*a* in the August experiment (Control mean = 0.11 nmol/L; N+P = 0.04 nmol/L; N+P+Si = 0.09 nmol/L) (*Figure 44*). Nitrogen and phosphorus addition resulted in higher mean concentrations of fucoxanthin (0.45 nmol/L), zeaxanthin (0.05 nmol/L) and lutein (0.04 nmol/L), compared to within the control (0.27, 0.01, 0.01 nmol/L respectively). The addition of nitrogen, phosphorus and silicon resulted in higher mean concentrations of zeaxanthin (mean = 0.32 nmol/L) compared to the control (mean = 0.02 nmol/L). Chlorophyll-*a* and fucoxanthin concentrations were not found to be significantly different between treatments within these experiments.

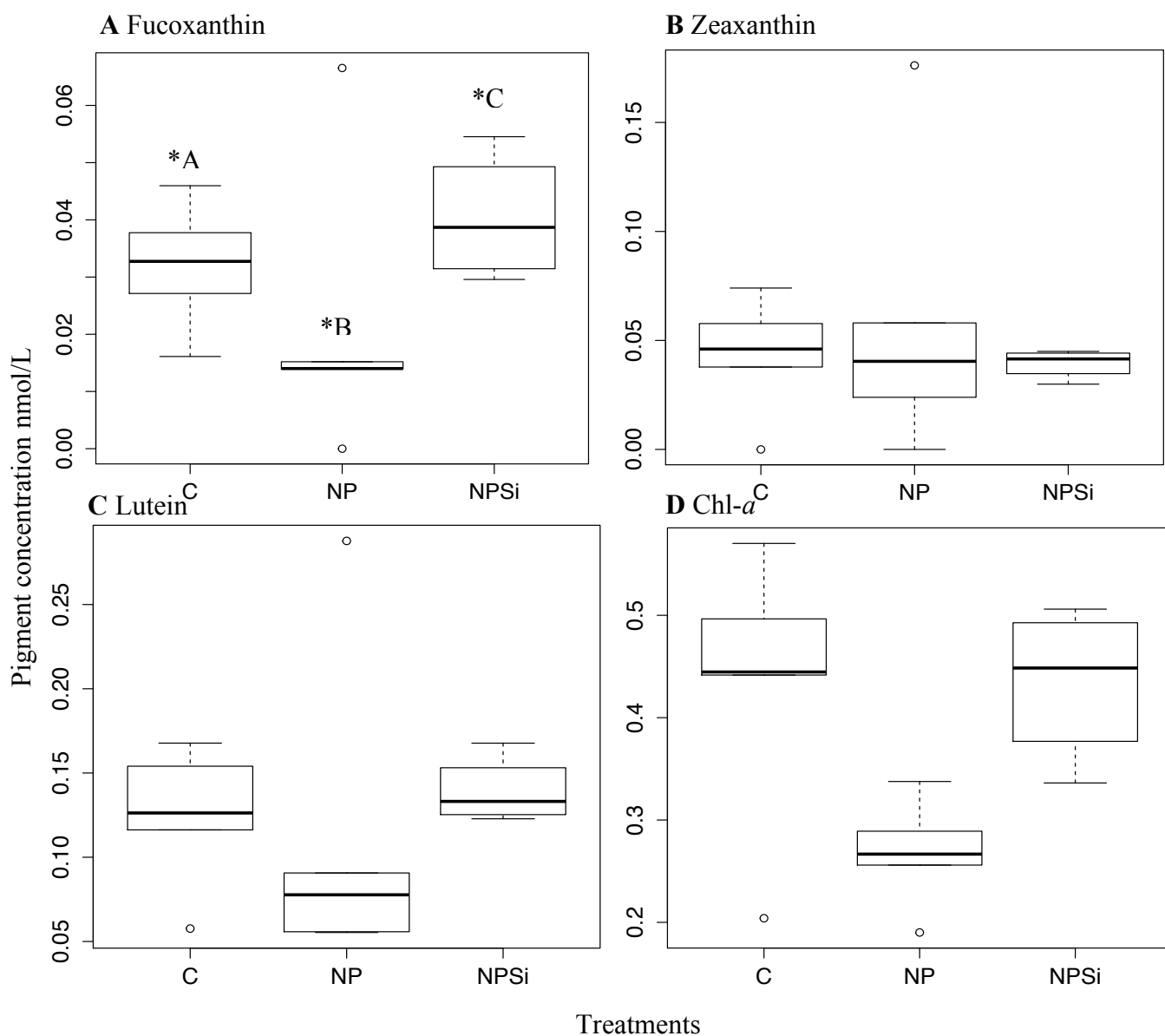


Figure 42: March 2013 under ice experiment 1 (A) fucoxanthin (B) Zeaxanthin (C) Lutein (D) Chl-a on day 7. ANOVA results show significant differences between treatments. (Fucoxanthin concentrations in *C are significantly higher than *A and *B).

Table 14: ANOVA results for March 2013 under-ice experiment 1 and Tukey test for assessing significant difference in pigment concentrations between treatments on day 7.

March 2013 Under-ice experiment in South basin

Treatment		F value	P value		
ANOVA	Fucoxanthin	1.19	0.34		
	Zeaxanthin	0.27	0.76		
	Lutein	0.17	0.85		
	Chl- <i>a</i>	4.61	0.04		
	diff	lwr	upr	P value	
Fucoxanthin					
	N+P - C	0.03	-0.19	0.26	0.82
	N+P+Si - C	0.30	0.08	0.53	0.02
	N+P+Si - N+P	0.27	0.04	0.49	0.03
Zeaxanthin					
	N+P - C	0.02	-0.06	0.09	0.83
	N+P+Si - C	0.00	-0.08	0.08	0.99
	N+P+Si - N+P	-0.02	-0.10	0.06	0.78
Lutein					
	N+P - C	-0.01	-0.12	0.10	0.96
	N+P+Si - C	0.01	-0.10	0.13	0.94
	N+P+Si - N+P	0.03	-0.09	0.14	0.83
Chl-<i>a</i>					
	N+P - C	-0.01	-0.12	0.10	0.96
	N+P+Si - C	0.01	-0.10	0.13	0.94
	N+P+Si - N+P	0.03	-0.09	0.14	0.83

Table 15: ANOVA results for March 2013 experiment 2 in field laboratory and Tukey test for assessing significant difference in pigment concentrations between treatments on day 6.

March 2013 experiment 2 in field laboratory on South basin shoreline

Treatment		F value	P value		
ANOVA	Fucoxanthin	5.35	0.05		
	Zeaxanthin	3.17	0.13		
	Lutein	1.61	0.29		
	Chl- <i>a</i>	0.89	0.47		
	diff	lwr	upr	P value	
Fucoxanthin					
	N+P - C	0.01	0.00	0.03	0.13
	N+P+Si - C	0.00	-0.02	0.01	0.65
	N+P+Si - N+P	-0.02	-0.03	0.00	0.06
Zeaxanthin					
	N+P - C	0.05	-0.09	0.19	0.53
	N+P+Si - C	0.12	-0.03	0.27	0.11
	N+P+Si - N+P	0.07	-0.08	0.23	0.37
Lutein					
	N+P - C	0.03	-0.03	0.08	0.31
	N+P+Si - C	0.00	-0.06	0.06	0.99
	N+P+Si - N+P	-0.03	-0.09	0.04	0.42
Chl-<i>a</i>					
	N+P - C	0.05	-0.11	0.21	0.58
	N+P+Si - C	-0.01	-0.19	0.16	0.96
	N+P+Si - N+P	-0.07	-0.24	0.11	0.50

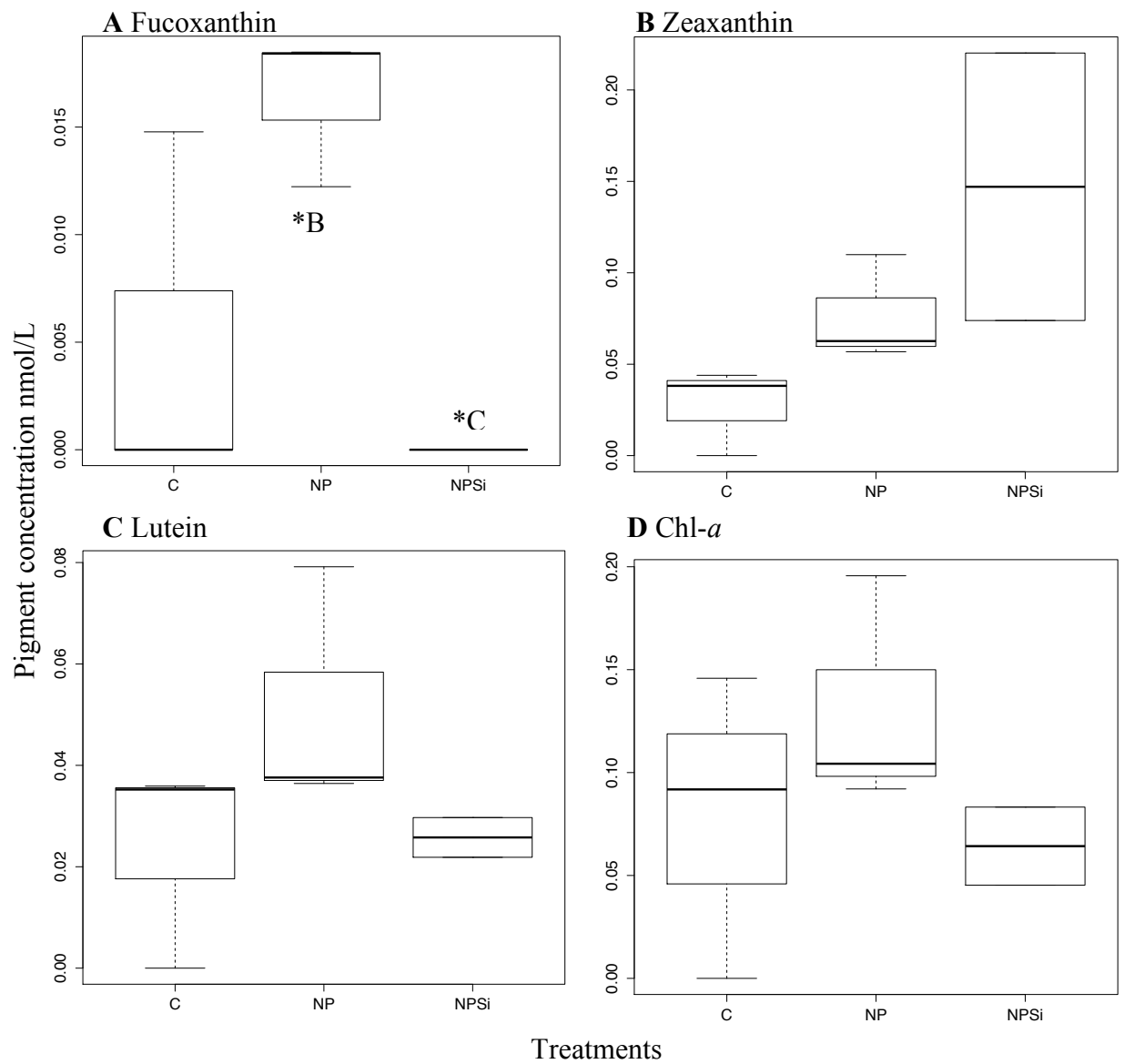


Figure 43: March 2013 experiment 2 carried out in the field laboratory and not under the ice (A) Fucoxanthin (B) Zeaxanthin (C) Lutein (D) Chl-a on day 6. ANOVA results show significant differences between treatments. (Fucoxanthin concentrations in *B are significantly higher than *C).

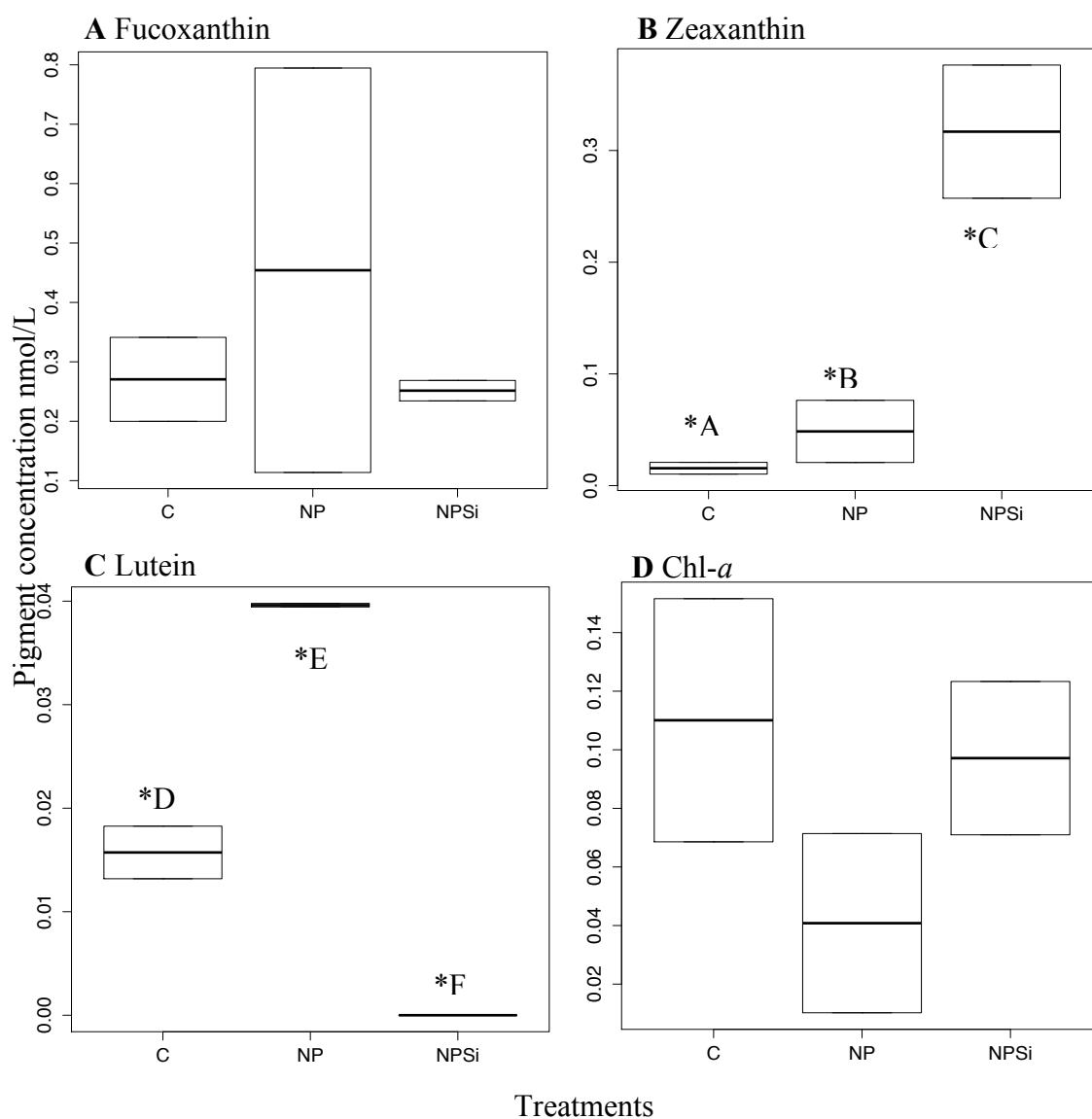


Figure 44: August 2013 experiment (A) fucoxanthin (B)

Zeaxanthin (C) Lutein (D) Chl-a on day 11. ANOVA results show significant differences between treatments. (Zeaxanthin concentrations in *C are significantly higher than *A and *B, and Lutein concentrations in *E and *F are significantly different from each other and from the control *D).

Table 16: ANOVA results for August 2013 experiment and Tukey test for assessing significant difference in pigment concentrations between treatments on day 11.

August 2013 experiment at Maloe More

Treatment		F value	P value		
ANOVA	Fucoxanthin	0.31	0.75		
	Zeaxanthin	18.18	0.02		
	Lutein	184.10	< 0.001		
	Chl- <i>a</i>	1.22	0.41		
	diff	lwr	upr	P value	
Fucoxanthin					
	N+P - C	0.18	-1.00	1.37	0.81
	N+P+Si - C	-0.02	-1.21	1.17	1.00
	N+P+Si - N+P	-0.20	-1.39	0.99	0.77
Zeaxanthin					
	N+P - C	0.03	-0.19	0.26	0.82
	N+P+Si - C	0.30	0.08	0.53	0.02
	N+P+Si - N+P	0.27	0.04	0.49	0.03
Lutein					
	N+P - C	0.02	0.02	0.03	< 0.001
	N+P+Si - C	-0.02	-0.02	-0.01	0.01
	N+P+Si - N+P	-0.04	-0.05	-0.03	< 0.001
Chl-<i>a</i>					
	N+P - C	-0.07	-0.27	0.13	0.42
	N+P+Si - C	-0.01	-0.21	0.18	0.96
	N+P+Si - N+P	0.06	-0.14	0.25	0.53

Growth rates for picocyanobacteria from the zeaxanthin pigment concentrations from day 0 of the treatments until the final day of the experiments were calculated (*Figure 45*). The growth rates were highest in the August experiment, increasing 0.03 nmol/L per day in the N+P+Si treatment, and March experiment 2, increasing 0.02 nmol/L per day, in the N+P+Si treatment (*Figure 45*). For the N+P treatment, growth rates in all the experiments was < 0.01 nmol/L per day. The March under ice experiment in the South basin found no changes in growth rates for picocyanobacteria with the treatments (*Figure 45*). The March experiment shows the highest growth rate with the N+P treatment, and the August experiment shows the highest growth rates with the N+P+Si treatment.

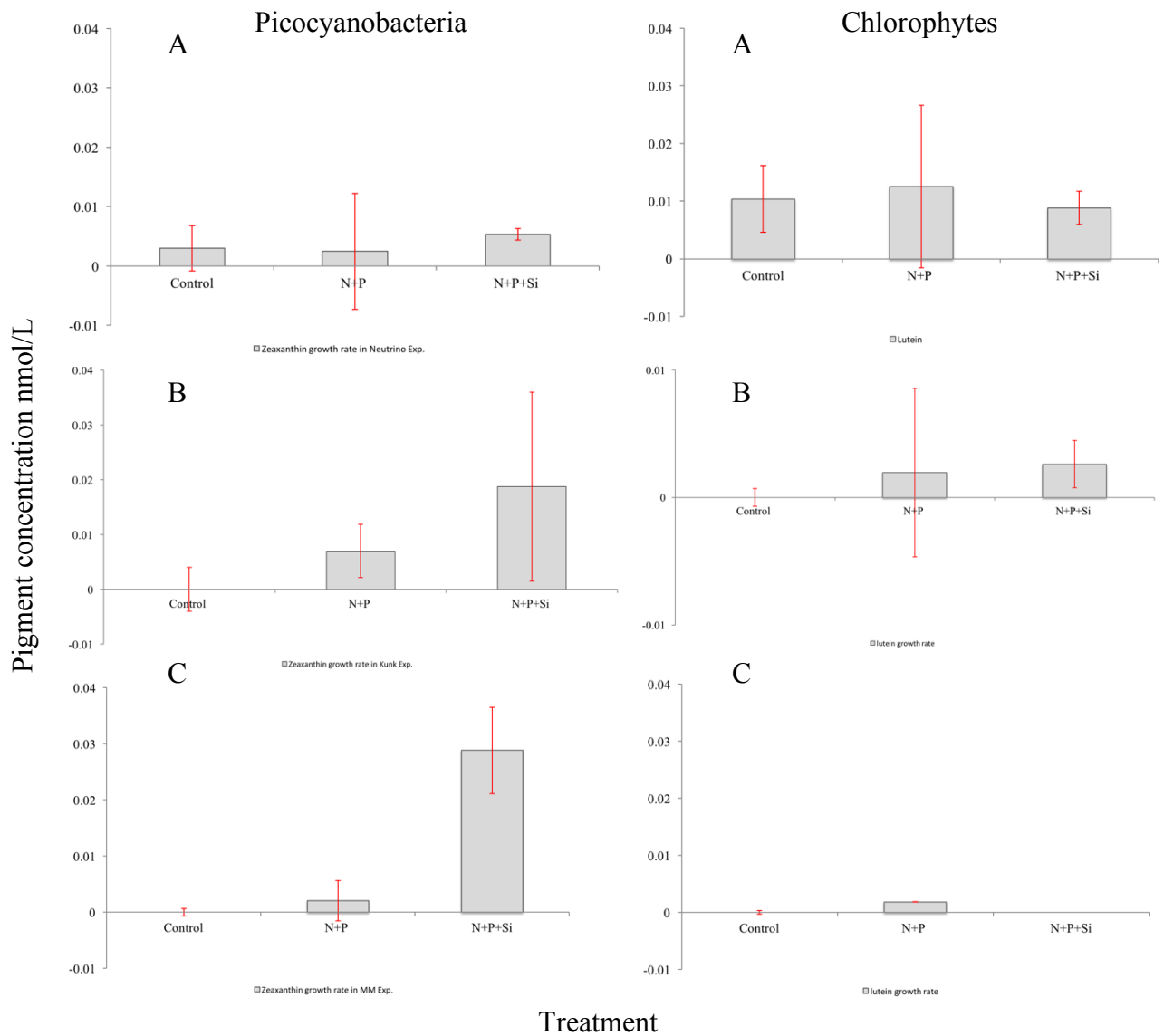


Figure 45: Growth rates for picocyanobacteria (inferred from zeaxanthin concentrations) chlorophytes (inferred from lutein concentrations) from the day 0 treatments until the final day of (A) March 2013 under ice experiment 1 (B) March 2013 experiment 2 (C) August 2013 experiment.

4.4 Discussion

4.4.1 Seasonal measurements and comparison with previous studies

Three different measures of chlorophyll-*a* have been taken in the winter and summer to compare the different methods (HPLC, spectrophotometric and fluorescence), to examine whether they show similar results and to test the accuracy of algal biomass measures in limnology. Differences within these analytical techniques are observed. The HPLC technique measures pure chlorophyll-*a* without interference from chlorophyll-*a* degradation products, whereas spectrophotometric and YSI techniques measure both chlorophyll-*a* and its derivatives. Results show that the HPLC technique gives lower chlorophyll-*a* values than spectrophotometric or fluorometric measurements. Hogan et al. (2014) similarly found lower chlorophyll-*a* values using HPLC techniques in comparison to spectrophotometric methods. Although the magnitude of chlorophyll-*a* changes down the water profile differs with each technique, the trends in concentrations are similar between the three measurements. YSI chlorophyll-*a* measurements have been chosen to present the chlorophyll-*a* data in this Chapter and Chapter Five, as it provides continuous measurements down the water column. This will provide a representative measurement of the chlorophyll-*a* concentration in the photic zone, rather than using spot samples at 1 m, 3 m, 5 m, 10 m, 20 m and 30 m.

Nutrient concentrations (silicate, nitrate and TP) in the photic zone are lower in August 2013 than March 2013 which is due to greater uptake within the summer months. DOC concentrations are higher in August 2013 than March 2013, which could be linked to greater phytoplankton production and/or greater fluvial input of terrestrial material. March 2013 algal biomass measured via chlorophyll-*a* concentrations is significantly (p value < 0.05) lower than August 2013 values, and is less than spot measurements (lower chlorophyll-*a* concentrations) taken a decade prior in 2002-2003 (Fietz et al. 2005) (*Figure 46*). It is important to consider, however, that these measurements taken in 2013 and 2003 represent a snap shot in time within the photic zone, and cannot be used to fully interpret chlorophyll-*a* concentration trends in March over time, especially due to the large size of Lake Baikal.

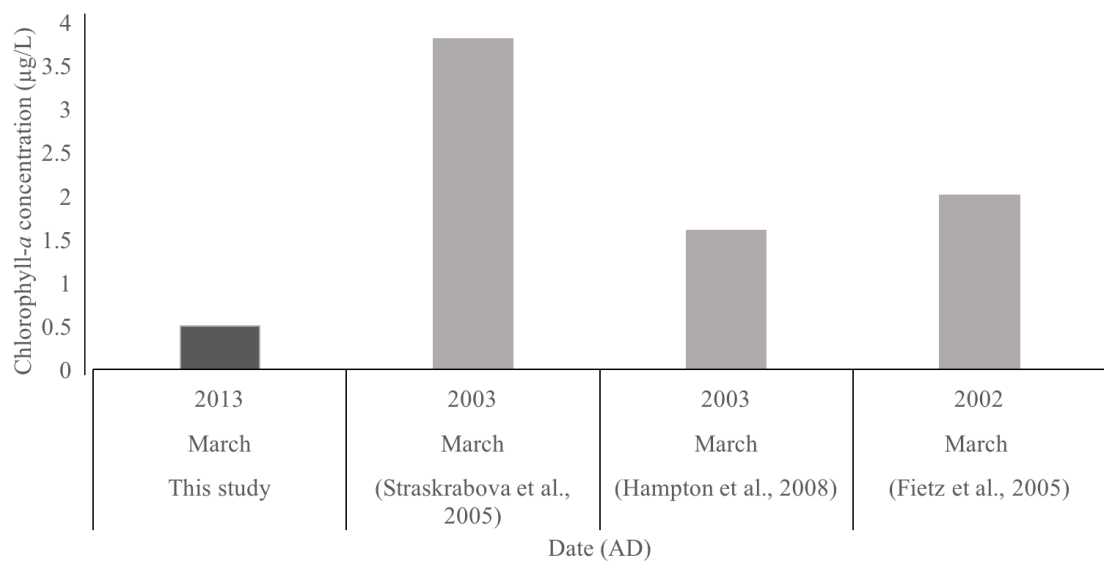


Figure 46: Spring chlorophyll-*a* concentrations in photic zone at Lake Baikal in March 2013 (this study) and from previous studies with chlorophyll-*a* measurements in March 2002 - 2003 (Fietz *et al.* 2005; Straskrabova *et al.* 2005; Hampton *et al.* 2008). These are spot sample measurement.

In comparison to historical chlorophyll-*a* data, measurements in March 2013 are still within the range of interannual variability (c. 0.2 – 3 µg/L), being closer to chlorophyll-*a* concentrations observed in December – February between 1979– 2003 (Hampton *et al.* 2008). Fietz (2005) measured under ice chlorophyll-*a* in March 2001 – 2003 which is slightly higher than chlorophyll-*a* measurements in March 2013. Diatom and cyanobacterial pigments concentrations appear to be lower in March 2013 than in March 2003, whereas chlorophyte pigments do not show any change between the two surveys in 2003 and 2013. This could potentially agree with the trend published by Silow *et al.* 2016 (Figure 47), which suggest a decline in under ice production of the dominant phytoplankton groups of Lake Baikal. Further monitoring work would be needed to confirm this, however if there is a declining trend it is likely that under ice production is likely to be a result of declining ice cover thickness and duration with increasing regional temperatures. The ice cover thickness in March 2013 was between 78.5 – 90 cm, which agrees with the decreasing trend of thickness values of c. 100 cm in 1950 to thickness values of c. 80 cm in 1995 (Todd and Mackay, 2003). Furthermore, increases in snow cover and lower light penetration would create a less favourable environment for *Aulacoseira baicalensis* growth (Jewson *et al.* 2009; 2015; Jewson and Granin, 2014). In contrast to *Aulacoseira baicalensis*, *Cylotella baicalensis* which similarly are unable to grow at high temperatures > 8.5 °C, can survive in low light levels (irradiance < 2 µmol m⁻² s⁻¹) from increased snow cover on the ice (Jewson *et al.* 2015). Phytoplankton

monitoring at Bolshie Koty in the South basin over the last 60 years shows declining trends in under ice diatom phytoplankton (Silow et al. 2016). Changes in the under-ice complex between 1951 – 2010 include a decrease in *Cyclotella baicalensis* ($R^2 = -0.047$) from c. 3.5 cells L^{-1} in 1950 to c. 1.8 cells L^{-1} in 2010, and a decrease in *Aulacoseira baicalensis* ($R^2 = -0.176$) from c. 5 cells L^{-1} in 1950 to c. 3.2 cells L^{-1} in 2010 (Silow et al. 2016) (Figure 47). The results presented in this chapter appear to be supporting these observed declining trends in under ice diatom production, and it is likely as result of climate warming which is leading to less snow and ice cover at Lake Baikal.

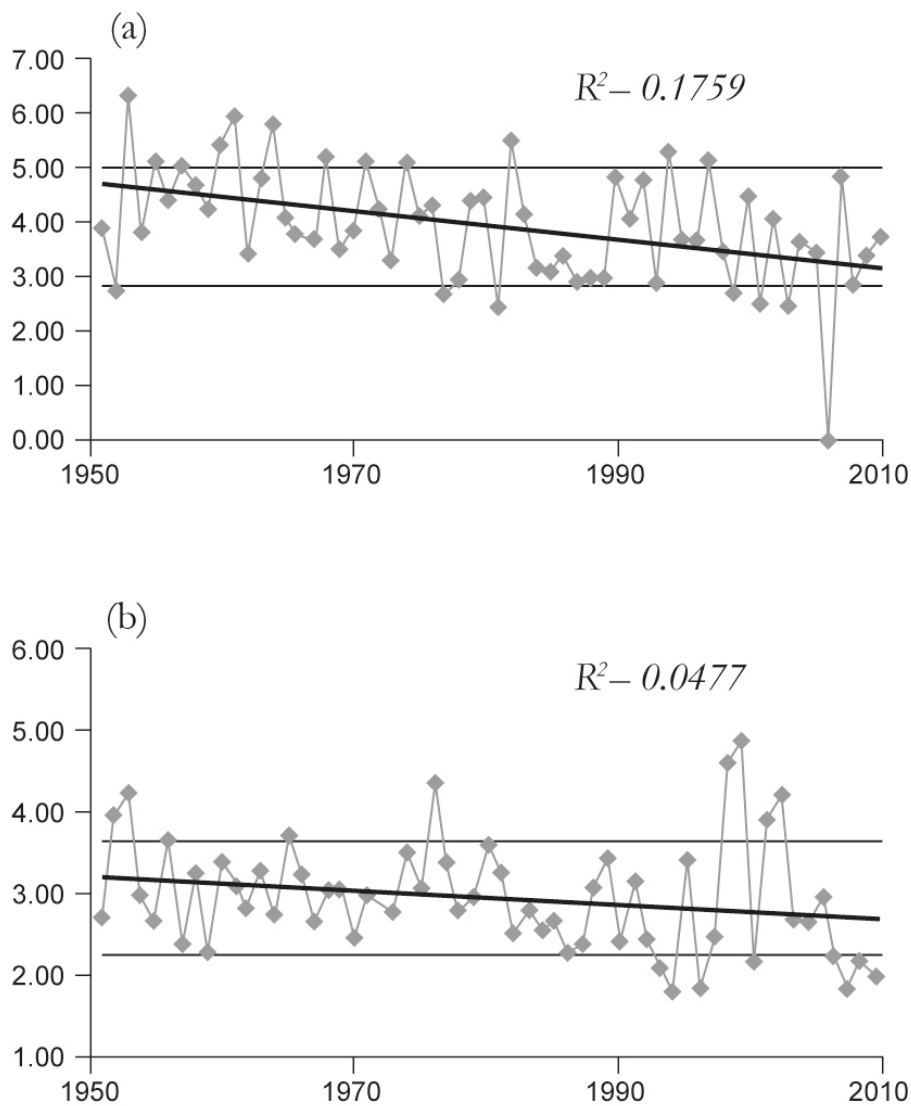


Figure 47: Trends in (A) *Aulacoseira baicalensis* (cells L^{-1}) and (B) *Cyclotella baicalensis* (cells L^{-1}) between 1950 - 2010 (modified from Silow et al. 2016).

4.4.2 Impact of nutrient enrichment on Baikal's pelagic phytoplankton

Nutrient enrichment experiments carried out in March 2013 show a shift in algal community composition from the algal pigment concentrations, from Day 0 to the end of the experiment (Day 6, Day 7 and Day 11 for the three experiments) in all three treatments (C, N+P and N+P+Si). This shift is from water samples dominated by diatoms, to being dominated by chlorophytes and picoplankton. In the August 2013 nutrient enrichment experiment, the addition of Silicon does seem to have an impact on algal community composition, with the increase in picoplankton populations which are not seen in the Control and N+P treatments. Thus, to validate these shifts within the algal pigment concentrations, phytoplankton counts are essential.

The nutrient enrichment experiments presented in this chapter are the first to be carried out at Lake Baikal which have investigated the impact of nutrient enrichment on major algal groups (diatoms and chrysophytes, picocyanobacteria and chlorophytes) using HPLC pigment analyses, rather than solely chlorophyll-*a* concentrations as a measure of total algae. This provides an insight into the algal community changes with changing nutrient concentrations. The study in this chapter found significant N, P and Si effects in the March 2013 experiments, as the N+P+Si treatment stimulated diatom growth, as shown from an increase in fucoxanthin concentrations. In the August 2013 experiment N+P additions stimulated an increase in only lutein concentrations. This suggests a response in chlorophytes with N+P enrichment in the August 2013 waters, and no response from diatoms or picocyanobacteria. Results show statistically significant increase in picocyanobacteria growth with N+P+Si additions in March 2013 and August 2013 experiments. Mean diatom pigments (fucoxanthin) increased in concentration in spring (March 2013 experiment 1) in the N+P+Si treatment, and fucoxanthin concentrations were significantly different between treatments, suggesting that diatoms were outcompeted by picocyanobacteria. Picocyanobacteria pigments (zeaxanthin) increased in concentrations in the August 2013 experiment, showing significantly higher concentrations in N+P+Si treatments than within the N+P and control treatments on the last day of the experiment, which suggests Si limitation. Overall the supply of N+P and N+P+Si in the March and August 2013 experiments did not significantly increase chlorophyll-*a* yield (p value > 0.05). The N+P+Si did increase the growth rate and concentrations of picocyanobacteria, and N+P did increase the concentrations of chlorophytes. Nutrient limitation differed amongst the algal groups, and was more pronounced in the summer than the spring. This is likely to be due to lower nutrient concentrations in summer from a greater nutrient demand from phytoplankton growth, largely picocyanobacteria growth, which dominate the water column in summer stratification.

All algal cells require silicon, however diatoms (siliceous algae) have generally been considered to require larger quantities of silicon for the growth of their frustules. Baines et al. (2012) however found silicon accumulation in marine picocyanobacteria from the eastern equatorial Pacific and the Sargasso Sea, using synchrotron X-ray fluorescence microscopy to determine the elemental composition of individual diatoms and cyanobacterial cells of *Synechococcus*, which dominate nutrient depleted waters. Similarly, the main picoplankton species in Lake Baikal are endemic *Synechocystis limnetica*, which are an chroococcoid phcoerythrin-rich cyanobacterium (Popovskaya, 1968; Belykh et al. 2006). Baines *et al.* (2012) suggests that picocyanobacteria can exert a previously unexpected influence on the oceanic silicon cycle (Baines *et al.* 2012). This is important to consider for Lake Baikal, as picocyanobacteria dominate the lake waters during thermal stratification (Belykh and Sorokovikova, 2003). These findings resemble some previous indication of significant silicon accumulations by colonial cyanobacteria in a freshwater lake, Rostherne Mere (Sigee and Levado, 2000; Krivtsov et al. 2005). The mechanism of silicon accumulation by *Synechococcus* (c. 1.5 μm in size) is unknown as methods cannot resolve the precise location of the silicon associated within the cell. It has been suggested that internal silica deposition might occur in the periplasmic space between the outer cell wall and the cell membrane, where it provides a protective function for the cell (Baines et al. 2012). There is uncertainty within this though, as little is known regarding silicon deposition in picocyanobacterial cells. To further investigate this result, elemental analyses need to be carried out on picocyanobacteria cells using, for example, a cryo-focussed Ion Beam Scanning Electron Microscopy (FIB SEM) and Transmission Electron Microscopy (TEM). Elemental analyses would assess the silicon content of picoplankton cells, by isolating picocyanobacterial cells from the sample and assess the chemical composition of the internal structure of these small cells. For single cell analyses of silicon, culture techniques need to be applied. Marine studies have found silicon content within these cells, however it has not been studied in freshwater systems. It is therefore important to examine this, as diatoms have previously been thought to be the only algal species that require sufficient silicon, to influence the silicon concentrations within Lake Baikal.

Primary production of phytoplankton at Lake Baikal has been measured since the 1960s (Votintsev et al. 1975; Back et al. 1991; Goldman et al. 1996), and between March – October the contribution of picoplankton to primary production ranged between 41 – 62 % (Yoshida et al. 2003). This highlights the importance of picocyanobacteria at Lake Baikal, and if silicon accumulation occurs within picoplankton cells then they also play a major role in the silicon cycling at Lake Baikal. If the Si is externally bound on picocyanobacterial cells then the influence of picocyanobacteria on Si cycling is suggested to be minimal, as it is easily exchangeable (Baines et al. 2012). If the Si is amorphous mineral silica within the

picocyanobacterial cell walls, then picocyanobacterial will influence the silicon cycle along with diatoms (Baines et al. 2012). Due to the high abundance of these small picocyanobacterial cells during the summer months at Lake Baikal and diverse distribution across the entire lake, in both pelagic and littoral regions, an increase in their biomass which is expected with lake warming could potentially have a large effect on future silicon cycling at Lake Baikal.

4.5 Summary

There is a difference between winter (March 2013) and summer (August 2013) algal production and community composition within the South basin, with higher total algae concentrations and a dominance of picocyanobacteria in the late summer. The spot samples of chlorophyll-*a* concentrations within this chapter and previous work suggest that winter (March 2013) chlorophyll-*a* measurements are lower than published values in 2003. It is important to note that these chlorophyll-*a* concentrations in March 2013 and March 2003 provides only a snap shot in time in winter limnology, and a single data point could be either noise or a trend in chlorophyll-*a*. Thus, further monitoring work is required to validate a declining trend in under ice chlorophyll-*a* concentrations. Given this caveat in the survey data, lower chlorophyll-*a* concentrations in March 2013 compared to March 2003 could be supporting a recent trend found in the South basin of Lake Baikal, by Silow et al. 2016, of declining under ice diatom production, over the last few decades.

Experiment results suggest that nitrogen, phosphorus and silicon are influencing algal communities, with nutrient treatments resulting in higher concentrations of diatom, chlorophyte and picocyanobacteria pigments. Nutrient enrichment, however, overall did not result in greater algal yield. As algal dominance is shifting in both control and nutrient enriched treatments, this suggests controls other than nutrient availability impacting algal communities, and suggests that climate (light and temperature) is playing a key role. From analysing the mesocosm samples on the last day of the experiment, nutrient treatments did not result in changes in the final chlorophyll-*a* yield, but resulted in difference in lutein and picocyanobacteria pigment concentrations and growth rates. Results from the nutrient enrichment experiments show that the addition of nitrogen and phosphorus did promote algal growth in Baikal's winter or summer waters. The response to nutrient treatments was from diatoms, picocyanobacteria and chlorophytes. Picocyanobacteria did not respond to N+P but responded to N+P+Si, which suggests silicon limitation. Chlorophytes responded to N+P, which suggests no silicon limitation, and diatoms did respond significantly to both N+P and N+P+Si in the March experiments. Nutrient treatments did not stimulate growth across all algal groups (diatoms and chrysophytes, chlorophytes and cyanobacteria), showing no

community-wide response with similar nutrient demands. Silicon promoted the growth of picocyanobacteria in both the winter and summer experiments, which is a non-siliceous organism, rather than largely promoting the growth of diatoms. This highlights the importance of silicon as a nutrient. Silicon concentrations are likely to increase with lake warming due to increased catchment erosion and river inflows. Further work is needed to examine silicon limitation at Lake Baikal in more detail, considering both spatial and seasonal aspects, as there are different algal community compositions in the winter and summer waters. It is therefore likely that nutrient limitation of phytoplankton growth varies across Lake Baikal, as found by O'Donnell et al. (2017) who reports difference in algal response to nutrients, between a pelagic south basin site and bay region close to the Selenga River inflow. Thus, due to Lake Baikal's great diversity from shallow bay regions to river influenced sites and pelagic deep basin sites, multiple sites are needed to assess lake-wide algal response to nutrient enrichments, under an experimental set-up in controlled conditions (constant temperature and light penetration). Phytoplankton cell counts are also needed to affirm or dispute these findings from the pigment data.

Chapter Five: Limnology II – Spatial and vertical summer limnological survey

5.1 Limnological surveys Lake Baikal

Lake Baikal has one of the longest phytoplankton monitoring records in the world, which extends back to the 1800s and detailed surveys since the mid 20th century (Popovskaya, 2000; Fietz et al. 2005; Hampton et al. 2008; Hampton et al. 2014; Izmesteva et al. 2016; Silow et al. 2016). A review of phytoplankton monitoring at Lake Baikal by Popovskaya (2000) reports the early investigations of algal flora to have been carried out by Gutwinsky (1891), Dorogostaisky (1904), Meier (1930), Yasnitsky (1930), Skvortzow (1937) and Antipova and Kozhov (1957). These studies were focussed within the South basin of Lake Baikal, at the biological station in the region of Bolshie Koty (*Figure 48*).

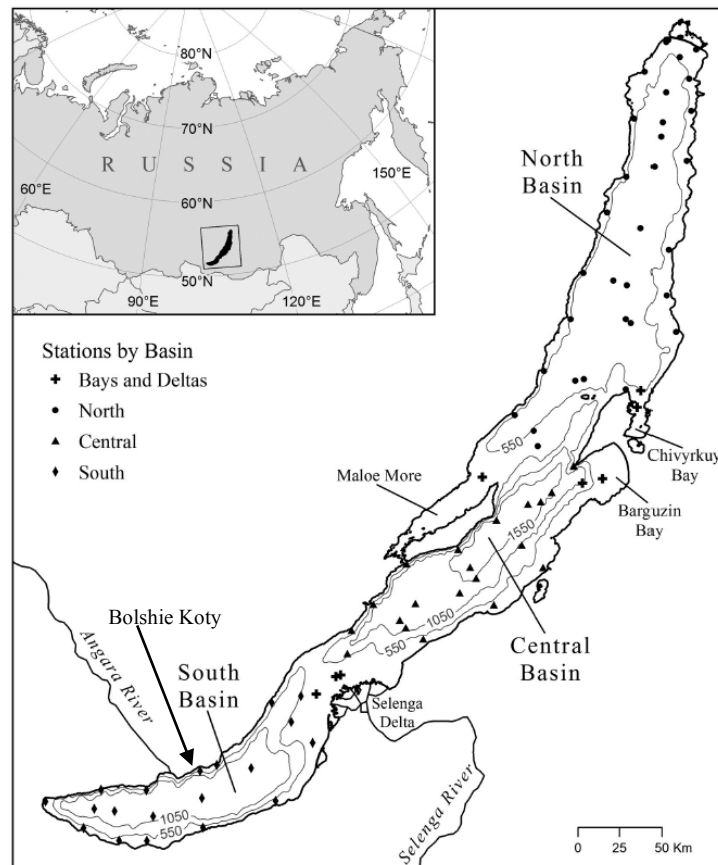


Figure 48: Location of Bolshie Koty sampling station on the shore of the South basin, and previous water sampling sites from past limnological surveys between 1977 – 2003 by Hampton et al. 2008 (modified from Izmesteva et al. 2016).

Sporadic phytoplankton monitoring has been carried out at Lake Baikal since the late 1800s, mainly focussing on the South basin, and since the early-1900s more systematic monitoring

has taken place near Bolshie Koty in the South basin. Inter-annual lake-wide monitoring then began from the 1960s onwards by Popovskaya (2000). The first spatial survey of phytoplankton was carried out, from 1964 to 1990 at an annual resolution (Popovskaya, 2000), at a total of 70 sampling stations across the lake. Monthly phytoplankton surveys were carried out at Bolshie Koty between 1977 to 2003 (Hampton et al. 2008), and between 1951 to 2010 (Silow et al. 2016). A multiparameter limnological study at Lake Baikal was conducted by Fietz (2005), and this survey examined regional, vertical and spatial variability in phytoplankton pigments between 2001- 2003. This was over a decade ago and provides measurements to compare with results presented in this chapter, to assess change over a 10-year period, as well as an insight into spatial, seasonal and annual variations in phytoplankton community composition and abundance, particularly over the last 60 years. Furthermore, Popovskaya et al. (2015) has carried out a survey between 2007 to 2011, to assess spring phytoplankton in the pelagic zones of Lake Baikal, and compared results with past records from 1964 – 1990 (Popovskaya, 2000). The comparison between these surveys shows that spring species composition (mainly *Aulacoseria baicalensis*, *Synedra acus* var. *radians*, *Aulacoseira islandica* and *Stephanodiscus meyerii*) has remained relatively stable, and any changes in phytoplankton biomass have been coincident with silicon concentrations, rather than nitrates, phosphates or temperature.

The first spatial survey of nutrients (total phosphorus, nitrate and silicate), DOC and phytoplankton pigments (chlorophylls and carotenoids) in Lake Baikal and major river inflows are presented in this chapter, being collected in August 2013. This survey, alongside the August 2013 spatial survey (26 sampling locations) of surface temperatures, nutrients (total phosphorus and total nitrogen), and chlorophyll-*a*, conducted by O'Donnell et al. (2017) in Lake Baikal provide a comprehensive insight into summer limnology at Lake Baikal. While the temporal coverage in these surveys is limited to late summer, these comprehensive surveys provide a benchmark for future monitoring work to compare to. Before this, the last extensive spatial surveys of autotrophic production at Lake Baikal (Fietz and Nicklisch, 2004; Fietz et al. 2005), regional algal community composition (Fietz and Nicklisch, 2004; Fietz et al. 2005), vertical algal assemblage (Hampton et al. 2008; 2014) and DOC (Yoshioka et al. 2002) were conducted in 2002-2003 (Fietz and Nicklisch, 2004; Fietz et al. 2005), 1955 - 2000 (Hampton et al. 2008; 2014) and 1999 (Yoshioka et al. 2002). The last detailed spatial survey of the lake in 2002-2003 found the South basin to be more productive based on chlorophyll-*a* concentrations than the North (Fietz, 2005), but the reasons behind this pattern are unclear and it is unknown as to whether they have changed over the last decade. High-resolution surveys, both spatially and temporally, are important measures to assess how increasing surface lake water temperatures are influencing Lake Baikal, as regional temperatures have been rising

rapidly over the last few decades (Jones et al. 2012), with rising regional average annual air temperatures from the 1970s, from c. $-0.5\text{ }^{\circ}\text{C}$ to $> 1\text{ }^{\circ}\text{C}$ (Shimaraev and Domysheva, 2013). Limnological changes include shifts in algal and zooplankton groups in terms of their depth distribution in pelagic regions (Hampton et al. 2014). Heavy diatoms have moved down the water column by 1.9 m y^{-1} between 1955 – 2000, whilst other phytoplankton groups have not shifted in their vertical position with the stronger thermal gradient within the upper 50 m of the water column (Hampton et al. 2014). Zooplankton groups moved to shallower positions within the water column ($0.57 - 0.75\text{ m y}^{-1}$) over the period of 1955 – 2000 (Hampton et al. 2014). Observed changes in primary production from chlorophyll-*a* concentrations and water transparency from secchi depth measurements are also noted over the last 60 years (Izmesteva et al. 2016). Mean lake-wide chlorophyll-*a* concentrations within the upper 50 m of the water column have increased from c. $0.75\text{ }\mu\text{g/L}$ to $1.2\text{ }\mu\text{g/L}$ and mean lake-wide secchi depth measurements increased from 6.8 m to 8 m between 1975 – 2005 (Izmesteva et al. 2016).

Monitoring studies have not just been restricted to the summer months, but have interannually monitored changes in algal production (chlorophyll-*a* concentrations) (Hampton et al. 2008). Long term monitoring studies over the last 60 years have captured the periodicity of large under-ice blooms, known as *Melosira* blooms, which are largely characterised by *Aulacoseira baicalensis* and occur approximately every 3 years (Hampton et al. 2008; Katz et al. 2015). The most extensive survey at Lake Baikal, in terms of temporal monitoring has recently been published (Izmesteva et al. 2016). This survey entailed annual summer sampling between 1977 to 2003 at 79 lake-wide stations (*Figure 48*), monitoring changes in chlorophyll-*a* concentrations, zooplankton assemblages, lake-water temperatures and water transparency (Izmesteva et al. 2016). Lake-wide differences in chlorophyll-*a* concentrations over the 26-year period highlight the influence of warming surface lake temperatures on production, from the trends of water temperature and chlorophyll-*a* concentration between 1975 - 2005 (Izmesteva et al. 2016). In contrast to this survey, a single station survey carried out in only the South basin shows very detailed changes in chlorophyll-*a* concentrations and secchi depths, with measurements taken every 10 - 14 days over a 60-year period since 1945 (Hampton et al. 2008). The increasing algal production and water transparency trends observed at this single site in the South basin every few weeks (Hampton et al. 2008) match those trends observed across the entire South basin from data collected once a year, and have been associated with lake warming (Izmesteva et al. 2016). For the rest of the lake though, the North and Central basins show different trends to the South. Water transparency deepened in the North and Central basins, with an increase of 1.4 m in mean secchi depth over the 26-year period. This spatial heterogeneity suggests a decline in productivity in the Central and North basin, and an increase in the South basin, emphasising the need for extensive monitoring in large lakes.

A large seasonal study of vertical phytoplankton assemblages down the water column in the South basin has also been carried out between 1994 – 2005 (Jewson et al. 2008; 2009; 2010; Jewson and Granin, 2014). Routine samples were collected to depths of 1,400 m on a monthly/bimonthly schedule, along with silicate and phosphate measurements (Jewson et al. 2008; 2009; 2010; Jewson and Granin, 2014). More recent spatial surveys include phytoplankton analyses at two depth profiles in the South basin and across the surface waters of the lake by Morley (2005) between 2001 - 2002, and surveys of photosynthetic pigments both vertically and spatially across the lake by Fietz (2005) between 2001 - 2003. Primary production is not uniform across Lake Baikal (Popovskaya, 2000) and differences in phytoplankton composition and gradient changes in phytoplankton biomass between the North and South basin have been mainly attributed to ice cover dynamics. For example, Popovskaya *et al.* 2015 shows that maximum concentrations of spring phytoplankton have been found in the South and Central basins, with the lowest phytoplankton biomass in the North basin. Additionally, Fietz and Nicklisch (2004) report a decrease in picocyanobacteria abundance from the South to the North. Fietz and Nicklisch (2004) also found greater summer production in the South basin and delayed ice break-up production in the North basin at the same time in 2001. This pattern is a result of differences in ice cover duration between the two basins.

Differences in algal communities between the North and South basin had previously been observed in June 1991 (Bondarenko et al. 1996) and May 2000 (Kozhova and Kobanova, 2002), with larger algal species (e.g. *Aulacoseira baicalensis*) in the North, and smaller algal species in the South and Central basins. Bondarenko et al. (1996) also reports that the regions of highest algal biomass were the sites by river inflows and within eutrophic littoral waters. Remote sensing has observed spatial patterns in chlorophyll-*a*, showing a latitudinal gradient in concentrations, from low to high chlorophyll-*a* concentrations from the North to South basin (Heim et al. 2005). The influence of river inputs is also highlighted from remote sensing, with intense fluvial inputs of suspended particulate matter concentrations from the Selenga River, Barguzin River and Upper Angara River (Heim et al. 2005). Thermal bars which form within littoral regions in Lake Baikal influence the distribution of algal species, as waters within these regions are warmer and more nutrient-rich (Likhoshway et al. 1996). These thermal bars form in the summer due to circulation dynamics, and bring nutrient rich deep water up to the surface via cabbelling (Botte and Kay, 2000). Higher abundances of certain diatom species, such as *Nitzschia acicularis* and *Aulacoseria skvortzowii* have been found at these locations, whereas within pelagic waters, beyond the thermal bars, higher abundances of *Cyclotella* spp and *A. baicalensis* were present (Likhoshway et al. 1996).

The main influences on Baikal's phytoplankton dynamics include the timing of ice break up and the river waters flowing into the lake which affect the strength and duration of summer thermal stratification (Goldman et al. 1996). Fietz (2005) found that thermal stratification was driving the lake-wide pigment distribution, with higher mean sum of carotenoids, mean chlorophyll-*a* concentrations and autotrophic picoplankton (APP) biovolume at sites with higher mean lake water temperatures due to stronger thermal stratification (Fietz, 2005). Hampton et al. (2015) reports lake warming over the last few decades to be driving depth distribution of major algal groups within the water column, in particular heavy diatoms. Heavy diatoms, which rely on mixing to remain suspended, shifted down the water column by 1.9 m y^{-1} (Hampton et al. 2014). As well as climate (water temperature, ice cover duration and snow depth), water chemistry and nutrient limitation could affect the spatial distribution of major algal groups across Lake Baikal (Goldman et al. 1996; Satoh et al. 2006).

5.2 Vertical distribution of phytoplankton

Phytoplankton biomass is vertically structured in Lake Baikal, with the formation of deep chlorophyll maxima (DCM) (Bondarenko et al. 1996; Popovskaya 2000). The DCM layer can form in deep transparent lakes, developing in some lakes after ice break-up due to ultraviolet radiation (UVR) avoidance (Sommaruga, 2001; Modenutti et al. 2013). Beyond this layer of maximum production, algal biomass generally declines although a secondary peak can be observed in the profile due to sinking algae. Fietz (2005) has published vertical profiles of total algae from continuous water column measurements, showing these DCM layers across Lake Baikal in July 2002 and July 2003. These show chlorophyll-*a* maxima within the mixing layer, at around 10 and 20 m water depth in the South basin (Fietz, 2005). In the North basin, this DCM was positioned between 10 and 50 m water depth, and within the mixing layer similar to the pelagic South basin DCM position (Fietz, 2005). More pronounced DCM were observed in pelagic basins compared to the littoral regions, with high concentrations in the South and Central basin ($2 - 3 \text{ nmol L}^{-1}$) than the North basin ($0.5 - 1 \text{ nmol L}^{-1}$) (Fietz, 2005). Eutrophication can cause DCM to move towards the surface as the algal biomass within the epilimnion increases, which causes shading and reduced light penetration (Klausmeier and Litchman, 2001; Zhang et al. 2012). This phenomenon has been observed in limnological studies from the Laurentian Great Lakes (Barbiero and Tuchman, 2001) (Lake Erie and Lake Ontario) which have a long history of excessive nutrient loading (Millie et al. 2009). However, knowledge on recent changes in the DCM in Lake Baikal is scarce.

This chapter will compare limnological parameters (mixing layer depth, DCM depth and light attenuation coefficients) and primary producers among the pelagic North, Central and South

basin sites. As well as abyssal sites, littoral sites such as Maloe More Bay, river influenced sites, such as by the Selenga Delta and water bodies within the Selenga Delta catchment area are included within the spatial survey in August 2013. The survey, across both the lake and catchment area, is to identify potential sources of nutrient enrichment deriving from the watershed. Chemical compositions of all major river inflows into Baikal were sampled in August 2013 from 36 different sites. Phytoplankton composition and biomass were examined across the three basins, at 15 lake sites, using chlorophyll and carotenoid pigments. The modern-day spatial patterns of phytoplankton pigments and environmental variables (nutrients and DOC concentrations, major ion concentrations, pH, dissolved oxygen, conductivity, temperature and light attenuation coefficient) will be explored, to further examine the mechanisms driving any observed differences in primary production, and help to understand algal autoecologies. Furthermore, this chapter provides an update on the pelagic algal community composition and biomass, across the lake and down the water column, a decade later from the last spatial survey conducted by Fietz (2005). The results from August 2013 have then been compared with previous work at Lake Baikal, and with other large lakes, and along with the distribution of the primary producers, their relation to light, nutrients and dissolved organic carbon (DOC) has been examined. This study represents a detailed spatial survey of summer nutrient concentrations in Lake Baikal. Although it provides a snapshot in time, the highest abundances of primary producers are observed in the summer months (Fietz, 2005) and this survey will provide a benchmark for future ones to compare against.

Limnological results from this chapter will also aid with interpreting the down-core sedimentary pigment records. Alongside assessing biological and water chemistry patterns, mercury pollution within the Selenga River and pelagic lake waters will be examined. This is as potentially toxic elements, such as mercury, have been increasing at Lake Baikal over the last few decades and bioaccumulate within the food chain (Ciesielski et al. 2016). Mercury analyses at selected sites have therefore been carried out to assess modern day water quality and examine if the Selenga River is a major source of mercury pollution.

5.3 Results

5.3.1 Lake-wide nutrient distributions

Mean TP concentrations within the lake mixing layer ranged from 10 – 32 µg/L across the lake, with distinct differences between South basin and North basin sites (p value = 0.010), and Central basin and North basin sites (p value = 0.002) (*Table 17; Table 18; Figure 49*). Highest pelagic TP concentrations were found close to major river inflows (Selenga River and Upper Angara rivers), and at the southernmost site closest to Baikalsk. TP concentrations were at least two-fold higher in the river inflows than the lake. Concentrations ranged from 50 – 130 µg/L in the Selenga River, 14.4 – 107.2 µg/L in the smaller South basin tributaries (Vydrino, Solzan, Khara-Murin, Snezhnaya, Mishika Rivers), and 67.3 – 71.3 µg/L in the Barguzin River, which enters the Central basin (*Figure 49*). Mean mixing layer silicate concentrations were not significantly different between the South and North basin (p value = 0.06), although the Central basin sites, including Maloe More Bay, generally had lower silicate concentrations (0.4 – 0.5 mg/L), being significantly different to the South and North basin (p value = 0.002 and < 0.001 respectively) (*Table 17; Table 18; Figure 49*). Mean silicate concentrations ranged from 0.4 – 0.9 mg/L, but were, on average, ten-fold higher within the inflowing rivers (*Figure 49*). Mean mixing layer DOC concentrations ranged between 1.72 – 2.51 mg/L and significantly different between the South and North basins (p value = < 0.01) (*Figure 49; Table 17; Table 18*). DOC concentrations are greater in the river waters than the pelagic lake water sites, ranging from 7.3 – 16.0 mg/L in the Selenga River waters, 4.3 – 7.1 mg/L in the smaller south basin tributaries, 13.0 – 15.9 mg/L in the Barguzin River waters and 3.1 – 4.3 mg/L in the Upper Angara River waters. Mean mixing layer nitrate concentrations ranged between 0 – 0.06 mg/L across the lake and were slightly higher in the South basin compared to the Central and North basin (*Figure 49*). The Central basin, including Maloe More, has significantly lower nitrate concentrations than the South (p value = < 0.001) and the South basin had significantly higher mean nitrate concentrations compared to the North basin (p value = 0.005) (*Table 17; Table 18; Figure 49*).

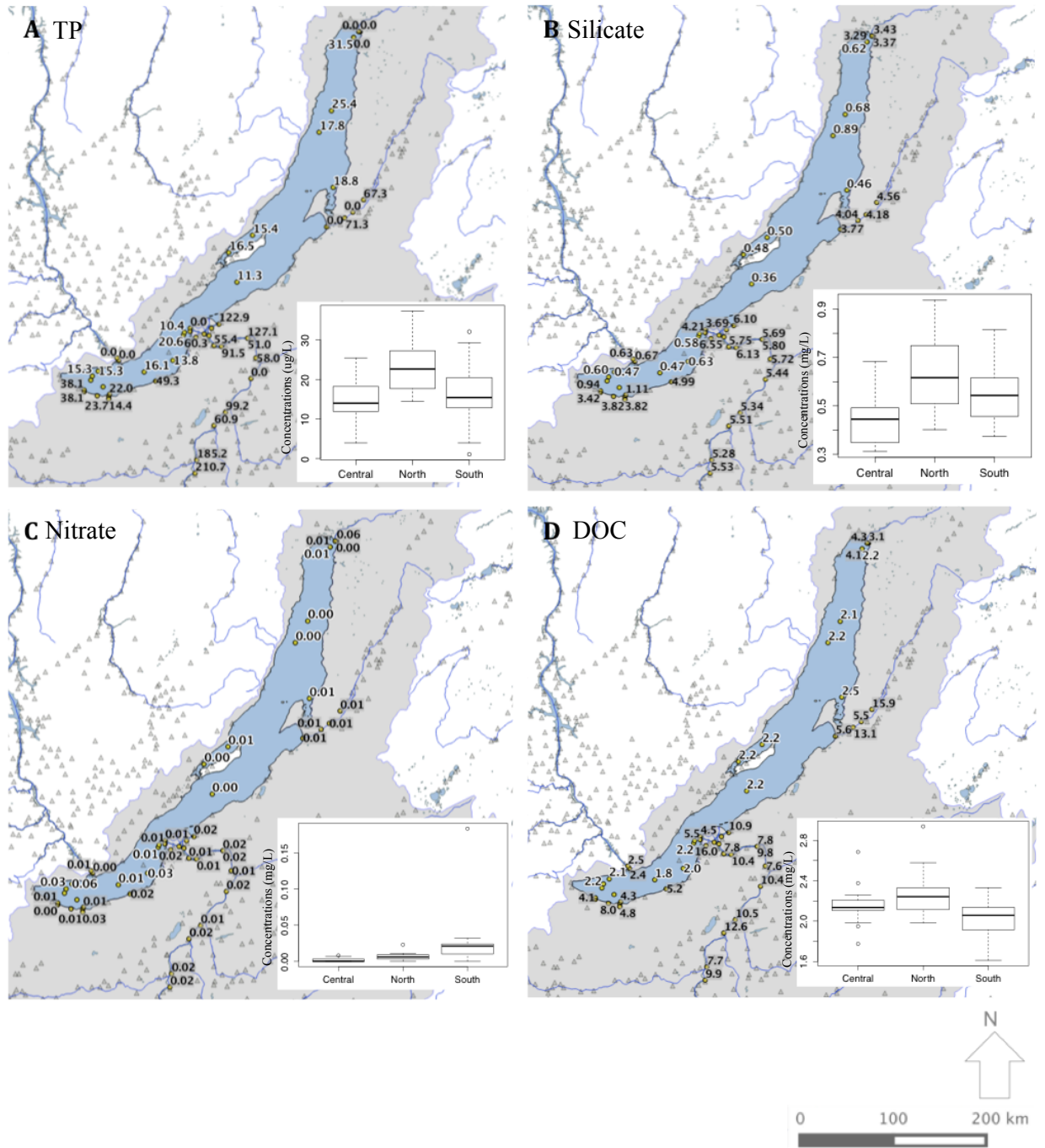


Figure 49: (A) Average total phosphorus ($\mu\text{g/L}$), (B) silicate (mg/L) (C) nitrate (mg/L) and (D) DOC (mg/L) concentrations in the mixing layer across the three basins and major river inflows. Triangles show the location of settlements in the catchment. Shading represents the Baikal catchment region.

Table 17: Results from normality, ANOVA, and KW tests performed on nutrient and DOC concentration datasets.

	Normality Test	P value	ANOVA P value	K-W Chi Squared	K-W P value
DOC	0.963	0.033	(-)	14.900	< 0.001
TP	0.837	< 0.001	(-)	14.137	< 0.001
Silicate	0.987	0.650	< 0.001	(-)	(-)
Nitrate	0.908	< 0.001	(-)	30.490	< 0.001

Table 18: P values presented from post-hoc tests for significant differences in nutrient concentrations between the South, Central and North basins.

	S - N	S - C	C - N
DOC	< 0.001	0.137	0.425
TP	0.010	0.527	0.002
Silicate	0.061	0.002	< 0.001
Nitrate	0.005	< 0.001	0.163

Major ion concentrations of lake waters were similar across the three basins (Figure 52; Table 19). Sulphate and chloride concentrations were approximately two-fold higher within the river water samples compared to the pelagic lake waters, with mean sulphate concentrations of 3.62 mg/L and mean chloride concentrations of 0.35 mg/L in the pelagic South basin mixing layer waters, and mean sulphate concentrations of 7.36 mg/L and mean chloride concentrations of 0.86 mg/L in the Selenga river waters (Table 19).

Table 19: Average major ion concentrations within the mixing layer across the three basins and in the major river inflows.

Site/Basin		Concentrations (mg/L)					
		Na ⁺	K ⁺	Mg ²⁺	Ca ²⁺	Cl ⁻	SO ₄ ²⁻
BAIK13-1	South	3.35	0.94	2.85	13.75	0.39	4.19
BAIK13-4	South	3.27	0.83	3.01	13.66	0.34	4.05
BAIK13-5	South	3.38	0.75	3.16	15.12	0.34	0.00
BAIK13-7	South	3.44	0.64	3.06	15.06	0.36	4.09
BAIK13-8	South	3.38	0.76	3.19	15.03	0.32	4.13
BAIK13-9	South	3.38	0.79	3.01	14.81	0.34	4.17
BAIK13-10	South	3.50	0.62	3.13	13.77	0.33	4.08
BAIK13-11	South	3.47	0.61	3.17	15.13	0.36	4.25
BAIK13-12	Central	3.26	0.66	3.13	14.70	0.33	4.14
BAIK13-13	Central	3.48	0.70	3.23	14.96	0.35	4.30
BAIK13-14	Central	3.48	0.63	3.14	15.23	0.32	4.01
BAIK13-16	North	3.40	0.80	3.11	15.43	0.39	4.59
BAIK13-17	North	3.35	0.77	3.01	13.97	0.32	4.05
BAIK13-18	North	3.65	0.63	3.13	16.08	0.33	4.07
BAIK13-19	North	5.57	0.73	5.30	13.61	0.36	4.12
Average in mixing layer	South	3.40	0.74	3.07	14.54	0.35	3.62
	Central	3.41	0.66	3.17	14.96	0.33	4.15
	North	3.99	0.73	3.64	14.77	0.35	4.21
Selenga river inflow average		5.85	0.83	5.47	21.86	0.86	7.36
Barguzin river inflow average		5.23	0.83	5.22	25.15	0.52	7.48
Upper Angara river inflow average		1.97	0.25	1.60	8.76	0.08	2.94

PCA shows higher mean mixing layer concentrations of sulphate, magnesium and sodium at BAIK13-19 in the North basin (*Figure 53*). Sites with the highest mean mixing layer silicate and DOC concentrations are BAIK13-7 in the South basin, BAIK13-10 by the Selenga Delta, BAIK13-16, BAIK13-17, BAIK13-18. in the North basin (*Figure 53*). Sites with the lowest mean mixing layer TP are Central basin (BAIK13-12), Selenga (BAIK13-11), Maloe More (BAIK13-13, BAIK13-14) and South basin (BAIK13-8) sites, in comparison to the North basin sites (*Figure 53*).

Vertical profiles of nutrients (TP, silicate and nitrate) from water column depths from 1 to 180 m show higher concentrations of TP within the deeper waters compared to within the mixing layer (*Figure 50*). TP concentrations reach values of 40 µg/L in one of the South basin sites (BAIK13-7). Silicate and nitrate concentrations are more homogeneously distributed down the water column, and no clear patterns of higher concentrations within the deeper waters are observed lake-wide (*Figure 50; Figure 51*).

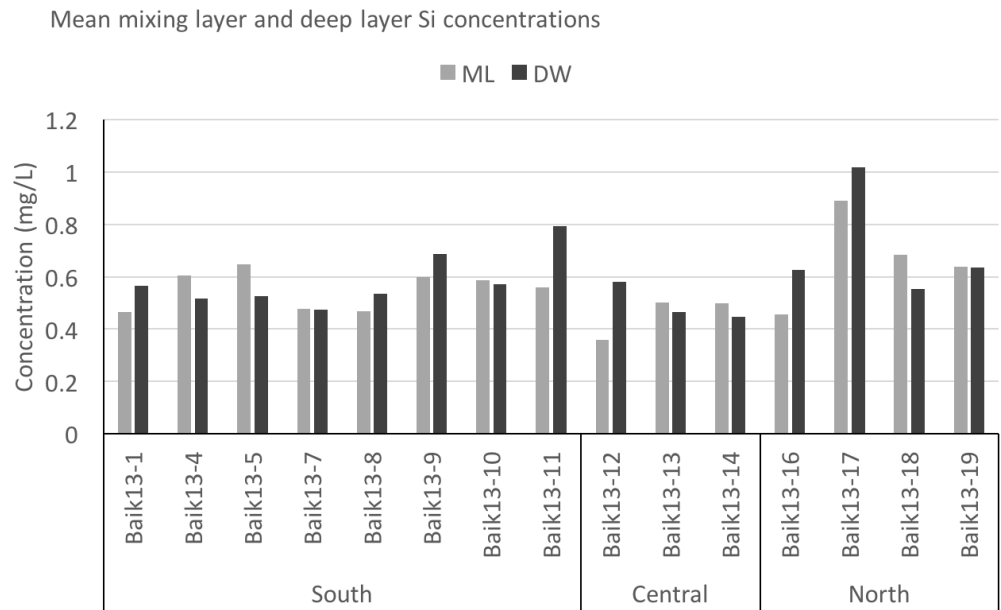
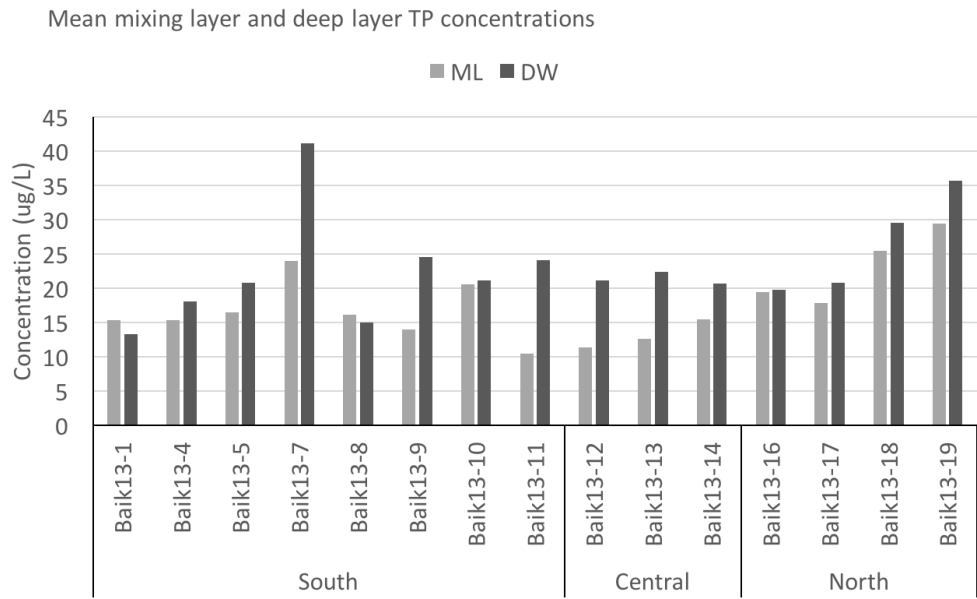


Figure 50: Mean mixing layer (ML) and mean deep water layer (DW) concentrations of total phosphorus and silicate concentrations.

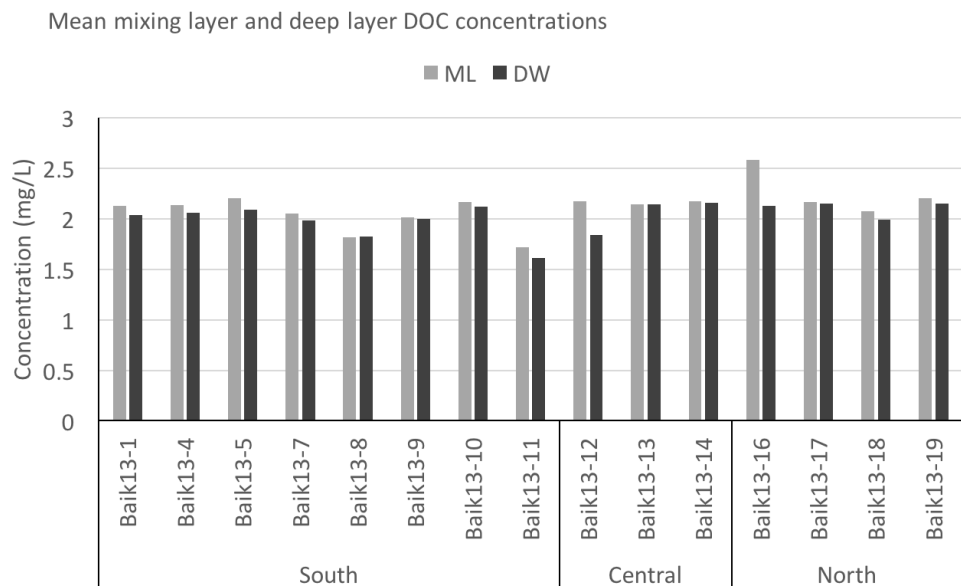
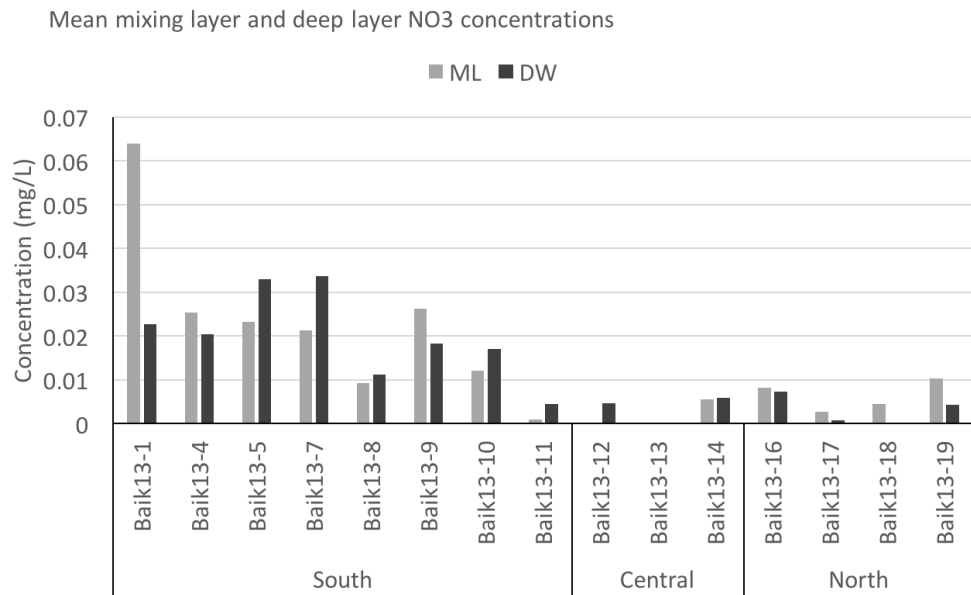


Figure 51: Mean mixing layer (ML) and mean deep water layer (DW) concentrations of nitrate and dissolved organic carbon concentrations.

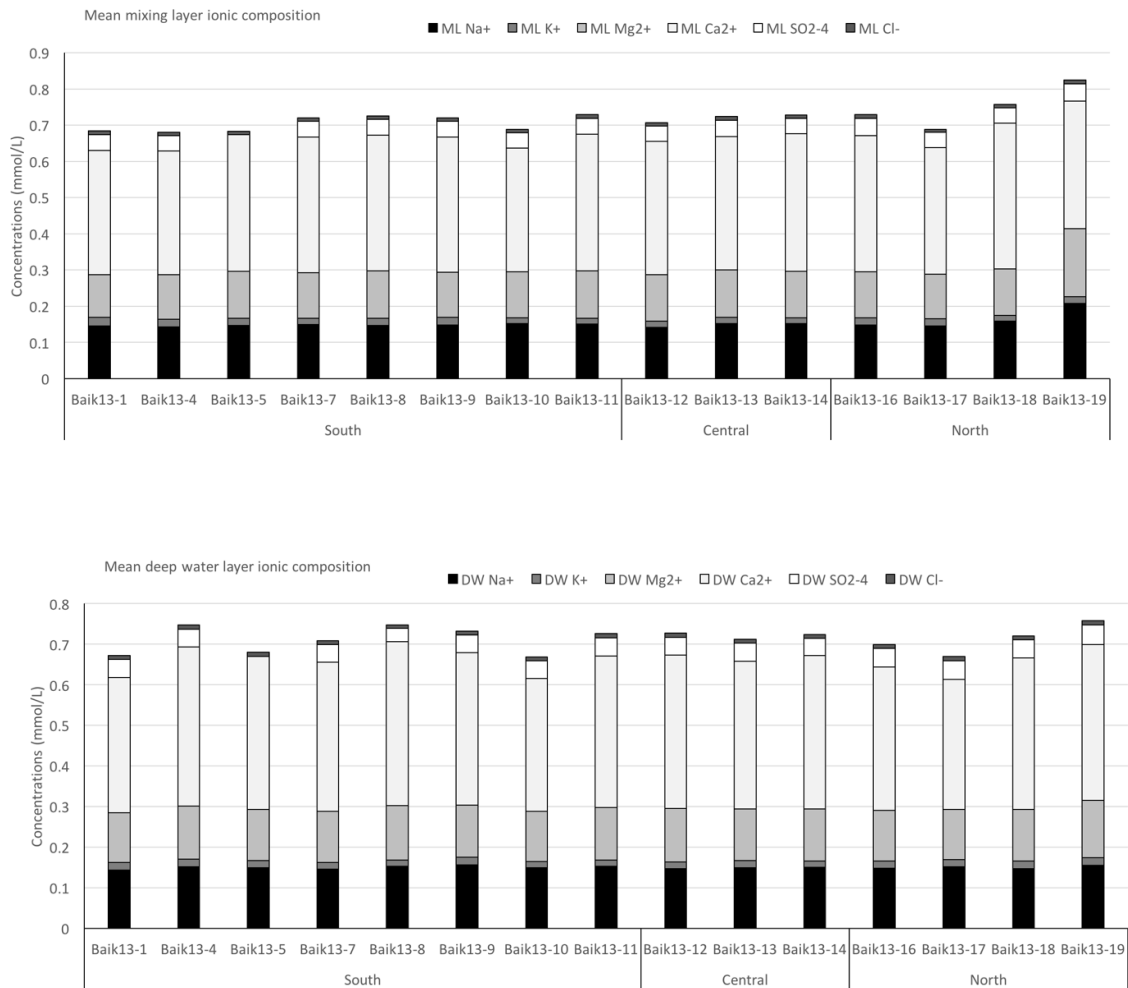


Figure 52: Mean mixing layer (ML) and mean deep water layer (DW) concentrations of major ion concentrations.

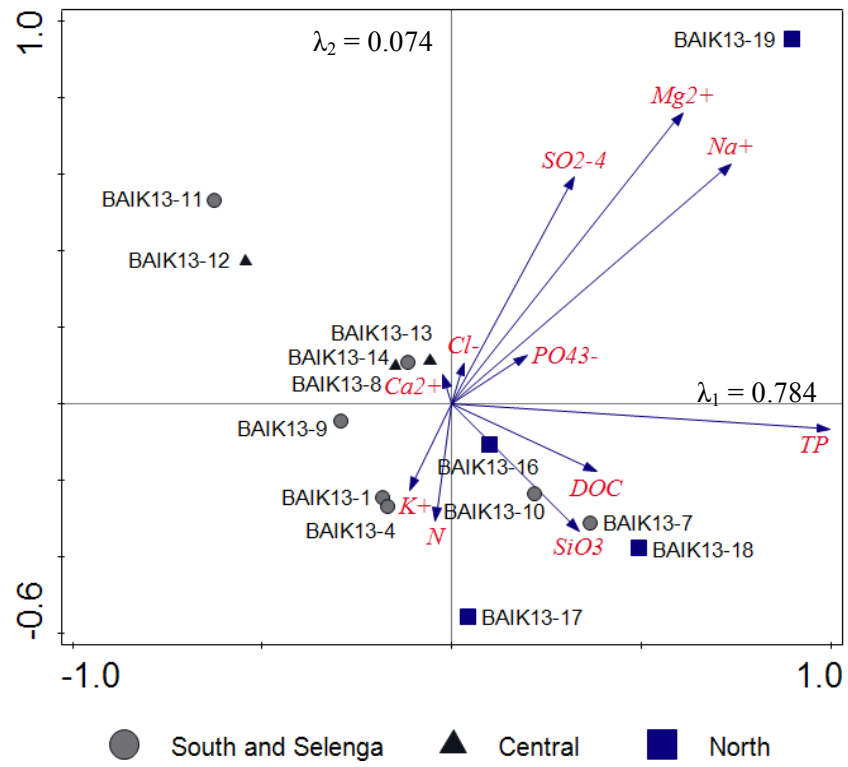


Figure 53: PCA of mean mixing layer nutrients, dissolved organic carbon and major ions.

Table 20: Comparisons of total phosphorus ($\mu\text{g/L}$), nitrate (mg/L) and sulphate (mg/L) from this study (2013) and past measurements from previous publications. TP data sources from Liebezeit, 1992; Granina and Sigg, 1995; Sorokovikova et al. 2015. Nitrate data sources from Zilov et al. 2012; Sorokovikova et al. 2012; 2015. Sulphate data sources from Falkner et al. 1991; Sorokovikova et al. 2015.

(-) means no available data

	This study (August 2013)	Previous studies	
TP ($\mu\text{g/L}$)	South	10.4 - 23.5	2.8
	Central	11.30	(-)
	Maloe More	15.3 - 16.5	(-)
	North	17.8 - 31.5	(-)
	Selenga River	47 - 211	18 - 346
	Upper Angara	(-)	9 - 23
	Barguzin River	67 - 71	12 - 181
	Snezhnaya River	14.4 - 27.2	(-)
	Khara-Murin River	107.2	(-)
	Lake Baikal, Vydrino	22	(-)
	Mishika River	49.3	(-)
	Solzan River	18.3	(-)
Nitrate (mg/L)	South	0.001 - 0.06	0.04 - 0.07 0.02 - 0.28
	Central	0.00	(-)
	Maloe More	0.005	(-)
	North	0.002 - 0.009	(-)
	Selenga River	0.006 - 0.021	0.002 - 0.4
	Upper Angara	0.003 - 0.061	0.02 - 0.27
	Barguzin River	0.015	0.03 - 0.21
	Snezhnaya River	0.013 - 0.034	(-)
	Khara-Murin River	0.012	(-)
	Lake Baikal, Vydrino	0.011	(-)
	Mishika River	0.016	(-)
	Solzan River	0.012	(-)
Sulphate (mg/L)	South	4.05 - 4.25	5.42
	Central	4.14	5.94
	Maloe More	4.01 - 4.30	(-)
	North	4.05 - 4.59	5.53
	Selenga River	7.31 - 10.41	7.6 - 18.7
	Upper Angara	0 - 6.124	5.5 - 8
	Barguzin River	6.58 - 10.17	7.1
	Snezhnaya River	4.27 - 6.59	5.5 - 11.6
	Khara-Murin River	4.490	4.8 - 12.6
	Lake Baikal, Vydrino	6.670	(-)
	Mishika River	0.000	(-)
	Solzan River	0.000	4.8 - 37.1

Table 21: Comparisons of silicate (mg/L) and DOC concentrations (mg/L) from this study (2013) and past measurements from previous publications. Silicate data sources from Jewson et al. 2010; Sorokovikova et al. 2012; Jewson and Granin, 2014. DOC data sources from Yoshioka et al. 2002; 2007.

(-) means no available data

		This study (August 2013)	Previous studies
Si (mg/L)	South	0.47 - 0.63	0.4 - 0.9
	Central	0.36	(-)
	Maloe More	0.48 - 0.50	(-)
	North	0.46 - 0.89	(-)
	Selenga River	5.28 - 11.33	(-)
	Upper Angara	3.29 - 3.43	(-)
	Barguzin River	4.04 - 4.56	(-)
	Snezhnaya River	3.82 - 3.83	(-)
	Khara-Murin River	4.38	(-)
	Lake Baikal, Vydrino	1.11	(-)
	Mishika River	4.99	(-)
	Solzan River	0.60	(-)
DOC (mg/L)	South	1.72 - 2.15	1.17 - 1.23
	Central	2.18	1.18 - 1.22
	Maloe More	2.17 - 2.19	(-)
	North	2.07 - 2.51	1.16 - 1.22
	Selenga River	7.29 - 17.93	6.5
	Upper Angara	3.14 - 4.42	(-)
	Barguzin River	13.07 - 15.87	1.77 - 6.07
	Snezhnaya River	4.77 - 7.14	(-)
	Khara-Murin River	8.04	(-)
	Lake Baikal, Vydrino	4.33	1.36
	Mishika River	5.17	1.34
	Solzan River	2.53	(-)

Table 22: TP concentrations within surface waters across Lake Baikal and upper waters from tributaries between 1995 to 2009 (unpublished data from Prof. E. Silow)

Site	Time of year	Total Phosphorus concentrations ($\mu\text{g/L}$)
Lake wide	January	5.9 – 13.0
Lake wide	February	6.2 – 16.2
Lake wide	March	7.5 – 9.8
Lake wide	April	5.5 – 14.0
Lake wide	May	5.2 – 14.2
Lake wide	June	4.9 – 14.3
Lake wide	July	3.9 – 13.0
Lake wide	August	0 – 7.8
Lake wide	September	0 – 7.2
Lake wide	October	2.9 – 7.5
Lake wide	November	2.9 – 7.5
Lake wide	December	4.6 – 10.1
Upper waters of tributaries	Summer	10 - 30

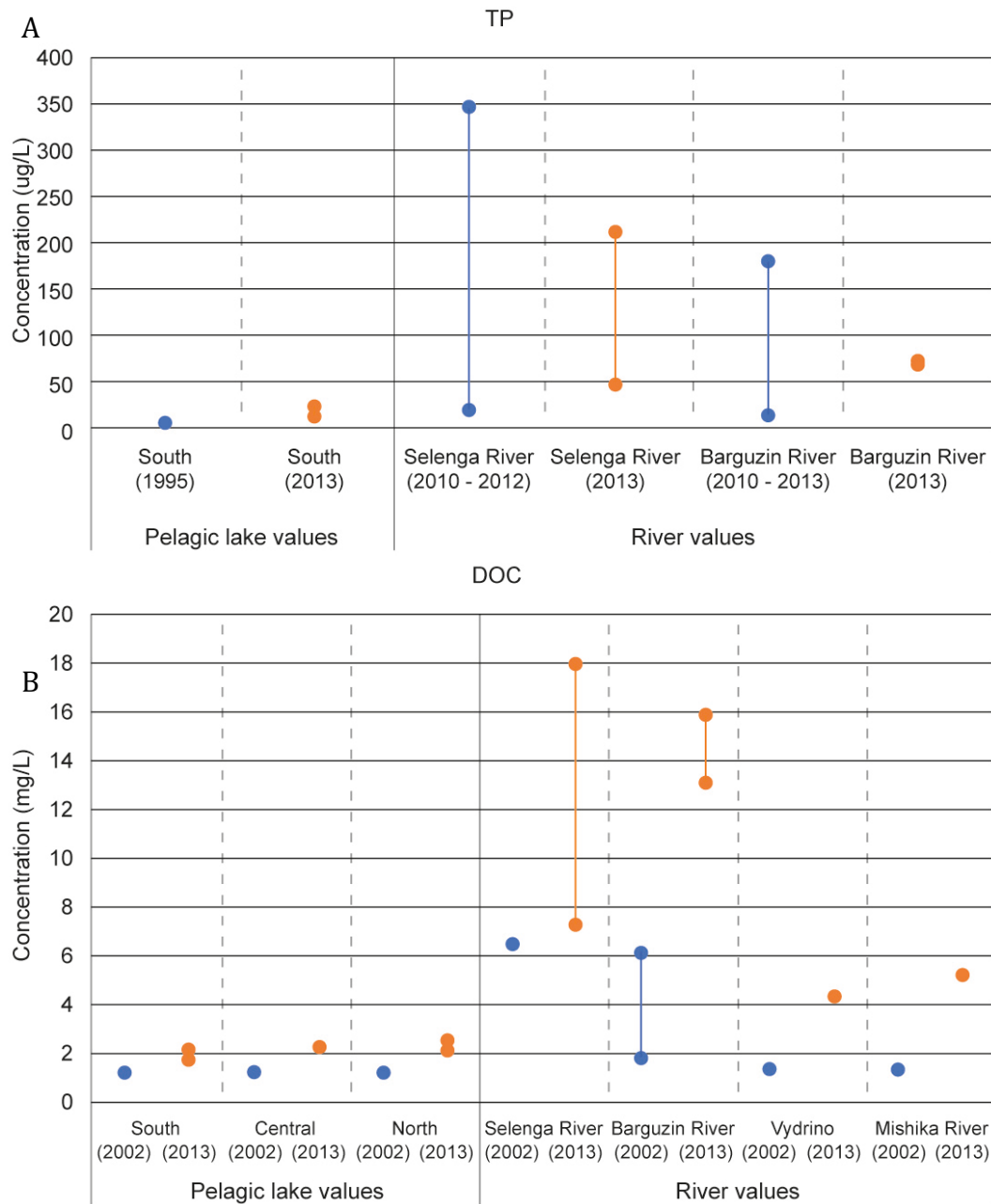


Figure 54: (A) TP concentrations from August 2013 and past measurements in 1995 and 2010 - 2012 (Liebzeit, 1992; Granina and Sigg, 1995; Sorokovikova et al. 2015) ($\mu\text{g/L}$); (B) DOC concentrations (mg/L) from August 2013 and past measurements from Yoshioka et al. 2002; 2007 from South, Central and North basin and river waters (Selenga, Barguzin, Vydrino and Mishika River).

5.3.2 Mercury concentrations

Mercury analyses was undertaken in this thesis, as a pilot study, to examine whether there are any signs of mercury contamination in the river waters, lake waters or preserved within the sediment records. As discussed in Chapter Two, mercury contamination is a growing threat at Lake Baikal, from both atmospheric and from local sources from mining activity along the Selenga River. Very little work has been carried out looking at mercury concentrations in Lake Baikal, with the most recent work published by Meuleman et al. 1995 and Leermakers et al. 1996. Thus, there is a gap in this knowledge, and the results presented in this chapter provide a benchmark for future work to compare mercury concentrations against.

Spot samples of mercury concentrations range between 6.0 – 8.1 ng L⁻¹ in the Selenga River waters, and within the Selenga Delta waters the values range between 0.3 – 5.5 ng L⁻¹ (Figure 55). In the pelagic lake waters, mercury concentrations reach 3.2 ng L⁻¹ in the North basin, near the Upper Angara and range between 0.0 – 1.6 ng L⁻¹ in the pelagic lake waters, with the lowest concentrations in the Central basin at BAIK13-12 and the highest nearby the Selenga Delta at BAIK13-10 (Figure 55).

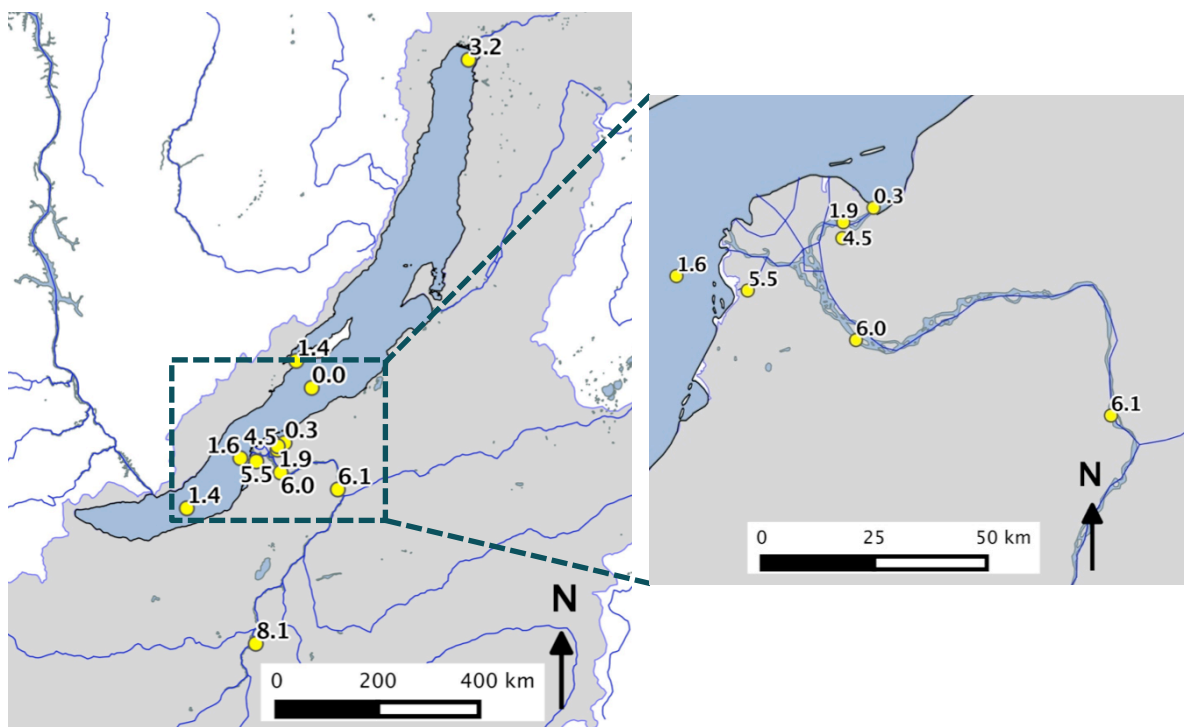


Figure 55: Mercury concentrations (ng L⁻¹) in pelagic lake sites in the South, Central and North basins and within the Selenga River.

Within the lake and river waters, mercury concentrations, were above detection limits within all the samples. The spot samples of mercury concentrations measured within the lake waters in August 2013 were higher than previously published values of 0.77 - 0.14 – ng L⁻¹ in June 1992 -1993 from pelagic Baikal waters (Meuleman et al. 1995; Baeyens et al. 2002), and comparable to mercury concentrations within the open ocean (0.2 – 0.7 ng/L) (Kim and Fitzgerald, 1986; Mason and Fitzgerald, 1990 cited in Meuleman et al. 1995). The highest mercury concentrations (3.2 ng L⁻¹) were found at BAIK13-19 in the North basin, the closest site to the Upper Angara River (distance of c. 10 km), which is two-fold higher than values within the pelagic South and Central basins.

Along with surface water mercury measurements, mercury concentrations were measured down-core on BAIK13-1C in the South basin, BAIK13-10A close to the Selenga River, and BAIK13-19B close to the Upper Angara River (*Figure 28*). Surface sediments were not showing a similar spatial trend to the water samples, as surface sediment mercury concentrations are higher in the South basin (67.3 ng/L) than close to the Selenga Delta (47.7 ng/L) or Upper Angara in the North basin (51.1 ng/L) (*Figure 56*).

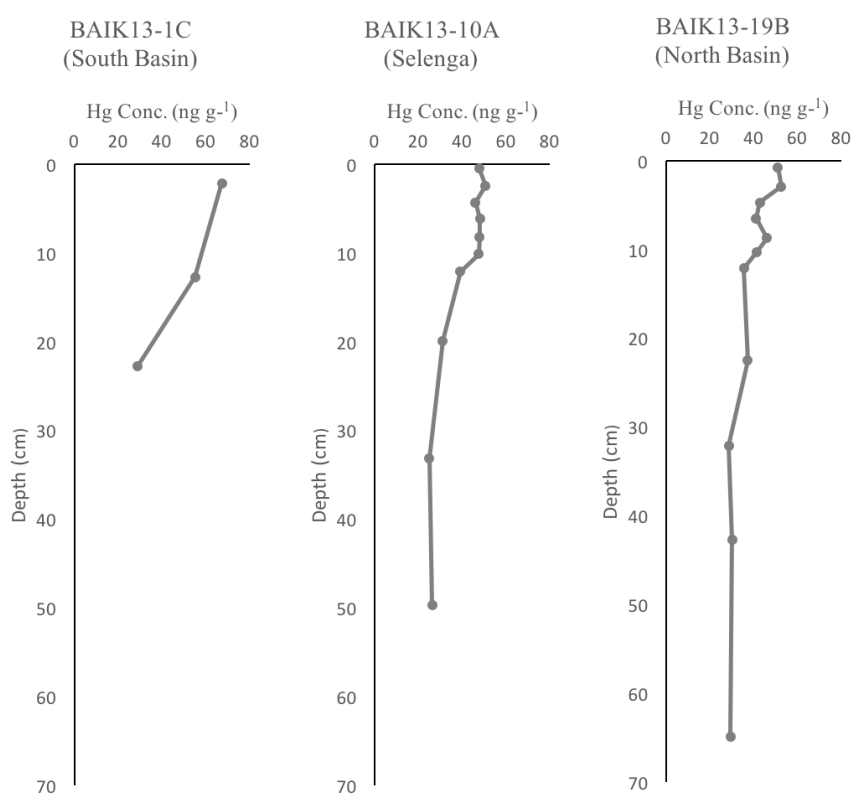


Figure 56: Down-core mercury concentrations at South basin (BAIK13-1C), Selenga (BAIK13-10A) and North basin (BAIK13-19B).

5.3.3 Limnological parameters and chlorophyll-*a* measurements

Chlorophyll-*a* concentrations presented within this chapter were collected using the YSI sonde, and provide continuous measurements down the water column to water depths of c. 120 m. The differences between the chlorophyll-*a* concentrations measured using YSI, HPLC and Spectrophotometry are discussed in Chapter Four. YSI chlorophyll-*a* concentrations range between 0.3 to 8.47 µg/L in the surface waters across Lake Baikal, which is comparable to chlorophyll-*a* measurements obtained from another spatial survey in August 2013 by O'Donnell et al. (2017) (range of 2.5 to 10 µg/L). In this thesis, spatial differences in mean chlorophyll-*a* concentrations within the mixing layer and deeper waters are observed within the dataset. Mean August mixing layer chlorophyll-*a* concentrations from the YSI sonde dataset were significantly (p value = < 0.01) higher in the South basin (mean 4.3 µg/L; maximum c. 8.5 µg/L) than the North basin (mean = 1.2 µg/L; maximum = 2 µg/L) sites (*Figure 57*). Central basin mixing layer chlorophyll-*a* concentrations were significantly lower than the South basin sites (p value = < 0.01) and similar to the North basin sites, with mean concentrations ranging between 0.34 – 0.90 µg/L. North basin deep water chlorophyll-*a* concentrations ranged from 1.1 – 2.7 µg/L, which is similar to the Central basin deep water chlorophyll-*a* concentrations. There was a marked difference in the distribution of chlorophyll-*a* in the North and Central basins where deepwater exceeded mixed layer concentrations in 6 of the 7 sites. This pattern was reversed in the South basin where mixed layer chlorophyll-*a* concentrations always exceeded those in the deepwater (*Figure 57*).

The vertical distribution of chlorophyll-*a* is heterogenous across the lake, with DCM positioned at different water depths. Distinct DCM are not present at all the sites across the lake. The sites which do not show a clear DCM are BAIK13-4, BAIK13-5 and BAIK13-7 in the South basin and BAIK13-10 in the Selenga Shallows (*Figure 58*; *Figure 59*). BAIK13-4, BAIK13-5 and BAIK13-7 in South basin show surface layers of high chlorophyll-*a* concentrations (> 3 µg/L), and BAIK13-10 in the Selenga Shallows shows high chlorophyll-*a* concentrations (c. 5 – 7 µg/L) between c. 10 – 30 m. The rest of the sites across the lake exhibit distinct DCM, especially at BAIK13-12 in the Central basin and BAIK13-14 in Maloe More, which reach chlorophyll-*a* concentrations of 10 – 12 µg/L (*Figure 60*). Thus, the DCM is most pronounced and the thickest in the Central basin (BAIK13-12) and Maloe More (BAIK13-14) than within the South and North basin or by the Selenga Delta (*Figure 60*). The DCM layer, forms further up the water column within all the South basin sites, compared to the Central and North basin. In all the South basin sites, the DCM formed within the top 4 m of the epilimnion, and extended to depths of 20.2 – 46.5 m, beyond the euphotic zone depth. BAIK13-7 in the South basin (*Figure 58*; *Table 23*) had the highest light attenuation

coefficient (0.28 m^{-1}) and a DCM layer between 0.5 – 20.7 m, which extended beyond the mixing layer depth at 6.2 m, with secondary chlorophyll-*a* maximum at 42.7 – 44.6 m, beyond the euphotic zone depth. In the Central basin sites the DCM layer formed lower down the water column, beginning at depths of 7.1 – 31.5 m and extended to depths of 32.5 – 79.7 m (*Figure 58; Table 23*). There is greater variability in the DCM layer thickness and position in the North basin, which started at depths of 2.8 – 9.0 m and extended to depths of 17.0 – 58.8 m (*Figure 61; Table 23*).

Pigment analyses suggest that diatoms and picocyanobacteria are the major algal groups across Lake Baikal. In the South basin, zeaxanthin is the largest contributor to algal biomass at the DCM layer (0.64 – 1.77 nmol/L), whereas, at the Selenga and North basin sites both fucoxanthin and zeaxanthin have similar concentrations (0.69 and 0.72 nmol/L respectively) (*Table 24*). At BAIK13-12 in the Central basin and BAIK13-14 at Maloe More, with the highest chlorophyll-*a* concentrations at the DCM (12.67 and 10.72 $\mu\text{g/L}$ respectively), fucoxanthin is the largest contributor to total algal biomass (0.28 and 0.63 nmol/L respectively). In the South basin, Chivsky Bay and near the Upper Angara, the sites with the shallower DCM, picocyanobacteria are dominant within the algal biomass in the DCM layer (*Table 24*).

In 2013, highest chlorophyll-*a* concentrations were detected within the mixing layer of the South basin sites. However, these average concentrations within the mixing layer do not consider the DCM, which develop in deep oligotrophic lakes in the summer (Camacho, 2006; Saros et al. 2005; Modenutti et al. 2013). This DCM generally sits close to the thermocline depth in the South basin sites, similar to the chlorophyll maxima in Lake Michigan and Lake Huron (Barbiero and Tuchman, 2001), but is positioned further below the mixing layer depth in the Central and North basin sites (*Figure 57*). This may be due to less algal shading in the mixing layer within the Central and North basin sites. The DCM layer varies in thickness across the three basins, forming further up the water column in the South basin sites, compared to the Central and North basin. This contrasts with the DCM measurements in 2002-2003 at Lake Baikal, which shows shallower DCM in the Central and North basin, and deeper DCM in the south basin (Nakano et al. 2003; Fietz et al. 2005), than the chlorophyll maxima positions in August 2013 (*Figure 57*).

DCM generally fall close to the mixing layer depth in the South and North basin sites, whereas in the Central basin sites the DCM is positioned the deepest relative to the mixing layer (*Figure 57*). Light attenuation coefficients (K_d) were highest in the South basin sites ($p > 0.05$), reaching values of c. 0.28 m^{-1} , mean 0.19 m^{-1} and the lowest summer light attenuation

coefficients of $< 0.1 \text{ m}^{-1}$ were found at the Central basin sites (mean 0.1 m^{-1}) (Figure 57). North basin sites had intermediate light attenuation (mean 0.18 m^{-1}). Photic zone depths extended to c. 40 m within the Central basin sites, and were shallower within the South and North basin sites, reaching depths of c. 20 – 30 m. The mixing layer depths (ranging between 4.3 – 23.7 m) were consistently shallower than the euphotic zone depths (ranging between 16.9 – 43.3 m) at all lake sites (Figure 57).

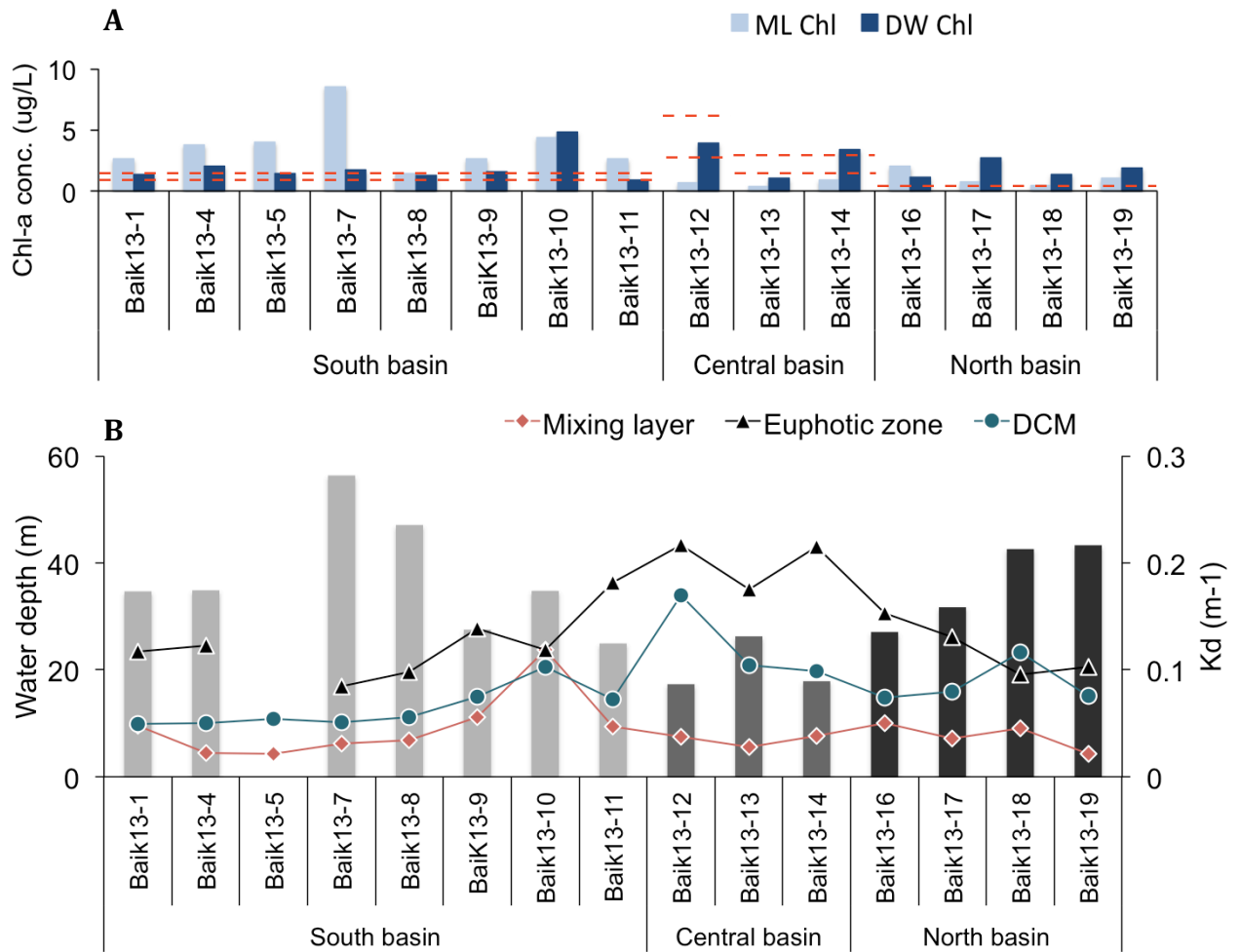


Figure 57: **(A)** Average YSI Chlorophyll-a concentrations within the mixing layer and deep water layers. Red dotted line: Mean chlorophyll-a concentrations at DCM within the south basin, central basin, Maloe More and north basin from previous study in 2002 – 2003 (Fietz, 2005). **(B)** Limnological parameters (euphotic zone depth, mixing layer depth and deep chlorophyll maxima) at each water-sampling site across the three basins. Grey bars represent the light attenuation coefficient (K_d) values across the lake. DCM represents the water depths of the maximum chlorophyll concentrations down the water column.

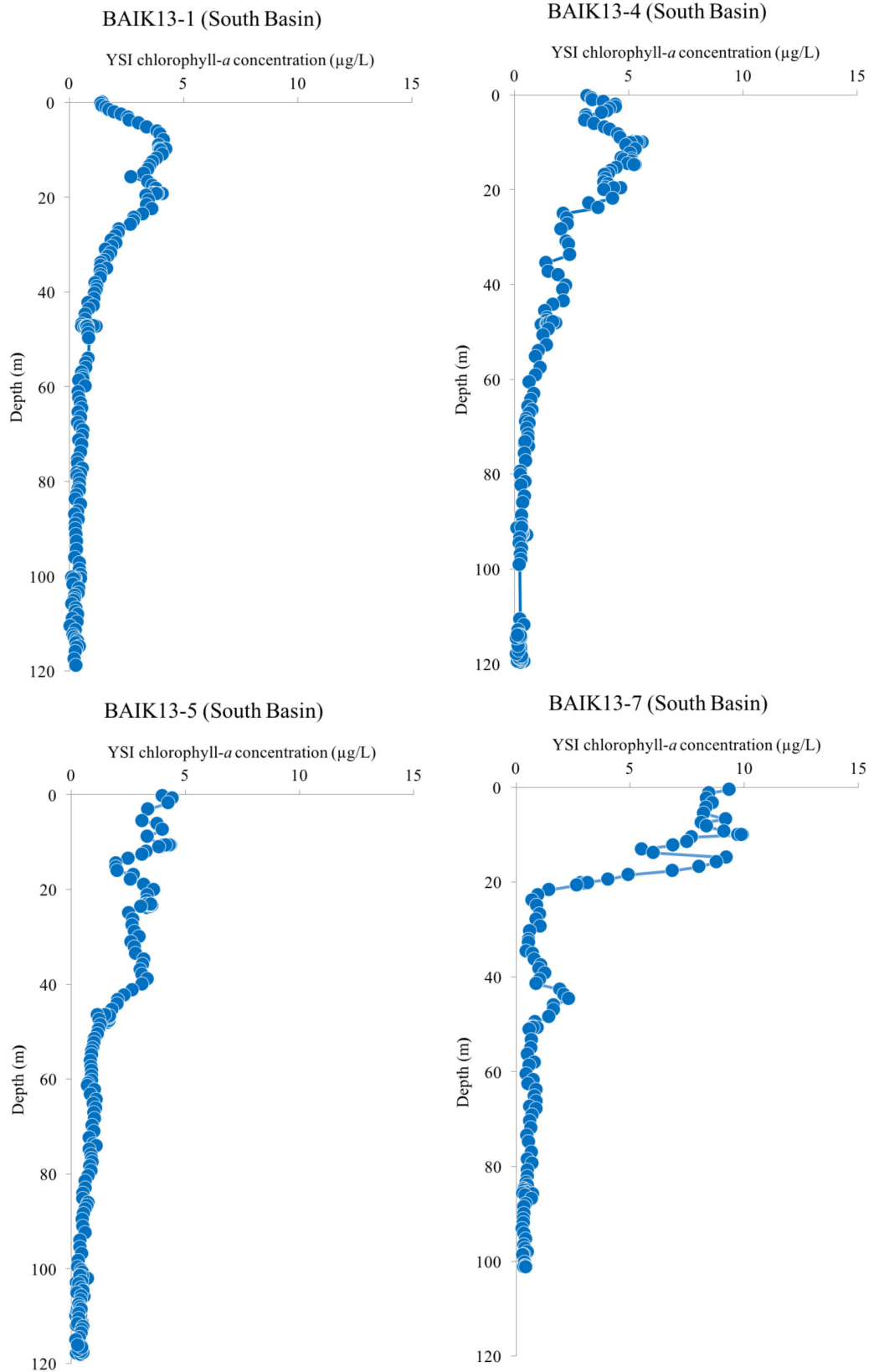


Figure 58: YSI chlorophyll-*a* concentrations ($\mu\text{g/L}$) showing the DCM profiles in the South basin. Sites which do not exhibit a distinct DCM (BAIK13-1, BAIK13-4, BAIK13-5 and BAIK13-7) are still presented.

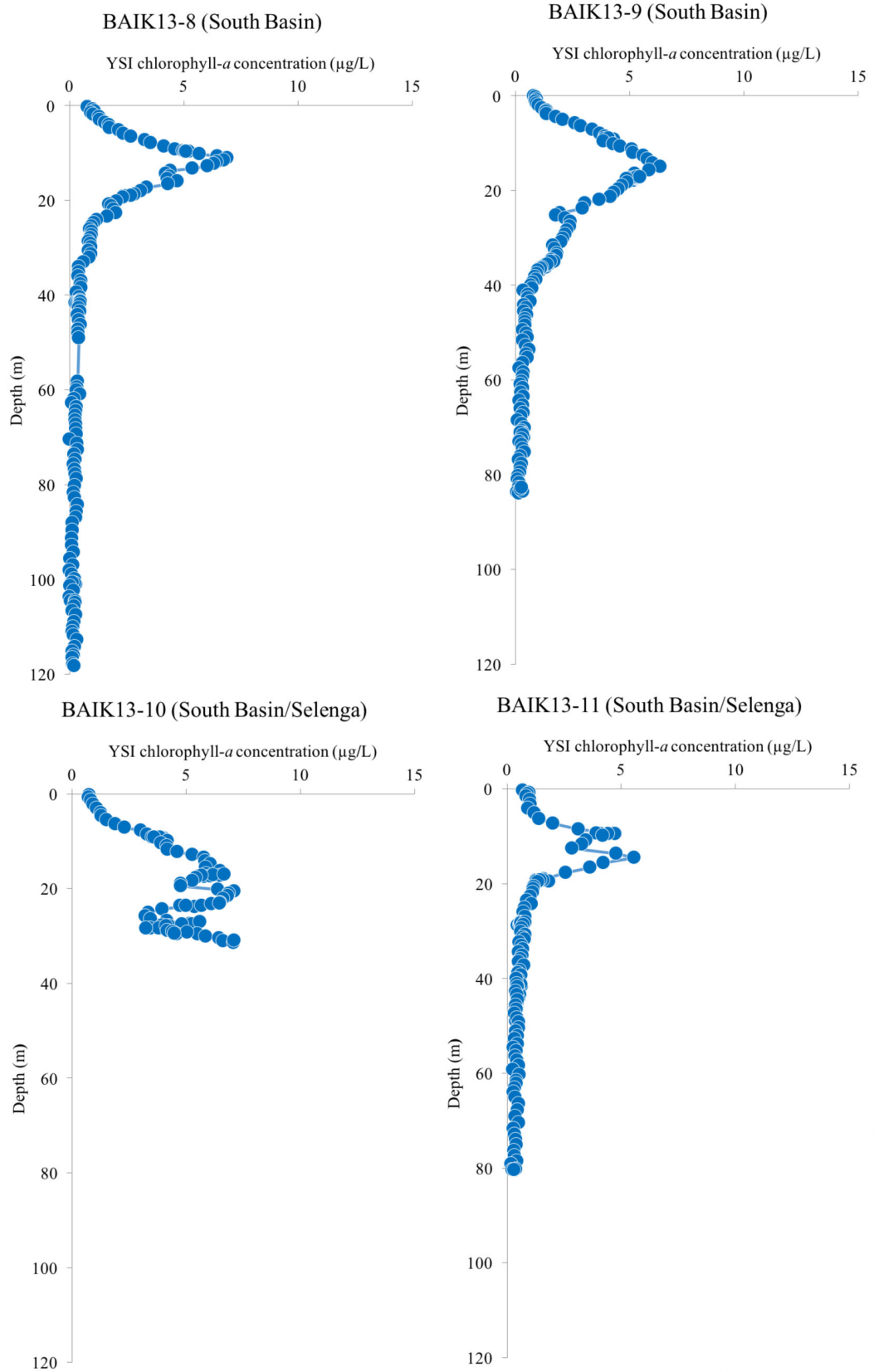


Figure 59: YSI chlorophyll-*a* concentrations (µg/L) showing the DCM profiles in the South basin. A site which does not exhibit a distinct DCM (BAIK13-10) is still presented.

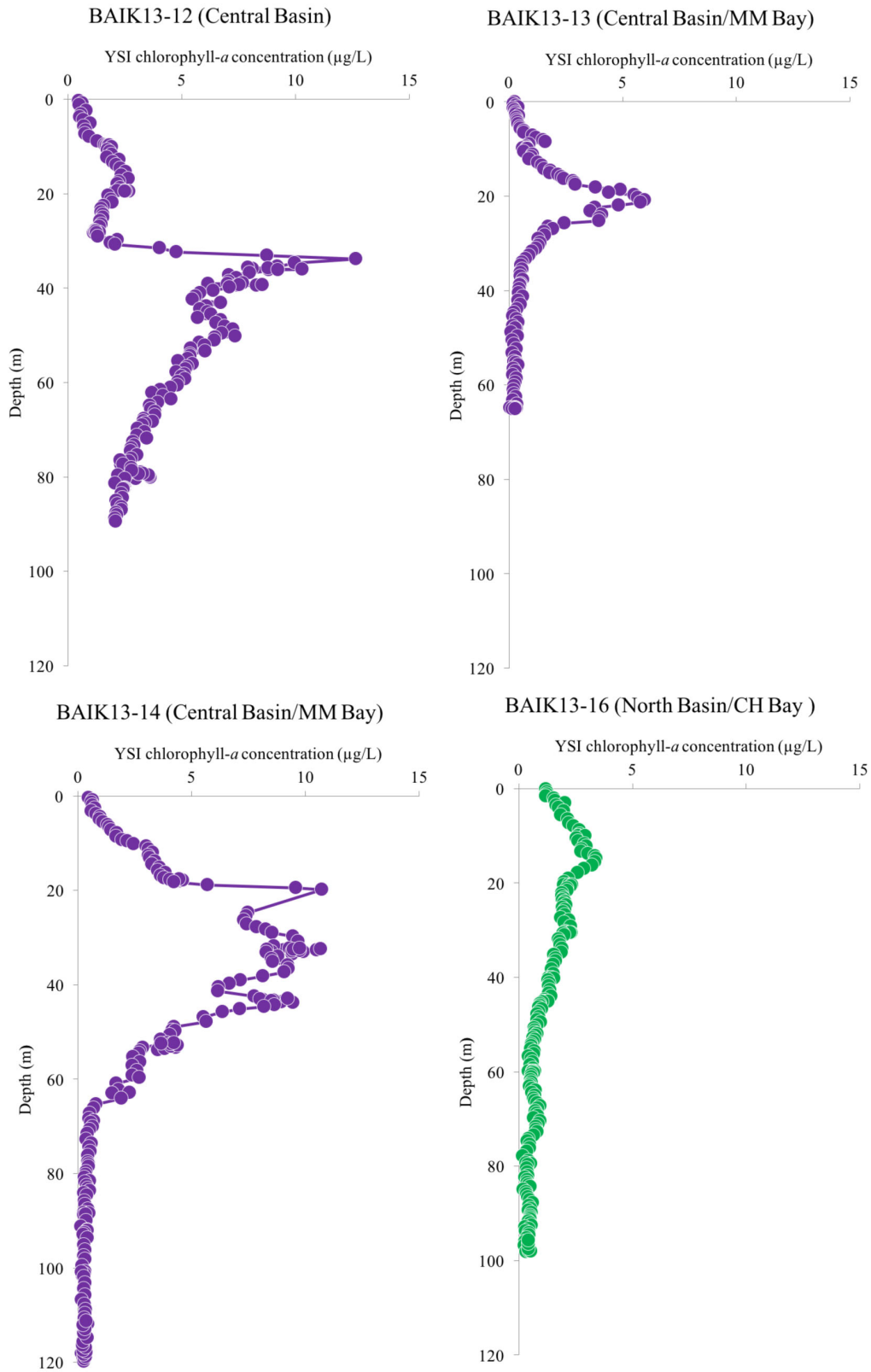


Figure 60: YSI chlorophyll-*a* concentrations (µg/L) showing the DCM profiles in the Central basin, Maloe More Bay (MM) and Chivsky Bay (CH) in the North basin.

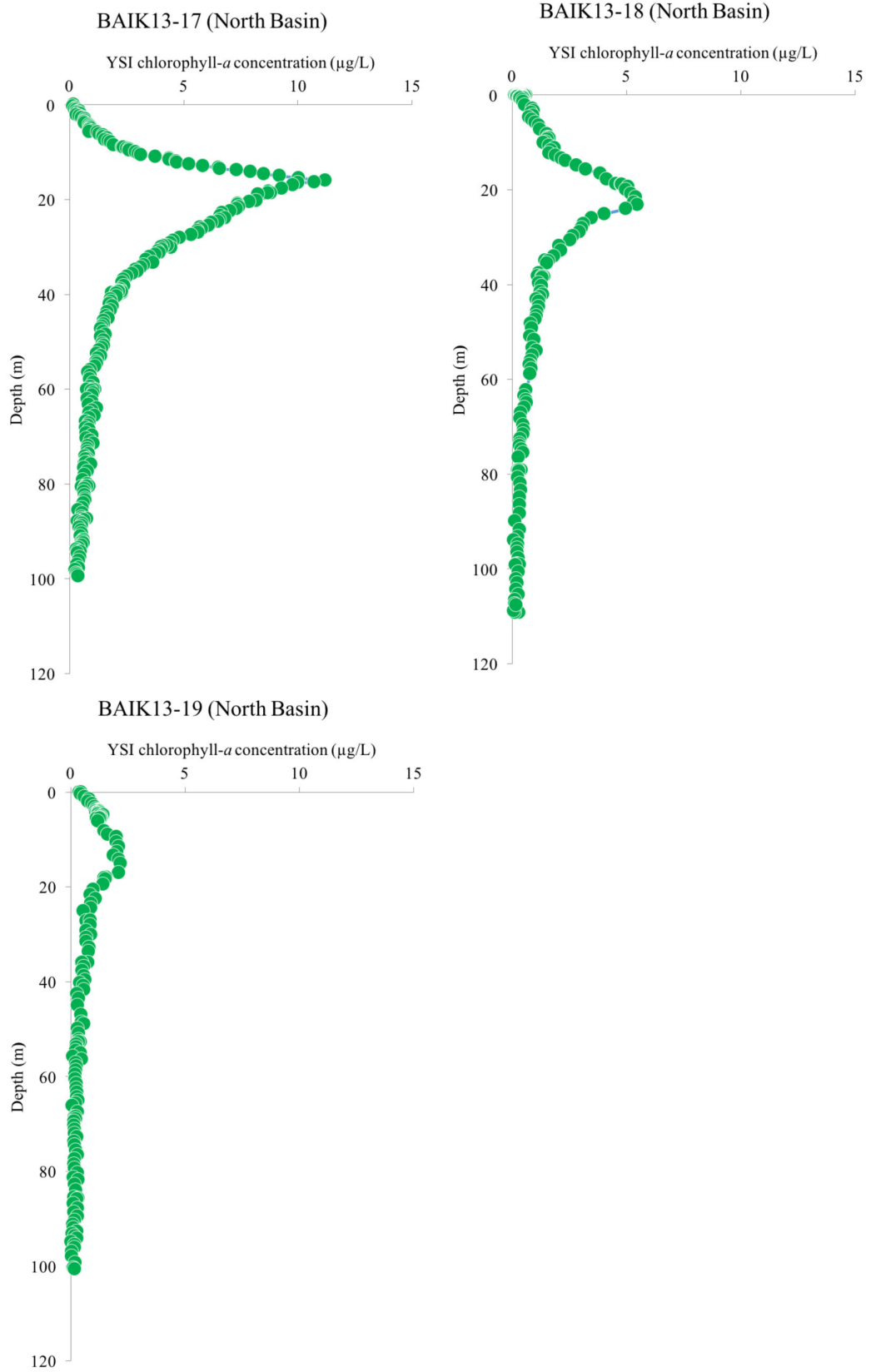


Figure 61: YSI chlorophyll-*a* concentrations ($\mu\text{g/L}$) showing the DCM profiles in the North basin.

Table 23: DCM layer thickness within the South, Central and North basins sampled in August 2013.

	Site	DCM layer			Average chl concentration (ug/L)
		Min depth (m)	Max depth (m)	Thickness (m)	
South basin	BAIK13-1	0	37	37	2.97
	BAIK13-4	0.2	43.5	43.3	4.07
	BAIK13-5	0.3	46.5	46.2	2.92
	BAIK13-7	0.5	20.7	20.2	7.34
	BAIK13-8	2.4	24.1	21.7	3.62
	BAIK13-9	4.4	35	30.6	3.39
	BAIK13-10	9.9	30.9	21	5.24
	BAIK13-11	2.3	24	21.7	2.53
Central basin	BAIK13-12	31.5	79.7	48.2	5.45
	BAIK13-13	7.1	32.5	25.4	2.3
	BAIK13-14	10.7	52.4	41.7	6.57
North basin	BAIK13-16	0.1	45	44.9	2.02
	BAIK13-17	9	39.5	30.5	5.26
	BAIK13-18	2.8	58.8	56	2.03
	BAIK13-19	8.9	17	8.1	1.97

Table 24: Zeaxanthin and fucoxanthin pigment concentrations at the DCM layer in the South, Selenga, Central, Maloe More and North basin sites in August 2013.

	Site	Zeaxanthin conc. (nmol/L)	Fucoxanthin conc. (nmol/L)
South	BAIK13-1	0.64	0.00
	BAIK13-4	1.71	0.00
	BAIK13-5	1.34	0.00
	BAIK13-7	1.77	0.00
	BAIK13-8	1.74	0.00
	BAIK13-9	1.17	0.00
Selenga	BAIK13-10	0.72	0.69
	BAIK13-11	1.68	0.00
Central	BAIK13-12	(-)	0.28
Maloe More	BAIK13-13	0.51	0.44
	BAIK13-14	(-)	0.63
North	BAIK13-16	0.42	0.32
	BAIK13-17	0.50	0.36
	BAIK13-18	0.60	0.44
	BAIK13-19	0.04	0.05

DCM across Lake Baikal in previous spatial surveys show different profiles (*Figure 65*), with DCM at 20 – 30 m in the South basin, 10 – 15 m at the Selenga, 15 m in the Central basin and no clear peak observed in the North basin (Nakano et al. 2003; Fietz et al. 2005). The peak in the chlorophyll-*a* concentrations range from 4 – 10 µg/L in the South basin, 7 µg/L at the Selenga, 3.5 µg/L in the Central basin, and 2 - 11 µg/L in the North basin. In comparison to previous studies, the August 2013 concentrations are higher, with values in the South, Selenga inflow, Central and North basin ranging between 1.25 – 1.5 µg/L, 2 – 3 µg/L, 3.5 µg/L and

0.5 – 0.6 µg/L respectively (Nakano et al. 2003; Fietz et al. 2005). In 2002/2003 the DCM reached deeper positions in the water column in the South basin, between 20 – 30 m, whereas in the North basin chlorophyll-*a* concentrations were relatively homogenous down the profile, with no clear peaks (Fietz et al. 2005). The DCM was positioned within the mixing layer in the South basin sites, and this chlorophyll-*a* concentration was higher than at all the nearshore sites (Fietz et al. 2005). Similar to the South basin sites, the DCM within the Central and North basin sites were found within the mixing layer (Fietz et al. 2005). Diatoms and chrysophytes were the major contributors to the total chlorophyll-*a*, except in the South, which largely comprised of chlorophytes (Fietz et al. 2005), and these regional trends are suggested to have been driven by temperature and stratification (Fietz et al. 2005). The August 2013 pigment data shows that since 2001-2003 there has been a shift from the South basin mixing layer waters being largely dominated by chlorophytes (Fietz et al. 2005), to picocyanobacterial pigments (*Figure 67; Figure 68*).

5.3.4 Distribution of phytoplankton pigments

PCA of pigment datasets in the mixing layer show that the highest pigment concentrations (carotenoids and chlorophylls) lie within the South basin and Selenga Delta sites, except for site BAIK13-1 in the South basin (*Figure 64*). The patterns are less distinct down the water column, with no distinct distribution of pigments amongst regions. The dominant carotenoids detected within the mixing layer were zeaxanthin (cyanobacteria), fucoxanthin (diatoms and chrysophytes), peridinin (dinoflagellates) and lutein (chlorophytes) (*Figure 62; Figure 63*). Other carotenoids (not presented) were also detected in lower concentrations including neoxanthin and violaxanthin (chlorophytes), alloxanthin (cryptophytes), diadinoxanthin (diatoms) and β-carotene. The highest concentrations of chlorophylls and carotenoids were found in the South basin sites (*Figure 62; Figure 63*). Mean mixing layer zeaxanthin concentrations in the South basin were 0.98 nmol/L, being higher compared with the Central and North basin sites (0.33 and 0.6 nmol/L respectively) (*Figure 62; Table 25; Table 26; Table 27*). Concentrations of fucoxanthin were significantly higher in the South than North basins (p value = < 0.01) with fucoxanthin concentrations in the South basin (0.38 nmol/L) being double those in the North (0.18 nmol/L) (*Figure 62; Table 25; Table 26; Table 27*). Lutein concentrations within the mixing layer were not significantly different between the three basins, despite higher values observed within the South basin site, reaching concentrations of 0.22 nmol/L, and average mixing layer concentrations of 0.11 nmol/L in the South basin compared to 0.02 nmol/L and 0.03 nmol/L in the Central and North basin respectively (*Figure 63*).

Table 25: Results from normality tests, ANOVA, and KW tests performed on mixing layer pigment datasets.

	Normality Test	P value	ANOVA P value	K-W Chi Squared	K-W P value
Zeaxanthin	0.846	< 0.001	(-)	21.137	< 0.001
Fucoxanthin	0.929	0.006	< 0.001	(-)	(-)
Lutein	0.970	0.177	0.667	(-)	(-)
Chl- <i>a</i>	0.950	< 0.001	(-)	199.879	< 0.001

Table 26: P values presented from post hoc tests which indicate if there is any significant difference in concentrations between the South, Central and North basins.

	S-N	S-C	C-N
Zeaxanthin	0.056	< 0.001	0.052
Fucoxanthin	< 0.001	< 0.001	0.226
Lutein	0.729	0.946	0.719
Chl- <i>a</i>	< 0.001	< 0.001	0.990

Table 27: Mean concentrations mixing layer HPLC pigments (nmol/L) (fucoxanthin, lutein and zeaxanthin) and YSI chlorophyll-*a* (nmol/L) data in the South, Central and North basins.

	South	Central	North
Zeaxanthin	0.98	0.33	0.59
Fucoxanthin	0.38	0.14	0.18
Lutein	0.11	0.02	0.03
Chl- <i>a</i>	3.42	1.02	1.46

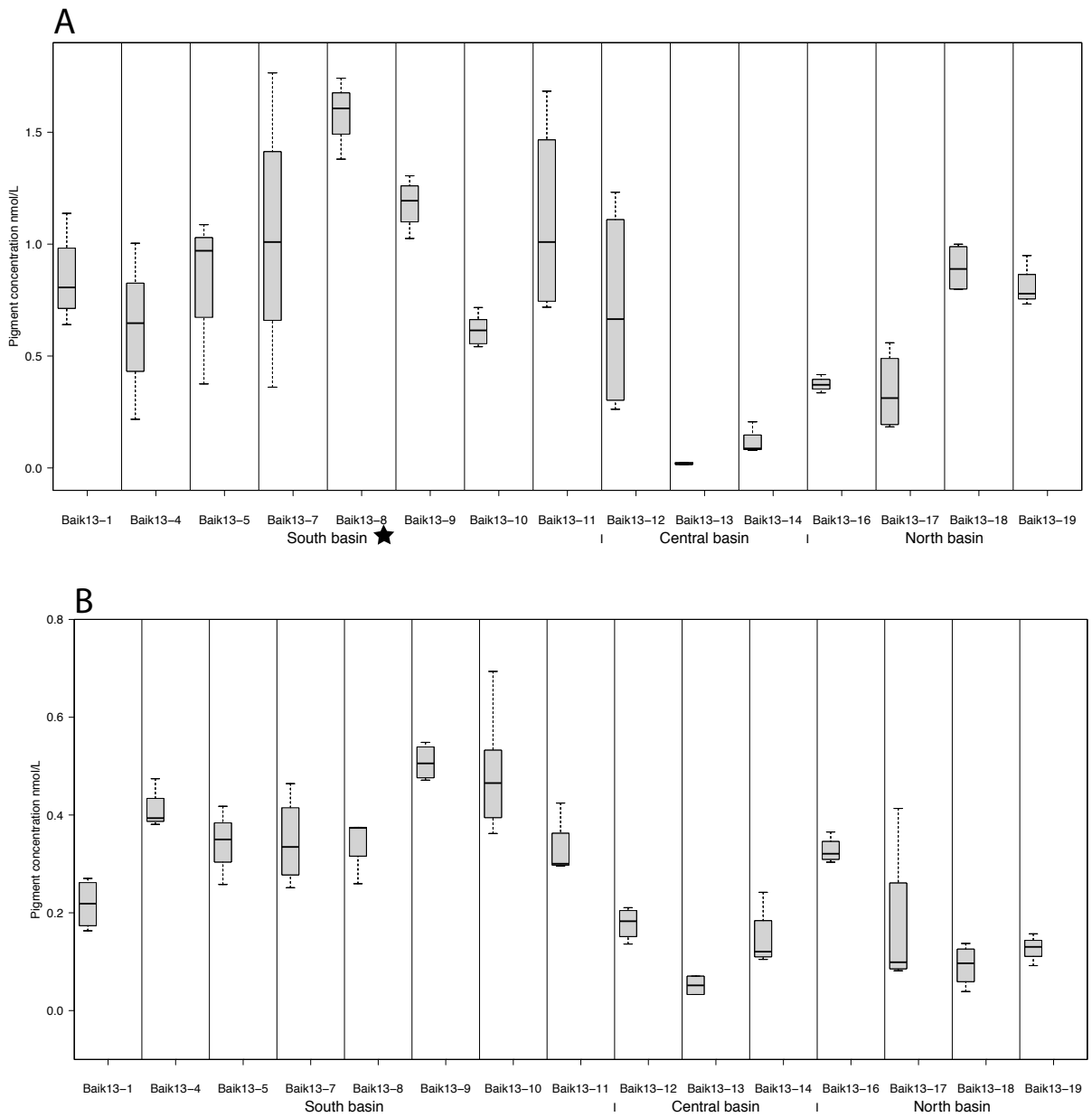
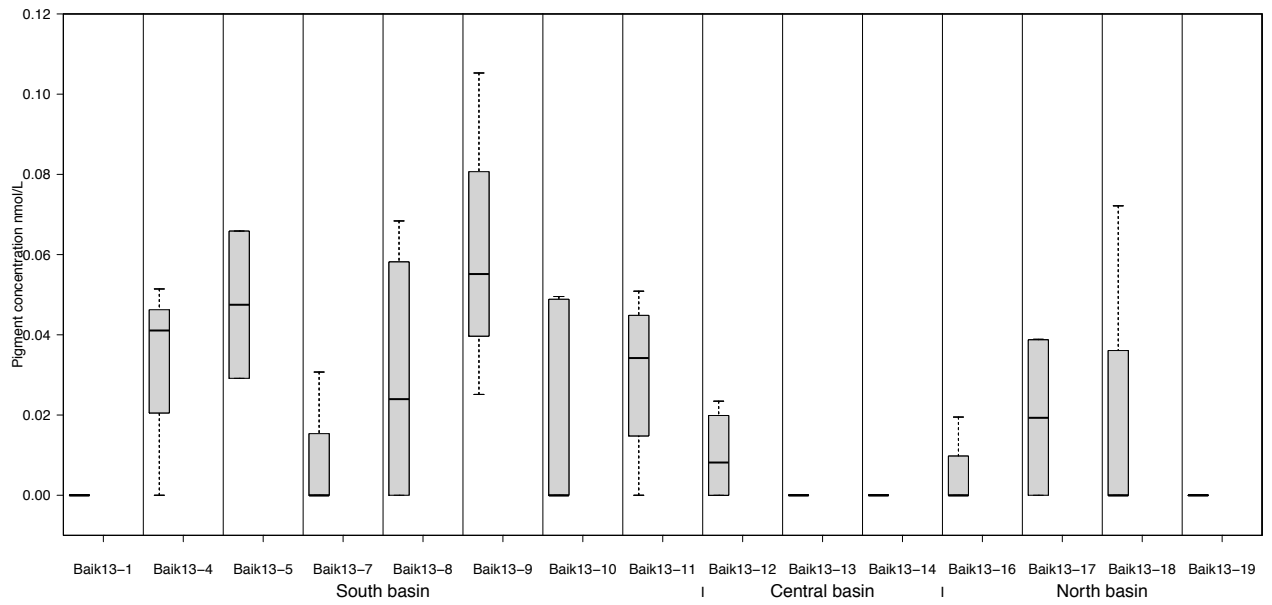


Figure 62: Mean phytoplankton pigment concentrations within the mixing layer; (A) zeaxanthin (cyanobacterial biomarker), (B) fucoxanthin (diatom and chrysophyte biomarker). South basin zeaxanthin concentrations are significantly different to the Central basin (black star).

A



B

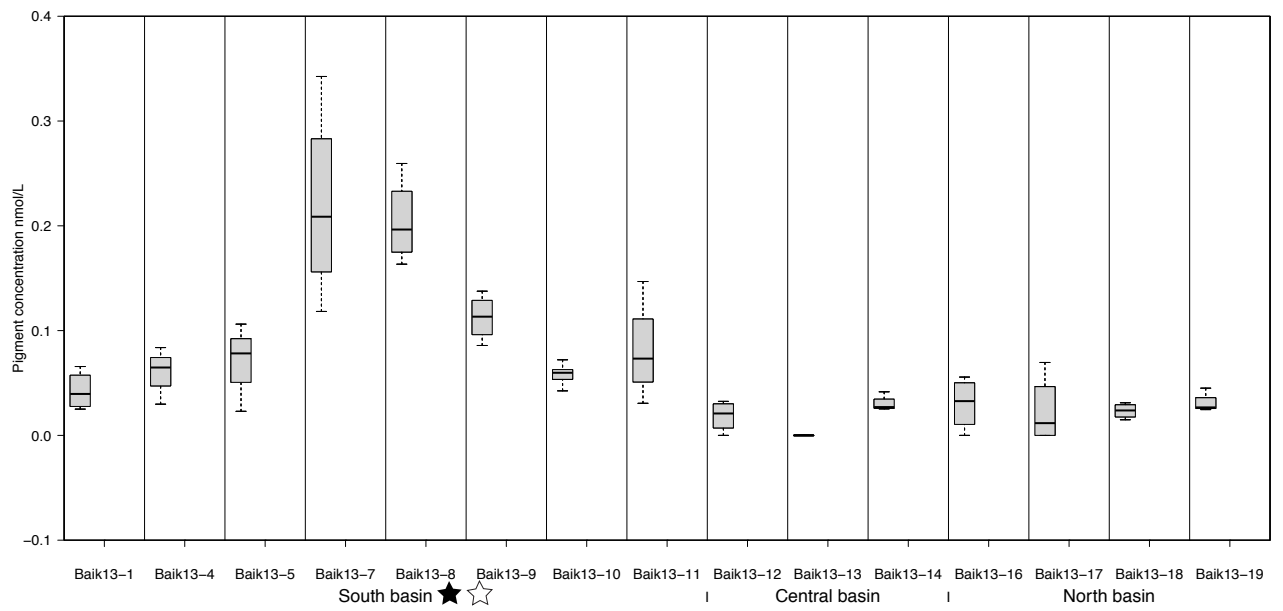


Figure 63: Mean phytoplankton pigment concentrations within the mixing layer; (A) Peridinin (dinoflagellate biomarker) and (B) lutein (chlorophyte biomarker).

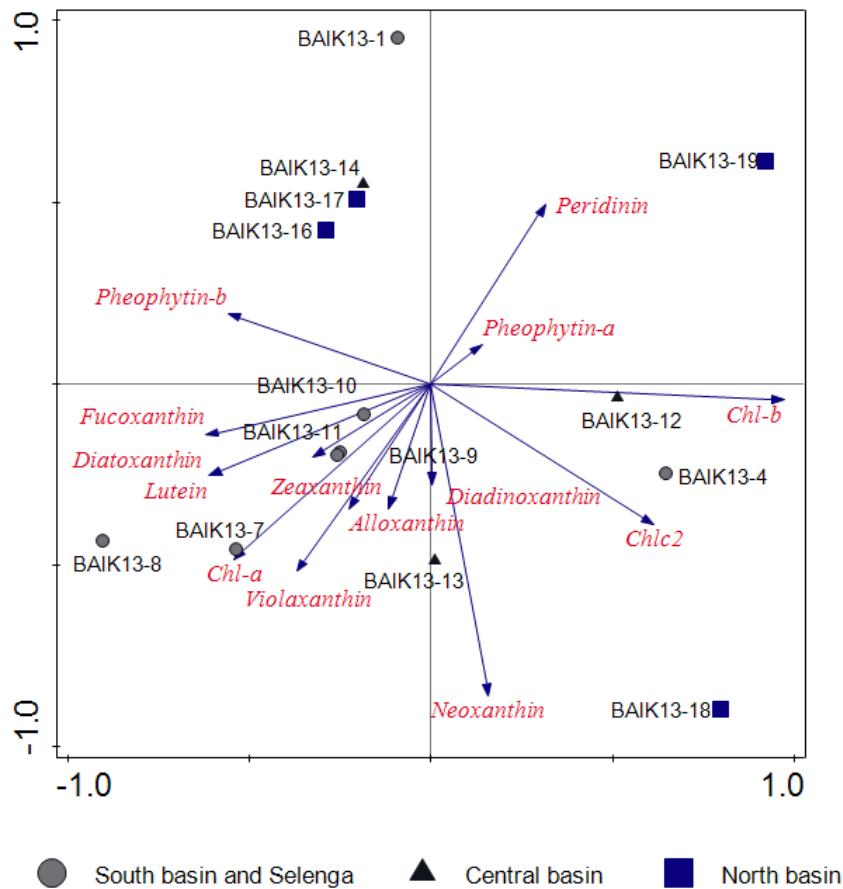


Figure 64: PCA of mean pigment concentrations in the mixing layer and each site.

In comparison to past limnological measurements taken in July 2001 – 2003 by Fietz et al. (2005), YSI chlorophyll-*a* concentrations within the mixing layer are greater in August 2013 than fluorometric chlorophyll-*a* concentrations measured in June 2001 – 2003 within the South, Selenga, Central and North basin sites. Chlorophyll-*a* concentrations increase from c. 1.5 nmol/L to c. 4.8 nmol/L, and from c. 2.4 nmol/L to c. 5.1 nmol/L in the South basin and Selenga Delta sites respectively (Figure 65). Central and North basin sites show a smaller magnitude of increase, and Maloe More shows a large decrease in chlorophyll-*a* concentrations, from c. 6.1 nmol/L to c. 1 nmol/L, within the mixing layer (Figure 65). At the DCM, chlorophyll-*a* concentrations are also higher in August 2013 than June 2001 – 2003, in the South basin, Central basin and North basin sites, including Maloe More (Figure 65). Chlorophyll-*a* concentrations at the DCM increase by more than two-fold within these regions, with concentrations between c. 0.5 – 6 µg/L in 2001-2003 and between c. 2 – 12.5 µg/L (Figure 65). Alongside changes in concentrations, the position of the DCM in the water column has deepened within the Central, Maloe More and North basin sites to depths > 40 m

(*Figure 66*). DCM within the South basin has remained similar, although the range has increased from c. 30 – 45 m to c. 20 – 48 m. Mixing layer depths have become shallower in the South basin and Maloe More sites, with ranges between c. 10 – 20 m to c. 4 – 24 m between 2001-2003 and 2013 respectively in the South basin, and a decrease in mixing depths from c. 30 m to 5 – 8 m in Maloe More (*Figure 66*). Fucoxanthin and zeaxanthin pigment concentrations show changes over this period at certain regions within the lake. Fucoxanthin concentrations within the mixing layer declined from c. 0.5 – 2 nmol/L to < 0.25 nmol/L in Maloe More, and from c. 0.25 – 0.75 nmol/L to < 0.8 nmol/L in the North basin sites (*Figure 67*). Zeaxanthin concentrations within the mixing layer increased from c. 0.3 – 0.75 nmol/L to 0.6 – 1.6 nmol/L in the South basin, c. 0.1 – 0.3 to 0.7 nmol/L in the Central basin and c. 0.1 nmol/L to 0.3 – 0.9 nmol/L in the North basin sites (*Figure 67*). Lutein concentrations are lower in August 2013 than previous measurements in 2001-2003 (Fietz, 2005), with lower mixing layer values in the Selenga, Maloe More, Central and North basin sites (*Figure 68*). The range of lutein concentrations within the South basin varies from c. 0.15 – 0.2 nmol/L in 2001-2003 (Fietz, 2005) to c. 0.04 – 0.22 nmol/L (*Figure 68*).

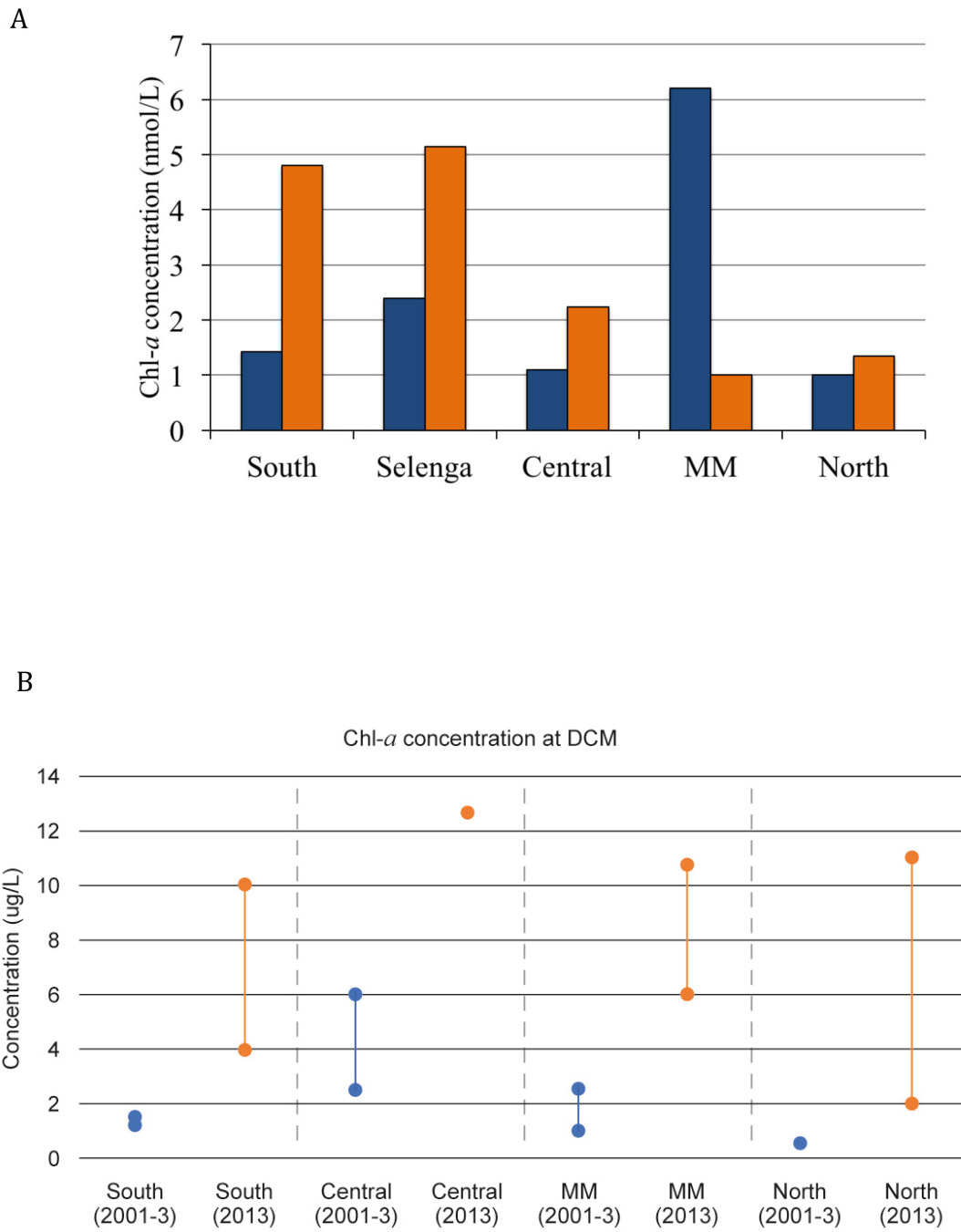


Figure 65: Comparison between results from this study (2013) and past measures between 2001 – 2003 (Fietz et al. 2005) of (A) mean range of chlorophyll-a concentrations; (B) mean range of YSI chlorophyll-a concentrations at the deep chlorophyll maxima across the three basins.

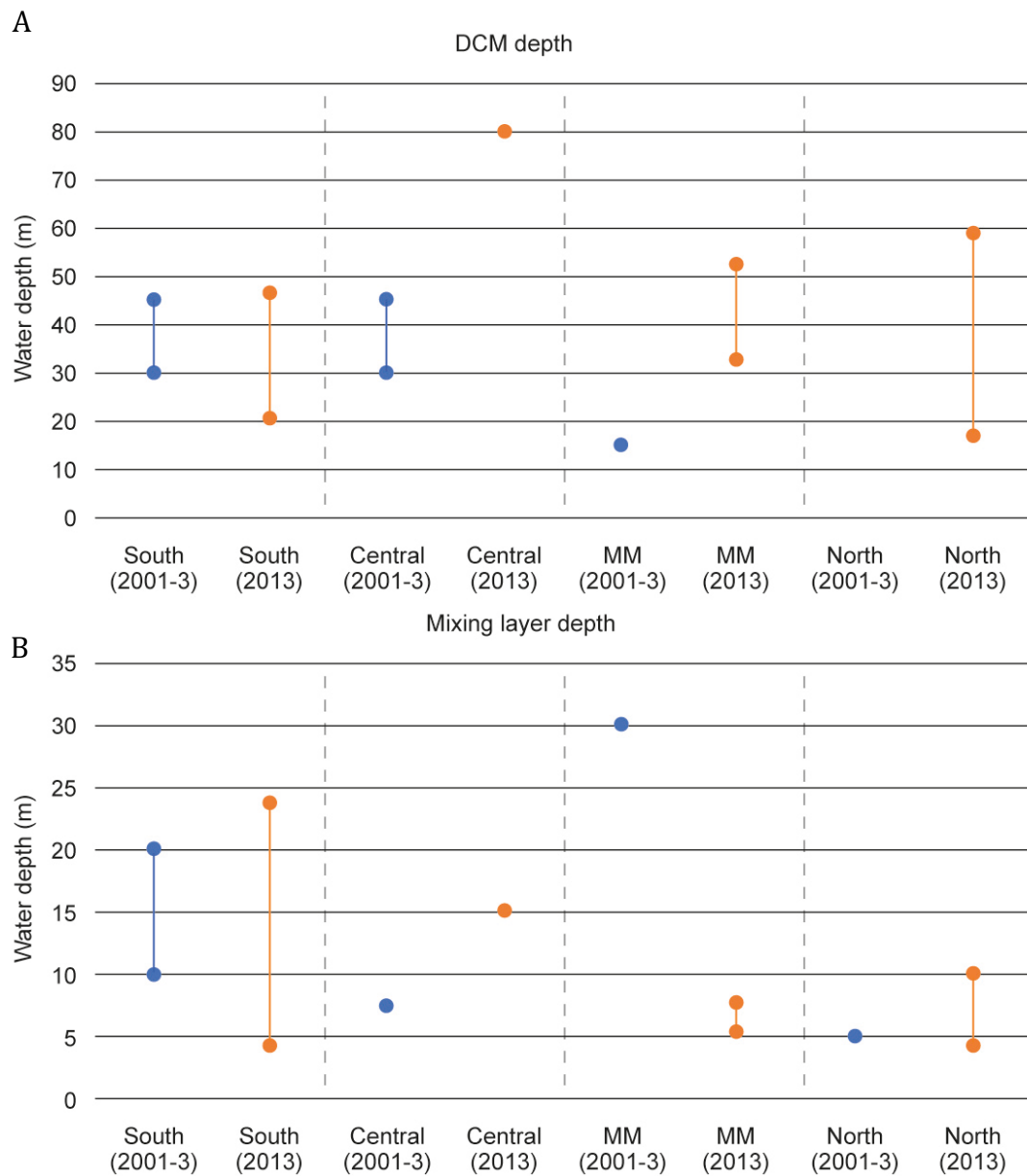


Figure 66: Comparison between results from this study (2013) and past measures between 2001 – 2003 (Fietz et al. 2005) of (A) deep chlorophyll maxima depth; (B) mixing layer depth across the three basins.

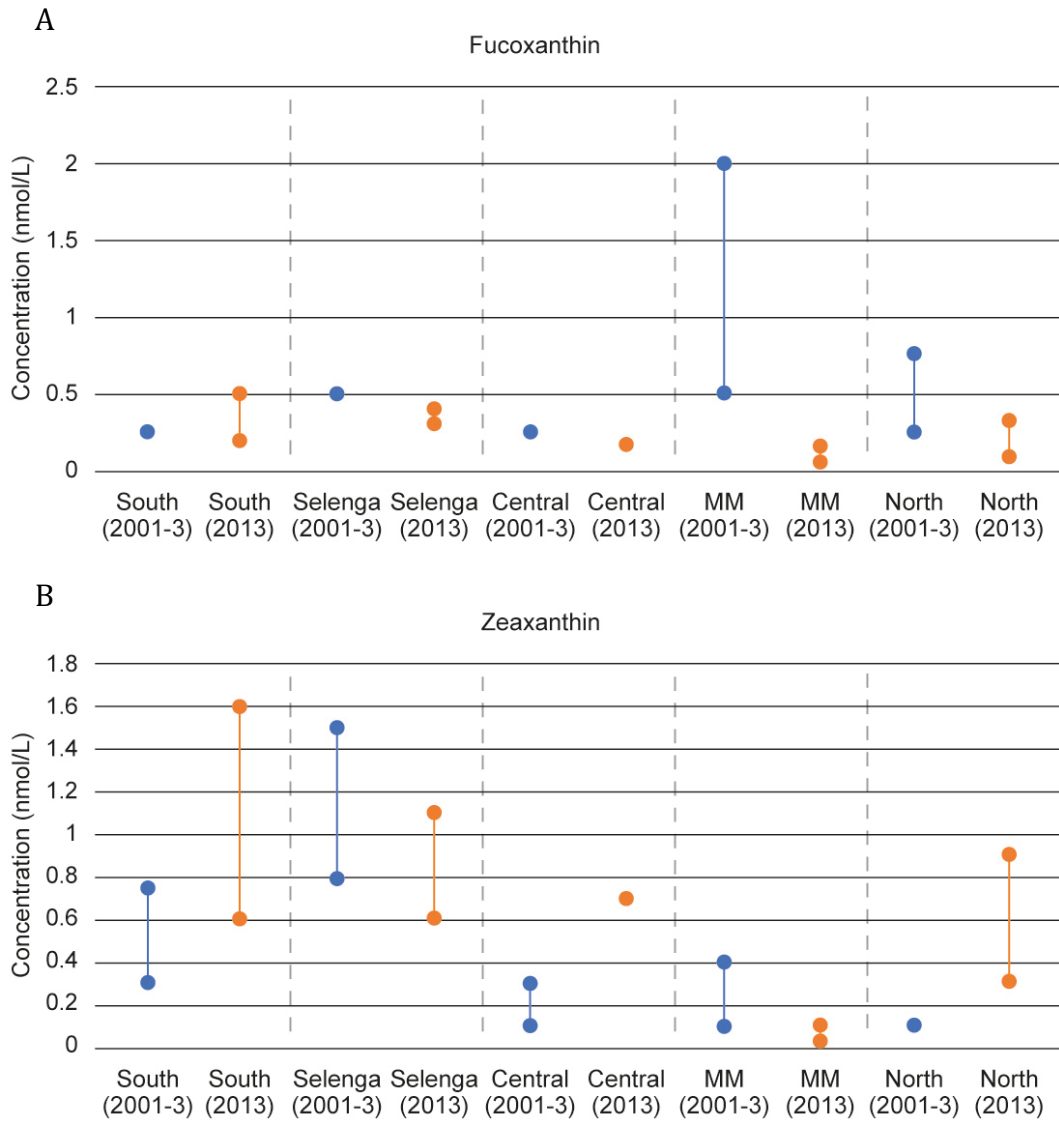


Figure 67: Comparison between results from this study (2013) and past measures between 2001 – 2003 (Fietz et al. 2005) of (A) fucoxanthin concentrations (nmol/L) and (B) zeaxanthin concentrations (nmol/L) across the three basins.

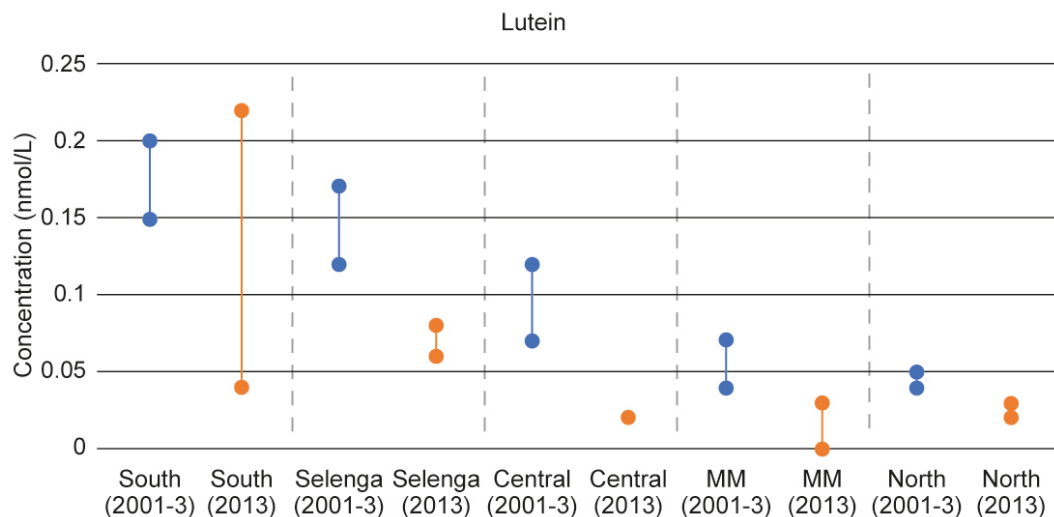


Figure 68: Comparison between results from this study (2013) and past measures between 2001 – 2003 (Fietz et al. 2005) of lutein concentrations (nmol/L) across the three basins.

5.3.5 Correlations between phytoplankton pigments and physico-chemical variables

Relationships between limnological (physical and chemical) variables and phytoplankton pigments within the mixing layer were explored via PCA methods to understand the distribution of pigments across the lake. From the RDA results, limnological variables (temperature, conductivity, pH, dissolved oxygen, oxidation-reduction potential and light attenuation coefficient) were not correlated with the phytoplankton pigment assemblages within the mixing layer across the basins. Similarly, nutrient concentrations (TP, silicate, nitrate and major ions) were not significantly correlated with total algae and carotenoids. DOC concentrations show a relationship with the pigment distribution, as inferred from the RDA analyses (p value = 0.02) using forward selection with Monte Carlo permutation tests (Figure 69). There is likely to be autocorrelation within these datasets, however the DOC concentrations appear to be related to picocyanobacteria (zeaxanthin) pigment. This trend suggests higher DOC concentrations are found alongside lower zeaxanthin pigment concentrations in the mixing layer ($R^2 = 0.41$, p value = 0.01) (Figure 70). DOC concentrations do not show a strong relationship with other pigments. Light attenuation coefficients show a positive correlation with total algae (Chl-*a*) ($R^2 = 0.28$, p value = 0.05) and no correlation with DOC concentrations ($R^2 = 0.04$, p value = 0.46).

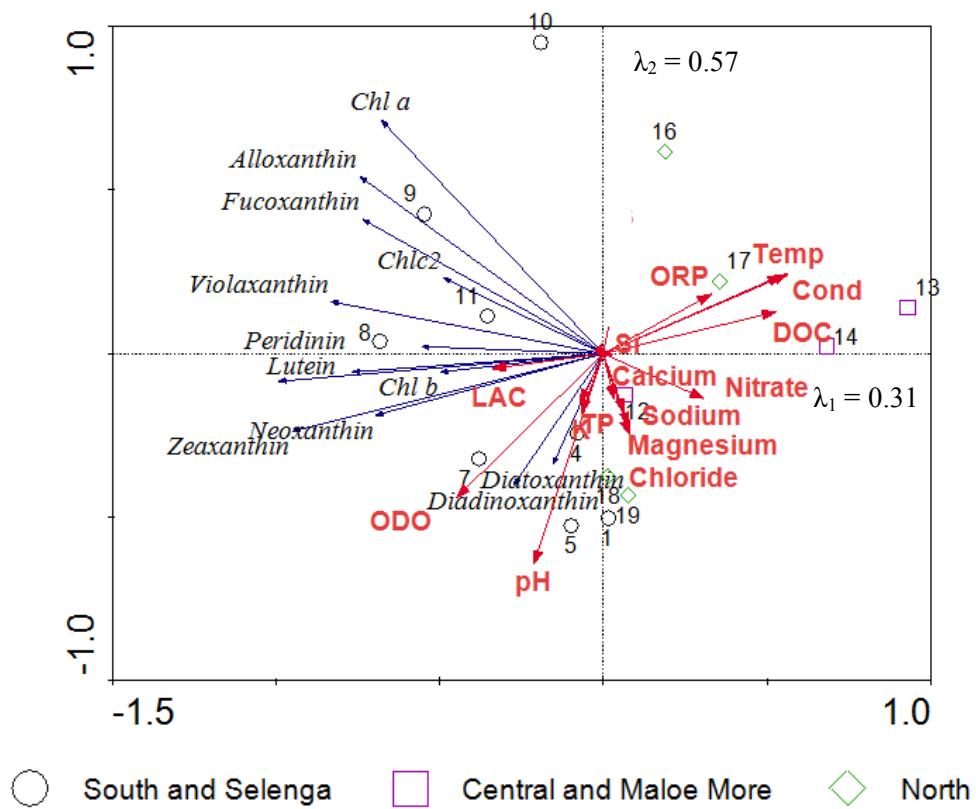


Figure 69: Results from RDA between average mixing layer limnological variables (physical and chemical) and phytoplankton pigments using forward selection with Monte Carlo permutation tests. DOC is the only environmental variable which is significantly correlated with the algal pigments (p value = 0.02). (ODO – dissolved oxygen, ORP – redox potential, LAC – light attenuation coefficient).

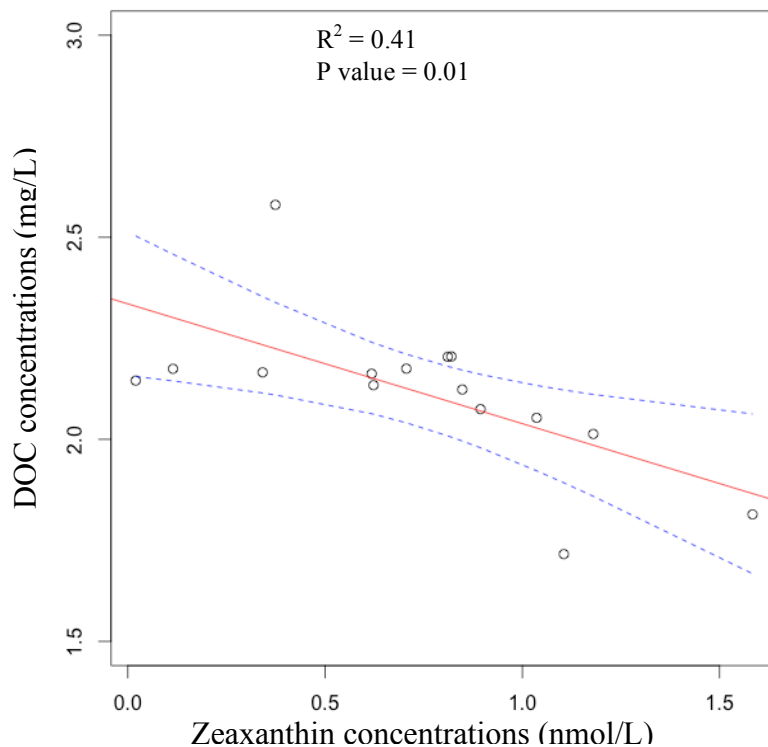


Figure 70: Regression correlation with 95% confidence regression lines between mixing layer DOC and zeaxanthin concentrations.

5.4 Discussion

5.4.1 Increased algal production in the mixing layer over the last decade

Picocyanobacteria (zeaxanthin pigment), diatom and chrysophytes (fucoxanthin pigment) and chlorophytes (lutein pigment) were the major algal groups detected within the August 2013 waters. Algal group assemblages, as inferred from pigments, shows differences between the August 2013 and 2001-2003 compositions from Fietz et al. (2005). The South basin, Selenga Shallows, Central basin, Maloe More and North basin mixing layer waters show higher concentrations of lutein (chlorophyte pigment) in July 2001-2003 than August 2013. Higher concentrations of zeaxanthin were found in the South basin, Central basin and North basin in August 2013 than July 2001 – 2003. Fucoxanthin concentrations are only higher in the South basin in August 2013 than July 2001- 2003. The difference in diatom pigment concentrations within the mixing layer over the last decade could be due to changes in the vertical distribution of algae, and therefore greater abundances of diatom forming below the mixing layer at the DCM in August 2013 compared to July 2001 – 2003. Higher picocyanobacteria pigments

could be a result of lake warming and stronger thermal stratification, although it is unclear why there is less chlorophyte pigment in the pelagic waters in August 2013 compared to July 2001 – 2003. Both the 2001-2003 July and August 2013 surveys found that the South basin has higher abundances of pigments, which is likely to be a result of earlier ice-break up within the South basin than the North basin, and the Selenga River influences the earlier onset of thermal stratification within the South basin.

Our 2013 study of summer-time autotrophic production confirmed the continued increase of chlorophyll-*a* concentrations in the South basin over recent decades. The largest difference in chlorophyll-*a* concentrations between the 2001/2003 (Fietz et al. 2005) and 2013 values was in the South basin and Maloe More (*Figure 65*). The South basin mixing layer chlorophyll-*a* concentrations increase by 2-fold, whereas, there is a decrease in the mixing layer chlorophyll-*a* concentrations in Maloe More by 6-fold (*Figure 65*). This is due to changes in the depth distribution of algae, as the DCM at Maloe More is deeper in 2013, and the mixing layer depth is c. 22 m shallower, compared to in 2002/2003 (*Figure 66*). The South basin has continued to be more productive than the Central and North basin. Mean summer (July/August) chlorophyll-*a* concentrations in the upper 50 m of the water column have increased in the South basin, from 0.5 µg/L to 1.6 µg /L between 1980 - 2005. This trend has continued with average mixing layer chlorophyll-*a* concentrations in the South basin of 3.8 µg /L in 2013 (this study). Lake-wide chlorophyll-*a* increases have also been found at Lake Baikal between 1977 and 2003, from 0.82 to 1.20 µg /L (Izmesteva et al. 2016). However, although this increasing trend was seen in all three basins, only the South basin showed a significant increase in chlorophyll-*a* (Izmesteva et al. 2016). Mean YSI chlorophyll-*a* concentrations in the South basin mixing layer in August 2013 are higher than the interannual variability of chlorophyll-*a* concentrations between 1979 and 2003 (Moore et al. 2009).

The largest fucoxanthin concentrations in the summer mixing layer were found in the South basin (*Figure 62*) and from sediment traps diatom populations at BAIK13-1 consisted largely of smaller more competitive species, namely *Synedra acus* (Panizzo et al. 2016). *Synedra acus* is one of the fastest growing planktonic diatoms in Lake Baikal (Jewson et al. 2015) which blooms under the ice and as ice breaks up (Izmest'eva et al. 2006). Below silicate values of 0.5 mg/L diatoms lose the ability to reproduce effectively (Jewson et al. 2010), and the average silicate concentrations within the South, Central and North basins in August 2013 were 0.6, 0.5 and 0.7 mg/L respectively (*Figure 49*). Low Si concentrations within the summer mixing layer can be explained by the sinking out of silica into the bottom waters, leaving only a small proportion of silica recycled in the mixing layer (Müller et al. 2005). Therefore, during summer stratification non-siliceous autotrophic picoplankton dominate the algal production

within the mixing layer, and diatoms are re-established in the water column by convective mixing in autumn and spring (Jewson et al. 2010). August 2013 pigment data in the South and North basin support this, as picocyanobacteria dominate the mixing layer as shown from the zeaxanthin pigment concentrations, which are more than double the fucoxanthin (diatom pigment) and lutein (chlorophyte pigment) concentrations (*Figure 62; Figure 63*). In Maloe More and the Selenga Shallows, mixing layer concentrations of zeaxanthin and fucoxanthin are similar (*Figure 62*). This could be a result of different mixing within the pelagic deep basins and shallower regions, such as Maloe More and the Selenga Shallows. The greatest zeaxanthin concentrations were detected in the mixing layer of the South basin, than the Central and North basins. Results show that higher zeaxanthin concentrations within the South basin than the Central and North basin, is not due to nutrient availability, as the concentrations of total phosphorus and silicate are not significantly higher within the South basin mixing layer compared to the Central and North basin. Thermal stratification is also not a factor explaining higher zeaxanthin concentrations within the mixing layer, as the mixing layer depth is not deeper within the South basin compared to the Central and North basin.

Diatom and picocyanobacterial abundance in the mixing layer has also increased over the last 10 years in the South basin; concentrations of fucoxanthin and zeaxanthin increasing from 0.25 – 0.37 nmol/L and 0.5 - 0.98 nmol/L respectively (*Figure 67*). This could be a result of changes in the ice cover dynamics, with earlier ice break up in the South basin compared to the North basin, resulting in a longer stratification period to enable the summer phytoplankton assemblages to establish and grow (Hampton et al. 2008). However, this could also be a result of a change in the depth distribution of the algae, as the DCM position is deeper in the Central basin in August 2013, and the mixing layer depths are shallower than in 2001/2002 (*Figure 66*). In Maloe More there are lower concentrations of diatom, picoplankton and chlorophyte pigments in the mixing layer in 2013 than 2001-2003, and again this could be a result of changes in the DCM to deeper positions, with higher concentrations of these algal groups being found below the mixing layer depth. A deeper DCM is a result of greater light penetration through the water column at Maloe More, as shown by the higher light attenuation values at the Maloe More, compared to the pelagic South and North basin. In the North basin, there are fewer diatoms in 2013 than in 2001-2003, but more picoplankton, which could be a result of changes in the ice cover duration, as air temperatures within the Baikal region continue to show an increasing trend over the last decade (Shimaraev and Domysheva, 2013). Therefore, the decrease in diatoms in the mixing layer might be linked to changes in the depth distribution of diatoms with a deeper DCM forming in August 2013.

5.4.2 Depth distributions of algae across the lake and changes in lake functioning over the last decade

The functioning of Lake Baikal over the last decade has changed, due to greater algal biomass in the mixing layer of the South basin, restricting production in the deeper waters. The data suggests that the deeper layers of maximal productivity in some of the Central and North basin sites, compared to the South basin, is a result of lower algal production within the mixing layer. Light attenuation coefficients were positively correlated with chlorophyll-*a* concentrations ($R^2 = 0.28$; p -value < 0.05), and not with DOC concentrations. Thus, phytoplankton biomass may be having a slight influence on light dynamics within the water column, rather than DOC concentrations.

Coloured dissolved organic matter (CDOM) can be an important determinant of light penetration through the water column, such as in boreal lakes (Thrane et al. 2014), alpine and subalpine lakes (Rose et al. 2009a) and North American lakes (Williamson et al. 1996). However, this is not the case in this study, as photodegradation destroys CDOM in Lake Baikal (Sugiyama et al. 2014). Over the last 10 years, the light dynamics within Lake Baikal have changed in the South basin, with secchi depth measurements decreasing from 7 to 4.5 m from 2003 to 2013 (Fietz et al. 2005). This is likely to be a result of increases in phytoplankton biomass since the last spatial survey in 2001-2003, from average concentrations of 1.43 nmol/L (Fietz et al. 2005) to 3.31 nmol/L (this study). This is supported by a recent study (Izmesteva et al. 2016), which found higher secchi transparency, between 1977 to 2003, in both the Central and North basins of Lake Baikal, but not in the South basin as the secchi depth measurements reduced over the 26-year period. This suggests an increase in productivity in the South basin, and a decline in productivity in the Central and North basin (Izmesteva et al. 2016).

Greater light penetration from reduced algal shading, and hence a lower light attenuation coefficient, moves the DCM layer deeper down the water column in Maloe More (BAIK13-14) and the Central basin (BAIK13-12). The DCM extended beyond the photic zone to depths of 52.4 – 79.7 m in all the Central basin sites. The algal cells accumulate at depths with higher nutrient concentrations and lower solar irradiance (Kiefer et al. 1972; Barbiero and Tuchman, 2004; Camacho, 2006). The recruitment of phytoplankton from the surface populations will then limit the rate of nutrient recycling into the mixing layer, and trap algal cells below the thermocline. This is observed at BAIK13-12 in the Central basin, where maximal productivity begins at 31.5 m, which is below the mixing layer depth at 7.5 m. Photoadaptation, which is the adaptation of an organism to changing light levels, has been suggested to play an important

role in the DCM formation at Lake Superior (Barbiero and Tuchman, 2001; Sterner, 2010), where the DCM sits close to the photic zone depth (Watson et al. 1975). However, the dominant mechanisms driving the DCM formation remains unclear in deep lakes such as Lake Baikal, as depth differential zooplankton grazing, photoinhibition of phytoplankton, nutrient distributions and UVR exposure also have an impact (White and Matsumoto, 2012).

Mean chlorophyll-*a* concentrations are greater than the previously published mean values of 1.43 nmol/L in the South basin, and 1.0 nmol/L in the North basin from a spatial survey 10 years ago (Fietz et al. 2005). Alongside increases in production (chlorophyll-*a* concentrations) over the last 10 years (Fietz et al. 2005; Hampton et al. 2008; Moore et al. 2009), this study also found that DOC concentrations, both across the lake and within river waters were greater than previously published values (Yoshioka et al. 2002; Yoshioka et al. 2007; Sugiyama et al. 2014). Mixing layer depths in the South and Central basin are currently shallower than previous surveys, and there is greater autotrophic production than previous surveys, and deeper algal production in the Central and North basin, compared to the South. Over the last 10 years observed disparities in the chlorophyll-*a* concentrations, within the water column and between sites, highlights the differences in algal production between the South and North basins. In comparison with the 2002-2003 spatial survey, the deep chlorophyll maximum was positioned within the mixing layer in the South basin, Central basin and North basin sites, and no deeper-water production was observed in the Central and North basin (Fietz et al. 2005). The data from this study shows that lake functioning has changed in the past 10 years, due to the shift towards shallower DCM positions in the South basin sites, and deeper DCM positions in Maloe More and the North basin sites (*Figure 66*), resulting in higher algal production in deeper waters compared to within the mixing layer (*Figure 57*).

5.4.3 Spatial distribution of nutrients and comparisons with previous measurements

Total phosphorus concentrations

A recent spatial survey which was also conducted in August 2013 (O'Donnell et al. 2017), found TP concentrations Lake Baikal to range between 4.9 to 42.7 µg/L. These values are comparable to some TP concentrations presented in this chapter, which range between 10 to 32 µg/L in the lake waters. O'Donnell et al. (2017) has reported that the above TP measurements agree with those from Votintsev et al. (1995) and Kozhova and Izmeteva (1998). Data collected in the 1990s, however, shows average mixing layer TP concentrations of 2.8 µg/L in the South basin (Liebezeit, 1992; Granina and Sigg, 1995 as cited in Callender et al. 1997a), compared with values of c. 15 µg/L in the South basin in August 2013, presented

in this study (*Figure 49*). Furthermore, TP concentrations measurements of surface waters between 1995 to 2009 range between 0 – 16.2 µg/L in lake waters across the year, with August measurements reaching 7.8 µg/L (Prof. E. Silow, unpublished data) (*Table 22*). TP concentrations of 0 – 16.2 µg/L are suggested to reflect natural variability of nutrients within Baikal's waters (per. comms. Prof. E. Silow). South basin and Central basin TP concentrations presented in this thesis (10.4 – 16.1 µg/L), collected in August 2013, are almost double the August values measured between 1995 – 2009 (7.8 µg/L; Prof. E. Silow unpublished data), but within the range measured by O'Donnell et al. (2017) in 2013 (4.9 – 25 µg/L). The highest TP concentrations presented in this chapter were measured close to the Selenga Delta (20.6 µg/L) and in the North basin (17.8 – 31.5 µg/L), being almost triple the values measured by Prof. E. Silow and slightly higher than values measured by O'Donnell et al. (2017) (15.5 µg/L).

These measurements show only a snap shot in time, and thus it is still not fully known whether the nutrient concentrations at Lake Baikal have remained similar or changed over the last 10 years, due to the lack of TP data available for Lake Baikal and its tributaries. Total phosphorus concentrations, presented in this thesis, in August 2013 show differences between basins, with higher mean mixing layer values in the North basin compared to the South and Central (*Figure 49*). The total phosphorus values measured from all the open lake-water sites in August 2013 were generally less than 25 µg/L, falling within the moderately eutrophic range (Yang et al. 2008). This is higher than expected but is comparable with recent TP measurements published at Lake Baikal (O'Donnell et al. 2017). The largest range and highest TP concentrations in the river inflows are found in the Selenga River waters, between 47 – 211 µg/L, which is similar to recent TP inflow data (2010 – 2012) reported in Sorokovikova et al. (2015), with Selenga River TP values between 18 – 346 µg/L (*Figure 49*). After the Selenga River, the Barguzin River has the next highest concentrations, 67 – 71 µg/L (in this study) and 12 – 181 µg/L (*Figure 49*) (Sorokovikova et al. 2015). However, the values measured in August 2013 are over two-fold higher than those measured by Prof. E. Silow between 1995 – 2009 in Baikal's tributaries (10 - 30 µg/L).

Despite the TP values at Lake Baikal suggesting an increasing trend in lake water concentrations over the last decade, it is important to note that the samples in this chapter are only a snap shot of Baikal's limnology at that time, and it is important to consider any analytical error during the undertaking of TP analyses. With both these considered, the TP measurements taken in August 2013 in this PhD research and by O'Donnell et al. (2017) in the pelagic South basin waters are similar and some measurements fall within the natural variability of TP concentration at Lake Baikal. The results in this chapter therefore highlight

the importance of future monitoring nutrient concentrations at Lake Baikal, to see if rivers and shoreline settlements are enriching the pelagic lake waters in phosphorus concentrations.

Nitrate, sulphate and silicate concentrations

Nitrate, sulphate and silicate concentrations within the lake waters are similar across the three basins in August 2013 (*Figure 49; Table 19*). This is comparable to previous work, as nitrate, sulphate and silicate concentrations measured in 1988 show no variability in concentrations across Lake Baikal or over the last 60 years (Falkner et al. 1991; 1997). Furthermore, in comparison to nitrate concentrations in the South basin (Zilov et al. 2012), the values in the upper 50 m of the water column in August 2013 have remained very similar to those between 1957 and 2008 (*Table 20*). In Lake Baikal's tributaries, measurements taken in 2010 – 2012 (Sorokovikova et al. 2015) show that the nitrate concentrations in the Selenga River are comparable to this study, and higher within the Upper Angara and Barguzin River in August 2013 (*Table 20*). Previous water quality investigations in Baikal's main tributaries from 2010 – 2012 found an increase in sulphate concentrations in the Selenga River waters from the mid-20th century to present day, from 6.2 – 8.6 mg/L to 7.6 – 18.7mg/L (Sorokovikova et al. 2015a; 2015b). In comparison August 2013 results show an average sulphate concentration of 7.36 mg/L in the Selenga River waters, with highest values of 10.4 mg/L. The major ions data from Sorokovikova et al. (2015a) reports the deterioration of the water quality in the Selenga River and in the small tributaries of South Baikal, due to wastewater discharges and atmospheric precipitation pollution. This study confirms these findings, with similar sulphate concentrations found in the Selenga River (7.31 – 10.41 mg/L), Snezhnaya River (4.27 – 6.59 mg/L) and Khara-Murin River (4.49 mg/L) (*Table 20*).

Silicate concentrations measured along a transect from the Selenga River Delta show decreasing values from 2 – 2.6 mg/L to 0.6 – 0.7 mg/L in 2003 – 2004 (Sorokovikova et al. 2012). Over the last 10-years seasonal silicate concentrations in the South basin have changed, with higher concentrations of 1 – 1.25 mg/L in 2003 (Jewson and Granin, 2014), than in August 2013 (mean mixing layer value of 0.54 mg/L). This decreasing trend in silicate concentrations has also been seen in the South, Central and North basin, between 1994 – 2001, with a decrease in average lake values from 1 mg/L to 0.6 – 0.8 mg/L (Shimaraev and Domysheva, 2013). Low silicate concentrations have been observed in periods of high diatom productivity at Lake Baikal, with the silicon reserves reflecting climatic variations (Shimaraev and Domysheva, 2013). The low silicon concentrations found in August 2013 could be a result of an *Aulacoseira* bloom in spring 2013, depleting the silicate levels for the summer stratification period. This is as a recent study has found that the *Aulacoseira* bloom has shifted

by 1.6 months between 1950 - 2000, due to later onset of ice-cover associated with climate change over the 50-year period (Katz et al. 2015). To further support this, the August 2013 silicate concentrations are comparable to previous measurements obtained during years of high biomass (0.3 – 0.5 mg/L) (Jewson et al. 2010; Jewson and Granin, 2014). During the last spatial survey in 2001-2003, there was no *Aulacoseira* bloom, as the spring peak in phytoplankton did not reach the biovolume of *Aulacoseira* years (Fietz et al. 2005). However due to the large store of silica in Lake Baikal's waters, and the vertical water exchange, it has been suggested that at present silica import cannot be a limiting factor for diatom production (Shimaraev and Domysheva, 2004).

Dissolved organic carbon concentrations

The DOC values within the pelagic lakes waters ranged from 1.7 to 2.6 mg/L, slightly higher than previously published values of 1.0 – 1.3 mg/L in the pelagic regions of Lake Baikal in 1997 – 1998 across all basins (*Table 21*) (Yoshioka *et al.* 2002) and 2006 in the South basin (Sugiyama *et al.* 2014). DOC mixing layer concentrations were significantly different between basins, with mean mixing layer values higher in the North basin compared to the South basin (*Figure 49*). In comparison with pelagic values, higher concentrations are found at the river influenced sites (*Figure 49*). Elevated DOC concentrations are found within the river inflows, with values reaching up to 17.9 mg/L in the Selenga River. These high DOC concentrations are not seen in the pelagic open lake region. Summer mixing layer DOC concentrations were higher than deeper water values (*Figure 51*), which is similar to previously published DOC values in Baikal's pelagic waters (Sugiyama *et al.* 2014). DOC concentrations in nutrient-poor alpine lakes have reported DOC concentrations between 0.5 – 17.4 mg/L (Perez and Sommaruga, 2006) and the average DOC concentration within Lake Superior is 1.2 mg/L (Waples *et al.* 2008). Pelagic DOC values in August 2013 are very low, despite much higher concentrations measured in the river inflows, ranging between 4 – 15 mg/L (*Figure 49*). Similarly, DOC studies at Lake Baikal found values of 4.3 mg/L within the Selenga, Barguzin and Upper Angara river inputs (*Table 21*) (Suzuki *et al.* 2008; Yoshioka *et al.* 2002). Over the last two decades, DOC concentrations in Lake Baikal's pelagic waters and river inflows, namely the Selenga, Barguzin, Vydrino and Mishika River have increased (*Figure 54*), as shown by the August 2013 data presented in this chapter (Yoshioka *et al.* 2002; 2007; Sugiyama *et al.* 2014).

5.4.4 Correlations between phytoplankton pigment distribution and environmental variables

There is no correlation between nutrients and the algal community composition across Lake Baikal, despite the finding that nutrient concentrations within the pelagic waters differ significantly between the basins. Within the South and North basins the TP concentrations were slightly higher close to the Selenga River and Upper Angara River respectively (*Figure 69*). Generally, there is no clear difference in silicate, nitrate, sulphate and other major ions (Na, K, Mg, Ca) concentrations between littoral, profundal and river-influenced sites across the lake. There is a correlation between DOC and phytoplankton pigments, in particular picocyanobacterial (P-value < 0.05). Any relationship between DOC and picocyanobacteria is not known in Baikal, although DOC inputs drive the microbial loop, which recycle nutrients for phytoplankton growth.

Higher DOC concentrations in August 2013 compared to a decade ago is likely to be due to precipitation and temperature increases within the Baikal area. This is as increased regional precipitation would result in greater fluvial input of DOC from the catchment into the pelagic lake waters, and increased regional temperatures would result in greater permafrost thaw and the release of DOC into the fluvial waters. Even though carbon cycling within Lake Baikal remains unclear, the mechanisms, which could be keeping DOC so low, could be photodegradation (Osburn et al. 2009) and microbial activity, which degrades DOM via respiration (McGowan et al. 2015). The findings support this, as DOC concentrations are not correlated with light attenuation coefficients, which suggest that the DOC is colourless and does not determine the 1% attenuation depth. There is a negative relationship between chlorophyll-*a* and DOC, and DOC has the strongest negative relationship with zeaxanthin concentrations ($R^2 = 0.41$, $p < 0.05$), the picocyanobacterial biomarker. Studies in small Scandinavian lakes have reported that the highest abundances of picocyanobacteria are within lakes with low DOC concentrations, and DOC explained the most variation in picocyanobacteria biomass and production (Drakare et al. 2003). The relationship between DOC and picoplankton highlights the important role of the microbial loop within Baikal's ecosystem. DOC inputs stimulate the microbial food web and result in increases within the nutrient recycling and carbon processing. As autotrophic phytoplankton cells leak DOC, higher heterotrophic bacterial activity is generally found with higher phytoplankton biomass in clear lakes (Drakare et al. 2003), and microbes will reduce DOC concentrations of these waters and release nutrients (phosphorus and nitrogen) to fuel greater phytoplankton growth. Furthermore, the potential relationship between DOC and picocyanobacteria may be a result of a switch from autotrophic to heterotrophic growth within the Baikal's picoplankton

populations, with the utilisation of DOC (Anderson and McIntosh, 1991; Calvo-Diaz et al. 2011; Parvathi et al. 2014). However, it is unknown to what extent Baikal phytoplankton may be mixotrophic (Hampton et al. 2008). Another possible explanation for this observed pattern might be viral activity, with viral induced picoplankton mortality resulting in higher DOC concentrations (Wilhelm and Suttle, 2014).

5.4.5 Spatial distribution mercury

The mercury concentrations show a gradient from higher concentrations in the Selenga River water to low concentrations in the pelagic lake waters. Mercury concentrations within the Selenga Delta in June 1992 -1993 (Meuleman et al. 1995) were lower (0.26 ng L^{-1}) than in August 2013 ($0.3 - 5.5 \text{ ng L}^{-1}$). Furthermore, mean mercury concentrations measured in the Selenga Shallows and Listvyanka Bay in March 2010 were 0.6 ng L^{-1} and 0.9 ng L^{-1} respectively (Ciesielski et al. 2016). These previous mercury concentrations within the Selenga Shallows and Listvyanka Bay (Ciesielski et al. 2016) were lower than concentrations within August 2013 of 1.6 ng L^{-1} near the Selenga Delta and 1.4 ng L^{-1} in the pelagic South basin (*Figure 55*). Thus, the results suggest a spatial gradient of mercury concentrations (Selenga River > Selenga delta > pelagic lake waters), with higher concentrations in the Selenga river and lowest values in the lake. This pattern is expected due to the mining activity along the Selenga River. Mercury concentrations within Lake Baikal's pelagic waters are very low, being comparable to oceans, and are comparable to concentrations of mercury in unpolluted waters (Kim and Fitzgerald, 1986; Mason and Fitzgerald, 1990; Meuleman et al. 1995). Whereas mercury concentrations in polluted lake waters are between $2 - 25 \text{ ng/L}$ (Bloom and Effler, 1990 as cited in Meuleman et al. 1995). Therefore, August 2013 mercury concentrations from the pelagic zone suggest unpolluted waters, while in the Selenga Delta and along the Selenga River, elevated concentrations highlight the influence of the Selenga River as a source of mercury pollution. The high mercury concentration observed in the North basin waters at BAIK13-19 also highlights the importance of the Upper Angara River, with contamination from industry in the North basin catchment. Sedimentary records of mercury show no significant contamination of the pelagic regions of Lake Baikal, due to the low concentrations preserved within the sediments from the South basin, Selenga and North basin. Sedimentary mercury concentrations are comparable with previous studies, between c. $40 - 70 \text{ ng g}^{-1}$ (Leermakers et al. 1996). These values within the surface sediments are likely to reflect global atmospheric background levels of deposition, which are c. 25 ng g^{-1} and 29 ng g^{-1} (Leermakers et al. 1996).

5.5 Summary

Results from the August 2013 spatial survey provide a detailed snap shot in time, in the late summer limnology at Lake Baikal. When comparing the data to previously published chlorophyll-*a* monitoring records at Lake Baikal, it needs to be taken into account that a single data point can represent either a trend or noise within the dataset. Thus, to validate these results, spatial surveys taken over a 2-3 year period would have been needed. With this in consideration, summer chlorophyll-*a* concentrations in the South basin appear to be continuing along the increasing trend published in Hampton et al. (2008), as they show higher concentrations than values measured in 2003. Over the last decade, average summer chlorophyll-*a*, diatom and picocyanobacterial pigment concentrations seem to have increased in the pelagic South basin mixing layer since 2001-2003 measurements (Fietz et al. 2005). Higher chlorophyll-*a* concentrations were detected within the mixing layer of the South basin sites, and the DCM layer formed within the upper 4 m of the epilimnion, extending to depths of 20.2 – 46 m, beyond both the mixing layer and euphotic zone. Picocyanobacteria were detected in highest abundances in the South basin sites, within the top 20 m of the water column, contributing the most to the chlorophyll maxima layer. Algal biomass affects the light dynamics within the lake and DOC concentrations appear to have little influence on the light penetration. DOC measurements show higher concentrations in the river and pelagic lake waters than previous measurements (Yoshioka et al. 2002), and forecasted increases in DOC inputs, from permafrost thaw and greater fluvial inputs into Lake Baikal are likely to influence the algal community composition, due to the recycling of nutrients from microbial activity (Moore et al. 2009), and an observed link between picocyanobacteria and DOC concentrations.

Over the last decade, the limnological functioning of Lake Baikal appears to have changed, due to greater algal biomass than previously in the mixing layer of the South basin, restricting algal production further down the water column. Both local thermal stratification and the inflow of more nutrient rich waters could be the cause of greater algal biomass and less deep-water production in the South basin sites, than the Central and North basins. TP concentrations within the pelagic waters of Lake Baikal are higher than expected, falling within the mesotrophic and bordering on the eutrophic range. The highest TP concentrations were measured close to the Selenga Delta and in the North basin, being two-fold higher than measured TP concentrations between 1995 to 2009 which reflect natural variability. As this suggests a potential increase in TP concentrations in over 10 µg/L between 2009 to 2013, it is important to consider any potential analytical error in these values. But it is similarly important to note that these values are comparable to the range of TP measurements collected from a

survey conducted at the same time, in late summer (2013) (O'Donnell et al. 2017), using a similar digestion method. Thus, the TP concentrations suggest a new phenomenon in the nutrient concentrations of Lake Baikal's pelagic waters, and the possibility of anthropogenic impact needs to be investigated further as it is unlikely that these values are not solely a natural cause.

Nitrate concentrations within the lake waters are very low, and largely below detection limits, and silicate concentrations appear to be lower than previously published values. Results also show no significant accumulation of mercury. From the survey data alone, the TP measurements are suggesting the input of nutrients into Lake Baikal, largely from the major river inflow, the Selenga River, and possible anthropogenic impact. However, to assess whether pelagic Lake Baikal is showing any signs of eutrophication, Chapter Seven will provide insight into historic algal trends. Chapter Seven also attempts to disentangle climate with anthropogenic impacts at Lake Baikal, by looking into palaeolimnological changes pre and post known anthropogenic impact in the region, in 1950, and by looking at past pollution records which include SCP records published at Lake Baikal. It is however likely, that due to the massive size and hydrodynamics of Lake Baikal, any anthropogenic impact on pelagic Lake Baikal, at the moment, is being diluted by the volume of water, and are only showing up in the littoral regions as found by previously published work with algal blooms on the shorelines. Findings from a recently published study (Izmesteva et al. 2016) supports this work, by showing no evidence of pelagic cultural eutrophication in Lake Baikal. Climate-driven processes, and possible anthropogenic impact as well, appear to be driving the changes in the functioning and production over the last decade, with greater deeper water production in the Central and North basin (deeper DCM) and higher biomass in the South basin with shallower DCM.

Chapter Six: Recent palaeoproductivity in context within Longer-term variability

6.1 Longer-term reconstruction of environmental change at Lake Baikal

The aims of this chapter are to compare modern (last 200 years) palaeolimnology at Lake Baikal to natural Holocene variability within the system and past environmental changes within the region. Recent production changes observed over the last 200 years as presented in (Chapter Seven) need to be put into a longer-term context. This chapter will be comparing the pigment and carbon isotope records over the last two centuries, to the records over the entire short cores, which extend to cover up to the last millennium. The upper sediments of these short cores have been ^{210}Pb dated (Chapter Seven), however dates have not been obtained for older sediments, due to the complexities of radiocarbon dating Baikal sediments (Piotrowska et al. 2004). Although these short cores have not been AMS ^{14}C dated, they still provide a method of comparing recent trends with longer-term changes. This chapter will also compare the production trends over the last 200 years with previous records at Lake Baikal within the Holocene and the Kazantsevo (Last interglacial) (Fietz, 2005; Fietz et al. 2007), which is equivalent to Marine Isotopic Stage (MIS) 5e. This will enable us to see if the recent trends observed are distinct or similar to past production changes at Lake Baikal. Pigment ratios (Diatoxanthin:Chlas, Canthaxanthin:Chlas, Lutein: Chlas and Chlb:Chlas) are used within this chapter to assess the contribution of algal groups to total algae, such as diatoms, picocyanobacteria and chlorophytes. Mean ratios have been calculated for sediments > 200 years and < 200 years to compare the two intervals, and examine changes in the algal group proportions. Regional production records will be examined to explore lake-wide response and/or basin response, to determine the spatial and temporal difference in trends within (or between) the records.

Lake Baikal has a wide variety of sedimentary environments, consisting of abyssal plains, delta fans, littoral bays and underwater highs. Tectonic large lakes, such as Lake Baikal, provide records which span from hundreds to millions of years, however the palaeoclimate record can be complicated by currents, turbidites and tectonics (Colman et al. 2003; Charlet et al. 2005). Due to secondary processes and large mass flows, coring locations were selected based on the deposition environment, to minimise the influence of turbidites. This further highlights the importance of site selection for coring, to collect a sediment core to analyse continuous environmental change, without large hiatuses which cannot be accounted for in the record and with suitable preservation conditions for pigment analyses. The three basins

(South, Central and North) are c. 200 km long with steep border-fault margins (Colman et al. 2003). Turbidites are prevalent on the deep basin floors (Nelson *et al.* 1995; 1999; Colman et al. 2003), and postglacial sediments typically consist of diatomaceous and fine-grained mud, interbedded with coarse silt or mud turbidite layers (Colman et al. 2003). Sedimentation rates vary greatly across Lake Baikal, and as discussed in Chapter Seven, this will have an impact on pigment preservation. The highest sedimentation rates are near the mouths of large rivers (2.32 – 10.7 mm/yr), and the lowest sedimentation rates within the deep basins (0.705 – 1 mm/year), and at underwater ridges (0.015 – 0.025 mm/year) (Vologina and Sturm, 2009). Thus, across Lake Baikal, the areas of different sedimentation are deep water pelagic regions with turbidites, littoral regions without turbidites, under water ridges with pelagic sediment accumulated under calm conditions, delta areas where sediments are largely terrigenous material and shallow water Maloe More region where there are abundant sands and poorly sorted terrigenous material (Sturm and Vologina, 2001; Vologina and Sturm, 2009).

Deep basin sites tend to be subject to turbidite sedimentation within Lake Baikal (Peck et al. 1994), and sedimentation rates vary across basins. Maximum rates of sedimentation are observed in the South basin (1 mm/year) and Central basin (0.91 mm/year), and the minimum sedimentation rates are observed in the North basin (0.705 mm/year) (Sturm and Vologina, 2001). The differences in the sedimentation rates in the basins is due to the different biologic productivities and different amounts of terrigenous material supplied to the lake. Regions in Lake Baikal which have been found to lack turbidites within the sediment cores are underwater ridges, such as the Academician Ridge, which separate the North and Central basin. The Holocene sedimentation rate at the Academician Ridge is c. 0.005 – 0.025 mm/year (Colman et al. 1993; Vologina et al. 2003; Vologina and Sturm, 2009). Similar to the Academician Ridge, the surface sediment of Buguldeika ridge lacks turbidites, and has higher sedimentation rate of 0.2 – 0.86 mm/year due to the Selenga River (Kuzmin et al. 2001). Regions with high sedimentation rates are delta sites near the mouths of large rivers, such as Proval Bay in the northern part of the Selenga Delta (Vologina and Sturm, 2009). Proval Bay was formed by an earthquake within the Selenga Delta region in 1862 (Vologina et al. 2010), and the sedimentation rates have been found to vary between 2.32 mm/year (Vologina et al. 2007b) to 10.7mm/year (Tulokhomov et al. 2006), depending on the proximity to the Selenga River.

High-resolution sedimentary records of environmental change over the last millennium at Lake Baikal can be affected by the presence of turbidite layers, although magnetic susceptibility techniques can be applied to help identify turbidites down a sediment core (Flower et al. 1995; Lee et al. 1998, Vologina et al. 2010). Sediment cores retrieved from across the whole lake have been studied since the early 1990s by the Baikal Drilling Project

and other palaeoclimate studies (Colman et al. 1995; Grachev et al. 1998; Kashiwaya et al. 2003; Kuzmin et al. 2000; Williams et al. 2001; Morley, 2005; Fietz et al. 2007), showing the large variation in sedimentation rates across Lake Baikal, between the deep basins, fluvial fans, underwater ridges and littoral bays. Sediment cores collected from littoral zones along the eastern shore in the North basin and the southern shore on the South basin do not show any distinct turbidites, and the sedimentation rates are 0.61 – 0.75 mm/year (Bangs et al. 2000; Sturm and Vologina, 2001). Previously the Academician ridge has been used as a coring site, as it is undisturbed and relatively shallow with slow sedimentation rates (Williams et al. 2001; Grygar et al. 2006; Watanabe et al. 2009; Kuzmin et al. 2014), and therefore provides detailed continuous records over the last 1,000 years. Other cores for high resolution palaeoclimate records have been taken from sites in shallower waters at isolated inter-basin highs which separate the sub-basins in Lake Baikal, within the Selenga Delta zone (such as Posolsky Bank), the Buguldeika Saddle, the Vydrino Shoulder, and the Continent Ridge (Prokopenko et al. 2001; Grygar et al. 2006; Fietz et al. 2007). However, sediment cores from these locations have also documented tectonic disruptions (Mats et al. 2000) and influence from bottom-water currents (Ceramicola *et al.* 2001), showing depositional, re-depositional and tectonic processes on these isolated highs and delta regions (Charlet et al. 2005). For example, the Vydrino Shoulder is the source of turbidites, but the underwater high from where the sediment cores were taken were free from turbidites as they were not taken from the slopes (Charlet et al. 2005). Also, the Posolsky Bank is a major tilted fault block and the Continent Ridge is affected by active faulting (Charlet et al. 2005).

Sediment cores presented within this chapter have been analysed for sedimentary pigments and carbon isotopes at high-resolution (c. 0.5 – 1 cm intervals which equates to c. 5 - 10 years). To reconstruct changes over the lake, turbidite sections within cores need to be accounted for and removed from the analyses. In most cores presented in this chapter, the total thickness of pelagic sediment is greater than the total thickness of turbidites. The sedimentation rate of turbidites is much higher than the rate of sediment accumulation, and therefore this suggests that the deposits within these deep-water plains formed mainly under calm sedimentation conditions (Sturm and Vologina, 2001).

To reconstruct past environmental change, accurate sediment core chronologies are important. Radiocarbon is frequently used on well-preserved remains of terrestrial plants such as wood fragments, seeds and leaves, or on plant biomarkers (Bertrand et al. 2012). Bulk sediments are used for radiocarbon dating when sediments lack well preserved plant remains or when there is not enough material for compound specific analyses (Bertrand et al. 2012). It has been previously proposed that radiocarbon ages from bulk sediments do not provide an accurate

chronology of sediment deposition, as bulk sediments contain a mixture of aquatic and terrestrial carbon (Bjork and Wohlfarth, 2001). The upper part of cores from Lake Baikal are not AMS ^{14}C dated, and tend to be ^{210}Pb dated, as the AMS ^{14}C ages of surface sediments can range between 0.5 – 1.5 ka years BP at Lake Baikal (Tani et al. 2002). This age discrepancy for surface sediments in Lake Baikal is due to the offset between atmospheric and lacustrine ^{14}C ages, known as the reservoir effect. However, the reservoir effect in Lake Baikal has not been fully evaluated (Tani et al. 2002). Radiocarbon dating is known to be difficult at Lake Baikal (Colman, 1996), and has been previously applied to bulk sediments from the Baikal Drilling Project cores. Whereas for the Continent Project work at Lake Baikal, pollen was used for radiocarbon dates (Piotrowska et al. 2004), rather than radiocarbon dating bulk sediments. TOC/N ratios have recently been suggested to be useful for correcting bulk radiocarbon ages from sediments from lakes in Northern Chilean Patagonia (Bertrand et al. 2012). Bertrand et al. (2012) found a link between the fraction of terrestrial carbon as inferred from TOC/N ratios, and the age offset of the sediments. TOC/N measurements could therefore be paired with radiocarbon dating of bulk sediments at Lake Baikal, to improve the chronologies based on radiocarbon dating of bulk lake sediments. There is still debate as to whether this approach can be used at all the sites across Lake Baikal, and uncertainty in the best way to carry out radiocarbon dating on Baikal sediments. This chapter does not present any dates beyond the last 200 years and radiocarbon dating of older sediments is future work for the project.

Radiocarbon dating will be applied to the sediment cores, instead of ^{32}Si dating, as high resolution analyses is required to explore recent changes in production. ^{32}Si dating technique has been applied to Lake Baikal sediments from the South basin which cover the last c. 1000 years (Morgenstern et al. 2013). ^{32}Si isotope has a half-life of c. 144 years (Fifield and Morgenstern, 2009), and is produced by the atmosphere via cosmic ray interactions (Morgenstern et al. 2013). Atmospheric precipitation transports ^{32}Si to earth's surface, and diatom utilise ^{32}Si within their frustules (Morgenstern et al. 2013). This technique can be applied to the dating gap between ^{210}Pb dating and ^{14}C dating, being used for sediments > 150 years (Morgenstern et al. 2013). The chronology for ^{32}Si has been found to be robust, however large quantities (> 10 g) of dry sediment are required which restricts the resolution as the sedimentation rates at Lake Baikal are low, generally c. 0.01 cm/yr (Morgenstern et al. 2013), and this technique has not been considered for this study.

6.2 Past carbon records over the Holocene at Lake Baikal

Studies have looked at carbon sequestration from CMAR (Mackay et al. 2016), and productivity from $\delta^{13}\text{C}$ and TOC/N ratios at Lake Baikal over the Holocene (Prokopenko et al. 1993; 2001; Horiuchi et al. 2000; Prokopenko and Williams, 2003; Ishiwatari et al. 2005; Morley, 2005; Watanabe et al. 2009; Mackay et al. 2016). A recent study by Mackay et al. (2016) has examined the influence of forest development in the early Holocene, lacustrine productivity and changes in permafrost cover in Baikal's catchment on the carbon dynamics over the Holocene period. This study has inferred carbon sequestration changes in correspondence with changes in permafrost conditions at the forest-steppe ecotone in the Baikal catchment. However, the variability within the $\delta^{13}\text{C}$ record from the pelagic South basin over the Holocene at Lake Baikal is proposed to be due to changes in pelagic and near-shore productivity, coupled with changes in delivery of carbon to the lake (Mackay et al. 2016). This carbon record at the Vydrino shoulder site in the South basin only extends to 800 yrs BP in the late Holocene. The data presented in this chapter fills this gap to examine recent Holocene changes in carbon dynamics over the last c. 1000 years in the South (BAIK13-7A), but also regionally across the lake from the other sites.

6.3 Results

6.3.1 Core lithology (data produced by E. Vologina)

South basin (BAIK13-1)

BAIK13-1A (51°46'04.2" N 104°24'58.6" E) in the South basin is comprised of largely biogenic-terrigenous sediment, with diatoms and clay (*Figure 71*). There are oxidised layers in the upper 3.6 cm of the core and at 7.3 – 8.5 cm, and turbidite layers with sandy sediments between 15 – 20 cm and 33 – 37 cm. Magnetic susceptibility is relatively consistent within the upper 15 cm of the core, and then becomes more variable with peaks between 28- 40 cm.

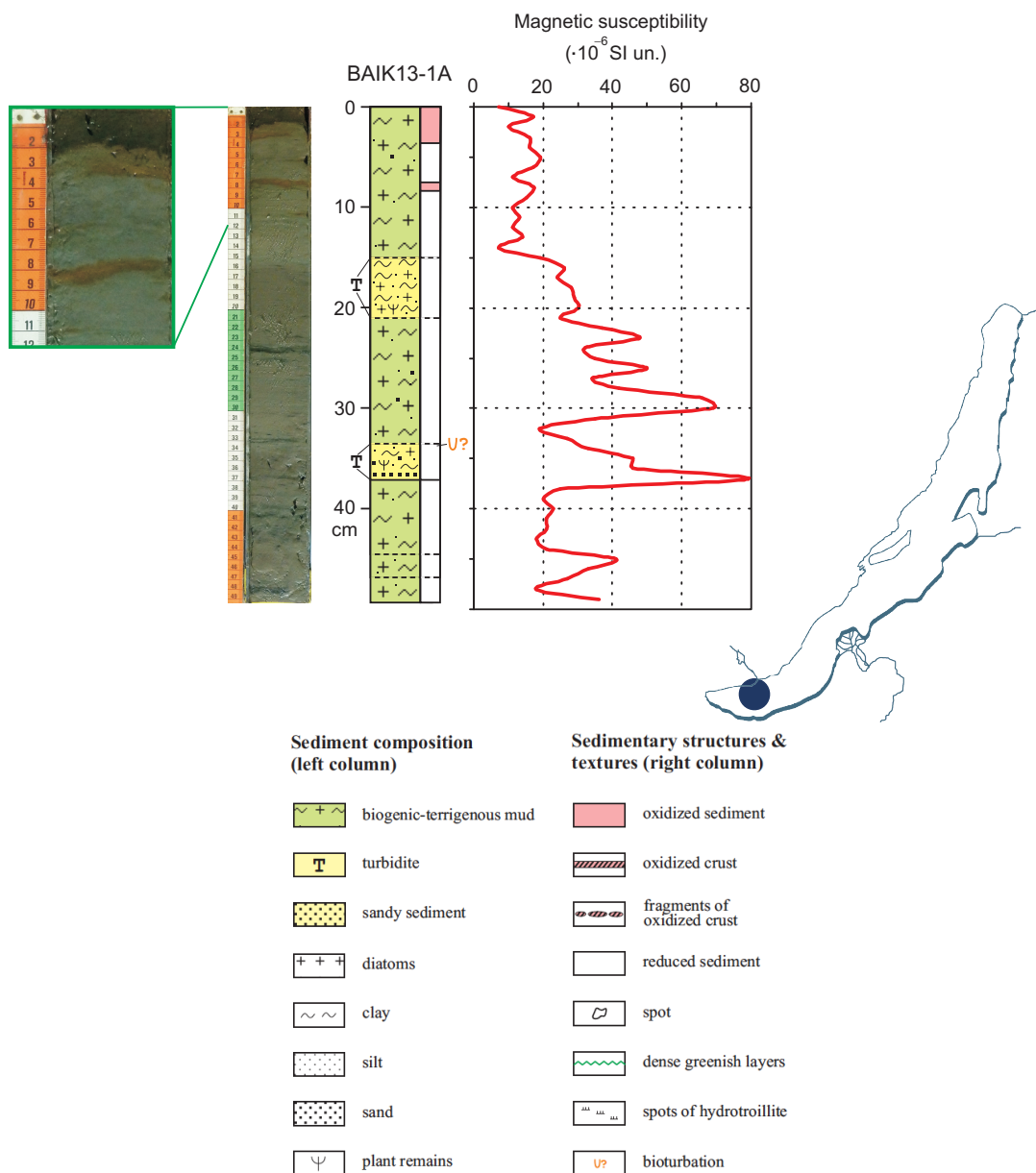


Figure 71: Lithology and magnetic susceptibility at BAIK13-1.

South basin (BAIK13-4)

BAIK13-4C (51°41'33.8" N 104°18'00.1" E) in the South basin is comprised of biogenic-terrigenous sediments and sandy turbidite deposits, with three turbidite layers, one being in the upper 10 cm of the core (Figure 72). There are also two oxidised layers, at 0 – 2.7 cm and 5.3 – 8.5 cm. Magnetic susceptibility is relatively consistent between 0 – 30 cm, and then peaks to values of c. 80 (10^{-6} SI un).

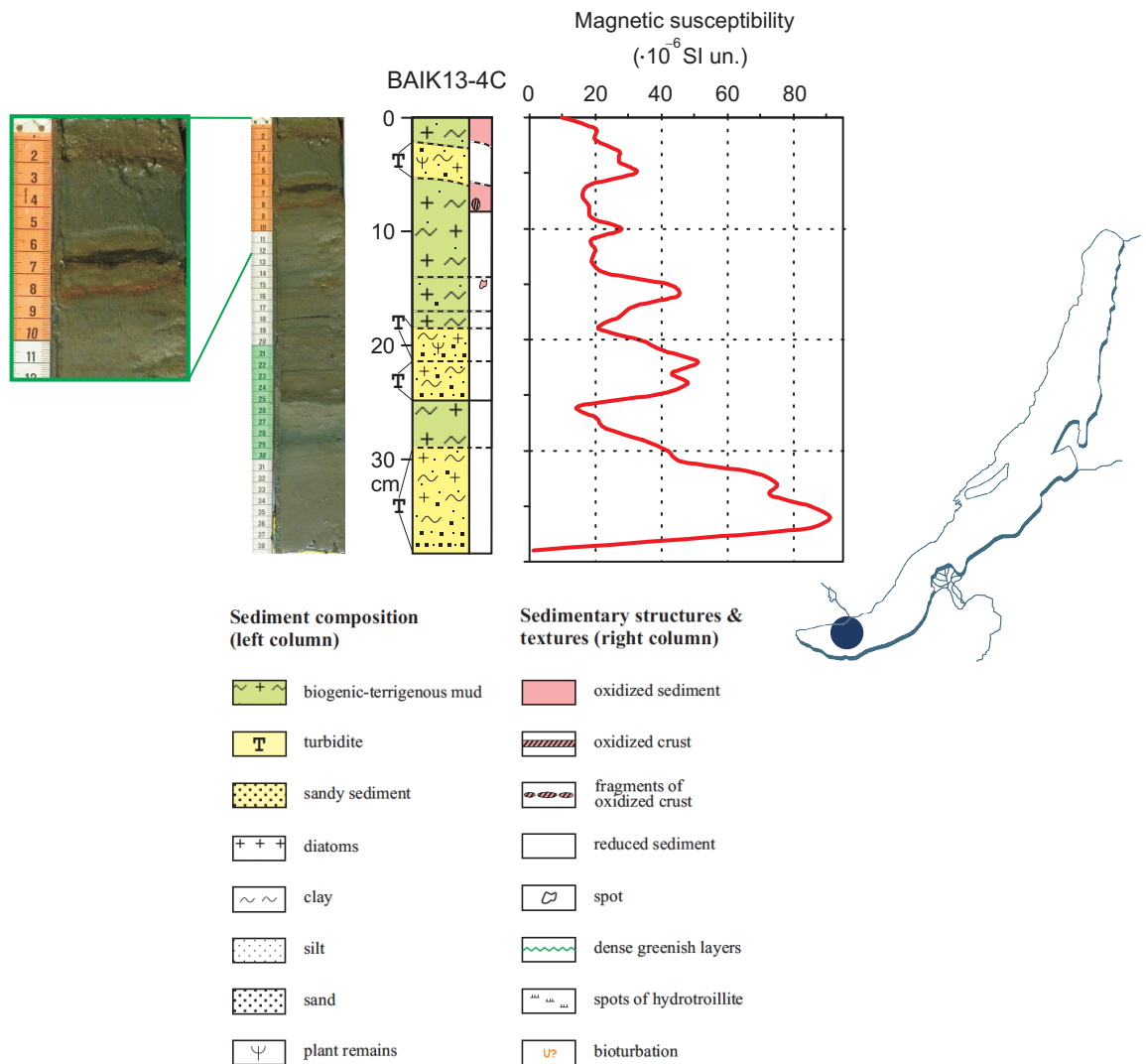


Figure 72: Lithology and magnetic susceptibility at BAIK13-4.

South basin (BAIK13-7)

BAIK13-7B (51°34'06" N 104°31'43" E) in the South basin is comprised mainly of biogenic-terrigenous sediment, with diatoms and clay (Figure 73). There are two oxidised layers, at 0 – 3cm, and 10.5 – 12.1 cm. Turbidites are present at the bottom of the sediment core, at c. 38 – 45 cm. Both magnetic susceptibility and water content are relatively constant down core.

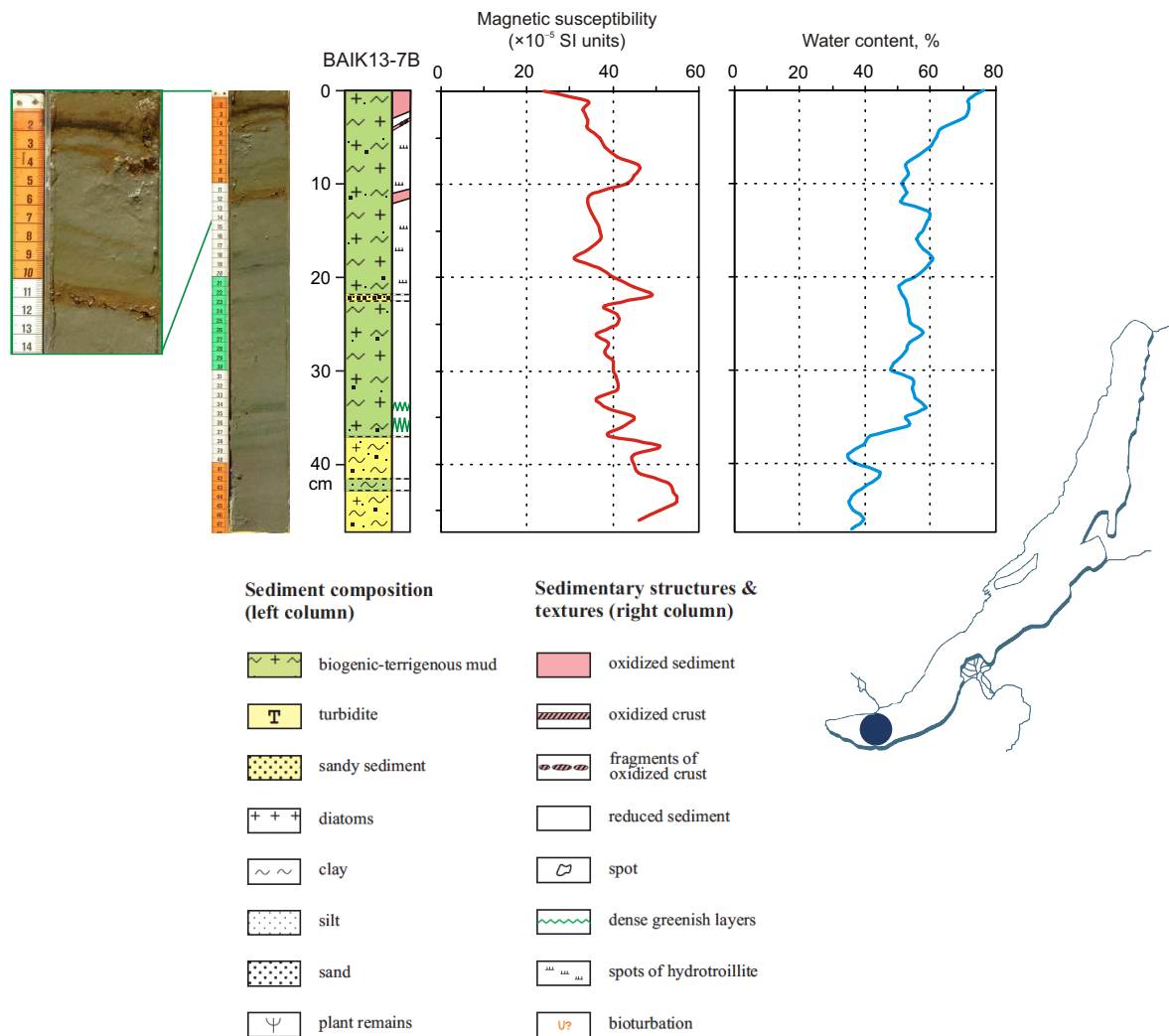


Figure 73: Lithology and magnetic susceptibility at BAIK13-7.

South basin/Selenga (BAIK13-10)

BAIK13-10B (52°11'07" N 106°05'38" E) nearby the Selenga Delta in the South basin is comprised predominately of biogenic-terrigenous sediments (*Figure 74*). There is one oxidised layer at the top of the core, 0 – 4 cm, and one turbidite at the bottom of the core 48 – 51 cm. Magnetic susceptibility and water content are relatively constant down-core.

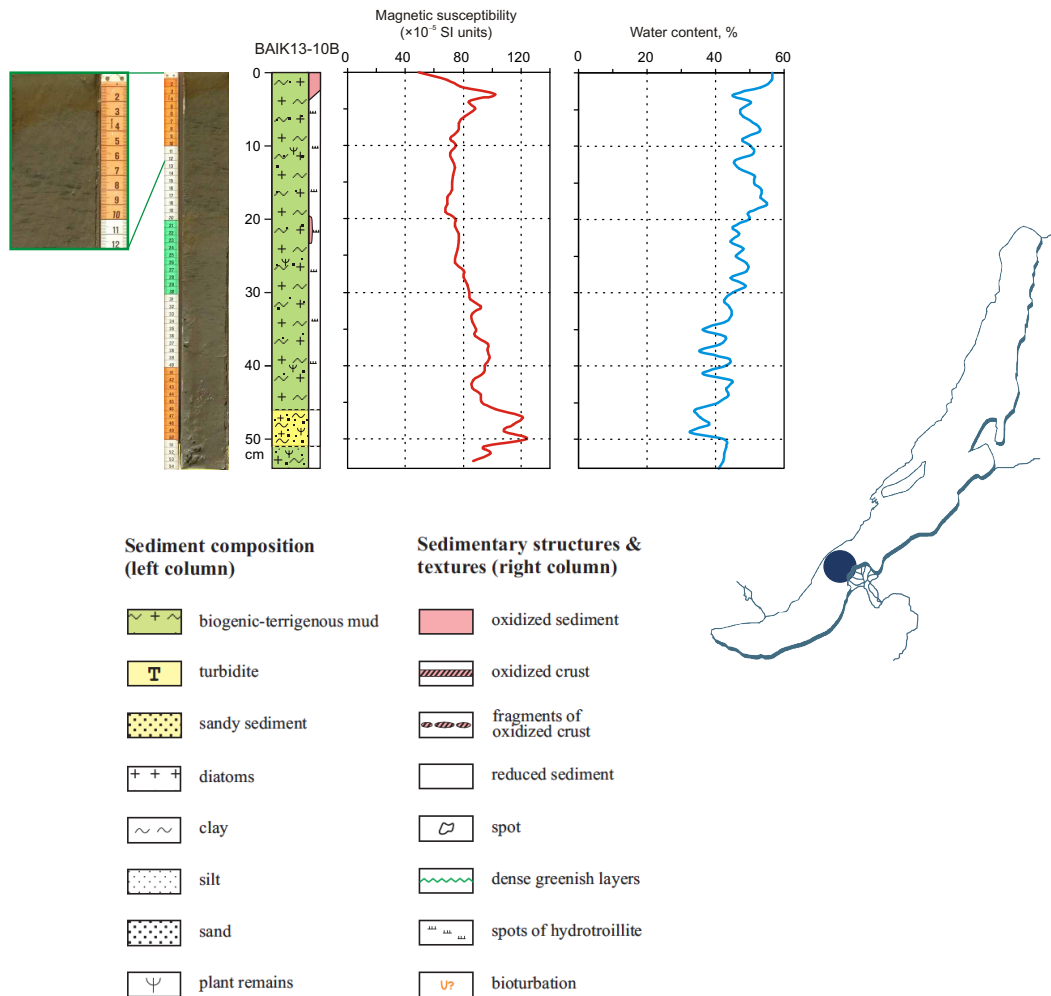


Figure 74: Lithology and magnetic susceptibility at BAIK13-10.

South basin/Selenga (BAIK13-11)

BAIK13-11A (52°27'00" N 106°07'32" E) at Buguldeika in the South basin is entirely comprised of biogenic-terrigenous sediments with no oxidised layers or turbidites present (Figure 75). The magnetic susceptibility and water content are constant down-core.

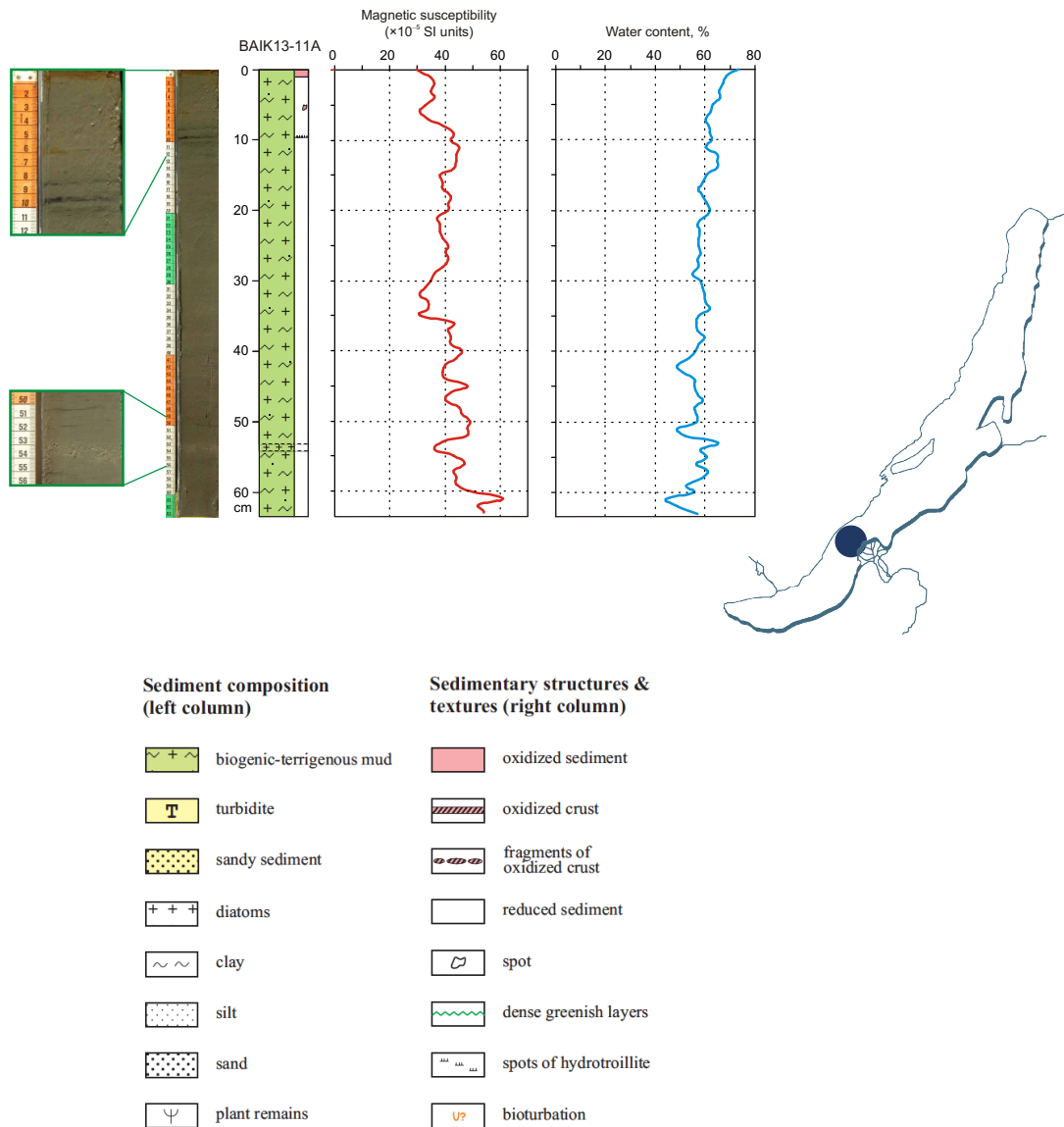


Figure 75: Lithology and magnetic susceptibility at BAIK13-11.

Central basin/Maloe More Bay (BAIK13-14)

BAIK13-14B (53°21.033 N 107°29.885' E) in Maloe More, off the Central basin, is entirely comprised of biogenic-terrigenous sediment in the top 18 cm of the core, and then it is entirely comprised of sandy turbidite sediment between 18 – 30 cm (Figure 76). There are no oxidised layers and the water content decreases simultaneously with increasing magnetic susceptibility at the transition from organic to sandy sediment.

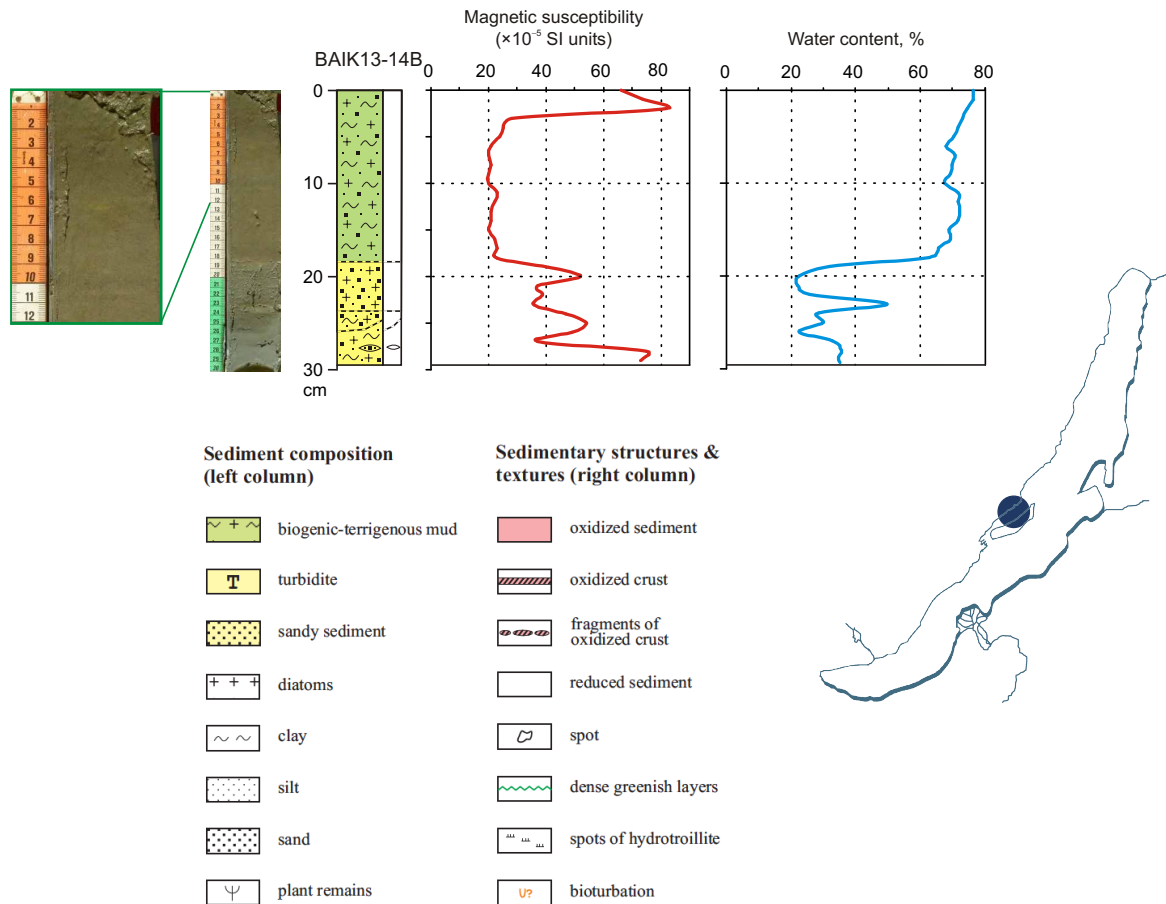


Figure 76: Lithology and magnetic susceptibility at BAIK13-14.

Central basin/Maloe More Bay (BAIK13-15)

BAIK13-15B (53°23.270 N 107°35.346' E) in Maloe More, off the Central basin. Similar to BAIK13-14B, BAIK13-15B is comprised of biogenic-terrigenous sediment in the top 14 cm of the core, and then entirely comprised of sandy turbidite sediment (*Figure 77*). There is an oxidised layer in the upper 5 cm, and water content and magnetic susceptibility mirror each other below 14 cm.

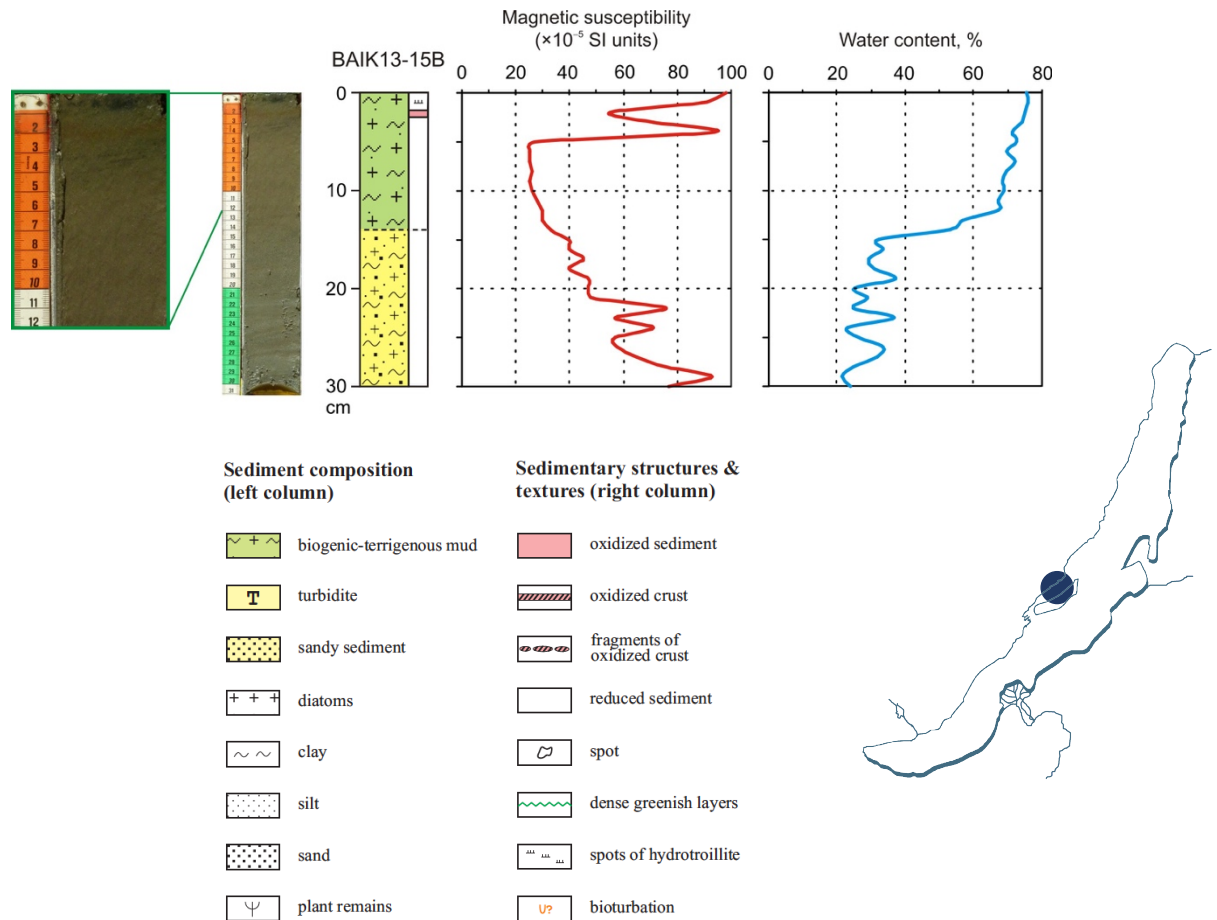


Figure 77: Lithology and magnetic susceptibility at BAIK13-15B.

North basin/Chivsky Bay (BAIK13-16)

BAIK13-16A (53°52'26" N 109°09'49" E) in Chivsky Bay in the North basin is comprised entirely of biogenic-terrigenous sediment in the top 21 cm with three oxidised layers (Figure 78). There are no sandy turbidite layers present within these Holocene sediments. The sediment core lithology shifts to late Pleistocene clays from 22 – 60 cm. Pleistocene clays are identified due to the presence of an endemic diatom species, *Stephanodiscus flabellatus*, which is now extinct and indicative of that period (Bradbury et al. 1994). The water content decreases down-core with c. 50 – 60 % in the Holocene sediments and c. 40 % in the Pleistocene clays, and magnetic susceptibility varies between c. 20 and 100 (10^{-6} SI un).

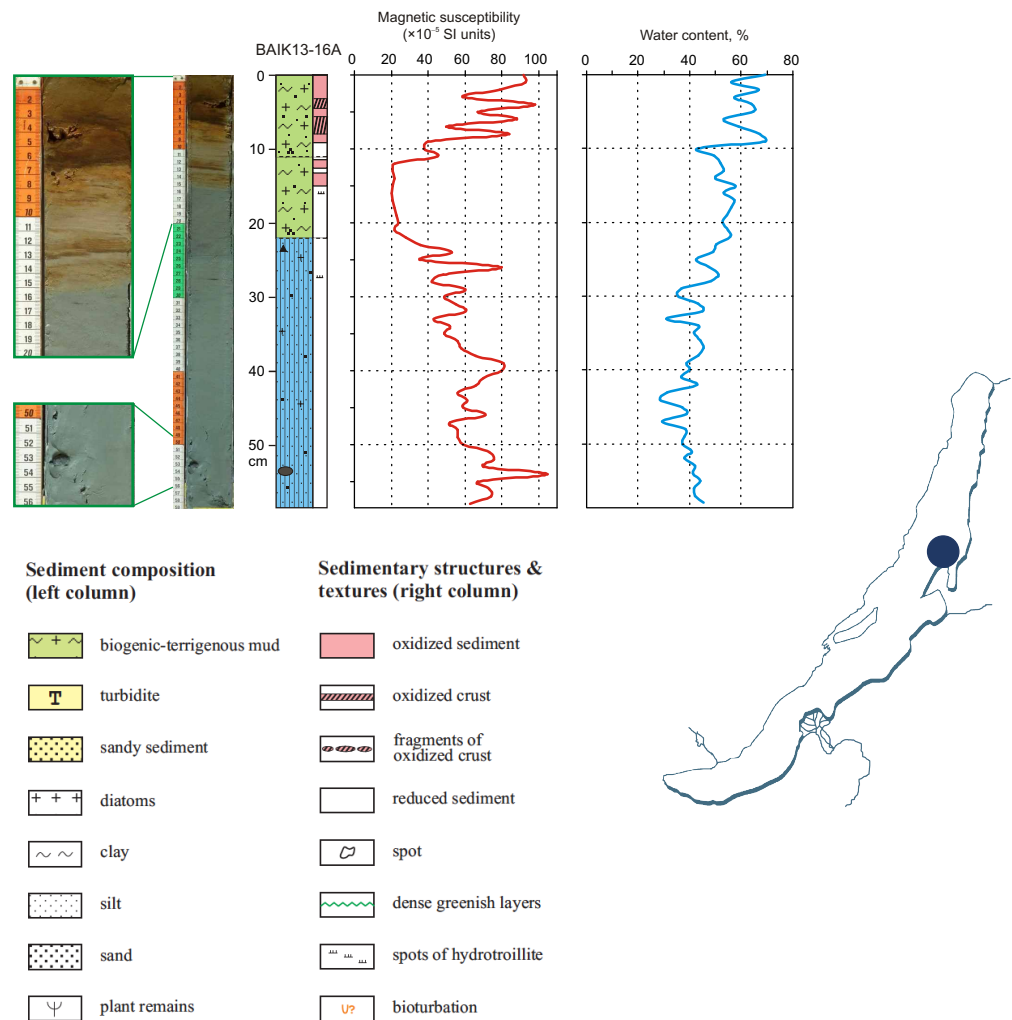


Figure 78: Lithology and magnetic susceptibility at BAIK13-16.

North basin (BAIK13-18)

BAIK13-18C (54°47'31.4" N 109°14'15.3" E) in the North basin has two oxidised layers in the top 22 cm, at 0 – 4.5 cm and 14 – 19.5 cm) in the sediment core, which is comprised entirely of biogenic-terrigenous sediment (*Figure 79*). There is a large sandy turbidite layer between 22 – 50 cm, and below this layer the sediments are predominately biogenic-terrigenous. The water content is constant down-core and the magnetic susceptibility is higher within the sandy sediments, peaking at 49 cm.

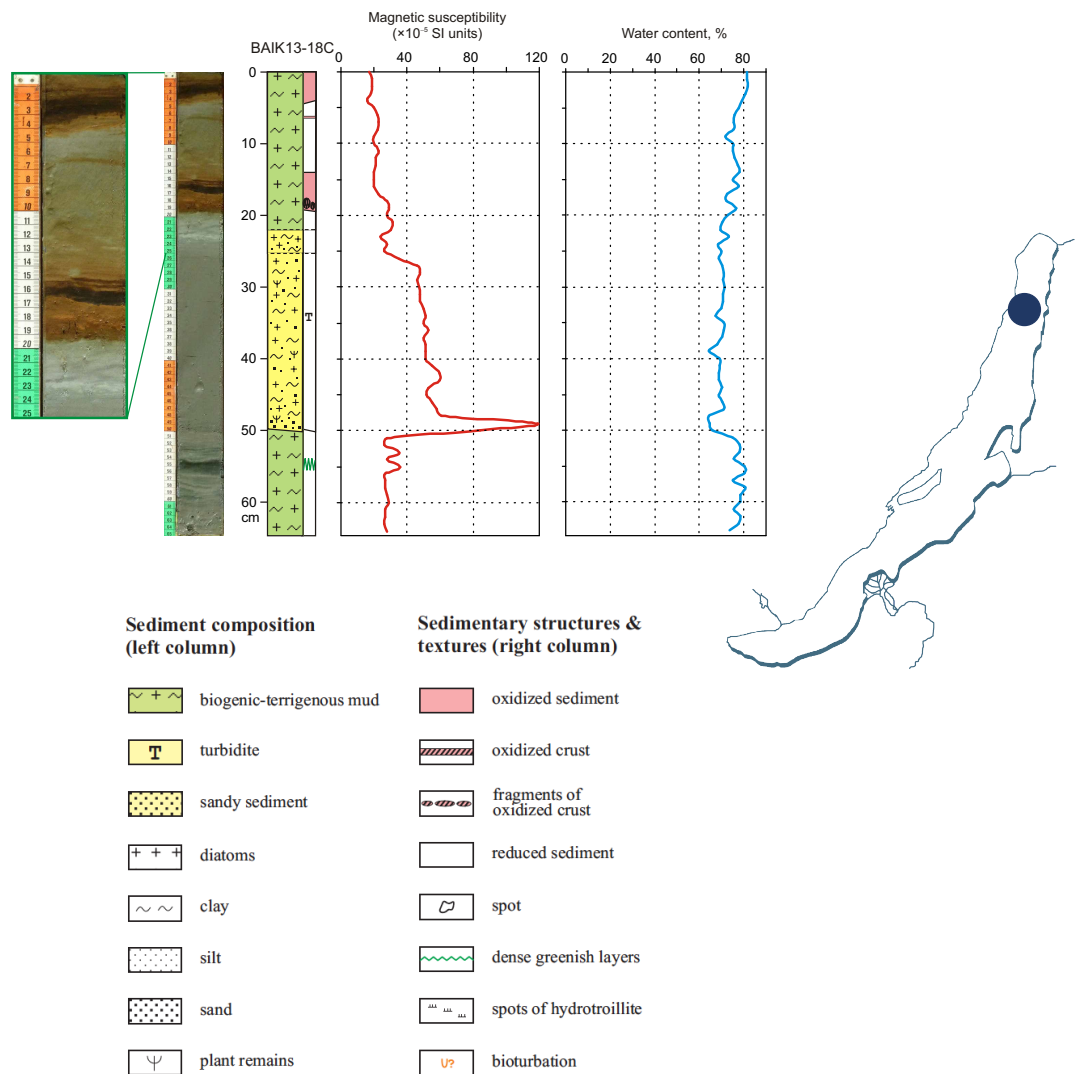
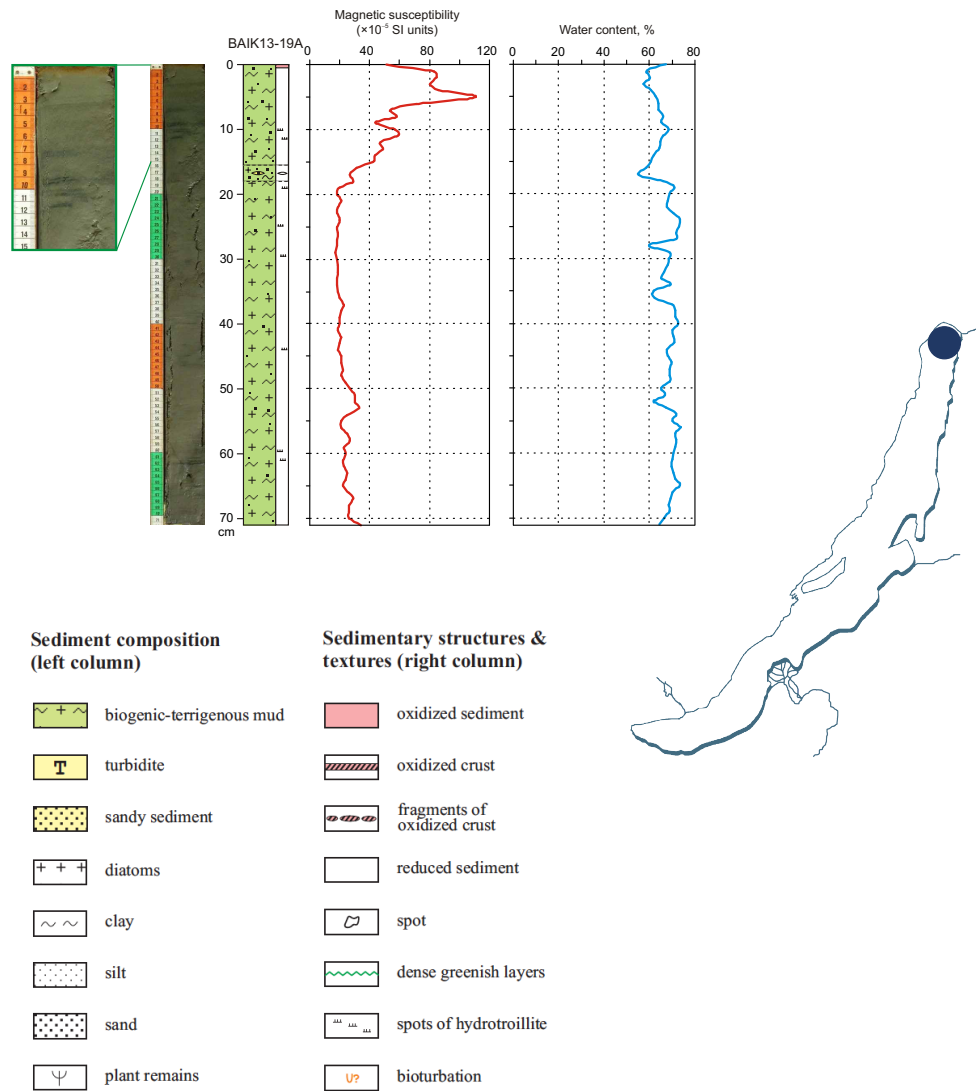


Figure 79: Lithology and magnetic susceptibility at BAIK13-18.

North basin (BAIK13-19)

BAIK13-19A (55°38'57.8" N 109°46'57.7" E) near the Upper Angara River in the North basin is entirely comprised of biogenic-terrigenous sediments, with no oxidised sediments or sandy turbidite layers present (Figure 80). Water content is constant down-core and the magnetic susceptibility decreased between 0 – 20 cm and then remains constant down-core.



6.3.2 Comparing recent production changes with the longer term

There are significantly (p value < 0.01) greater mean Chlas concentrations over the last 200 years compared within sediments > 200 years, across all the sites (*Table 28; Figure 81*). South and North basin sites have a mean Chlas concentration between $84.9 - 246 \text{ nmol g}^{-1} \text{ OC}$ and $89.8 - 138.3 \text{ nmol g}^{-1} \text{ OC}$ respectively, the Selenga sites have a mean Chlas concentration between $120.4 - 567.5 \text{ nmol g}^{-1} \text{ OC}$ and Maloe More has a mean Chlas concentration of $306.6 \text{ nmol g}^{-1} \text{ OC}$. The largest differences in Chlas concentrations between pre and post 1800 AD, are in the South basin, Selenga and Maloe More sites. The sediments > 200 years BP range between 5.3 to $73.7 \text{ nmol g}^{-1} \text{ OC}$ in mean Chlas concentration across the lake. Lake wide, there were lower diatoxanthin:Chlas ratios in sediments < 200 years. Chlb:Chlas ratios are higher in sediments < 200 years BP within the South basin, Selenga and Maloe More sites, but not detected within the North basin. Canthaxanthin:Chlas ratio values were similar within sediments pre and post 1800 AD. Mean Chlas concentrations are highest in the Selenga Delta sites and lowest in the North basin sites, in both time intervals (Selenga $>$ Maloe More $>$ South basin $>$ North basin) (*Table 29*).

The proportion of diatoms to total algae was greater in sediments > 200 years, than < 200 years, in the Selenga and Maloe More sites, as inferred from the Diatoxanthin:Chlas ratios (*Table 28*). In sediments < 200 years diatoms contribute to 12% at both sites, and this declined to 1.6 % and 2.7 % respectively post 1800 AD. Canthaxanthin:Chlas ratios also show higher contribution of picocyanobacteria in sediments > 200 years in the South, Selenga, Maloe More and North basin sites, with values of 1.9 %, 7.9 %, 6 % and 3.5% respectively (*Table 28*). In sediments < 200 years the contribution of picocyanobacteria decreased to 0 – 1.3 % within these sites. In contrast to these algal groups, chlorophyte contribution to total algae, as inferred from Chlb:Chlas, is higher in sediments < 200 years in the South basin, Selenga and Maloe More sites, with an increase from 1 % to 13 % in BAIK13-1C sediments, 0.4 % to 1.5 % in BAIK13-10A sediments and 0.1 % to 0.9 % in BAIK13-14C sediments (*Table 28*). Lutein:Chlas ratios show that the proportion of chlorophytes to total algae was greater in sediments > 200 years than < 200 years (*Table 28*). The proportion of chlorophytes to total algae has decreased between the two time intervals, from 20 % to 7% in Maloe More (BAIK13-14C), 28% to 3% in the Selenga (BAIK13-10A) and 2.5 % to 0.3 % in the South basin (BAIK13-1C). Total carotenoid concentrations are significantly higher in sediments < 200 years, than > 200 years in the South basin (BAIK13-1C and BAIK13-4F), Selenga (BAIK13-10A) and Maloe More (BAIK13-14C). In the North basin site (BAIK13-19B), total carotenoid concentrations are significantly lower in sediments > 200 years, than < 200 years (*Figure 82*).

Table 28: Mean and SD values of Chlas concentrations, Chlbs/Chlas, Diatox/Chlas, Cantha/Chlas over the last 200 years and in sediments > 200 years. Turbidite sections have been removed within the pigment records. (*BAIK13-7A and *BAIK13-18A show high levels of degradation).

		Chlas	Chlbs/Chlas	Diatox/Chlas	Lutein/Chlas	Cantha/Chlas
BAIK13-1	< 200 years BP					
	Mean	246.0	0.131	0.004	0.003	0.003
	SD	108.0	0.414	0.010	0.008	0.005
	> 200 years BP					
Mean	62.9	0.010	0.007	0.025	0.019	
SD	51.5	0.053	0.013	0.055	0.032	
BAIK13-4	< 200 years BP					
	Mean	183.2	0.009	0.000	0.017	0.003
	SD	142.6	0.009	0.000	0.008	0.002
	> 200 years BP					
Mean	39.6	0.084	0.025	0.129	0.003	
SD	30.4	0.086	0.067	0.099	0.011	
BAIK13-7	< 200 years BP					
	Mean	84.9	0.002	(-)	(-)	0.003
	SD	85.6	0.004	(-)	(-)	0.004
	> 200 years BP					
Mean	11.2	0.000	(-)	(-)	0.003	
SD	21.9	0.000	(-)	(-)	0.021	
BAIK13-10	< 200 years BP					
	Mean	567.5	0.015	0.016	0.028	0.010
	SD	204.4	0.011	0.016	0.031	0.007
	> 200 years BP					
Mean	73.7	0.004	0.124	0.281	0.079	
SD	35.9	0.011	0.062	0.140	0.053	
BAIK13-11	< 200 years BP					
	Mean	120.4	(-)	0.002	0.014	0.018
	SD	97.3	(-)	0.005	0.021	0.013
	> 200 years BP					
Mean	37.5	(-)	0.023	0.090	0.038	
SD	20.3	(-)	0.041	0.056	0.013	
BAIK13-14	< 200 years BP					
	Mean	306.6	0.009	0.027	0.074	0.010
	SD	182.8	0.010	0.021	0.025	0.005
	> 200 years BP					
Mean	48.8	0.001	0.127	0.208	0.060	
SD	24.0	0.003	0.065	0.058	0.030	
BAIK13-18	< 200 years BP					
	Mean	89.8	(-)	0.004	0.000	0.000
	SD	84.4	(-)	0.015	0.000	0.000
	> 200 years BP					
Mean	5.4	(-)	0.001	0.018	0.009	
SD	9.9	(-)	0.008	0.076	0.034	
BAIK13-19	< 200 years BP					
	Mean	138.3	(-)	0.003	0.018	0.013
	SD	83.4	(-)	0.005	0.024	0.007
	> 200 years BP					
Mean	60.7	(-)	0.014	0.025	0.035	
SD	41.2	(-)	0.022	0.023	0.020	

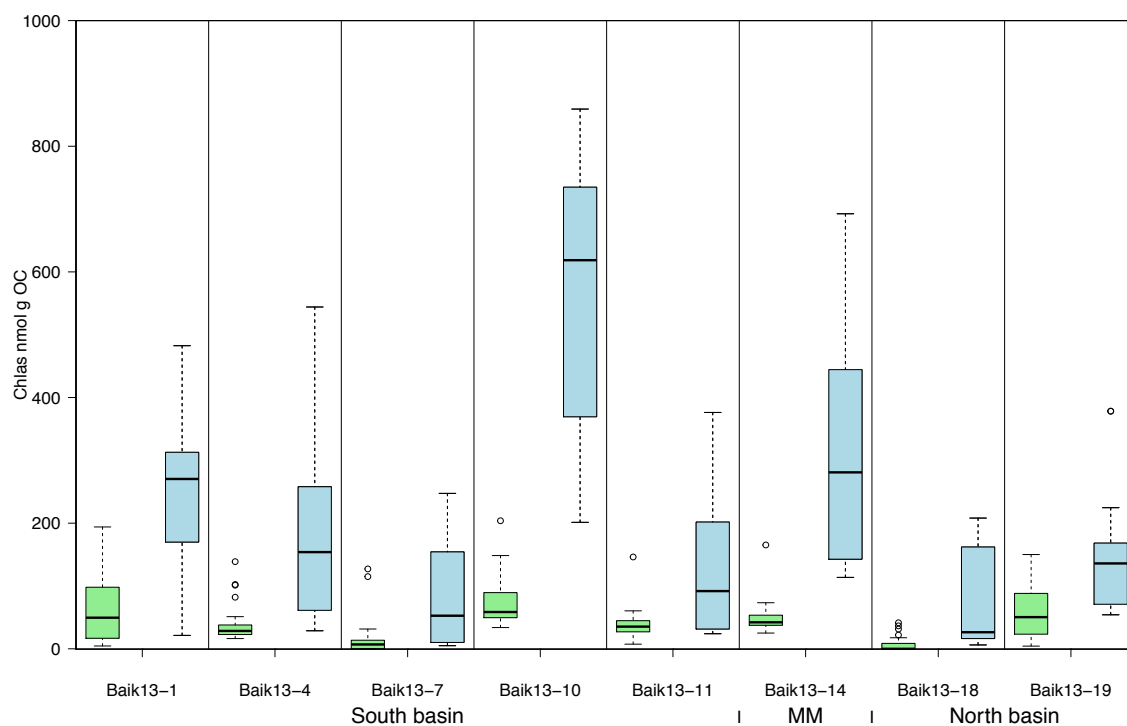


Figure 81: Chlas concentration ($\text{nmol g}^{-1} \text{OC}$) (green > 200 years and blue < 200 years). Turbidite sections are removed within the pigment record. (*BAIK13-7A and *BAIK13-18A show high levels of degradation).

Table 29: Mean values of Chlas concentrations, Chlbs/Chlas, Diatox/Chlas, Cantha/Chlas over the last 200 years and in sediments > 200 years for the South basin, Selenga, Maloe More and North basin. Turbidite sections have been removed within the pigment records.

	Chlas	Chlbs/Chlas	Diatox/Chlas	Lutein/Chlas	Cantha/Chlas
< 200 years BP					
South basin	171.36	0.05	0.00	0.01	0.00
Selenga	343.96	0.02	0.01	0.02	0.01
Maloe More	306.64	0.01	0.03	0.07	0.01
North basin	114.09	(-)	0.00	0.01	0.01
> 200 years BP					
South basin	37.89	0.03	0.02	0.08	0.01
Selenga	55.62	0.00	0.07	0.19	0.06
Maloe More	48.81	0.00	0.13	0.21	0.06
North basin	33.04	(-)	0.01	0.02	0.02

Table 30: Results from t-test to examine if Chlas concentrations are significantly different between the two intervals (> and < 200 years). (*BAIK13-7A and *BAIK13-18A show high levels of degradation).

Basin	Site	T-test	P value
South basin and Selenga	BAIK13-1	6.92	< 0.01
	BAIK13-4	4.65	< 0.01
	BAIK13-7	3.39	< 0.01
	BAIK13-10	17.45	< 0.01
Maloe More	BAIK13-11	3.62	< 0.01
	BAIK13-14	5.89	< 0.01
North basin	BAIK13-18	3.41	< 0.01
	BAIK13-19	5.54	< 0.01

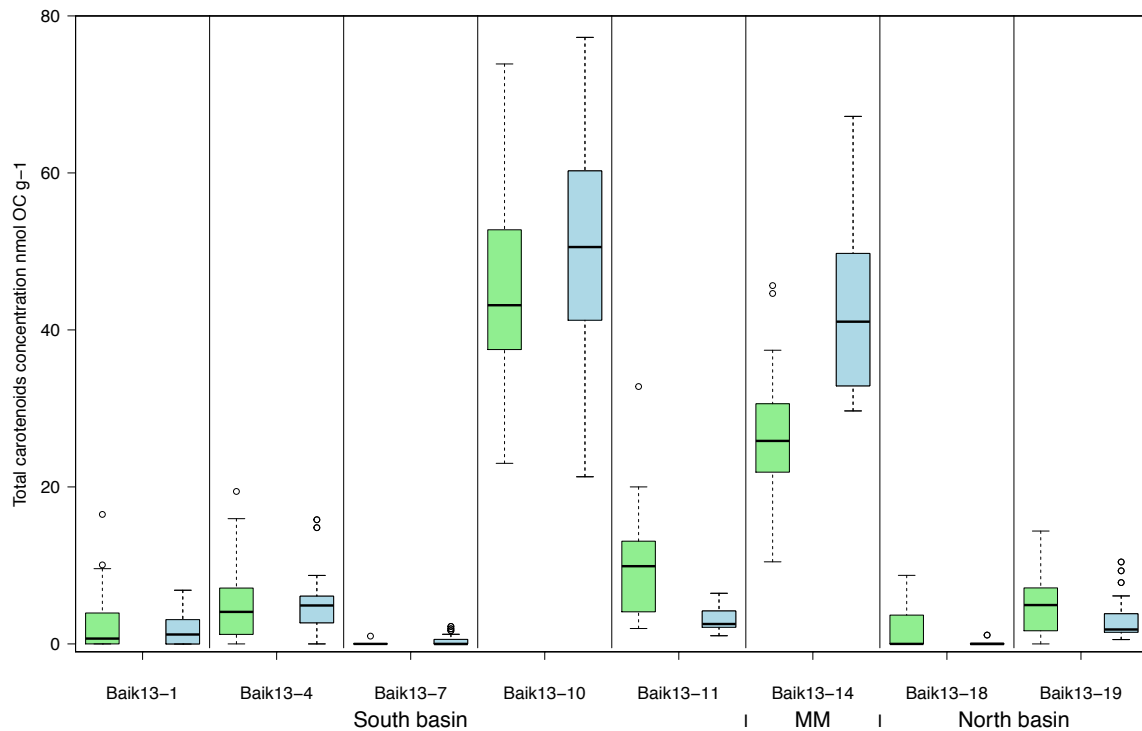


Figure 82: Total carotenoids concentration (nmol g⁻¹ OC) (green > 200 years and blue < 200 years). Turbidite sections are removed from the pigment record. (*BAIK13-7A and *BAIK13-18A show high levels of degradation).

Mean $\delta^{13}\text{C}$ values post 200 years ranged between -27.4 ‰ to 28.9 ‰ in the South basin, -25.9 ‰ to -27.2 ‰ at the Selenga, -27.0 ‰ at Maloe More, and -26.8 ‰ to -29.1 ‰ in the North basin (Figure 83; Table 32). Before 1800 AD, mean $\delta^{13}\text{C}$ values range between 27.2 ‰ to -28.1‰ in the South basin, -26.4 ‰ – 26.9 ‰ at the Selenga, -25.8 ‰ at Maloe More and

between -27.7 ‰ to -28.5 ‰ in the North basin. The largest variation in $\delta^{13}\text{C}$ values pre 1800 AD is observed within South basin sites; BAIK13-7A and Maloe More (BAIK13-14C), and post 200 years the largest variation is observed at BAIK13-4F and BAIK13-7A. Mean $\delta^{13}\text{C}$ values are more positive post 1800 AD than pre 1800 AD at only BAIK13-10A and BAIK13-19B (Table 32). In contrast, mean $\delta^{13}\text{C}$ values pre 1800 AD are more positive than post 1800 AD at a large number of sites across the lake; BAIK13-1C, BAIK13-11C, BAIK13-14C and BAIK13-18A. At sites BAIK13-4F and BAIK13-7A, mean $\delta^{13}\text{C}$ values are similar pre and post 1800 AD.

Table 31: Results from t-test to examine if total carotenoid concentrations are significantly different between the two intervals (> and < 200 years). (*BAIK13-7A and *BAIK13-18A show high levels of degradation).

Basin	Site	T-test	P value
	BAIK13-1	8.46	< 0.01
South basin and Selenga	BAIK13-4	-5.72	< 0.01
	BAIK13-7	-0.28	0.79
	BAIK13-10	7.89	< 0.01
	BAIK13-11	-1.85	0.08
Maloe More	BAIK13-14	-4.73	< 0.01
North basin	BAIK13-18	-2.63	0.02
	BAIK13-19	8.46	< 0.01

Mean TOC content post 1800 AD ranged between 1.9 – 3.1 % in the South basin, 2.6 – 3.0 % at the Selenga, 3% at Maloe More and 2.1 – 2.5 % in the North basin. Pre 1800 AD, mean TOC content range between 1.4 – 2.2 % in the South basin, 2.2 – 2.6 % at the Selenga, 1.9% at Maloe More and 1.6 – 1.9 % in the North basin (Figure 84; Table 32). The largest variation in TOC content pre 1800 AD is seen in the South basin at BAIK13-4, and post 200 years the variation is similar across the sites. Mean TOC content is higher post 1800 AD than pre 1800 AD, at BAIK13-1C, BAIK13-7A, BAIK13-10A, BAIK13-11C, BAIK13-14C, BAIK13-18A and BAIK13-19B, and no difference in mean TOC content between these two time intervals is seen at BAIK13-4 (Figure 84; Table 32). Mean TOC/N ratios post 1800 AD range between 10.4 – 11 in the South basin, 9.0 – 10.1 at the Selenga, 9.0 at Maloe More and 8.9 – 11.0 in the North basin. Pre 1800 AD, mean TOC/N values range between 11.0 – 12.6 in the South basin, 9.8 – 10.1 at the Selenga, 9.1 at Maloe More and 9.5 - 11.3 in the North basin (Figure 84; Table 32). The largest variation in TOC/N ratios pre and post 1800 AD is observed in the South basin at BAIK13-4F. Mean TOC/N ratios are lower post 1800 AD than pre 1800 AD, at BAIK13-1C, BAIK13-7A, BAIK13-10A, BAIK13-11C, BAIK13-14C, BAIK13-18A and BAIK13-19B, and no difference in mean TOC/N ratios between these two time intervals is seen at BAIK13-4F (Figure 84; Table 32).

Table 32: Mean and SD values of $\delta^{13}\text{C}$, TOC content and TOC/N ratios over the last 200 years and in sediments > 200 years. Turbidite sections have been removed within the pigment records.

		$\delta^{13}\text{C}$	TOC	TOC/N
BAIK13-1	< 200 years BP			
	Mean	-28.9	3.1	10.6
	SD	0.2	0.4	0.4
	> 200 years BP			
	Mean	-28.1	2.0	11.0
	SD	0.8	0.5	0.8
BAIK13-4	< 200 years BP			
	Mean	-27.4	2.2	11.0
	SD	0.6	0.6	1.0
	> 200 years BP			
	Mean	-27.4	2.2	11.0
	SD	0.6	0.6	1.0
BAIK13-7	< 200 years BP			
	Mean	-27.4	1.9	10.4
	SD	1.6	0.6	0.6
	> 200 years BP			
	Mean	-27.2	1.4	12.6
	SD	0.7	0.3	3.0
BAIK13-10	< 200 years BP			
	Mean	-25.9	3.0	10.1
	SD	0.5	0.3	0.2
	> 200 years BP			
	Mean	-26.4	2.6	10.6
	SD	0.2	0.2	0.4
BAIK13-11	< 200 years BP			
	Mean	-27.2	2.6	9.0
	SD	0.4	0.5	0.2
	> 200 years BP			
	Mean	-26.9	2.2	9.8
	SD	0.3	0.2	0.5
BAIK13-14	< 200 years BP			
	Mean	-27.0	3.0	9.0
	SD	0.4	0.5	0.2
	> 200 years BP			
	Mean	-25.8	1.9	9.1
	SD	1.0	0.2	0.3
BAIK13-18	< 200 years BP			
	Mean	-29.1	2.5	8.9
	SD	0.3	0.9	2.7
	> 200 years BP			
	Mean	-28.5	1.6	9.5
	SD	0.5	0.5	0.6
BAIK13-19	< 200 years BP			
	Mean	-26.8	2.1	11.0
	SD	0.2	0.3	0.3
	> 200 years BP			
	Mean	-27.7	1.9	11.3
	SD	0.3	0.2	0.7

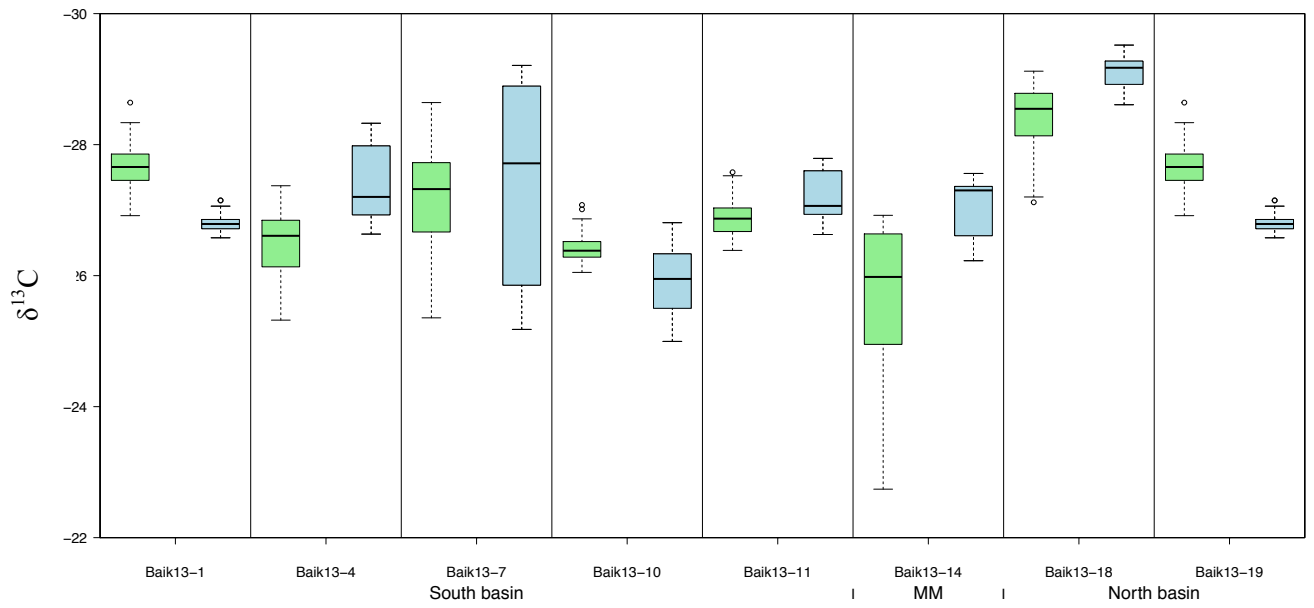


Figure 83: $\delta^{13}\text{C}$ values (green > 200 years and blue < 200 years) at sites in the South basin, Maloe More (MM) and North basin. Turbidite sections are removed within the $\delta^{13}\text{C}$ record.

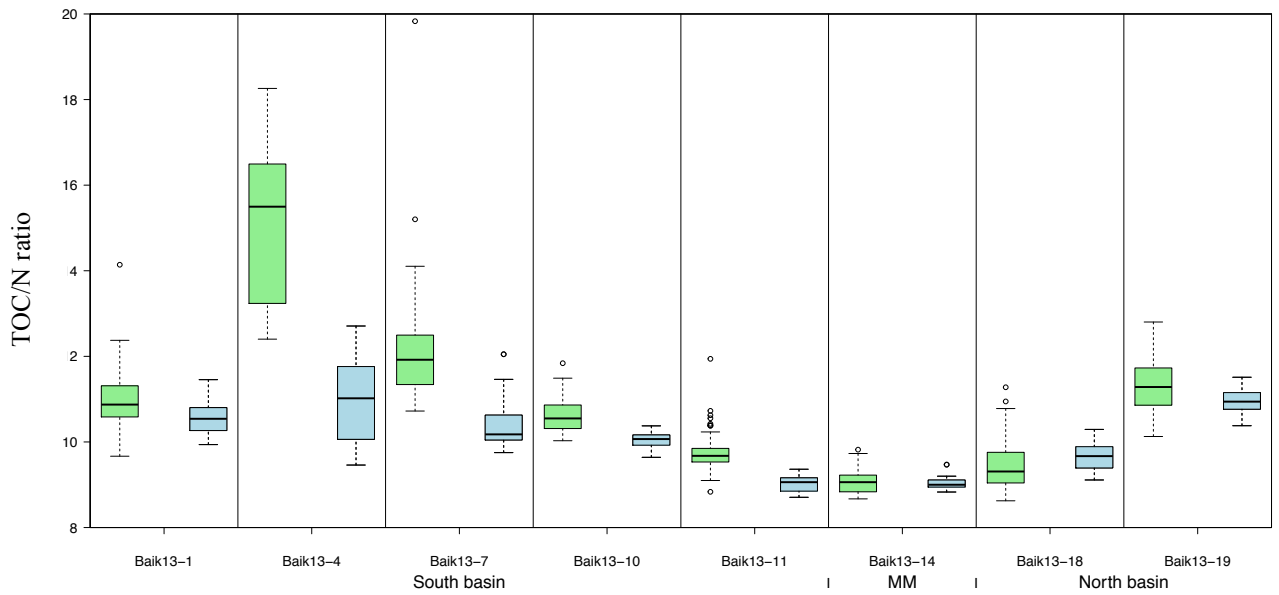


Figure 84: TOC/N ratio (green > 200 years and blue < 200 years) at sites in the South basin, Maloe More (MM) and North basin. Turbidite sections are removed within the TOC/N record.

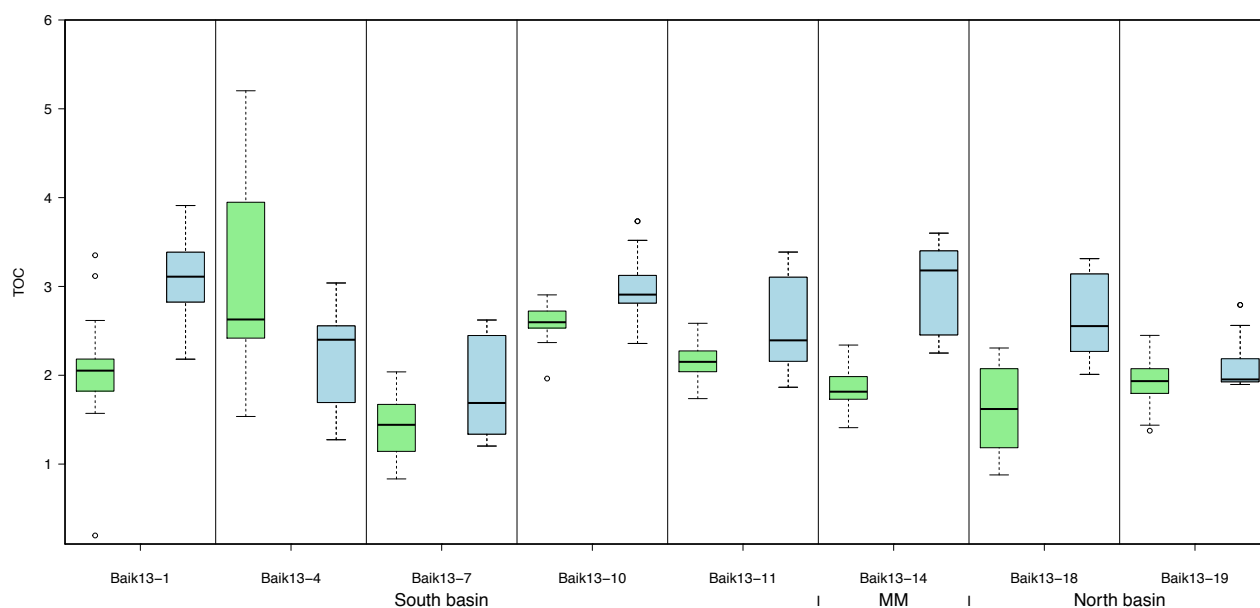


Figure 85: TOC content (green > 200 years and blue < 200 years) at sites in the South basin, Maloe More (MM) and North basin. Turbidite sections are removed within the TOC/N record.

Table 33: Results from t-test to examine if TOC, TOC/N ratio and $\delta^{13}\text{C}$ values are significantly different between the two intervals (> and < 200 years).

Basin	Site	TOC %		TOC/N (%)		$\delta^{13}\text{C}$	
		T-test	P value	T-test	P value	T-test	P value
South basin and Selenga	BAIK13-1	10.31	< 0.01	-1.85	0.07	8.46	< 0.01
	BAIK13-4	-2.77	0.01	-6.57	< 0.01	-5.72	< 0.01
	BAIK13-7	0.21	0.83	-4.57	< 0.01	-0.28	0.78
	BAIK13-10	7.66	< 0.01	-7.47	< 0.01	7.89	< 0.01
Maloe More	BAIK13-11	4.72	< 0.01	-7.14	< 0.01	-1.84	0.08
	BAIK13-14	9.99	< 0.01	0.32	0.76	-4.73	< 0.01
North basin	BAIK13-18	3.95	< 0.01	-0.91	0.38	-2.62	0.02
	BAIK13-19	4.05	< 0.01	4.53	< 0.01	8.46	< 0.01

6.3.3 Spatial comparison of short cores across Lake Baikal

The sites close to major rivers, the Selenga (BAIK13-11C) and Upper Angara (BAIK13-19B) have no turbidites (Figure 86). These sediment cores have the least interference from turbidites and smaller oxidised layers which is likely to be due to the higher sedimentation rates, in comparison to the pelagic deep south and north basin sites. The coring sites within the South basin are very variable, with turbidite layers throughout and large oxidised layers in the upper 10 cm (Figure 86). BAIK13-4F in South basin is the only sediment core which shows the presence of turbidite layers within the sediment interval which covers the last 200

years (*Figure 86*). The smallest oxidised layers within the upper sediments of the cores are found within the Maloe More sediments (BAIK13-14C and BAIK13-15B), BAIK13-19B by the Upper Angara in the North basin and BAIK13-11C opposite the Selenga Delta (*Figure 86*). Despite the presence of turbidites in the South basin, Maloe More, Selenga and North basin sediment cores, proxy records can still be used to reconstruct past changes in primary production, by removing the associated intervals within the pigment and $\delta^{13}\text{C}$ records. BAIK13-16B in Chivsky Bay in the North basin is the only sediment record which is known to cover all the Holocene period, due to the presence of Pleistocene clays, identified from the sedimentary lithology profiles (*Figure 86*). Despite the shallower depths at this site (650 m) compared to the pelagic basins ($> 1,000$ m), this core however has a large oxidised layer extending over the upper 15 cm of the sediment core, and the pigment records largely consists of chlorophyll degradation products, if any pigments at all. This core therefore does not provide a reliable pigment record to reconstruct longer term changes in primary production. As found in Chapter Seven, the cores which provide the most reliable pigment records are BAIK13-1C (South basin), Baik13-10A (Selenga Shallows), BAIK13-14C (Maloe More) and BAIK13-19B (North basin). For the $\delta^{13}\text{C}$ records, these sediment cores can be used for longer term reconstructions, if the turbidite sections are removed, and the diatom records within the surface sediments of BAIK13-4F, BAIK13-11C, BAIK13-14C, BAIK13-18A and BAIK13-19B can still be used.

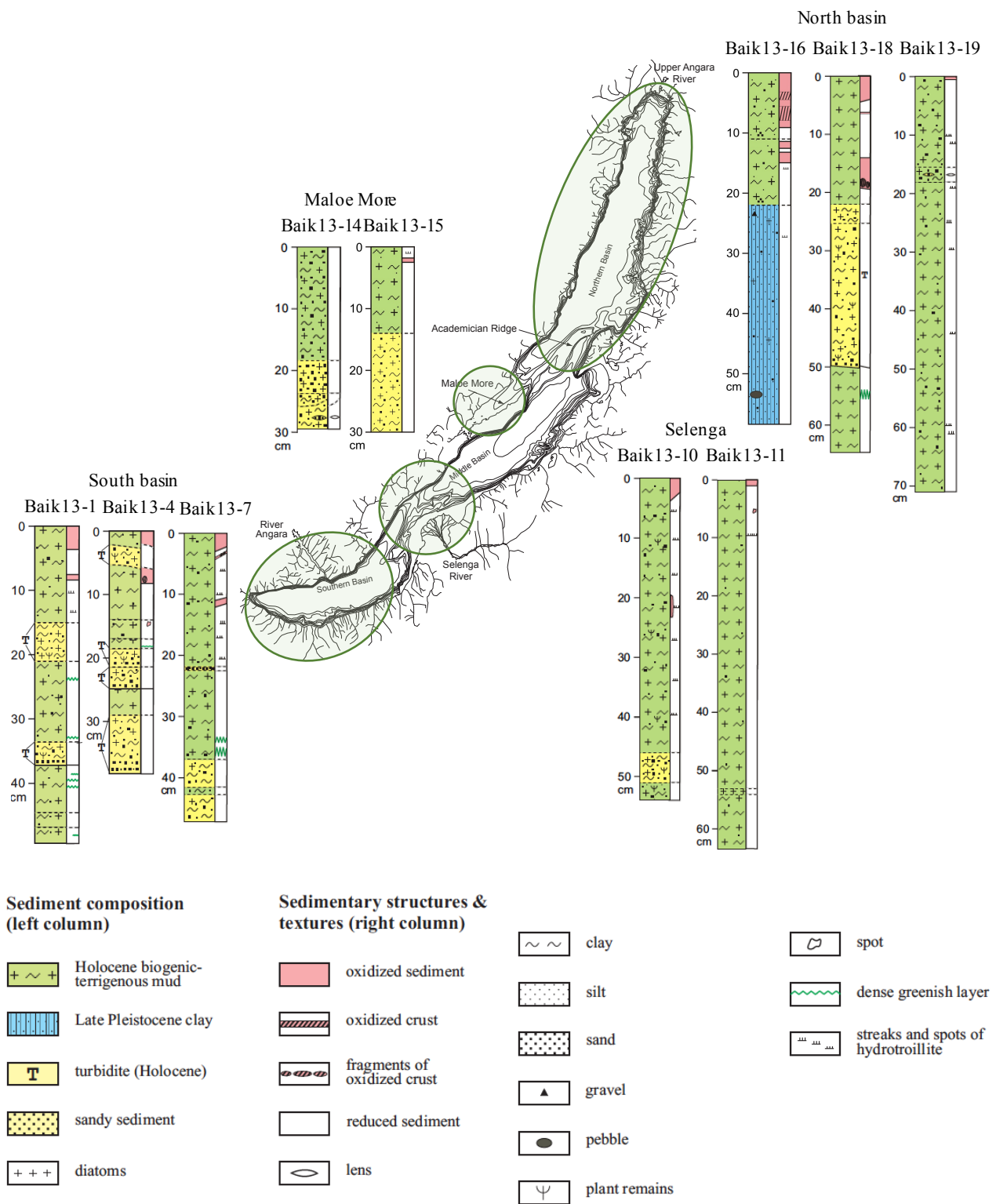


Figure 86: Sediment cores collected in March 2013 and August 2013 in the South basin, Maloe More, Selenga and North basin. (*BAIK13-7 and *BAIK13-18 show high levels of degradation).

The sediment depths analysed below are associated with the section of the core > 200 years BP. These depths are focussed upon within this chapter to compare the results from the ^{210}Pb dated sediment cores presented in Chapter Seven (< 200 years) to these records (> 200 years).

BAIK13-1C South basin (6 – 22 cm sediment depth)

BAIK13-1C shows peaks in Chla concentrations and chlorophyll degradation products between 9 – 12 cm to c. $4 \text{ nmol g}^{-1} \text{ OC}$ (Figure 87). Lutein, diatoxanthin and canthaxanthin peak between between 9 – 12 cm, to concentrations of c. 8, 3 and 3.5 nmol g^{-1} respectively. $\delta^{13}\text{C}$ also peak to more positive values between 9 – 12 cm to -27.6 ‰ and -27.2 ‰ . TOC/N values range between 10 – 12, and peak to values of 14 at c. 21 cm. TOC value generally range between 1 – 2.5 %.

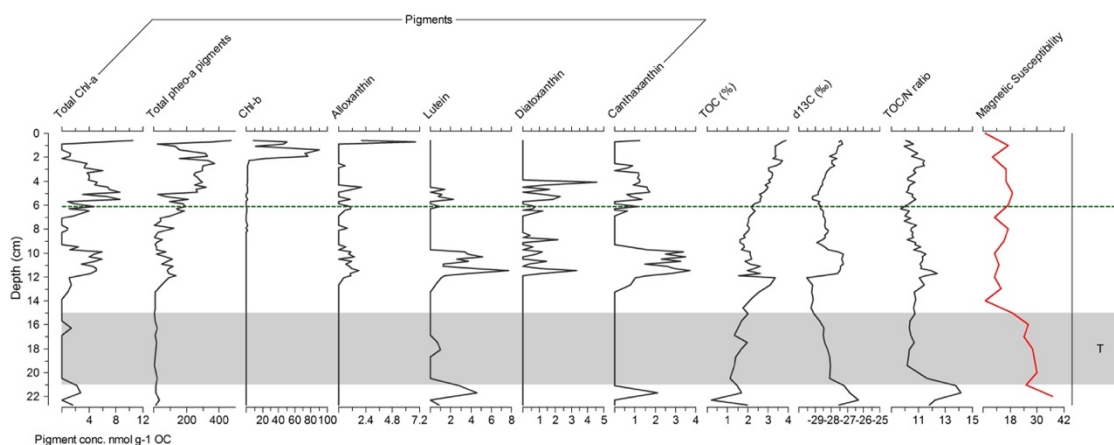


Figure 87: Pigment concentrations (nmol per g OM), pigment ratios, TOC %, $\delta^{13}\text{C}$, TOC/N ratio values and magnetic susceptibility values (10^{-6} SI un) in the entire BAIK13-1C sediment core. Grey shaded areas represent turbidite layers. Green line represents the sediment depth for the last 200 years from ^{210}Pb dating. (T – turbidites).

BAIK13-4F South basin (10 – 20 cm sediment depth)

BAIK13-4F shows a peak in Chlas, Chlb and lutein concentrations between c. 13 – 16 cm to values of c. 5 -10, 5 – 7 and 6 – 14 $\text{nmol g}^{-1} \text{ OC}$ respectively (Figure 88). TOC % and TOC/N ratios also increase between c. 13 – 16 cm to values of 4 – 5 and c. 17 – 20 respectively. $\delta^{13}\text{C}$ values range between -28.2 ‰ to -25.3 ‰ .

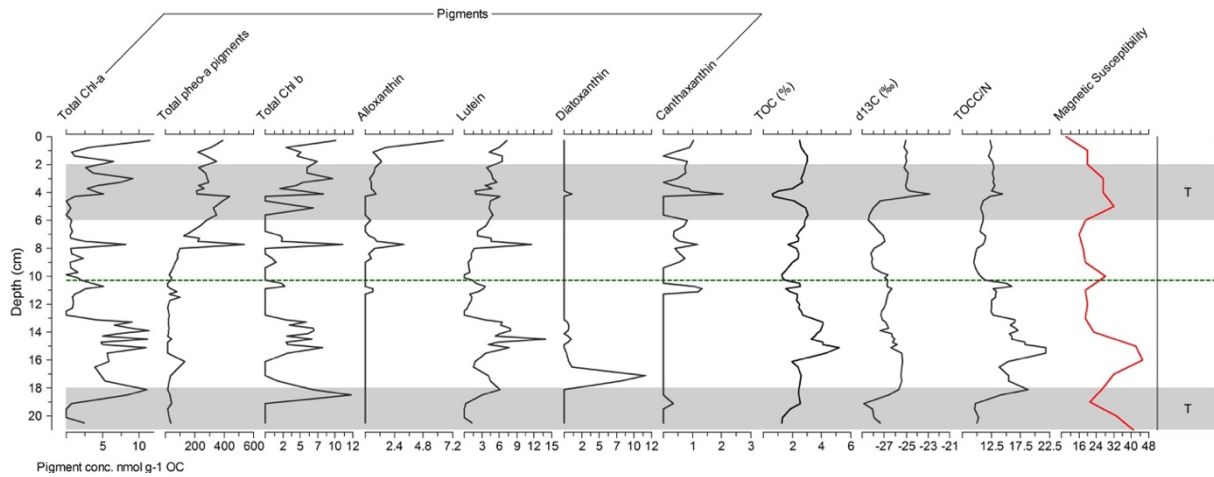


Figure 88: Pigment concentrations (nmol per g OM), pigment ratios, TOC %, $\delta^{13}\text{C}$, TOC/N ratio values and magnetic susceptibility values (10^{-6} SI un) in the entire BAIK13-4F sediment core. Grey shaded areas represent turbidite layers. Green line represents the sediment depth for the last 200 years from ^{210}Pb dating (T – turbidites).

BAIK13-7A South basin (5 – 45 cm sediment depth) (*show high levels of degradation)

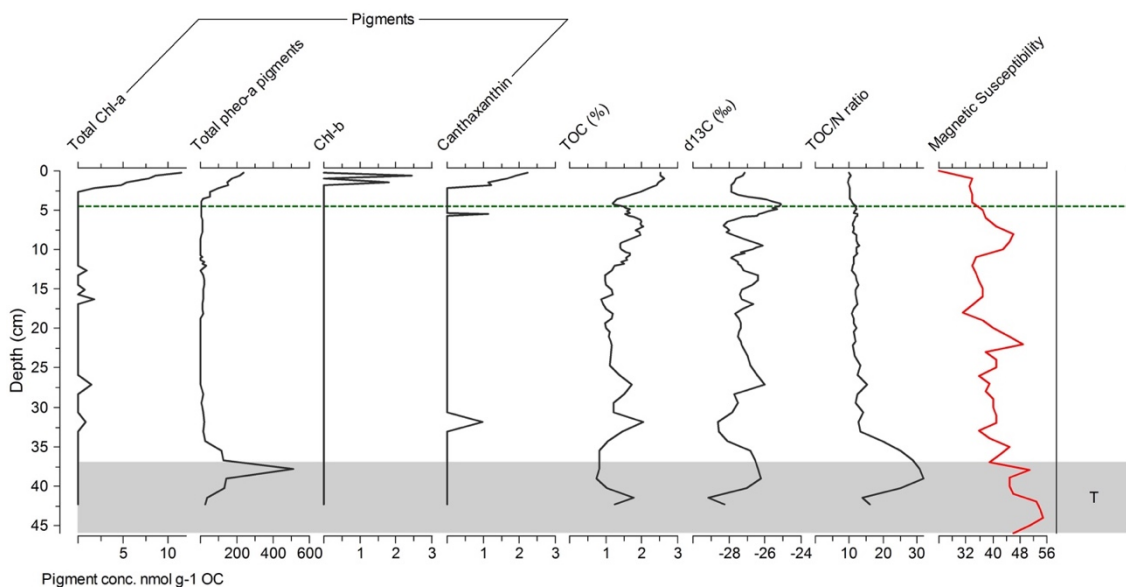


Figure 89: Pigment concentrations (nmol per g OM), pigment ratios, TOC %, $\delta^{13}\text{C}$, TOC/N ratio values and magnetic susceptibility values (10^{-6} SI un) in the entire BAIK13-7A sediment core. Grey shaded areas represent turbidite layers. Green line represents the sediment depth for the last 200 years from ^{210}Pb dating. (T – turbidites).

BAIK13-7A shows slight peaks in Chla concentrations downcore to low concentrations of 0.8 – 2 nmol g⁻¹ OC (Figure 89). $\delta^{13}\text{C}$ varies downcore, ranging between -26.0 ‰ to -28.6 ‰. TOC/N ratio values are consistently between 10 – 12, and then peak to values > 30 between 33 – 40 cm.

BAIK13-10A Selenga (11 – 50 cm sediment depth)

In BAIK13-10A Chla concentrations range between 8 – 26 nmol g⁻¹ OC, and total pheo a pigment concentrations range between 40 – 200 nmol g⁻¹ (Figure 90). Chlb concentrations peak between 14 – 18 cm to concentrations of 1.2 – 7.5 nmol g⁻¹ OC. Alloxanthin, diatoxanthin, lutein and canthaxanthin concentrations vary downcore and show no obvious increasing or decreasing trends. Alloxanthin concentrations range between 28 – 35 nmol g⁻¹ OC, diatoxanthin concentrations range between 1.5 – 16 nmol g⁻¹ OC, lutein concentrations range between 8 – 26 nmol g⁻¹ OC and canthaxanthin concentrations range between 1.4 – 10 nmol g⁻¹ OC. δ¹³C are relatively constant between -27.0 ‰ to -26.0 ‰, and TOC values are consistently between 2.5 – 3 %. TOC/N values show an increasing trend down-core from 10 to 12.

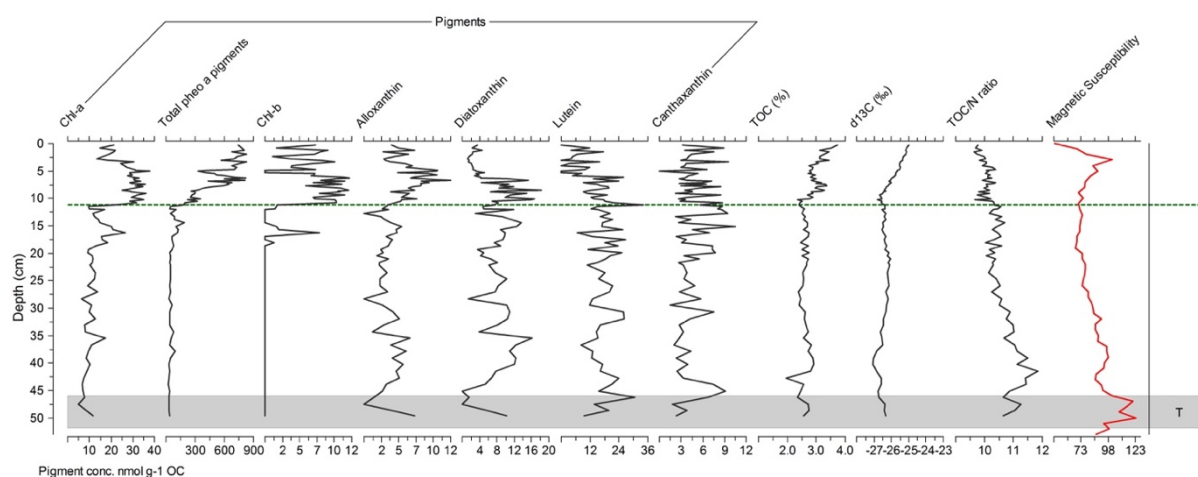


Figure 90: Pigment concentrations (nmol per g OM), pigment ratios, TOC %, δ¹³C, TOC/N ratio values and magnetic susceptibility values (10⁻⁶ SI un) in the entire BAIK13-10A sediment core. Grey shaded areas represent turbidite layers. Green line represents the sediment depth for the last 200 years from ²¹⁰Pb dating. (T – turbidites).

BAIK13-11C Selenga (9 – 50 cm sediment depth)

At BAIK13-11C Chla, lutein, diatoxanthin and alloxanthin concentrations show higher concentrations between 20 – 42 cm of 6 – 10, 3 – 9, 4 – 12 and 1.5 – 4 nmol g⁻¹ respectively (Figure 91). Canthaxanthin concentrations vary between 0.9 – 1.5 nmol g⁻¹ OC downcore and total pheo a pigments range between 20 – 30 nmol g⁻¹ OC, with a peak at 21 cm to 150 nmol g⁻¹ OC. δ¹³C values vary between -27.5 ‰ and -26.5 ‰, down-core, with TOC % values between 1.7 – 2.3 % and TOC/N ratio values between 9 – 12.

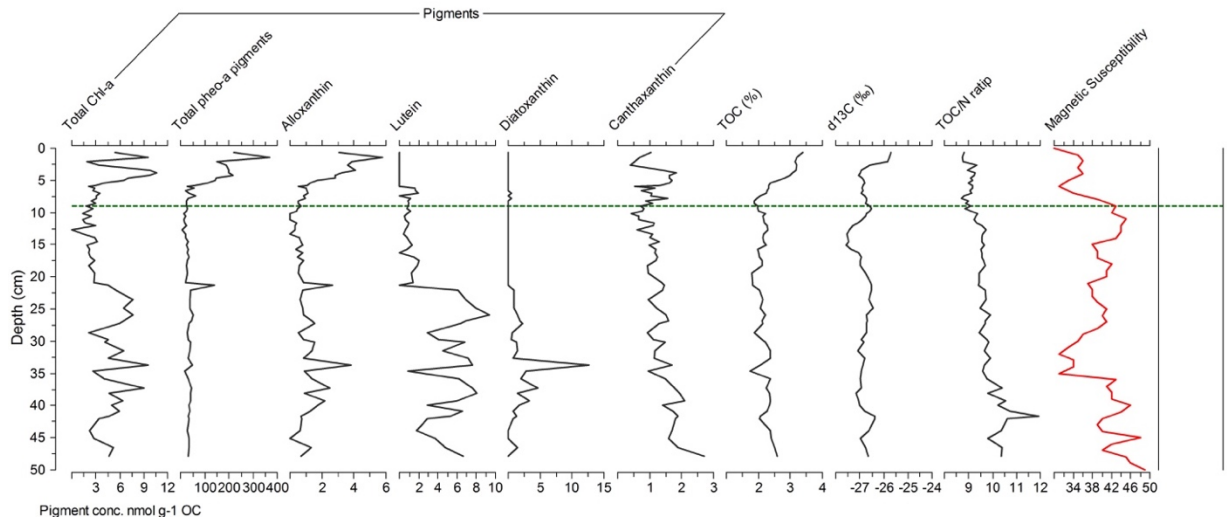


Figure 91: Pigment concentrations (nmol per g OM), pigment ratios, TOC %, $\delta^{13}\text{C}$, TOC/N ratio values and magnetic susceptibility values (10^{-6} SI un) in the entire BAIK13-11C sediment core. No turbidites in sediment core. Green line represents the sediment depth for the last 200 years from ^{210}Pb dating.

BAIK13-14C Maloe More (7 – 24 cm sediment depth)

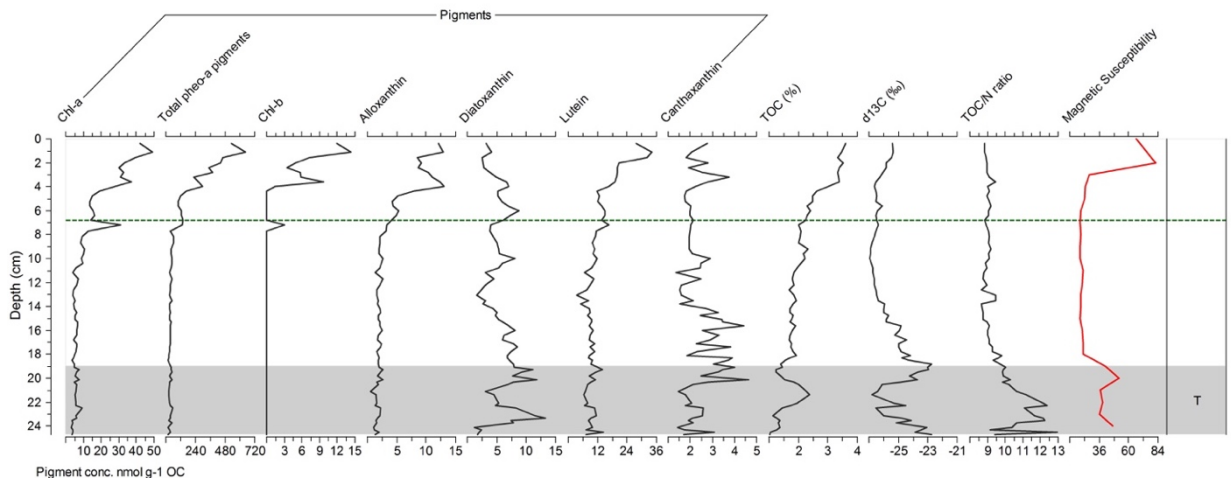


Figure 92: Pigment concentrations (nmol per g OM), pigment ratios, TOC %, $\delta^{13}\text{C}$, TOC/N ratio values and magnetic susceptibility values (10^{-6} SI un) in the entire BAIK13-14C sediment core. Grey shaded areas represent turbidite layers. Green line represents the sediment depth for the last 200 years from ^{210}Pb dating. (T – turbidites).

There is a peak in Chlorophyll-*a* concentrations at 7 cm to 30 nmol g⁻¹ OC, and declining trend in concentrations down-core (Figure 92). Alloxanthin concentrations show little change down core, ranging between 1.7 – 2.5 nmol g⁻¹ OC, and lutein concentrations show an increasing trend from 3.5 to 10 nmol g⁻¹ towards the 200-year horizon. Both canthaxanthin and diatoxanthin concentrations are higher in the bottom sediments, between 15 – 24 cm, ranging

in concentrations between 1.5 – 5 and 1.5 – 13 nmol g⁻¹ OC respectively. $\delta^{13}\text{C}$ and TOC/N values increase towards the bottom of the core, peaking to values of -24.8 ‰ to -22.7 ‰ (becoming more positive) and ratio value between 10 - 13. TOC % values show a slight decreasing trend down core, from 2.3 % to 1%.

BAIK13-15B Maloe More (No ²¹⁰Pb dates; 0 – 22 cm sediment depth)

BAIK13-15B shows decreasing trends in Chla, total pheo-*a* pigments, Chlb, alloxanthin, lutein, diatoxanthin and canthaxanthin pigment concentrations down-core, as well as TOC % (Figure 93).

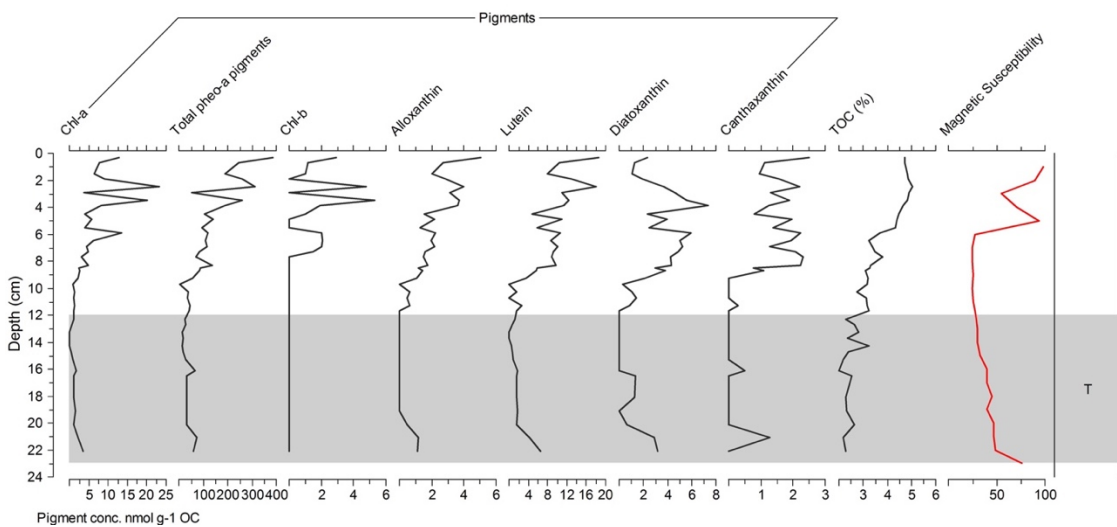


Figure 93: Pigment concentrations (nmol per g OM), pigment ratios, TOC % and magnetic susceptibility values (10^{-6} SI un) in the entire BAIK13-15B sediment core. Grey shaded areas represent turbidite layers. (T – turbidites).

BAIK13-16B North basin (No ²¹⁰Pb dates; 0 – 55 cm sediment depth)

The surface sediments of BAIK13-16B have high concentrations of Chla, total pheo *a* pigments, alloxanthin and canthaxanthin pigments which then decrease to undetectable concentrations between 5 – 22 cm (Figure 94). Lutein concentrations are undetectable and then peak at 3.7 cm to 0.6 nmol g⁻¹ OC. The Pleistocene clay sediments (22 – 55 cm) show higher concentrations of lutein and canthaxanthin, reaching values of 1.5 nmol g⁻¹ OC. TOC content decreases from 3.5 % in the surface sediments to 0.2 % at 10.3 cm and remain low between 1 – 1.8 %. $\delta^{13}\text{C}$ values rise to values of -24.2 ‰ from -28.7 ‰ between 0 – 22 cm, and then remain between -29.9 ‰ and -28.7 ‰ downcore. TOC/N ratios range between 7 – 10.6 between 0 – 22 cm, peaking at 10.3 to values of 13.2. Between 22 – 55 cm TOC/N ratios remain at c. 9.6 - 11.4.

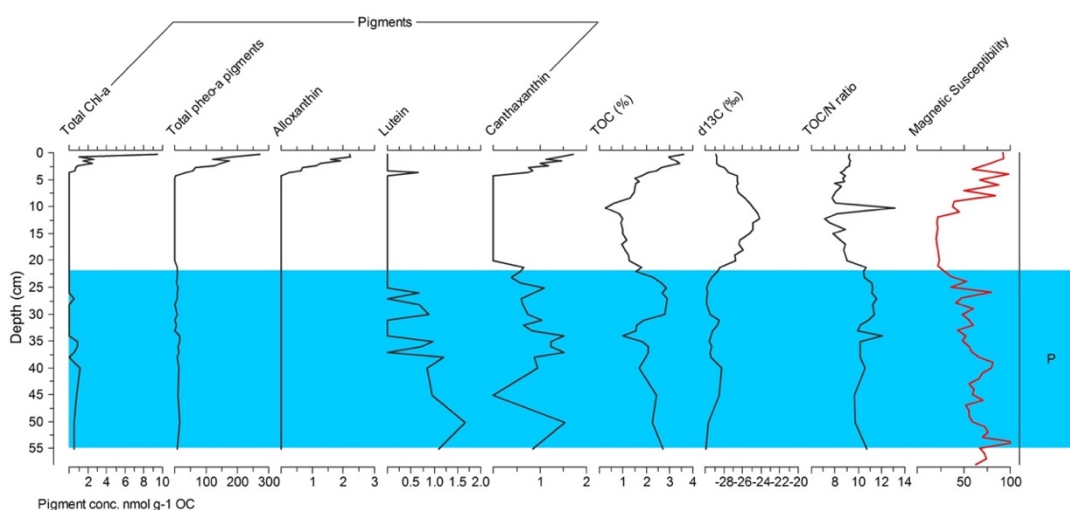


Figure 94: Pigment concentrations (nmol per g OM), pigment ratios, TOC % and magnetic susceptibility values (10^{-6} SI un) in the entire BAIK13-16B sediment core. No turbidites in sediment core. Blue shaded area represents Pleistocene clays.

BAIK13-18A North basin (4 – 55 cm sediment depth) (*show high levels of degradation)

BAIK13-18A shows peaks in Chla, lutein, diatoxanthin and canthaxanthin concentrations between 25 – 55 cm (Figure 95). Pheo-a pigments are not detected between 8 – 20 cm. Between these sediment depths diatoxanthin and canthaxanthin peak to concentrations of 10 – 13 nmol g⁻¹ OC and lutein is undetectable. TOC content decreases from 2.3 % to 0.8 % between 8 – 20 cm in the turbidite free sediment interval, and $\delta^{13}\text{C}$ values increase from -29.1 ‰ to -27.2 ‰. TOC/N ratios range between 8.6 – 10.7 between 8 – 20 cm.

BAIK13-19B North basin (8 – 65 cm sediment depth)

BAIK13-19B shows little change in Chla and total pheo a pigment concentrations down core, which range between 1.6 – 7.0 nmol g⁻¹ OC and 23.5 – 143.5 nmol g⁻¹ OC respectively (Figure 96). Higher concentrations of diatoxanthin and lutein occur between 30 – 55 cm, reaching values of > 4 nmol g⁻¹ OC. Canthaxanthin concentrations rise between 17- 60 cm, and reach concentrations of 3.4 nmol g⁻¹ OC. TOC content range between 1.4 – 2.5 %, TOC/N ratios

peak between 15 – 30 cm to values > 12, and then stay consistent between 10 – 11.7. $\delta^{13}\text{C}$ values range between -27.5 ‰ and -28.6 ‰.

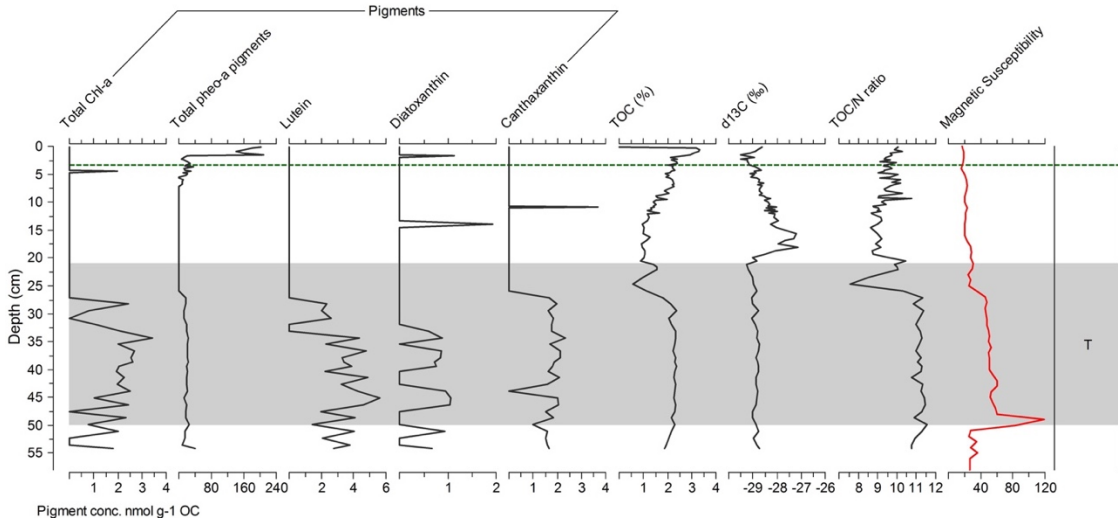


Figure 95: Pigment concentrations (nmol per g OM), pigment ratios, TOC %, $\delta^{13}\text{C}$, TOC/N ratio values and magnetic susceptibility values (10^{-6} SI un) in the entire BAIK13-18A sediment core. Grey shaded areas represent turbidite layers. Green line represents the sediment depth for the last 200 years from ^{210}Pb dating. (T – turbidites).

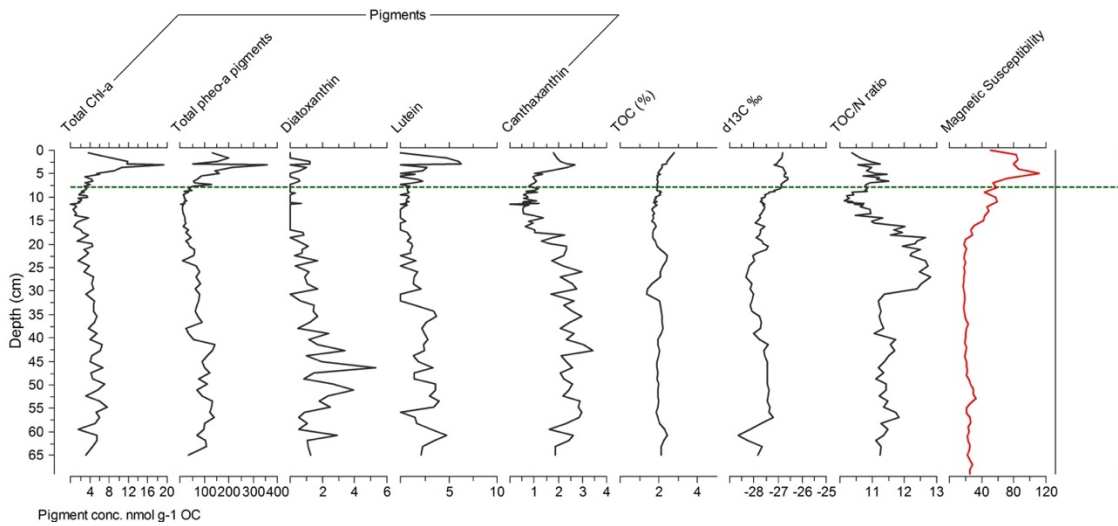


Figure 96: Pigment concentrations (nmol per g OM), pigment ratios, TOC %, $\delta^{13}\text{C}$, TOC/N ratio values and magnetic susceptibility values (10^{-6} SI un) in the entire BAIK13-19B sediment core. No turbidites in sediment core. Green line represents the sediment depth for the last 200 years from ^{210}Pb dating.

Diatoxanthin:canthaxanthin pigment concentration ratios were highest in the Selenga cores (BAIK13-10A and BAIK13-11C) and showed a decreasing trend towards the surface sediments (*Figure 97*). This decreasing trend is also seen in the Maloe More sites (BAIK13-14C and BAIK13-15B), at a smaller magnitude and later on. South basin and North basin sites do not show this decreasing trend, only slightly at BAIK13-1C in the South basin. This is likely to be a reflection of ice cover changes, which could explain the regional differences, and an explanation for the Selenga having an earlier response and larger change could possibly be due to the input of Selenga waters.

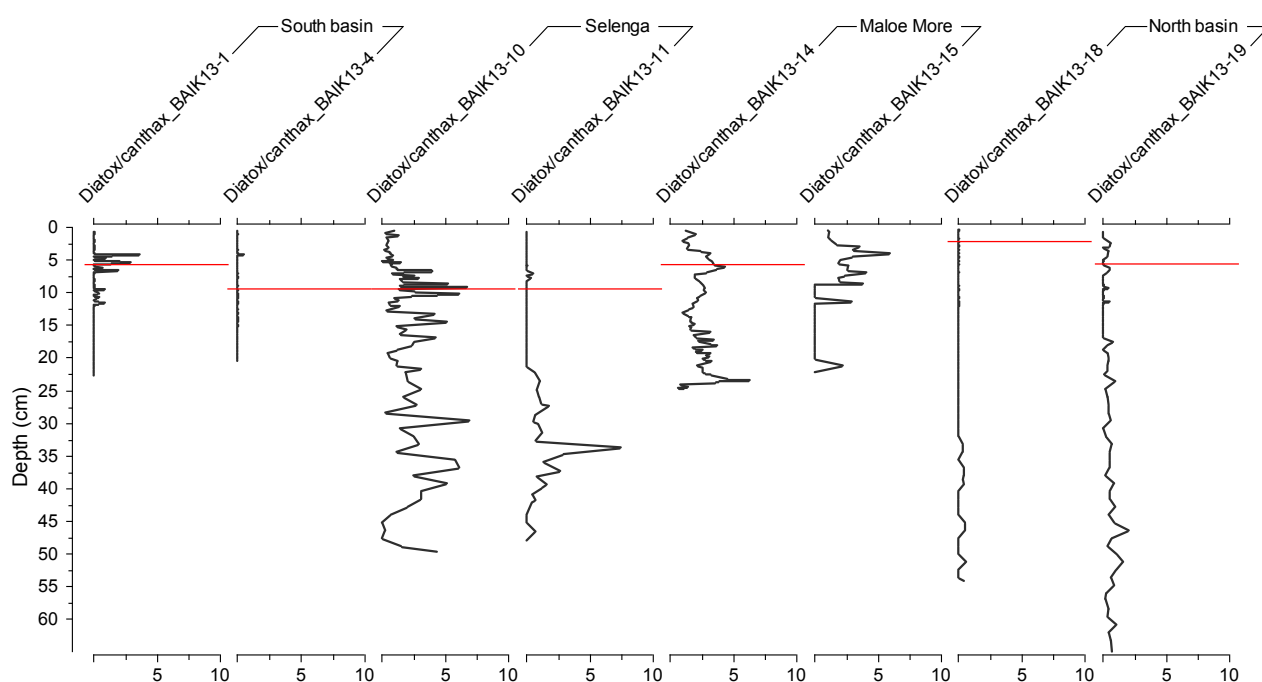


Figure 97: Diatoxanthin:canthaxanthin ratio. Red line represents sediment depth of last 200 years from ^{210}Pb dating chronologies.

6.3.4 Comparison with previous studies

In general TOC is low at Lake Baikal because of the slow accumulation rates and oxygenated upper sediments (Horiuchi et al. 2000; Ishiwatari et al. 2005; Watanabe et al. 2009; Mackay et al. 2016). Over the Holocene, TOC % values ranged between c. 1-3 % (Mackay et al. 2016), and TOC/N ratio values fluctuated between 9.8 and 13.8 (mean = 11.6). The $\delta^{13}\text{C}$ values from bulk sediments are influenced by several sources, as discussed in Chapter One, but what makes Lake Baikal unusual is that cold climates e.g. glacial periods, result in higher $\delta^{13}\text{C}$ values than in warm periods, e.g. interglacials (Watanabe et al. 2004). It is unclear why this is, but Mackay et al. (2016) has suggested that the most reasonable explanation is to do with changes in pelagic and littoral communities. Over the Holocene, $\delta^{13}\text{C}$ values ranged between -27 ‰ to –

30.5 ‰, with the lowest $\delta^{13}\text{C}$ values of c. -30 ‰ (least positive) found between c. 4 – 8 k BP (Mackay et al. 2016) (*Figure 98*). The $\delta^{13}\text{C}$ values are less positive (lower) in the early and mid-Holocene compared to the late Holocene (c. -27 ‰ to -29 ‰) (Mackay et al. 2016). The $\delta^{13}\text{C}$ records from the North basin and academician ridge from other studies at Lake Baikal over the Holocene also show a general trend towards more positive $\delta^{13}\text{C}$ values, although these are at lower resolution (Ishiwatari et al. 2005; Watanabe et al. 2009) (*Figure 98*; *Figure 99*). All these records show a similar range in $\delta^{13}\text{C}$ values (Ishiwatari et al. 2005; Watanabe et al. 2009; Mackay et al. 2016). TOC records at these sites show similar trends over the Holocene, and ranges in values (Ishiwatari et al. 2005; Horiuchi et al. 2000; Watanabe et al. 2009; Mackay et al. 2016) (*Figure 100*).

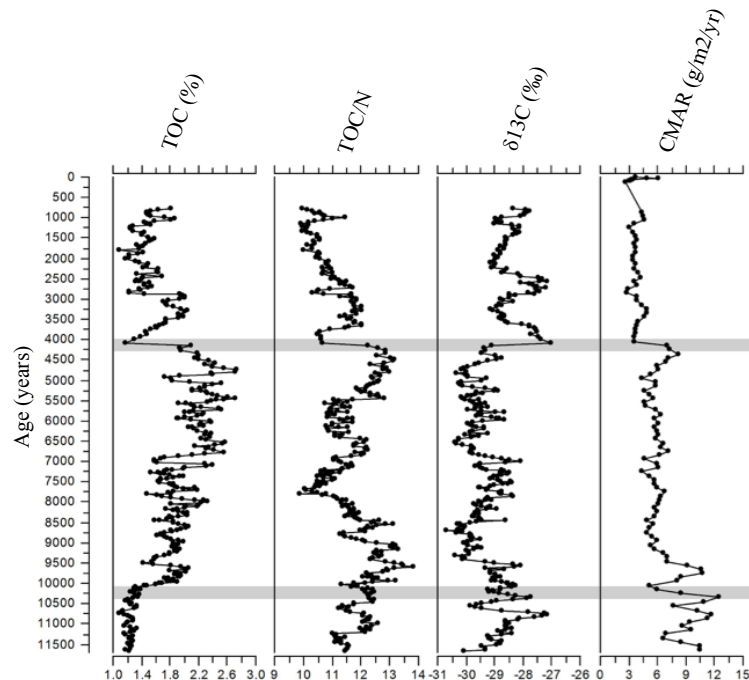


Figure 98: $\delta^{13}\text{C}$, C/N % ratios, TOC % and CMAR values over the Holocene at the Vydrino site in the South basin (modified from Mackay et al. 2016).

$\delta^{13}\text{C}$ values show the greatest variability down-core in the South basin, Maloe More and Chivsky Bay in the North basin (BAIK13-16B), in comparison to the Selenga and pelagic North basin sites (*Figure 101*). TOC content and TOC/N values both show the greatest variability down-core in the South basin (*Figure 102*; *Figure 103*). In comparison to Fietz et al. (2007), mean $\delta^{13}\text{C}$ values in the South basin of -21.5 ‰ to -26.1 ‰ over the last 7,000 years are higher (more positive) than mean South basin $\delta^{13}\text{C}$ values of -27 ‰ to -28.9 ‰ presented pre and post 200 years in this chapter. This is also the case for mean $\delta^{13}\text{C}$ values in

Selenga of -22.8 ‰ to -26.2 ‰ over the last 10,000 years and North basin of -22.8 ‰ to -47 ‰ over the last 11,000 years (Fietz et al. 2007), as the mean $\delta^{13}\text{C}$ values pre and post 200 years range between -25.9 ‰ and -27.2 ‰ and -26.8 ‰ and -29.1 ‰.

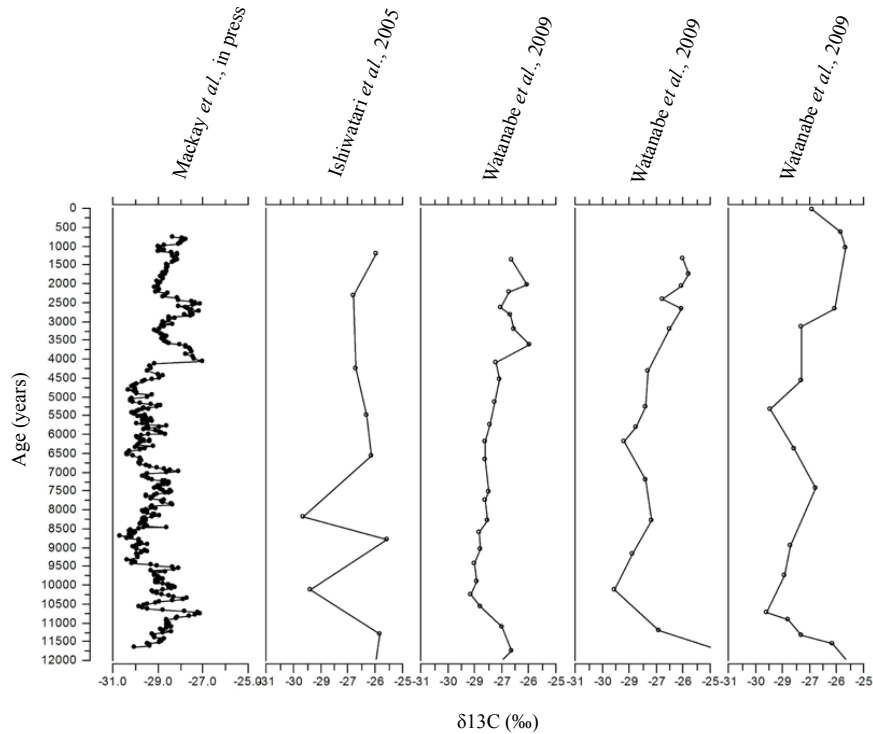


Figure 99: Previous $\delta^{13}\text{C}$ records at Lake Baikal over the Holocene (from Ishiwatari et al. 2005; Watanabe et al. 2009; Mackay et al. 2016) (modified from Mackay et al. 2016).

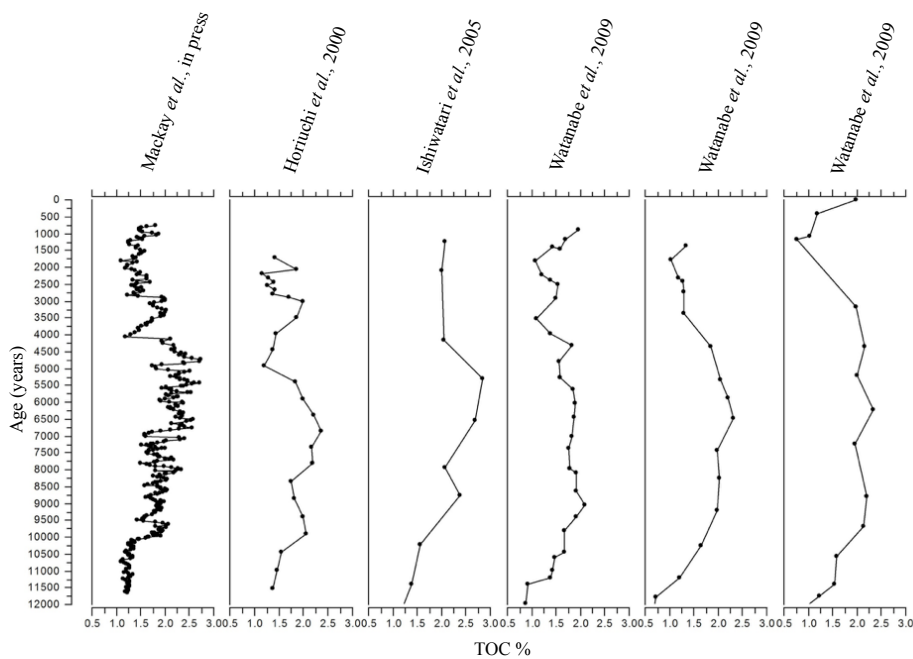


Figure 100: Previous TOC % records at Lake Baikal over the Holocene (from Ishiwatari et al. 2005; Horiuchi et al. 2000; Watanabe et al. 2009; Mackay et al. 2016) (modified from Mackay et al. 2016).

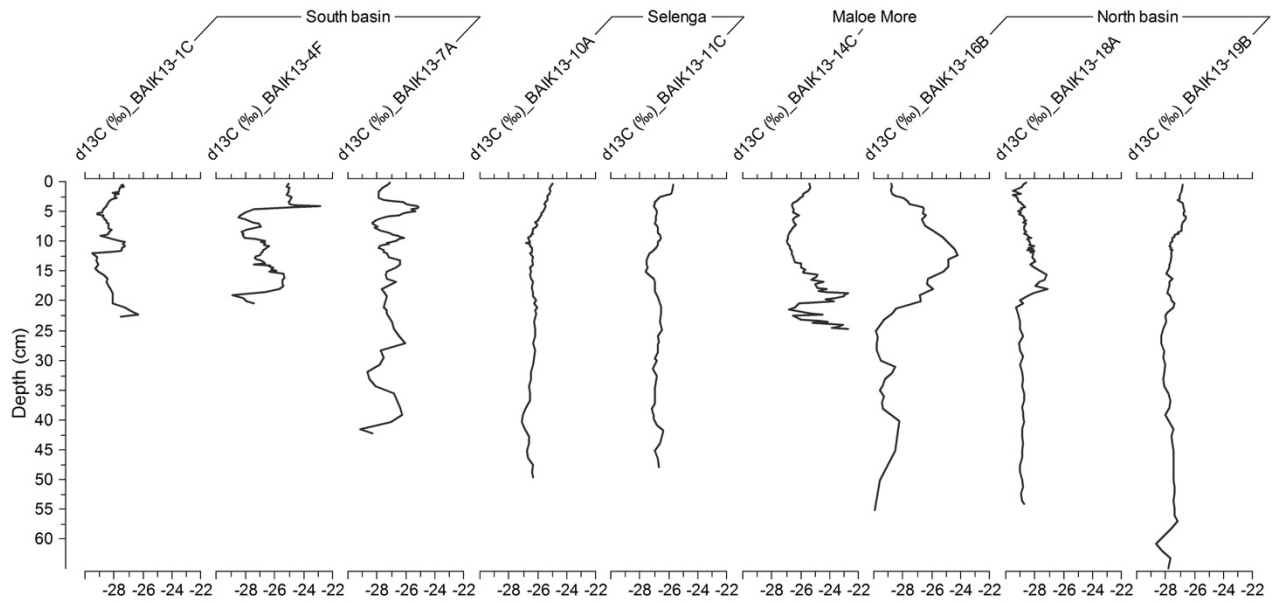


Figure 101: $\delta^{13}\text{C}$ values from South basin, Selenga, Maloe More and North basin sediment cores.

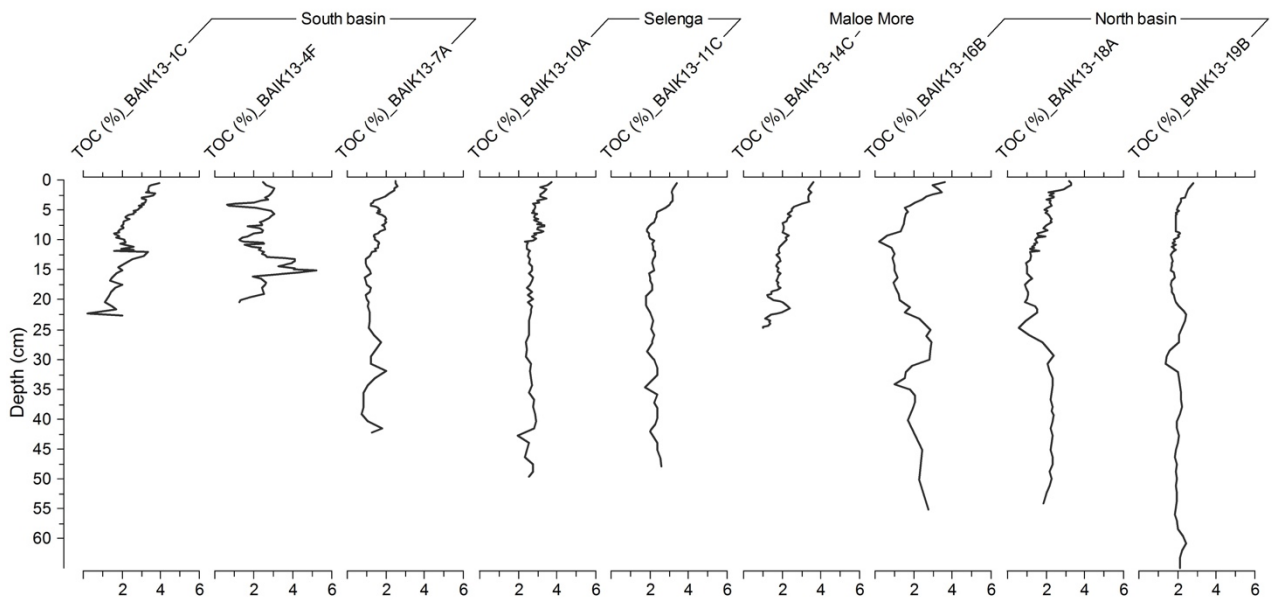


Figure 102: TOC content from South basin, Selenga, Maloe More and North basin sediment cores.

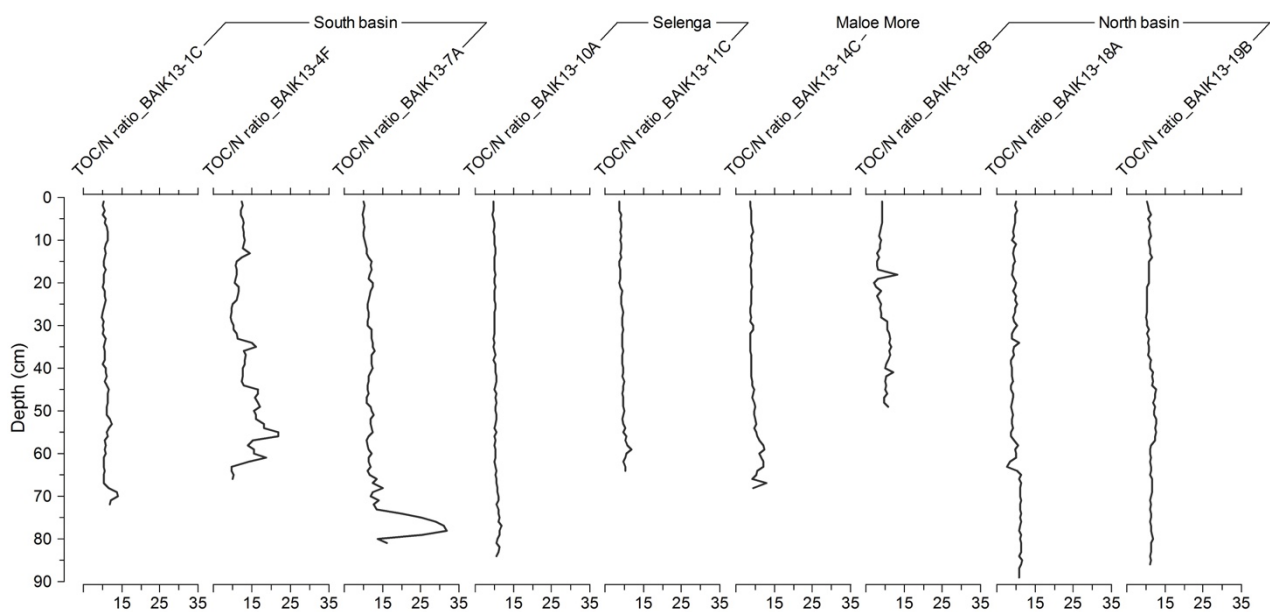


Figure 103: TOC/N ratio from South basin, Selenga, Maloe More and North basin sediment cores.

Previous sedimentary pigment records from Lake Baikal have largely used Steryl Chlorin Esters (SCE) as phytoplankton markers (Naylor and Keely, 1998; Soma et al. 1996; Tani et al. 2001). Large quantities of SCEs, formed through zooplankton grazing (Harradine et al. 1996; Talbot et al. 2000), have been observed in Baikal's sediments (Soma et al. 1996; Tani et al. 2001). Earlier studies (Soma et al. 1996; Tani et al. 2001) could not compare SCE with other photosynthetic pigments, as chlorophyll derivatives and carotenoids were not detected within the sediments. Comparisons between SCE and other pigments were investigated by Tani et al. (2002) and Fietz et al. (2007) using dated undisturbed sediment cores for pigments, and found chl degradation products (pyropheophytin-*a*, pheophytin-*a* and pheophorbide-*a*) and carotenoids (β -carotene, canthaxanthin, zeaxanthin, diatoxanthin, alloxanthin). Past pigment studies at Lake Baikal have largely examined environmental change over the Pleistocene period, and within sediments older than 15,000 years BP, pyropheophytin-*a* and SCE-*a* are the dominant chlorophyll-*a* derivatives (Soma et al. 2001; Tani et al. 2002). These pigments have been suggested to be the best for reconstructing long-term history of phytoplankton productivity at Lake Baikal (Soma et al. 2001; Tani et al. 2002). The order of stability of the main pigments detected within Baikal's Pleistocene sediments are SCEs-*a* > pyropheophytin-*a* > pheophytin-*a* > pheophorbide-*a* (Tani et al. 2002). This order corresponds to the lipophilicities of these derivatives, i.e the order of reverse-phase HPLC elution.

Records covering the Last Glacial-Interglacial Transition (LGIT) (Tani et al. 2002) and Holocene (Fietz et al. 2007) were however at low resolution of 200 – 300 years (Tani et al. 2002) and c. 150 years (Fietz et al. 2005). Sediment cores analysed by Tani et al. 2002 were taken on steep slopes in the South basin, which may not be representative of pelagic lake conditions. Tani et al. (2002) shows that pigment profiles (SCE, carotenoids, chl derivatives) during this period are significantly different from that of biogenic silica records in sediments, which reflects solely diatom production. Tani et al. (2002) found a decrease in algal activity during the Younger Dryas period, but this is only in the South basin, and it is uncertain if the same trend is observed in the North basin. This study found that photosynthetic pigments including carotenoids indicated a general increase in phytoplankton, which started as early as 15, 000 years BP at the beginning of the post-glacial period. This rise in Chlas concentrations occurred much earlier than the onset of the diatom record from biogenic silica, which increased after 10, 000 years BP, largely after 5, 000 years BP.

Pigment records from this study have been compared with records over the Holocene from Fietz et al. (2007) from Vydrino in the South basin, Posolski in the Selenga shallows and the Continent Ridge in the North basin (*Figure 107, Figure 108 and Figure 109*). Age models constructed based on AMS ¹⁴C dates on pollen from parallel cores from the same sites (Piotrowska et al. 2004). Fietz et al. (2007) presents temporal and spatial variations of fossil phytoplankton pigments and organic carbon during the Holocene at the South, Selenga Delta and North basins, and during the last interglacial in the North basin. During the Kazantsevo interglacial, Fietz et al. (2007) suggests that higher Chlas correspond with higher phytoplankton production and therefore higher water temperatures compared to the glacial periods. Fietz et al. (2007) also found that highest phytoplankton production during the Holocene occurred at c. 9 kyr BP at the time of climate amelioration following the Younger Dryas and short productivity maxima occurred during the late Atlantic and at the Subboreal/Subatlantic transition (*Figure 104*). The comparison between Holocene and Kazantsevo indicated that nutrient availability was different and influenced the recorded phytoplankton production as well.

At the same sites as these, pollen, diatom, biogenic silica and oxygen isotope analyses have been performed (Boes et al. 2005; Demske et al. 2005; Granoszewski et al. 2005; Morley et al. 2005; Rioual and Mackay, 2005). A cooling period at the Atlantic Subboreal transition (5.7 – 4.5 kyr BP) was indicated by a decrease in TOC content and Chlas concentrations, and a shift in pollen assemblages to lower abundances of Spruce (*Picea obovata*) (Demske et al. 2005) and decrease in diatom abundances (Karabanov et al. 2000) in the North basin. From c. 4.5 kyr BP to 3.5 kyr BP the Chlas and pheophorbide-*a* concentrations increased, alongside

changes in the pollen assemblages, which indicate a Subboreal optimum (Boes et al. 2005; Demske et al. 2005). At the Subboreal optimum, high diatom productivity and biogenic silica accumulation has previously been found (Qui et al. 1993; Karabanov et al. 2000). The Subboreal optimum has been proposed to be the warmest period of the Holocene within the Baikal region (Karabanov et al. 2000), but the pigment record at the Continent Ridge site from Fietz et al. (2007) does not support this finding. Instead higher Chlas concentrations are observed at the Boreal optimum, representing climatic warming (*Figure 104*). The cores at Vydrino and Posolski did not reach the Boreal period and hence no comparison with the Subboreal optimum could be made. Higher Chlas concentrations were found during the Subboreal compared to Subatlantic at all three sites (*Figure 104*). Subsequently between 3 kyr BP and 1 kyr BP at Continent Ridge and between 2 and 1 kyr BP in the South basin and Selenga cores, cooling periods may be assumed, as Fietz et al. (2007) recorded lowest concentrations of Chlas and pheophorbide-*a*, and lowest carotenoids/Chlas ratios during this period. This was also found by Tani et al. (2001), with the lowest Chlas and carotenoid concentrations during approximately the same period in a core from the South basin. At the Continent Ridge site, this cooling was possibly related to the Subatlantic cooling, which is reflected by the pollen assemblage changes between 3 kyr BP and 2.5 kyr BP (Demske et al. 2005). Thus, these three cores all show strong climate oscillations during the Holocene, showing lake-wide response to regional climatic changes. Before c. 10, 000 years BP there were very low Chlas (Fietz et al. 2007) and biogenic silica concentrations (Prokopenko et al. 2007), indicating low aquatic productivity. Lower production at Lake Baikal during glacial periods is due to extended periods of snow and ice cover and reduced growing season for planktonic diatoms. These previous Holocene studies provide a context to examine the results presented within this chapter, enabling recent limnological changes to be assessed alongside longer term changes at Lake Baikal.

The records from Fietz et al. (2007) show the steep decline in pigment concentrations within the upper 10 cm at the Vydrino (*Figure 105*), Posolski (*Figure 107*) and Continent Ridge site (*Figure 106*). The pigment record in the Vydrino core below 10 cm is poor, with slight fluctuations in Chl-*b* concentrations (*Figure 107*). In contrast the Posolski site shows large shifts in carotenoids down-core, with higher concentrations of diatoxanthin, lutein and canthaxanthin in the mid-Holocene between c. 3 – 4 kyr BP (*Figure 108*). Similarly, the pigment record from the Continent Ridge site (*Figure 109*) show peaks in both carotenoids and Chlas down-core, although these occur in mid-early Holocene. Turbidites were not observed within sections of the cores sampled for pigment analyses, and oxidised layers in the upper 10 cm of the cores has been proposed to be significantly influencing the pigment

preservation (Fietz et al. 2007). The pigment sections within these cores below 10 cm can be used to compare with the pigments records presented in this chapter.

Radiocarbon dates have marked the last 1,000 years to cover the upper c. 18 cm at the Vydrino site, the upper c. 7 cm at the Posolski site and the upper c. 12 cm at the Continent Ridge site (Piotrowska et al. 2004). Assuming similar sedimentation rates, the last 200 years is covered by approximately the upper c. 5 cm, c. 2 cm and c. 3 cm at the Vydrino, Posolski and Continent Ridge sites respectively. This is similar within the ^{210}Pb dated cores at BAIK13-1C and BAIK13-7A in the South basin, and BAIK13-18A in the North basin. The Posolski site does not match the sedimentation rates of the cores from the Selenga shallows in this study, as the upper c. 12 cm at BAIK13-10A and BAIK13-11C covers the last 200 years. Sedimentation rates are also different between cores from this study and Fietz et al. (2007), as BAIK13-4F in the South basin has large turbidite layers in the upper c. 6 cm and BAIK13-19B in the North basin is closer to the Upper Angara shallows. This highlights the differences in sedimentation rates and the difficulties in comparing sediment cores based on sediment depths rather than ages. The upper c. 10 cm of the cores collected by Fietz et al. (2007) in the South basin, Selenga and North basin are considered unreliable, due to the strong degradation of Chl *a* within the oxidised layers. The upper c. 10 cm of the cores cover the last c. 500 years at the Vydrino site, > 1000 years at the Posolski site and the last c. 1000 years at the Continent Ridge site (Piotrowska et al. 2004). Cores from Fietz et al. (2007) therefore do not provide useful pigment records to cover the last millennium, to assess algal response to late Holocene climatic events such as the LIA. Pigment records in this study can only be compared to older sediments in the Holocene and from the last interglacial (Fietz et al. 2007).

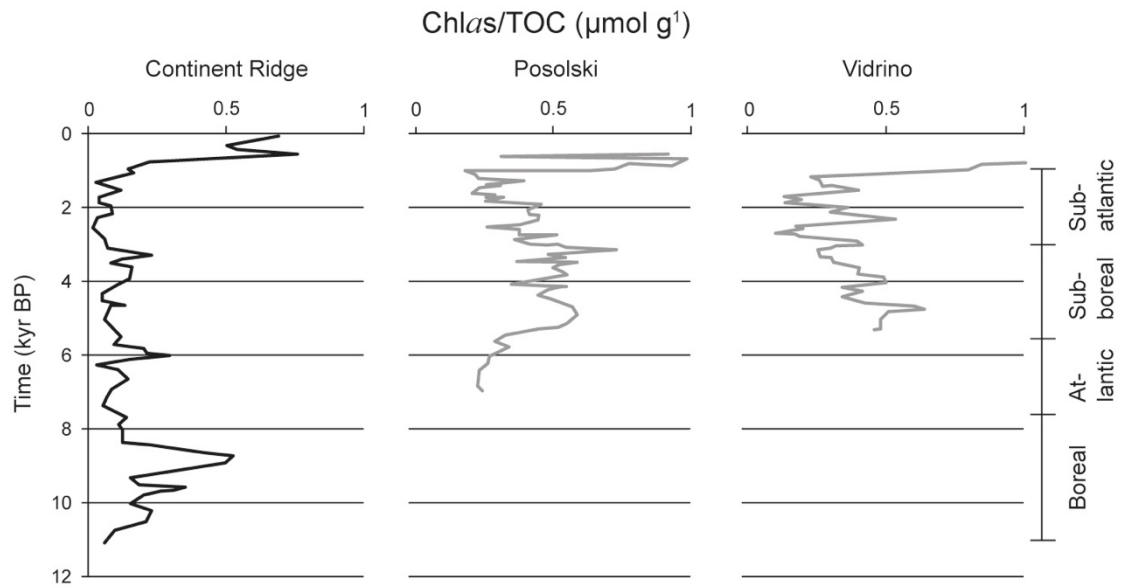


Figure 104: Chlas concentrations in the North, Selenga and South basin sites over the Holocene (Fietz et al. 2007).

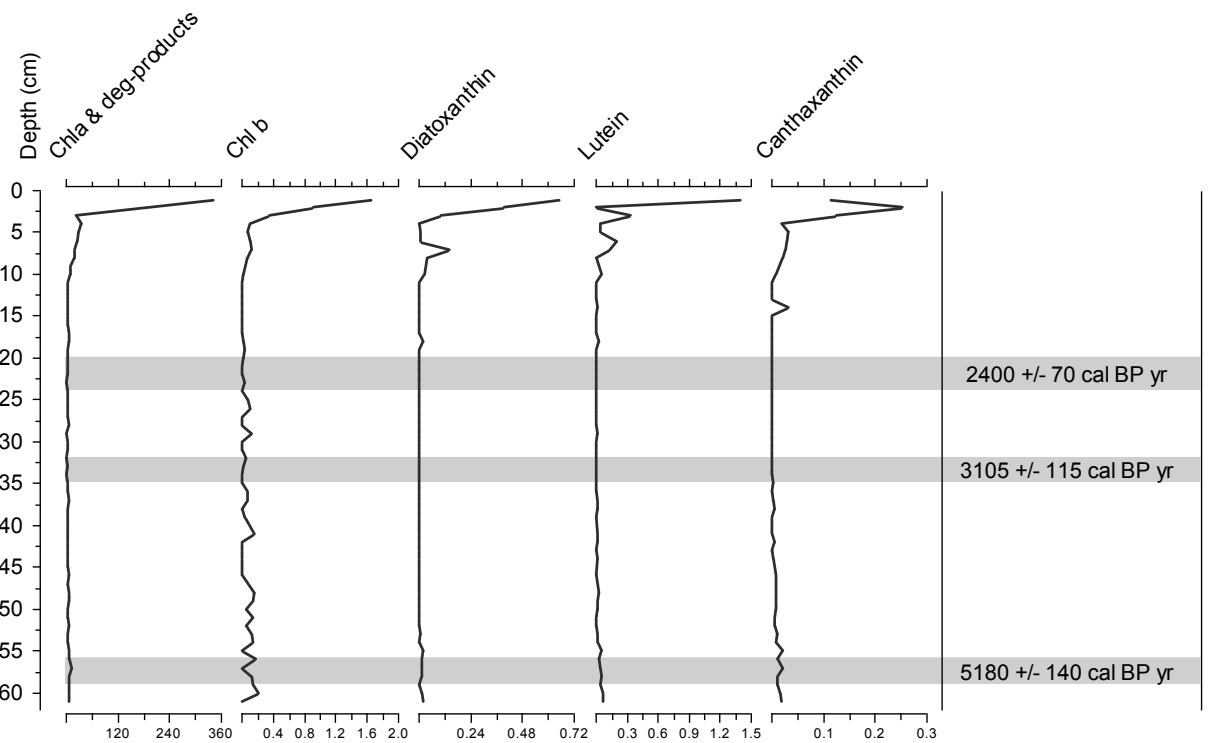


Figure 105: Fossil pigment concentrations (µmol g⁻¹ OC) from the Vydrino coring site in the South basin (Fietz et al. 2007).

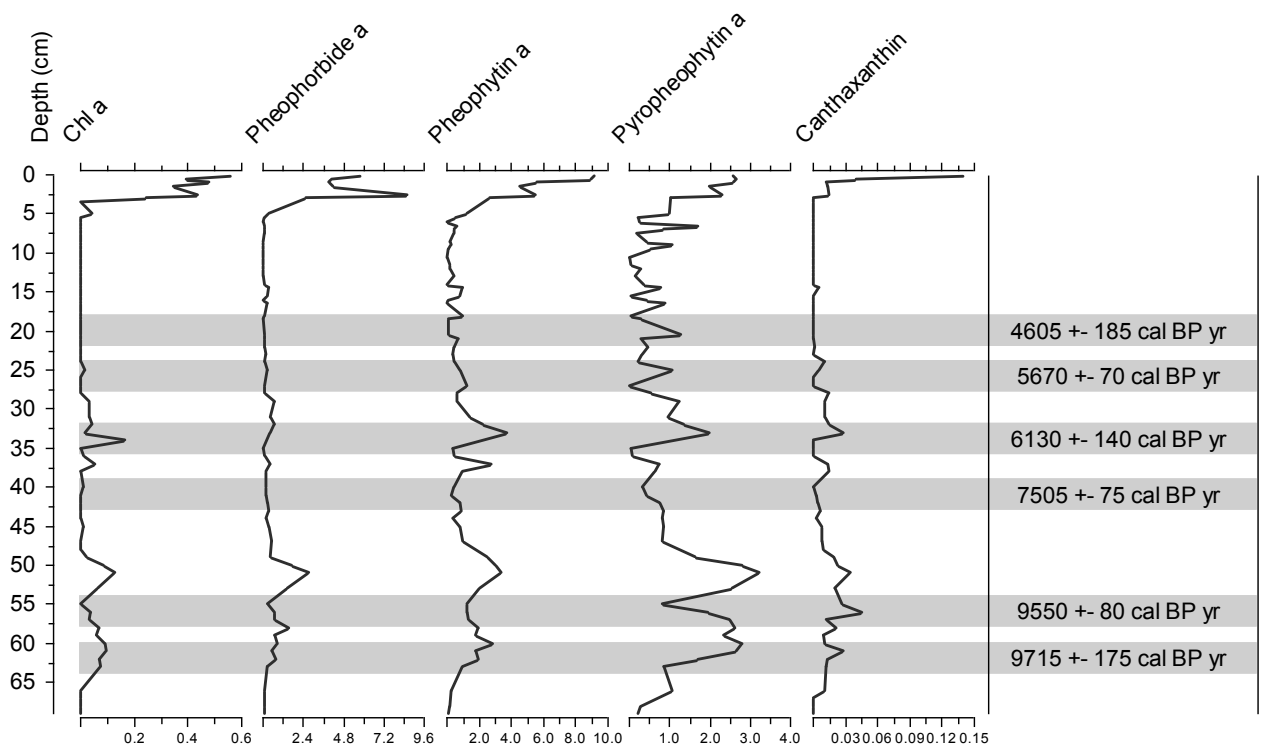


Figure 106: Fossil pigment concentrations ($\mu\text{mol g}^{-1} \text{OC}$) from the Continent Ridge coring site in the North basin (Fietz et al. 2007).

Fietz et al. (2007) found the mean Chlas concentrations over the last 5,000 years to be $0.33 \mu\text{mol g}^{-1}$ (330 nmol g^{-1}) at Vydrino, $0.42 \mu\text{mol g}^{-1}$ (420 nmol g^{-1}) at Posolski and $0.09 \mu\text{mol g}^{-1}$ (90 nmol g^{-1}) at Continent Ridge (Selenga > South > North). Over the entire Holocene period, Fietz et al. (2007) found Chlas concentrations between $200 - 1000 \text{ nmol g}^{-1}$ in the South basin, $200 - 2000 \text{ nmol g}^{-1}$ in the Selenga sites and $100 - 800 \text{ nmol g}^{-1}$ in the North basin over the Holocene. Mean Chlas concentrations in this study are also higher in the Selenga and South basin sites and lowest in the North basin (Selenga > South > Maloe More > North). In comparison to the last interglacial period, Chlas concentrations are higher, at $0.26 \mu\text{mol g}^{-1}$ (260 nmol g^{-1}) in the North basin (Fietz et al. 2007). This is higher than all the sites, except Maloe More (BAIK13-14C).

Pigments (diatoxanthin and canthaxanthin concentrations) from the South basin, Selenga Delta and North basin sites in this study and from Fietz et al. (2007) do not show similar down-core trends (Figure 107, Figure 108 and Figure 109). Chlas concentrations show similar down-core profiles in the Selenga Delta and North basin sites within this study and Fietz et al. (2007), but differ in the South basin sites. The pigment concentrations measured in Fietz et al. (2007) are also lower than those presented in this chapter. In the South basin, diatoxanthin peaks to 1.2 nmol g^{-1} , canthaxanthin peaks to 0.5 nmol g^{-1} and Chlas peak to $383.6 \text{ nmol g}^{-1}$.

in Fietz et al. (2007). In the Selenga delta, diatoxanthin peaks to 0.12 nmol g^{-1} , canthaxanthin peaks to 0.11 nmol g^{-1} and Chlas peak to 44.7 nmol g^{-1} in Fietz et al. (2007). In the North basin, diatoxanthin is sparse downcore, canthaxanthin peaks to 0.2 nmol g^{-1} and Chlas peak to 20.3 nmol g^{-1} Fietz et al. (2007). The radiocarbon dates from Fietz et al. (2007) suggest that the upper 30 cm of the sediment cores cover the last c. 2,500 cal BP years in the South basin and Selenga sites, and in the North basin the upper 20 cm of the sediment core covers the last c. 4,600 cal BP years. The cores from this study potentially cover longer time scales than previously thought of c. 1000 years.

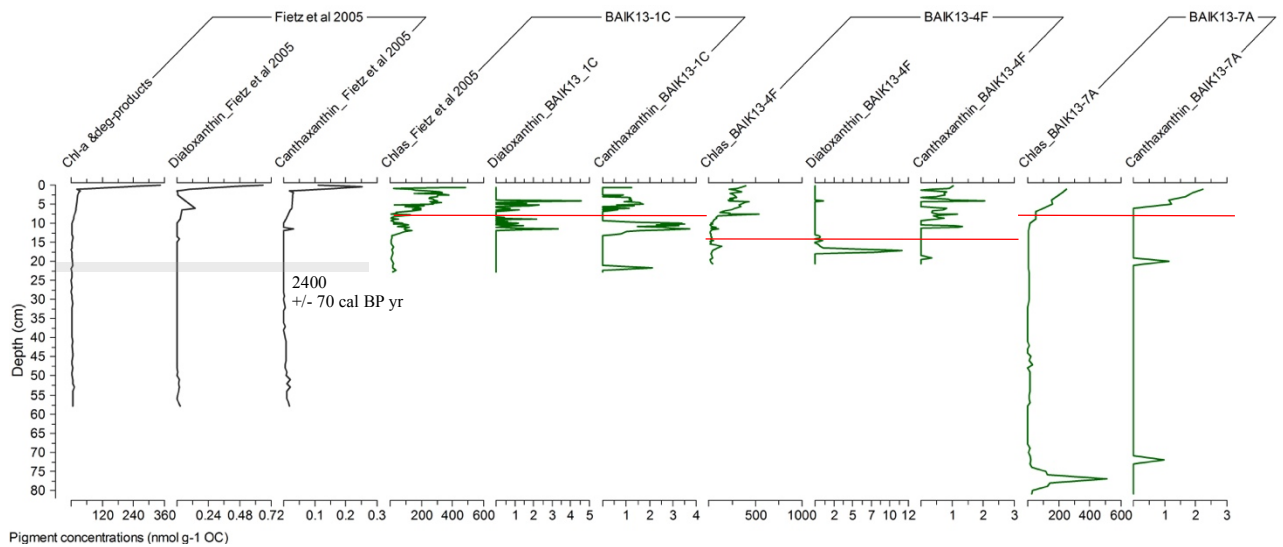


Figure 107: South basin sedimentary pigment profiles at Vydrino site (Fietz et al. 2007) and BAIK13-1C, BAIK13-4F and BAIK13-7A (this study: nmol g^{-1}). Red line represents sediment depth of last 200 years from ^{210}Pb dating chronologies. Grey line represents horizon for radiocarbon dating. (*BAIK13-7A shows high levels of degradation).

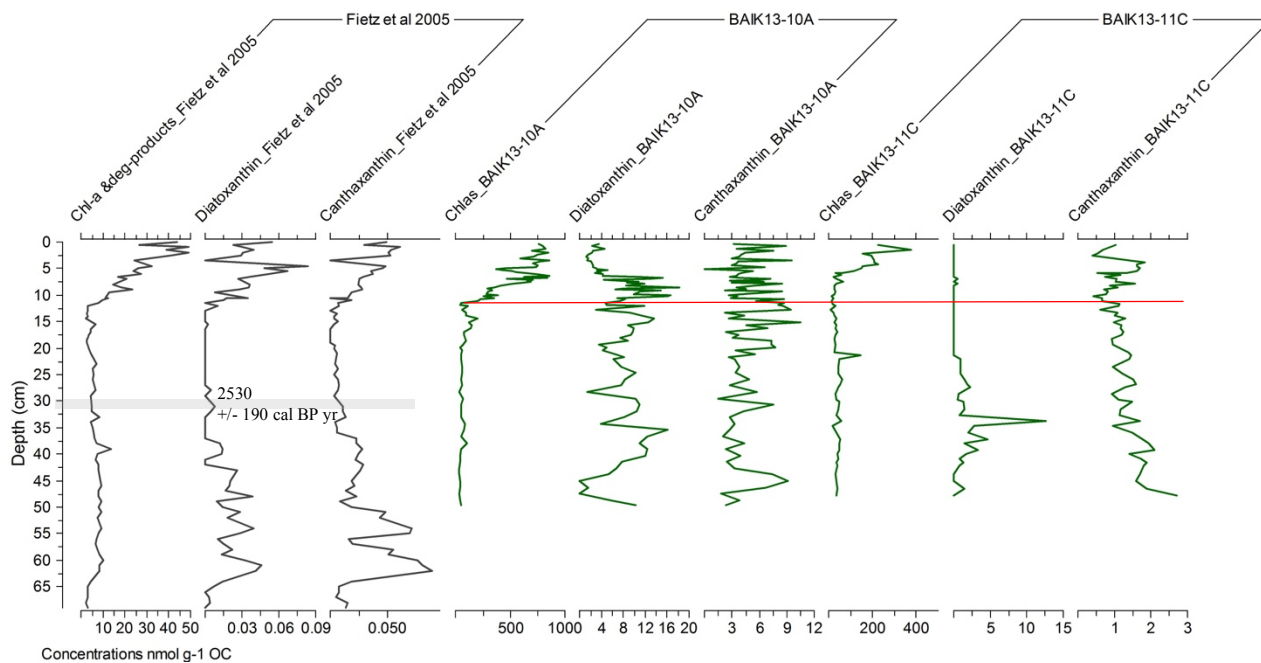


Figure 108: Selenga sedimentary pigment profiles at Posolski site (Fietz et al. 2007) and BAIK13-10A and BAIK13-11C (this study: nmol g). Red line represents sediment depth of last 200 years from ^{210}Pb dating chronologies. Grey line represents horizon for radiocarbon dating.

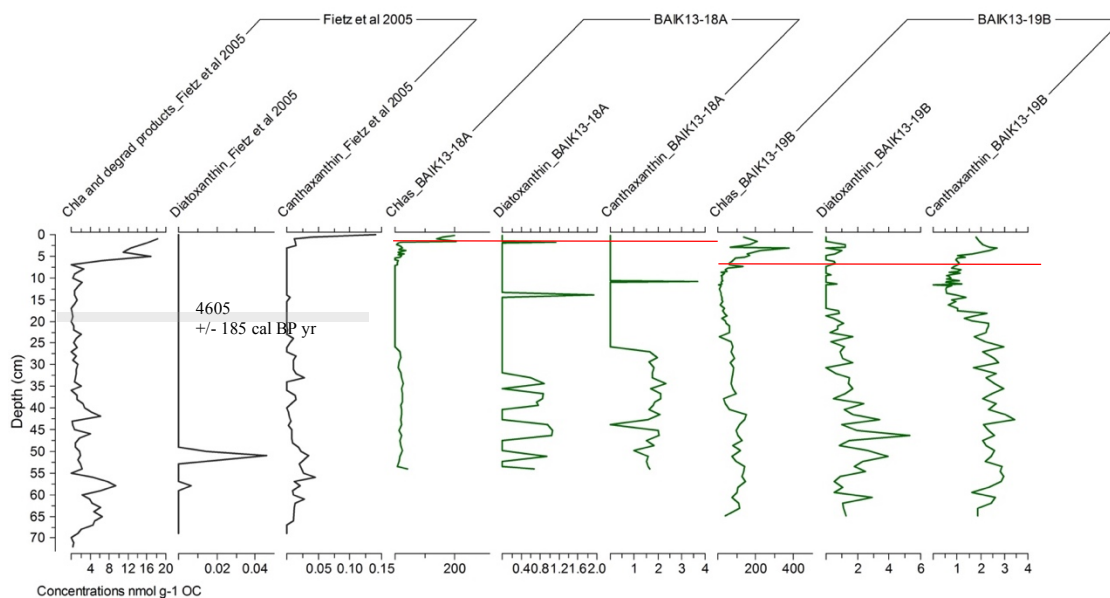


Figure 109: North basin sedimentary pigment profiles at Continent Ridge site (Fietz et al. 2007) and BAIK13-18A and BAIK13-19B (this study: nmol g). Red line represents sediment depth of last 200 years from ^{210}Pb dating chronologies. Grey line represents horizon for radiocarbon dating. (*BAIK13-18A shows high levels of degradation).

6.4 Discussion

6.4.1 Recent production changes in context with longer term variability at Lake Baikal

The pigment records show that over the last 200 years there were higher pigment concentrations compared to earlier in the sediment record. This is seen across all the sites, although the magnitude is greater in the South basin, Selenga Shallows and Maloe More, than the North basin sites. In comparison to Fietz et al. (2007) the Chlas concentrations in the last interglacial period are higher than the Chlas measured within the sediment records in this study, except for BAIK13-14C in Maloe More. Previous pigment records from Fietz et al. (2007) found that the pigment records over the last few centuries were not reliable in the upper 10 cm due to strong degradation within the oxidised layer. In contrast the sediment records presented in this chapter are higher resolution and results found that Chlas concentrations within oxidised layer were not significantly lower than concentrations within anoxic layers, as presented in Chapter Seven. Pigment concentrations within the oxidised layers were therefore not removed when comparing pigment samples pre and post 1800 AD. One reason as to why pigment concentrations within the oxic layers are higher might be as degradation is incomplete.

The longer-term trends which are observed in these short cores, are decreasing diatom pigment concentrations at all the cores, but particularly at BAIK13-1C, BAIK13-10A, BAIK13-11C and BAIK13-14C in the South basin, Selenga and Maloe More sites. This decreasing trend in diatom pigment concentrations is supported by declining diatom concentrations observed within sediment records from across Lake Baikal (Mackay et al. 1998). This could be linked to ice cover changes, and the amelioration from the Little Ice Age (LIA). High lutein concentrations and Chlb/Chlas ratios in the upper 10 cm are found only at the Maloe More sites (BAIK13-14C and BAIK13-15B). This suggests a recent increase in chlorophytes, with higher concentrations in comparison to over the longer record at Maloe More, but not at the rest of the lake sites. Recent floristic changes with greater abundances of chlorophytes at Maloe More Bay could be an indication of human influence within the Maloe More region, supporting the findings by Timoshkin et al. (2015) of early signs of littoral eutrophication. Recent increase in alloxanthin concentrations are distinctively different to longer term changes, being higher than sediments older than the last 200 years in all the cores, except in the North basin. The increasing trends in canthaxanthin seen over the last 200 years in the South basin and North basin (Chapter Seven) are not distinct, as higher canthaxanthin concentrations are observed in sediments older than the last 200 years.

Carbon isotope records show more positive $\delta^{13}\text{C}$ values in the last 200 years compared to earlier in the sediment record, at a few sites only, in the South (BAIK13-4F), Selenga Shallows (BAIK13-10A and BAIK13-11C) and North basin (BAIK13-19B). This differs to the Chlas concentrations temporal trends. TOC/N ratios down-core suggest that organic matter is predominantly derived from algal production, except for shifts to higher TOC/N values (> 12) at BAIK13-4F, BAIK13-16B and BAIK13-19B. This could possibly be a result of degradation of nitrogen in the sediments, rather than greater terrestrial input, at these pelagic sites as these sites are > 5 km from the shoreline. In comparison to previous carbon records at Lake Baikal, the $\delta^{13}\text{C}$ values in this study are generally more positive. The $\delta^{13}\text{C}$ values at BAIK13-7A in the South basin follow on from the $\delta^{13}\text{C}$ values in the Vydrino record (Mackay et al. 2016). Values between -29 ‰ and -26 ‰ are previously found in the late Holocene (Ishiwatari et al. 2005; Watanabe et al. 2009; Mackay et al. 2016), and the values in this study generally fall within this range, except for higher values at BAIK13-4F in the South basin and BAIK13-14C at Maloe More. This suggests that possibly greater production over the last 200 years than in the late Holocene at BAIK13-4F and BAIK13-14C, if the carbon isotopic composition is predominately driven by algal production. Alternatively, it could be suggesting greater abundances of picocyanobacteria, which is shown in the pigment records, with higher concentrations of canthaxanthin pigments towards the top of the core, and decreasing diatoxanthin:canthaxanthin pigment ratios. Another reason for higher $\delta^{13}\text{C}$ values could be related to the shift between algal groups, e.g. diatoms to other algae. This is as diatoms have lower $\delta^{13}\text{C}$ values (Yoshii et al. 1999), so a decline in diatom abundance could result in an increase in $\delta^{13}\text{C}$ values.

TOC/N ratio values range between 10 – 12 in the late Holocene sediments (Mackay et al. 2016), being similar to values presented within the sediment cores in this chapter. This suggests no change in the carbon source between the late Holocene and last 200 years, with no shifts to predominately terrestrial input (values > 12). TOC values within the sediment cores presented in this chapter are higher than values in the late Holocene from previous studies, being > 2 % in the surface sediments, and reaching values of c. 6 % in the South basin, Selenga and Maloe More sites. TOC values measured on late Holocene sediments range between 1 – 1.8 % (Mackay et al. 2016). TOC values might be higher over the last 200 years than in the late Holocene, due to greater aquatic production.

In comparison to Fietz et al. (2007), mean $\delta^{13}\text{C}$ values in the South basin over the last 7,000 years are higher (more positive) than mean South basin $\delta^{13}\text{C}$ presented pre and post 200 years in this chapter. This is also the case for mean $\delta^{13}\text{C}$ values in the Selenga over the last 10,000 years and North basin over the last 11,000 years (Fietz et al. 2007). This could be due to the

influence of dissolved organic matter from catchment rivers, as DOM has higher $\delta^{13}\text{C}$ values (-26 ‰ to -27 ‰) (Yoshioka et al. 2002) than $\delta^{13}\text{C}$ values of diatoms (-28 ‰ to -35 ‰) (Yoshii et al. 1999). In contrast to the aforementioned, the Holocene core from the Vydrino site in the South basin presented in Mackay et al. (2016) shows more negative $\delta^{13}\text{C}$ values in the early Holocene compared to the late Holocene period, which is proposed to be a result of forest development and lower abundances of picoplankton in early Holocene. Furthermore, diatom fluxes are very high in the early Holocene sediments which could be driving the lower $\delta^{13}\text{C}$ values (Mackay et al. 2016).

The pigment and $\delta^{13}\text{C}$ records shown in this chapter provide possible evidence of climate variability, with warming from the LIA and recent climate warming across all regions. Previous work at Lake Baikal has reported evidence for the LIA period within the region, with climatic cooling inferred from diatom assemblage changes (Mackay et al. 2005). However, the algal production proxies do not show any evidence for the MCA within the region, which supports findings of previous studies (Morley, 2005). The full extent to which the sediment cores presented in this chapter cover the Holocene period is unknown, and therefore radiocarbon dating of sediments > 200 years will enable further examination of the production proxies in relation to the late Holocene climatic events. The only core which certainly covers all the Holocene is BAIK13-16B due to the presence of Pleistocene clays at the bottom of the core. However, the sediment lithology suggest that this core is likely to have suffered from a hiatus, as the TOC and $\delta^{13}\text{C}$ values are relatively high during the Pleistocene clays (*Figure 94* in this Chapter).

Most of the sediment cores have turbidite sections within the bottom sediments (below c. 15 cm), but no distinct algal changes occur down-core. The occurrence of turbidite layers disrupt the reliability of longer term reconstructions of environmental change at these sites. There is no clear evidence for the onset of the LIA within these sediment cores, although increasing trend in Chl_a concentrations and decreasing diatoxanthin: canthaxanthin pigment ratios might be reflecting amelioration from the LIA. Nonetheless Morley (2005) detected the LIA from diatom assemblage changes, not diatom concentrations within the diatom record. It might be that only certain proxies can be used to detect these smaller scale climatic events, and diatoms (certain species) are more responsive due to ice cover dynamics rather than other algal groups detected from pigments. Another explanation could also be the effect of pigment preservation on the ability of algal pigments to detect the LIA. The carbon record shows peaks towards higher (more positive) $\delta^{13}\text{C}$ values within the sediment cores at BAIK13-1C and BAIK13-14C. This could possibly be reflecting the LIA, as previous studies show higher $\delta^{13}\text{C}$ values in the colder periods (Mackay et al. 2016). The $\delta^{13}\text{C}$ values within glacial periods has

been found to range between -22 ‰ and -20 ‰, and within the Holocene period they ranged between -30 ‰ and -26 ‰ (Prokopenko and Williams, 2003). Higher $\delta^{13}\text{C}$ values down-core could be a result of increased picoplankton abundance, such as at BAIK13-1C and BAIK13-14C which shows higher canthaxanthin concentrations alongside a peak to more positive $\delta^{13}\text{C}$ values. The peaks in $\delta^{13}\text{C}$ values at BAIK13-1C and BAIK13-14C could be due to the picoplankton concentrations. This peak could be the LIA, as longer periods of ice cover would result in shorter periods of turnover when diatoms dominate the primary production, this would result in less diatoms and more picoplankton, as the summer stratification periods would be longer than the turnover period (Mackay et al. 2016). Greater ice cover could possibly result in more positive $\delta^{13}\text{C}$ values, due to reduced interaction of the lake waters with atmospheric carbon dioxide (Prokopenko and Williams, 2001; Morley, 2005). Other published studies suggest that CO_2 is actually more soluble in colder water and primary production is lower, which would result in no discrimination between carbon isotopes with greater ice cover (Prokopenko et al. 1999; Watanabe et al. 2004) (*Table 5* in Chapter One). More positive $\delta^{13}\text{C}$ values could also result from the reduction of terrestrial input which is depleted in $\delta^{13}\text{C}$ due to the ice cover on the lake, although this is not supported by the TOC/N ratio values with an increase in values to > 12 or supported by the Rock Eval data for BAIK13-1C presented in Chapter Seven, with no decrease in the HI values.

6.5 Summary

Difficulties are present when comparing records using sediment depths due to large variation in sedimentation rates across the lake, and chronologies are essential for time interval comparisons. Down-core pigment and carbon isotope records presented in this chapter cannot be used to accurately examine if the LIA or MCA climatic events occurred at Lake Baikal. Despite this, they do provide a way to examine if recent palaeolimnological changes are distinct from past production changes over the late Holocene. Dated sediment cores from Fietz et al. (2007) additionally provide comparisons with Holocene sediments older than the last 1000 years and the last interglacial. The next steps of this research are therefore to obtain radiocarbon dates for these short cores presented in this chapter to further examine these observed regional and down-core trends and provide a temporal context.

Algal pigment concentrations over the last 200 years are higher than over longer time scales at all the sites across the lake, and there is a lake-wide trend to higher recent production as inferred from Chl_as concentrations. There is also a lake-wide response from the $\delta^{13}\text{C}$ records over the last 200 years, showing an increasing trend to more positive $\delta^{13}\text{C}$ values. Down-core, over longer time scales the trends in the Chl_as concentrations are similar, however there is

large variability in the $\delta^{13}\text{C}$ trends across the sites. Some of the sediment cores in the South basin and Maloe More show peaks of higher $\delta^{13}\text{C}$ values than within the last 200 years, and these coincide with higher picoplankton pigment concentrations. Thus, these peaks to more positive $\delta^{13}\text{C}$ values could be due to decreased interaction of lake waters with atmospheric carbon dioxide, and increased picoplankton abundances. The $\delta^{13}\text{C}$ record could potentially be showing the onset of the LIA at certain sites, and climatic amelioration from the LIA. In contrast, Chlas concentrations are only showing distinctive trends over the last two centuries, and thus potentially showing the amelioration from the LIA similar to the $\delta^{13}\text{C}$ record as significant positive correlations have been observed at certain sites as presented in Chapter Seven. $\delta^{13}\text{C}$ values over the last 200 years are higher than over longer term in the sediment core at only at the Selenga site (BAIK13-10A) and South basin (BAIK13-4F) sites, as the rest of the sites show higher $\delta^{13}\text{C}$ values lower down the sediment core. The $\delta^{13}\text{C}$ values are similar to past studies, and show more positive values than Vydrino site. Pigments are different to past records by Fietz et al. (2007), although they show similarities in Chlas in the South, Selenga and North basin. Floristic changes do occur downcore, with a decreasing trend in diatoxanthin:canthaxanthin pigment concentrations observed towards the surface sediments lake-wide, in the South, Selenga and Maloe More. This suggests decreasing abundances of diatoms in relation to picocyanobacterial populations, which is likely to be a reflection of declining ice cover duration and thickness. When putting these production proxies into context with natural variability, Chlas and diatoxanthin:canthaxanthin pigment concentrations are clearly different between the two time intervals, before and after the last 200 years, with higher Chlas concentrations and lower diatoxanthin:canthaxanthin ratio values over the last two centuries. In contrast, the $\delta^{13}\text{C}$ values are not significantly different before and after the last 200 years, as large shifts within the $\delta^{13}\text{C}$ values are observed down-core.

The carbon isotope record shows a lake wide response over the last 200 years, with increasing values, as presented in Chapter Seven. On longer time scales, there is variation in the $\delta^{13}\text{C}$ values across the sites, with no lake wide response or basin specific response. The $\delta^{13}\text{C}$ values over the last 200 years are not more positive than previous values down the sediment core. Thus, there is an increase in $\delta^{13}\text{C}$ values before the last 200 years in records from the South basin, Maloe More and North basin. These increases in $\delta^{13}\text{C}$ values could be reflecting changes in the ice cover and algal community composition, and might be indicating the LIA. Over the last two centuries, there is a lake-wide response in $\delta^{13}\text{C}$ values and recent trends are likely to be due to lake warming and/or anthropogenic nutrient enrichment at certain sites, as suggested in Chapter Seven.

Chapter Seven: Reconstructing palaeoproductivity over the last 200 years

7.1 Exploring limnological change over the last 200 years within the Baikal region

Limnological change since 1800 A.D. has been analysed, to look prior to the natural baseline of the ecosystem (1900 – 1950 A.D.) and the impact of anthropogenic changes from the 1950s onwards. This chapter reports temporal trends in production over the last 200 years, using bulk organic stable carbon isotope ($\delta^{13}\text{C}_{\text{organic}}$) compositions as well as algal pigments, contained in the sediments of Lake Baikal. Diatom assemblages have been analysed within selected sediment tops of cores to compare with past records at Lake Baikal. The sites have been compared to examine both basin response and lake-wide response to any changes over the past two centuries, and the preservation of algal biomarkers has been assessed. The aims of this chapter are to compare past biological production across the South basin, Central basin and North basin, and to identify the timings of algal changes, over the last two centuries. Palaeolimnological findings within this chapter will also be compared to previous work by Fietz (2005), which found higher production in the South basin than the North basin of Lake Baikal. This difference is suggested to be due to the influences of the weather systems (the North Atlantic Westerlies and the Siberian High). These weather systems control the ice season at Lake Baikal, and a northward shift would result in the South basin becoming ice-free earlier than the North basin.

Difference between the North and South basin of Lake Baikal have been found in pigment preservation (Fietz, 2005), with higher levels of degradation in North basin compared to the South. This was similarly discussed in Chapter Five. Factors which affect pigment preservation within lake sediments are burial rates, water column depth, microbial activity and exposure to oxygen (Leavitt et al. 1993; Cuddington and Leavitt, 1999; Fietz et al. 2005). Sedimentation rates are generally low within the pelagic regions of Lake Baikal, and previous studies have found Holocene sediment accumulation rates (SARs) (cm yr^{-1}) to vary spatially, with sedimentation rates of less than 0.003 cm yr^{-1} in the ridges and banks, and sedimentation rates of more than 0.03 cm yr^{-1} in the deep basins (Colman et al. 2003). All the sites (BAIK13-1C, BAIK13-4F, BAIK13-7A, BAIK13-10A, BAIK13-11C, BAIK13-14C, BAIK13-19B) except for BAIK13-18A in the North basin have SARs $> 0.03 \text{ cm yr}^{-1}$. Overall the South basin (BAIK13-1C; BAIK13-4F; BAIK13-7A) has higher average SARs (0.08 cm yr^{-1}), than the North basin (0.02 cm yr^{-1}). These values are within the reported range of SAR in the South

basin (0.02 – 0.1 cm yr¹) (Vologina et al. 2007). Previously published work has found higher Holocene SARs in the pelagic South basin (0.035 cm yr¹) compared to sediments near the steep north-slopes of southern Lake Baikal (0.003 cm yr¹) (Sturm et al. 2015). Vologina and Sturm (2009) also found the SARs to be higher in the South basin than the Central and North basin, with average recent SARs of 0.1, 0.09 and 0.07 cm yr¹ respectively. This variance is a result of differences in the biological productivities and amounts of terrigenous material supplied to the basins (Vologina and Sturm, 2009). Sedimentation rates close to large river inflows have been found to vary between 0.23 – 1.07 cm yr¹, and are higher than SARs in the deep lake basins at Lake Baikal (0.07 – 0.1 cm yr¹) and on underwater ridges (0.001 – 0.002 cm yr¹) (Vologina and Sturm, 2009). Previously measured ²¹⁰Pb sedimentation rates at Lake Baikal show similar mean burial rates at sites within the South basin and Buguldieka Saddle sites (0.01 – 0.02 g cm⁻² yr⁻¹) between c. 1930 – 1990 AD (*Table 34*) (Mackay et al. 1998). The lowest mean sedimentation rates were measured in the North basin and Academician Ridge sites (0.009 g cm⁻² yr⁻¹) between c. 1930 – 1990 AD (*Table 34*) (Mackay et al. 1998).

Table 34: Previous ²¹⁰Pb derived sedimentation rates at Lake Baikal between c. 1930 – 1990 AD (Mackay et al. 1998).

Region	Site	Location	Water depth (m)	Mean sedimentation rates (g cm ⁻² yr ⁻¹)	
South basin	BAIK6	51°48'38"N 104°51'38"E	1425		0.021
Buguldieka Saddle	BAIK19	52°27'00"N 106°07'32"E	342		0.017
Central basin	BAIK22	52°59'17"N 107°39'58"E	1624	(post-1934)	0.052
				(pre-1934)	0.011
Academician Ridge	BAIK25	53°33'18"N 107°58'00"E	307		0.009
North basin	BAIK29	54°48'01"N 109°12'58"E	910		0.009
South basin	BAIK38	51°34'06"N 104°31'43"E	690		0.011

Sedimentary analyses allow temporal trends over the last 200 years, prior to main anthropogenic influence from c. 1950 AD onwards within the Baikal region (Brunello et al. 2004) to be examined. This chapter will explore if there have been any changes within the algal production and/or composition via pigments (chlorophylls and carotenoids). Diatom concentrations and assemblages will also be explored along with any changes in carbon sequestration from carbon mass accumulation rates (CMARs) and carbon isotopic values, in response to climate. These records will be compared with ice cover changes from Listvyanka (between 1868 - 1996) (Todd and Mackay, 2003) and regional mean annual temperature

changes from Irkutsk station in the South basin (between 2013 – 1821). Ice cover data from Listvyanka station in the South basin is used as an ice cover record for all the cores, as the variability, but not exact timing, in ice cover at this station is highly representative of that across all the lake (Todd and Mackay, 2003).

Floristic, production and $\delta^{13}\text{C}$ changes before and after industrial influence at Lake Baikal will be compared, to explore basin and lake-wide response to regional anthropogenic impact. Industrial activity, mining and shoreline settlements are the main anthropogenic pressures which began after 1950 AD within the catchment area (Brunello et al. 2004). Thus, the algal production records from the deep-water pelagic sites (> 800 m) will be compared with those from the shallower littoral and river-influenced sites, to see if all the pelagic South and North basins, as well as nearshore regions have a similar response to climate and/or anthropogenic influence. Spatial differences in pigment assemblages within basins and between basins will be explored from surface sediments, which are averaged to cover the last 20 years. The last 20 years has been chosen because the largest change in average annual regional temperatures at Irkutsk are seen over this period, with an increase in average annual temperatures from -5.8 to 0.32°C (Shimaraev and Domysheva, 2013).

Sediment cores were collected from across Lake Baikal, to address the aims of this thesis by examining sedimentary algal records from sites vulnerable to human influence in the South basin, Maloe More Bay and close to the Selenga Delta, and 'pristine' sites in the North basin. Multiple sediment cores were collected from each coring station across Lake Baikal to conduct lithological analyses, algal pigments, $\delta^{13}\text{C}$, ^{210}Pb and diatom analyses. It is important to note however that multiple cores were not taken in the exact same location, especially during the summer (August 2013) expedition when cores were taken from on-board the research vessel. In the winter (March 2013) however, sediment cores taken from BAIK13-1 and BAIK13-4 coring stations, would be relatively nearby one another due to the stability of the coring stations on the ice above. Lithology of the sediment cores shows the presence of turbidites, which are mass structures of slumped material within a sediment core. Turbidites and their spatial variability across Lake Baikal were discussed previously in Chapter Six. Amongst the sediment cores collected in March and August 2013, core BAIK13-4 shows a turbidite within the upper sediments which cover the last 200 years. Pigment and $\delta^{13}\text{C}$ data has therefore been removed at these sediment depth intervals in the BAIK13-4 sediment core, despite the ^{210}Pb age model curve showing a good fit in the upper sediments of the sediment core (*Figure 121*).

7.2 Results

7.2.1 Age models and Sedimentation rates

The sediment cores are mainly comprised of biogenic-terrigenous muds, with turbidite and oxidised layers, which are distinguished by layers of coarse-grained sands and accumulations of Fe and Mn oxides respectively. The upper 4 - 11 cm of the sediment cores cover the last 200 years, and within these upper sediments there are oxidised layers present in all cores except for the Maloe More core (BAIK13-14C). This Maloe More sediment core shows higher sedimentation rates (c. 0.005 – 0.03 g cm⁻² yr⁻¹) than pelagic deep basin cores (c. 0.002 – 0.02 g cm⁻² yr⁻¹), which might account for the absence of a defined oxidised layer in the upper sediments of BAIK13-14C. The oxidised layers within the rest of the short cores range in thickness between 0.5 - 4.5 cm. There are also no turbidite layers, except for within a South basin core (BAIK13-4F).

Turbidites are sedimentary structures formed by mass movement of sediments at the bottom of the basins. Turbidites result in an increase in sedimentation rates, and these structures need to be considered during sediment core interpretations. The influence of turbidites on palaeolimnological work was further discussed previously in Chapter Six. Within this thesis, the largest range in SARs over this period was found at Baik13-4F in the South basin (0.002 – 0.316 g cm⁻² yr⁻¹), which is mostly due to one high value (0.316 g cm⁻² yr⁻¹) in 1998. Sedimentation accumulation rates (SARs) were the greatest over the last 150 years at the Selenga Delta (BAIK13-10A and BAIK13-11C) (average SAR of 0.041 g cm⁻² yr⁻¹ and 0.016 g cm⁻² yr⁻¹) and Maloe More Bay (BAIK13-14C) (average SAR of 0.011 g cm⁻² yr⁻¹) (*Figure 120*). The lowest average SAR was found in the North basin 0.004 g cm⁻² yr⁻¹ at a pelagic deep basin site (BAIK13-18A). BAIK13-10A (0.005 – 0.132 g cm⁻² yr⁻¹) has a large range in SAR, along with BAIK13-14C (0.002 – 0.300 g cm⁻² yr⁻¹) and BAIK13-11C (0.005 – 0.032 g cm⁻² yr⁻¹). The other deep basin pelagic South basin sites (BAIK13-1C and BAIK13-7A) have very low sediment accumulation rates over the last 150 years (0.001 – 0.014 and 0.002 – 0.020 g cm⁻² yr⁻¹ respectively), and the other North basin site (BAIK13-19B) has a smaller SAR range of 0.004 – 0.021 g cm⁻² yr⁻¹ in comparison to the Selenga Delta site (*Figure 120*). The lowest SAR was found at BAIK13-18A in the North basin (0.002 – 0.008 g cm⁻² yr⁻¹).

Sedimentation rates were used to calculate the ²¹⁰Pb chronology for each sediment core, age-depth models were constructed to obtain the sediment intervals which cover the last c. 200 years (*Figure 121*). Uncertainties within the age-depth models are largest for the BAIK13-11C sediment core in the Selenga and BAIK13-19B core in the North basin (*Figure 121*).

Sediment cores with the smallest errors in age are BAIK13-1C, BAIK13-4F and BAIK13-7A in the South basin, BAIK13-10A in the Selenga Shallows and BAIK13-14C in Maloe More (*Figure 121*).

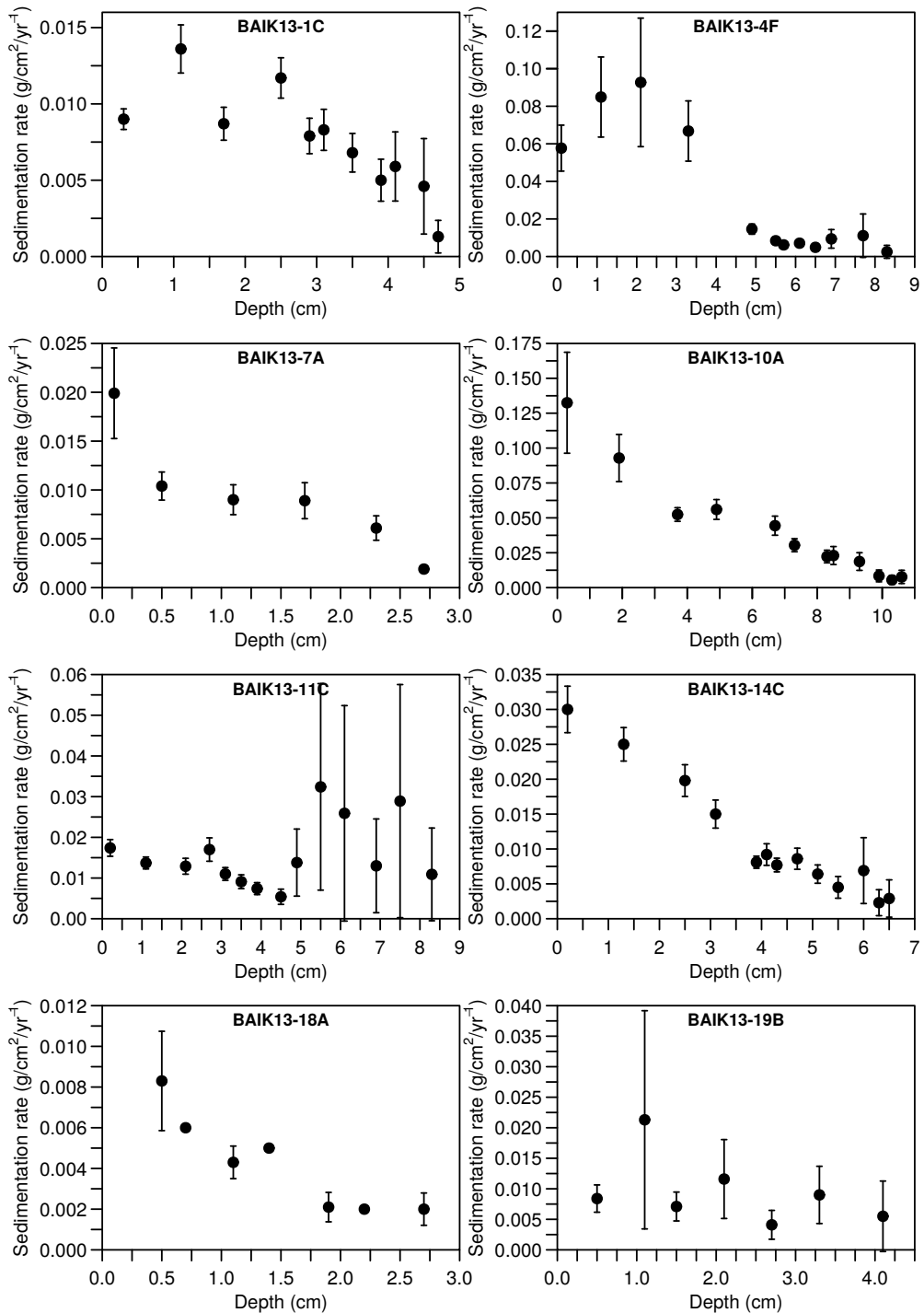


Figure 110: Sedimentation rates for each ²¹⁰Pb dated sediment core in the South basin, Selenga, Maloe More and North basin.

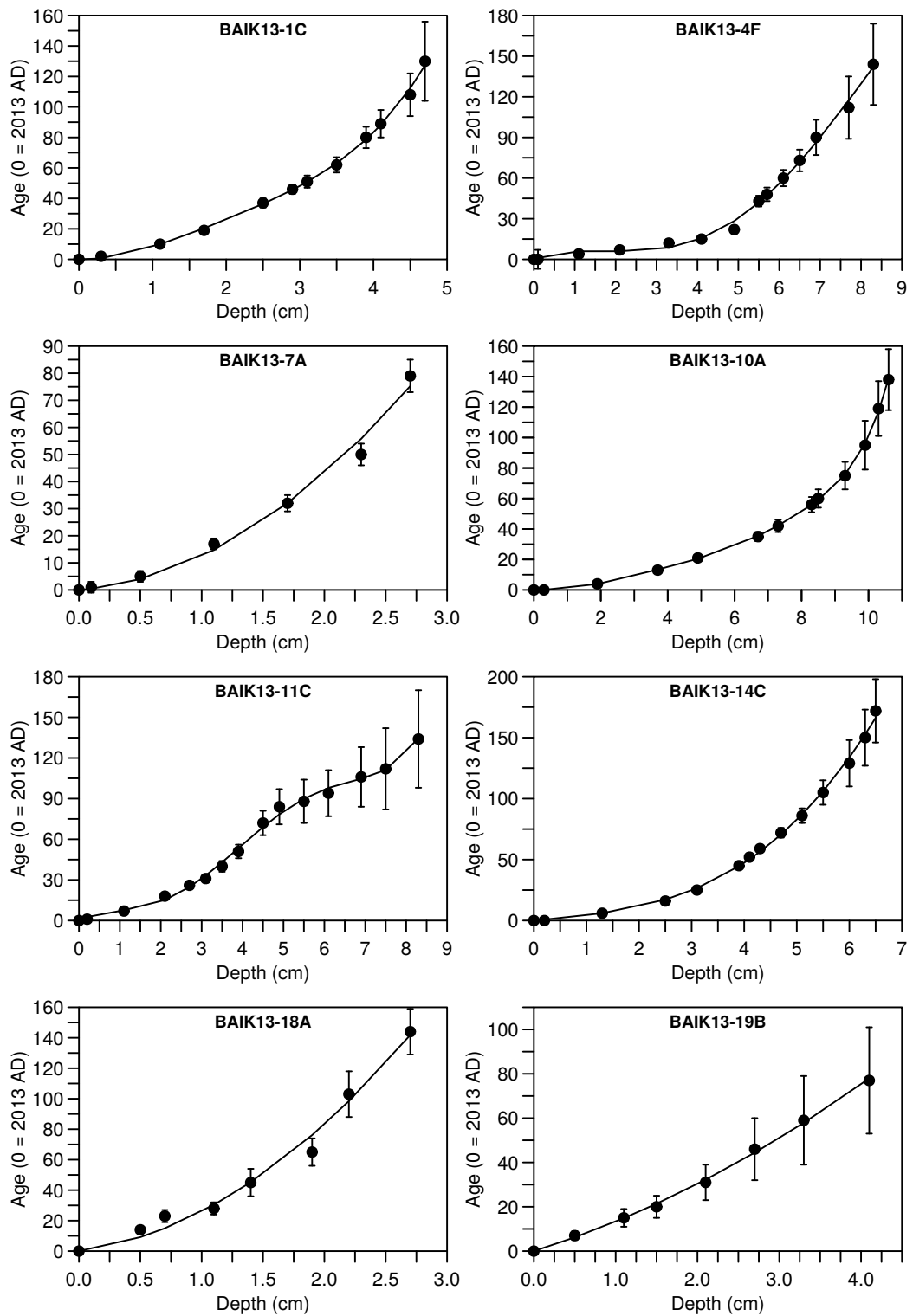


Figure 111: Age-depth models with polynomial line-fitting for each ^{210}Pb dated sediment core in the South basin, Selenga, Maloe More and North basin. The age units are years before 2013.

7.2.2 Investigating pigment preservation

To examine past primary production changes, it is vital to assess whether the pigment records are predominantly a reflection of production or degradation, by calculating a range of pigment measures (pigment flux, pigment concentrations nmol per g dry weight and nmol per g of OC), and comparing pigment concentrations to burial rates (Hurley and Armstrong, 1990; Leavitt and Findlay, 1994). Pigment preservation measures can then be used to examine if pigment concentrations are influenced by sedimentation rates, and therefore pigment preservation is site-specific, being lower in regions where pigments are exposed to oxic conditions for a longer period, such as in the pelagic deep basins. Leavitt and Findlay (1994) suggests that pigment concentrations corrected by organic content should be used, rather than pigment accumulation rates, to assess phytoplankton abundance in surface sediments, as it incorporates the mineralisation of labile organic material. TOC corrected pigment concentrations consider the percentage of total organic carbon preserved within the sediments, assuming carbon degradation is similar to pigment degradation. Pigment preservation within oxic and anoxic sediment layers were also assessed by comparing Chlas concentrations, Chlas accumulation rates and chl-*a*:pheo-*a* pigment ratios within these layers at each coring site. Similarly, carbon mass accumulation rates (CMAR) were compared between oxic and anoxic sediments. These comparison tests were carried out to assess if pigment and/or carbon concentrations/flux are significantly different between oxic and anoxic sediments, or if there is no significant difference between these sediments.

Pigment preservation in oxic and anoxic layers

Mean Chlas (chlorophyll-*a* and its derivatives) concentrations in the oxic layers are higher than mean Chlas concentrations in anoxic layers in the South basin, Selenga and Maloe More Bay and North basin sediment cores. Mean Chlas concentrations in the South basin oxic layers ranged between 159.1 – 271.3 nmol g⁻¹ OC, and between 20.0 – 208.2 nmol g⁻¹ OC in the anoxic layers (*Figure 153*). Mean Chlas concentrations in the North basin oxic layer ranged between 81.2 – 137.8 nmol g⁻¹ OC and are 138.4 nmol g⁻¹ OC in the anoxic layer (*Figure 122*). A t-test analysis showed significant (*p* value < 0.01) differences in Chlas concentrations between oxic and anoxic layers, with higher concentrations in the oxic layers in two of the South basin sites (BAIK13-4F and BAIK13-7A), one of the Selenga sites (BAIK13-10A) and in the Maloe More (BAIK13-14C) sediment record (*Table 35*). Comparison tests could not be carried out on one of the Selenga cores (BAIK13-11C) and one of the North basin cores (BAIK13-19B) as only one sample at the top of these cores was oxic, and the sediments at the other North basin core (BAIK13-18A) were fully oxidised. In the Selenga sites mean Chlas

concentrations ranged between 159.1 – 224.9 nmol g⁻¹ OC in the oxic layer and 20.0 – 119.7 nmol g⁻¹ OC in the anoxic layers (Figure 122). The highest mean Chlas concentrations in the oxic layers were found in Maloe More, which are 505.5 nmol g⁻¹ OC and c. 187.3 nmol g⁻¹ OC in the anoxic layer (Figure 122).

Mean Chlas accumulation rate (AR) in the oxic layers were higher than mean Chlas AR in anoxic layers in all the South basin sites, Selenga, Maloe More Bay and North basin sites. Mean South basin Chlas AR ranged between 0.008 – 0.347 nmol pigment cm⁻² yr⁻¹ in the oxic layers and between 0.000 – 0.121 nmol pigment cm⁻² yr⁻¹ in the anoxic layers (Figure 123). Mean Chlas AR in the North basin ranged between 0.035 – 0.037 nmol pigment cm⁻² yr⁻¹ in the oxic layer and are c. 0.02 nmol pigment cm⁻² yr⁻¹ in the anoxic layer (Figure 123). In the Selenga sites mean Chla AR ranged between 0.28 – 2.35 nmol pigment cm⁻² yr⁻¹ in the oxic layer and between 0.05 – 0.50 nmol pigment cm⁻² yr⁻¹ in the anoxic layer (Figure 123). Mean Chlas AR at Maloe More Bay were c. 0.37 nmol pigment cm⁻² yr⁻¹ in the oxic layer and c. 0.04 nmol pigment cm⁻² yr⁻¹ in the anoxic layer of the sediments (Figure 123). A t-test analysis showed significant differences in Chlas AR between oxic and anoxic layers in one of the Selenga sites (BAIK13-10A) and at Maloe More (BAIK13-14C) (Table 36).

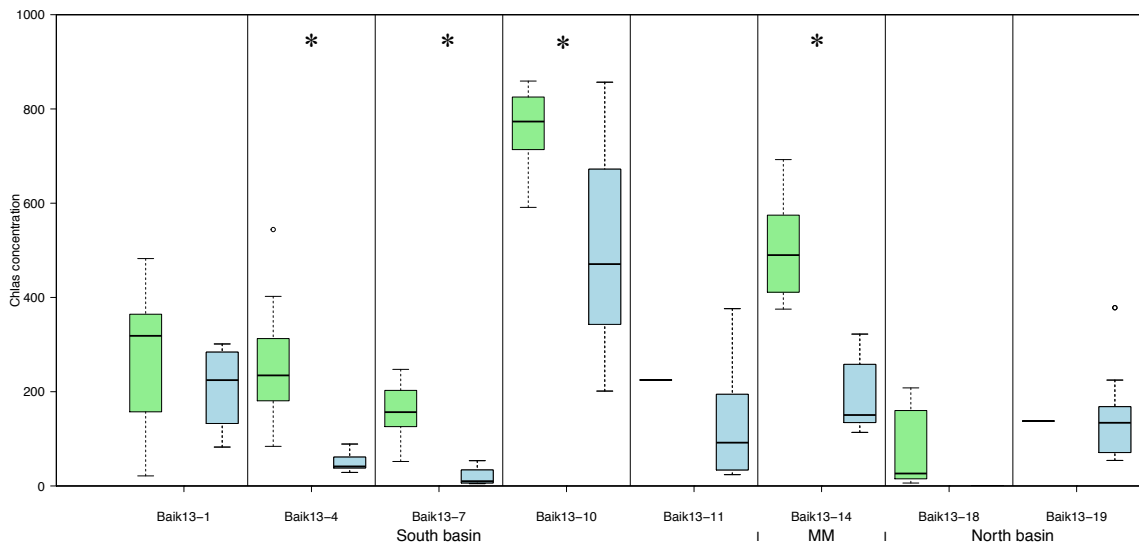


Figure 112: Comparison of Chlas concentration (nmol g⁻¹ OC) between oxic (green) and anoxic (blue) layers in the sediment cores across the lake over the last 200 years. ANOVA results showed significant differences (as indicated by an asterisk).

Mean CMAR were higher in oxic layers than anoxic layers in all sites (Figure 124), but only significantly different (p value of 0.013 and 0.009 respectively) between these two layers at BAIK13-10A and BAIK13-14C (Table 37). The highest mean CMAR were at the Selenga

(BAIK13-10A and BAIK13-11C) (0.003 and $0.001 \text{ g C m}^{-2} \text{ yr}^{-1}$), Maloe More Bay (BAIK13-14C) ($0.001 \text{ g C m}^{-2} \text{ yr}^{-1}$) and South basin, at BAIK13-1C ($0.001 \text{ g C m}^{-2} \text{ yr}^{-1}$) (Figure 124). Thus, significant differences in Chlas concentrations, Chlas AR and CMAR were found at BAIK13-10A and BAIK13-14C, between oxic and anoxic sediments, with higher values consistently in the oxic sediments.

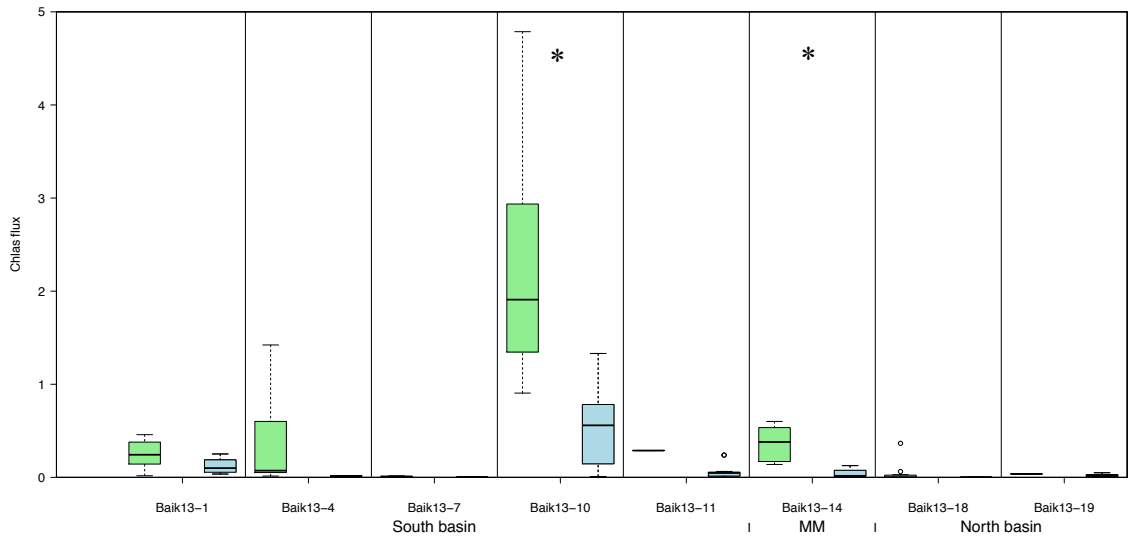


Figure 113: Comparison of Chlas AR ($\text{nmol pigment cm}^{-2} \text{ yr}^{-1}$) between oxic (green) and anoxic (blue) layers in the sediment cores across the lake over the last 200 years. ANOVA results showed significant differences (as indicated by an asterisk).

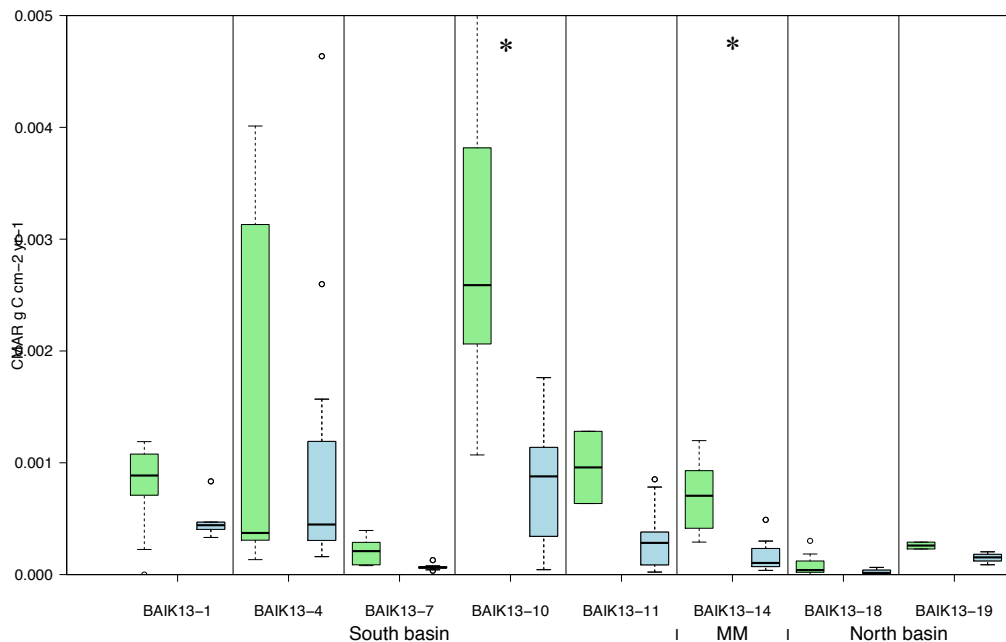


Figure 114: Comparison of CMAR ($\text{g C cm}^{-2} \text{ yr}^{-1}$) between oxic (green) and anoxic (blue) layers in the sediment cores across the lake over the last 200 years. ANOVA results showed significant differences (as indicated by an asterisk).

Table 35: Results from *t*-test and *p* values for comparing Chlas concentrations (nmol g OC⁻¹) between oxic and anoxic layers in the sediment cores across the lake over the last 200 years. Sites include South basin, South/Selenga, Central/MM (Maloe More Bay) and North basin.

Basin	Site	Chlas concentration T-test	Chlas concentration P-value
South	BAIK13-1	0.71	0.53
South	BAIK13-4	11.74	< 0.001
South	BAIK13-7	7.08	< 0.001
South/Selenga	BAIK13-10	3.74	< 0.001
South/Selenga	BAIK13-11	x	x
Central/MM	BAIK13-14	9.91	< 0.001
North	BAIK13-18	x	x
North	BAIK13-19	x	x

Table 36: Results from *t*-test and *p* values for comparing Chlas AR values (nmol pigment g OC cm⁻² yr⁻¹) between oxic and anoxic layers in the sediment cores across the lake over the last 200 years. Sites include South basin, South/Selenga, Central/MM (Maloe More Bay) and North basin.

Basin	Site	Chlas AR T-test	Chlas AR P-value
South	BAIK13-1	2.07	0.129
South	BAIK13-4	3.37	0.015
South	BAIK13-7	3.03	0.022
South/Selenga	BAIK13-10	3.87	0.003
South/Selenga	BAIK13-11	x	x
Central/MM	BAIK13-14	4.59	0.006
North	BAIK13-18	x	x
North	BAIK13-19	x	x

Table 37: Results from *t*-test and *p* values for comparing CMAR values (g C m⁻² yr⁻¹) between oxic and anoxic layers in the sediment cores across the lake over the last 200 years. Sites include South basin, South/Selenga, Central/MM (Maloe More Bay) and North basin.

Basin	Site	CMAR T-test	CMAR P-value
South	BAIK13-1	1.83	0.126
South	BAIK13-4	2.09	0.052
South	BAIK13-7	2.87	0.028
South/Selenga	BAIK13-10	3.08	0.013
South/Selenga	BAIK13-11	2.14	0.279
Central/MM	BAIK13-14	4.15	0.009
North	BAIK13-18	2.78	0.018
North	BAIK13-19	2.41	0.250

The pigment preservation ratio is the amount of intact chlorophyll-*a* relative to the amount of chlorophyll-*a* degradation products. Preservation ratio was higher in anoxic sediments than oxic, except for BAIK13-7A (Figure 125). There was a significant difference between oxic and anoxic sediments at this site (BAIK13-7A), and significantly higher chl-*a*:pheo-*a* ratio values in the anoxic sediments at BAIK13-10A and BAIK13-14C (Table 38). From this finding the reliability of the pigment preservation index within Lake Baikal's sediments has been explored in the 'Pigment preservation ratio, burial rates and pigment flux' section.

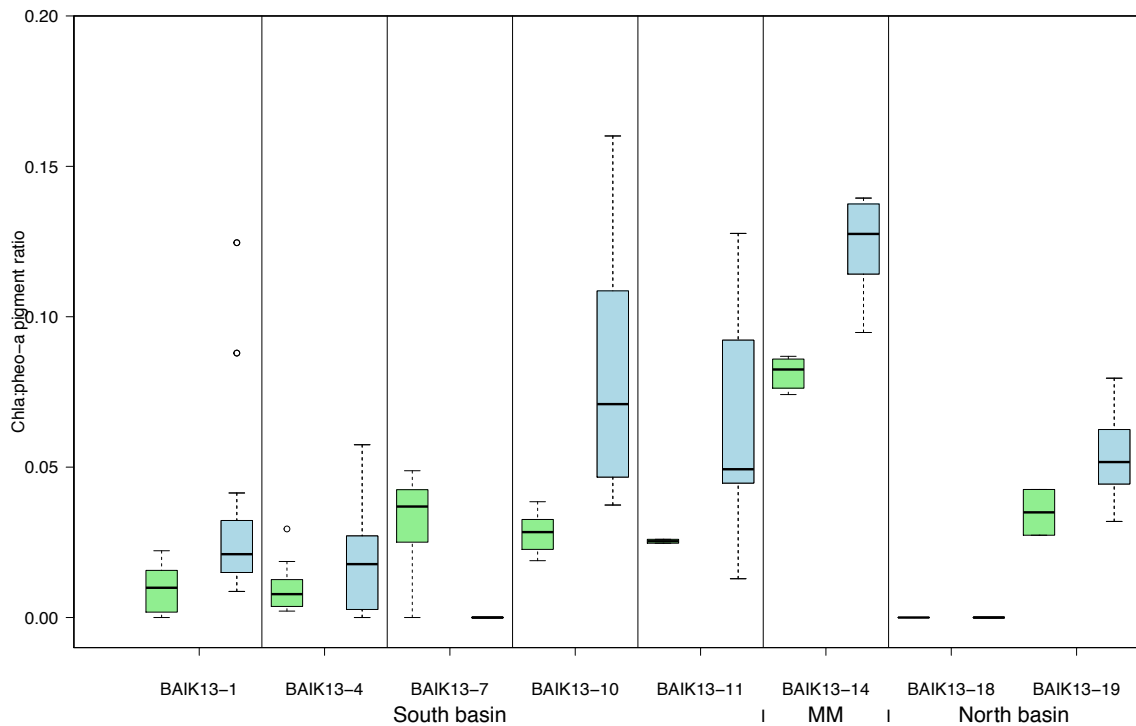


Figure 115: Comparison of chl-*a*:pheo-*a* pigment preservation ratio between oxic (green) and anoxic (blue) layers in the sediment cores across the lake over the last 200 years. T-test results show significant differences (as indicated by an asterisk).

Table 38: Results from *t*-test and *p* values for comparing chl-*a*:pheo-*a* pigment preservation ratio between oxic and anoxic layers in the sediment cores across the lake over the last 200 years. Sites include South basin, South/Selenga, Central/MM (Maloe More Bay) and North basin.

Basin	Site	Chl- <i>a</i> :pheo- <i>a</i> pigment ratio T-test	Chl- <i>a</i> :pheo- <i>a</i> pigment ratio P-value
South	BAIK13-1	-2.48	0.029
South	BAIK13-4	-2.27	0.038
South	BAIK13-7	4.89	0.003
South/Selenga	BAIK13-10	-4.11	0.002
South/Selenga	BAIK13-11	5.74	0.110
Central/MM	BAIK13-14	5.54	0.003
North	BAIK13-18	(-)	(-)
North	BAIK13-19	-1.79	0.324

Burial rates and pigment concentrations

Significant positive correlations (p value < 0.01) were observed between Chl-*a* concentration (nmol g^{-1} OC and nmol g^{-1} DW) and burial rates (CMAR and DMAR) at one of the South basin sites (BAIK13-4F), one of the Selenga sites (BAIK13-10A), Maloe More Bay (BAIK13-14C) and one of the North basin sites (BAIK13-18A) (Table 39; Table 40). This significant trend was also seen in the canthaxanthin concentrations (nmol g^{-1} OC) in one of the South basin sites (BAIK13-1C) and in the diatoxanthin concentrations (nmol g^{-1} OC) in one of the Selenga sites (BAIK13-10A) and Maloe More (BAIK13-14C) (Table 41; Table 42). These results suggest that burial was influencing pigment concentrations, within deep basin sites (at BAIK13-4F, BAIK13-7A and BAIK13-18A), river-influenced sites (at BAIK13-10A) and at littoral bay sites (at BAIK13-14C).

Table 39: Correlations between CMAR/DMAR and Chlas concentration per organic content. *Red* = negative relationship. Sites include South basin, South/Selenga, Central/MM (Maloe More Bay) and North basin.

Basin	Site	CMAR/DMAR	Chlas concentration nmol g ⁻¹ OC Correlation Coefficient	Chlas concentration nmol g ⁻¹ OC P value
South	BAIK13-1	CMAR	0.190	0.136
South	BAIK13-1	DMAR	0.096	0.304
South	BAIK13-4	CMAR	0.196	0.051
South	BAIK13-4	DMAR	0.099	0.189
South	BAIK13-7	CMAR	0.783	< 0.001
South	BAIK13-7	DMAR	0.607	< 0.001
South/Selenga	BAIK13-10	CMAR	0.300	< 0.001
South/Selenga	BAIK13-10	DMAR	0.179	0.006
South/Selenga	BAIK13-11	CMAR	0.046	0.378
South/Selenga	BAIK13-11	DMAR	0.001	0.918
Central/MM	BAIK13-14	CMAR	0.630	< 0.001
Central/MM	BAIK13-14	DMAR	0.570	< 0.001
North	BAIK13-18	CMAR	0.776	< 0.001
North	BAIK13-18	DMAR	0.290	0.038
North	BAIK13-19	CMAR	< 0.001	0.993
North	BAIK13-19	DMAR	0.146	0.144

Table 40: Correlations between CMAR/DMAR and Chlas concentration per dry matter. Sites include South basin, South/Selenga, Central/MM (Maloe More Bay) and North basin.

Basin	Site	CMAR/DMAR	Chlas concentration nmol g ⁻¹ DW Correlation Coefficient	Chlas concentration nmol g ⁻¹ DW P value
South	BAIK13-1	CMAR	0.223	0.103
South	BAIK13-1	DMAR	0.112	0.263
South	BAIK13-4	CMAR	0.359	0.004
South	BAIK13-4	DMAR	0.251	0.028
South	BAIK13-7	CMAR	0.656	< 0.001
South	BAIK13-7	DMAR	0.822	< 0.001
South/Selenga	BAIK13-10	CMAR	0.432	< 0.001
South/Selenga	BAIK13-10	DMAR	0.274	< 0.001
South/Selenga	BAIK13-11	CMAR	0.059	0.316
South/Selenga	BAIK13-11	DMAR	< 0.001	0.982
Central/MM	BAIK13-14	CMAR	0.636	< 0.001
Central/MM	BAIK13-14	DMAR	0.573	< 0.001
North	BAIK13-18	CMAR	0.741	< 0.001
North	BAIK13-18	DMAR	0.292	0.037
North	BAIK13-19	CMAR	0.039	0.462
North	BAIK13-19	DMAR	0.136	0.160

Table 41: Correlations between CMAR/DMAR and Diatoxanthin concentrations. *Red* = negative relationship. Sites include South basin, South/Selenga, Central/MM (Maloe More Bay) and North basin.

Basin	Site	CMAR/DMAR	Diatoxanthin concentration nmol g ⁻¹ OC Correlation Coefficient	Diatoxanthin concentration nmol g ⁻¹ OC P value
South	BAIK13-1	CMAR	0.003	0.667
South	BAIK13-1	DMAR	0.002	0.653
South	BAIK13-4	CMAR	x	x
South	BAIK13-4	DMAR	x	x
South	BAIK13-7	CMAR	x	x
South	BAIK13-7	DMAR	x	x
South/Selenga	BAIK13-10	CMAR	0.250	< 0.001
South/Selenga	BAIK13-10	DMAR	0.145	0.013
South/Selenga	BAIK13-11	CMAR	x	x
South/Selenga	BAIK13-11	DMAR	x	x
Central/MM	BAIK13-14	CMAR	0.550	0.001
Central/MM	BAIK13-14	DMAR	0.529	0.001
North	BAIK13-18	CMAR	x	x
North	BAIK13-18	DMAR	x	x
North	BAIK13-19	CMAR	0.105	0.221
North	BAIK13-19	DMAR	0.439	0.005

Table 42: Correlations between CMAR/DMAR and Canthaxanthin concentrations. *Red* = negative relationship. Sites include South basin, South/Selenga, Central/MM (Maloe More Bay) and North basin.

Basin	Site	CMAR/DMAR	Canthaxanthin concentration nmol g ⁻¹ OC Correlation Coefficient	Canthaxanthin concentration nmol g ⁻¹ OC P value
South	BAIK13-1	CMAR	< 0.001	0.645
South	BAIK13-1	DMAR	0.017	0.298
South	BAIK13-4	CMAR	0.009	0.691
South	BAIK13-4	DMAR	0.011	0.672
South	BAIK13-7	CMAR	0.831	< 0.001
South	BAIK13-7	DMAR	0.710	< 0.001
South/Selenga	BAIK13-10	CMAR	0.006	0.621
South/Selenga	BAIK13-10	DMAR	0.013	0.486
South/Selenga	BAIK13-11	CMAR	0.020	0.562
South/Selenga	BAIK13-11	DMAR	0.016	0.610
Central/MM	BAIK13-14	CMAR	0.021	0.594
Central/MM	BAIK13-14	DMAR	0.009	0.731
North	BAIK13-18	CMAR	x	x
North	BAIK13-18	DMAR	x	x
North	BAIK13-19	CMAR	0.010	0.707
North	BAIK13-19	DMAR	0.398	0.009

Chl-*a*:pheo-*a* pigment ratio

Regression analyses were carried out between chl-*a*:pheo-*a* pigment ratios and water depth, to examine whether the water column depth is having an influence on pigment preservation. Average chl-*a*:pheo-*a* pigment ratios in the surface sediments (upper 2 cm) were highest at Maloe More (BAIK13-14C; chl-*a*: pheo-*a* = 0.08) compared to the rest of the sites, and intact chlorophyll-*a* was detected at all sites except for BAIK13-18A in the North basin (Figure 126). Pigment preservation was found to be site specific, being higher at Maloe More Bay (Maloe More Bay > Selenga > South and North basin), with higher pigment preservation at littoral sites shallower than 600 m in comparison to deep pelagic sites (Figure 126). River influenced sites (BAIK13-10A and BAIK13-11C; chl-*a*:pheo-*a* = 0.03) had similar average chl-*a*:pheo-*a* pigment ratios to one of the South basin sites (BAIK13-7A; chl-*a*: pheo-*a* = 0.04) and one of the North basin sites (BAIK13-19B; chl-*a*:pheo-*a* = 0.03). The Selenga sites (BAIK13-10A and BAIK13-11C) ranged in water depths between 60 m to 345 m, and the lower chl-*a*: pheo-*a* pigment ratios compared to Maloe More (BAIK13-14C) could be due to transportation of degraded material along the Selenga River. Furthermore, one of the pelagic North basin sites (BAIK13-19B) had a water depth of 460 m, and a similar average chl-*a*:pheo-*a* pigment ratio to a deep pelagic South basin site (BAIK13-7A) with a water depth of 1360 m (Figure 126). This is also likely to be due to the influence of the Upper Angara river waters into the North basin.

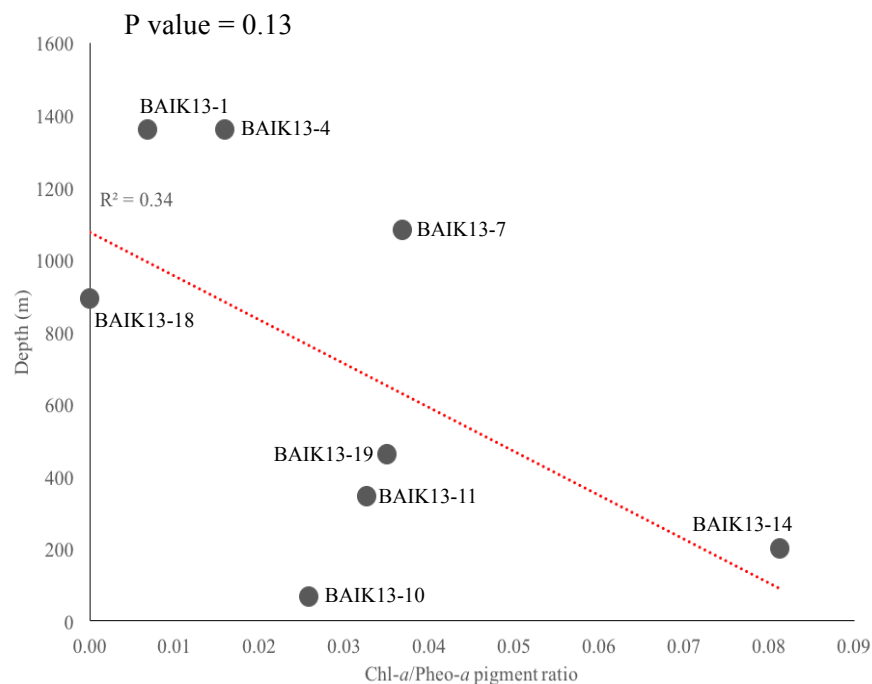


Figure 116: Chl-*a*: pheo-*a* pigment ratio in surface sediments (upper 2 cm) and water column depth at coring sites across the lake.

Pigment preservation ratio, burial rates and pigment flux

The pigment preservation ratio can be influenced by pigment flux (Chlas flux) and burial rate (CMAR, DMAR), as higher burial rate and pigment flux will result in higher chl-*a*:pheo-*a* ratio. Regression correlation coefficients between the chl-*a*:pheo-*a* pigment ratio vs chlas AR, chl-*a*:pheo-*a* pigment ratio vs CMAR, and chl-*a*:pheo-*a* pigment ratio vs DMAR all showed a significant (p value < 0.001) positive relationship in two of the South basin sites (BAIK13-4F and BAIK13-7A) ($R^2 = 0.72$ and 0.75), but not in the rest of the sites across the lake (*Table 43; Table 44; Table 45*). North basin and Maloe More do not show significant trends between chl-*a*:pheo-*a* pigment ratios vs chlas AR, chl-*a*:pheo-*a* pigment ratio vs CMAR, and chl-*a*:pheo-*a* pigment ratio vs DMAR. A significant (p value < 0.001) negative relationship ($R^2 = 0.35$) was found in one of the Selenga sites (BAIK13-10A), between chl-*a*:pheo-*a* pigment ratio vs chlas AR, chl-*a*:pheo-*a* pigment ratio vs CMAR, and chl-*a*:pheo-*a* pigment ratio vs DMAR (*Table 43; Table 44; Table 45*). This showed that higher pigment flux, carbon burial and sedimentation rates were not coinciding with higher concentrations of intact chlorophyll-*a* at BAIK13-10A. Thus, burial rate was not resulting in higher pigment preservation at the Selenga Shallows site, whereas at BAIK13-4F and BAIK13-7A in the South basin, higher burial rate was coinciding with a higher pigment preservation index value.

Table 43: Regression correlation coefficients and significance values between the chl-*a*:pheo-*a* pigment ratio and Chlas AR. *Red* = negative relationship. Sites include South basin, South/Selenga, Central/MM (Maloe More Bay) and North basin.

Basin	Site	Preservation Ratio	Chlas flux nmol pigment OC cm ⁻² yr ⁻¹ Correlation Coefficient	Chlas flux nmol pigment OC cm ⁻² yr ⁻¹ P-value
South	BAIK13-1	Chl- <i>a</i> :Pheo- <i>a</i> pigment ratio	0.041	0.509
South	BAIK13-4	Chl- <i>a</i> :Pheo- <i>a</i> pigment ratio	0.717	< 0.001
South	BAIK13-7	Chl- <i>a</i> :Pheo- <i>a</i> pigment ratio	0.754	< 0.001
South/Selenga	BAIK13-10	Chl- <i>a</i> :Pheo- <i>a</i> pigment ratio	0.347	< 0.001
South/Selenga	BAIK13-11	Chl- <i>a</i> :Pheo- <i>a</i> pigment ratio	0.235	0.036
Central/MM	BAIK13-14	Chl- <i>a</i> :Pheo- <i>a</i> pigment ratio	0.379	0.011
North	BAIK13-18	Chl- <i>a</i> :Pheo- <i>a</i> pigment ratio	x	x
North	BAIK13-19	Chl- <i>a</i> :Pheo- <i>a</i> pigment ratio	0.116	0.196

Table 44: Regression correlation coefficients and significance values between the chl-*a*:pheo-*a* pigment ratio and CMAR. *Red* = negative relationship. Sites include South basin, South/Selenga, Central/MM (Maloe More Bay) and North basin.

Basin	Site	Preservation Ratio	CMAR g C m ⁻² yr ⁻¹ Correlation Coefficient	CMAR g C m ⁻² yr ⁻¹ P-value
South	BAIK13-1	Chl- <i>a</i> :Pheo- <i>a</i> pigment ratio	0.060	0.418
South	BAIK13-4	Chl- <i>a</i> :Pheo- <i>a</i> pigment ratio	0.681	< 0.001
South	BAIK13-7	Chl- <i>a</i> :Pheo- <i>a</i> pigment ratio	0.671	< 0.001
South/Selenga	BAIK13-10	Chl- <i>a</i> :Pheo- <i>a</i> pigment ratio	0.357	< 0.001
South/Selenga	BAIK13-11	Chl- <i>a</i> :Pheo- <i>a</i> pigment ratio	0.036	0.436
Central/MM	BAIK13-14	Chl- <i>a</i> :Pheo- <i>a</i> pigment ratio	0.343	0.017
North	BAIK13-18	Chl- <i>a</i> :Pheo- <i>a</i> pigment ratio	x	x
North	BAIK13-19	Chl- <i>a</i> :Pheo- <i>a</i> pigment ratio	0.028	0.534

Table 45: Regression correlation coefficients and significance values between the chl-*a*:pheo-*a* pigment ratio and DMAR. *Red* = negative relationship. Sites include South basin, South/Selenga, Central/MM (Maloe More Bay) and North basin.

Basin	Site	Preservation Ratio	DMAR g DW cm ⁻² yr ⁻¹ Correlation Coefficient	DMAR g DW cm ⁻² yr ⁻¹ P-value
South	BAIK13-1	Chl- <i>a</i> :Pheo- <i>a</i> pigment ratio	0.174	0.156
South	BAIK13-4	Chl- <i>a</i> :Pheo- <i>a</i> pigment ratio	0.643	< 0.001
South	BAIK13-7	Chl- <i>a</i> :Pheo- <i>a</i> pigment ratio	0.504	0003
South/Selenga	BAIK13-10	Chl- <i>a</i> :Pheo- <i>a</i> pigment ratio	0.203	0.003
South/Selenga	BAIK13-11	Chl- <i>a</i> :Pheo- <i>a</i> pigment ratio	< 0.001	0.993
Central/MM	BAIK13-14	Chl- <i>a</i> :Pheo- <i>a</i> pigment ratio	0.309	0.025
North	BAIK13-18	Chl- <i>a</i> :Pheo- <i>a</i> pigment ratio	x	x
North	BAIK13-19	Chl- <i>a</i> :Pheo- <i>a</i> pigment ratio	0.166	0.118

There was no correlation between chl-*a*:pheo-*a* pigment ratio and CMAR at all the sites (*Figure 127*), i.e. no correlation between pigment preservation and carbon accumulation rate. Therefore, burial might not be a major factor on pigment preservation at sites other than BAIK13-4F and BAIK13-7A, if the chl-*a*: pheo-*a* pigment ratio is a reliable preservation indicator. This is a tentative finding though as Lake Baikal's sediments largely consist of chlorophyll degradation products with minimal concentrations of intact chlorophyll-*a* due to the large water column depths, especially within the pelagic deep basins (> 1,000 m water depth).

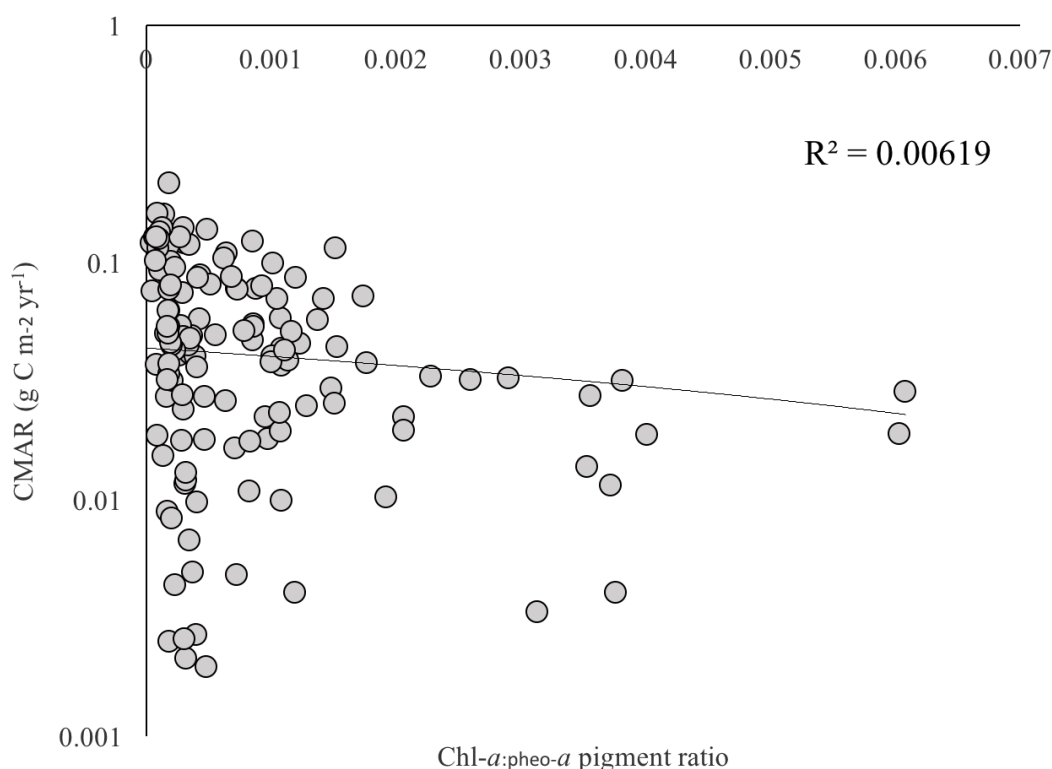


Figure 117: Chl-a:pheo-a pigment ratio and CMAR (g C m⁻² yr⁻¹) plotted on a log scale at all the sites in the South basin, Selenga, Maloe More Bay and North basin

Testing pigment co-variation

Pigment co-variation was tested to assess pigment preservation. If all the trends were similar then it suggests a possible degradation profile, whereas if the pigment concentration trends differed, then this suggests possible production signals. This is tested between Chlas, diatoxanthin (diatom pigment) and canthaxanthin (picocyanobacteria pigment), i.e total algae and two of the major algal groups. Chlas and diatoxanthin concentrations, and diatoxanthin and canthaxanthin concentrations were not significantly positively correlated in the South basin, Selenga, Maloe More or North basin sediment cores over the last 200 years (*Table 46*;

Table 47). However, Chlas and canthaxanthin concentrations have a significant (p value < 0.001) positive relationship in one of the South basin (BAIK13-7A) ($R^2 = 0.91$) and one of the North basin sites (BAIK13-19B) ($R^2 = 0.48$) (Table 46). In the Selenga and Maloe More sediment records pigments do not co-vary, and showed different trends, suggesting a production signal rather than a preservation signal.

Table 46: Correlation coefficients and significance testing between Chlas, diatoxanthin and canthaxanthin pigment concentrations. BAIK13-18A in the North basin has not been included as no intact chlorophyll-a or diatoxanthin/canthaxanthin pigments were detected. *Red* = negative relationship. Sites include South basin, South/Selenga, Central/MM (Maloe More Bay) and North basin.

Basin	Site	Pigment concentration nmol g ⁻¹ OC	Chlas concentration nmol g ⁻¹ OC Correlation Coefficient	Chlas concentration nmol g ⁻¹ OC P value
South	BAIK13-1	Diatoxanthin	0.004	0.832
South	BAIK13-1	Canthaxanthin	0.053	0.450
South	BAIK13-4	Diatoxanthin	x	x
South	BAIK13-4	Canthaxanthin	< 0.001	0.968
South	BAIK13-7	Diatoxanthin	x	x
South	BAIK13-7	Canthaxanthin	0.907	< 0.001
South/Selenga	BAIK13-10	Diatoxanthin	0.283	< 0.001
South/Selenga	BAIK13-10	Canthaxanthin	0.002	0.769
South/Selenga	BAIK13-11	Diatoxanthin	0.104	0.177
South/Selenga	BAIK13-11	Canthaxanthin	0.002	0.852
Central/MM	BAIK13-14	Diatoxanthin	0.504	0.002
Central/MM	BAIK13-14	Canthaxanthin	0.069	0.325
North	BAIK13-19	Diatoxanthin	0.009	0.725
North	BAIK13-19	Canthaxanthin	0.480	0.002

Table 47: Correlation coefficients and significance testing between diatoxanthin and canthaxanthin pigment concentrations. BAIK13-18A in the North basin has not been included as no intact diatoxanthin/canthaxanthin pigments were detected. Red = negative relationship. Sites include South basin, South/Selenga, Central/MM (Maloe More Bay) and North basin.

Basin	Site	Pigment concentration nmol g ⁻¹ OC	Diatoxanthin concentration nmol g ⁻¹ OC Correlation Coefficient	Diatoxanthin concentration nmol g ⁻¹ OC P value
South	BAIK13-1	Canthaxanthin	0.335	0.038
South	BAIK13-4	Canthaxanthin	x	x
South	BAIK13-7	Canthaxanthin	x	x
South/Selenga	BAIK13-10	Canthaxanthin	0.001	0.836
South/Selenga	BAIK13-11	Canthaxanthin	0.012	0.642
Central/MM	BAIK13-14	Canthaxanthin	0.030	0.519
North	BAIK13-19	Canthaxanthin	0.235	0.056

There is also a strong relationship between SAR and pigment flux in both oxic and anoxic sediments (Figure 128), which suggests that burial rate is a main factor in determining pigment flux.

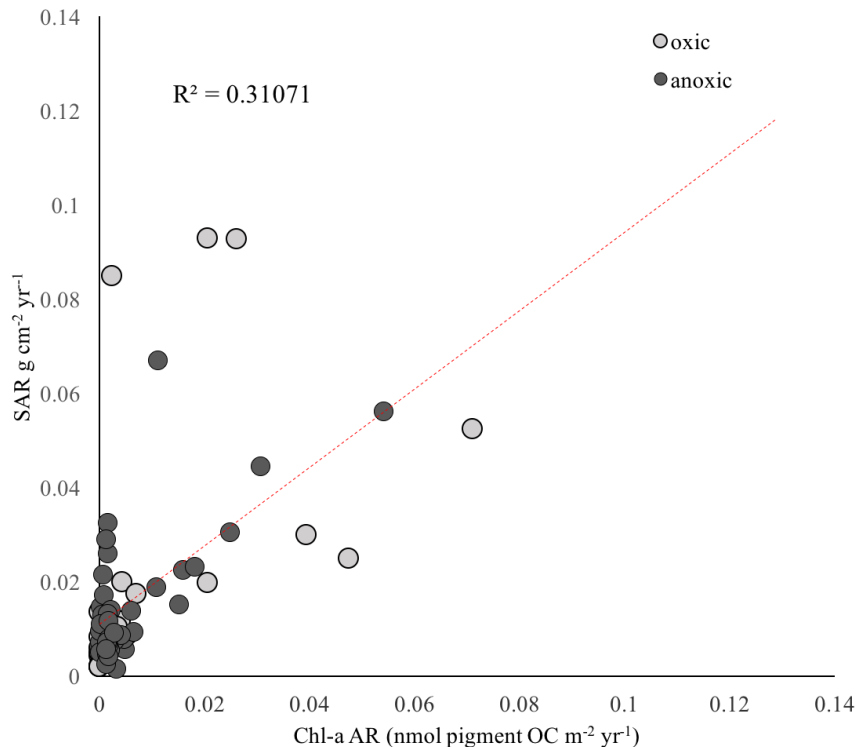


Figure 118: Mean Chla AR and SAR within oxic and anoxic sediments at all sites in the South basin, Selenga, Maloe More and North basin.

From the analyses discussed above, the pigment records which can be used to address the aims of this chapter are BAIK13-1C and BAIK13-4F in the South basin, BAIK13-10A and BAIK13-11C in the Selenga, BAIK13-14C in Maloe More and BAIK13-19B in the North basin (*Table 48*). The pigment records which have not been selected for interpretation are BAIK13-7A in the South basin and BAIK13-18A in the North basin (*Table 48*). Pigment flux at BAIK13-1C, BAIK13-4F, BAIK13-10A, BAIK13-11C, BAIK13-14C and BAIK13-19B were not positively correlated with burial rate, and pigment flux and concentrations were not significantly higher in anoxic sediments, compared to oxic sediments. Pigments within these records do not show exponential decline in concentrations, and do not show pigment co-variation down-core (*Figure 133; Figure 134; Figure 136; Figure 137; Figure 138; Figure 140*). Whereas both BAIK13-7A and BAIK13-18A have very low sedimentation rates ($< 0.002 \text{ cm}^2/\text{yr}^1$) and the pigment records largely consisted of chlorophyll degradation products (*Figure 135; Figure 139*). Thus BAIK13-7A and BAIK13-18A are likely to be reflecting degradation profiles, rather than production trends.

Table 48: Summary table of sediment cores to highlight which pigment records are suitable for interpretation. Grey indicates pigment records which can be interpreted.

Basin	Core	Turbidites	Oxidised layers	SAR	Pigment composition
South basin	BAIK13-1	No	Yes	Low ($< 0.02 \text{ g cm}^{-2} \text{ yr}^{-1}$)	Chls, carotenoids and degrad products
	BAIK13-4	Yes	Yes	Variable	Chls, carotenoids and degrad products
Selenga	BAIK13-7	No	Yes	Low ($< 0.02 \text{ g cm}^{-2} \text{ yr}^{-1}$)	Mainly degradation products x
	BAIK13-10	No	Yes	High ($> 0.02 \text{ g cm}^{-2} \text{ yr}^{-1}$)	Chls, carotenoids and degrad products
Maloe More	BAIK13-11	No	Yes	Variable	Chls, carotenoids and degrad products
	BAIK13-14	No	No	High ($> 0.02 \text{ g cm}^{-2} \text{ yr}^{-1}$)	Chls, carotenoids and degrad products
North basin	BAIK13-18	No	Yes	Low ($< 0.01 \text{ g cm}^{-2} \text{ yr}^{-1}$)	Mainly degradation products x
	BAIK13-19	No	Yes	Low ($< 0.01 \text{ g cm}^{-2} \text{ yr}^{-1}$)	Chls, carotenoids and degrad products

7.2.3 Lake-wide spatial variability in surface sediment TOC, carbon isotopes, TOC/N ratios, pigments and diatom assemblages over the past 20 years

Total organic carbon (TOC), stable carbon isotopes ($\delta^{13}\text{C}$), TOC/N ratios, algal pigments and diatom assemblages from core tops from across the lake show spatial variability in aquatic production. Mean values within the ^{210}Pb dated surface sediments over the last 20 years were taken (*Table 49*), to compare the profundal, littoral and river-influenced sites.

Table 49: The upper cms which cover the last 20 years at each coring site and the age of the upper 1 cm at each coring site.

Site	Upper cms which cover the last 20 years	Age of the upper 1 cm (years)	Date of the upper 1 cm (AD)
BAIK13-1	2.0	5	2008
BAIK13-4	4.5	6	2007
BAIK13-7	1.5	12	2001
BAIK13-10	5.0	1	2012
BAIK13-11	2.5	7	2006
BAIK13-14	2.5	4	2009
BAIK13-18	1.0	26	1987
BAIK13-19	1.5	13	2000

TOC, TOC/N and $\delta^{13}\text{C}$

TOC values within the surface sediments (*Figure 129*) of Lake Baikal ranged between 0.64 % and 3.91 %, with the largest range in the South basin sites. BAIK13-1C had the highest mean TOC values over the last 20 years (c. 3.3 %) and the largest variation was seen within BAIK13-4F (c. 1 to 3 %) (*Figure 129*). Mean TOC values were greatest at Maloe More (mean = 3.46 %; max = 3.60 %), than the pelagic basin sites (South basin mean = 2.71 %; max = 3.20 % and North basin mean = 3.04 %; max = 3.31 %) and Selenga site (mean = 3.13 %; max = 3.73 %) (Maloe More > Selenga > North basin > South basin) (*Figure 129*). Although there was spatial variation in TOC values, there was no significant difference (p value > 0.01) between the different regions.

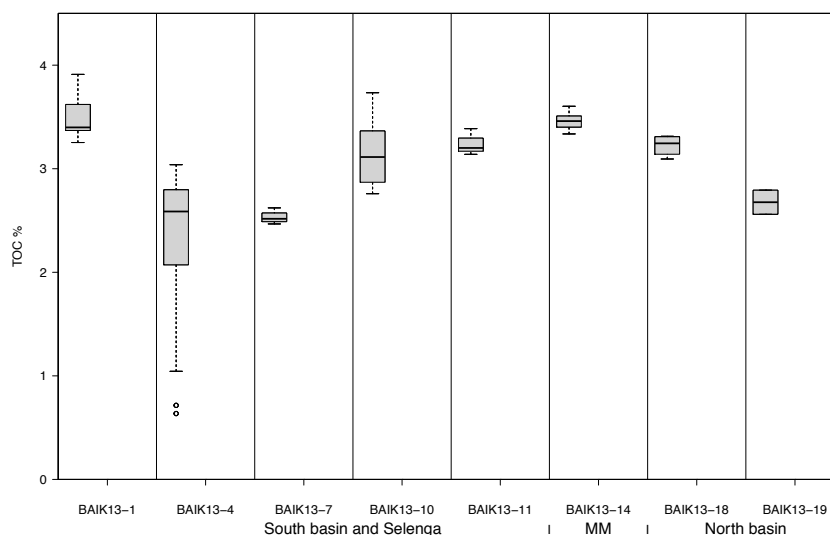


Figure 119: TOC % in the surface (upper 2 cm) sediments (over the last 20 years) in the South, Selenga, Maloe More (MM) and North basin sites.

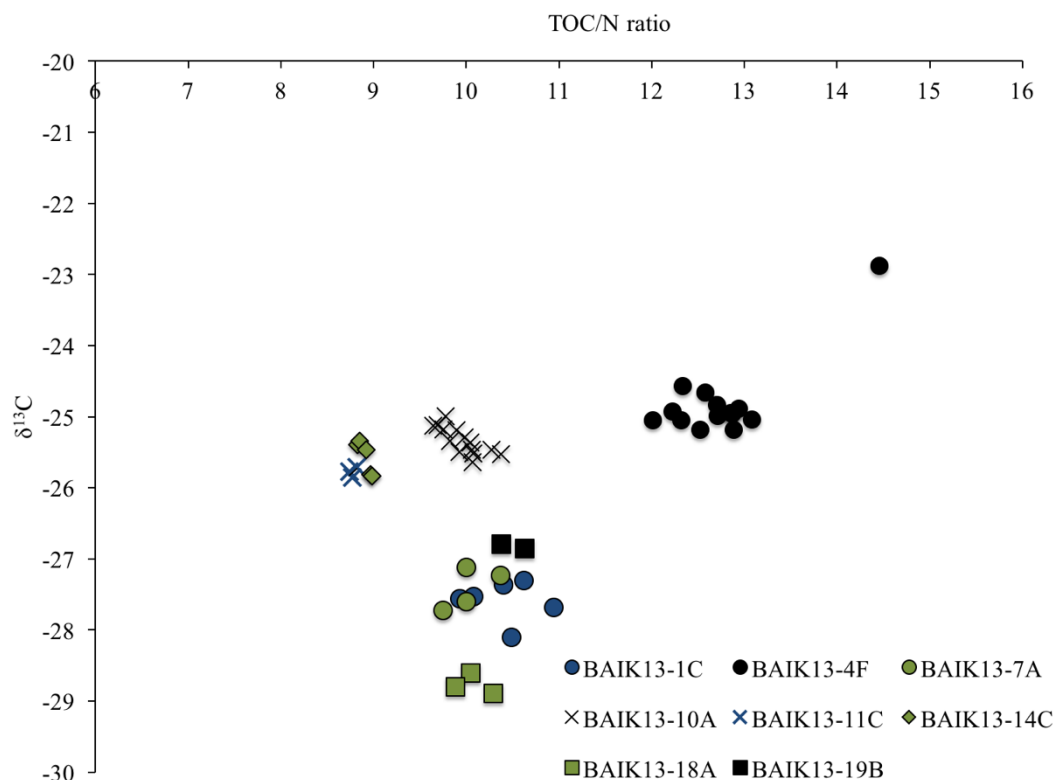


Figure 120: Biplot of surface sediment $\delta^{13}\text{C}$ and TOC/N ratio values over the last 20 years in the South (BAIK13-1C; BAIK13-4F; BAIK13-7A), Selenga (BAIK13-10A; BAIK13-11C), Maloe More (BAIK13-14C) and North basin (BAIK13-18A; BAIK13-19B) sites. TOC/N ratio values < 12 indicates predominately algal sources (Prokopenko et al. 1993).

Results showed inter core variability in surface sediment $\delta^{13}\text{C}$ values, especially in the South basin (BAIK13-1C and BAIK13-4F), Selenga (BAIK13-10A) and Maloe More (BAIK13-14C). Pelagic deep basin sites (BAIK13-1C; BAIK13-7A; BAIK13-18A), except for BAIK13-4F in the South basin, had the lowest average $\delta^{13}\text{C}$ values (-28.6 to -27.1 ‰) in the surface sediments (Figure 130), compared to river influenced sites (BAIK13-10A; BAIK13-19B) (-26.8 to -24.9 ‰) and littoral bay regions (BAIK13-14C) (-25.8 to -25.3 ‰). The highest $\delta^{13}\text{C}$ values within the surface sediments were found at BAIK13-4F (max = -22.8 ‰) in the South basin, BAIK13-10A near the Selenga Delta (-24.9 to -25.6 ‰), BAIK13-11C (-25.8 to -25.7 ‰) and BAIK13-14C in Maloe More. TOC/N ratio values ranged between 8.74 to 14.45, with the largest range in the South basin sites (Figure 130). The lowest TOC/N ratio values were at BAIK13-11C (8.74 – 8.82) and Maloe More (BAIK13-14C; 8.83 – 9.98), and the highest TOC/N ratio values were at BAIK13-4F (mean = 12.74; max = 14.45). All sites, except BAIK13-4F, had TOC/N ratio values < 12 , indicating predominately algal sources (Prokopenko et al. 1993).

Sedimentary pigments

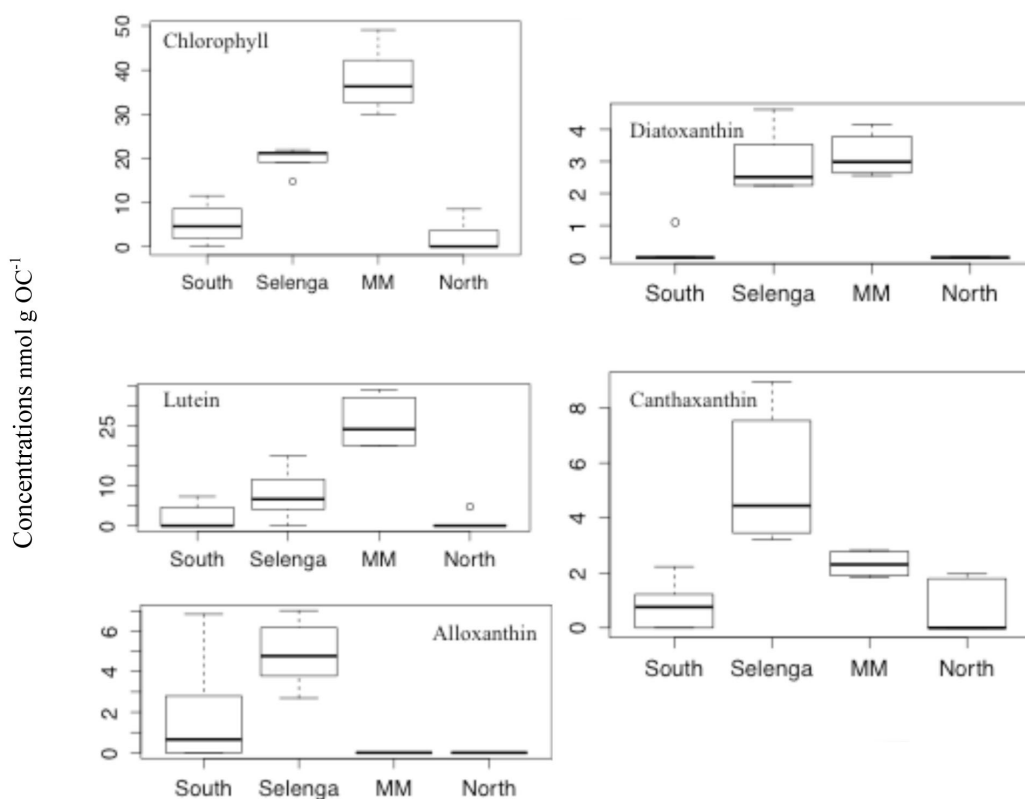


Figure 121: Chlorophyll-*a* and major carotenoid concentrations in the surface sediments over the last 20 years in the South, Selenga, Maloe More and North basin sites. (BAIK13-7A and BAIK13-18A pigment data removed).

Table 50: *P*-values from ANOVA to test if there is a significant difference in pigment concentrations between regions (South basin, Selenga Shallows, Maloe More and North basin).

	P- values				
	Chlorophyll- <i>a</i>	Diatoxanthin	Lutein	Canthaxanthin	Alloxanthin
Selenga - South	< 0.001	< 0.001	0.007	< 0.001	0.001
MM - South	< 0.001	< 0.001	< 0.001	0.006	0.215
North - South	0.353	0.998	0.883	0.987	0.215
MM - Selenga	< 0.001	0.922	< 0.001	< 0.001	< 0.001
North - Selenga	< 0.001	< 0.001	0.011	< 0.001	< 0.001
North - MM	< 0.001	< 0.001	< 0.001	0.027	1.000

Lake-wide, the total chlorophyll-*a* concentrations ranged between 0.75 and 49.07 nmol g⁻¹ OC within the surface sediments covering the last 20 years (*Figure 131*). There was lake-wide variability within the mean chlorophyll-*a* concentrations (Maloe More > Selenga > South basin > North basin), and the largest range (29.98 – 49.07 nmol g⁻¹ OC) in chlorophyll-*a* concentration were found at Maloe More (BAIK13-14C). Surface sediment chlorophyll-*a* concentrations at Maloe More were significantly higher than the Selenga (p value < 0.01), South basin (p value < 0.01) and North basin sites (p value < 0.01) (*Table 50*). Surface sediment chlorophyll-*a* concentrations at the Selenga were significantly higher than both the pelagic South basin sites (p value < 0.01) and North basin sites (p value < 0.01). The main carotenoids measured within the surface sediments were lutein, canthaxanthin, alloxanthin and diatoxanthin. Lutein concentrations ranged from 1.88 to 34.19 nmol g⁻¹ OC, being highest at Maloe More (mean = 25.87 nmol g⁻¹ OC; 20.09 – 34.19 nmol g⁻¹ OC) (Maloe more > Selenga > South and North basin). Maloe More and Selenga lutein concentrations were significantly higher than the South basin sites (p value = < 0.01 and 0.01 respectively) and North basin sites (p value = < 0.01 and 0.01 respectively). Canthaxanthin concentrations were significantly higher (mean = 5.52 nmol g⁻¹ OC; 3.23 – 8.94 nmol g⁻¹ OC) in the Selenga than Maloe More (p value = < 0.01) and both the South (p value = < 0.01) and North basin sites (p value < 0.01) (Selenga > Maloe more > South basin > North basin). Alloxanthin concentrations had the largest range in the South basin sites (mean = 2.34 nmol g⁻¹ OC; 0.39 – 6.84 nmol g⁻¹ OC), and the Selenga concentrations were significantly higher than the rest of the sites (Selenga > South basin > Maloe more and North basin). Mean diatoxanthin concentrations were highest in Maloe More (mean = 3.18 nmol g⁻¹ OC) (Maloe more > Selenga > South and North basin), and the largest range in diatoxanthin concentrations were at the Selenga (2.24 – 4.62 nmol g⁻¹ OC). The Maloe More and Selenga surface sediment diatoxanthin concentrations were significantly higher than both the pelagic South (p value < 0.01) and North basin sites (p value < 0.01) (*Table 50*).

Diatom assemblages

Surface sediment (0 – 2 cm) diatom assemblages were largely comprised of *Aulacoseira baicalensis*, *Aulacoseira skvortzowii*, *Crateriportula inconspicua*, *Cyclotella minuta/ornata*, *Stephanodiscus meyerii* and *Synedra acus* var. *radians*. *Aulacoseira baicalensis* had the highest abundances, ranging between (9.5 – 74.7 %) across the sites (Figure 132). Surface sediment abundances of *Aulacoseira baicalensis* were significantly higher in the North basin sites compared to the South basin, Maloe More and Selenga site (p value < 0.01) (Table 51) (North basin > South basin > Maloe More > Selenga). *Cyclotella minuta/ornata* abundances had the largest range in the South basin sites (22.2 – 51.3 %), mean abundances are highest within Maloe More (39.2 %) (Maloe More > South basin > Selenga and North basin), and the South basin abundances were significantly higher than the North basin (p value < 0.01) (Table 51). Similarly, *Synedra acus* var. *radians* abundances had the largest range in the South basin sites (mean = 15.2 %; 4.5 – 30.4 %), and mean abundances were significantly higher than the North basin (p value < 0.01) (Table 51). Mean abundances of *Synedra acus* var. *radians* within the surface sediments were similar within the South basin, Selenga and Maloe More (15.2%, 13.9% and 12.2% respectively). *Aulacoseira skvortzowii* abundances were significantly higher at the Selenga than the rest of the sites (p value < 0.01) (Table 51), and the South basin abundances were significantly higher than the North basin (p value < 0.01) (Selenga > South basin > Maloe More > North basin).

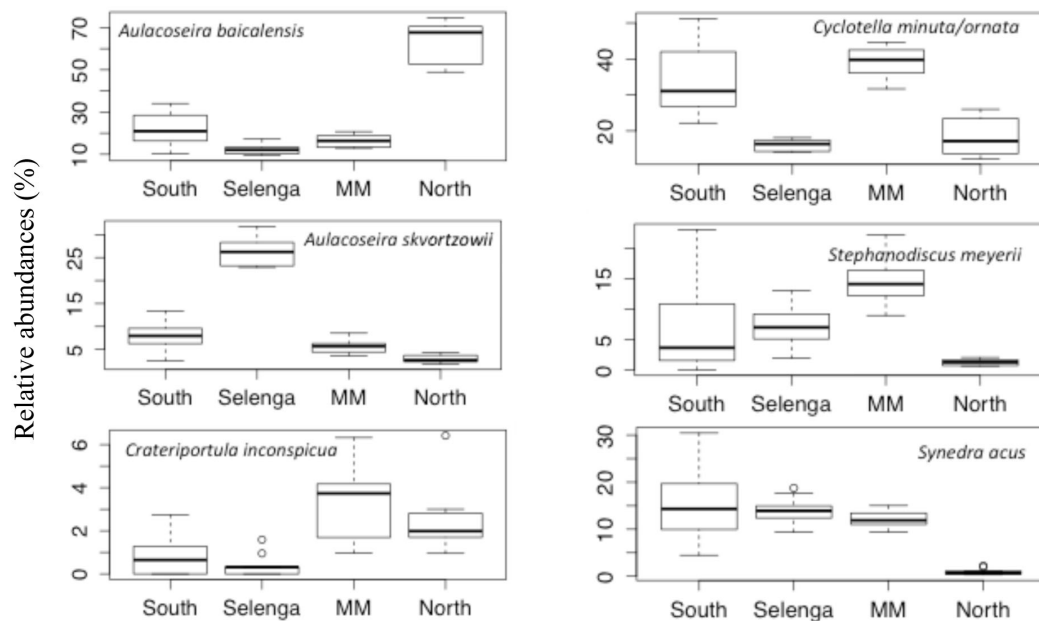


Figure 122: Main diatom species abundances in the surface sediments over the last 20 years in the South, Selenga, Maloe More and North basin sites.

Mean *Stephanodiscus meyerii* abundances are lowest at the North basin sites (1.2 %) (Maloe More > Selenga > South basin > North basin), and the Maloe More abundances are significantly higher than the rest of the sites (p values < 0.01 - 0.01) (Table 51). Mean abundances of *Crateriportula inconspicua* are the lowest at the Selenga (mean = 0.4 %), and the South basin abundances are significantly lower than the North basin (p value < 0.01) (Maloe More > North basin > South basin > Selenga).

Table 51: P-values from ANOVA to test if there is a significant difference in diatom species abundances between regions (South basin, Selenga Shallows, Maloe More (MM) and North basin).

	P- values					
	<i>Synedra acus</i>	<i>S. meyerii</i>	<i>C. inconspicua</i>	<i>C. minuta/ornata</i>	<i>A. baicalensis</i>	<i>A. skvortzowii</i>
Selenga - South	0.898	0.984	0.706	< 0.001	0.002	< 0.001
MM - South	0.439	0.001	< 0.001	0.227	0.146	0.145
North - South	< 0.001	0.061	0.005	< 0.001	< 0.001	< 0.001
MM - Selenga	0.876	0.016	< 0.001	0.000	0.662	< 0.001
North - Selenga	< 0.001	0.075	0.002	0.921	< 0.001	< 0.001
North - MM	< 0.001	< 0.001	0.406	< 0.001	< 0.001	0.127

7.2.4 Temporal trends over the last 200 years

South basin (BAIK13-1C)

Zonation was carried out on the pigment concentration data using CONISS and b-stick analyses in R (see Chapter Two for methods). A significant zone boundary falls at 4.5 cm (110 yrs) (Figure 133), and this is the only significant zone over the last 200 years. The pigment record from BAIK13-1C largely consists of pheo-*a* pigments (pheophorbide-*a*, pheophytin-*a* and pyropheophytin-*a*), which range in concentrations between 21.34 – 472.02 nmol g⁻¹ OC. Chlorophyll-*a* concentrations range between 0.84 – 10.48 nmol g⁻¹ OC. The chlorophyll-*a*:pheo-*a* pigment ratio values are low (0.003 – 0.088), with a peak at 5.1 cm (0.125 nmol g⁻¹ OC). Chlorophyll-*b* concentrations increase from 3.33 to 90.07 nmol g⁻¹ OC in the upper 2 cm, between 2.3 cm and 1.1 cm. The carotenoids present in low concentrations (< 10 nmol g⁻¹ OC) are alloxanthin, diatoxanthin, lutein and canthaxanthin. The Diatoxanthin/canthaxanthin ratio declines from 2.90 – 3.66 at 3.9 cm. Alloxanthin:chl-*a* ratio values peak at 5.5 cm, 4.5 cm and 0.7 cm, with the highest values in the surface sediment. Chl-*b*:Chl-*a* ratio similarly peaks in the upper 1 cm, from 0.57 to 2.14. TOC percentages range between 2.18 % and 3.71 %, with an increasing trend towards the surface and TOC/N ratios range between 9.96 and 11.42. δ¹³C values increase from -29.15 ‰ to -27.31 ‰ towards the surface.

South basin (BAIK13-4F)

There is only one significant zone boundary in the pigment over the last 200 years, which lies at 7.7 cm (120 yrs) (*Figure 134*). Total pheo-*a* pigments show an increasing trend, ranging between 28.71 and 535.93 nmol g⁻¹ OC, similar to the chlorophyll-*a* concentrations, which range between 0.504 and 11.51 nmol g⁻¹ OC. The chlorophyll-*a*:pheo-*a* pigment ratio values vary down-core, with peaks at 0 - 4.1 cm and 8.7 - 10.3 cm. Chlorophyll-*b* concentrations increase to values of 6.57 - 9.28 nmol g⁻¹ OC within the top 6 cm. The carotenoids present in low concentrations (< 10 nmol g⁻¹ OC) are alloxanthin, lutein and canthaxanthin. Alloxanthin:chl-*a* is low throughout, with a peak at 9 - 8 cm and 0.8 - 0.3 cm. Chl-*b*:chl-*a* ratio values vary down-core, with generally higher ratio values in the top 5 cm. TOC varies between 0.71 % and 3.07 %, and TOC/N ratios range between 9.46 to 14.45. δ¹³C values increase from -28.45 ‰ to -22.87 ‰ at 4.6 cm. Surface sediment diatom assemblages show abundance changes, within the dominant diatom species; *Aulacoseira baicalensis*, *Cyclotella minuta/ornata* and *Synedra acus var. radians*, with an increasing trend in *Synedra acus var. radians* abundance from 6.95 to 30.44 %. Diatom concentrations range between 85.1 to 147.1 (10⁴ valves/g dry wt).

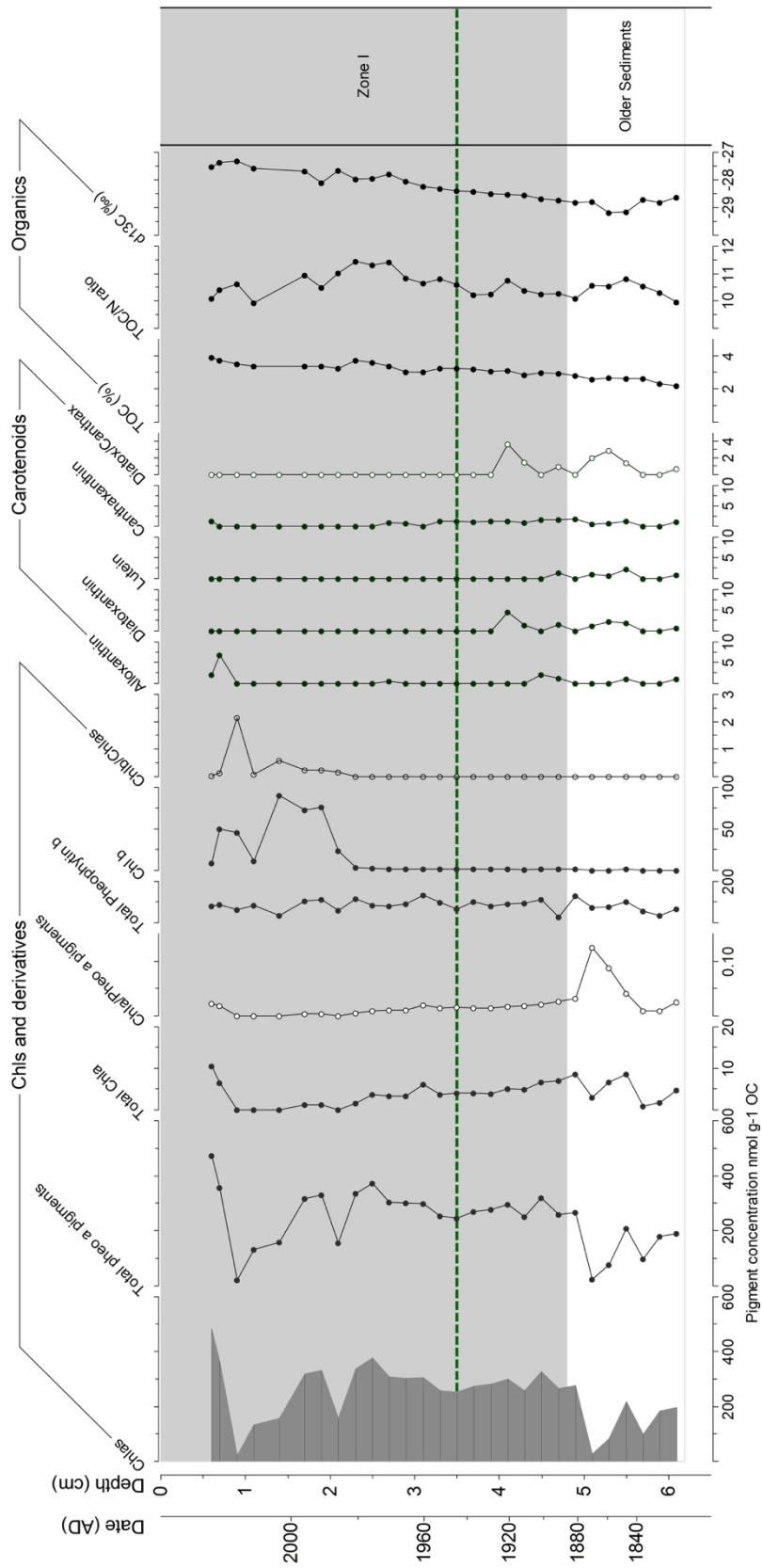


Figure 123: BAIK13-1C in the South basin. Chl-a and derivatives, carotenoids and organics (only major algal pigments) are shown. Dashed green line indicates onset of human influence in the Baikal region (Brunello et al. 2004). Grey shading represents recent sediments (Zone 1).

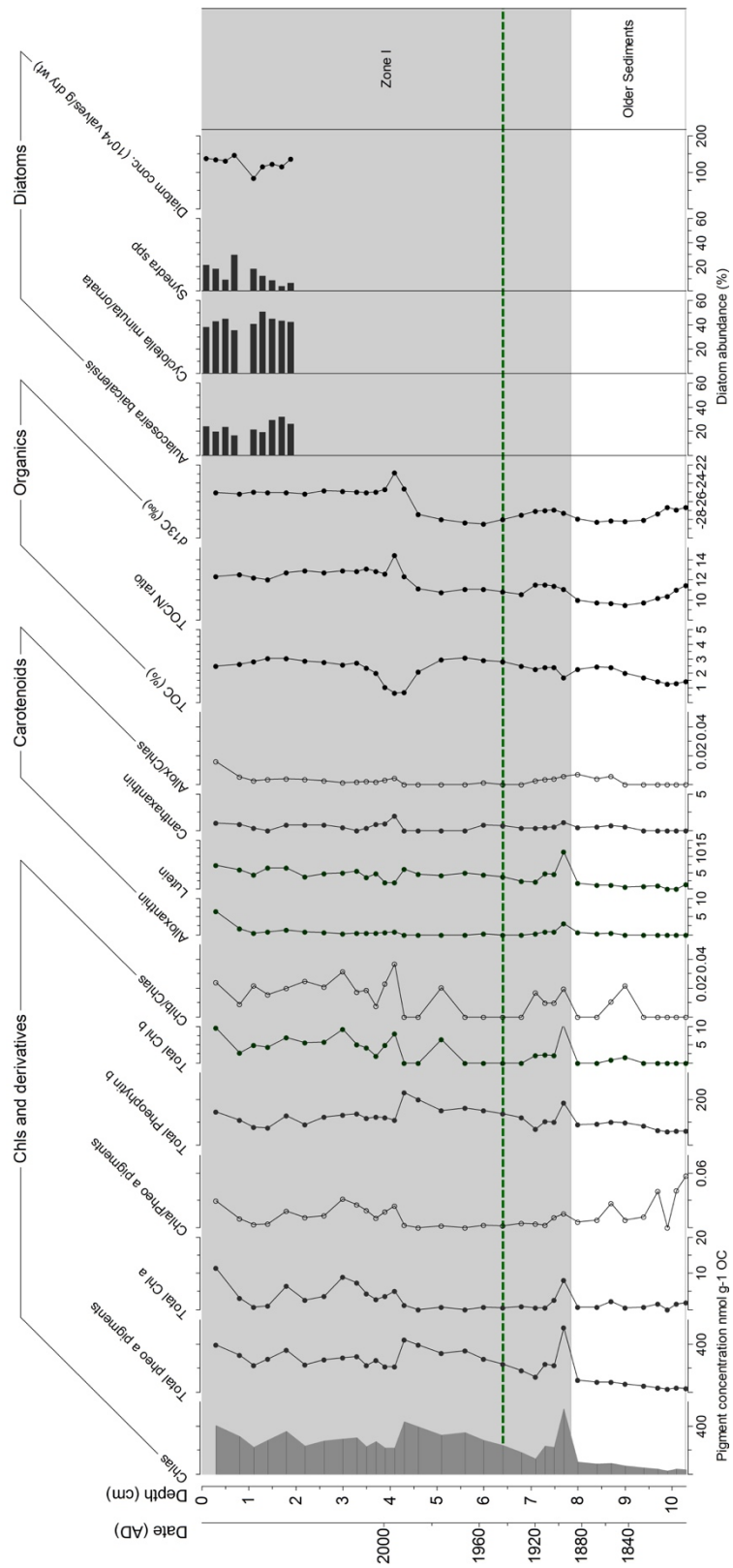


Figure 124: BAIK13-4F in the South basin. Chl-a and derivatives, carotenoids, organics and diatoms (only major algal pigments and diatom species) are shown. Dashed green line indicates onset of human influence in the Baikal region (Brunello et al. 2004). Grey shading represents recent sediments (Zone 1).

South basin (BAIK13-7A) (*likely pigment degradation profile)

A significant zone boundary in the pigment data falls at 3.3 cm (110 yrs) (*Figure 135*), and no other significant zone are observed over the last 200 years. Total pheo-*a* pigments increase to concentrations of 53.68 – 235.8 nmol g OC⁻¹ from 4.96 – 15.23 nmol g⁻¹ OC, between 3.3 and 3.5 cm. Similarly, chlorophyll-*a* concentrations increase to concentrations of 1.81 – 11.5 nmol g⁻¹ OC between 2.7 – 2.2 cm. The chlorophyll-*a*:pheo-*a* pigment ratio values increases alongside the total pheo-*a* pigments and chlorophyll-*a* concentrations. Chlorophyll-*b* is detected within the upper 2 cm of the core, with concentrations of 1.81 and 2.43 nmol g⁻¹ OC at 1.4 and 0.6 cm respectively. The main carotenoid detected in Baik13-7A is canthaxanthin, which increases to concentrations of 1.23 – 2.23 nmol g⁻¹ OC from 2.2 – 1.8 cm. TOC percentages increase from 4.3 % to 1.4 % and TOC/N ratios decrease from values of 12.05 to 1.4. $\delta^{13}\text{C}$ values range between -25.16 ‰ to -27.89 ‰, with more positive values down-core. Surface sediment diatom assemblages show a slight increase in *Synedra acus* var. *radians* from abundances of 13.3 % to 17.6 %, and *Aulacoseria baicalensis* decrease in abundance from 40.6 % to 25.4 – 34.1 %. *Cyclotella minuta/ornata* diatom species range between 38.6% and 24.7%. Diatom concentrations show a decreasing trend from 540.8 to 148.9 – 352.9 (10⁴ valves/g dry wt). DDI values range between 0.6 to 0.2, showing a decreasing trend.

Selenga Delta (BAIK13-10A)

There are two significant zone boundaries within the pigment data over the last 200 years, with the first zone boundary falling at 7.6 cm (50 yrs) (*Figure 136*), and the second zone boundary at 11.2 cm (140 yrs). Total pheo-*a* pigments increase in concentrations from 179.7 – 263.7 nmol g⁻¹ OC between 11.2 – 8.7 cm, to concentrations of 809.3 – 778.9 nmol g⁻¹ OC in the upper 7 cm. Chlorophyll-*a* concentrations range between 13.6 – 38.0 nmol g⁻¹ OC, with no clear pattern. The chlorophyll-*a*:pheo-*a* pigment ratio values show a slight decreasing trend from 0.16 to 0.02 between 11.2 – 0.3 cm. Chlorophyll-*b* concentrations range between 1.05 and 11.67 nmol g⁻¹ OC, with no clear pattern. The carotenoids which are detected are alloxanthin, diatoxanthin, lutein, zeaxanthin and canthaxanthin. Alloxanthin concentrations increase from 4.35 to 12.0 nmol g⁻¹ OC, with higher concentrations in zone 1. Diatoxanthin concentrations decrease from c. 18 to 1.2 nmol g OC⁻¹ and lutein, zeaxanthin and canthaxanthin concentrations range between (c. 3 – 25 nmol g⁻¹ OC, c. 6 – 16 nmol g⁻¹ OC, and c. 2 – 9 nmol g⁻¹ OC respectively). Diatoxanthin:canthaxanthin ratios decreases at c. 6 cm from c. 4 to c. 0.2. UV absorbing compound is detected within these sediments, and the UV index reaches values of > 15 at c. 9 cm and in the surface sediments.

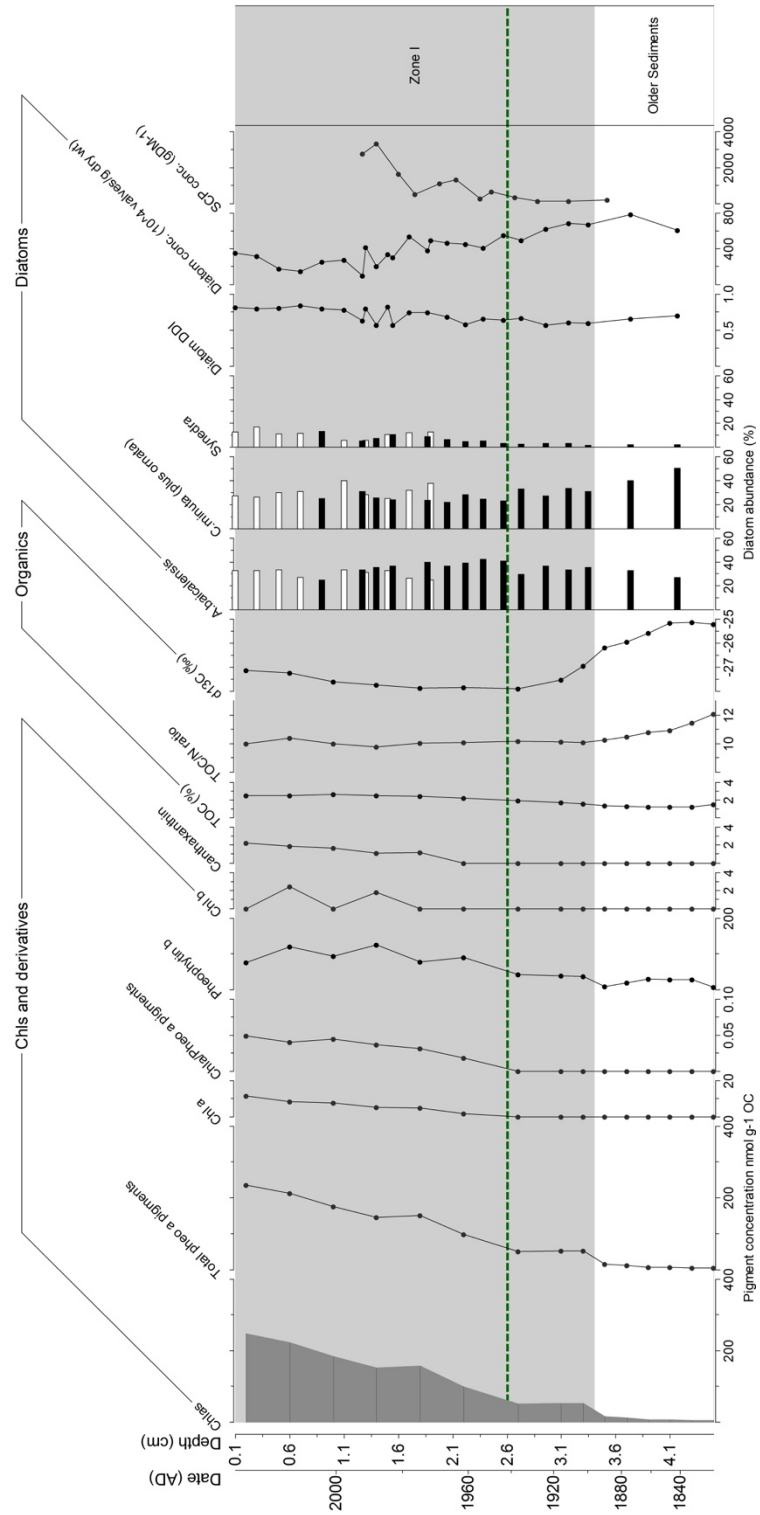


Figure 125: BAIK13-7A in the South basin. Chl-a and derivatives, carotenoids, organics, diatoms (only major algal pigments and diatom species) and Spheroidal Carbonaceous Particles (SCP) are shown. SCP data from Prof. N. Rose. Diatom counts made by author are shown as white bars, and those made by Prof Anson Mackay are shown as black bars (as published in Mackay et al. 1998). Dashed green line indicates onset of human influence in the Baikal region (Brunello et al. 2004). Grey shading represents recent sediments (Zone I).

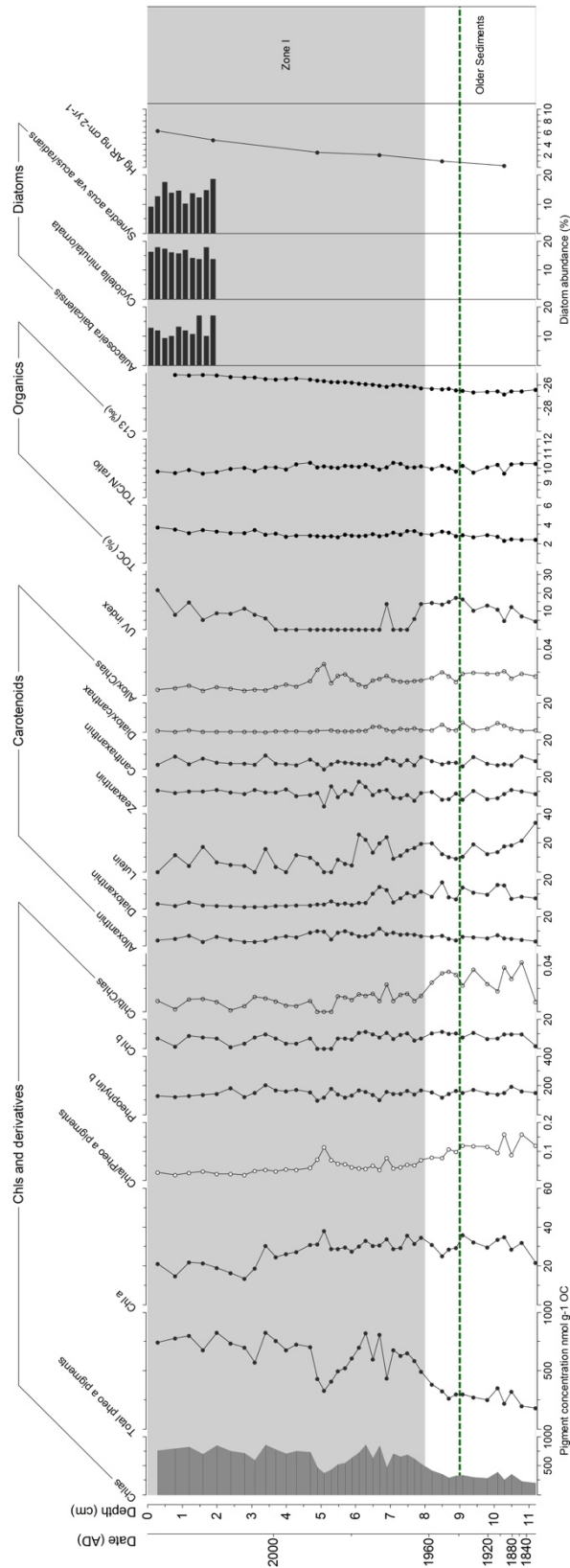


Figure 126: BAIK13-10A by the Selenga Delta. Chl-a and derivatives, carotenoids, organics, diatoms (only major algal pigments and diatom species) and mercury (Hg) Accumulation Rate (AR) are shown. Dashed green line indicates onset of human influence in the Baikal region (Brunello et al. 2004). Grey shading represents recent sediments (Zone 1).

$\delta^{13}\text{C}$ values range between -26 ‰ to -25.1 ‰, showing an increasing trend towards the surface sediments. TOC is consistent between 2 – 3 % and TOC/N values range between 9.6 to 10.3.

Selenga Delta (BAIK13-11C)

The only significant zone boundary in the pigment data over the last 200 years falls at 5.8 cm (90 yrs) (*Figure 137*). Pheo-*a* pigments rise from c. 26 to > 300 nmol g⁻¹ OC and show an increasing trend towards the surface sediments. Chlorophyll-*a* concentrations show a similar pattern, and increase from c. 3 nmol g⁻¹ OC at c. 6 cm to c. 10 nmol g⁻¹ OC in the upper 4 cm. The main carotenoids detected are alloxanthin, lutein and canthaxanthin (concentrations < 0.5 nmol g⁻¹ OC). UV absorbing compound is also detected within these sediments, and the UV index shows peaks (c. 30 – 40) between 5 – 9 cm in the sediment core. Diatom assemblages within the upper 2 cm show a slight decreasing trend in *Aulacoseira baicalensis* to abundances of c. 14 % and *Cyclotella minuta/ornata* to abundances of c. 20 %, and increasing abundances of *Synedra acus* var. *radians* to abundances of > 20 %. Diatom concentrations show a decreasing trend towards the surface sediments, from concentrations of c. > 700 (10⁴ valves/g dry wt) to < 300 (10⁴ valves/g dry wt). DDI values fluctuate between 0.4 to 0.7. $\delta^{13}\text{C}$ values range between -26.9 ‰ to -25.7 ‰, with more positive values within the upper sediments. TOC shows a subtle increasing trend from 1.8 to 3 % towards the top of the core, and TOC/N values fluctuate between 8 – 9.

Maloe More (BAIK13-14C)

One significant zone boundary is observed within the pigment data covering the last 200 years, which lies at c. 4 cm (60 yrs) (*Figure 138*). Pheo-*a* pigments increase from 100 nmol g⁻¹ OC to concentrations > 600 nmol g⁻¹ OC towards the top of the core. Chlorophyll-*a* concentrations also show this trend, which increase from c. 12 to 50 nmol g⁻¹ OC. The chlorophyll degradation ratio fluctuates, with higher values at c. 3 cm. Chlorophyll-*b* rises in concentrations from c. 1.4 to 15 nmol g⁻¹ OC in the upper 4 cm. The main carotenoids detected are alloxanthin, diatoxanthin, lutein and canthaxanthin. The diatoxanthin/canthaxanthin ratio decreases at c. 3 cm from c. 4 to 1. Diatom assemblages show decreasing abundances of *Stephanodiscus meyerii* (from c. 20 % to c. 13 %) and *Synedra acus* var. *radians* (from c. 15 % to 10%) within the upper 2 cm and a general increasing trend in *Aulacoseira baicalensis* (from c. 15 % to 20 %) and *Cyclotella minuta/ornata* (from c. 25 % to c. 30 %).

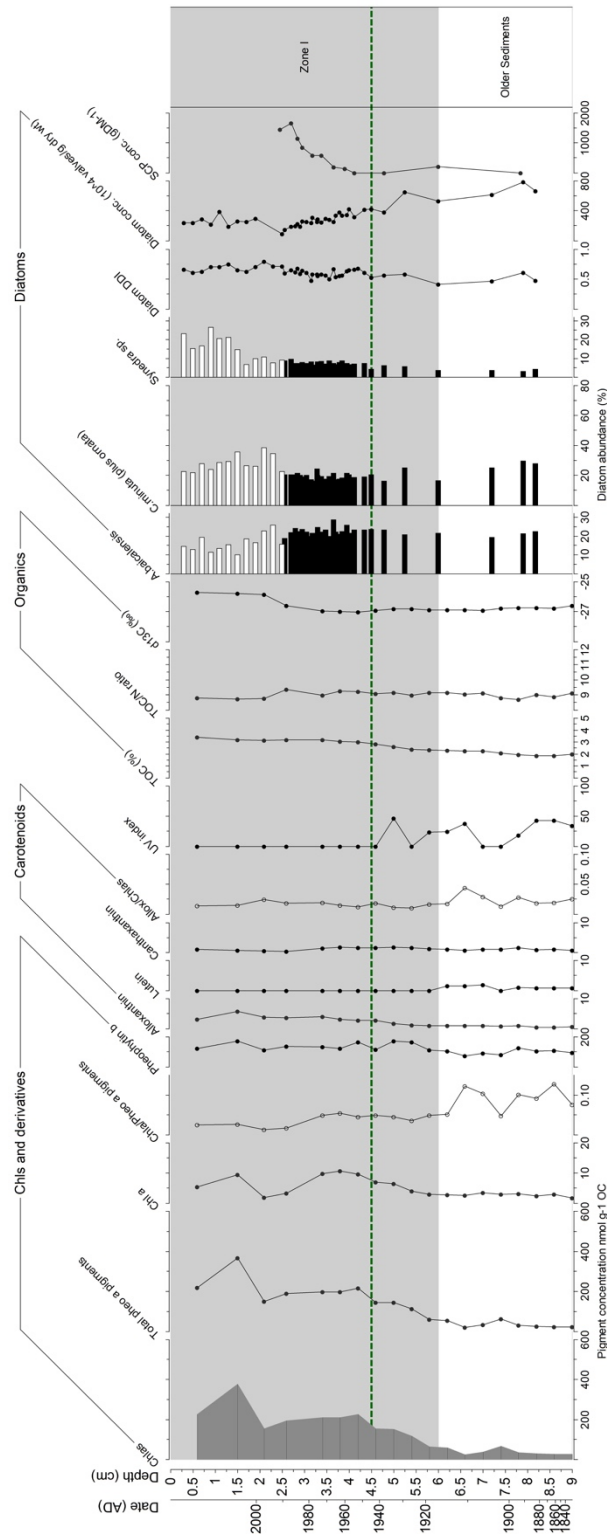


Figure 127: BAIK13-11C in the South basin, opposite the Selenga Delta. Chl-a and derivatives, carotenoids, organics, diatoms (only major algal pigments and diatom species) and Spheroidal Carbonaceous Particles (SCP) are shown. SCP data from Prof. N. Rose. Diatom counts made by author are shown as white bars, and those made by Prof Anson Mackay are shown as black bars (as published in Mackay et al. 1998). Dashed green line indicates onset of human influence in the Baikal region (Brunello et al. 2004). Grey shading represents recent sediments (Zone 1).

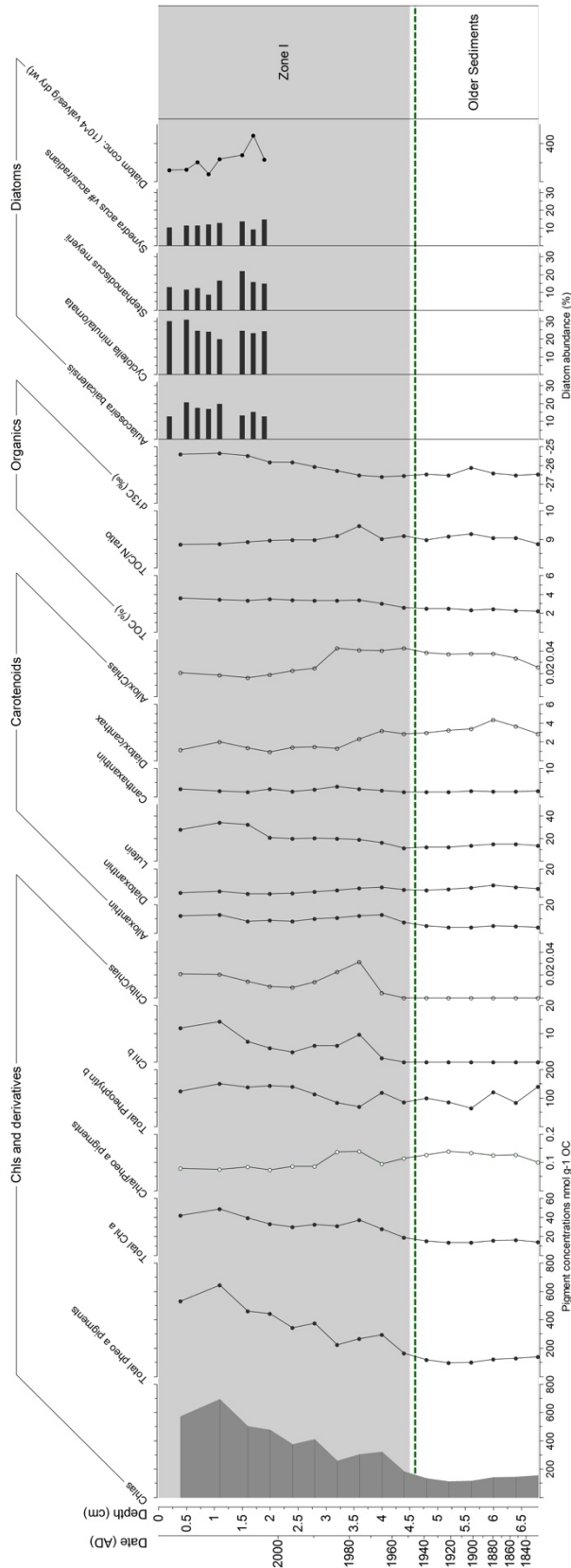


Figure 128: BAIK13-14C in Maloe More Bay. Chl-a and derivatives, carotenoids, organics, diatoms (only major algal pigments and diatom species) are shown. Dashed green line indicates onset of human influence in the Baikal region (Brunello et al. 2004). Grey shading represents recent sediments (Zone I).

Diatom concentrations also show a decreasing trend from c. 500 to c. 130 (10^4 valves/g dry wt). TOC values show a slight increasing trend from 2 to 3 %, and $\delta^{13}\text{C}$ values range between -26.4 ‰ to -25.3 ‰ with higher values towards the surface sediments. TOC/N ratio values range between 8 to 9.4.

North basin (BAIK13-18A) (*likely pigment degradation profile)

Over the last 200 years, the only significant zone boundary in the pigment data falls at 1.5 cm (50 yrs) (*Figure 139*). Pheo-*a* pigments increase at 1.7 cm from c. 20 nmol g OC⁻¹ to c. 200 nmol g⁻¹ OC. No chlorophyll-*a*, chlorophyll-*b* or are carotenoids detected within this core. Diatom assemblages within the upper 2 cm show a decreasing trend in *Aulacoseira baicalensis* (from c. 60 % to c. 50 %), *Synedra acus* var. *radians* (from c. 6 % to 1 %). *Cyclotella minuta/ornata* diatom species range in abundance between c. 20 to 30 %. TOC values are consistently at c. 2 %, and TOC/N ratios range between 9 to 10. $\delta^{13}\text{C}$ values remain relatively constant, ranging between -29.5 ‰ and -28 ‰.

North basin (BAIK13-19B)

Only one significant zone boundary in the pigment data was observed in the pigment data, which falls at 7.8 cm (230 yrs) (*Figure 140*). Pheo-*a* pigments and chlorophyll-*a* increase from 60 nmol g⁻¹ OC to 350 nmol g⁻¹ OC, and c. 3 nmol g⁻¹ OC to c. 20 nmol g⁻¹ OC respectively. The chlorophyll degradation ratio mirrors this. The main carotenoids detected are diatoxanthin, lutein and canthaxanthin, which all increase between 2 – 3 cm. Diatoxanthin/canthaxanthin ratio shows variation, with several peaks downcore. Diatom assemblages show decreasing abundances of *Aulacoseria baicalensis* (from c. 70 to 60 %), slight increases in the abundance of *Cyclotella minuta/ornata* (from c. 12 % to 20 %), and low abundances of *Synedra acus* var. *radians* between 0.3 and 1 %. Diatom concentrations range between 150 and 500 (10^4 valves/g dry wt). Mercury accumulation rates are relatively constant and are < 1 ng cm⁻² yr⁻¹. TOC remains similar at c. 2 % throughout, and TOC/N ratios range between 10.9 and 11.2. $\delta^{13}\text{C}$ values also remain similar, between - 27 ‰ and -26.8 ‰.

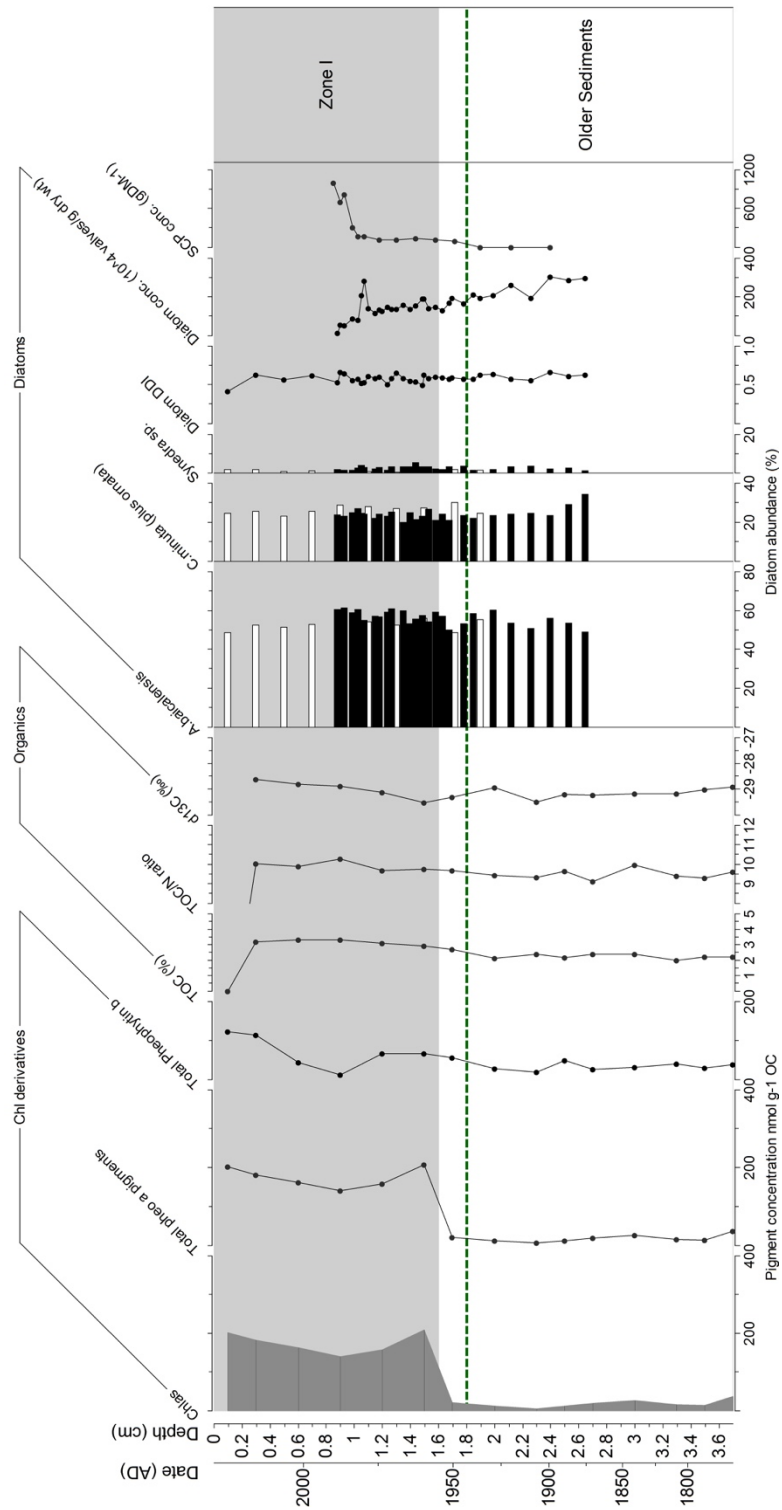


Figure 129: BAIK13-18A in the North basin. Chl-a and derivatives, carotenoids, organics, diatoms (only major algal pigments and diatom species) and Spheroidal Carbonaceous Particles (SCP) are shown. SCP data from Prof. N. Rose. Diatom counts made by author are shown as white bars, and those made by Prof Anson Mackay are shown as black bars (as published in Mackay et al. 1998). Dashed green line indicates onset of human influence in the Baikal region (Brunello et al. 2004). Grey shading represents recent sediments (Zone 1).

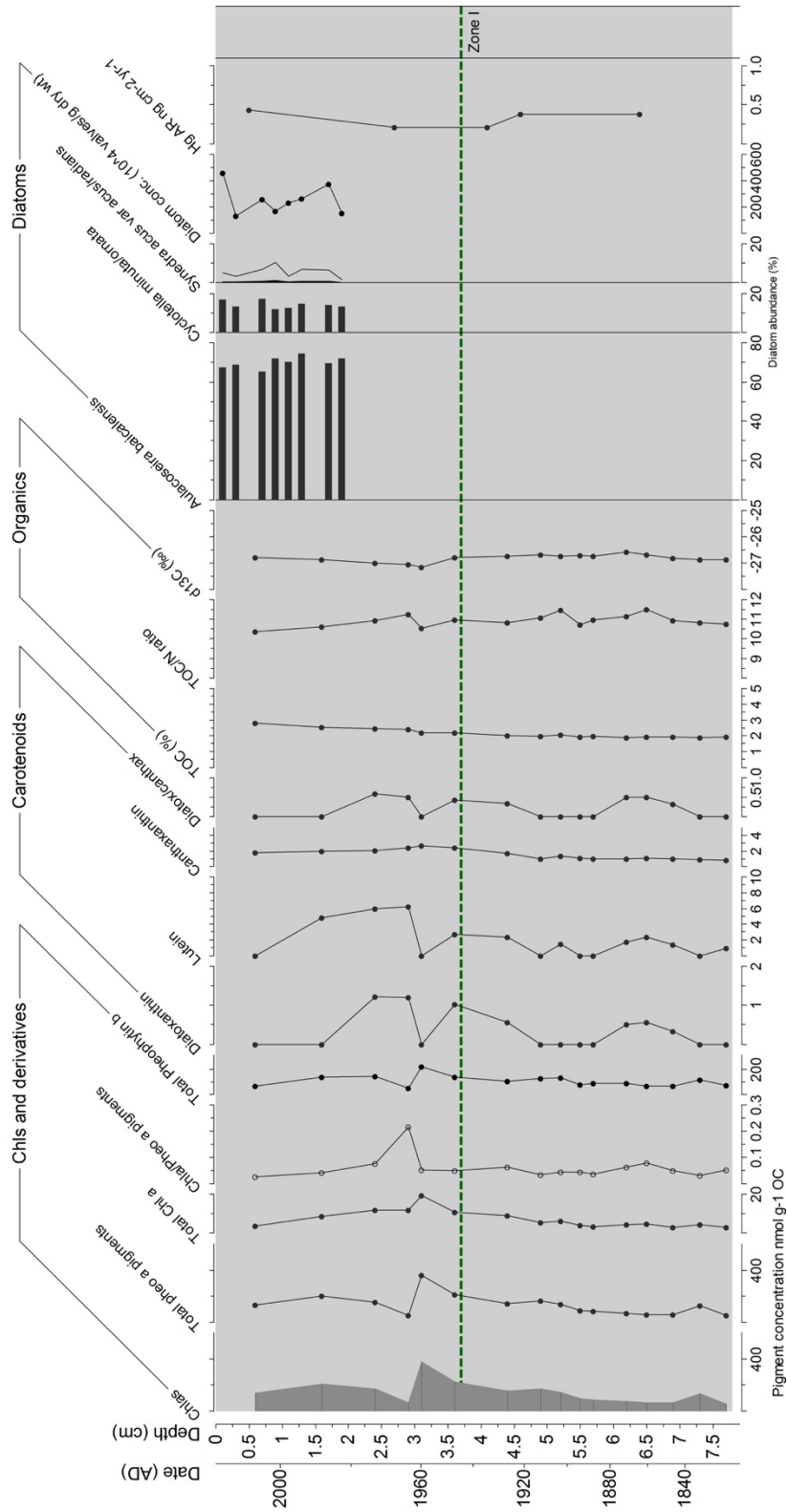


Figure 130: BAIK13-19B in the North basin. Chl-a and derivatives, carotenoids, organics, diatoms (only major algal pigments and diatom species) and mercury (Hg) Accumulation Rate (AR) are shown. Dashed green line indicates onset of human influence in the Baikal region (Brunello et al., 2004). Exaggeration factor (x10) applied to *Synedra* abundances. Grey shading represents recent sediments (Zone I).

7.2.5 Carbon accumulation over the last two centuries

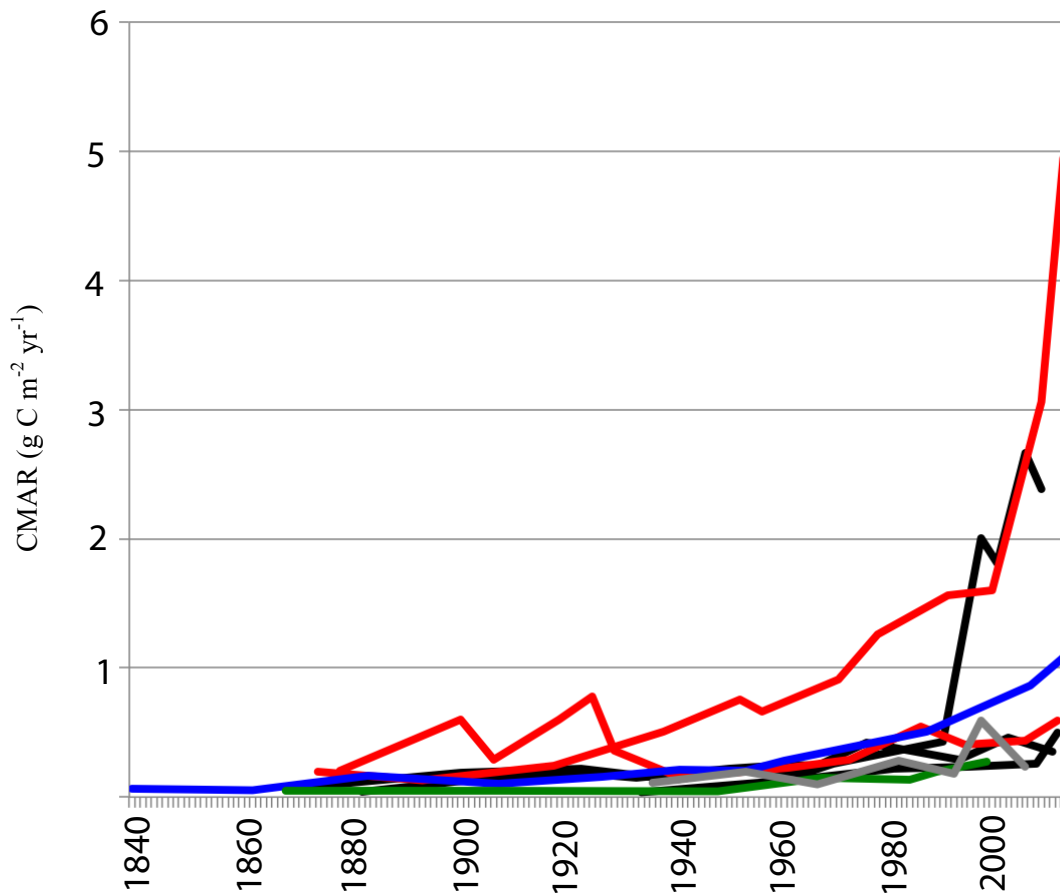


Figure 131: CMARs between 1840 – 2013 in the Selenga (red line), South basin (black line), Maloe More (blue line) and North basin (green and grey line).

Carbon mass accumulation rates (CMAR) were calculated for each of the sites, and average CMAR rates over the last 200 years are highest at the Selenga (BAIK13-10A and BAIK13-11C) ($13.20 \text{ g C m}^{-2} \text{ yr}^{-1}$ and $4.21 \text{ g C m}^{-2} \text{ yr}^{-1}$) and in the South basin ($2.31 - 8.79 \text{ g C m}^{-2} \text{ yr}^{-1}$) and Maloe More Bay ($3.64 \text{ g C m}^{-2} \text{ yr}^{-1}$) (Figure 141). The lowest average CMARs were found in the North basin, with $2.43 \text{ g C m}^{-2} \text{ yr}^{-1}$ and $1.28 \text{ g C m}^{-2} \text{ yr}^{-1}$ in the pelagic deep-water basin (Figure 141). All records show a recent increase in carbon sequestration. However, the magnitude of this increase varies spatially across the lake, with CMARs at the Selenga Delta site increasing 50-fold over the last 200 years, 30-fold in the South basin and 15-fold in Maloe More. In contrast the CMAR at the North basin sites have increased by 2 to 6-fold over the last 200 years. An exception to this is the site opposite the Selenga delta (BAIK13-11C), which has higher CMARs in the late 1800s, which may be due to the earthquake reported in 1862 (Vologina et al. 2010). This earthquake occurred in Proval Bay by the Selenga Delta region

and it is possible that the impact of this earthquake would have led to greater sediment deposition within the Selenga region and result in peaks within CMAR (Vologina et al. 2010).

7.2.6 Carbon isotopic data over the last 200 years

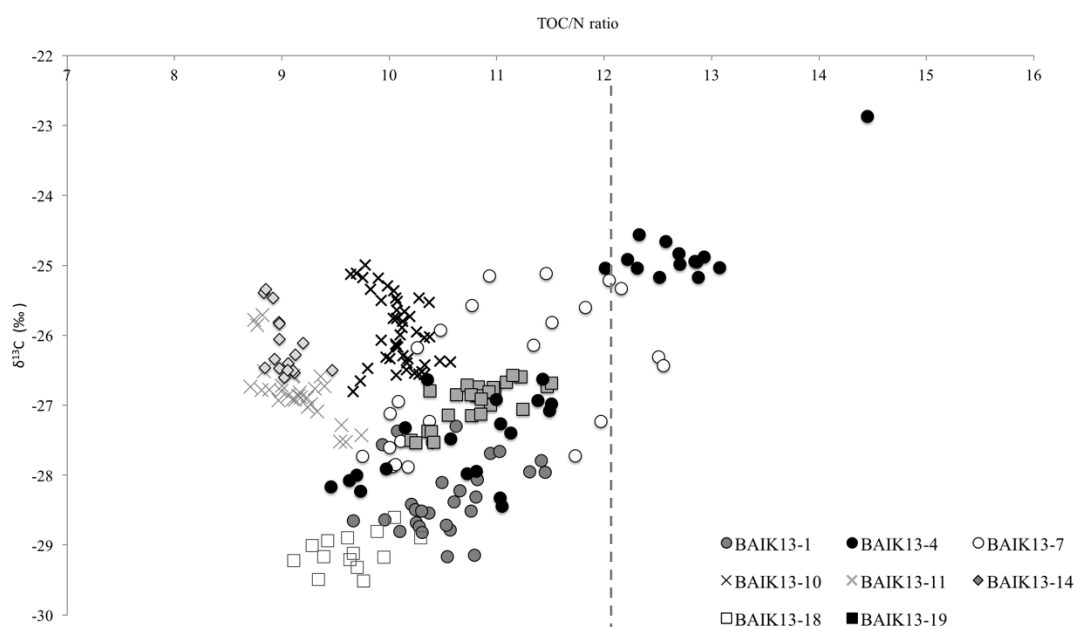


Figure 132: $\delta^{13}\text{C}$ and TOC/N values over the last 200 years from sediment cores taken in the South basin (BAIK13-1C, BAIK13-4F, BAIK13-7A), North basin (BAIK13-18A, BAIK13-19B), Maloe More (BAIK13-14C) and Selenga (BAIK13-10A, BAIK13-11C). TOC/N ratio values < 12 indicates predominately algal sources (Prokopenko et al. 1993).

Spatial trends in $\delta^{13}\text{C}$ and TOC/N values over the last 200 years (Figure 142) were similar to those displayed in the surface sediments over the last 20 years (Figure 130). The carbon isotope values ranged between -22.9‰ to -29.5‰ across the lake within sediments covering the last 200 years (Figure 142). The highest carbon isotope values were within the sediments from the South basin (BAIK13-4F; BAIK13-7A), the Selenga (BAIK13-10A; BAIK13-11C) and Maloe More (BAIK13-14C). The largest range in carbon isotope values was within Baik13-4 in the South basin (-22.9‰ to -28.4‰). The lowest carbon isotope values were from sediments in the pelagic North basin site (BAIK13-18A). The largest shifts ($> 1\text{‰}$) in $\delta^{13}\text{C}$ values, towards more positive values, over the last 200 years were seen in the South basin (at BAIK13-4F) (5.5‰ shift), at Maloe More (BAIK13-14C) (1.3‰) and at the Selenga (BAIK13-11C) (1.2‰ shift). The TOC/N ratios can be used to further pinpoint the organic carbon sources and these ranged between 8.7 to 14.4, and largely fell within the aquatic source

range (< 12) (Prokopenko et al. 1993). The highest TOC/N values were in the South basin (BAIK13-4F), and this sediment core had the largest range over the last 200 years (9.5 to 14.5). The lowest TOC/N values were in the Selenga and Maloe More sediments, which ranged between 8.8 to 9.5 and 8.7 to 10.6 respectively. North basin TOC/N values ranged between 9.1 to 11.5.

7.2.7 Rock Eval data

To further interpret the carbon source and extent of degradation, Rock Eval analyses has been carried. The highest hydrogen index (HI) (degree of algal material) and oxygen index (OI) (degree of degradation) values were in the South basin sediments, ranging between 98 - 306, and 158 - 356 respectively (Figure 143, Figure 144). North basin sediment samples had the lowest OI values, ranging between 194 - 262 and HI values ranging between 165 - 297. The smallest range in HI values was within the Selenga sediment core, between 143 - 197 and the smallest range in OI values, between 194 - 262. The HI and OI values of the sediment samples suggest both Type II (algal) and Type III (woody plant) organic matter. The variations in the OI values suggested differential amounts of oxidation, either from carbon source changes or degradation.

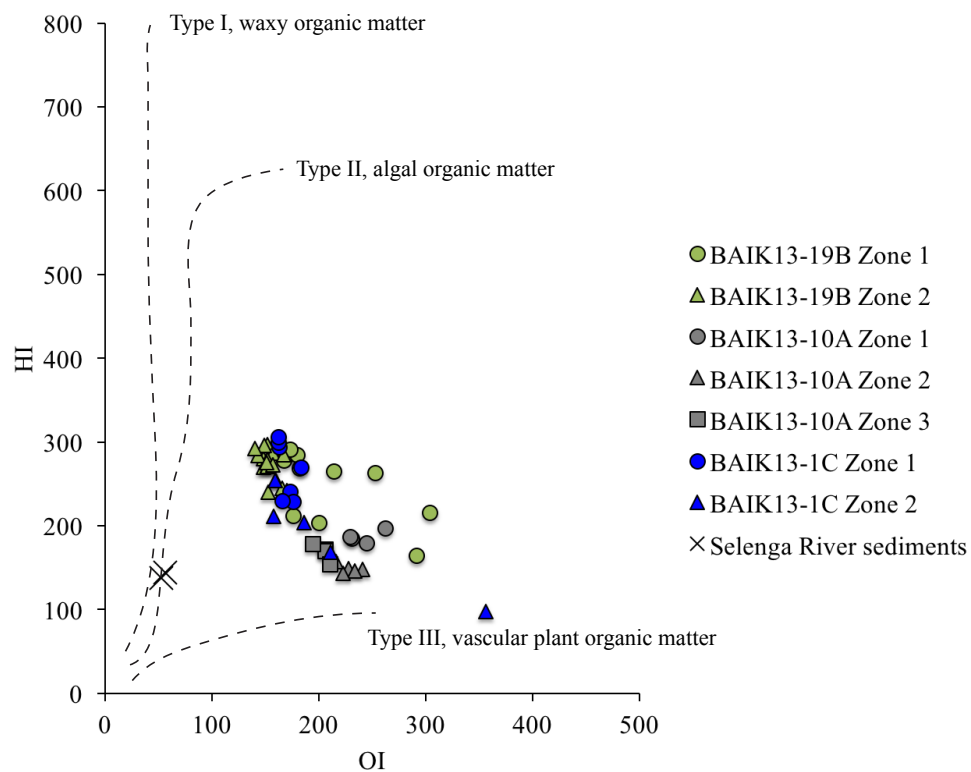


Figure 133: HI and OI data grouped into significant zones down-core. Data is presented for sediment cores in the South basin (Baik13-1C), North basin (Baik13-19B) and Selenga (Baik13-10A). Note that the low resolution for this analysis is due to this being a pilot study.

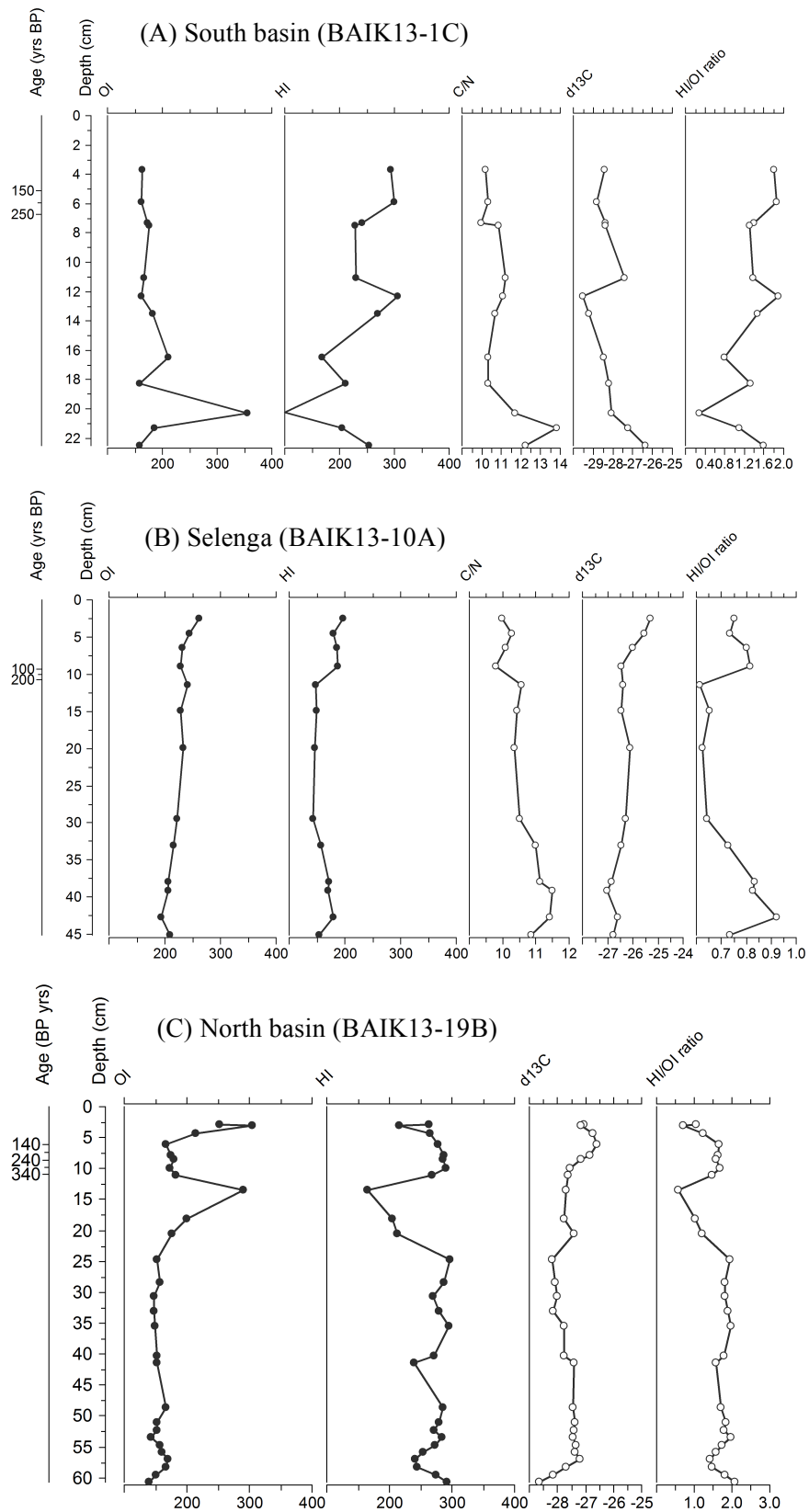


Figure 134: Down-core HI, OI, HI/OI ratio values, $\delta^{13}C$ and TOC/N values for sediment cores taken in the (A) Selenga (BAIK13-10A), (B) South basin (BAIK13-1C) and (C) North basin (BAIK13-19B).

7.2.8 Trends in algal production and climate

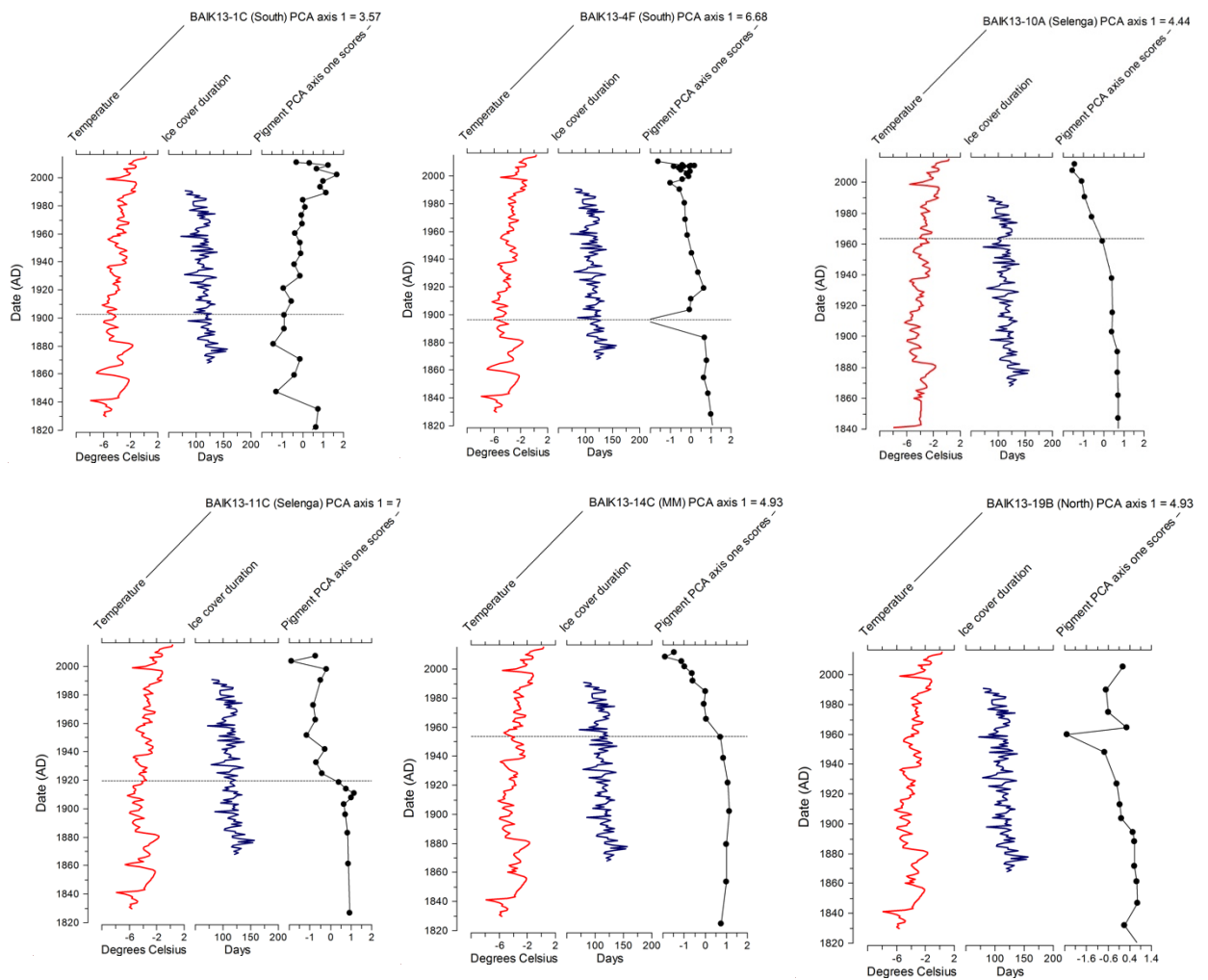


Figure 135: Average annual temperature at Irkutsk, ice cover duration at Lystvyanka station in the South basin and PCA axis one scores on pigment datasets from sediment cores in the South, North, Maloe More (MM) and Selenga sites. Dashed line represents a significant zone within the pigment data.

PCA axis one scores provide a summary of compositional changes within the pigment data. The PCA axis one scores showed the main pigment compositional changes occurred over the past c. 30 years in the South basin (BAIK13-1C and BAIK13-4F) (Figure 145). At the Selenga sites, PCA axis one scores suggested a gradual increasing trend in compositional change at BAIK13-10A over the last century, and the main compositional changes in the early 20th century at BAIK13-11C (Figure 145). At Maloe More (BAIK13-14C) and the North basin (BAIK13-19B), PCA axis one scores showed a decreasing trend over the last c. 60 years (Figure 145). Floristic change with increasing regional temperatures and decreasing ice cover

duration over the past 200 years was therefore seen only at the South, and not in all the Selenga, Maloe More and North basin sites.

Mann-Kendall coefficients on the Chlas concentrations showed a significant increasing trend in the South basin, Selenga, Maloe More and North basin sites. Break-point analyses showed that a significant increase in Chlas concentrations occurred earlier at the Selenga Delta sites (break point at 1935 AD; p value = 0.01), and over the last 60 years in the South basin sites (break point at 1946 AD; p value = < 0.01) (*Table 52*). There was also a significant increase in Chlas in the North basin, and most recently at Maloe More (break point at 1984 AD; p value = < 0.01). Chlorophyll-*b* concentrations showed an increasing trend over the last 200 years in the South basin (break point at 1965 AD; p value = 0.02), and a more recent increase at Maloe More (break point at 2002 AD; p value = 0.02) (*Table 52*). Mann-Kendall coefficients for alloxanthin suggested a significant increasing trend at the Selenga sites (break point at 1912 AD; p value = 0.02) and Maloe More. M-K coefficients for diatoxanthin suggested a significant decreasing trend in the South basin and Selenga Delta (break point at 1940 AD; p value = < 0.01) (*Table 52*). Lutein concentrations were significantly decreasing in the South basin, and Selenga Delta, and significantly increasing at Maloe More (break point at 1958 AD; p value = 0.00). Canthaxanthin showed a significant increasing trend in the South basin (break point at 1957 AD; p value = < 0.01), and a decreasing trend in the North basin. Mann-Kendall coefficient trends on the carbon isotope data suggested a significant increasing trend in the South basin (break point at 1975 AD; p value = < 0.01), Selenga Delta (break point at 1952 AD; p value = < 0.01), Maloe More (break point at 1980 AD; p value = < 0.01). In contrast, in the North basin there was no significant trend in $\delta^{13}\text{C}$ values.

Table 52: MK trend test coefficients and p-values, and timing of break-point with p-value. BAIK13-4F is removed due to turbidite layer (* likely pigment degradation profiles).

	M-K coefficient values	P-value	Trend	Break point	P-value
South Basin (BAIK13-1)					
Alloxanthin	-0.024	0.896	NONE	2007	< 0.001
Diatoxanthin	-0.421	0.006	DECREASING	1858	0.15
Lutein	-0.437	0.005	DECREASING	1847	0.39
Chlas	0.307	0.020	NONE	2009	0.09
Chlb	0.681	< 0.001	INCREASING	1965	0.02
$\delta^{13}\text{C}$	0.373	0.006	INCREASING	1975	< 0.001
South Basin (BAIK13-4)					
Alloxanthin	0.437	< 0.001	INCREASING	2008	< 0.001
Lutein	0.559	< 0.001	INCREASING	1900	0.19
Canthaxanthin	0.254	0.040	NONE	1854	0.27
Chlas	0.542	< 0.001	INCREASING	1990	0.18
Chlb	0.468	< 0.001	INCREASING	1993	0.08
$\delta^{13}\text{C}$	0.110	0.377	NONE	1969	< 0.001
South Basin (BAIK13-7) *					
Canthaxanthin	0.731	< 0.001	INCREASING	1957	< 0.001
Chlas	0.905	< 0.001	INCREASING	1946	< 0.001
Chlb	0.394	0.090	NONE	1956	0.48
$\delta^{13}\text{C}$	-0.543	< 0.001	DECREASING	1954	< 0.001
Selenga (BAIK13-10)					
Alloxanthin	0.004	0.973	NONE	1988	< 0.001
Diatoxanthin	-0.593	< 0.001	DECREASING	1940	< 0.001
Lutein	-0.405	< 0.001	DECREASING	1979	0.32
Canthaxanthin	0.070	0.955	NONE	1991	0.45
Zeaxanthin	0.205	0.060	NONE	1949	0.15
Chlas	0.600	< 0.001	INCREASING	1935	0.01
$\delta^{13}\text{C}$	0.922	< 0.001	INCREASING	1952	< 0.001
Selenga (BAIK13-11)					
Alloxanthin	0.747	< 0.001	INCREASING	1912	0.02
Lutein	-0.494	0.006	DECREASING	1881	0.66
Chlas	0.747	< 0.001	INCREASING	1894	0.10
$\delta^{13}\text{C}$	0.020	0.880	NONE	1980	< 0.001
Maloe More (BAIK13-14)					
Alloxanthin	0.500	0.007	INCREASING	1908	0.39
Diatoxanthin	-0.650	< 0.001	DECREASING	1974	0.05
Lutein	0.650	< 0.001	INCREASING	1958	< 0.001
Canthaxanthin	0.233	0.224	NONE	1922	0.61
Chlas	0.700	< 0.001	INCREASING	1984	< 0.001
Chlb	0.706	< 0.001	INCREASING	2002	0.02
$\delta^{13}\text{C}$	0.550	0.003	INCREASING	1980	< 0.001
North Basin (BAIK13-18) *					
Chlas	0.363	0.070	NONE	1917	0.02
$\delta^{13}\text{C}$	0.121	0.584	NONE	1954	< 0.001
North Basin (BAIK13-19)					
Diatoxanthin	0.179	0.396	NONE	1976	0.13
Canthaxanthin	0.633	< 0.001	INCREASING	1964	0.08
Chlas	0.533	0.004	INCREASING	1961	0.40
$\delta^{13}\text{C}$	0.183	0.344	NONE	1871	0.08

Diatom pigments (diatoxanthin) declined over the last 200 years in the South basin and Selenga sites, along with lutein (chlorophyte) pigments, and picocyanobacterial pigments were showing an increasing trend in both the South basin and North basin. There was more floristic change in the South basin, Maloe More and Selenga sites than the North basin, as supported by PCA results (*Figure 146*), with significant increasing trends in alloxanthin, lutein and canthaxanthin and significant decreasing trends in diatoxanthin (*Table 52*). In the North basin the only significant trends were observed in canthaxanthin concentrations (*Table 52*). In comparison to the carbon isotopic data, increasing trends were seen in the South basin, Selenga and Maloe More, occurring earlier at the Selenga Delta, with the most recent changes at Maloe More. This is similar to the lake-wide Chlas trend. These Mann-Kendall coefficient trends could be linked to warming over the last 50 years, with greater abundances of picocyanobacteria in both the South and North basin. The decreasing diatom pigment trend in the South basin provides evidence of a decline in under-ice diatom production over the last 60 years, as seen in monitoring studies (Silow et al. 2016).

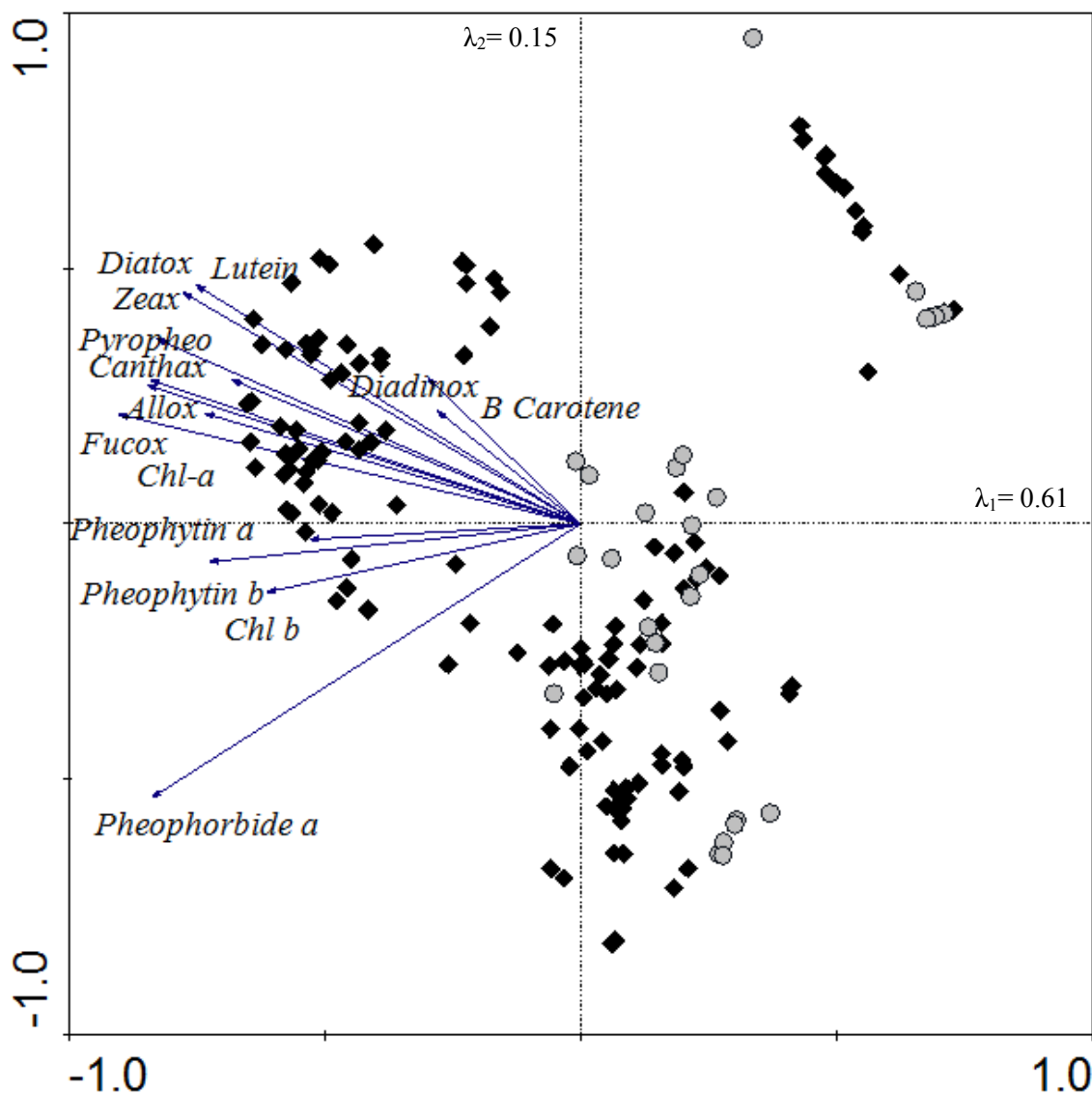


Figure 136: PCA of pigments over the last 200 years at all sites in South basin, Selenga, Maloe More and North basin. Grey circles indicate North basin sites and black diamonds indicate South, Selenga and Maloe More sites. (Removed pigment data from BAIK13-7A and BAIK13-18A).

7.2.9 Pre and post- 1950 AD

Air temperatures within the Baikal region have risen rapidly over the last 50 years and main anthropogenic influence from industrial activity within the watershed began in the 1950s (Brunello et al. 2004). Algal production measures (Chlas concentrations, $\delta^{13}\text{C}$, diatom concentrations, total carotenoid concentrations) have therefore been compared pre and post 1950 AD to examine trends before and after this time period.

Mean pelagic deep basin Chlas concentrations pre-1950 ranged between 4.96 and 544.1 nmol g⁻¹ OC in the South basin (mean = 119.9 nmol g⁻¹ OC), and between 6.17 and 168.6 nmol g⁻¹ OC in the North basin (mean = 65.3 nmol g⁻¹ OC), and at the Selenga Delta and Maloe More mean Chlas concentrations are 293.3 nmol g⁻¹ OC and 134.1 nmol g⁻¹ OC respectively (*Figure 147*). All sites across the lake showed higher mean Chlas concentrations post-1950 than pre-1950, and the largest increase in Chlas concentrations post-1950 occurred at the Selenga Delta (Selenga Delta > Maloe More > South Basin > North Basin). Similarly, after 1950, the Chlas concentrations were highest in the Selenga Delta, ranging from 292.3 – 859.2 nmol g⁻¹ OC (Selenga Delta > Maloe More > South Basin > North Basin). Chlas concentrations pre and post-1950 were significantly different in the South basin, Selenga Delta and Maloe More sites (p value = < 0.001), but not the North basin (p values = 0.184).

Mean δ¹³C values became more positive after 1950 at the South basin sites (except BAIK13-7A), the Selenga site, Maloe More site, and Baik13-18A in the North basin (not BAIK13-19B close to the Upper Angara) (*Figure 147*). However, the mean post-1950 δ¹³C values in the North basin, Selenga Delta and Maloe More were not significantly higher than the pre-1950 values (p values = 0.99, 0.22 and 0.96 respectively).

Mean diatom concentrations were significantly lower post-1950 in the South basin and North basin, compared to pre-1950 (p value = < 0.01) (*Figure 148*). Diatom concentrations pre-1950 range between c. 500 – 700 10⁴ valves/g dry wt at BAIK13-7A and BAIK13-11C, and c. 200 – 300 10⁴ valves/g dry wt at BAIK13-18A. Post-1950, diatom concentrations decreased to c. 250 – 400 10⁴ valves/g dry wt in the South basin, and < 200 10⁴ valves/g dry wt in the North basin (*Figure 148*).

Total carotenoid concentrations were highest at the Selenga (BAIK13-10A) and Maloe More (BAIK13-14C) (between c. 25 – 60 nmol g⁻¹ OC), which is more than two-fold higher than concentrations within the pelagic deep basin sites (< 10 nmol g⁻¹ OC) (*Figure 148*). Concentrations were higher post-1950 than pre-1950 at the Selenga and Maloe More sites, and significant difference in concentrations between these two time-intervals were only seen in the Selenga sites (p values < 0.01) (*Figure 148*).

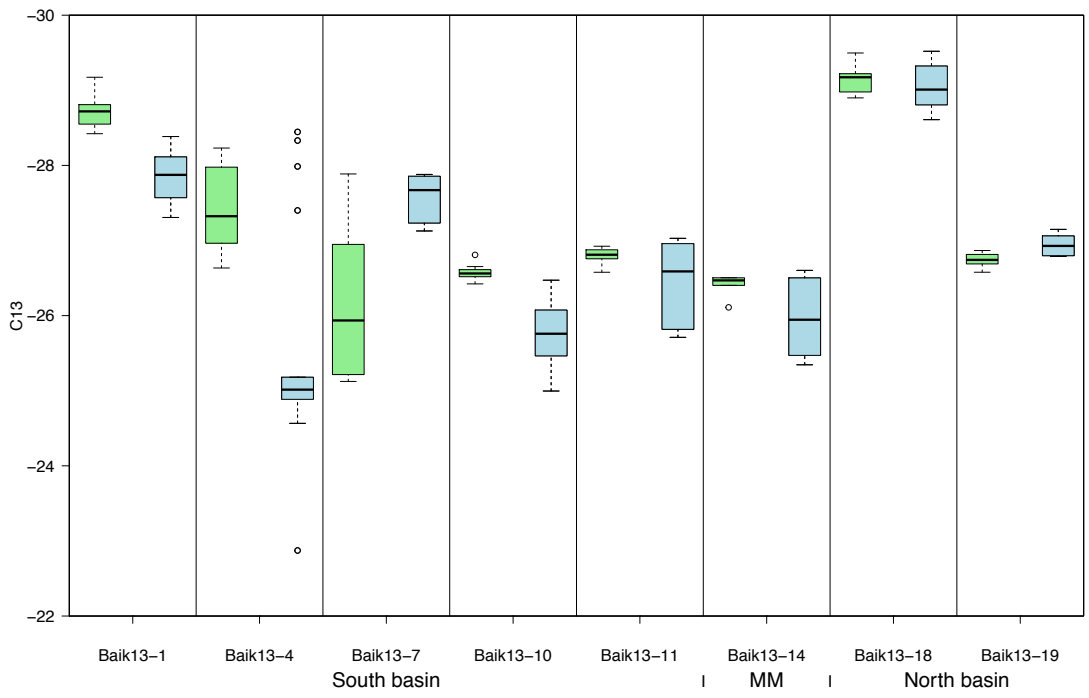
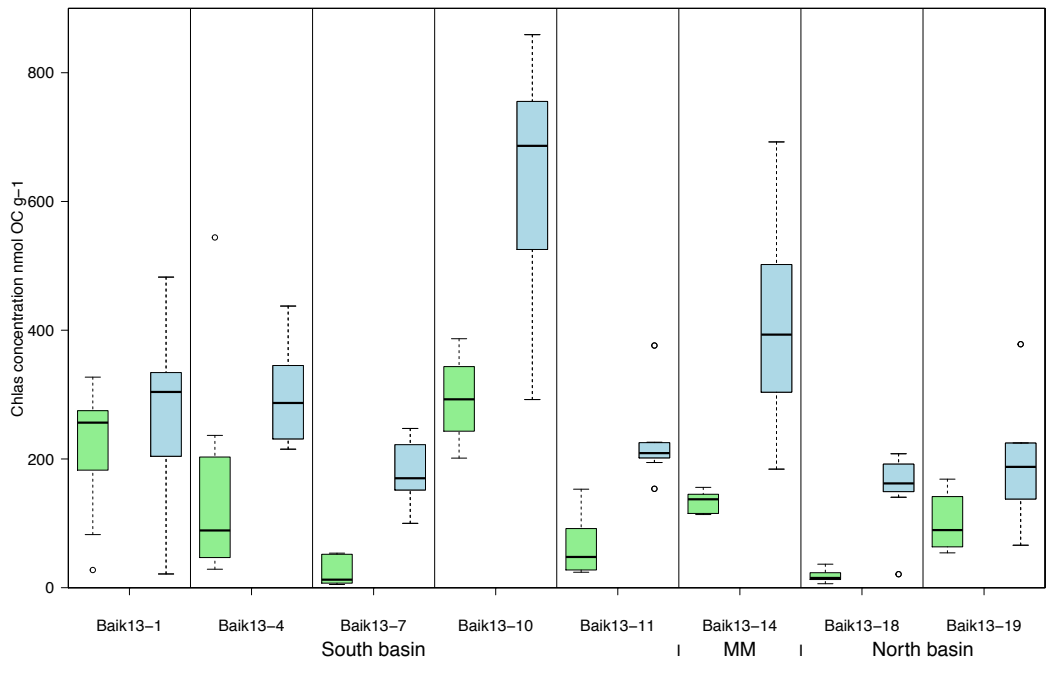


Figure 137: Chl a concentrations and $\delta^{13}C$ values (suess corrected) pre (green) and post (blue) 1950 AD across the lake. (*BAIK13-7A and *BAIK13-18A show high levels of degradation).

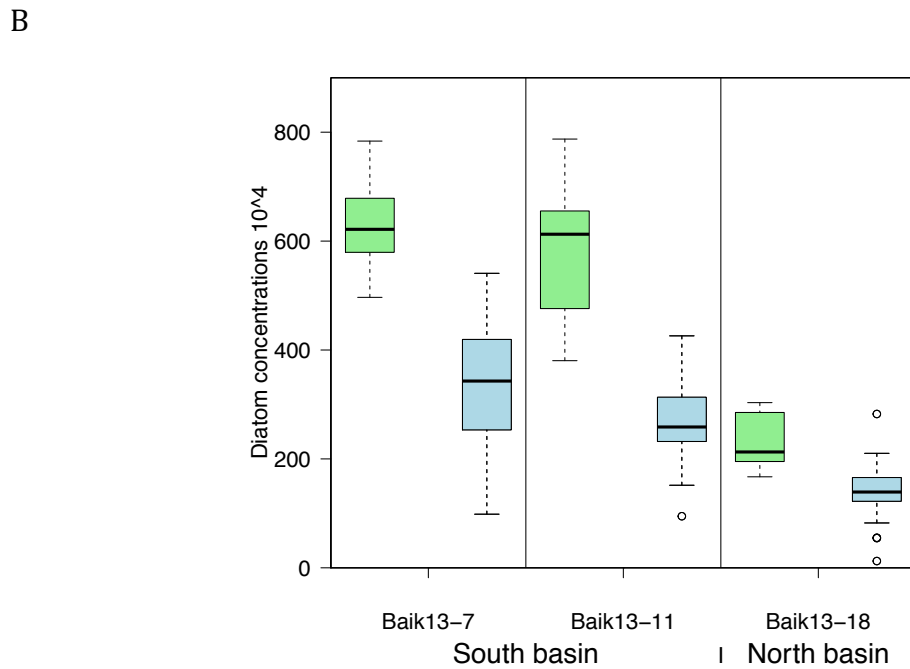
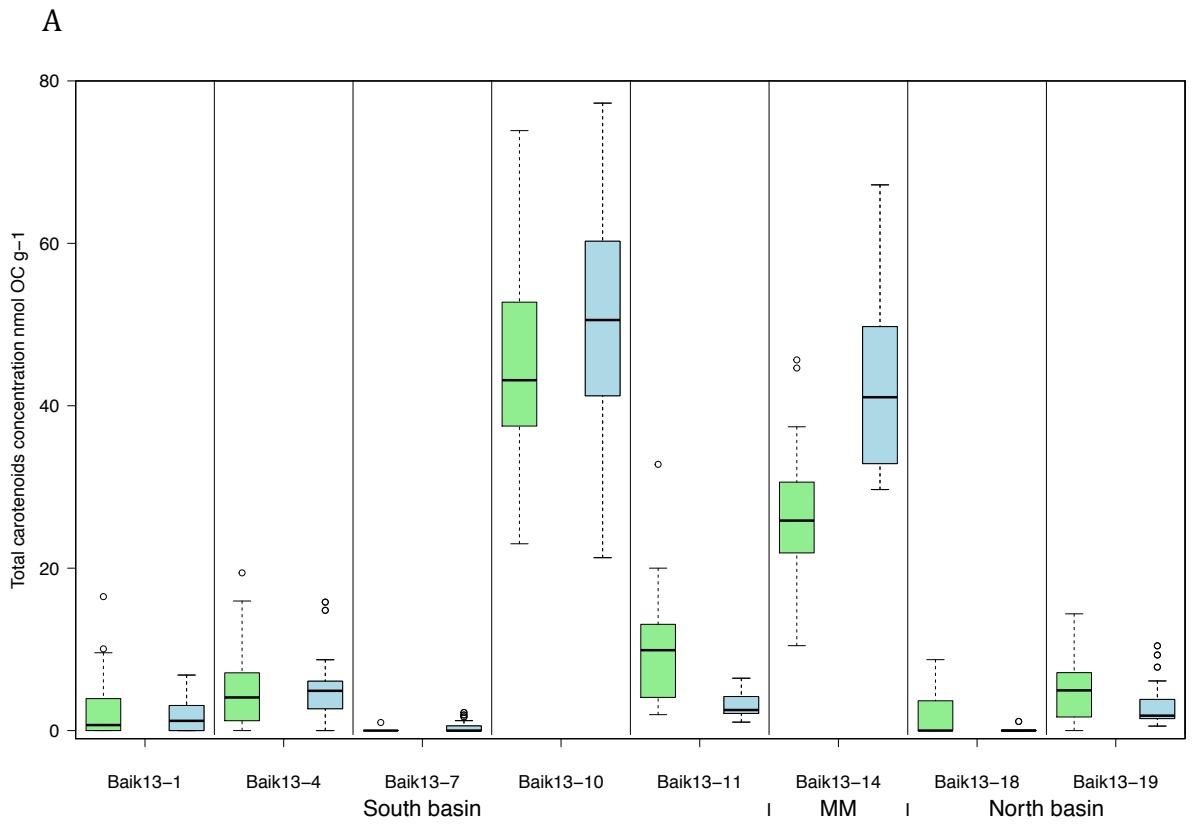


Figure 138: (A) Total carotenoids concentrations pre (green) and post (blue) 1950 across the lake. (B) Diatom valve concentrations (10^4 valves/g dry wt) pre (green) and post (blue) 1950 across the lake.

7.2.10 Correlations between Chlas and $\delta^{13}C$

Correlations were carried out between Chlas concentrations and carbon isotopes to examine whether these proxies are showing similar trends over the last 200 years. This was tested at all sites in the South basin (except BAIK13-7A), Selenga, Maloe More and North basin (except BAIK13-18A), to assess whether there was regional variation in correlations over the last 200 years, and if they are both potentially showing response to climate and/or anthropogenic nutrient enrichment or neither.

Significant positive relationships between Chlas concentration and $\delta^{13}C$ values over the last 200 years were only found at Selenga ($R^2 = 0.50$; p value= 0.005) and Maloe More ($R^2 = 0.55$; p value= 0.01) (Table 53). In contrast to these littoral and river influenced sites, the pelagic South and North basin did not show a significant positive relationship between these two proxies.

Table 53: Regression coefficients and p-values for correlations between Chlas concentrations and $\delta^{13}C$ across the lake. Core data within the South basin and North basin have been merged.

Chlas concentrations and $\delta^{13}C$		
	R^2	P value
South basin	0.15	0.131
Selenga Shallows	0.50	0.005
Maloe More	0.55	0.014
North basin	0.51	0.067

7.2.11 Pigments, $\delta^{13}C$ and regional annual temperatures

Correlations were carried out between Chlas and regional annual temperature, diatom concentrations and regional annual temperature, carbon isotopes and regional annual temperature and pigment ratios (diatoxanthin:canthaxanthin and Chlb:Chlas) and regional annual temperature. This is in order to examine whether any of the above show similar and synchronous changes with increasing regional temperatures over the last 200 years. Correlations have been carried out between Chlas concentrations vs mean annual temperatures and $\delta^{13}C$ vs mean annual temperatures at sites within the South basin (BAIK13-1C, BAIK13-4F), Selenga (BAIK13-10A, BAIK13-11C), Maloe More (BAIK13-14C) and North basin (BAIK13-19B) (see Chapter Two for methods on matching sediment measures with temperatures). Correlations were conducted to assess whether trends in Chlas concentrations or $\delta^{13}C$ values over the last 200 years are associated regional warming trends, and to examine if increasing mean annual temperatures coincide with increasing Chlas concentrations and

increasing $\delta^{13}\text{C}$ values (more positive). If the datasets were not correlated then this suggested that climate is not driving changes within the pigment and carbon isotope records, which is likely to be a result of lag in response due to the sensitivity of diatoms to environmental change.

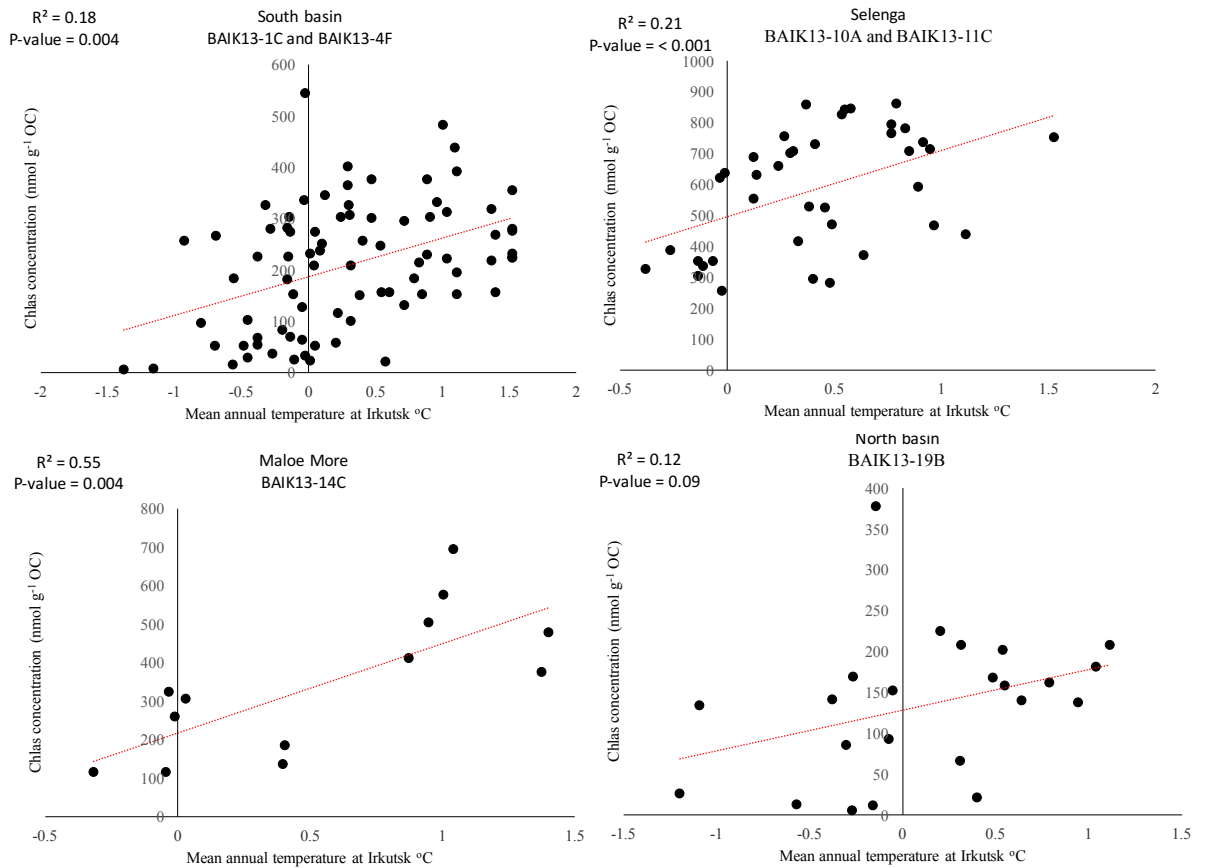


Figure 139: Regression correlations and p-values between average annual temperature at Irkutsk and Chl a concentrations in the South basin, Maloe More, Selenga and North basin. (BAIK13-7A pigment data removed from South basin correlation and BAIK13-18A pigment data removed from North basin correlation).

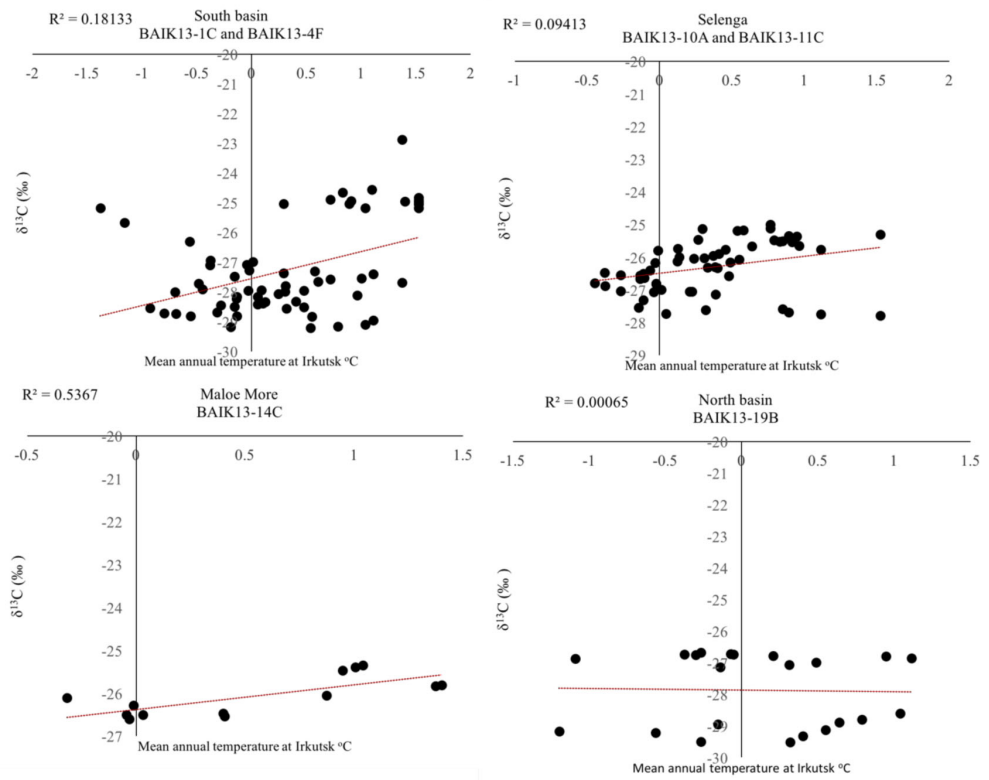


Figure 140: Regression correlations and p -values between average annual temperature at Irkutsk and $\delta^{13}\text{C}$ values in the South basin, Maloe More, Selenga and North basin.

Table 54: Correlation coefficients and p-values for correlations between average annual temperature at Irkutsk and Chlas concentrations, $\delta^{13}\text{C}$, diatom concentrations, diatoxanthin: canthaxanthin pigment ratio and chl_b: chlas pigment ratio in the South basin, Selenga, Maloe More and North basin.

	Chlas and temperature		$\delta^{13}\text{C}$ and temperature		Diatom conc. and temperature	
	R ²	P value	R ²	P value	R ²	P value
South basin	0.16	0.004	0.18	< 0.001	0.57	< 0.001
Selenga Shallows	0.19	< 0.001	0.09	0.020	0.29	< 0.001
Maloe More	0.55	0.004	0.54	0.004	0.07	0.522
North basin	0.12	0.098	0.00	0.910	0.02	0.352
	Diatox:canthax and temperature		Chlb:Chlas and temperature			
	R ²	P value	R ²	P value		
South basin	(-)	(-)	0.03	0.125		
Selenga Shallows	0.32	< 0.001	0.45	< 0.001		
Maloe More	0.63	0.001	0.04	0.498		
North basin	(-)	(-)	(-)	(-)		

There were positive relationships between Chlas concentrations (nmol g⁻¹ OC) and average annual regional temperatures in the South basin (R² = 0.16; p value = 0.004), Selenga (R² = 0.19; p value = < 0.001) and Maloe More (R² = 0.55; p value = 0.004), but not the North basin (R² = 0.12; p value = 0.098) (Maloe more > Selenga > South > North) (Figure 140; Table 55). There were positive relationships between $\delta^{13}\text{C}$ and average annual regional temperatures in the South basin (R² = 0.66; p value = < 0.001), Maloe More (R² = 0.57; p value = 0.004), but not in the Selenga (R² = 0.45; p value = 0.02) or North basin (R² = 0.64; p value = 0.910) (Figure 150; Table 54). There was a significant negative relationship between diatom concentrations and average annual regional temperatures in the South (R² = 0.57; p value = < 0.001) and Selenga (R² = 0.29; p value = < 0.001), but not at Maloe More (R² = 0.07; p value = 0.522) or in the North basin (R² = -0.02; p value = 0.352). Furthermore there was a significant negative relationship between diatoxanthin: canthaxanthin pigment ratios and average monthly regional temperatures at the Selenga (R² = 0.32; p value = < 0.001) and Maloe More (R² = 0.63; p value = 0.001), and a significant positive relationship between Chlb:Chlas and average monthly regional temperatures at the Selenga site (R² = 0.45; p value = < 0.001) but not the South basin or Maloe More sites.

Diatoxanthin:canthaxanthin ratios showed a declining trend at BAIK13-1C in the South basin and BAIK13-10A in the Selenga over the last 60 years, a slight decreasing trend at Maloe More (BAIK13-14C) and no clear pattern in the North basin (at BAIK13-19B) (Figure 151). The diatoxanthin:canthaxanthin ratio trend coincides with declining ice cover duration and increasing mean spring (March/April) temperatures (Figure 151). Diatom concentrations similarly showed decreasing trends over the last 60 years in the South basin (at BAIK13-7A) and Selenga (at BAIK13-11C) (Figure 151).

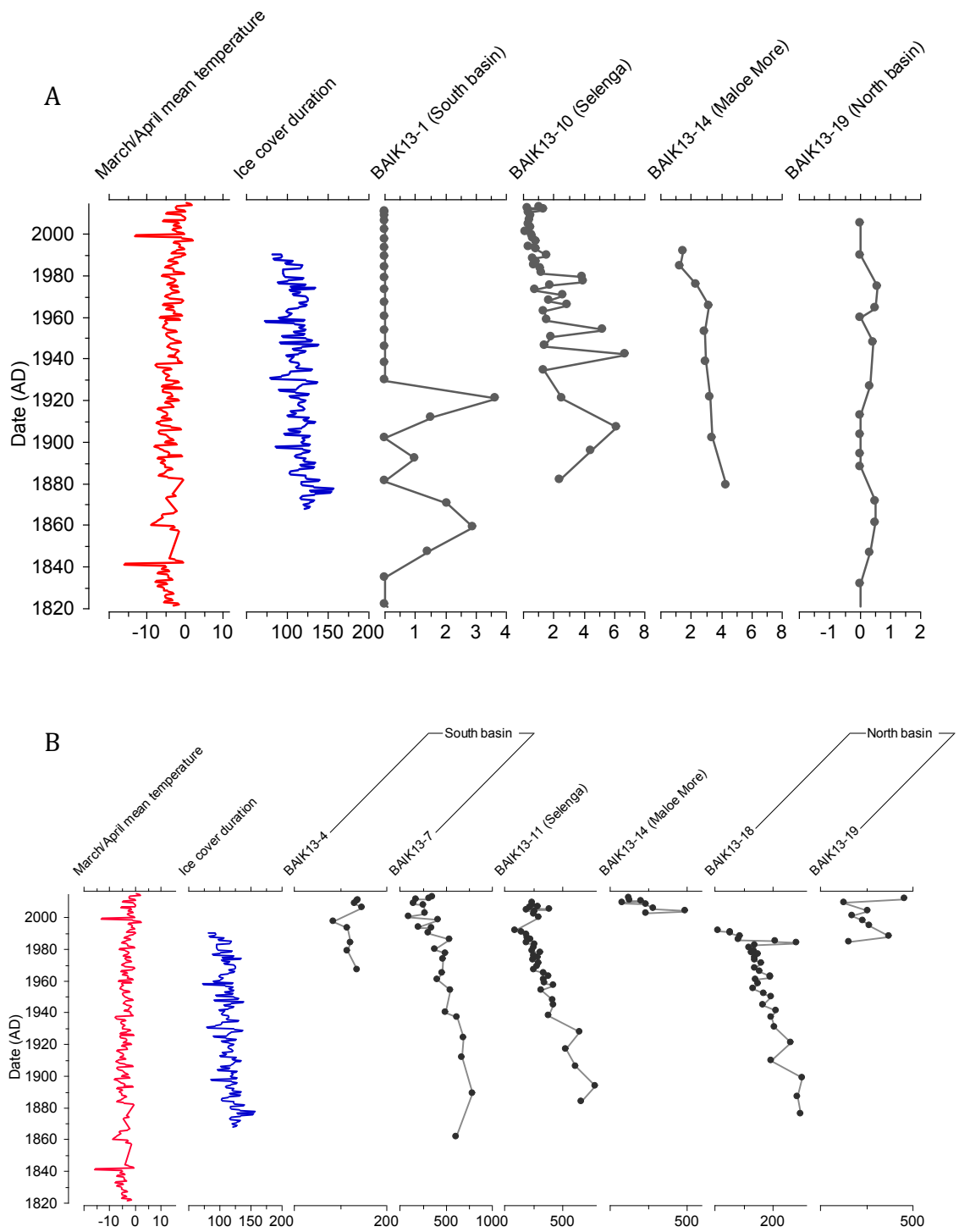


Figure 141: (A) Diatoxanthin:canthaxanthin pigment ratio, Irkutsk regional air temperature ($^{\circ}\text{C}$) and ice cover duration (days), (B) Diatom concentrations (10^4 valves/g dry wet), Irkutsk regional air temperature ($^{\circ}\text{C}$) and ice cover duration (days).

To further assess whether temperature or anthropogenic catchment change are driving algal pigment distribution, RDA analysis was performed on selected cores. The sediment cores

selected were BAIK13-11C in the South basin, near the Selenga Delta, and BAIK13-14C in Maloe More Bay. Due to limited historical records, available for anthropogenic data over the last few decades within the Lake Baikal catchment, such as population records, tourist numbers, and agricultural output records, a record of tourist activity was created based on known tourist activity from the literature.

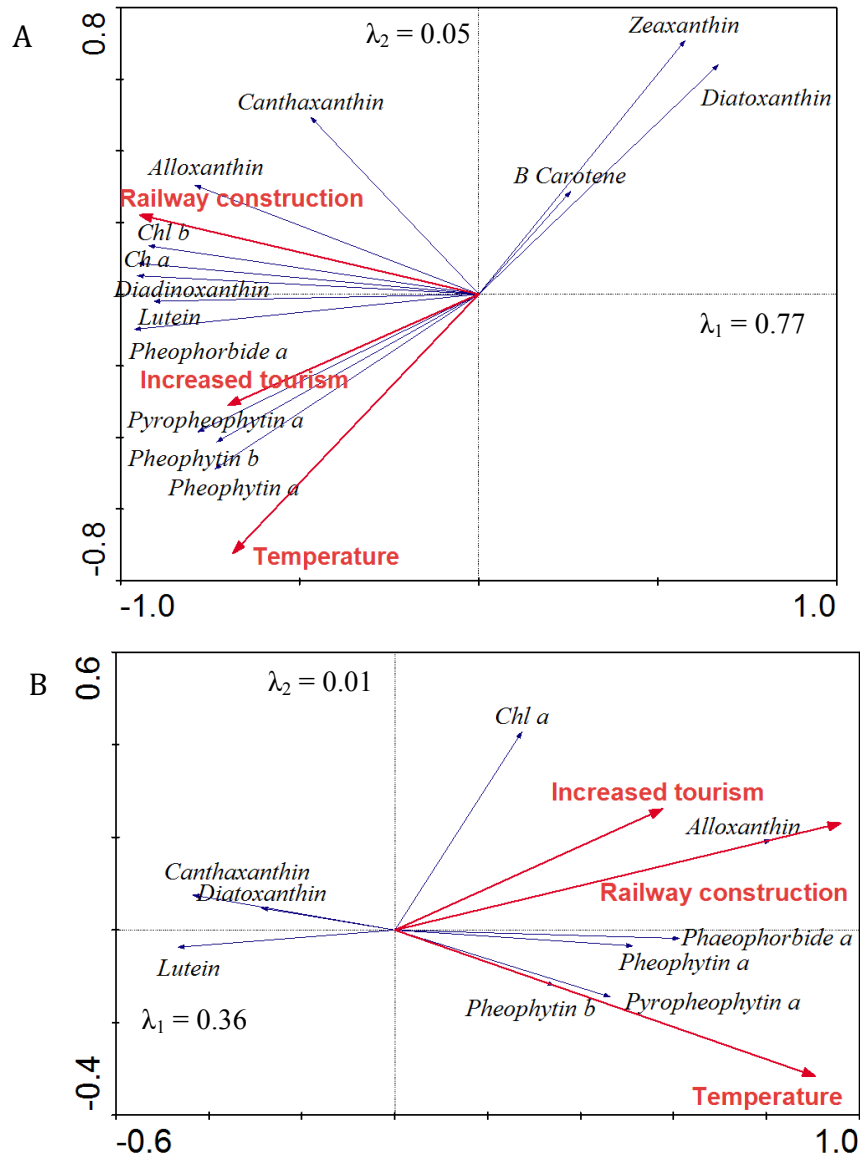


Figure 142: RDA analysis results of (A) BAIK13-11 in the South basin and (B) BAIK13-14 at Maloe More Bay, examining the influence of air temperature and tourist activity on down-core sedimentary algal pigments since c. 1950AD. Tourism is significantly (p value > 0.05) correlated with algal pigments in both BAIK13-11C and BAIK13-14, and temperature (p value > 0.05) in BAIK13-14C. Forward selection with Monte Carlo permutation tests were applied. 'Railway construction' refers to sediments post 1950 AD, 'Increased tourism' refers to sediments post 1990 AD and 'Temperature' refers to Irkutsk air temperatures.

A value of '1' was applied to sediment dating back earlier than the construction of the Amur Railway in c.1950, a value of '2' was applied to sediment between c. 1950 to c. 1990, and a

value of '3' was applied to sediment intervals post c. 1990. This is applied to help disentangle the impact of climate and human pollution on the algal community assemblages in Lake Baikal. Results show that at BAIK13-11 there is no significant link between pigment distribution and temperature (p value > 0.05), but significant relationship between tourist activity (since the construction of the railway) and algal community composition, with increases in alloxanthin pigments (cryptophytes) (*Figure 152*). At BAIK13-14 in Maloe More Bay, RDA analyses shows a significant relationship between temperature, tourist activity and algal community composition (p value < 0.05), with increasing concentrations of chlorophylls, lutein, canthaxanthin, and decreasing concentrations of diatoxanthin (diatom pigment) (*Figure 152*). These results suggest that both climate and tourist activity are influencing the algal community with the shallower bay regions, compared to the deeper pelagic sites.

7.3 Discussion

7.3.1 Assessment of reliability of pigment records

The cores which meet the aims of this chapter, providing pigment records, are from the pelagic South basin (BAIK13-1C and BAIK13-4F), Maloe More (BAIK13-14C), Selenga (BAIK13-10A and BAIK13-11C) and pelagic North basin (BAIK13-19B). These cores can be used for interpretation as pigment concentrations (Chl a , diatoxanthin and canthaxanthin) do not covary, and these cores do not show an exponential decay in pigment concentrations which is indicative of degradation profiles (Fietz et al. 2007). With turbidites removed from BAIK13-4F the pigment records can be used. BAIK13-11C does not have any turbidites in the sediment interval covering last 200 years, although similarly to BAIK13-4F the sedimentation rates are variable. The pigment records which are likely to be showing degradation profiles and were not interpreted include BAIK13-7A and BAIK13-18A. This is due to the very low sedimentation rates ($< 0.01\text{ g cm}^{-2}\text{ yr}^{-1}$) and pigment compositions of solely degradation products. Although BAIK13-1C and BAIK13-19B have similarly low sedimentation rates, the pigment composition consists of chlorophylls, carotenoids and derivatives.

Pigment preservation measures highlight that the pigment record from BAIK13-1C, BAIK13-4F, BAIK13-10A, BAIK13-11C, BAIK13-14C and BAIK13-18A can provide useful primary production reconstructions, as the oxidised layers are not significantly influencing the Chl a concentrations and flux. However, despite this the pigment preservation ratios (chl- a :pheo- a) are significantly higher in anoxic than oxic sediments at BAIK13-7A, BAIK13-10A and BAIK13-14C. This is due to the higher concentrations of pheo- a pigments (pheophorbide- a , pheophytin- a and pyropheophytin- a), which exceed chlorophyll- a concentrations by at least

10-fold in the upper sediments (0.5 – 5 cm) which are oxidised. BAIK13-7A is likely to be a degradation profiles, however at BAIK13-10A and BAIK13-14C the chl-*a*:pheo-*a* pigment ratios could be reflecting algal production rather than pigment preservation in the surface sediments.

The sediment cores with the highest diversity of chlorophylls and carotenoids within the pigment record are from the Maloe More (BAIK13-14C) and Selenga sites (BAIK13-10A). The higher preservation state of sedimentary pigments at the Maloe More and Selenga sites are likely to be due to shallower water depths and greater production, which causes increased direct deposition rates and better preservation in the sediment. This has also been found by Fietz (2005) at Lake Baikal, as chlorophyll and carotenoid deposition. Preservation was more pronounced at sites with high productivity in the euphotic zone, resulting in lower residence time under oxic conditions due to higher sedimentation rates. Thus, this is the case at BAIK13-14C, at Maloe More Bay, which has higher sedimentation rates compared to pelagic basin sites, and higher algal production in the photic zone (as presented in Chapter Five).

One of the pelagic South basin cores (BAIK13-1C) and one of the pelagic North basin cores (BAIK13-19B) also show high pigment preservation, with intact chlorophyll-*a*. At these deep pelagic sites, (1,360 and 460 m respectively), burial rates are not significantly influencing pigment preservation, despite the sedimentation rates being similar ($0.012 - 0.02 \text{ g cm}^{-2} \text{ yr}^{-1}$) to the other deep basin sites, which have poor pigment records (BAIK13-7A and BAIK13-18A) due to sediment focussing and low sediment accumulation. There is no co-variation between Chl*a*s, diatoxanthin and canthaxanthin pigments at the South basin (BAIK13-1C), Maloe More and Selenga (BAIK13-10A) sites. However, there is significant co-variation between Chl*a*s and canthaxanthin at the North basin site (BAIK13-19B). These sediment cores in the South basin, Maloe More, Selenga sites and North basin (BAIK13-1C, BAIK13-10A, BAIK13-14C and BAIK13-19B) have robust age models, with small age errors (2 – 9 years) in the upper sediments, which cover the last 200 years. These pigment records can therefore be used to address the aims of this chapter, to examine past production trends in the South and North basins, and at shallow water sites such as Maloe More and the Selenga. Although the burial rates are influencing the pigment preservation at Maloe More (BAIK13-14C) and one of the Selenga sites (BAIK13-10A) of Chl*a*s and diatoxanthin, these sites have shallower water depths (200 and 60 m respectively) and the highest sedimentation rates ($0.03 - 0.13 \text{ g cm}^{-2} \text{ yr}^{-1}$). Therefore, pigments at these sites spend less time within the water column, being incorporated into the sediment records faster, being removed from the oxidised layer within the upper sediments.

From the literature, differences in pigment degradation have been found between the South and North basins of Lake Baikal, with higher degradation in the North basin, assessed from fluxes of major lipid biomarkers in the water column and sediments (Russell and Rosell-Mele, 2005). This is a result of differences in sedimentation rates, basin morphometry, ice cover duration, productive season duration, temperatures and algal productivity (Shimaraev, 1994; Kozhova and Imesteva, 1998). The results presented within this thesis do show the lowest sedimentation rates at BAIK13-18A in the North basin, and the highest sedimentation rates at BAIK13-4F in the South basin, and BAIK13-10A close to the Selenga delta in the South basin. Stronger degradation of algal pigments in the North basin than the Central and South basin and Selenga Delta, prior to final burial within the sediments, was also found by Fietz (2005). This difference is shown by steeper exponential decay curves of Chlas/TOC down the sediment cores in the North basin (Fietz, 2005). Furthermore, less than 10% of the original chlorophyll-*a* within the bottom sediment traps was preserved in the South basin surface sediments, and less than 5% in the North basin surface sediments (Fietz, 2005). The main factor suggested to be causing this difference is sedimentation rates, which is causing pigments to remain within oxic conditions for longer in the North basin (Fietz, 2005). In addition, it is suggested that both chemical and enzymatic oxidation by microbial activity are having a larger effect on pigment degradation in the North basin than the South basin and Selenga Delta (Fietz, 2005).

In alignment with the above, Cuddington and Leavitt (1999) have predicted correlations between oxic layer thickness and rates of pigment deposition. In support of this, higher pigment accumulation rates have been observed at sites with smaller oxic layer thickness within the surface sediments. The pelagic South (BAIK13-1C, BAIK13-4F and BAIK13-7A) and North basin sites (BAIK13-18A) have the thickest oxidised layers and lowest Chlas accumulation rates in comparison to Maloe More (BAIK13-14C), one of the Selenga sites (BAIK13-11C) and one of the North basin sites (BAIK13-1B9). However, an exception to this is one of the Selenga sites (BAIK13-10A), which has a thick oxidised layer and a high Chlas accumulation. The results suggest that within the sediment cores there are only significant differences in Chlas AR between oxic and anoxic layers at Maloe More (BAIK13-14C) and the Selenga sites (BAIK13-10A), with the difference being higher Chlas AR within oxic layers. Thus, oxic layers within a sediment core do not appear to be significantly influencing pigment preservation. This contrasts with Fietz (2005), which reports sharp decreases with the Chlas and carotenoids within the oxidised layers (upper 10 cm) of the short cores in the South basin (675 m water depth), Selenga (133 m water depth) and North basin (386 m water depth). The upper 10 cm within the sediment cores presented in this chapter cover the last 200 years at BAIK13-4F in the South basin and BAIK13-10A close to the

Selenga Delta. However, in the rest of the cores (BAIK13-1C, BAIK13-7A, BAIK13-11C, BAIK13-14C, BAIK13-18A and BAIK13-19B) the upper 10 cm within the sediment cores extends over the last 200 year time period.

Florian et al. (2015) found that if chl-*a*: pheo-*a* pigment ratio is correlated with factors (such as sedimentation rate, TOC flux, or Chl*a* flux), which can be used to indicate a change in pigment preservation, then the chl-*a*: pheo-*a* pigment ratio is showing pigment preservation. However, the pigment preservation ratio is not positively correlated with DMAR, CMAR or Chl*a* flux. Instead the preservation ratio is negatively correlated with these factors at the Selenga and Maloe More sites. This finding suggests that perhaps in Baikal sediments the preservation ratio is not solely reflecting pigment preservation, which may be due to pheo-*a* pigments being used as a good indicator for production (Fietz, 2005) rather than to measure the extent of degradation. Fietz (2005) reports that sedimentary pigments can be used to assess relative changes in phytoplankton groups, but not to determine past phytoplankton abundance, due to degradation at Lake Baikal, which has also been suggested by Leavitt (1993) within smaller lakes. However, the results presented do not show exponential decay of Chl*a*s and carotenoids, and do not show significant pigment co-variation between Chl*a*s and the dominant carotenoids. Instead, the pigment records analysed (BAIK13-1C, BAIK13-4F, BAIK13-10A, BAIK13-11C, BAIK13-14C and BAIK13-19B) are likely to be showing both a production signal and a degradation profile.

7.3.2 *Diatom assemblages and correction factors*

In conjunction with the sedimentary pigment records, the reliability of the diatom valve assemblage records was assessed via the use of correction factors and diatom dissolution indices. Correction factors have been applied to the major diatom species in two of the South basin surface sediments (BAIK13-4F and BAIK13-7A) (Table 55), to correct diatom abundances for dissolution (Battarbee et al. 2005). These two cores have been chosen to apply correction factors to the diatom abundance datasets, as they have the highest abundances of *Synedra acus* var. *radians* within the surface sediments. These species make up over 80% of the total uncorrected diatom assemblage. The largest differences in raw diatom abundances and corrected diatom abundances are seen within the *Synedra acus* var. *radians*, with increases from 12.5 - 14.6 % to 63.7 - 65.8 %, and *Cyclotella minuta/ornata*, with decreases from 30.5 - 42.9 % to 2.7 - 3.7 % (Table 55). There are also shifts in *Aulacoseira baicalensis* species, with decreases from 24.0 - 31.3 % to 7.2 - 9.1 %. Slight changes are seen in the abundances of *Stephanodiscus meyerii* and *Aulacoseira skvortzowii* between the raw and corrected data,

with increases from 0.6 – 2.9 % to 1.5 – 8.7 % and 5.4 – 10.3 % to 6.7 – 11.8% respectively (Table 55).

The large differences between the raw and corrected data for *Synedra acus* var. *radians* and *Cyclotella minuta/ornata* are due to the lightly silicified cells in comparison to *Aulacoseira baicalensis* and *Aulacoseira skvortzowii* (Battarbee et al. 2005). Therefore, the interpretation of the raw diatom assemblages in the surface sediments may be complicated due to the higher levels of dissolution on these species (Ryves et al. 2003). However, despite this, raw data will be analysed within this chapter instead of applying correction factors down-core across the sites, and dissolution impacts will be considered. This is as the patterns are still the same, spatial trends and temporal trends, and the corrected abundances do not include all the diatom assemblages (84 – 95 % of diatom assemblage have applied correction factor), only the major diatom species.

Table 55: Raw and corrected diatom abundances; average surface sediment abundances (0 – 2 cm); two cores in South basin; BAIK13-4F and BAIK13-7A. These cores have been selected as they have the highest abundances of *Synedra acus* var. *radians*, which is a lightly silicified diatom species.

	BAIK13-4F		BAIK13-7A	
	Raw abundance data (%)	Corrected abundance data (%)	Raw abundance data (%)	Corrected abundance data (%)
<i>Aulacoseria skvortzowi</i>	5.4	6.7	10.3	11.8
<i>Aulacoseria baicalensis</i>	24.0	7.2	31.3	9.1
<i>Cyclotella minuta/ornata</i>	42.9	3.7	30.5	2.7
<i>Stephanodiscus meyerii</i>	2.9	8.7	0.6	1.5
<i>Synedra acus</i>	14.6	65.8	12.5	63.7

7.3.3 Spatial differences in algal assemblage and production from surface sediments

Littoral regions, i.e. Maloe More Bay (BAIK13-14C), and river-influenced sites, i.e. Selenga Delta site (BAIK13-10A), have a greater percentage of TOC within the surface sediments, compared to the deeper pelagic South and North basins. The Selenga and Maloe More site have more positive $\delta^{13}\text{C}$ values, higher concentrations of chlorophyll-*a* and carotenoids (diatoxanthin, lutein and canthaxanthin) pigments, and higher abundances of *Stephanodiscus meyerii* and *Crateriportula inconspicua* diatom species. *Stephanodiscus meyerii* builds up in shallow waters and then extends into pelagic regions in the spring, and higher abundances can suggest greater nearshore nutrient input, in particular phosphorus (Bradbury et al. 1994; Morley, 2005). In surface sediments, these diatom species are largely found in Maloe More due to shallower and more nutrient-rich waters (Müller et al. 2005). Maloe More is also in a drier region than the South, Central and North basins (Atlas Baikal 1993), and has shallow

snow depths during the winter (Shimaraev et al. 1994), and so light penetration might be an important factor. Furthermore, in phytoplankton surveys in 2001-2002 higher abundances of *Stephanodiscus meyerii* were found in the South and Central basins, and rarely in the North (Morley, 2005). This is as *Stephanodiscus meyerii* have a high temperature optimum of 15 - 17.5°C (Jewson et al. 2015), and prefer warmer waters with shorter ice cover duration (Morley, 2005). High abundances of this diatom species within sediments has been associated with climate driven nutrient enrichment (Bangs et al. 2000) and anthropogenic pollution (Bradbury et al. 1994) in other lakes. *Crateriportula inconspicua* is suggested to grow in warm, shallow mesotrophic waters (Edlund et al. 1995) as found in Maloe More. Thus, from the surface sediments, the Selenga and Maloe More sites are warmer, more nutrient-rich and productive sites, than the pelagic South and North basin sites.

Within the deep basins, TOC percentages are not significantly different, however the South basin sites have more positive $\delta^{13}\text{C}$ values than the North basin, when excluding BAIK13-19B, which is close to the Upper Angara River. Alongside higher $\delta^{13}\text{C}$ isotopic compositions, the South basins sites have higher chlorophyll-*a* and carotenoid (alloxanthin and canthaxanthin) concentrations, than the North basin sites. This suggests higher abundances of cryptophytes and picocyanobacteria in the pelagic South basin, which predominantly grow in the summer months, reflecting a longer growing season than in the North basin. The South basin sites show the largest variability in $\delta^{13}\text{C}$ values, *Synedra acus* var. *radians* and *Cyclotella minuta/ornata* diatom species abundance over the last 20 years. *Synedra acus* var. *radians* is a lightly silicified diatom species, which can outcompete larger diatoms and grow in more silicon-limited conditions, and has previously been associated with increased river discharges (Bradbury et al. 1994). This diatom species grows in nearshore areas and behind thermal bars after ice break-up, and extends into the pelagic zone in spring/early summer. *Synedra acus* var. *radians* has also been found to grow best under high irradiances resulting from lower snow depths on the ice, and shorter periods of opaque ice. Previous studies which have found higher abundances of *Synedra acus* var. *radians* in the South and Central basin, and rare abundances in the North basin, have associated this pattern to shorter opaque ice cover durations and warmer waters in the South and Central basins, making this diatom species more competitive (Bondarenko et al. 1996; Morley, 2005). Similar abundances of *Synedra acus* var. *radians* are detected in the South, Selenga and Maloe More surface sediments, which are much higher than in the North basin. Higher abundances of *Synedra acus* var. *radians* previously detected in the upper sediments of cores taken 20 years ago in the South basin sites, compared to the North basin (Mackay et al. 1998), were attributed to areas of clearer ice or nutrient input from rivers. Recent rises in the abundance of *Synedra acus* var. *radians* has been associated with anthropogenic pollution (Julius et al. 1997; Bangs et al. 2000), however these species are

present in past diatom assemblages, and are not just a recent occurrence. *Synedra acus* var. *radians* occur within the sediment record over the Holocene, being linked to warmer climate in the Medieval Climate Anomaly (Bangs et al. 2000; Karabanov et al. 2000). Although *Synedra acus* var. *radians* have a temperature optimum of c. 15 – 17.5 °C, they also have a broad temperature range for growth, and can bloom in both the spring and summer months (Jewson et al. 2015).

Cyclotella minuta diatom species bloom in the autumn months at Lake Baikal, and have a lower temperature optimum compared to *Synedra acus* var. *radians*, of c. 8.5°C (Jewson et al. 2015). Higher abundances of *Cyclotella minuta* in the South basin suggest shorter ice cover duration than the North basin. North basin sites have the highest abundances in *Aulacoseira baicalensis*, which is a pelagic spring diatom species adapted to colder water temperatures, with a temperature optimum of c. 4°C (Jewson et al. 2009), and blooms under the ice. This diatom species is tolerant to low light levels (optimum of c. 35 $\mu\text{mol m}^{-2}\text{s}^{-1}$) (Jewson et al. 2009) and needs irradiance and turbulence to maintain its position in the water column (Granin et al. 2000). *Aulacoseira baicalensis* is also a large diatom, which requires silica for its heavily silicified cells (Julius et al. 1996). Higher abundances of *Aulacoseira baicalensis* therefore suggest longer ice cover duration, higher spring insolation and colder waters in the North compared to the rest of the lake (Bradbury et al. 1994), which was similarly found by Morley (2005). *Aulacoseira skvortzowii* also blooms under the ice in spring, although this diatom species is not fully pelagic like *Aulacoseira baicalensis* and starts growing in the near shore zones behind thermal bars before it extends into the pelagic zone in spring (Edlund and Stoermer, 2000). This diatom species is highest in abundances in the Selenga, and lowest in the North basin sites. This suggests that *Aulacoseira skvortzowii* have extended into the pelagic waters sooner in the Selenga and South basin sites, suggesting differences in seasonal dynamics between the South and North basin, with earlier ice out time and warmer waters in the South basin. Highest abundances of *Aulacoseira skvortzowii* have previously been noted in the South basin from phytoplankton analyses in 2001 - 2002 and surface sediments (Jewson et al. 2015)

Overall the South basin surface sediments have lower abundances of endemic diatoms associated with ice-cover (i.e. *Aulacoseira baicalensis*) than the North basin, and higher abundances of *Synedra acus* var. *radians*, *Stephanodiscus meyerii* and *Aulacoseira skvortzowii*, which are all associated with warmer waters. *Synedra acus* var. *radians* have previously been associated with nutrient-rich waters, and higher abundances of these species within the South, along with lower *Aulacoseira baicalensis* abundances suggests the South basin has a longer ice-free period than the North basin.

7.3.4 Production trends over the last 200 years

Previously mean Holocene CMAR at Vydrino in the South basin were found to be $5.87 \text{ g C m}^{-2} \text{ yr}^{-1}$, (Mackay et al. 2016), which is low in comparison to the range of CMAR values found within other large lakes, between $1 - 20 \text{ g C m}^{-2} \text{ yr}^{-1}$ (Alin and Johnson, 2007). In comparison to other Lake Baikal studies, the CMAR values presented in this chapter are similar to those published in Ishiwatari et al. (2005) and Müller et al. (2005). Recent increases in CMAR over the past 100 years have been seen in other large lakes, such as Lake Ontario, and this has been linked to anthropogenic nutrient enrichment (Hodell and Schelske, 1998).

Over the last 50 years, CMAR has increased lake-wide, with the greatest change observed in the Selenga and South basin sites (*Figure 141*). The South basin shows an increase from c. $0.25 \text{ g C m}^{-2} \text{ yr}^{-1}$ to c. $2.8 \text{ g C m}^{-2} \text{ yr}^{-1}$ in 2012, and the Selenga shows an increase from c. $1.3 \text{ g C m}^{-2} \text{ yr}^{-1}$ to $5.0 \text{ g C m}^{-2} \text{ yr}^{-1}$ in 2012 (*Figure 141*). This trend towards increasing CMAR is likely to be a result of permafrost thaw in Baikal's catchment during the warm, wet summers (Mackay et al. 2016). The $\delta^{13}\text{C}$ values similarly show an increasing trend towards more positive values over the last 50 years in the Selenga (BAIK13-10A) and Maloe More (BAIK13-14C) (*Figure 136*; *Figure 138*). The factors which could be explaining the $\delta^{13}\text{C}$ values over the last 200 years in Lake Baikal are pelagic productivity, catchment input, and it has been suggested that gas hydrates could be an influence. The presence of large reservoirs of gas hydrates has been detected in Baikal's sediments from seismic profiling, and are thought to be a potential source of low $\delta^{13}\text{C}$ to the TDIC pool (Klerkx et al. 2003). The location of gas hydrates within Lake Baikal has been suggested to be within the abyssal areas near the Selenga Delta in the South and Central basins, extending over 4000 km^2 and ranging between $34 - 450 \text{ m}$ in depth (Golmshtok et al. 1997; Kuzmin et al. 2000). It is thought that the methane gas hydrates became unstable due to warming lake waters, providing a depleted carbon source (c. -60 ‰) from bacterial activity, lowering the isotopic composition of the TDIC pool utilised by algae (Klerkx et al. 2003 Prokopenko and Williams, 2004). Baikal's bulk sediments may be influenced by methane release, with low $\delta^{13}\text{C}$ values in glacial periods and higher $\delta^{13}\text{C}$ values in interglacial periods, due to increased aquatic production and methane release (Prokopenko and Williams, 2004). Fluctuations in $\delta^{13}\text{C}$ values over the last 130 years correspond to global methane levels detected within the Vostok ice core (Prokopenko and Williams, 2004). In Lake Baikal, it is unclear as to whether gas hydrate release is due to climatically induced changes in mixing regimes (Prokopenko and Williams, 2004) or by tectonic activity via thermal pulses (Granin and Granina, 2002; Vanneste et al. 2003; Van Rensbergen et al. 2003). Furthermore, $\delta^{13}\text{C}$ records from sediment cores taken in the North basin (Ishiwatari et al. 1992), where no gas hydrates have been detected, show similar trends

to the cores taken within the gas hydrate areas (Prokopenko et al. 1993; Prokopenko and Williams, 2004). If methane release is influencing the $\delta^{13}\text{C}$ signal, then this lake-wide similarity in $\delta^{13}\text{C}$ trends suggest that gas hydrates are not a local effect on $\delta^{13}\text{C}$ values of bulk sediments, and are transported throughout the lake by mixing (Morley, 2005). However, despite the aforementioned studies, it is unlikely that gas hydrates are a significant factor in controlling the $\delta^{13}\text{C}$ values (Mackay et al. 2016).

Higher $\delta^{13}\text{C}$ values could possibly be showing the LIA in some of the pigment records presented within this chapter. This is as carbon isotope records over the last glacial to interglacial transition show that the $\delta^{13}\text{C}$ values were higher in the glacial periods (c. -18 to -24 ‰) than the interglacial periods (c. -28 to -30 ‰) (Brincat et al. 2000; Prokopenko and Williams, 2001; Wantanabe et al. 2004; Mackay et al. 2016) suggesting greater productivity in colder climatic conditions than warmer, if primary production is driving the $\delta^{13}\text{C}$ signal. Less positive $\delta^{13}\text{C}_{\text{organic}}$ values in the interglacial periods could be due to more ^{12}C being available in the warm intervals compared to the glacial periods, with changes in the terrestrial ecosystem. These changes include taiga forest expansion (Demske et al. 2005), which would result in greater soil respiration and therefore more carbon dioxide depleted in ^{13}C entering the lake waters from river inflows (Hammarlund et al. 1992). Less ^{13}C enriched sediments in the Holocene could also be due to algal compositional changes in the lake waters (Mackay et al. 2016). Higher levels of diatom production in the Holocene compared to the glacial period would lead to lower $\delta^{13}\text{C}$ values of bulk sediments, due to the isotopic composition of diatoms. *Aulacoseria baicalensis*, has a carbon isotopic composition between -28.8 and -29.5 ‰ (Yoshii et al. 1999). Thus, both forest expansion and increase diatom production is suggested to be driving the $\delta^{13}\text{C}$ signal in the early Holocene.

In the late Holocene, the $\delta^{13}\text{C}_{\text{organic}}$ values become more positive with higher TOC/N ratios and TOC % values, like in the early Holocene, and so the forest expansion is not driving the $\delta^{13}\text{C}$ signal. Instead, a decline in diatom production, and a rise in picocyanobacterial abundance is suggested to be the cause of the late Holocene $\delta^{13}\text{C}$ signal (Mackay et al. 2016). This is as, in contrast to diatoms, picocyanobacteria dominate the summer-stratified waters of Lake Baikal (Belykh and Sorokovikova, 2010), and this algal group have a higher carbon isotopic composition than diatoms (c. -22.7 ‰). Therefore, higher abundances of picocyanobacteria could result in more positive $\delta^{13}\text{C}$ values within Baikal's sediments, as $\delta^{13}\text{C}$ values of picoplankton have been found to range between -22 ‰ to -30 ‰ (Sakata et al. 1997). Higher $\delta^{13}\text{C}$ values in some of the sediment records (beyond the last 200 years) presented in Chapter Six coincide with higher picocyanobacterial abundances. Over the last 200 years, increasing

picocyanobacterial pigment abundances are not seen lake-wide within the sediment records presented in this chapter, alongside rising $\delta^{13}\text{C}$ values.

To further analyse the carbon source, Rock Eval analyses carried out on sediments from BAIK13-1C and BAIK-19B shows that the carbon within the South and North basin sediments is likely to be more algal-derived due to the higher HI values and lower OI values than the Selenga sediments. However, the peaks in the OI and subsequent decreases in the HI at the North basin may be a result of the river inputs from the Upper Angara. The peak in the TOC/N ratios at the South basin (BAIK13-1C) corresponds with an increase in OI values and decrease in HI at c. 20 cm depth, suggesting a shift to more terrestrial carbon sources (*Figure 144*). The carbon source from the Selenga core is likely to be more mixed, due to the generally higher OI values and lower HI values. Therefore, this possibly reflects degradation via transport and terrestrial input from the Selenga River. Overall the TOC/N ratios in the Selenga core are not showing degradation, but reflecting the mixture in carbon sources, as it matches the trend in HI values rather than OI values (*Figure 144*). Rock Eval measurements from the Selenga delta sediments (*Figure 144*) show similar HI values (138 – 144) to the Selenga core, but lower OI values (53 – 56). The lower OI values suggest higher degradation of organic matter in the Selenga River sediment, compared to the lake site close to the Selenga. HI/OI ratios are generally > 1 in the South, North and Selenga sites, and the HI/OI ratio are higher in the South and North basin sediments than at the Selenga site. However, in the South basin, the HI/OI ratio decreases to < 1 at c. 20 cm, supporting the interpretations of greater degradation inferred from the higher TOC/N values and OI values.

Results in this chapter show that the oxidised layers are not significantly influencing pigment preservation, and the pigment concentrations are not exponentially declining. There are production trends over the last 200 years, and differences across the lake. There are lake-wide increasing Chlas concentrations and increasing CMARs and carbon isotopic values. Previous studies have found that in deep lakes, such as Lake Baikal, accumulated Chlas (concentrations of chlorophyll-*a* and its degradation products) represent total algal biomass (Fietz et al. 2007), providing a good reflection of the historic phytoplankton standing crop and autochthonous productivity, and used as an indicator for global climatic changes (Fietz et al. 2007). The sedimentary pigment profiles do not show an exponential decline in Chlas or carotenoids, but show variation in concentrations down-core over the last 200 years. This contrasts with previous pigment work at Lake Baikal (Fietz, 2005; Fietz et al. 2007). Fietz et al. (2007) found that the Chlas within the upper 10 cm of the sediment cores from the South, Selenga and North basins showed degradation profiles, as the Chlas decrease was greater than the TOC decline down-core, declining exponentially. This is suggested to be due to strong degradation within

the oxidised layer of the three short cores, rather than changing productivity, with degradation below the oxidised layer in these cores is minimal (Fietz et al. 2007).

The South basin, Selenga and Maloe More have higher Chlas concentrations than the North basin. Fietz (2005) also found differences in phytoplankton production between the North and South basin, with higher chlorophyll-*a* concentrations in the South basin and Selenga sites. Chlas concentrations increase over the last 200 years, showing higher mean concentrations post-1950 than pre-1950. However, Chlas begin to rise prior to 1950 in the South basin and Selenga Delta sites (significant break point at 1935 AD), unlike the sites in Maloe More Bay (significant break point at 1984 AD) and in the North basin where Chlas begin to rise in concentrations at or after 1950. Therefore, the South and North basins are not showing synchronous changes in total algal production. The $\delta^{13}\text{C}$ values are becoming more positive over the last 200 years across the lake (except at BAIK13-7A), however the increase is only synchronous with the Chlas increase at Maloe More and the Selenga and not the rest of the lake (*Table 54*).

The production increase seen from the $\delta^{13}\text{C}$ data could be algal derived, as the TOC/N ratios indicate the carbon source is predominately algal derived. $\delta^{13}\text{C}$ has been found to provide a reliable proxy for productivity as carbon degradation does not alter the $\delta^{13}\text{C} / \delta^{12}\text{C}$ ratio of the bulk material, and does not modify the fractionation, which occurs at the surface waters. Microbial reworking of organic matter can potentially alter the $\delta^{13}\text{C}$ signal of bulk carbon (Meyers and Ishiwatari. 1993; Torres et al. 2012), however studies which have a TOC content (1.8 – 4.6 %) similar to Lake Baikal, such as Lake Michigan (Rea et al. 1980), Lake Ontario (Schelske and Hodell, 1991), Lake Superior (O'Beirne et al. 2015) and New Zealand fjords (Schüller and Savage, 2011) show no diagenetic alterations to the $\delta^{13}\text{C}$ ratio of total organic carbon. Rock Eval data suggests that the bulk carbon in the pelagic South and North basin cores were dominated to a greater extent by algal material than carbon within the Selenga delta core, due to the higher HI values. However, the TOC/N values are not higher in the Selenga cores compared to the pelagic basin cores. TOC/N values in the Selenga cores appear to be reflecting carbon source, as the TOC/N fluctuation coincide with HI variations. In contrast the TOC/N values in the South basin core appear to be reflecting degradation, as higher TOC/N values occur alongside higher OI values. The HI values in Baikal's sediments are similar to those measured in modern marine sediments (HI values c. 200 – 300 mg HC/g TOC) (Hare et al. 2014), and the threshold which characterises the transition to mainly terrestrial material is c. 100 mg HC/g TOC. Sediments from Lake Ohrid, which is a deep ancient lake, has HI values of 250 mg HC/g TOC and OI values of 150 during the Holocene (Lacey et al. 2014). Similarly, RE measurements from Hudson Bay sediments have low HI

values (100 – 250 mg HC/g TOC) and a low HI/OI ratio (< 1), which suggest either a high degree of degradation or large contributions from terrigenous organic matter in both Lake Ohrid and Hudson Bay (Hare et al. 2014).

7.3.5 Composition trends over the last 200 years

The decreasing diatom pigment (diatoxanthin) concentrations, and decreasing diatom valve concentrations, indicate declining diatom production in the South basin. Diatoxanthin to canthaxanthin ratio shows the relative contribution of diatoms and chrysophytes (diatoxanthin) and picocyanobacteria (canthaxanthin). The Selenga, Maloe More and South basin show a decreasing diatoxanthin: canthaxanthin ratio with increasing regional temperatures and decreasing ice cover, whereas, these trends are not shown in the North basin at BAIK13-19B. The results presented in this thesis suggest a declining diatom crop at Lake Baikal, which could be due lake water temperatures and/or nutrient concentrations. This corresponds to monitoring records in the South basin, which have found decreasing trend abundances of under-ice diatoms over the last few decades (Silow et al. 2016).

Higher TP concentrations have been measured in August 2013 (as shown in Chapter Five), which are higher than previous measurements in pelagic waters at Lake Baikal. As seen in Chapter Four, nutrient enrichment could result in algal competition under changing nutrient levels. Thus, higher TP concentrations could lead to picoplankton and chlorophytes outcompeting diatoms. Limnological surveys in August 2013 also show that there are higher abundances of picocyanobacteria pigments (zeaxanthin) in August 2013, compared to previous measurements in summer 2001 – 2003 by Fietz (2005), which could be a result of nutrient enrichment and/or longer thermal stratification period at Lake Baikal. Also from work published by Timoshkin et al. 2015, it is known that there have been recent changes in the coastal regions at Lake Baikal, due to nutrient input, resulting in the growth of algal blooms of cyanobacteria and chlorophytes. Alongside anthropogenic impact, there have been ice cover changes recorded at Lake Baikal, with a declining trend in ice cover duration and thickness. Thus, a decline in under ice diatom production, and changes within the thermal stratification of Lake Baikal's pelagic waters which are a recorded trend of shallowing of the mixing layer, would impact Baikal's diatom crop. Another factor to consider is the dissolved silica reservoir. Silicate concentrations measured in August 2013 (as shown in Chapter Five) are at the silica limitation level, which could be a result of diatom growth depleting the silica reservoirs, and thus the silica depletion hypothesis. The Selenga River, however, is a large inflow of silicate into Lake Baikal, and it is unlikely that silicate will become limited within the pelagic waters. It is more likely that changes in both climate (ice cover and stratification)

and nutrients (algal competition) are driving the declining diatom crop trend seen at Lake Baikal. This has been addressed by RDA analysis in Chapter Seven, which shows decreasing diatoxanthin concentrations (diatom pigment) with increased air temperatures and tourist activity at BAIK13-14, in Maloe More.

There are also diatom compositional changes observed over the last few decades, with decreasing abundances of *Aulacoseira baicalensis* in the South basin, Selenga and North basin. Sedimentary diatom assemblages within the upper sediments across the lake show small increases in the non-endemic *Synedra acus* var. *radians* diatom species within the South basin surface sediments, whereas no increases in *Synedra acus* var. *radians* were found in the North basin surface sediments. Phytoplankton monitoring has found a decreasing trend in Baikal endemics (*Aulacoseira baicalensis*, *Aulacoseira skvortzowii* and *Stephanodiscus meyerii*), and an increasing trend in *Synedra acus* var. *radians* abundance between 1955 and 2005 (Silow, 2014). Increases in the number of non-endemic small diatom species have been observed since 1973, and the decreases in the large endemic diatom species is associated with declining under ice production (Silow, 2014). Popovskaya (2000) also found an increase in *Synedra acus* var. *radians* in phytoplankton over the last decade in the South basin, along with *Nitzschia acicularis*, which is not found in Baikal's sediments. These observed changes agree with diatom assemblages presented in this chapter in the surface sediments.

Similar carotenoids (alloxanthin, diatoxanthin, lutein and canthaxanthin) have been detected in the South basin, Selenga Delta and North basin short cores as found by Fietz (2005). Fietz (2005) found highest pigment diversity in the South and Selenga cores, similar to the results presented in this chapter, and fucoxanthin were found in the Selenga Delta sites. However, fucoxanthin was only detected in the Selenga Delta site, whereas Fietz et al. (2007) found this diatom pigment in the South basin sites (Fietz et al. 2007).

7.3.6 Linking production and floristic changes to anthropogenic pollution and/or climate response

Temperatures within the Baikal region have increased rapidly over the last 20 years (Shimaraev and Domysheva, 2013). Average surface water temperature between May-September in the South basin rose by 0.25 – 0.35°C per decade over the last 100 years, with a rapid rise by the mid-1990s (Shimaraev and Domysheva, 2013). These trends are similar across the whole lake, however average surface water temperatures rose faster in the Central and North basin, by c. 0.5 - 0.6 °C per decade (Shimaraev and Domysheva, 2013). Over the last few decades there has been a rise in lake warming and development within Baikal's

watershed (Brunello et al. 2004; Shimaraev and Domysheva, 2013), and sediment records show recent production and floristic changes within the primary producers via algal pigment, diatom assemblages and carbon isotopic changes of bulk sediments. Increases in carbon sequestration since the 1990s, as shown by CMAR changes, are more pronounced in the Selenga and Maloe More sites, than in the pelagic South and North basins.

Results from the spatial-temporal analyses suggest that biological changes may have occurred in Lake Baikal associated with lake warming and reduced seasonal ice-cover, but there is no evidence of wide-spread pelagic eutrophication within the sediment record, except for perhaps at Maloe More Bay. The Maloe More pigment record showed the highest chlorophyll-*b* and lutein concentrations, which are biomarkers of chlorophytes, compared to concentrations in sediment records from rest of the sites. Mann-Kendall coefficients also show significant increasing trends in chlorophyte pigments since c. 1960 AD in the South basin and Maloe More. Recent monitoring at Lake Baikal have found blooms of filamentous green algae, namely *Spirogyra*, along the coastal zones in the South and North basin, and have associated their occurrence with nutrient input from settlements (Timoshkin et al. 2016). However, the pelagic South and North basin sites are likely to be too far from the shoreline to detect the benthic algal blooms found by Timoshkin et al. (2016), providing evidence that the deep pelagic system is not yet affected. Subtle increases in total algae (chlorophyll-*a* concentrations) are seen prior to regional human influence (pre-1950) in the pelagic South and North basin, whereas at the Selenga and in the littoral regions, such as Maloe More, total algae begins to increase post-1950 and the rise in concentrations is more pronounced. The production trends seen in the South basin over the last 200 years from the chlorophyll-*a* concentrations, chlas flux, $\delta^{13}\text{C}$ values and CMAR are likely to be a result of lake warming since the LIA, which has been reported within limnological studies at Lake Baikal over a 26-year period between 1977 – 2003 (Izmesteva et al. 2015). Decreasing diatoxanthin: canthaxanthin ratios in the Selenga and Maloe More sites, and decreasing diatom concentrations in the South basin and Selenga over the last 200 years also suggest changes in ecological structure which could be linked to ice cover changes. After the LIA, reduced ice-cover duration would have decreased the abundances of large endemic diatoms, which grow under the ice, and the longer summer growing seasons would promote higher abundances of picocyanobacteria. Furthermore, Mann-Kendall coefficients show significant decreasing trends in the diatom pigment (diatoxanthin) from sediments at the Selenga and Maloe More sites, suggesting a decline in under ice diatom production (between 1940 – 1970 AD), and significant increasing trends in picocyanobacteria pigment (canthaxanthin) at c. 1960 in the South basin. However, overall floristic changes with temperature are largely seen in the Selenga and Maloe More sites, as indicated by PCA axis one scores and MK coefficients.

Carbon isotopic data suggests that both the South basin, Selenga and Maloe More are responding to climate, with increase $\delta^{13}\text{C}$ values over the last 200 years, which is also seen in correlations between Chlas concentrations and temperature. However, Chlas concentrations and $\delta^{13}\text{C}$ values in sediment from the North basins sites were not responding to the climate changes presented in the South basin record. The two basins are behaving differently in terms of algal production and floristic change. The South basin is responding more to increasing regional air temperatures than the North basin, which could be due to the influence of the Selenga River waters and changing ice cover parameters e.g. later ice on and shortened duration. Maloe More Bay shows distinct differences compared to the pelagic sites, and suggests that this site may be showing evidence of human influence due to the recent rises in chlorophytes, which match monitoring findings across the littoral regions of the lake.

The rise in Chlas concentrations occurs before the increase in SCP concentrations in South basin and the Selenga sites, further supporting that primary production changes in the pelagic basins is prior to main industrial influence within the region. However, SCPs are derived from high temperature fossil fuel combustion linked to metal smelting and generation of power from burning of fossil fuel combustion, and therefore agricultural impacts may have been an influence on aquatic primary production before the SCP rise.

RDA analyses shows that tourist activity is likely to be having an influence on algal community composition, especially within shallower bay regions, such as Maloe More Bay. It is likely that Maloe More exhibits a greater influence by anthropogenic activity over the last few decades, in comparison to the pelagic south basin sites. But it is likely that both climate and anthropogenic activity are impacting all regions of the lake now, and although there are no human records to test these results, anthropogenic activity cannot be ruled out. Anthropogenic impacts need to be taken into consideration, especially seen as shoreline regions show cultural eutrophication and the total phosphorus concentrations measured in August 2013 are higher than expected. These phosphorus values are only a snap shot in time, but they are comparable to measurements taken at the same time (August 2013) by O'Donnell et al. (2017) and do suggest values higher than those previously measured in 1995 – 2009 of natural variability (Silow, unpublished). As anthropogenic data cannot be included, instead trends pre and post 1950 are taken into account, to look at timing of changes, although it is important to note that this does not attempt to disentangle climate from human influence, and both could be acting on the algal communities over the last few decades.

Findings from Chapter Five also show increasing concentrations within chlorophyll-*a* concentrations which follow a trend from previous monitoring work, and a rise in the abundance of chlorophyte pigments in Maloe More Bay. Chlorophyll-*a* profiles (from August 2013) show higher algal production in the upper waters and no distinct DCM, which is characteristic of eutrophication, as the DCM moves upwards. This could be as the South basin is more productive naturally but as the chlorophyll-*a* trends show a continuing trend over the last few decades and production is now higher it cannot be ruled out that this is both anthropogenic and climate influenced. Alongside the chlorophyll-*a* water column profiles there are the phosphorus concentrations which show values which fall within the mesotrophic and eutrophic range. Furthermore, the rise in lutein concentrations, which are seen in sedimentary record of BAIK13-14 in Maloe More could be due to changes in thermal stratification and/or nutrient concentrations. Nutrient levels could be driving this algal community change, as experimental studies presented in Chapter Four show an increase in chlorophyte pigments with N+P enrichment. Thus, more monitoring work is needed, but the survey work presented in Chapter Five along with this palaeo work presented in this chapter suggest that climate is not solely influencing the pelagic regions of the lake.

7.4 Summary

Results show that pigment preservation within the sediments is site-specific, being affected by sedimentation rates and water column depth. One of the North and South basin sites show extensive degradation, and are not suitable for further analyses. Suitable pigment records from the South and North basin, Maloe More Bay and the Selenga Shallows, were interpreted in terms of production rather than degradation profiles. Oxic layers are not significantly influencing the pigment preservation in these sediment cores, and the pigments are not co-varying and showing exponential decay profiles. These records are similar to those previously published at Lake Baikal by Fietz (2005), in terms of the carotenoids detected across the lake and spatial production patterns, however the research presented in this thesis found intact chlorophyll-*a* within the sediments and the pigment profiles do not show exponential decay in the oxidised layers. Results in this chapter suggest that the carbon in the pelagic basins is predominantly derived from phytoplankton production rather than terrestrial input at Lake Baikal. Both TOC/N and Rock Eval data suggests predominantly algal source in the South, North, Maloe More and Selenga sites, with more mixed sources and greater oxidation of material at the Selenga site. The $\delta^{13}\text{C}$ signal is likely to be largely influenced by phytoplankton composition and production, and ice cover dynamics at Lake Baikal, and can therefore be used as a proxy to investigate past production in these sediments. The pigment records and carbon isotopic records correlate at the Selenga and Maloe More sites, showing increasing Chl_a

concentrations with increasing $\delta^{13}\text{C}$ values, and the timing is relatively synchronous suggesting they are responding to the same drivers of climate change as increasing trends begin prior to anthropogenic influence within the Baikal region. This positive relationship between Chlas concentration and $\delta^{13}\text{C}$ values is not shown in the South or North basin. In the North basin, there is no significant increase in $\delta^{13}\text{C}$ values, and in the South basin, there is no significant increase in Chlas concentrations over the last 200 years as reflected from the Mann-Kendall trend test. Pigments also match the diatom assemblage changes, with both suggesting decreasing diatom production in the South, Selenga and Maloe More sites, but not in the North basin. Overall, the Selenga and Maloe More pigment records show greater production, along with floristic change, over the last 200 years. Production changes are seen between two intervals over the last 200 years, as pre-1950 the Chlas concentrations are lower, the $\delta^{13}\text{C}$ values are more negative and the diatom concentrations are higher in the pelagic South and North basin sites, Maloe More and Selenga sites. MK coefficients show significant trends in pigments occurring the earliest at the Selenga site (between 1930 – 1950 AD) and then significant trends are detected in the pelagic South and North basin sites between 1960 – 1970 AD. The timing of significant trends in Maloe More occur at the same time as in the pelagic basins, however more recent changes are also observed, with significant trends in pigments between 1980 – 2002 AD. Therefore, the river influenced site shows the earliest signs of algal change, and the algal changes within the pelagic waters occur at similar times within the South and North basin. However, Maloe More Bay additionally shows more recent trends in algal production, differing from the trends seen in the pelagic basin and river influenced sites. Results from Maloe More could potentially be showing recent eutrophication evidence, with increasing abundances of chlorophytes over the last 60 years.

Pigments can be used as a proxy for reconstructing past algal community structure and abundance, at sites which are productive, such as within shallow littoral bay regions and close to major river inflows (< 200 m water depth). Lake-wide increases in production have been observed from algal pigment and $\delta^{13}\text{C}$ records, which occur prior to human influence in the South basin only. Production increases in the North basin are less pronounced than the South basin. Compositional changes are largely seen over the last 60 years in the South basin, Selenga and Maloe More Bay. There is a decreasing trend in diatom production with lake warming in the South basin and Selenga, and increases in picocyanobacteria concentrations in both North and South basin. Recent compositional change in Maloe More Bay might be showing signs of eutrophication, with increasing concentrations of chlorophyte pigments.

Chapter Eight: Synthesis and future research at Lake Baikal

The main objective of this thesis was to employ limnological and palaeolimnological techniques to examine if there is evidence of eutrophication and/or climate change impacts at Lake Baikal. Sites were selected across the South basin, Selenga Shallows, Maloe More Bay, Chivsky Bay and North basin. Recent observations of increases in aquatic primary production (chlorophyll-*a* concentrations) in the pelagic South basin have been seen by Izmeteva et al. (2016). There have also been recent observations of blooms of chlorophytes in the coastal regions (Timoshkin et al. 2016), which has prompted questions about whether the pelagic waters of Lake Baikal are showing signs of eutrophication. Another question raised, was whether sedimentary fossil pigment and $\delta^{13}\text{C}$ records can be used to track limnological change and historic trends in primary production, and whether enhanced primary production is due to nutrient enrichment (nitrogen and phosphorus) from regional anthropogenic activity or from recent climatic changes. Experimental studies of nutrient enrichment have been carried out within this thesis (Chapter Four), to explore the influence of nutrients (nitrogen + phosphorus and nitrogen + phosphorus + silicon treatments) on Baikal's algal groups, and examine the nutrient-driven changes in pelagic phytoplankton. Water column profiles of chlorophyll-*a*, nutrients and other algal group pigments, such as diatoms, chlorophytes and picocyanobacteria, were collected from 15 water sampling sites across the lake to examine modern day conditions and spatial differences in limnological parameters (i.e mixing layer depth, light penetration, DCM formation, euphotic zone depth) (Chapter Five). The sediments covering the last 200 years within the ^{210}Pb dated cores are undisturbed, except for in one South basin core (BAIK13-4F) where turbidite sections have been removed. Pigment, $\delta^{13}\text{C}_{\text{organic carbon}}$ and diatom concentration trends have been examined pre and post 1950 AD, to explore patterns in production before and after the timing of main anthropogenic influence within the Baikal region (Brunello et al. 2004) (Chapter Seven). Long-term trends in primary production have been analysed from the sediment cores, to put limnological changes observed over the last 200 years into context with natural variability, and to explore any evidence of late Holocene climatic events (Chapter Six).

8.1 Site selection for environmental reconstruction at Lake Baikal

Short cores collected show spatial variation in sedimentation rates, oxidised layers and turbidites across Lake Baikal. Cores from these regions were found to be suitable for investigating past production trends over the last c. 200 years. Pelagic South (BAIK13-1C;

BAIK13-4F; BAIK13-7A), North basin (BAIK13-18A) and Maloe More (BAIK13-14) sites were found to be the most influenced by turbidites. However, sediment cores from the Selenga Shallows (BAIK-10A), opposite the Selenga Delta (BAIK13-11C), and close to the Upper Angara River in the North basin (BAIK13-19B) had no or minimal turbidite disturbance within the bottom sediments. Even though sedimentation rates and sediment formation varies across Lake Baikal, sediment cores from the sites presented in this thesis show that cores can be used for reconstructions over longer time periods within the late Holocene. Baikal's sediments can be used for primary production reconstructions as the sediment accumulation rate allows high resolution studies covering the last 200 years. For longer term reconstructions, the turbidite sections at the bottom of these cores would need to be removed, and these cores would also need to be radiocarbon dated as it is problematic to extend the ^{210}Pb chronologies over the entire sediment core due to assumptions with sedimentation rates.

The varying fossil pigment record highlights the importance of coring site location, as burial rate and water column depth influence the reliability of the pigment record preserved. Oxidation of organic matter at sites with low sedimentation rates, i.e. at deep water sites (> 1,000m in water depth) in the South (BAIK13-7A) and North basin (BAIK13-18A), also have implications on the use of $\delta^{13}\text{C}$ and Chl *a* concentrations as production records. ^{210}Pb dated sedimentary fossil pigment records from 6 of the 10 selected coring sites suggest that pigments can be used to reconstruct past floristic changes and production. This is because the pigment records do not show an exponential decay in concentrations but instead a variation in the concentrations down-core. Furthermore, the pigments do not show significant co-variations and are not greatly influenced by the presence of oxidised layers within the upper sediments. Thus, pigments can be used as a production proxy at all the regions to test the hypothesis and look at spatial variation and historic trends in production. Only two sites (BAIK13-7A and BAIK13-18A) were found to be unsuitable for interpretation of the pigment record and had high levels of degradation. Alongside pigments, $\delta^{13}\text{C}$ records can be used to examine algal production changes as TOC/N ratios and Rock Eval analyses indicate the source of carbon to be largely derived from phytoplankton production.

8.2 Is Lake Baikal eutrophying and showing anthropogenic impacts and/or responding to climatic changes?

Winter limnology suggests a possible decline in under ice diatom production in the South basin over the last decade, with lower total algal biomass and diatom pigment concentrations in 2013 compared to previous under ice measurements in 2001 – 2003. However, the sampling only represents a snapshot in time, and more extensive measurements over the winter period

are required to validate this finding. Summer autotrophic biomass was greatest within the South basin sites, and predominantly higher within the mixing layer. Summer chlorophyll-*a* concentrations in the South basin were higher than values measured a decade ago, along with higher abundances of diatoms and picoplankton, as inferred from fucoxanthin and zeaxanthin pigment concentrations respectively. Findings from Chapter Five also suggest a change in the vertical chl-*a* profiles over the last decade, with greater algal production in the mixing layer of the South basin that restricts algal biomass in the deeper waters. Results from Chapter Four suggest that much of the variation between this study and previous published work is due to climate-driven reductions in ice duration on the lake. For example, over the last 130 years the length of the ice-free season has increased by 16 days in the southern basin (Hampton et al. 2008). In Chapter Five, environmental variables (i.e nutrients) were not significantly correlated (p value > 0.01) to the phytoplankton pigment distributions. Interestingly, a significant positive relationship was observed between picocyanobacterial pigment and DOC concentrations. This highlights the importance of DOC with Baikal's primary production, especially as DOC concentrations are likely to rise with regional climate warming, as fluvial inflows increase and regional permafrost continue to degrade.

Despite limnological surveys (Chapter Five) showing no correlation between lake water nutrient concentrations and algal community composition, it is important to note the high pelagic TP concentrations measured in August 2013. The TP concentrations measured at this time, both within this thesis and recently published work at Lake Baikal by O'Donnell et al. (2017), are higher than past values between 1995 to 2009, by c. 10 $\mu\text{g/L}$ at some sites. Given the large difference in the TP concentrations over these four years, the nutrient enrichment which has been seen within the coastal regions (Timoshkin et al. 2016), and the high TP concentrations measured within Selenga River waters in August 2013 (values over 50 $\mu\text{g/L}$) it is likely that humans are influencing pelagic algal communities. Furthermore, limnological surveys presented in Chapter Five show a difference in the summer chlorophyll-*a* profiles, with no distinct DCM detected within the South basin in August 2013, in comparison to the Central and North basin sites. A shift to shallower algal production within the water column suggests nutrient enrichment within the surface waters, and catchment measurements in August 2013 show high nutrient concentrations within the river inflows into the South basin. Thus, it is possible that the South basin is showing a greater response to climatic changes and human activity in comparison to the North basin sites, due to the greater changes seen in ice cover duration and water temperatures, and the inflow of the nutrient rich Selenga River waters.

In comparison to the bay regions, however, results from Maloe More Bay (BAIK13-14) show signs of nutrient enrichment, with a shift towards more sedimentary chlorophyte algal pigments. RDA analyses presented in Chapter Seven highlight a significant correlation between both air temperature and tourist activity on sedimentary algal pigments at BAIK13-14, with diatom pigment concentrations (diatoxanthin) declining and Chl *a* and picoplankton pigment concentrations (canthaxanthin) increasing in concentration with rising air temperatures and increased tourism. The timing of sedimentary algal pigment change within the BAIK13-14 sediment core also suggest a shift in abundance and composition post 1950 AD, when human influence within the region is known. It is, however, difficult to disentangle the impact of climate and anthropogenic activity on Baikal's algal community composition given the limited sources available for anthropogenic data (i.e. long term records for population, tourist numbers and agricultural output).

Palaeolimnological studies can be used to effectively compare conditions before and after disturbances, such as industrial activity, and can be used in absence of and in combination with monitoring data. Sedimentary pigment records (Chapter Seven) show increasing Chl *a* and are similar to monitoring studies over the last c. 30 years. These record increasing chlorophyll-*a* concentrations and decreasing diatom production in the South basin (Izmesteva et al. 2016). August 2013 results (Chapter Five) further suggest that this increasing trend in chlorophyll-*a* concentrations is continuing as well. This is as chlorophyll-*a* concentrations measured in August 2013 in the upper 50 m of the water column in the South basin are more than two-fold higher than values measured in 2005 (Hampton et al. 2008; Moore et al. 2009; Izmesteva et al. 2016). Dated lake sediment cores demonstrate chlorophyll-*a* and its diagenetic products, a proxy for whole lake primary production, have increased significantly over the last century. The Mann-Kendall analyses that were presented in Chapter Five show increasing trends in Chl *a* concentrations across the lake, and significant breakpoints were found at 1935 in the Selenga Shallows and 1984 in Maloe More Bay. Similarly, the Mann-Kendall analyses show increasing $\delta^{13}\text{C}$ values across the lake, with significant breakpoints at; 1975 in the South basin, 1952 in the Selenga Shallows and 1980 in the North basin. Although, t-test analyses show consistently higher $\delta^{13}\text{C}$ values pre-1950 than post-1950. Significant positive relationships were observed between Chl *a* concentrations and $\delta^{13}\text{C}$ values in the Selenga Shallows and Maloe More sites, suggesting response to similar drivers between these two primary production proxies. CMAR and pigment flux were analysed for patterns of primary production over the last 200 years, and show consistently increasing trends lake-wide, with highest values in the South basin, Selenga Shallows and Maloe More sites, compared to the North basin. Pigment concentrations, flux, and $\delta^{13}\text{C}$ values at pelagic sites located up to 5 km away from the main catchment area, were also consistently higher post-1950 lake-wide,

suggesting a rise in primary production prior to main anthropogenic influence. Mann-Kendall analysis showed significant increasing trends in chlorophyte pigments over the last 200 years in the South basin and Maloe More Bay, with significant breakpoints at 1965, 1958 and 2002. This very recent increase observed at Maloe More Bay supports recent work by Timoshkin et al. (2016), on eutrophication at Lake Baikal.

The findings from the chapters thus far have suggested anthropogenic influence on the pelagic regions of Lake Baikal cannot be ruled out, due to aforementioned points around; the increase in TP concentrations, known coastal nutrient enrichment and shifts within the algal community composition. Results suggest that the nutrient levels might be influenced by both climate and anthropogenic activity, however mercury contamination from the Selenga River into Lake Baikal from mining activity does not appear to be happening. Mercury concentrations within Lake Baikal's waters are similar to background global atmospheric deposition levels and do not suggest mercury pollution, but results highlight the importance of the Selenga River as a possible source of toxic trace metals. Low lake levels of mercury are also likely to be a result of dilution effects due to the huge size of Lake Baikal. Sedimentary mercury concentrations suggest no significant mercury pollution over the last century within the lake waters from industrial atmospheric deposition and/or river inflows. In terms of eutrophication, there appears to be a site-specific response, with potentially only Maloe More Bay showing evidence of both climate impacts and eutrophication over the last c. 30 years. This evidence, consisting of a rise in chlorophyte pigments over the last 30 years, which may be due to sewage inputs from expanding tourism and settlements within the Maloe More Bay region and rising temperatures.

The temperature-mediated processes which can affect primary production and subsequent concentrations of chlorophyll-*a* include reduced ice cover, lengthened growing seasons, altering light availability and nutrient dynamics and changes in lake mixing (Williamson et al. 2014). Precipitation mediated processes can also affect transport of allochthonous materials into the lake, influencing water colour and nutrient availability. Thus, observed DOC trends from limnological surveys show increasing concentrations in both the pelagic lake and river waters of Lake Baikal over the last decade, and are likely to be climate driven (Yoshioka et al. 2002; Sugiyama et al. 2014). Records also show basin specific responses to ice cover duration changes, with declining trends in under ice diatom production observed in the South basin and Selenga Shallows from diatom valve and diatom pigment concentrations. These findings support recent monitoring studies in pelagic Lake Baikal (Izmesteva et al. 2016; Silow et al. 2016). There are also significant positive relationships between average annual air temperatures in the region and Chl_a concentrations and $\delta^{13}\text{C}$ values in the South basin,

Selenga and Maloe More sites, and a decrease in diatom concentrations (valve) and diatom:canthaxanthin pigment ratios in these regions. This suggests the South basin, Selenga Shallows and Maloe More sites are responding differently to recent climatic changes and/or anthropogenic nutrient enrichment, compared to the North basin. This disparity in the response to climate is likely to be a result of; differences in the timing of ice on and off, and the influence of the Selenga River in the South basin, from the inflow of warmer river waters with elevated nutrient and DOC concentrations. Furthermore, PCA axis one scores from the pigment compositions reflect higher floristic change in the South basin over the last 30 years, and a reducing species composition over the last few decades in the Selenga and Maloe More sites, with no change in the North basin sites. Lastly, longer-term sedimentary pigment records suggest warming from LIA, and the correspondence between picoplankton pigment concentrations and $\delta^{13}\text{C}$ values might be an indication of cooler climatic conditions during the LIA. This is due to higher $\delta^{13}\text{C}$ values during cooler periods and increased picoplankton abundance.

8.3 How could Baikal's pelagic phytoplankton respond to nutrient enrichment?

Nutrient enrichment experiments show that silicon is not limiting diatom growth at Lake Baikal, instead silicon additions are influencing the growth of picocyanobacteria, which is seen in the August 2013 experiment. Nitrogen and phosphorus additions are only promoting the growth of chlorophytes in one of the March 2013 experiments, and there is no response in chlorophyll-*a* concentrations within any of the experiments. This suggests that there was no community wide response to nutrient limitation, and the algal groups have different nutrient demands. The treatments did affect the pigment concentrations and growth rates of picocyanobacteria, and chlorophytes, but not diatoms.

8.4 Further work

Short sediment cores need to be radiocarbon dated, preferably on pollen extracts (Piotrowska et al. 2004), to explore the down-core trends in more detail over the late Holocene, and any evidence of climatic events, the LIA and MCA. Although this study and others (Soma et al. 1996; Tani et al. 2002; Fietz et al. 2007) show that pigments can be used at Lake Baikal as a proxy for production, more detailed studies expanding on previous work by Fietz (2005) into pigment preservation using sediment traps is required. This would assess pigment flux into the sediments, and enable correction factors to be established and applied to pigments down-core. The contemporary limnological work of this thesis highlights a gap in the knowledge of

DOC within Lake Baikal, and its influence on microbial and phytoplankton communities. It would therefore be of interest to explore the influence of DOC on picocyanobacteria further. Findings from the experimental studies show silicon accumulation within picocyanobacterial cells. The results in this thesis highlight a gap in the knowledge of the role of picocyanobacteria within the silicon cycling in large lakes, such as Lake Baikal. The application of nutrient enrichment experiments is key to understanding the influence of nutrients on algal community dynamics. Thus, a more extensive network of nutrient enrichment experiments across Lake Baikal, and across the seasons, would be beneficial in assessing the impact of anthropogenic driven changes in lake water nutrient concentrations on Baikal's phytoplankton.

8.5 End note

The spatial survey of phytoplankton pigments, nutrients (total phosphorus, nitrate) and DOC concentrations conducted in August 2013 provides a benchmark for future surveys. Pigments have been shown to reflect phytoplankton variation caused by climatic changes and/or anthropogenic activity, over the last 50 years. The limnological findings from comparisons between data from the August 2013 and previous surveys, and the palaeolimnological findings both highlight the urgency to monitor pelagic waters along with coastal and bay regions, for the protection of Lake Baikal. Palaeolimnological results show that $\delta^{13}\text{C}$ can be used as a production proxy, and algal pigment, with caution, dependent on coring site selection in Lake Baikal (largely sedimentation rates and occurrence of turbidites within records).

Overall, given the results from the experiments (Chapter Four), Lake Baikal is susceptible to eutrophication, and sedimentary pigment records from Maloe More Bay are showing a rise in chlorophyte pigment concentrations. Results from Chapter Seven suggest that Maloe More Bay could be showing signs of nutrient enrichment, however it is more unclear what the extent of anthropogenic impact is upon the deeper pelagic basin sites. It could be that the lake is big enough to buffer any anthropogenic impact, or potentially delay its response. However, it would be unreasonable to conclude that humans have had no impact upon the open waters, given that it is known that they have in the shallow waters. Furthermore, the total phosphorus measurements in August 2013 present a new phenomenon at Lake Baikal, as these TP concentrations are higher than seen before. These nutrient values could be naturally and/or human driven, but most likely to be human driven given the extent of the increase, and the high TP concentrations measured within the Selenga River waters. Alongside TP, DOC concentrations within Lake Baikal's waters are showing an increasing trend in comparison to past studies, and are likely to be due to catchment changes. Changes in the DOC

concentrations could affect the limnological structure of the lake, impacting light penetration, but also the microbial loop, which in turn will affect the nutrient levels and algal community composition.

Overall there are no drastic algal shifts in the pelagic waters, but chlorophyll-*a* concentrations are rising (higher than they have been before). Diatom concentrations appear to be continuing the declining trend, as seen in previous work (which is seen in both waters and sediments). Diatoms could be declining due to ice cover duration (decreasing), with smaller winter blooms perhaps (smaller under ice production). Decline could also be due to changes in thermal stratification driven by increasing water temperatures, and/or changes in nutrient levels, with competition from other algal groups (more competitive picoplankton) with nutrient enrichment, and could be due to the silicate concentrations. Although unlikely to be solely due to silicate concentrations due to the inflow of Selenga waters, and diatom dissolution within the waters. All the above findings suggest the importance of undertaking further research on the impact of both humans and climate have had upon our world's largest freshwater lake.

References

Abbott, M.B., Binford, M.W., Brenner, M., Kelts, K.R. (1997). ‘A 3500 14C high-resolution record of water-level changes in Lake Titicaca, Bolivia/Peru.’ *Quaternary Research*, **47**, 169 – 180.

Adrian, R., O’Reilly, C.M., Zagarese, H., Baines, S.B., Hessen, D.O., Keller, W., Livingstone, D.M., Sommaruga, R., Straile, D., Van Donk, E., Weyhenmeyer, G.A., Winder, M. (2009). ‘Lakes as sentinels of climate change.’ *Limnology Oceanography*, **54**, (6), 2283- 2297.

Airs, R.L., Jie, C., Keely, B.J. (2000). ‘A novel sedimentary chlorin: structural evidence for a chlorophyll origin for aetioporphyrins.’ *Organic Geochemistry*, **31**, 1253 – 1256

Aizenshtat, Z. (1973). ‘Perylene and its geochemical significance’. *Geochim Cosmochim Ac.*, **37**, 559-567.

Alin, S.R., Cohen, A.S., Bills, R., Gashagaza, M.M., Michel, E., Tiercelin, J-J., Martens, K., Coveliers, P., Mboko, S.K., West, K., Soreghan, M., Kimbadi, S., Ntakimazi, G. (1999). ‘Effects of landscape distribution on animal communities in Lake Tanganyika, East Africa.’ *Conservation Biology*, **13**, (5), 1017-1033.

Alin, S.R., Johnson, T.C. (2007). ‘Carbon cycling in large lakes of the world: A synthesis of production, burial, and lake-atmosphere exchange estimates.’ *Global Biogeochemical Cycles*, **21**, 1-12.

Allan, J.D., McIntyre, P.B., Smith, S.D.P., Halpern, B.S., Boyer, G.L., Buchsbaum, A., Burton, G.A., Campbell, L.M., Chadderton, L.W., Ciborowski, J.J.H., Doran, P.J., Eder, T., Infante, D.M., Johnson, L.B., Joseph, C.A., Marino, A.L., Prusevich, A., Read, J.G., Rose, J.B., Rutherford, E.S., Sowa, S.P., Steinan, A.D. (2013). ‘Joint analysis of stressors and ecosystem services to enhance restoration effectiveness’. *Proceedings of the National Academy of Sciences*, **110**, 372-377.

Allinger, L.E, Reavie, E.D. (2013). ‘The ecological history of Lake Erie as recorded by the phytoplankton community.’ *Journal of Great Lakes Research*, **39**, 365-382

Andersen, R.A., Bidigare, R.R., Keller, M.D., Latasa, M. (1996). ‘A comparison of HPLC pigment signatures and electron microscopic observations for oligotrophic waters of the North Atlantic and Pacific Oceans.’ *Deep Sea Research II*, **43**, (2-3), 517-537.

Anderson, S.L., McIntosh, L. (1991). ‘Light-activated heterotrophic growth of the cyanobacterium *Synechocystis* sp. Strain PCC 6803: a blue-light-requiring process.’ *Journal of Bacteriology*, **173**, (9), 2761 - 2767

Anderson, N.J., Dietz, R.D., Engstrom, D.R. (2013). ‘Land-use change, not climate, controls organic carbon burial in lakes.’ *Proceedings of the Royal Society B*, **280**, 2-7.

Antipova, N.L., Kozhov, M.M. (1957). Data on seasonal and annual fluctuations of dominant forms of phytoplankton of Lake Baikal. *Proceedings of Irkutsk State University, Irkutsk*, 7 (1), 263–268.

Antipova, N. L. (1963). ‘Seasonal and annual phytoplankton changes in Lake Baikal’. *Proceeding of Limnological Institute*, **22**, 12–28.

Appleby, P.G. (2001). ‘Chronostratigraphic techniques in recent sediments.’ In: Last, W.M. & Smol, J.P. (eds.) *Tracking Environmental Change Using Lake Sediments, Volume 1: Basin Analysis, Coring, and Chronological Techniques*. Kluwer Academic Publishers, Dordrecht, 171–203.

Appleby, P.G. (2008). ‘Three decades of dating recent sediments by fallout radionuclides: a review.’ *The Holocene*, **18**, (1), 83–93.

Appleby, P.G., Oldfield, F. (1978). ‘The calculation of ^{210}Pb dates assuming a constant rate of supply of unsupported ^{210}Pb to the sediment’. *Catena*, **5**, 1-8.

Appleby, P. G., Nolan, P. J., Gifford, D. W., Godfrey, M. J., Oldfield, F., Anderson, N. J. & Battarbee, R. W. (1986). ‘Pb-210 Dating by Low Background Gamma-Counting.’ *Hydrobiologia*, **143**, 21-27.

Asaeda, T., Shinohara, R. (2012). ‘Japanese lakes. In: Bengtsson L, Herschy RW, Fairbridge RW (eds) *Encyclopedia of lakes and reservoirs*.’ Springer, New York, pp 415–421

Atlas Baikalia (1993). *Baikal Atlas*. Federal Service of Surveying and Cartography, Moscow [in Russian].

Attermeyer, K., Hornick, T., Kayler, Z.E., Bahr, A., Zwirnmann, E., Grossart, H-P., Premke, K. (2014). ‘Enhanced bacterial decomposition with increasing addition of autochthonous to allochthonous carbon without any effect on bacterial community composition.’ *Biogeosciences*, **11**, 1479-1489.

Austin, J. & Colman, S. (2008). ‘A century of temperature variability in Lake Superior.’ *Limnology and Oceanography*, **53**, 2724–2730.

Babanazarova, O., Sidelev, S., Schischeleva, S. (2013). ‘The structure of winter phytoplankton in Lake Nero, Russia, a hypertrophic lake dominated by Planktothrix-like Cyanobacteria.’ *Aquatic Biosystems*, **9**, 1 – 11.

Back, R. C., Bolgrien, D.W. (1991). ‘Phytoplankton Photosynthesis in Southern Lake Baikal: Size-Fractioned Chlorophyll a and Photosynthetic Parameters.’ *Internat. Assoc. Great Lakes Res.*, **17**, (2), 194 – 202.

Bade, D.L., Carpenter, S.R., Cole, J.J., Pace, M.L., Kritzberg, E., Van de Bogert, M.C., Cory, R.M., McKnight, D.M. (2007). ‘Sources and fates of dissolved organic carbon in lakes as determined by whole-lake carbon isotope additions.’ *Biogeochemistry*, **84**, 115-129

Baeyens, W., Dehandschutter, B., Leermakers, M., Bobrov, V.A., Hus, R., Baeyens-Volant, D. (2003). ‘Natural mercury levels in geological enriched and geological active areas: case study of Katun River and Lake Teletskoye, Altai (Siberia).’ *Water, Air and Soil Pollution*, **142**, 375-393

Bagheri, S., Mansor, M., Turkoglu, M., Makaremi, M., Omar, W.M.W., Negarestan, H. (2012). ‘Phytoplankton species composition and abundance in the southwestern Caspian Sea.’ *Ekoloji* **21**, **83**, 32 – 43.

Baines, S.B., Twining, B.S., Brzezinski, M.A., Krause, J.W., Vogt, S., Assael, D., McDaniel, H. (2012). ‘Significant silicon accumulation by marine picocyanobacteria.’ *Nature Geoscience*, **5**, 886 – 891.

Bangs M., Battarbee R.W., Flower R.J., Jewson D., Lees J.A., Sturm M., Vologina E.G. and Mackay A.W. (2000). ‘Climate change in Lake Baikal: diatom evidence in an area of continuous sedimentation.’ *International Journal of Earth Sciences*, **89**, 251-259.

Barbiero, R.P., Tuchman, M.L. (2001). ‘Results from the U.S. EPA’s Biological Open Water Surveillance Program of the Laurentian Great Lakes: II. Deep Chlorophyll Maxima.’ *Journal of Great Lakes Research*, **27**, (2), 155-166

Barlow, R.G., Burkill, P.H., Mantoura, R.F.C. (1988). ‘Grazing and degradation of algal pigments by marine protozoan *Oxyrrhis marina*.’ *J. Exp. Mar. Biol. Ecol.*, **119**, 119-129

Battarbee R.W. and Kneen M. (1982). ‘The use of electronically counted microspheres in absolute diatom analysis.’ *Limnology and Oceanography*, **27**, 184-188.

Battarbee, R.W., Mackay, A.W., Jewson, D.H., Ryves, D.B., Sturm, M. (2005). ‘Differential dissolution of Lake Baikal diatoms: correction factors and implications for palaeoclimatic reconstruction.’ *Global and Planetary Change*, **46**, 75-86.

Batimaa, P., Myagmarjav, B., Batnasan, N., Jadambaa, N., Khishgsuren, P. (2011). ‘Urban water vulnerability to climate change in Mongolia.’ In: Ministry of Nature, Environment and Tourism report, p 78.

Bayamba B, Todo Y (2011). ‘Technological impact of placer gold mine on water quality: case of Tuul river valley in the Zaamar Goldfield, Mongolia.’ *Eng Tech*, **75**, 167–17.5

Beardall, J., Young, E., Roberts, S. (2001). ‘Approaches for determining phytoplankton nutrient limitation.’ *Aquatic Science*, **63**, 44-69.

Beeton, A.M. (2002). ‘Large freshwater lakes: present state, trends, and future.’ *Environmental Conservation*, **29**, (1), 21 – 38.

Belykh, O.I., Sorokovikova, E.G. (2003). ‘Autotrophic picoplankton in Lake Baikal: Abundance, dynamics, and distribution.’ *Aquatic Ecosystem Health and Management*, **6**, (3), 251-261.

Belykh, O.I., Ekaterina, G., Sorokovikova, T., Saphonova, A., Tikhonova, I.V. (2006). ‘Autotrophic picoplankton of Lake Baikal: composition, abundance and structure.’ *Hydrobiologia*, **568**, 9-17.

Bertilsson, S., Burgin, A., Carey, C.C., Fey, S.B., Grossart, H-P., Grubisic, L.M., Jones, I.D., Kirillin, G., Lennon, J.T., Shade, a., Smyth, R.L. (2013). ‘The under-ice microbiome of seasonally frozen lakes.’ *Limnol. Oceanogr.*, **58**, (6), 1998 – 2012.

Bertrand, S., Sterken, M., Vargas-Ramirez, L., De Batist, M., Vyverman, W., Lepoint, G., Fagel, N., (2010). ‘Bulk organic geochemistry of sediments from Puyehue Lake and its watershed (Chile, 40°S. Implications for paleoenvironmental reconstructions.’ *Palaeogeography, Palaeoclimatology, Palaeoecology*, **294**, 56-71.

Bertrand, S., Araneda, A., Vargas, P., Jana, P., Fagel, P., Urrutia, R. (2012). ‘Using the N/C ratio to correct bulk radiocarbon ages from lake sediments: Insights from Chilean Patagonia.’ *Quaternary Geochronology*, **12**, 23 – 29.

Bezrukova, E.V., Belov, A.V., Abzaeva, A.A., Letunova, P.P., Orlova, L.A., Sokolova, L.P., Kulagina, N.V., Fisher, E.E. (2006). ‘First high-resolution dated records of vegetation and climate changes on the Lake Baikal northern shore in the middle-late Holocene.’ *Doklady Earth Sciences*, **411**, (8), 1331-1335.

Bezrukova, E.V., Hildebrandt, S., Letunova, P.P., Ivanov, E.V., Orlova, L.A., Müller, S., Tarasov, P.E. (2013). ‘Vegetation dynamics around Lake Baikal since the middle Holocene reconstructed from the pollen and botanical composition analyses of peat sediments: Implications for paleoclimatic and archaeological research.’ *Quaternary International*, **290-291**, 35-45.

Bianchi, T.S., Johansson, B., Elmgren, R. (2000). ‘Breakdown of phytoplankton pigments in Baltic sediments: effects of anoxia and loss of deposit – feeding macrofauna.’ *Journal of Experimental Marine Biology and Ecology*, **251**, 161 – 183.

Bianchi, T. S. (2007). Biogeochemistry of estuaries. Oxford University Press, Oxford, New York.

Bianchi, T., Canuel, E. (2011). Chemical biomarkers in aquatic ecosystems. Princeton University Press, Princeton and Oxford.

Björck, S., Wohlfarth, B. (2001). 14C chronostratigraphic techniques in paleolimnology. In: Last, W.M., Smol, J.P. (Eds.), Tracking Environmental Change Using Lake Sediments. Basin Analysis, Coring, and Chronological Techniques, Vol. 1. Kluwer, Dordrecht, pp. 205 - 245.

Boes, X., Piotrovskaya, N., Fagel, N. (2005). 'High-resolution diatom/clay record in Lake Baikal from grey-scale and magnetic susceptibility over Termination I.' *Global Planet Change*, **46**, 299 – 314.

Bradbury, J. P., Bezrukova, Y. V., Chernyaeva, G. P., Colman, S. M., Khursevich, G., King, J. W. & Likhoshway, Ye. V. (1994). 'A synthesis of post-glacial diatom records from Lake Baikal.' *Journal of Paleolimnology*, **10**, 213-252.

Bradley, R.S. (2003). Climate forcing during the Holocene. In: Mackay, A.W., Battarbee, R.W., Birks, H.J.B., Oldfield, F. (Eds.), *Global Change in the Holocene*. Arnold, London, pp. 10–19.

Bradbury, J.P., Colman, S.M., Dean, W.E. (2004). 'Limnological and climatic environments at Upper Klamath Lake, Oregon during the past 45,000 years.' *Journal of Palaeolimnology*, **31**, 167-188.

Brenner, M., Whitmore, T.J., Curtis, J.H., Hodell, D.A., Schelske, C.L. (1999). 'Stable isotope ($\delta^{13}\text{C}$ and $\delta^{15}\text{N}$) signatures of sedimented organic matter as indicators of historic lake trophic state.' *Journal of Paleolimnology*, **22**, 205-221.

Brincat, D., Yamada, K., Ishiwatari, R., Uemura, H., Naraoka, H. (2000). 'Molecular-isotopic stratigraphy of long-chain *n*-alkanes in Lake Baikal Holocene and glacial age sediments.' *Organic Geochemistry*, **31**, 287-294.

Brunello, A.J., Molotov, V.C., Dugherkhuu, B., Goldman, C., Khamaganova, E., Strijhova, T., Sigman, R. Buchaca (2004). Lake Baikal: Lake Basin Management Initiative Experience and Lessons Learned Brief. 1 – 26.

Bondarenko N.A., Gusel'nikova N.E., Logacheva N.F. and Pomazkina G.V. (1996). 'Spatial distribution of phytoplankton in Lake Baikal, spring 1991.' *Freshwater Biology*, **35**, 517-23.

Bondarenko, N.A. (1999). 'Floral shift in the phytoplankton of Lake Baikal, Siberia: Recent dominance of *Nitzschia acicularis*.' *Plankton Biol. Ecol.*, **46**, (1), 18 – 23.

Bondarenko, N.A., Evstafev, V.K. (2006). 'Eleven and ten year basic cycles of Lake Baikal

spring phytoplankton conformed to solar activity cycles.' *Hydrobiologia*, **568**, 19 – 24.

Bondarenko, N.A., Belykh, O.I., Golobokova, L.P., Artemyeva, O.V., Logacheva, N.F., Tikhonova, I.V., Lipko, I.A., Kostornova, T.Y., Parfenova, V.V., Khodzher, T.V., Ahn, T-S., Zo, Y-G. (2012). 'Stratified distribution of nutrients and extremophile biota within freshwater ice covering the surface of Lake Baikal.' *The Journal of Microbiology*, **50**, (1), 8 – 16.

Bonilla, S., Villeneuve, V., Vincent, W.F. (2005). 'Benthic and planktonic algal communities in a high arctic lake: pigment structure and contrasting responses to nutrient enrichment.' *Journal of Phycology*, **41**, 1120-1130.

Bopp, L., Aumont, O., Cadule, P., Alvain, S., Gehlen, M. (2005). 'Response of diatoms distribution to global warming and potential implications: a global model study.' *Geophysical Research Letters*, **32**, (19), 1-4.

Boyle, J., Mackay, A.W., Rose, N.L., Appleby, P.G. (1998). 'Sediment heavy metal record in Lake Baikal: Natural and anthropogenic sources.' *Journal of Paleolimnology*, **20**, (2), 135-150.

Brincat, D., Yamada, K., Ishiwatari, R., Uemura, H., Naraoka, H. (2000). 'Molecular-isotopic stratigraphy of long-chain *n*-alkanes in Lake Baikal Holocene and glacial age sediments.' *Organic Geochemistry*, **31**, 287-294.

Buchaca, T., Felip, M., Catalan, J. (2005). 'A comparison of HPLC pigment analyses and biovolume estimated of phytoplankton groups in an oligotrophic lake.' *Journal of plankton research*, **27**, (1), 91 – 101.

Bufal, V.V., Linevich, N.L., Bashalkhanova, L.B. (2005). *Klimat Priolkhonie. Geografiya I prirodnye resursy* 1, 66-73.

Büntgen, U., Tegel, W., Nicolussi, K., McCormick, M., Frank, D., Trouet, V., Kaplan, J.O., Herzig, F., Heussner, K.-U., Wanner, H., Luterbacher, J., Esper, J. (2011). '2500 years of European climate variability and human susceptibility.' *Science*, **371**, 578–582.

Burkill, H., Mantoura, R.F.C., Llewellyn, C.A., Owens, N.J.P. (1987). 'Microzooplankton grazing and selectivity of phytoplankton coastal waters.' *Mar. Biol.*, **93**, 581– 590.

Callender, E., Granina, L. (1997a). ‘Biogeochemical phosphorus mass balance for Lake Baikal, southeastern Siberia, Russia.’ *Marine Geology*, **139**, 5 – 19.

Callender, E., Granina, L. (1997b). ‘Geochemical mass balances of major elements in Lake Baikal.’ *Limnology and Oceanography*, **42**, (1), 148 – 155.

Callieri, C. (2007). ‘Picophytoplankton in freshwater ecosystems: the importance of small-sized phototrophs.’ *Freshwater Reviews*, **1**, 1-28.

Calvo-Diaz, A., Diaz-Perez, L., Suarez, L.A., Moran, X.A.G., Teira, E., Maranon, E. (2011). ‘Decrease in the autotrophic to heterotrophic biomass ratio of picoplankton in oligotrophic marine waters due to bottle enclosure.’ *Applied and Environmental Microbiology*, 5739-5746.

Carpenter, S.R., Cole, J.J., Hodgson, J.R., Kitchell, J.F., Pace, M.L., Bade, D., Cottingham, K.L., Essington, T.E., Houser, J.N., Schindler, D.E. (2001). ‘Trophic cascades, nutrients, and lake productivity: Whole-lake experiments.’ *Ecol. Monogr.*, **71**, 163–186.

Camacho, A., Wurtsbaugh, W.A., Miracle, M.R., Armengol, X., Vicente, E. (2003). ‘Nitrogen limitation of phytoplankton in a Spanish karst lake within a deep chlorophyll maximum: a nutrient enrichment bioassay approach.’ *Journal of Plankton Research*, **25**, (4), 397-404.

Camacho, A. (2006). ‘On the occurrence and ecological features of deep chlorophyll maxima (DCM) in Spanish stratified lakes.’ *Limnetica*, **25**, (1-2), 453 – 478.

Campbell, I.D., Campbell, C., Apps, M., Rutter, N.W., Bush, A.B.G., (1998). ‘Late Holocene ~ 1500 yr climatic periodicities and their implications.’ *Geology*, **26**, 471–473.

Ceramicola, S., Rebesco, M., De Batist, M., Khlystov, O. (2001). ‘Seismic evidence of small-scale lacustrine drifts in Lake Baikal (Russia).’ *Mar. Geophys. Res.*, **22**, 445-464.

Ciesielski, T., Pastukhov, M.V., Fodor, P., Bertenyi, Z., Namies´nik, J., Szefer, P. (2006). ‘Relationships and bioaccumulation of chemical elements in the Baikal seal (*Phoca sibirica*).’ *Environ. Pollut.*, **139**, 372–384.

Ciesielski, T.M., Pastukhov, M.V., Leeves, S.A., Farkas, J., Lierhagen, S., Poletaeva, V.I., Jenssen, B.M. (2016). 'Differential bioaccumulation of potentially toxic elements in benthic and pelagic food chains in Lake Baikal.' *Environ Sci Pollut Res.*, **23**, 15, 15593-15604.

Chalov, S.R., Zavadsky, A.S., Belozerova, E.V., Bulacheva, M.P. Jarsjo, J., Thorslund, J.T., Yamkhin, J. (2012). 'Suspended and dissolved matter fluxes in the upper Selenga River basin: Synthesis.' *Geography, Environment, Sustainability*, **2**, (5), 78 – 94.

Charlet, F., Fagel, N., De Batist, M., Hauregard, F., Minnebo, B., Meischner, D., SONIC Team. (2005). 'Sedimentary dynamics on isolated highs in Lake Baikal: evidence from detailed high-resolution geophysical data and sediment cores.' *Global Planet. Change*, **46**, 125-144.

Charlton, M.N., Milne, J.E., Booth, W.G., Chiocchio, F. (1993). 'Lake Erie offshore in 1990 restoration and resilience in the central basin.' *J. Great Lakes Res.*, **19**, 291–309.

Charlton, M.N., Milne, J.E. (2005). 'Review of thirty years of change in Lake Erie water quality.' NWRI contribution. National Water Research Institute, Environment, Canada, 4-167.

Chen C.T. and Millero F.J. (1986). 'Precise thermodynamic properties for natural waters covering the limnological range.' *Limnology and Oceanography*, **31**, 657-662.

Chen, N., Bianchi, T.S., McKee, B.A., Bland, J.M. (2001). 'Historic trends of hypoxia on the Louisiana shelf: application of pigments as biomarkers.' *Organic Geochemistry*, **32**, 543 – 561.

Chen, N., Bianchi, T.S., Bland, J.M. (2003a). 'Implications for the role of pre-versus post depositional transformation of chlorophyll-a in the Lower Mississippi River and Louisiana shelf.' *Marine Chemistry*, **81**, 37 – 55.

Chen, N., Bianchi, T.S., Bland, J.M. (2003b). 'Novel decomposition products of chlorophyll-a in continental shelf (Louisiana shelf) sediments: Formation and transformation of Carotenol chlorin esters.' *Geochimica et Cosmochimica Acta*, **67**, (11), 2027 – 2042.

Cofala, J., Amann, M., & Mechler, R. (2005). Scenarios of world anthropogenic emissions of air pollutants and methane up to 2030. Report of the Transboundary Air Pollution (TAP)

programme, International Institute for Applied Systems Analysis, Laxenburg, Austria.

Cohen, A.S., Soreghan, M.J., Scholz, C.A. (1993). ‘Estimating the age of formation of lakes: An example from Lake Tanganyika, East African Rift System.’ *Geology*, **21**, 511 – 514.

Colman S.M., Peck J.A., Hatton J., Karabanov E.B., and King J.W. (1999). ‘Biogenic silica records from the BDP-93 site and adjacent areas of the Selenga Delta, Lake Baikal, Siberia.’ *J. Paleolimnol.*, **21**, 9-17.

Cole, J., and others. (2007). ‘Plumbing the global carbon cycle: Integrating inland waters into the terrestrial carbon budget.’ *Ecosystems*, **10**, 171–184.

Coleman, S.M., Peck, J.A., Karabanov, E.B., Carter, S.J., Bradbury, J.P., King, J.W., Williams, D.F. (1995). ‘Continental climate response to orbital forcing from biogenic silica records in Lake Baikal.’ *Nature*, **378**, 769 – 771.

Coleman S.M., Jones G.A., Rubin M., King J.W., Peck J.A. and Orem W.H. (1996). ‘AMS radiocarbon analyses from Lake Baikal, Siberia: challenges of dating sediments from a large, oligotrophic lake.’ *Quaternary Science Reviews*, **15**, 669-684.

Colman, S.M., Karabanov, E.B., Nelson, C.H. (2003). ‘Quaternary sedimentation and subsidence history of Lake Baikal, Siberia, based on seismic stratigraphy and coring.’ *Journal of Sedimentary Research*, **73**, (6), 941-956.

Conley, D.J., Schelske, C.L., Stoermer, E.F. (1993). ‘Modification of the biogeochemical cycle of silica with eutrophication.’ *Marine ecology progress series*, **101**, 179 – 192.

Conley, D.J., Björck, S., Bonsdorff, E., Carstensen, J., Destouni, G., Gustafsson, B.G., Hietanen, S., Kortekaas, M., Kuosa, H., Meier, H.E.M., Müller-Karulis, B., Nordberg, K., Norkko, A., Nürnberg, G., Pitkänen, H., Rabalais, N.N., Rosenberg, R., Savchuk, O.P., Slomp, C.P., Voss, M., Wulff, F., Zillen, L. (2009). ‘Hypoxia-related processes in the Baltic Sea.’ *Environmental Science & Technology*, **43**, (10), 3412-3420.

Cottingham, K.L., Knight, S.E. Carpenter, S.R., Cole, J.J., Pace, M.L., Wagner, A.E. (1997). ‘Response of phytoplankton and bacteria to nutrients and zooplankton: a mesocosm experiment.’ *Journal of Plankton Research*, **19**, (8), 995-1010.

Conway, H.L., Parker, J.I., Yaguchi, E.M., Mellinger, D.L. (1977). ‘Biological utilization of silicon in Lake Michigan.’ *J. Fish. Res. Bd Can.*, **34**, 537-544.

Cook, E.R., Krusic, P.J., Anchukaitis, K.J., Buckley, B.M., Nakatsuka, T., Sano, M., PAGES Asia2k Members. (2013). ‘Tree-ring reconstructed summer temperature anomalies for temperate East Asia since 800 C.E.’ *Clim Dyn*, **41**, 2957-1972.

Cretaux, J.-F., Letolle, R., Bergé-Nguyen, M.(2013). ‘History of Aral Sea level variability and current scientific debates.’ *Global and Planetary Change*, **110**, 99-113.

Cristescu, ME., Adamowicz, S.J., Vaillant, J.J., Haffner, D.G. (2010). ‘Ancient lakes revisited: from the ecology to the genetics of speciation.’ *Molecular Ecology*, **19**, 4837 – 4851.

Cuddington, K., Leavitt, P.R. (1999). ‘An individual-based model of pigment flux in lakes: implications for organic biogeochemistry and paleoecology.’ *Canadian Journal of Fisheries and Aquatic Sciences*, **56**, 1964 – 1977.

Czaplicki, S. (2013). ‘Chromatography in bioactivity analysis of compounds.’ Chapter 4 Column Chromatography, Dr. Dean Martin (Ed.).

Daley, R. J., Brown, S. R. (1973). ‘Experimental characterization of lacustrine chlorophyll diagenesis. 1. Physiological and environmental effects.’ *Archiv für Hydrobiologie*, **72**, 277–304.

D’Arrigo, R., Jacoby, G., Pederson, N., Frank, D/, Buckley, B., Nachin, B., Mijiddorj, R., Dugarjav, C. (2000). ‘Mongolian tree-rings, temperature sensitivity and reconstructions of Northern Hemisphere temperature.’ *The Holocene*, **10**, 6, 669-672.

Deike, R.G., Granina, L., Callender, E., McGee, J.J. (1997). ‘Formation of ferric iron crusts in Quaternary sediments of Lake Baikal, Russia, and implications for paleoclimate.’ *Marine Geology*, **139**, 21-46.

De Batist, M., Canals, M., Sherstyankin, P., Alekseev, S. (2002). A New Bathymetric Map of Lake Baikal. Intas 99-1669 Project Team.

De La Rocha, C. L. (2006). ‘Opal-based isotopic proxies of Paleoenvironmental conditions.’ *Global Biogeochemical Cycles*, **20**, (4), 1-11.

DeLuca, T., Boisvenue, C. (2012). ‘Boreal forest soil carbon: distribution, function and modelling.’ *Forestry*, **85**, 161-184.

Demske, D., Mohr, B., Oberhänsli, H. (2002). ‘Late Pliocene vegetation and climate of the Lake Baikal region, southern East Siberia, reconstructed from palynological data.’ *Palaeogeography, Palaeoclimatology, Palaeoecology*, **184**, 107-129.

Demske, D., Heumann, G., Granoszewski, W., Nita, M., Mamakowa, K., Tarasov, P.E., Oberhänsli, H. (2005). ‘Late glacial and Holocene vegetation and regional climate variability evidenced in high-resolution pollen records from Lake Baikal.’ *Global and Planetary Change*, **46**, 255-279.

Dentener, F., Kinne, S., Bond, T., Boucher, O., Cofala, J., Generoso, S., Ginoux, P., Gong, S., Hoelzemann, J.J., Ito, A., Marelli, L., Penner, J.E., Putaud, J-P., Textor, C., Schulz, M., van der Werd, G.R., Wilson, J. (2006). ‘Emissions of primary aerosol and precursor gases in the years 2000 and 1750 prescribed data-sets for AeroCom.’ *Atmos. Chem. Phys.*, **6**, 4321-4344.

Drakare, S., Blomqvist, P., Bergstrom, A-K., Jansson, M. (2003). ‘Relationships between picophytoplankton and environmental variables in lakes along a gradient of water colour and nutrient content.’ *Freshwater Biology*, **48**, 729 – 740.

Driedger, A.G.J., Dürr, H.H., Mitchell, K., Van Cappellen, P. (2015). ‘Plastic debris in the Laurentian Great Lakes: A review.’ *Journal of Great Lakes Research*, **41**, 9-19.

Dobiesz, N.E., Hecky, R.E., Johnson, T.B., Sarvala, J., Dettmers, J.M., Lehtiniemi, M., Rudstam, L.G., Madenjian, C.P., Witte, F. (2010). ‘Metrics of ecosystem status for large aquatic systems – A global comparison.’ *Journal of Great Lake Research*, **36**, 123-138.

Dobretsov, N.L., Grachev, M.A., Kuzmin, M.I. (2000). ‘Unique Ecosystem of Lake Baikal and Paleoclimate of Central Asia.’ *Terra Nostra*, **9**, 12-25.

Dong, X., Anderson, N.J., Yang, X., Chen, X., Shen, J. (2012). ‘Carbon burial by shallow lakes on the Yangtze floodplain and its relevance to regional carbon sequestration.’ *Global Change Biology*, **18**, 2205-2217.

Dorogostaisky, V.G. (1904). ‘Data for algology of Lake Baikal and its basin. News of Eastern

Siberian Department of Russian Geographic Society', **35**, (3), 1–11.

Dudgeon, D., Arthington, A.H., Gessner, M.O., Kawabata, Z-I., Knowler, D.J., Leveque, C., Naisman, R.J., Prieur-Richard, A-H., Soto, D., Stiassny, M.L.J., Sullivan, C.A. (2006). 'Freshwater biodiversity: importance, threats, status and conservation challenges.' *Biol. Rev.*, **81**, 163-182.

Eaton, A. D., Clesceri, L. S. and Greenberg, A. E., Eds. (1995). Standard Methods for the Examination of Water and Wastewater. Washington, APHA.

Edlund, M. B., Stoermer, E. F. & Pilskaln, C. H. (1995). 'Siliceous microfossil succession in the recent history of two basins in Lake Baikal, Siberia.' *Journal of Paleolimnology*, **14**, 165-184.

Edlund M.B. and Stoermer E.F. (2000). 'A 200,000-year, high-resolution record of diatom productivity and community makeup from Lake Baikal shows high correspondence to the marine oxygen-isotope record of climate change.' *Limnology and Oceanography*, **45**, 948-962.

Effler, S.W., Blooms, N.S. (1990). 'Seasonal variability in the mercury speciation of Onondaga Lake (New York).' *Water, Air and Soil Pollution*, **53**, (3), 251-265.

Elser, J.J., Kimmel, B.L. (1986). 'Alteration of phytoplankton phosphorus status during enrichment experiments: implications for interpreting nutrient enrichment bioassay results.' *Hydrobiologia*, **133**, 217-222.

Elser, J.J., Marzolf, E.R., Goldman, C.R. (1990). 'Phosphorus and nitrogen limitation of phytoplankton growth in the fresh-waters of North America – a review and critique of experimental enrichments.' *Can. J. Fish. Aquat. Sci.*, **47**, 1468-1477.

Environmental monitoring of Lake Baikal (2013) (<http://baikalake.ru/en/>).

Eriksen, M., Mason, S., Wilson, S., Box, C., Zellers, A., Edwards, W., Farley, H., Amato, S. (2013). 'Microplastic pollution in the surface waters of the Laurentian Great Lakes.' *Marine Pollution Bulletin*, **77**, (1-2), 177-182.

Falkner, K.K., Measures, C.I., Herbelin, S.E., Edmond, J.M. (1991). ‘The major and minor element geochemistry of Lake Baikal.’ *Limnology and Oceanography*, **36**, (3), 413 – 423.

Falkner, K.K., Church, M., Measures, C.I., LeBaron, G., Thouron, D., Jeandel, C., Stordal, M.C., Gill, G.A., Mortlock, R., Froelich, P., Chan, L-H. (1997). ‘Minor and trace element chemistry of Lake Baikal, its tributaries, and surrounding hot springs.’ *Limnology and Oceanography*, **42**, (2), 329 – 345.

Fee J.E., Schindler, D.W. (2011). ‘Experimental Lakes Area: Whole-Lake Experiments in Eutrophication.’ *Journal of the Fisheries Research Board of Canada*, **31**, (5), 937 – 953.

Felisberto, S.A., Leandrini, J.A., Rodrigues, L. (2011). ‘Effects of nutrients enrichment on algal communities: an experimental in mesocosms approach.’ *Acta Limnologica Brasiliensia*, **23**, (2), 128 – 137.

Fenchel T., King G. M., and Blackburn T. H. (1998). Bacterial biogeochemistry: The ecophysiology of mineral cycling. Academic Press.

Fietz, S., Nicklisch, A. (2004). ‘An HPLC analysis of the summer phytoplankton assemblage in Lake Baikal.’ *Freshwater Biology*, **49**, 332 – 345.

Fietz, S. (2005). 'Recent and fossil phytoplankton pigments in Lake Baikal as markers for community structure and environmental changes.' Humboldt University Berlin, Germany. PhD Thesis.

Fietz, S., Kobanova, G., Izmesteva, L., Nicklisch, A. (2005). 'Regional, vertical and seasonal distribution of phytoplankton and photosynthetic pigments in Lake Baikal.' *Journal of Plankton Research*, **27**, (8), 793 – 810.

Fietz, S., Nicklisch, A., Oberhansli, H. (2007). ‘Phytoplankton response to climate changes in Lake Baikal during the Holocene and Kazantsevo Interglacials assessed from sedimentary pigments.’ *Journal of Paleolimnology*, **37**, 177-203.

Fifield, L.K., Morgenstern, U. (2009). ‘Silicon-32 as a tool for dating the recent past.’ *Quat Geochronol.*, **4**, 400 – 405.

Findlay, D. L., Kasian, S. E. M., Stainton, M. P., Beaty, K., Lyng, M. (2001). ‘Climatic influences on algal populations of boreal forest lakes in the experimental lakes area.’ *Limnol. Oceanogr.* **46**, 1784–1793.

Francis, T.B., Wolkovitch, E.M., Scheurell, M.D., Katz, S.L., Holmes, E.E., Hampton, S.E. (2014). ‘Shifting regimes and changing interactions in the Lake Washington, USA, plankton community from 1962 – 1994.’ *Plos One*, **9**, (10), 1932 – 6203.

Free, C.M., Jensen, O.P., Mason, S. a, Eriksen, M., Williamson, N.J., Boldgiv, B. (2014). ‘High- levels of microplastic pollution in a large, remote, mountain lake.’ *Mar. Pollut. Bull.*, **85**, 156–163.

Florian, C.R., Miller, G.H., Fogel, M.L., Wolfe, A.P., Vinebrooke, R.D., Geirsdottir, A. (2015). ‘Algal pigments in Arctic lake sediments record biogeochemical changes due to Holocene climate variability and anthropogenic global change.’ *Journal of Palaeolimnology*, **54**, 53-69.

Flower R.J. (1993). ‘Diatom preservation: experiments and observations on dissolution and breakage in modern and fossil material.’ *Hydrobiologia*, **269/270**, 473-484.

Flower, R. J. & Likhoshway, Ye. V. (1993). ‘Diatom preservation in Lake Baikal. In Diatom algae as indicators of the changes of climate and environment. Fifth workshop on diatom algae (ed. M. A. Grachev), pp. 77^78. Irkutsk: Russian Botanical Society Publications.

Flower R.J., Mackay A.W., Rose N.L., Boyle J.L., Dearing J.A., Appleby P.G., Kuzmin, A.E., and Granina L.Z. (1995). ‘Sedimentary records of recent environmental-change in Lake Baikal, Siberia.’ *The Holocene*, **5**, 323-327.

Free, C.M., Jensen, O.P., Mason, S. a, Eriksen, M., Williamson, N.J., Boldgiv, B. (2014). ‘High- levels of microplastic pollution in a large, remote, mountain lake.’ *Mar. Pollut. Bull.*, **85**, 156–163.

Furlong, E. T. and Carpenter, R. (1988). ‘Pigment preservation and remineralization in oxic coastal marine sediments.’ *Geochimica et Cosmochimica Acta*, **52**, 87-99.

Galaziy, G.I. (Ed.). (1993). Baikal Atlas. Federalnaya sluzhba geodezii i kartografii Rossii, Moscow (in Russian).

Galloway, J.N., Townsend, A.R., Erisman, J.W., Bekunda, M., Cai, Z., Freney, J.R., Martinelli, L.A., Seitzinger, S.P., Sutton, M.A. (2008). ‘Transformation of the nitrogen cycle: recent trends, questions, and potential solutions.’ *Science*, **320**, 889-892.

Genkai-Kato, M., Sekino, T., Yoshida, T., Miysaka, H., Khodzher, T.V., Belykh, O.A., Melnik, N.G., Kawabata, Z., Higashi, M., Nakanishi, M. (2002). ‘Nutritional diagnosis of phytoplankton in Lake Baikal.’ *Ecological Research*, **17**, 135-142.

Gilpin, L.C., Davidson, K., Roberts, E. (2004). ‘The influence of changes in nitrogen: silicon ratios on diatom growth dynamics.’ *Journal of Sea Research*, **51**, 21-35.

Gobler, C.J., Buck, N.J., Sieracki, M.E., Sanudo-Wilhelmy, S.A. (2006). ‘Nitrogen and silicon limitation of phytoplankton communities across an urban estuary: The East river-Long Island Sound system.’ *Estuarine, Coastal and Shelf Science*, **68**, 127-138.

Goldman, C.R., Elser, J.J., Richards, R.C., Reuter, J.E., Priscu, J.C., Levin, A.L. (1996). ‘Thermal stratification, nutrient dynamics, and phytoplankton productivity during the onset of spring phytoplankton growth in Lake Baikal, Russia.’ *Hydrobiologia*, **331**, 9 – 24.

Golmshtok, A.Y., Duchkov, A.D., Hutchinson, D.R., Khanukaev, S.B., Einikov, A.I. (1997). ‘Estimation of heat flow on Baikal from seismic data on the lower boundary of the gas hydrate layer.’ *Russ. Geol. Geophys.*, **38**, 1714-1727.

Gong, D.Y., Ho, C.H. (2002). ‘The Siberian High and climate change over middle to high latitude Asia.’ *Theoretical and Applied Climatology*, **72**, 1-9.

Grachev, M. A. et al. (1989). Distemper virus in Baikal seals. *Nature, London*, **338**, 209.

Grachev, M.A., Vorobyova, S.S., Likhoshway, Y.V., Goldberg, E.L., Ziborova, G.A., Levina, O.V., Khlystov, O.M. (1998). ‘A high-resolution diatom record of the palaeoclimates of East Siberia for the last 2.5 My from Lake Baikal.’ *Quaternary Science Reviews*, **17**, 1101-6.

Graneli, E., Carlsson, P., Turner, J.T., Tester, P.A., Bechemin, C., Dawson, R., Funari, E. (1999). ‘Effects of N:P:Si ratios and zooplankton grazing on phytoplankton communities in the northern Adriatic Sea. I. Nutrients, phytoplankton biomass, and polysaccharide production.’ *Aquatic Microbial Ecology*, **18**, 37-54.

Granin, N.G., Jewson, D.H., Gnatovsky, R.Y., Levin, L.A., Zhdanov, A.A., Gorbunova, L.A., Tsekhanovsky, V.V., Doroschenko, L.M., Mogilev, N.Y. (2000). ‘Turbulent mixing under ice and the growth of diatoms in Lake Baikal.’ *Verhandlungen International Vereinigung Limnologie*, **27**, 2812-2814.

Granin, N.G. and Others (1991). Distribution of Baikal pelagial ecosystem characteristics in spring convection. Krasnoyarsk.

Granina, L., Sigg, L. (1995). New data on the composition of suspended particles in Lake Baikal and its tributaries. 2nd Vereshchagin Baikal Conf., Irkutsk, Oct. 5-10, 1995, Abstr., p.51.

Granina, L.Z., Baryshev, V.B., Grachev, A.M. (1995). ‘Study of elemental composition of suspended sediments in Lake Baikal and its tributaries by X-ray fluorescent analysis based on synchrotron radiation.’ *Nuclear Instr. Meth. Phys. Res. A.*, **359**, 302-304.

Granina, L., Müller, B., Wehrli, B. (2004). ‘Origin and dynamics of Fe and Mn sedimentary layers in Lake Baikal.’ *Chem. Geol.*, **205**, (1-2), 55-72.

Granoszewski, W., Demske, D., Nita, M., Heumann, G., Andreev, A.A. (2005). ‘Vegetation and climate variability during the Last Interglacial evidenced in the pollen record from Lake Baikal.’ *Global Planet Change*, **46**, 187 – 198.

Greisberger, S., Teubner, K. (2007). ‘Does pigment composition reflect phytoplankton community structure in differing temperature and light conditions in a deep alpine lake? An approach using HPLC and delayed fluorescence techniques.’ *Journal of Phycology*, **43**, 1108 – 1119.

Grimm, E.C. (1987). ‘CONISS: a Fortran 77 program for stratigraphically constrained cluster analysis by the method of incremental sum of squares.’ *Computers & Geosciences*, **13**, (1), 13-35.

Grosswald, M.G., Kuhle, M. (1994). ‘Impact of glaciations on Lake Baikal. International Project on Palaeolimnology and Lake Cenozoic Climate.’ *Newsletter*, vol. 8, pp. 48-60.

Grosheva, E.I., Voronskaya, G.N., Pastukhova, M.V. (2000). ‘Trace element bioavailability in Lake Baikal.’ *Aquatic Ecosystem Health and Management*, **3**, 229-234.

Gryar, T., Kadlec, J., Pruner, P., Swann, G., Bezdicka, P., Hradil, D., Lang, K., Novotna, K., Oberhansli, H. (2006). ‘Paleoenvironmental record in Lake Baikal sediments: Environmental changes in the last 160 ky.’ *Palaeogeography, Palaeoclimatology, Palaeoecology*, **237**, 240 – 254.

Guilizzoni, P., Bonomi, G., Galanti, G., Ruggiu, D. (1983). ‘Relationship between sedimentary pigments and primary production: Evidence from core analyses of twelve Italian lakes.’ *Hydrobiologia*, **103**, (1), 103–106.

Gustokashina, N.N., Bufal, V.V. (2003). Mnogoletnie Izmeneniia Osnovnykh elementov Klimata Na Territorii Predbaikalia. Institute of Geography Publishing House, Irkutsk (in Russian).

Gutwinski, R. (1891). ‘Algarum e lacu Baykal ete paeninsula Kamtschatka a.c.prof. Dybowski anno 1877 reportarum enumeratio.’ *La nuova Natarisia, Consacrata allo Studio delle Alghe*, **11**, 300–305.

Hammarlund D (1992). ‘A distinct $\delta^{13}\text{C}$ decline in organic lake sediments at the Pleistocene-Holocene transition in southern Sweden.’ *Boreas*, **22**, 236-243.

Hampton, S.E., Izmesteva, L.R., Moore, M.V., Katz, S.L., Dennis, B., Silow, E.A. (2008). ‘Sixty years of environmental change in the world’s largest freshwater lake – Lake Baikal, Siberia.’ *Global Change Biology*, **14**, 1947 – 1958.

Hampton, S.E., Gray, D.K., Izmesteva, L.R., Moore, M.V., Ozersky, T. (2014). ‘The Rise and Fall of Plankton: Long-term changes in the vertical distribution of algae and grazers in Lake Baikal, Siberia.’ *PLOS ONE*, **9**, (2), 1 – 10.

Hampton, S.E., Moore, M.V., Ozersky, T., Stanley, E.H., Polashenski, C.M., Galloway, A.W.E. (2015). ‘Heating up a cold subject: prospects for under-ice plankton research in lakes.’ *Journal of plankton research*, **0**, (0), 1- 8.

Handong, Y., Appleby, P.G. (2016). ‘Use of lead-210 as a novel tracer for lead (Pb) sources in plants.’ *Scientific Reports*, **6**, 1-9.

- Hare, A.A., Kuzyk, Z.Z., Macdonald, R.W., Sanei, H., Barber, D., Stern, G.A., Wang, F. (2014).** ‘Characterization of sedimentary organic matter in recent marine sediments from Hudson Bay, Canada, by Rock-Eval pyrolysis.’ *Organic Geochemistry*, **68**, 52-60.
- Harradine, P., J., Peakman, T.M., Maxwell, J.R. (1996).** ‘Triterpenoid Chlorin Esters: Water Column Transformation Products of Chlorophyll a.’ *Tetrahedron*, **52**, (42), 13427 – 13440.
- Heathcote, A.J., Anderson, N.J., Prairie, Y.T., Engstrom, D.R., del Giorgio, P.A. (2015).** ‘Large increases in carbon burial in northern lakes during the Anthropocene.’ *Nature*, 1-6.
- Hecky, R.E., Kilham, P. (1988).** ‘Nutrient limitation of phytoplankton in freshwater and marine environments: A review of recent evidence on the effects of enrichment.’ *Limnol. Oceanogr.*, **33**, (4, part 2), 796 – 822.
- Hecky, R.E., Smith, R.E., Barton, D.R., Guildford, S.J., Taylor, W.D., Charlton, M.N., and Howell, T. (2004).** ‘The nearshore phosphorus shunt: a consequence of ecosystem engineering by dreissenids in the Laurentian Great Lakes.’ *Canadian Journal of Fisheries and Aquatic Sciences*, **61**, (7), 1285-1293.
- Heisler, J., Glibert, P.M., Burkholder, J.M. Anderson, D.M., Cochlan, W., Dennison, W.C., Dortch, Q., Gobler, C.J., Heil, C.A., Humphries, E., Lewitus, A., Magnien, R., Marshall, H.G., Sellner, K., Stockwell, D.A., Stoecker, D.K., Suddleson, M. (2008).** ‘Eutrophication and harmful algal blooms: a scientific consensus.’ *Harmful Algae*, **8**, 3 – 13.
- Hanson, P.C., Pollard, A.I., Bade, D.L., Predick, K., Carpenter, S.R., Foley, J.A. (2004).** ‘A model of carbon evasion and sedimentation in temperate lakes.’ *Global Change Biology*, **10**, 1285 – 1298.
- Hamilton, D.H. (1969).** ‘Nutrient limitation of summer phytoplankton growth in Cayuga Lake.’ *Limnol. Oceanogr.*, **14**, 579-590.
- Head, E. J. H., Harris, L. R. (1992).** ‘Chlorophyll and carotenoid transformation and destruction by *Calanus* spp. grazing on diatoms.’ *Marine Ecology Progress Series*, **86**, (3), 229–238.

Heim, B. (2005). ‘Qualitative and Quantitative analyses of Lake Baikal’s surface waters using ocean colour satellite data (SeaWiFS).’ PhD Thesis.

Heim, B., Oberhaensli, H., Fietz, S., Kaufmann, H. (2005). ‘Variation in Lake Baikal’s phytoplankton distribution and fluvial input by SeaWiFS satellite data.’ *Global and Planetary Change*, **46**, 9-27.

Heim, B., Klump, J., Schulze, A., Schneider, S., Swiercz, S., Dachnowski, G., Fagel, N. (2007). Lithological map of the Lake Baikal catchment. Deutsches GeoForschungsZentrum GFZ. <http://doi.org/10.1594/GFZ.SDDB.1213>.

Hendry, K. R. and Brzezinski, M. A. (2014). ‘Using silicon isotopes to understand the role of the Southern Ocean in modern and ancient biogeochemistry and climate’. *Quaternary Sci. Rev.*, **89**, 13–26.

Higgins, S.N., Malkin, S.Y., Todd Howell, E., Guildford, S.J., Campbell, L., Hiriart-Baer, V., and Hecky, R.E. (2008). ‘An ecological review of *Cladophora glomerata* (Chlorophyta) in the Laurentian Great Lakes.’ *Journal of Phycology*, **44**, (4), 839-854.

Hirakawa, S., Imaeda, D., Nakayama, K., Udaka, M., Kim, E-Y., Kunisue, T., Ogawa, M., Matsuda, T., Matsui, S., Petrov, E.A., Batoev, V.B., Tanabe, S., Iwata, H. (2011). ‘Integrative assessment of potential effects of dioxins and related compounds in wild Baikal seals (*Pusa sibirica*): Application of microarray and biochemical analyses’. *Aquatic Toxicology*, **105**, 89-99.

Hodell, D.A., Schelske, C.L. (1998). ‘Production, sedimentation, and isotopic composition of organic matter in Lake Ontario.’ *Limnol Oceanogr*, **43**, (2), 200–214.

Hodgson, D.A., Wright SW, Tyler PA, and Davies N. (1998). ‘Analysis of fossil pigments from algae and bacteria in meromictic Lake Fidler, Tasmania, and its application to lake management.’ *J Paleolimnol.*, **19**, 1-22.

Hogan, E.J., Anderson, N.J. (2014). ‘Nutrient limitation of periphyton growth in arctic lakes in south-west Greenland.’ *Polar Biology*, **37**, 1331-1342.

Hohmann, R., Kipfer, R., Peeters, F., Piepke, G., Imboden, D.M., Shimaraev, M.N. (1997). ‘Processes of deep-water renewal in Lake Baikal.’ *Journal of Limnology and Oceanography*, **42**, (5), 841-855.

Horiuchi, K., Minoura, K., Hoshino, K., Oda, T., Nakamura, T., Kawai, T. (2000). ‘Palaeoenvironmental history of Lake Baikal during the last 23000 years.’ *Palaeogeography, Palaeoclimatology, Palaeoecology*, **157**, 95-108.

Howarth, R. W., Marino, R., Lane, J., Cole, J.J. (1988). ‘Nitrogen fixation in freshwater, estuarine, and marine ecosystems. 1. Rates and importance.’ *Limnol. Oceanogr.*, **33**, 669–687.

Hsieh, C.H., Ishikawa, K., Sakai, Y., Ishikawa, T., Ichise, S., Yamamoto, Y., Kuo, T.C., Park, H.D., Yamamura, N., Kumagai, M. (2010). ‘Phytoplankton community reorganization driven by eutrophication and warming in Lake Biwa.’ *Aquatic Science*, **72**, 467 – 483.

Humborg, C., V. Ittekkot, A. Cociasu, B. V. Bodungen, (1997). ‘Effect of Danube River dam on Black Sea biogeochemistry and ecosystem structure.’ *Nature*, **386**, 385–388.

Humborg, C., D. J. Conley, L. Rahm, F. Wulff, A. Cociasu, V. Ittekkot. (2000). ‘Silicon retention in river basins: Far-reaching effects on biogeochemistry and aquatic food webs in coastal marine environments.’ *Ambio*, **29**, 45–50.

Hurley, J.P., Armstrong, D.E. (1990). ‘Fluxes and transformations of aquatic pigments in Lake Mendota, Wisconsin.’ *Limnology and Oceanography*, **35**, (2), 384-398.

Imaeda, D., Kunisue, T., Ochi, Y., Iwata, H., Tsydenova, O., Takahashi, S., Amano, M., Petrov, E.A., Batoev, V.B., Tanabe, S. (2009). ‘Accumulation features and temporal trends of PCDDs, PCDFs and PCBs in Baikal seals (*Pusa sibirica*).’ *Environmental Pollution*, **157**, 737 – 747.

Ishiwatari R., Uzaki M., Yamada K., and Ogura K. (1992). ‘Organic matter records of environmental changes in Lake Baikal sediments. 1: carbon isotopes, organic carbon and nitrogen.’ *IPPCCE Newsletter*, **6**, 80-88.

Ishiwatari, R., Yamamoto, S., Uemura, H. (2005). ‘Lipid and lignin/cutin compounds in Lake Baikal sediments over the last 37 kyr: implications for glacial-interglacial palaeoenvironmental change.’ *Organic Geochemistry*, **36**, 327-347.

Isobe, T., Ochi, Y., Imaeda, D., Sakai H., Hirakawa, S., Tsydenova, O., Amano, M., Petrov, E., Batoev, V., Iwata, H., Takahashi, S., Tanabe, S. (2009). ‘Contamination status of brominated flame retardants (BFRs) in Baikal Seals (*Pusa sibirica*).’ *Interdisciplinary Studies on Environmental Chemistry – Environment Research in Asia*, 119-124.

Iwata, H., Tanabe, S., Ueda, K., Tatsukawa, R. (1995). ‘Persistent organochlorine residues in air, water, sediments, and soils from the Lake Baikal Region, Russia.’ *Environ. Sci. Technol.*, **29**, 792-801.

Izmeteva, L.R., Moore, M.V., Hampton, S.E., Ferwerda, C.J., Gray, D.K., Woo, K.H., Pislegina, H.V., Krashchuk, L.S., Shimaraeva, S.V. Silow, E.A. (2015). ‘Lake-wide physical and biological trends associated with warming in Lake Baikal.’ *Journal of Great Lakes Research*, **42**, (1), 6 – 17.

Jagus, A., Rzetala, M.A., Rzetala, M. (2015). ‘Water storage possibilities in Lake Baikal and in reservoirs impounded by the dams of the Angara River cascade.’ *Environ Earth Sci.*, **73**, 621-628.

Jambers, W., van Grieken, R. (1997). ‘Single particle characterization of inorganic suspension in Lake Baikal, Siberia.’ *Environmental Science and Technology*, **31**, 1525-1533.

Jeffrey, S. W., Mantoura, R. F. C. (1997). Development of pigment methods for oceanography. In: Jeffrey, S., Mantoura, R., Wright, S. (Eds.), *Phytoplankton pigments in oceanography*. UNESCO Publishing, Paris, pp. 19–36.

Jewson, D.H., Granin, N.G., Zhdanov, A.A., Gorbunova, L.A., Bondarenko, N.A., Gnatovsky, R.Y. (2008). ‘Resting stages and ecology of the planktonic diatom *Aulacoseira skvortzowii* in Lake Baikal.’ *Limnology and Oceanography*, **53**, (3), 1125-1136.

Jewson, D.H., Granin, N.G., Zhdanov, A.A., Gnatovsky, R.Y. (2009). ‘Effect of snow depth on under-ice irradiance and growth of *Aulacoseira baicalensis* in Lake Baikal.’ *Aquatic Ecology*, **43**, 673 – 679.

Jewson, D.H., Granin, N.G., Zhdarnov, A.A., Gorbunova, L.A., Yu, R. (2010). ‘Vertical mixing, size change and resting stage formation of the planktonic diatom *Aulacoseria baicalensis*.’ *European Journal of Phycology*, **45**, (4), 354 – 364.

Jewson, D.H., Granin, N.G. (2014). ‘Cyclical size change and population dynamics of a planktonic diatom, *Aulacoseira baicalensis*, in lake Baikal.’ *European Journal of Phycology*, **50**, 1 – 19.

Jewson, D.H., Granin, N.G., Gnatovsky, R.Y., Lowry, S.F., Teubner, K. (2015). ‘Coexistence of two *Cyclotella* diatom species in the plankton of Lake Baikal.’ *Freshwater Biology*, **60**, 10, 2113-2126.

Jones, P.D., Mann, M.E. (2004). ‘Climate over past millennia.’ *Reviews of Geophysics*, **42**, 1–42.

Jones, V.J., Solovieva, N., Self, A.E., McGowan, S., Rosen, P., Salonen, J.S., Seppä, H., Väiliranta, M., Parrott, E., Brooks, S. (2011). ‘The influence of Holocene tree-line advance and retreat on an arctic lake ecosystem: a multi-proxy study from Kharinei Lake, North Eastern European Russia.’ *Journal of Palaeolimnology*, **46**, 123 – 137.

Jones, P.D., Lister, D.H., Osborn, T.J., Harpham, C., Salmon, M., Morice, C.P. (2012). ‘Hemispheric and large-scale land surface air temperature variations: an extensive revision and an update to 2010.’ *Journal of Geophysical Research*, **117**, 1-29.

Johnson, T.C., Brown, E.R., McManus, J., Barry, S., Barker, P., Gasse, F. (2002). ‘A high-resolution paleoclimate record spanning the past 25,000 years in southern East Africa.’ *Science*, **296**, 113 -132.

Julius, M. L., Stoermer, E. F., Colman, S. M. & Moore, T. C. (1997). ‘A preliminary investigation of siliceous microfossil succession in late Quaternary sediments from Lake Baikal, Siberia.’ *Journal of Paleolimnology* **18**, 187-204.

Karabanov, E.B., Prokopenko, A.A., Williams, D.F., Khursevich, G.K. (2000). ‘A new record of Holocene climate change from the bottom sediments of Lake Baikal.’ *Palaeogeography Palaeoclimatology Palaeoecology*, **156**, 211-224.

Kashiwaya, K., Ryugo, M., Horii, M., Sakai, H., Nakamura, T., Kawai, T. (1999). ‘Climato-limnological signals during the past 260 000 years in physical properties of bottom sediments from Lake Baikal.’ *Journal of Paleolimnology*, **21**, 143-150.

Kashiwaya, K., Ryugo, M., Horii, M., Sakai, H., Nakamura, T., Kawai, T. (1999). ‘Climato-limnological signals during the past 260 000 years in physical properties of bottom sediments from Lake Baikal.’ *Journal of Paleolimnology*, **21**, 143-50.

Kashiwaya, K., Ochiai, S., Sakai, H., Kawai, T. (2003). ‘Onset of current Milankovitch-type climatic oscillations in Lake Baikal sediments at around 4 Ma.’ *Earth Planet. Sci. Lett.*, **213**, (3-4), 185-190.

Katano, T., Nakano, S., Mitamura, O., Yoshida, H., Azumi, H., Matsuura, Y., Tanaka, Y., Maezono, H., Satoh, Y., Satoh, T., Sugiyama, Y., Watanabe, Y., Mimura, T., Akagashi, Y., Machida, H., Drucker, V.V., Tikhonova, I., Belykh, O., Fialkov, V.A., Han, M-S., Kang, S-H., Sugiyama, M. (2008). ‘Abundance and pigment type composition of picocyanobacteria in Barguzin Bay, Lake Baikal.’ *Limnology*, **9**, 105-114.

Katz, S.L., Izmet'eva, L.R., Hampton, S.E., Ozersky, T., Shchapov, K., Moore, M.V., Shimaraeva, S.V., Silow, E.A. (2015). ‘The “Melosira years” of Lake Baikal: Winter environmental conditions at ice onset predict under-ice algal blooms in spring.’ *Limnology and Oceanography*, **60**, 1950-1964.

Kaufman, D.S., Schneider, D.P., McKay, N.P., Ammann, C.M., Bradley, R.S., Briffa, K.R., Miller, G.H., Otto-Bliesner, B.L., Overpeck, J.T., Vinther, B.M., Arctic Lakes 2k Project Members (2009). ‘Recent warming reverses long-term Arctic cooling.’ *Science*, **325**, 1236-1239.

Khursevich G.K., Karabanov E.B., Prokopenko A.A., Williams D.F., Kuzmin M.I., Fedenya S.A. and Gvozdkov A.A. (2001). ‘Insolation regime in Siberia as a major factor controlling diatom production in Lake Baikal during the past 800,000 years.’ *Quaternary International*, **80-1**, 47-58.

Kiefer, D.A., Holm-Hansen, O., Goldman, C.R., Richards, R., Berman, T. (1972). ‘Phytoplankton in Lake Tahoe: Deep-living populations.’ *Limnology and Oceanography*, **17**, (3), 418 – 422.

Kilham, P. (1971). ‘A hypothesis concerning silica and the freshwater planktonic diatoms.’ *Limnol. Oceanogr.*, **16**, 10-18.

Kim, J.P., Fitzgerald, W.F. (1986). ‘Air partitioning of mercury in the Tropical Pacific Ocean.’ *Science*, **23**, 1131-1133.

King, L. L., Repeta, D. J. (1994). ‘Phorbol sterol esters in Black Sea sediment traps and sediments: A preliminary evaluation of their paleoceanographic potential.’ *Geochimica et Cosmochimica Acta*, **58**, (20), 4389–4399.

Kjørboe, T., Lundsgaard, C., Olesen, M., Hansen, J. L. S. (1994). ‘Aggregation and sedimentation processes during a spring phytoplankton bloom: A field experiment to test coagulation theory.’ *Journal of Marine Research*, **52**, (2), 297–323.

Klausmeier, C.A., Litchman, E. (2001). ‘Algal games: The vertical distribution of phytoplankton in poorly mixed water columns.’ *Limnol. Oceanogr.*, **46**, 1998–2007.

Klein, B., Gieskes, W.W.C., Kraay, G.G. (1986). ‘Digestion of chlorophylls and carotenoids by the marine protozoan *Oxyrrhis marina* by H.P.L.C. analysis of algal pigments.’ *J. Plankton Res.*, **8**, 827–836.

Klerkx, J., Batist, M.D., Poort, J., Hus, R., Rensbergen, P.V., Khlystov, O., Granin, N. (2003). ‘Tectonically controlled methane escape in Lake Baikal.’ *Advances in the Geological Storage of Carbon Dioxide*, **65**, 203-219.

Kluijver, A., Schoon, P.L., Downing, J.A., Schouten, S., Middelburg, J.J. (2014). ‘Stable carbon isotope biogeochemistry of lakes along a trophic gradient.’ *Biogeosciences*, **11**, 6265-6276.

Kokorin, A. O., Politov, S. V. (1991). ‘Wet deposition in the south Baikal region.’ *Soviet Meteorol. Hydrol.*, **1**, 39-44. (In Russian).

Kopp, J.F., Longbottom, M.C., Lobring, L.B. (1972). ‘Cold vapor method for determining mercury.’ *Journal (American Water Works Association)*, **64**, (1), 20-25.

Kotelevtsev, S.V., Hänninen, O.O.P., Lindström-Seppä, P.A., Huuskonen, S.E., Stephanova, L.I., Glaser, V.M., Beim, A.M. (2000). ‘Mutagenicity of bleached and

unbleached effluents from Baikalsk pulp and paper mill at Lake Baikal, Russia.’ *Aquatic Ecosystem Health and Management*, **3**, 95-104.

Koval, P.V., Kalmychkov, G.V., Gelety, V.F., Leonova, G.A., Medvedev, V.I., Andrulaitis, L.D. (1999). ‘Correlation of natural and technogenic mercury sources in the Baikal polygon, Russia.’ *Journal of Geochemical Exploration*, **66**, 277-289.

Koval, P.V., Kalmychkov, G.V., Geletyi, V.F., Andrulaitis, L.D. (2000). ‘Mercury distribution in the bottom and stream sediments of Lake Baikal, water reservoirs of the Angara river cascade, and adjacent drainage basins.’ K.Minoura (editor).

Kowalewska, G. (2005). ‘Algal pigments in sediments as a measure of eutrophication in the Baltic environment.’ *Quaternary International*, **130**, 141 – 151.

Kozhov, M. M. (1955). ‘Seasonal and annual changes in the plankton of Lake Baikal.’ [In Russian]. *Proc. Sov. Hydrobiol. Soc.*, **6**, 133–157.

Kozhov, M.M. (1963). Lake Baikal and its life. W. Junk Publishers, The Hague, The Netherlands.

Kozhova, O.M., Izmet’eva, L.R. (1998). Lake Baikal: Evolution and Biodiversity. Backhuys.

Kravtsova, L.S., Izhboldina, L.A., Khanaev, I.V., Pomazkina, G.V., Rodionova, E.V., Domysheva, V.M., Sakirko, M.V., Tomberg, I.V., Kostornova, T.Y., Kravchenko, O.S., Kupchinsky, A.B. (2014). ‘Nearshore benthic blooms of filamentous green algae in Lake Baikal.’ *Journal of Great Lakes Research*, **40**, 4441 – 448.

Kozhova, O. M. (1961). ‘On the periodical changes in the development of phytoplankton in Lake Baikal.’ [In Russian]. *Proc. Sov. Hydrobiol. Soc.*, **1**, 28–43.

Kozhova, O.M., Izhboldina, L.A. (1994). ‘Phytocenoses of the Bolshiye Koty River (Baikal tributary, Russia).’ *Algology*, **4**, 84–87.

Kozhova O.M. and Kobanov G.I. (2001). ‘Ecological peculiarities of diatoms in Lake Baikal. In: Economou-Amilli A. (ed.).’ *Proceedings of the 16th International Diatom Symposium. University of Athens, Greece.*, 279-290.

Kristiansen, S., Hoell, E.E. (2002). ‘The importance of silicon for marine production.’ *Hydrobiologia*, **484**, 21 – 31.

Krivtsov, V., Bellinger, E. G., Sigeo, D. C. (2005). ‘Elemental composition of *Microcystis aeruginosa* under conditions of lake nutrient depletion.’ *Aquat. Ecol.*, **39**, 123-134.

Kuzmin, M.I., Geletij, V.F., Kalmychkov, G.V., Kuznetsov, F.A., Larionov, E.G., Manakov, A.Y., Mironov, Y.I., Smolyakov, B.S., Dyadin, Y.A., Duchov, A.D., Bazin, N.M. and Mahov, G.A. (2000). ‘The discovery of the first gas hydrates in the sediments of Lake Baikal.’ In: Holder G.D. and Bishnoi P.R. (eds.). *Gas Hydrates. Challenges for the Future*. Annals of the New York Academy of Science 912, 112-115.

Kuz'min, M.I., Karabanov, E.B., Kawai, T., Williams, D., Bychinsky, V.A., Kerber, E.V., Kravchinsky, V.A., Bezrukova, E.V., Prokopenko, A.A., Geletii, V.F., Kalmychkov, G.V., Goreglyad, A.V., Antipin, V.S., Khomutova, M.Yu., Soshina, N.M., Ivanov, E.V., Khursevich, G.K., Tkachenko, L.L., Solotchina, E.P., Ioshida, N., Gvozdkov, A.N. (2001). ‘Deep drilling on Lake Baikal: main results.’ *Geologiya i Geofizika (Russian Geology and Geophysics)*, **42**, (1), 8–34.

Kuz'min, M.I., Bychinsjii, V.A., Kerber, E.V., Oschepkova, A.V., Goreglyad, A.V., Ivanov, E.V. (2014). ‘Chemical composition of sediments in Baikal deep-water boreholes as a basis for reconstructions of climatic and environmental changes.’ *Russian Geology and Geophysics*, **55**, 1-17.

Lacey, J.H., Francke, A., Leng, M.J., Vane, C.H., Wagner, B. (2014). ‘A high-resolution Late Glacial to Holocene record of environmental change in the Mediterranean from Lake Ohrid (Macedonia/Albania).’ *International Journal of Earth Sciences*, **104**, 1623-1638.

LaFlamme, R., Hites, R.A. (1978). ‘The global distribution of polycyclic aromatic hydrocarbons in recent sediments.’ *Geochim Cosmochim Ac.*, **42**, 289–303.

Lagus, A., Suomela, J., Weithoff, G., Heikkilä, K., Helminen, H., Sipura, J. (2004). ‘Species-specific differences in phytoplankton responses to N and P enrichments and the N:P ratio in the Archipelago Sea, northern Baltic Sea.’ *Journal of Plankton Research*, **26**, 779-798.

Lamb, A.J., Leng, M.J., Lamb, H.F., Telford, R.J., Mohammed, M.U. (2002). ‘Climatic and non-climatic effects on the $\delta^{18}\text{O}$ and $\delta^{13}\text{C}$ compositions of Lake Awassa, Ethiopia, during the last 6.5 ka.’ *Quaternary Science Reviews*, **21**, 2199-2211.

Lamb, A.L., Leng, M.J., Mohammed, M.U. Lamb, H.F. (2004). ‘Holocene climate and vegetation change in the Main Ethiopian Rift Valley, inferred from the composition (C/N and delta C-13) of lacustrine organic matter.’ *Quaternary Science Reviews*, **23**, 881-891.

Laws, E.A., Popp, B.N., Bidigare, R.R., Kennicutt, M.C., Macko, S.A. (1995). ‘Dependence of phytoplankton carbon isotopic composition on growth rate and $[\text{CO}_2]_{\text{aq}}$: Theoretical considerations and experimental results.’ *Geochimica et Cosmochimica Acta*, **59**, (6), 1131 – 1138.

Leavitt, P.R. (1993). 'A review of factors that regulate carotenoid and chlorophyll deposition and fossil pigment abundance.' *Journal of Palaeolimnology*, **9**, 109 – 127.

Leavitt, P.R., Findlay, D.L. (1994). ‘Comparison of fossil pigments with 20 years of phytoplankton data from eutrophic lake 227, experimental lakes area, Ontario.’ *Canadian Journal of Fisheries and Aquatic Sciences*, **51**, 2286 – 2299.

Leavitt, P.R., Vinebrooke, R.D., Donald, D.B., Smol, J.P., Schindler, D.W. (1997). ‘Past ultraviolet radiation environments in lakes derived from fossil pigments.’ *Nature*, **388**, 457 – 459.

Leavitt, P.R., Findlay, D.L., Hall, R.I., Smol, J.P. (1999). ‘Algal responses to dissolved organic carbon loss and pH decline during whole-lake acidification: Evidence from paleolimnology.’ *Limnology and Oceanography*, **44**, (3), 757-773.

Leavitt, P.R., Hodgson, D.A. (2001). ‘Sedimentary pigments.’ In: Smol, J.P., Birks, H.J.B., Last, W.M. (eds.) *Tracking Environmental Changes using Lake Sediments. Terrestrial, Algal and Siliceous Indicators 3*: Dordrecht: Kluwer.

Leavitt, P. R., Brock, C. S., Ebel, C., Patoine, A. (2006). ‘Landscape- scale effects of urban nitrogen on a chain of freshwater lakes in central North America.’ *Limnol. Oceanogr.* **51**, 2262–2277.

Lee, J.A., Flower, R.J., Appleby, P.G. (1998). ‘Mineral magnetic and physical properties of

surficial sediments and onshore samples from the southern basin of Lake Baikal, Siberia.' *Journal of Paleolimnology*, **20**, 175 – 186.

Lee YJ, Yun ST, Badarch M, Lee J, Ayur O, Kwon JS, Kim DM (2006). Joint research between Korea and Mongolia on water quality and contamination of transboundary watershed in Northern Mongolia. Korea Environmental Institute. Mongolian Nature and Environment Consortium.

Leermakers, M., Meuleman, C., Baeyens, W. (1996). 'Mercury distribution and fluxes in Lake Baikal.' In: Global and Regional mercury Cycles: Sources, Fluxes and Mass Balances. Eds Baeyens et al. Kluwer Academic Publishers. 303 – 315.

Lehmann, M.F., Bernasconi, S.M., Barbieri, A., McKenzie, J.A. (2002). 'Preservation of organic matter and alteration of its carbon and nitrogen isotope composition during simulated and in situ early sedimentary diagenesis.' *Geochemica et Cosmochimica Acta*, **66**, (20), 3573 – 3584.

Leng, M.J., Marshall, J.D. (2004). 'Palaeoclimate interpretation of stable isotope data from lake sediment archives.' *Quaternary Science Reviews*, **23**, 811-831.

Leng, M. J., Swann, G. E. A., Hodson, M. J., Tyler, J. J., Patwardhan, S. V., and Sloane, H. J. (2009). 'The potential use of silicon isotope composition of biogenic silica as a proxy for environmental change'. *Silicon*, **1**, 65–77.

Levine, M.A., Whalen, S.C. (2001). 'Nutrient limitation of phytoplankton production in Alaska Arctic foothill lakes.' *Environmental Science and Engineering*, **455**, 189-201.

Lewis Jr., W.M., Wurtsbaugh, W.A. (2008). 'Control of Lacustrine phytoplankton by nutrients: erosion of the phosphorus paradigm.' *Internationale Revue der gesamten Hydrobiologie und Hydrographie*, **93**, 446-465.

Liebezeit, G. (1992). 'Water and porewater chemistry of a Lake Baikal central basin station.' In: Degens, E.T., Levin, A., Sorokin, Y.I. (Editors). Interactions of Biogeochemical cycles in aqueous ecosystems. Mitt. Geol. Pallontol. Inst. Univ. Hamburg, Heft 72, 41 – 50.

Likhoshway, Y.V., Kuzmina, A.Y., Potyemkina, T.G., Potyemkin, V.L., Shimaraev, M.N. (1996). 'The distribution of diatoms near a thermal bar in Lake Baikal.' *J. Great Lakes Res.*, **22**, 5–14.

Lindström-Seppä, P., Huuskonen, S., Kotelevtsev, S., Mikkelsen, P., Raanen, T., Stepanova, L., Hanninen, A. (1998). 'Toxicity and Mutagenicity of Waste Waters from Baikalsk Pulp and Paper Mill: Evaluation of Pollutant Contamination in Lake Baikal.' *Marine Environmental Research*, **46**, (1 - 5), 213 – 211.

Livingstone D.M. (1999). 'Ice break-up on southern Lake Baikal and its relationship to local and regional air temperatures in Siberia and to the North Atlantic oscillation.' *Limnology and Oceanography*, **44**, 1486-1497.

Lorenschat, J., Zhang, X., Anselmetti, F.S., Reed, J.M., Wessels, M., Schwalb. (2014). 'Recent anthropogenic impact in ancient Lake Ohrid (Macedonia/Albania): a palaeolimnological approach.' *Journal of Palaeolimnology*, **52**, 139 – 154.

Lücke, A., Schleser, G.H., Zolitschka, B., Negendank, J.F.W. (2003). 'A lateglacial and Holocene organic carbon isotope record of lacustrine palaeoproductivity and climatic change derived from varved lake sediments of Lake Holzmaar, Germany.' *Quaternary Science Reviews*, **22**, 569-580.

Lücke, A., Brauer, A. (2004). 'Biogeochemical and micro-facial fingerprints of ecosystem response to rapid Late Glacial climatic changes in varved sediments of Meerfelder Maar (Germany).' *Palaeogeography, Palaeoclimatology, Palaeoecology*, **211**, 139-155.

Luniger, G., Schwark, L. (2002). 'Characterisation of sedimentary organic matter by bulk and molecular geochemical proxies: an example from Oligocene maar-type Lake Enspel, Germany.' *Sedimentary Geology*, **148**, 275-288.

Mackay, A.W., Flower, R.J., Kutmina, A.E., Granina, L., Rose, N.L., Appleby, P.G., Boyle, J.F., Battarbee, R.W. (1998). 'Diatom succession trends in recent sediments from Lake Baikal and their relation to atmospheric pollution and to climate change.' *Phil. Trans. R. Soc. Lond. B.*, **353**, 1011-1055.

Mackay, A.W., Battarbee, R.W., Flower, R.J., Granin, N.G., Jewson, D.H., Ryves, D.B., Sturm, M. (2003). 'Assessing the potential for developing internal diatom-based transfer functions for Lake Baikal.' *Limnology and Oceanography*, **48**, (3), 1183-1192.

Mackay, A.W., Ryves, D.B., Battarbee, R.W., Flower, R.J., Jewson, D., Rioual, P.M.J., Sturm, M. (2005). '1000 years of climate variability in central Asia: assessing the evidence

using Lake Baikal diatom assemblages and the application of a diatom-inferred model of snow thickness.' *Global and Planetary Change*, **46**, 281–297.

Mackay, A.W., Ryves, D.B., Morley, D.W., Jewson, D.H., Riouals, P. (2006). 'Assessing the vulnerability of endemic diatom species in Lake Baikal to predicted future climate change: a multivariate approach.' *Global Change Biology*, **12**, 2297 – 2315.

Mackay, A.W. (2007). 'The paleoclimatology of Lake Baikal: A diatom synthesis and prospectus.' *Earth-Science Reviews*, **82**, 181-215.

Mackay, A.W., Swann, G.E.A., Brewer, T.S., Morley, D.W., Piotrowska, N., Rioual, P., White, D. (2011). 'A late glacial-Holocene record of hydrological variability in Lake Baikal inferred from oxygen isotope analysis of diatom silica.' *Journal of Quaternary Science*, **26**, (6), 627-634.

Mackay, A.W., Bezrukova, E.V., Boyle, J.F., Holmes, J.A., Panizzo, V.N., Piotrowska, N., Shchetnikov, A., Shilland, E.M., Tarasov, P., White, D. (2013). 'Multiproxy evidence for abrupt climate change impacts on terrestrial and freshwater ecosystems in the Ol'khon region of Lake Baikal, central Asia.' *Quaternary International*, **290-291**, 46-56.

Mackay, A.W., Seddon, A.W.R., Leng, M.J., Heumann, G., Morley, D.W., Piotrowska, N., Rioual, P., Roberts, S., Swann, G.E.A. (2016). 'Holocene carbon dynamics at the forest-steppe ecotone of southern Siberia.' *Global Change Biology*, doi:10.1111/gcb.13583.

Maerki, M., Müller, B., Wehrli, B. (2006). 'Microscale mineralization pathways in surface sediments: A chemical sensor study in Lake Baikal.' *Limnology and Oceanography*, **51**, (3), 1342-1354.

Malderen, H.V., Grieken, R.V., Khodzher, T., Obolkin, V., Potemin, V. (1996). 'Composition of individual aerosol particles above Lake Baikal, Siberia.' *Atmospheric Environment*, **30**, (9), 1453-1465.

Magnuson, J.J., Robertson, D.M., Benson, B.J. (2000). 'Historical trends in lake and river ice cover in the northern hemisphere.' *Science*, **289**, 1743 – 1746.

- Marcarelli, A.M., Wurtsbaugh, W.A., Griset, O. (2006).** ‘Salinity controls phytoplankton response to nutrient enrichment in the Great Salt Lake, Utah, USA.’ *Can. J. Fish. Aquat. Sci.*, **63**, 2236-2248.
- Marchetto, A., Lami, A., Musazzi, S., Massafiero, J., Lanone, L., Guilizzoni, P. (2004).** ‘Lake Maggiore (N. Italy) trophic history: fossil diatom, plant pigments, and chironomids, and comparison with long-term limnological data.’ *Quaternary International*, **113**, 97 – 110.
- Marchitto, T.M. (2007).** ‘Nutrient Proxies.’ *Palaeoceanography, physical and chemical proxies/Nutrient proxies*, 1732-1739.
- Mason, R.P., Fitzgerald, W.F. (1990).** ‘Alkylmercury species in the equatorial pacific.’ *Nature*, **347**, 457-459.
- Mats, V.D., Khlystov, O.M., De Batist, M., Ceramicola, S., Lomonosova, T.K., Klimansky, A. (2000).** ‘Evolution of the Academician Ridge accommodation zone in the central part of the Baikal Rift, from high-resolution reflection seismic profiling and geological field investigations.’ *Int. J. Earth Sci.*, **89**, 229-250.
- Matzinger, A., Spirkovski, Z., Patceva, S., Wüest, A. (2006).** ‘Sensitivity of Ancient Lake Ohrid to local anthropogenic impacts and global warming.’ *J. Great Lakes Res.*, **32**, 158 – 179.
- Matzinger, A., Schmid, M., Veljanoska-Sarafiloska, E. Patceva, S., Guseska, D., Wagner, B., Müller, B., Sturm, M., Wüest, A. (2007).** ‘Eutrophication of ancient Lake Ohrid: Global warming amplifies detrimental effects of increased nutrient inputs.’ *Limnology and Oceanography*, **52**, (1), 338 – 353.
- McConnell, L.L., Kucklick, J.R., Bidleman, T.F., Ivanov, G.P., Chernyak, S.M. (1996).** ‘Air-water gas exchange of organochlorine compounds in Lake Baikal, Russia.’ *Enviro. Sci. Technol.*, **30**, 2975-2983.
- McFadden, M.A., Mullins, H.T., Patterson, W.P., Anderson, W.T. (2004).** ‘Paleoproductivity of eastern Lake Ontario over the past 10,000 years.’ *Limnology and Oceanography*, **49**, (5), 1570-1581.

McGowan, C., Barker, P., Haworth, E.Y., Leavitt, P.R., Maberly, S.C., Pates, J. (2012). ‘Humans and climate as drivers of algal community change in Windermere since 1850.’ *Freshwater Biology*, **57**, 260 – 277.

McGowan, S. (2013). Pigment Studies. In: Elias S.A. (ed.) *The Encyclopaedia of Quaternary Science*, vol. 3, pp. 326 - 338. Amsterdam: Elsevier.

McGowan, S., Anderson, N.J., Edwards, M.E., Langdon, P.G., Jones, V.J., Turner, S., van Hardenbroek, M., Whiteford, E., Wiik, E. (2015). ‘Long-term perspectives on terrestrial and aquatic carbon cycling from palaeolimnology.’ *Wires*, **3**, 211 – 234.

McKenzie J.A. (1985). ‘Carbon isotopes and productivity in the lacustrine and marine environment.’ In Stumm W. (ed). *Chemical Processes in Lakes*. Wiley, New York.

McKnight, D.M., Howes, B.L., Taylor, C.D., Goehring, D.D. (2000). ‘Phytoplankton dynamics in a stably stratified Antarctic lake during winter darkness.’ *J Phycol.*, **36**, 852 - 861.

McLeod, A.I. (2011). Kendall: Kendall Rank Correlation and Mann-Kendall trend test, R package version 2.2. Available at: <http://cran.rproject.org/package=Kendall>.

McMaster, N.L., Schindler, D.W. (2005). ‘Planktonic and epipelagic algal communities and their relationship to physical and chemical variables in alpine ponds in Banff National Park, Canada.’ *Arctic Antarctic Alpine Research*, **37**, 337–347.

Meier, K.I. (1930). ‘Introduction into algal flora of Lake Baikal. Bull.’ *MOIP*, New Series 39 (3–4), 179–396.

Melnik, N.G., Lazarev, M.I., Pomazkova, G.I., Bondarnko, N.A., Obolkina, L.A., Penzina, M.M., Timoshkin, O.A. (2008). ‘The cryophilic habitat of micrometazoans under the lake –ice in Lake Baikal.’ *Fundamental and Applied Limnology*, **170**, (4), 315 – 323.

Meuleman, C., Leermakers, M., Baeyens, W. (1995). ‘Mercury speciation in Lake Baikal.’ *Water, Air and Soil Pollution*, **80**, 539-551.

Meyers, P.A., Eadie, B.J. (1993). ‘Sources, degradation and recycling of organic matter associated with sinking particles in Lake Michigan.’ *Org. Geochem.*, **20**, (1), 47-56.

Meyers, P.A., Ishiwatari, R. (1993). ‘Lacustrine organic geochemistry – an overview of indicators of organic matter sources and diagenesis in lake sediments.’ *Org. Geochem*, **20**, (7), 867 – 900.

Meyers P.A. (1994). ‘Preservation of elemental and isotopic source identification of sedimentary organic-matter.’ *Chemical Geology*, **114**, 289-302.

Meyers, P.A., Ishiwatari, R. (1995). Organic matter accumulation records in lake sediments. In: Lerman A, Imboden D, Gat J (eds) *Physics and chemistry of lakes*. Springer, Berlin, pp 279–328.

Meyers, P.A., Lallier-Verges, E. (1999). ‘Lacustrine sedimentary organic matter records of Late Quaternary paleoclimates.’ *Journal of Paleolimnology*, **21**, 345-372.

Meyers, P.A., Teranes, J.L. (2001). ‘Sediment organic matter.’ In: *Tracking Environmental Change Using Lake Sediments, Volume 2, Physical and Geochemical Methods*, Eds Last, W.M., Smol, J.P. Kluwer Academic Publishers, The Netherlands.

Meyers, P.A. (2003). ‘Applications of organic geochemistry to palaeolimnological reconstructions: a summary of examples from the Laurentian Great Lakes.’ *Org Geochem*, **34**, (2), 261–289.

Michalak, A.M., Anderson, E.J., Beletsky, D., Boland, S., Bosch, N.S., Bridgeman, T.B., Chaffin, J.D., Cho, K., Confessor, R., Daloglu, I., DePinto, J.V., Evans, M.A., Fahnenstiel, G.L., He, L., Ho, J.C., Jenkins, L., Johengen, T.H., Kuo, K.C., LaPorte, E., Liu, X., McWilliams, M.R., Moore, M.R., Posselt, D.J., Richards, R.P., Scavia, D., Steiner, A.L., Verhamme, E., Wright, D.M., Zagorski, M.A. (2013). ‘Record-setting algal bloom in Lake Erie caused by agricultural and meteorological trends consistent with expected future conditions.’ *Proceedings of the National Academy of Sciences*, **110**, 6448-6452.

Micklin, P. (2007). ‘The Aral Sea Disaster.’ *Annual Review of Earth and Planetary Science*, **35**, 47 – 72.

Millie, D.F., Paerl, H.W., Hurley, J.P. (1993). ‘Microalgal pigment assessments using high-performance liquid chromatography: A synopsis of organismal and ecological applications.’ *Canadian Journal of Fisheries and Aquatic Sciences*, **50**, 2513 – 2527.

Millie, D.F., Fahnenstiel, G.L., Bressie, J.D., Pigg, R.J., Rediske, R.R., Klarer, D.M., Tester, P.A., Litaker, R.W. (2009). ‘Late-summer phytoplankton in western Lake Erie (Laurentian Great Lakes): bloom distributions, toxicity, and environmental influences.’ *Aquat. Ecol.*, **43**, 915–934.

Modenutti, B., Balseiro, E., Navarro, M.B., Laspoumaderes, C., Souza, M.S., Cuassolo, F. (2013). ‘Environmental changes affecting light climate in oligotrophic mountain lakes: the deep chlorophyll maxima as a sensitive variable.’ *Aquatic Science*, **75**, 361 – 371.

Moore, M.V., Hampton, S.E., Izmesteva, L.R., Silow, E.A., Peshkova, E.V., Pavlov, B.K. (2009). ‘Climate Change and the World’s “Sacred Sea” – Lake Baikal, Siberia.’ *BioScience*, **59**, (5), 405 – 417.

Morley, D.W. (2005). Reconstructing past climate variability in continental Eurasia. PhD Thesis (unpublished).

Morley, D.W., Leng, M.J., Mackay, A.W., Sloane, H.J. (2005). ‘Late glacial and Holocene environmental change in the Lake Baikal region documented by oxygen isotopes from diatom silica.’ *Global and Planetary Change*, **46**, 221-233.

Morgenstern, U., Ditchburn, R.G., Vologina, E.G., Sturm, M. (2013). ‘³²Si dating of sediments from Lake Baikal.’ *Journal of Paleolimnology*, **50**, (3), 345-352.

Müller, B., Maerki, M., Schmid, M., Vologina, E.G., Wehrli, B., Wuest, A., Sturm, M. (2005). ‘Internal carbon and nutrient cycling in Lake Baikal: sedimentation, upwelling, and early diagenesis.’ *Global and Planetary Change*, **46**, 101 – 124.

Muggeo, V.M. (2008). ‘Segmented: An R package to fit regression models with broken-line relationships.’ *R news*, **8**, 20-25.

Muylaert, K., Gonzales, R., Franck, M., Lionard, M., Van der Zee, C., Cattrijse, A., Sabbe, K., Chou, L., Vyverman, W. (2006). ‘Spatial variation in phytoplankton dynamics in the Belgian coastal zone of the North Sea studied by microscopy, HPLC-CHEMTAX and underway fluorescence recordings.’ *Journal of Sea Research*, **55**, 253 – 265.

Muylaert, K., Sanchez-Perez, J.M., Teissier, S., Sauvage, S., Dauta, A., Vervier, P. (2009). ‘Eutrophication and its effect of dissolved Si concentrations in the Garonne Rober (France).’ *Journal of Limnology*, **68**, (2), 368-374.

Nakata, H., Tanabe, S., Tatsukawa, R., Amano, M., Miyazaki, N., Petrov, E.A. (1995). ‘Persistent organochlorine residues and their accumulation kinetics in Baikal Seal (*Phoca sibirica*) from Lake Baikal, Russia.’ *Environmental Science and Technology*, **29**, 2877–2885.

Nakata, H., Tanabe, S., Tatsukawa, R., Amano, M., Miyazaki, N., Petrov, E.A., (1997). ‘Bioaccumulation profiles of polychlorinated biphenyls including coplanar congeners and possible toxicological implications in Baikal seal (*Phoca sibirica*).’ *Environmental Pollution*, **95**, 57–65.

Nakano, S., Mitamura, O., Sugiyama, M., Maslennikov, A., Nishibe, Y., Watanabe, Y., Drucker, V. (2003). ‘Vertical planktonic structure in the central basin of Lake Baikal in summer 1999, with special reference to the microbial food web.’ *Limnology*, **4**, 155-160.

Naylor, C.C., Keely, B.J. (1998). ‘Sedimentary porphyrins: oxidative transformation products of chlorophylls.’ *Org. Geochem.*, **28**, (7-8), 417 – 422.

Nelson, C.H., Karabanov, E.B., and Colman, S.M. (1995). ‘Late Quaternary Lake Baikal turbidite systems, Russia, in Pickering, K.T., Ricci Lucchi, F., Smith, R., Hiscott, R.N., and Kenyon, N., eds., *An Atlas of Deep-Water Environments*: London, Chapman & Hall, p. 29–33.

Nelson, C.H., Karabanov, E.B., Colman, S.M., Escutia, C. (1999). ‘Tectonic and sediment supply control of deep rift lake turbidite systems: Lake Baikal, Russia.’ *Geology*, **27**, (2), 163 – 166.

Nesje, A., Jansen, E., Birks, H.J.B., Bjune, A.E., Bakke, J., Andersson, C., Dahl, S.O., Kristensen, D.K., Lauritzen, S.-E., Lie, Ø., Risebrobakken, B., Svendsen, J.-I., (2005). Holocene climate variability in the northern North Atlantic region: a review of terrestrial and marine evidence. *The Nordic Seas: An integrated Perspective*. Geophysical Monograph Series, vol. 158, pp. 289–322.

Neukom, R., Gergis, J. (2011). ‘Southern Hemisphere high-resolution palaeoclimate records of the last 2000 years.’ *The Holocene*, **22**, 501-524.

Nomokonova, T., Losely, R.J., Weber, A., Goriunova, L.I., Novikov, A.G. (2010). ‘Late Holocene subsistence practices among cis-Baikal pastoralists, Siberia: zooarchaeological insights from Sagan-Zaba II.’ *Asian Perspectives*, 49, 157-179.

O’Beirne, M.D., Strzok, L.J., Werne, J.P., Johnson, T.C., Hecky, R.E. (2015). ‘Anthropogenic influences on the sedimentary geochemical record in western Lake Superior (1800-present).’ *Journal of Great Lakes Research*, 41, 20-29.

Obolkina, L.A., Bondarenko, N.A., Doroshenko, L.F., Molozhavaya, O.A. (2000). ‘Finding of a cryophilic community in Lake Baikal.’ *Doklady Akademii Nauk*, 371, 815 – 817.

Obolkin, V.A., Netsvetaeva, O.G., Golobokova, L.P., Potemkin, V.L., Zimnik, E.A., Filippova, U.G., Khodzher, T.V. (2013). ‘Results of long-term investigations on acid deposition in the area of south Baikal.’ *Geography and Natural Resources*, 34, (2), 151-157.

Obolkin, V.A., Potemkin, V.L., Makukhin, V.L., Chipanina, Y.V., Marinayte, I.I. (2014). ‘Low-level atmospheric jets as main mechanism of long-range transport of power plant plumes in the Lake Baikal region.’ *International Journal of Environmental Studies*, 71, (3), 391-397.

Obolkin, V., Khodzher, T., Sorokovikova, L., Tomberg, I., Netsvetaeva, O., Golobokova, L. (2016). ‘Effect of long-range transport of sulphur and nitrogen oxides from large coal power plants on acidification of river waters in the Baikal region, East Siberia.’ *International Journal of Environmental Studies*, 73, 452-461.

O’Brien W.J., Hershey A.E., Hobbie J.E., Hullar M.A., Kipphut G.W., Miller M.C., Moller B. & Vestal J.R. (1992). ‘Control mechanisms of arctic lake ecosystems: a limnocorral experiment.’ *Hydrobiologia*, 240, 143–188.

Och, L., Müller, B., Wichser, A., Ulrich, A., Vologina, E.G., Sturm, M. (2014). ‘Rare earth elements in the sediments of Lake Baikal.’ *Chemical Geology*, 376, 61-75.

O’Donnell, D.R., Wilburn, P., Silow, E.A., Yampolsky, L.Y., Litchman, E. (2017). ‘Nitrogen and phosphorus colimitation of phytoplankton in Lake Baikal: Insights from a spatial survey and nutrient enrichment experiments.’ *Limnology and Oceanography*, 62, (4), 1383-1392.

Officer, C.B., Ryther, J.H. (1980). ‘The possible importance of Silicon in marine eutrophication.’ *Marine Ecology – Progress Series*, **3**, 83-91.

O’Leary, MH. (1988). ‘Carbon isotopes in photosynthesis, fractionation techniques may reveal new aspects of carbon dynamics in plants.’ *BioScience*, **38**, (5), 328-335.

O’Reilly, C.M., Alin, S.R., Plisnier, P-D., Cohen, A.S., McKee, B.A. (2003). ‘Climate change decreases aquatic ecosystem productivity of Lake Tanganyika, Africa.’ *Nature*, **424**, 766 – 768.

Osburn, C.L., Retamal, L., Vincent, W.F. (2009). ‘Photoreactivity of chromophoric dissolved organic matter transported by the Mackenzie River to the Beaufort Sea.’ *Mar Chem.*, **115**, 10 – 20.

Ostrom, N.E., Carrick, H.J., Twiss, M.R., Piwinski. (2005). ‘Evaluation of primary production in Lake Erie by multiple proxies.’ *Oecologia*, **144**, 115-124.

Oviatt, C.A. Keller, A.A., Sampou, P.A., Beatty, L.L. (1986). ‘Patterns of productivity during eutrophication: a mesocosm experiment.’ *Marine Ecology – Progress Series*, **28**, 69-80.

Paerl, H.W. (2009). ‘Controlling eutrophication along the freshwater-marine continuum: Dual nutrient (N and P) reductions are essential.’ *Estuaries and Coasts*, **32**, 593-601.

Paerl, H.W., Hall, N.S., Calandrino, E.S. (2011). ‘Controlling harmful cyanobacterial blooms in a world experiencing anthropogenic and climatic-induced change.’ *Science of the Total Environment*, **409**, 1739-1745.

Paerl, H.W., Nathan, H.X., Hall, N.S., Zhu, G., Qin, B., Wu, Y., Rossignol, K.L., Dong, L., McCarthy, M.J., Joyner, A.R. (2014). ‘Controlling cyanobacterial blooms in hypertrophic Lake Taihu, China: Will nitrogen reductions cause replacement of non-N₂ fixing by N₂ fixing taxa?’ *Plus One*, **9**, (11), 1-13.

PAGES 2k Consortium (2013). ‘Continental-scale temperature variability during the past two millennia.’ *Nature Geoscience*, **6**, 339-346.

Panizzo, V.N., Swann, G.E.A., Mackay, A.W., Vologina, E., Sturm, M., Pashley, V.H., Hortswood, M.S.A. (2016) ‘Tracing the fate of transfer of silicon isotopes to the sediment record.’ *Biogeosciences*, **13**, 147-157.

Panizzo, V.N., Roberts, S., Swann, G.E.A., McGowan, S., Mackay, A.W., Vologina, E., Pashley, V., Hortswood, M.S.A. ‘Spatial differences in dissolved silicon utilisation in Lake Baikal, Siberia: evidence of high diatom bloom events and localised eutrophication.’ (Submitted).

Parker, J.I., D.N. Edgington. (1976). ‘Concentration of diatom frustules in Lake Michigan sediment cores.’ *Limnology and Oceanography*, **21**, 887-893.

Parplies, J., Lücke, A., Vos, H., Mingram, J., Stebich, M., Radtke, U., Han, J., Schleser, G.H. (2008). ‘Late glacial environment and climate development in northeastern China derived from geochemical and isotopic investigations of the varved sediment record from Lake Sihailongwan (Jilin Province).’ *Journal of Paleolimnology*, **40**, 471-487.

Parvathi, A., Zhong, X., Pradeep Ram, A.S., Jacquet, S. (2014). ‘Dynamics of auto- and heterotrophic picoplankton and associated viruses in Lake Geneva.’ *Hydrol. Earth Syst. Sci.*, **18**, 1073-1087.

Paterson, M.J., Schindler, D.W., Hecky, R.E., Findlay, D.L., Rondeau, K.J. (2011). ‘Comment: Lake 227 shows clearly that controlling inputs of nitrogen will not reduce or prevent eutrophication of lakes.’ *Limnology and Oceanography*, **56**, (4), 1545-1547.

Patoine, A., Leavitt, P.R. (2008). ‘Landscape analysis of the role of N₂ fixation in satisfying algal demand from nitrogen in eutrophic lakes.’ *Verh. Internat. Verein. Limnol.*, **30**, (3), 366-370.

Peck, J. A., King, J. W., Colman, S. M., Kravchinsky, V. A. (1994). ‘A rock magnetic record from Lake Baikal, Siberia: Evidence for Late Quaternary climate change.’ *Earth Plan. Sci. Lett.*, **122**, 221–238.

Perez, M.T., Sommaruga, R. (2006). ‘Differential effect of algal and soil derived dissolved organic matter on alpine lake bacterial community composition and activity.’ *Limnol. Oceanogr.*, **51**, (6), 2527 – 2537.

Perrot, V., Epov, V.N., Pastukhov, M.V., Grebenshikova, V.I., Zouiten, C., Sonke, J.E., Husted, S., Donard, O.F.X., Amouroux, D. (2010). ‘Tracing sources and bioaccumulation of mercury in fish of Lake Baikal – Angara River using Hg isotopic composition.’ *Environ. Sci. Technol.*, **44**, 8030-8037.

Peeters E, G. Piepke, R. Kipfer, R. Hohmann and D. M. Imboden, (1997). ‘Modelling transport rates in Lake Baikal: gas exchange and deep water renewal.’ *Environ. Sci. Technol.*, **31**, 2973-2982.

Phoenix, G.K., Hicks, W.K., Cindeberry, S., Kuylenstierna, J.C.I., Stock, W.D., Dentener, F.J., Giller, K.E., Austin, A.T., Lefroy, R.D.B., Gimeno, B.S., Ashmore, M.R., Ineson, P. (2006). ‘Atmospheric nitrogen deposition in world biodiversity hotspots: the need for a greater global perspective in assessing N deposition impacts.’ *Global Change Biology*, **12**, 470-476.

Pienitz, R., Smol, J.P., Last, W.M., Leavitt, P.R., Cumming, B.F. (2000). ‘Multi-proxy Holocene palaeoclimatic record from a saline lake in the Canadian Subarctic.’ *The Holocene*, **10**, (6), 673 – 686.

Piotrowska, N., Bluszez, A., Demske, D., Granoszewski, W., Heumann, G. (2004). ‘Extraction and AMS Radiocarbon dating of pollen from Lake Baikal sediments.’ *Radiocarbon*, **46**, (1), 181 – 187.

Popovskaya, G.I. (1968). ‘New species of *Synechocystis* Sauv. Genus in Lake Baikal plankton. In Savich, V.P. (ed.), *The Lowest Plant Systematics News*. Nauka, Leningrad: 3-5 (in Russian).

Popovskaya, G.I. (2000). ‘Ecological monitoring of phytoplankton in Lake Baikal.’ *Aquatic Ecosystem Health and Management*, **3**, 215 – 225.

Popovskaya, G.I., Likhoshway, Y.V., Genkal, S.I., Firsova. (2006). ‘The role of endemic diatom algae in the phytoplankton of Lake Baikal.’ *Hydrobiologia*, **568**, 87 – 94.

Popovskaya, G.I., Usol'tseva, M.V., Domysheva, V.M., Sakirko, M.V., Blinov, V.V., Khodzer, T.V. (2015). ‘The spring phytoplankton in the pelagic zone of Lake Baikal during 2007 – 2011’ *Geography and Natural Resources*, **36**, (3), 253-262.

Porra, R., Pfündel, E., Engel, N. (1997). Metabolism and function of photosynthetic pigments. In: Jeffrey, S., Mantoura, R., Wright, S. (Eds.), *Phytoplankton pigments in oceanography*. UNESCO Publishing, Paris, pp. 85–126.

Prokopenko, A., Williams, D. F., Koval, P., Karabanov, E. (1993). ‘The organic indexes in the surface sediments of Lake Baikal water system and the processes controlling their variation.’ *IPPCCE Newsletter*, **7**, 49-55.

Prokopenko, A.A., Williams, D.F., Karabanov, E.B., Khursevich, G.K. (1999). ‘Response of Lake Baikal ecosystem to climate forcing and pCO₂ change over the last glacial / interglacial transition.’ *Earth and Planetary Science Letters*, **172**, 239-253.

Prokopenko, A. A., Karabanov, E. B., Williams, D. F., Kuzmin, M. I., Shackleton, N. J., Crowhurst, S. J., Peck, J. A., Gvozdkov, A. N., King J. W. (2001a). ‘Biogenic silica record of the Lake Baikal response to climatic forcing during the Brunhes.’ *Quaternary Research*, **55**, 123-132.

Prokopenko, A.A., Karabanov, E.B., Williams, D.F., Kuzmin, M.I., Khursevich, G.K., Gvozdkov, A.A. (2001b). ‘The detailed record of climatic events during the past 75,000 yrs BP from the Lake Baikal drill core BDP-93-2.’ *Quaternary International*, **80-1**, 59-68.

Prokopenko, A.A., Williams, D.F., Karabanov, E.B., Khursevich, G.K. (2001c). ‘Continental response to Heinrich events and Bond cycles in sedimentary record of Lake Baikal, Siberia.’ *Global and Planetary Change*, **28**, 217 – 226.

Prokopenko, A.A., Williams, D.F. (2003). ‘Glacial/interglacial changes in carbon cycle of Lake Baikal.’ *Long Continental Records from Lake Baikal*, pp 163-185.

Prokopenko A.A. and Williams D.F. (2004). ‘Deglacial methane emission signals in the carbon isotopic record of Lake Baikal.’ *Earth and Planetary Science Letters*, **218**, 135-147.

Prokopenko, A.A., Khursevich, G.K., Bezrukova, E.V., Kuzmin, M.I., Boes, X., Williams, D.F., Fedenya, S.A., Kulagina, N.V., Letunova, P.P., Abzaeva, A.A. (2007). ‘Paleoenvironmental proxy records from Lake Hovsgol, Mongolia, and a synthesis of Holocene climate change in the Lake Baikal watershed.’ *Quaternary Research*, **68**, 2-17.

Qiu, L. Q., Williams, D. F., Gvozdkov, A., Karabanov, E. and Shimaraeva, M. (1993).

‘Biogenic silica accumulation and paleoproductivity in the northern basin of Lake Baikal during the Holocene.’ *Geology*, **21**, 25-28.

Ravens, T.M., Kocsis, O., Wüest, A. (2000). ‘Small-scale turbulence and vertical mixing in Lake Baikal.’ *Limnology and Oceanography*, **45**, (1), 159-173.

Rea, D.K., Bourbonniere, R.A., Meyers, P.A. (1980). ‘Southern Lake Michigan sediments: changes in accumulation rate, mineralogy, and organic content.’ *Journal of Great Lakes Research*, **6**, 321-330.

Reavie, E.D., Barbiero, R.P., Allinger, L.E., Warren, G.J. (2014a). ‘Phytoplankton trends in the Great Lakes, 2001-2011.’ *Journal of Great Lakes Research*, **40**, 618-639.

Repeta, D.J., Simpson, D.J. (1990). ‘The distribution and recycling of chlorophyll, bacteriochlorophyll and carotenoids in the Black Sea.’ *Deep-Sea Research*, **38**, (2), 969 – 984.

Reuss, N. (2005). ‘Sediment pigments as biomarkers of environmental changes.’ National Environment Research Institute, Ministry of the Environment, Denmark. PhD Thesis.

Reuss, N., Conley, D.J., Bianchi, T.S. (2005). ‘Preservation conditions and the use of sediment pigments as a tool for recent ecological reconstruction in four Northern European estuaries.’ *Marine Chemistry*, **95**, 283-302.

Riedinger-Whitmore, M.A., Whitmore, T.J., Smoak, J.M., Brenner, M., Moore, A., Curtis, J., Schelske, C.L. (2005). ‘Cyanobacterial proliferation is a recent response to eutrophication in many Florida Lakes: A Paleolimnological Assessment.’ *Lake and Reservoir Management*, **21**, (4), 423-435.

Richardson T.L., Gibson C.E. and Heaney S.I. (2000). ‘Temperature, growth and seasonal succession of phytoplankton in Lake Baikal, Siberia.’ *Freshwater Biology*, **44**, 431-440.

Rioual, P., Mackay, A.W. (2005). ‘A diatom record of centennial resolution for the Kazantsevo Interglacial stage in Lake Baikal (Siberia).’ *Global and Planetary Change*, **46**, 199-219.

Romanovsky, V.E., Drozdov, D.S., Oberman, N.G. Malkova, G.V., Kholodov, A.L., Marchenko, S.S., Moskalenko, N.G., Sergeev, D.O., Ukraintseva, N.G., Abramov A.A.,

Gilichinsky, D.A., Vasiliev, A.A. (2010). ‘Thermal state of permafrost in Russia.’ *Permafrost and Periglacial Processes*, **21**, 136-155.

Rose, N.L., Appleby, P.G., Boyle, J.F., Mackay, A.W., Flower, R.J. (1998). ‘The spatial and temporal distribution of fossil-fuel derived pollutants in the sediment record of Lake Baikal, eastern Siberia.’ *Journal of Paleolimnology*, **20**, 151 – 162.

Rose, K.C., Williamson, C.E., Saros, J.E., Sommaruga, R., Fischer, J.M. (2009). ‘Differences in UV transparency and thermal structure between alpine and subalpine lakes: implications for organisms.’ *Photochem. Photobiol. Sci.*, **8**, 1244 – 1256.

Rucinski, D., DePinto, J.V., Scavia, D., Beletsky, D. (2014). ‘Modeling lake Erie’s hypoxia response to nutrient loads and physical variability.’ *Journal of Great Lakes Research*, **40**, (3), 151-161.

Russell, M., Rosell-Melé, A. (2005). ‘Preliminary study of fluxes of major lipid biomarker classes in the water column and sediments of Lake Baikal, Russia.’ *Global and Planetary Change*, **46**, 45 – 56.

Russian Federal State Statistics Service. (2011)

(http://www.gks.ru/wps/wcm/connect/rosstat_main/rosstat/en/main/)

Rychkov I.L., Kuzevanova E.N. and Pomazkova G.I. (1989) Long-term natural changes in plankton of the southern Baikal. In: Salánki J, Herodek S (eds.). Akadémiai Kiadó, Budapest, 361-6.

Ryves, D.B., Jewson, D.H., Sturm, M., Battarbee, R.W., Flower, R. J., Mackay, A.W. (2003). ‘Quantitative and qualitative relationships between planktonic diatom communities and diatom assemblages in sedimenting material and surface sediments in Lake Baikal, Siberia.’ *Limnology and Oceanography*, **48**, (4), 1643 – 1661.

Ryves, D.B., Battarbee, R.W., Frit, S.C., (2009). 'The Dilemma of Disappearing Diatoms: Incorporating Diatom Dissolution Data into Paleoenvironmental Modelling and Reconstruction.' *Quaternary Science Reviews*, **28**, (1 – 2), 120 – 136

Salonen, K., Lepparanta, M., Viljanen, M., Gulati, R.D. (2009). ‘Perspectives in winter limnology: closing the annual cycle of freezing lakes.’ *Aquatic Ecology*, **43**, 609 – 616.

Saros, J.E., Interlandi, S.J., Doyle, S., Michel, T.J., Williamson, C.E. (2005). ‘Are the deep chlorophyll maxima in alpine lakes primarily induced by nutrient availability, not UV avoidance?’ *Arctic, Antarctic and Alpine Research*, **37**, (4), 557-563.

Satoh, Y., Katano, T., Satoh, T., Mitamura, O., Anbutsu, K., Nakano, S., Ueno, H., Kihira, M., Drucker, V., Tanaka, Y., Mimura, T., Watanabe, Y., Sugiyama, M. (2006). ‘Nutrient limitation of the primary production of phytoplankton in Lake Baikal.’ *Limnology*, **7**, 225 – 229.

Savage, C., Leavitt, P.R., Elmgren, R. (2010). ‘Effects of land use, urbanization, and climate variability on coastal eutrophication in the Baltic Sea.’ *Limnology and Oceanography*, **55**, (3), 1033 – 1046.

Searle, R.C. (2008). ‘Magnetic susceptibility as a tool for investigating igneous rocks – experience from IODP expedition 304.’ *Technical Developments*, **6**, 52-54.

Schelske, C.L., Robbins, J.A., Gardner, W.D., Conley, D.J., Bourbonniere, R.A. (1988). ‘Sediment record of biogeochemical responses to anthropogenic perturbations of nutrient cycles in Lake Ontario.’ *Can. J. Fish. Aquat. Sci.*, **45**, 1291-1303.

Schelske, C.L. and E.F. Stoermer. (1971). ‘Eutrophication, silica depletion, and predicted changes in algal quality in Lake Michigan.’ *Science*, **173**, 423-424.

Schelske, C.L. and E.F. Stoermer. (1972). ‘Phosphorus, silica, and eutrophication of Lake Michigan. In: G.E. Likens (ed.), Nutrients and eutrophication, Special Symposia Vol. 1, American Society of Limnology and Oceanography. pp. 157-171. Allen Press, Lawrence, Kansas.

Schelske, C.L., Conley, D.J., Robbins, J.A., Glover, R. (1983). ‘Early eutrophication of the lower Great Lakes: New evidence from biogenic silica in sediments.’ *Science*, **222**, 320– 322.

Schelske, C.L. (1985). ‘Biogeochemical silica mass balances in Lake Michigan and Lake Superior.’ *Biogeochemistry*, **1**, 197 – 218.

Schelske, C.L., Stoermer, E.F., Fahnenstiel, G.L., Haibach, M. (1986). ‘Phosphorus enrichment, silica utilization, and biogeochemical silica depletion in the Great Lakes.’ *Can. J. Fish Aquat. Sci.*, **43**, 407-415.

Schelske, C.L., Hodell, D.A. (1991). ‘Recent changes in productivity and climate of Lake Ontario detected by isotopic analysis of sediments.’ *Limnol. Oceanogr.*, **36**, 961–975.

Schelske, C.L., Hodell, D.A. (1995). ‘Using carbon isotopes of bulk sedimentary organic matter to reconstruct the history of nutrient loading and eutrophication in Lake Erie.’ *Limnol. Oceanogr.*, **40**, (5), 918 – 929.

Schelske, C.L., Stoermer, E.F., Kenney, W.F. (2006). ‘Historic low-level phosphorus enrichment in the Great Lakes inferred from biogenic silica accumulation in sediments.’ *Limnology and Oceanography*, **51**, 728 – 748.

Schindler, D. W. (1971). ‘Carbon, nitrogen, phosphorus and the eutrophication of freshwater lakes.’ *J. Phycol.*, **7**, 321–329.

Schlinder, D.W. (1977). ‘The evolution of phosphorus limitation in lakes.’ *Science*, **195**, 260-262.

Schindler, D. W. (1974). ‘Eutrophication and recovery in experimental lakes: implications for lake management.’ *Science*, **184**, 897–899.

Schindler, D.W., Hecky, R. E., Findlay, D. L., Stainton, M. P., Parker, B. R., Paterson, M., Beaty, K. G., Lyng, M., Kasian, S. E. M. (2008). ‘Eutrophication of lakes cannot be controlled by reducing nitrogen input: results of a 37-year whole ecosystem experiment.’ *Proc. Natl Acad. Sci. USA*, **105**, 254–258.

Schüller, S.E., Savage, C. (2011). ‘Spatial distribution of diatom and pigment sedimentary records in surface sediments in Doubtful Sound, Fiordland, New Zealand.’ *New Zealand Journal of Marine and Freshwater Research*, **45**, (4), 591-608.

Schüller, S.E., M.A. Allison, T.S. Bianchi, F. Tian, and C. Savage. (2013). ‘Historical variability in past phytoplankton abundance and composition in Doubtful Sound, New Zealand.’ *Continental Shelf Research*, **69**, 110–122.

Schüller, S.E. (2014). ‘Mechanisms governing degradation of phytoplankton pigments in fjords.’ Department of Marine Science, University of Otago, Dunedin, New Zealand, PhD thesis.

Schüller, S.E., Bianchi, T.S., Li, X., Allison, M.A., Savage, C. (2014). ‘Historical reconstruction of phytoplankton composition in estuaries of Fiordland, New Zealand: the application of plant pigment biomarkers.’ *Estuaries and Coasts*, **38**, 56-71.

Schuster, S., Grismer, M.E. (2004). ‘Evaluation of water quality projects in the Lake Tahoe basin.’ *Environ Monit Assess.*, **90**, (1-3), 225-242.

Scott, J.T., McCarthy, M.J. (2011). ‘Response to Comment: Nitrogen fixation has not offset declines in the Lake 227 nitrogen pool and shows that nitrogen control deserves consideration in aquatic ecosystems.’ *Limnol. Oceanogr.*, **56**, (4), 1548-1550.

Seehausen, O., Witte, F., Katunzi, E.F., Smits, J., Bouton, N. (1997). ‘Patterns of the remnant cichlid fauna in southern Lake Victoria.’ *Conservation Biology*, **11**, 890–904.

Sharkuu, N. (1998). ‘Trends in permafrost development in the Selenga River basin, Mongolia.’ *Collection Nordicana*, **55**, 979-985.

Shimaraev, M. N. (1971). ‘Hydrometeorological factors and variation in the abundance of Baikal plankton. [In Russian].’ *Proc. Limnol. Inst. Sib. Branch USSR Acad. Sci.*, **12**, 259–267.

Shimaraev, M.N. (1977). Thermal regime of Lake Baikal. Nauka, Novosibirsk.

Shimaraev, M. N. and Granin, N. G. (1991). Temperature stratification and the mechanisms of convection in Lake Baikal.’ *Doklady Akademii Nauk*, **321**, 831 – 835.

Shimaraev M.N, Granin N.G. and Zhdanov A.A (1993). ‘Deep ventilation of Lake Baikal waters due to spring thermal bars.’ *Limnology and Oceanography*, **38**, 1068-72.

Shimaraev, M.N., Verbolov, V.I., Granin, N.G., Sherstyankin, P.P. (1994). ‘Physical Limnology of Lake Baikal: A review.’ In Baikal International Center for Ecological Research (BICER). Eds Shimaraev, M.N., Okuda, S. Irkutsk.

Shimaraev, M.N., Kuimova, L.N., Sinyukovich, V.N., Tsekhanovskii, V.V. (2002). ‘Manifestation of global climatic changes in Lake Baikal during the 20th century.’ *Doklady Earth Sciences*, **383A**, 288–291.

Shimaraev, M.N., Domysheva, V.M. (2004). ‘Climate and long-term silica dynamics in Lake Baikal.’ *Rus. Geol. Geophys.*, **45**, 310–316.

Shimaraev, M.N., Domysheva, V.M. (2013). 'Trends in hydrological and Hydrochemical processes in Lake Baikal under conditions of modern climate change.' In: Climate change and global warming of inland waters. Impacts and mitigation for ecosystems and societies. Eds Goldman, C.R., Kumagai, M., Robarts, R.D.

Sigee, D. C., Levado, E. (2000). 'Cell surface elemental composition of *Microcystis aeruginosa*: High-Si and low-Si subpopulations within the water column of a eutrophic lake.' *J. Plankt. Res.*, **22**, 2137-2153.

Silliman, J.E., Meyers, P.A., Eadie, B.J. (1998). 'Perylene: an indicator of alteration processes or precursor materials?' *Org Geochem*, **29**, 1737-1744.

Silow, E.A. (2014). 'Lake Baikal: Current Environmental Problems.' *Encyclopaedia of Environmental Management*, 1-9.

Silow, E.A., Krashchuk, L.S., Onuchin, K.A., Pislegina, H.V., Rusanovskaya, O.O., Shimaraeva, S.V. (2016). 'Some recent trends regarding Lake Baikal phytoplankton and zooplankton.' *Lakes and Reservoirs and Management*, **21**, 40 – 44.

Sizykh, A.P. (2007). 'Models of Taiga-Steppe communities on the western coast of Lake Baikal.' *Russian Journal of Ecology*, **38**, (4), 234-237.

Skvortzow, B.W. (1937). 'Bottom diatoms from Olkhon gate of Baikal Lake, Siberia.' *The Philippine Journal of Science*, **3**, 293–377.

Sobek, S., Durisch-Kaiser, E., Zurbrügg, R., Wongfun, N., Wessels, M., Pasche, N., Wehrli, B. (2009). 'Organic carbon burial efficiency in lake sediments controlled by oxygen exposure time and sediment source.' *Limnology and Oceanography*, **54**, (6), 2243-2254.

Soma, Y., Tanaka, A., Soma, M., Kawai, T. (1996). 'Photosynthetic pigments and perylene in the sediments of southern basin of lake Baikal.' *Org. Geochem.*, **24**, (5), 553-561.

Soma, Y., Tanaka, A., Soma, M., Kawai, T. (2001). '2.8 million years of phytoplankton history in Lake Baikal recorded by the residual photosynthetic pigments in its sediment core.' *Geochemical Journal*, **35**, 377 – 383.

Soma, Y., Itoh, n., Tani, Y. (2005). ‘Sterol composition of steryl chlorin esters (SCEs) formed through grazing of algae by freshwater crustaceans: relevance to the composition of sedimentary SCEs.’ *Limnology*, **6**, 45-51.

Soma, Y., Tani, Y., Soma, M., Mitake, H., Kurihara, R., Hashimoto, S., Watanave, T., Nakamura, T. (2007). ‘Sedimentary steryl chlorin esters (SCEs) and other photosynthetic pigments as indicators of palaeolimnological change over the last 28,000 years from the Buguldeika Saddle of Lake Baikal.’ *Journal of Palaeolimnology*, **37**, 163-175.

Sommaruga, R. (2001). ‘The role of solar UV radiation in the ecology of alpine lakes.’ *Journal of Photochemistry and Photobiology B: Biology*, **62**, 35 – 42.

Sorokovikova, L.M., Avdeev, V.V. (1992). ‘Primary production and distribution of organic matter of the Selenga River.’ *Vodn. Resurs.*, **19**, 163-165.

Sorokovikova, L.M., Sinyukovich, V.N. (1995). Human activity and quality of the waters of Baikal tributaries. 2nd Vereshchagin Baikal Conf., Irkutsk, Oct. 5-10, 1995, Abstr., p.192.

Sorokovikova, L.M., Popovskaya, G.I., Belykh, O.I., Tomberg, I.V., Maksimenko, S.Y., Bashenkhaeva, N.V., Ivanov, V.G., Zemskaya, T.I. (2012). ‘Plankton composition and water chemistry in the mixing zone of the Selenga River with Lake Baikal.’ *Hydrobiologia*, **695**, 329 – 341.

Sorokovikova, L.M., Sinyukovich, V.N., Khodzher, T.V., Golobokova, L., Bashenkhaeva, N.V., Netsvetaeva, O.G. (2001). ‘The Inflow of Biogenic Elements and Organic Matter into Lake Baikal with River Waters and Atmospheric Precipitation.’ *Russian Meteorology and Hydrology*, **4**, 57-62.

Sorokovikova, L.M., Sinyukovich, V.N., Tomberg, I.V., Marinaite, I.I., Khodzher, T.V. (2015a). ‘Assessing the water quality in the tributary streams of Lake Baikal from chemical parameters.’ *Geography and Natural Resources*, **36**, (1), 31 – 39.

Sorokovikova, L.M., Sinyukovich, V.N., Netsvetaeva, O.G., Tomberg, I.V., Sezko, N.P., Lopatina, I.N. (2015b). ‘Chemical composition of snow water and river water on the southeastern shore of Lake Baikal.’ *Russian Meteorology and Hydrology*, **40**, (5), 334 – 342.

Stager, J.C., Cumming, B.F., Meeker, L.D. (2003). ‘A 10,000-year high-resolution diatom record from Pilkington Bay, Lake Victoria, East Africa.’ *Quaternary Research*, **59**, 172 – 181.

Steenbergen, C.L.M., Korthals, H.J., Dobrynin, E.G. (1994). ‘Algal and bacterial pigments in non-laminated lacustrine sediment: Studies of their sedimentation, degradation and stratigraphy.’ *FEMS Microbiology Ecology*, **13**, 335-352.

Steffen, M.M., Belisle, B.S., Watson, S.B., Boyer, G.L., Wilhelm, S.W. (2014). ‘Status, causes and controls of cyanobacterial blooms in Lake Erie.’ *Journal of Great Lakes Research*, **40**, (2), 215-225.

Stein, R., Fahl, K. (2004). ‘The Laptev Sea: distribution, sources, variability and burial of organic carbon.’ In: Stein, R., Macdonald, R.W. (Eds.), *The Organic Carbon Cycle in the Arctic Ocean*. Springer, Berlin, pp. 213–236.

Stein, R., Macdonald, R. (2004). *The Organic Carbon Cycle in the Arctic Ocean*. Springer, Berlin.

Stepanova, L.I., Lindstrom-Seppa, P., Hanninen, O.O.P., Kotelevtseva, S.V., Glasera, V.M., Novikova, C.N., Beim, A.M. (2000). ‘Lake Baikal: biomonitoring of pulp and paper mill wastewater.’ *Aquatic Ecosystem Health and Management*, **3**, 259 – 269.

Sterner, R.W., Smutka, T.M., McKay, R.M.L.M., Xiaoming, Q., Brown, E.T., Sherrell, R.M. (2004). ‘Phosphorus and trace metal limitation of algae and bacteria in Lake Superior.’ *Limnology and Oceanography*, **49**, (2), 495-507.

Sterner, R.W. (2010). ‘In situ-measured primary production in Lake Superior.’ *J. Great Lakes Res.*, **36**, 139–149.

Straskrabova, V., Izmestyeva, L.R., Maksimova, E.A., Fietz, S., Nedoma, J., Borovec, J., Kobanova, G.I., Shchetinina, E.V., Pislegina, E.V. (2005). ‘Primary production and microbial activity in the euphotic zone of Lake Baikal (Southern Basin) during late winter.’ *Global and Planetary Change*, **46**, 57 – 73.

Stoermer, E.F., Kocielek, J.P., Schelske, C.L., Conley, D.J. (1985a). ‘Siliceous microfossil succession in the recent history of Lake Superior.’ *Proc. Acad. Nat. Sci. Phila.*, **137**, 106–118.

Strom, S.L., Morello, T.A., Bright, K.J. (1998). ‘Protozoan size influences algal pigment degradation during grazing.’ *Marine Ecology Progress Series*, **164**, 189-197.

Stubblefield, A., Chandra, S., Eagan, S., Tuvshinjargal, D., Davaadorzh, G., Gilroy, D., Sampson, J., Thorne, J., Allen, B., Hogan, Z. (2005). ‘Impacts of gold mining and land use alterations on the water quality of central mongolian rivers.’ *Integrated Environmental Assessment Management*, **1**, (4), 365-373.

Sturm, M., Vologina, E.G. (2001). Characteristics of the uppermost sediments in Lake Baikal, in: International Workshop for the Baikal and Hovsgol drilling project in Ulaanbaatar (Abstracts). Ulaanbaatar, Mongolia, pp. 69 – 70.

Sturm, M., Vologina, E.G., Vorob’eva, S.S. (2016). ‘Holocene and Late Glacial sedimentation near steep slopes in southern Lake Baikal.’ *Journal of Limnology*, **75**, (1), 24-35.

Sugiyama, Y., Hatcher, P.G., Sleighter, R.L., Suzuki, T., Wada, C., Kumagai, T., Mitamura, O., Katano, T., Nakano, S., Tanaka, Y., Drucker, V.V., Fialkov, V.A., Sugiyama, M. (2014). ‘Developing an understanding of dissolved organic matter dynamics in the giant Lake Baikal by ultrahigh resolution mass spectrometry.’ *Limnology*, **15**, 127 – 139.

Sun, M.Y., Lee, C., Aller, R.C. (1993). ‘Anoxic and oxic degradation of C-labeled Chloropigments and a ¹⁴C-labeled diatom in Long Island Sound sediments.’ *Limnol. Oceanogr.*, **38**, 1438 – 1451.

Suzuki, T., Sugiyama, Y., Wada, C., Kumagai, T., Nagao, S., Katano, T., Nakano, S., Mitamura, O., Matsuura, Y., Drucker, V.V., Fialkov, V.A., Sugiyama, M. (2008). ‘Role of allochthonous organic matter in Lake Baikal investigated by a three-dimensional fluorescence excitation-emission matrix spectroscopy and high performance liquid chromatography-mass spectrometry.’ *Int Ver Theor Angew Limnol Verh*, **30**, 469–476.

Swann, G.E.A., Mackay, A.W., Leng, M.J., Demory, F. (2005). ‘Climatic change in Central Asia during MIS 3/2: a case study using biological responses from Lake Baikal.’ *Global and Planetary Change*, **46**, 235-253.

Swann, G.E.A., Mackay, A.W. (2006). 'Potential limitation of biogenic silica as an indicator of abrupt climate change in Lake Baikal, Russia.' *Journal of Paleolimnology*, **36**, 81-89.

Symons, C.C., Arnott, S.E., Sweetman, J.N. (2012). 'Nutrient limitation of phytoplankton communities in Subarctic lakes and ponds in Wapusk National Park, Canada.' *Polar Biol.*, **35**, 481–489.

Talbot MR, Livingstone DA (1989). 'Hydrogen index and carbon isotopes of lacustrine organic-matter as lake level indicators.' *Palaeogeography, Palaeoclimatology, Palaeoecology*, **70**, (1–3), 121–137.

Talbot, M.R., Johannessen, T. (1992). 'A high resolution palaeoclimatic record for the last 27,500 years in tropical West Africa from the carbon and nitrogen isotopic composition of lacustrine organic matter.' *Earth Planet Sci Lett.*, **110**, (1–4), 23–37.

Talbot, H. M., Head, R. N., Harris, R. P., Maxwell, J. R. (1999b). 'Distribution and stability of steryl chlorin esters in copepod faecal pellets from diatom grazing.' *Organic Geochemistry*, **30**, (9), 1163–1174.

Talbot, H.M., Head, R.N., Harris, R.P., Maxwell, J.R. (2000). 'Discrimination against 4-methyl sterol uptake during steryl chlorin ester production by copepods.' *Organic Geochemistry*, **31**, 871 – 880.

Tani, Y., Yoshii, K., Itoh, N., Nara, F., Soma, M., Tanaka, A.A., Soma, Y., Yonada, M., Hirota, M., Shibata, Y. (2001). 'Distribution of photosynthetic pigments and other biogenic compounds in the sediments from the southern basin of Lake Baikal.' *Geol Geofiz*, **2**, 206 – 212.

Tani, Y., Kurihara, K., Nara, F., Itoh, N., Soma, M., Soma, Y., Tanaka, A., Yoneda, M., Hirota, M., Shibata, Y. (2002). 'Temporal changes in the phytoplankton community of the southern basin of Lake Baikal over the last 24,000 years recorded by photosynthetic pigments in a sediment core.' *Organic Geochemistry*, **33**, 1621 – 1634.

Tani, Y., Nara, F., Soma, Y., Soma, M., Itoh, N., Matsumoto, G.I., Tanaka, A., Kawai, T. (2009). 'Phytoplankton assemblage in the Plio-Pleistocene record of Lake Baikal as indicated by sedimentary steryl chlorin esters.' *Quaternary International*, **205**, 126 – 136.

Taranu, Z.E., Gregory-Eaves, I., Leavitt, P.R., Bunting, L., Buchaca, T., Catalan, J., Domaizon, I., Guilizzoni, P., Lami, A., McGowan, S., Moorhouse, H., Morabito, G., Pick, F.R., Stevenson, M.A., Thompson, P.L., Vinebrooke, R.D. (2015). ‘Acceleration of cyanobacteria dominance in north temperate-subarctic lakes during the Anthropocene.’ *Ecology Letters*, **18**, (4), 375 – 384.

Tarasova E.N. et al. (1997). ‘Polychlorinated dibenzo-p-dioxins (PCDDs) and dibenzofurans (PCDFs) in Baikal seal.’ *Chemosphere*, **34**, 2419 - 2427.

Tarasov, P.A., Bezrukova, E.V., Krivonogov, S.K. (2009). ‘Late Glacial and Holocene changes in vegetation cover and climate in southern Siberia derived from a 15 kyr long pollen record from Lake Kotokel.’ *Clim. Past*, **5**, 285-295.

Tarasova, E.N., Mescheryakova, A.I. (1992). Modern state of hydrochemical regime of Lake Baikal [in Russian]. Nauka, Novosibirsk.

Teranes, J.L., Bernasconi, S.M. (2005). ‘Factors controlling $\delta^{13}\text{C}$ values of sedimentary carbon in hypertrophic Baldeggersee, Switzerland, and implications for interpreting isotope excursions in lake sedimentary records.’ *Limnology and Oceanography*, **50**, (3), 914-922.

Thackeray, S.J., Nöges, P., Dunbar, M.J., Dudley, B.J., Skjelbred, B., Morabito, G., Carvalho, L., Phillips, G., Mischke, U., Catalan, J., de Hoyos, C., Laplace, C., Austoni, M., Padedda, B.M., Maileht, K., Pasztaleniec, A., Järvinen, M., Solheim, A.L., Clarke, R.T. (2013). ‘Quantifying uncertainties in biologically-based water quality assessment: A pan-European analysis of lake phytoplankton community metrics.’ *Ecological Indicators*, **29**, 34 – 47.

Thorslund, J., Jarsjo, J., Chalov, S.R., Belozeroва, E.V. (2012). ‘Gold mining impact on riverine heavy metal transport in a sparsely monitored region: the upper Lake Baikal Basin case.’ *Journal of Environmental Monitoring*, **14**, 10, 2780 - 2792

Thrane, J-E., Hessen, D.O., Anderson, T. (2014). ‘The absorption of light in lakes: negative impacts of dissolved organic carbon on primary productivity.’ *Ecosystems*, **17**, 1040 – 1052.

Tréguer, P. J. and De La Rocha, C. L. (2013). ‘The world ocean silica cycle.’ *Ann. Rev. Mar. Sci.*, **5**, 477–501.

Tian, F., Herzsuh, U., Mischke, S., Schlütz, F. (2014). ‘What drives the recent intensified vegetation degradation in Mongolia- Climate change or human activity?’ *The Holocene*, 1-10.

Timoshkin, O. A. (2001). Lake Baikal: diversity of fauna, problems of its immiscibility and origin, ecology and “exotic” communities. In: Index of Animal Species Inhabiting Lake Baikal and Its Catchment Area. Nauka Publishers, Novosibirsk, Russia.

Timoshkin, O.A., Malnik, V.V., Sakirko, M.V., Boedeker, C. (2014 not 2015). ‘Ecological crisis on Lake Baikal: diagnosed by scientists.’ *Science* (<http://scfh.ru/en/news/ecological-crisis-on-lake-baikal-diagnosed-by-scientists-4105201512/>).

Timoshkin, O.A., Samsonov, D.P., Yamamuro, M., Moore, M.V., Belykh, O.I., Malnik, V.V., Sakirko, M.V., Shirokaya, A.A., Bondarenko, N.A., Domysheva, V.M., Fedorova, G.A., Kochetkov, A.I., Kuzmin, A.V., Lukhnev, A.G., Medvezhonkova, O.V., Nepokrytykh, A.V., Pasynkova, E.M., Poberezhnaya, A.E., Potapskaya, N.V., Rozhkova, N.A., Sheveleva, N.G., Tikhonova, I.V., Timoshkina, E.M., Tomberg, I.V., Volkova, E.A., Zaitseva, E.P., Zvereva, Y.M., Kupchinsky, A.B., Bukshuk, N.A. (2016). ‘Rapid ecological change in the coastal zone of Lake Baikal (East Siberia): Is the site of the world’s greatest freshwater biodiversity in danger?’ *Journal of Great Lakes Research*, **42**, (3), 487-497.

Toda, K., Obata, T., Obolkin, V.A., Potemkin, V.L., Hirota, K., Takeuchi, M., Arita, S., Khodzher, T.V., Grachev, M.A. (2010). ‘Atmospheric methanethiol emitted from a pulp and paper plant on the shore of Lake Baikal.’ *Atmospheric Environment*, **44**, 2427 – 2433.

Todd, M.C., Mackay, A.W. (2003). ‘Large-Scale climate controls on Lake Baikal ice cover.’ *Journal of Climate*, **16**, 3186 – 3199.

Toms, J. D. and Lesperance, M. L. (2003). ‘Piecewise regression: a tool for identifying ecological thresholds.’ *Ecology*, **84**, 2034-2041.

Törnqvist, R., Jarsjö, J., Pietron, J., Bring, A., Rogberg, P., Asokan, S.M. (2014). ‘Evolution of the hydro-climate system in the Lake Baikal basin.’ *Journal of Hydrology*, **519**, 1953-1962.

Torres, I.C., Inglett, P.W., Brenner, M., Kenney, W.F., Reddy, K.R. (2012). ‘Stable isotope ($\delta^{13}\text{C}$ and $\delta^{15}\text{N}$) values of sediment organic matter in subtropical lakes of different trophic status.’ *Journal of Palaeolimnology*, **47**, 693-706.

Torres, N.T., Och, L.M., Hauser, P.C., Furrer, G., Brandl, H., Vologina, E., Sturm, M., Bürgmann, H., Müller, B. (2014). ‘Early diagenetic processes generate iron and manganese oxide layers in the sediments of Lake Baikal, Siberia.’ *Environmental Science Processes & Impacts*, **16**, 879-889.

Touchart, L. (2012). ‘Lake Baikal. In: Bengtsson L, Herschy RW, Fairbridge RW (eds) Encyclopedia of lakes and reservoirs. Springer, New York, pp 83–91.

Trommer, G., Leynaert, A., Klein, C., Naegelen, A., Beker, B. (2013). ‘Phytoplankton phosphorus limitation in a North Atlantic coastal ecosystem not predicted by nutrient load.’ *Journal of Plankton Research*, **0**, 1 – 13.

Trouet, V. et al. (2013). ‘A 1500-year reconstruction of annual mean temperature for temperate North America on decadal-to-multidecadal time scales.’ *Environmental Research Letters*, **8**, (2), 1-10.

Tsugeki, N., Oda, H., Urabe, J. (2003). ‘Fluctuation of the zooplankton community in Lake Biwa during the 20th century: a Paleolimnological analysis.’ *Limnology*, **4**, 101–107.

Tulokhonov, A.K., Andreev, S.G., Batoev, V.B., Tsydenova, O.V., Khlystov, O.M. (2006). ‘Natural microchronicle of recent events in the basin of Lake Baikal.’ *Russian Geology and Geophysics (Geologiya i Geofizika)*, **47**, (9), 1030–1034.

Tumenbayar, B., Batbayar, M., Grayson, R. (2000). ‘Environmental hazard in Lake Baikal watershed posed by mercury placer in Mongolia.’ *World Placer Journal*, **1**, 134-159.

Turner, R. E., N. N. Rabalais. (1994). ‘Coastal eutrophication near the Mississippi river delta.’ *Nature*, **368**, 619–621.

UNEP, 2013. Global mercury Assessment 2013: Sources, Emissions, Releases and Environmental Transport. UNEP Chemicals Branch, Geneva, Switzerland

Vadeboncoeur, Y., Lodge, D.M., Carpenter, S.R. (2001). ‘Whole-lake fertilization effects on distribution of primary production between benthic and pelagic habitats.’ *Ecology*, **82**, 1065–1077.

Vadeboncoeur, Y., Jeppesen, E., Vander Zanden, M.J., Schierup, H-H., Christoffersen, K., Lodge, D.M. (2003). ‘From Greenland to green lakes: Cultural eutrophication and the loss of benthic pathways in lakes.’ *Limnology and Oceanography*, **48**, (4), 1408-1418.

Van de Vel, K., Mensink, C., Ridder, K.D., Deutsch, F., Maes, J., Vliegen, J., Aloyan, A., Yermakov, A., Arutyunyan, V., Khodzher, T., Mijling, B. (2009). ‘Air-quality modelling in the Lake Baikal region.’ *Environmental Monitoring Assessment*, **165**, 665 – 674.

Vanneste M., Poort J., De Batist M. and Klerkx J. (2003). ‘Atypical heat-flow near gas hydrate irregularities and cold seeps in the Baikal Rift Zone.’ *Marine and Petroleum Geology*, **19**, 1257-1274.

van Rensbergen P., de Batist M., Criel W., Klerkx J., Granin N., Gnatovsky R. and Krinitsky P. (2003). ‘An inventory of hydrate-related gas seeps in Lake Baikal.’ *EGS-AGU-EUG Joint Assembly*.

Vander Zanden, M.J., Shuter, B.J., Lester, N., Rasmussen, J.B. (1999). ‘Patterns of food chain length in lakes: a stable isotope study.’ *The American Naturalist*, **154**, (4), 406 – 416.

Veraart, A.J., Romani, A.M., Tornes, E., Sabater, S. (2008). ‘Algal response to nutrient enrichment in forested oligotrophic stream.’ *Journal of Phycology*, **44**, 564-572.

Verburg, P. (2007). ‘The need to correct for the Suess effect in the application of $\delta^{13}\text{C}$ in sediment of autotrophic Lake Tanganyika, as a productivity proxy in the Anthropocene.’ *J Paleolimnol.*, **37**, 591 – 602.

Verburg, P., Hecky, R.E. (2009). ‘The physics of the warming of Lake Tanganyika by climate change.’ *Limnology and Oceanography*, **54**, (2), 2418 – 2430.

Verkhozina, V.A., Kozhova, O.M., Kusner, Y.S. (2000). ‘Hydrodynamics as a limiting factor in the Lake Baikal ecosystem.’ *Aquatic Ecosystem Health and Management*, **3**, 203-210.

Verschuren, D., Johnson, T.C., Kling, H.J., Edgington, D.N., Leavitt, P.R., Brown, E.T., Talbot, M.R., Hecky, R.E. (2002). ‘History and timing of human impact on Lake Victoria, East Africa.’ *Proceedings of the Royal Society London B.*, **269**, 289-294.

Villanueva, J., Hastings, D.W. (2000). ‘A century-scale of the preservation of chlorophyll and its transformation products in anoxic sediments.’ *Geochimica et Cosmochimica Acta*, **64**, 13, 2281 – 2294.

Vollenweider, R.A. (1968). Scientific Fundamentals of the Eutrophication of Lakes and Flowing Waters, with Particular Reference to Nitrogen and Phosphorus as Factors in Eutrophication. Tech. Rep. DAS/CSI/68-27, OECD, Paris, France.

Vollenweider, R. A. (1976). ‘Advances in defining critical loading levels for phosphorus in lake eutrophication.’ *Memorie Dell’Istituto Italiano Di Idrobiologia*, **33**, 53–83.

Vologina, E.G., Sturm, M., Vorobeva, S.S., Granina, L.Z. (2000). ‘New results of high-resolution studies of surface sediments of Lake Baikal.’ *Terra Nostra*, **9**, 115 – 130

Vologina, E.G., Sturm, M., Vorob’eva, S.S., Granina, L.Z., Toshchakov, S.Yu. (2003). ‘Character of sedimentation in Lake Baikal in the Holocene.’ *Geologiya i Geofizika (Russian Geology and Geophysics)*, **44**, (5), 407–421.

Vologina, E.G., Kashik, S.A., Sturm, M., Vorob’eva, S.S., Lomonosova, T.K., Kalashnikova, I.A., Khramtsova, T.I., Toshchakov, S.Yu. (2007). ‘Results of research into Holocene sediments of the South and Central basins of Lake Baikal.’ *Russian Geology and Geophysics*, **48**, 312 – 322.

Vologina, E.G., Sturm, M. (2009). ‘Types of Holocene deposits and regional pattern of sedimentation in Lake Baikal.’ *Russian Geology and Geophysics*, **50**, 1 – 6.

Vologina, E.G., Kalugin, I.A., Osukhovskaya, Yu.N., Sturm, M., Ignatova, N.V., Radziminovich, Ya.B., Dar’in, A.V., Kuz’min, M.I. (2010). ‘Sedimentation in Proval Bay (Lake Baikal) after earthquake-induced subsidence of part of the Selenga River delta.’ *Russian Geology and Geophysics*, **51**, 1275 – 1284.

Votintsev, K.K., Glazunov, I.V., Tohnacheva, A.P. (1965). Hydrochemistry of Rivers in the Basin of Lake Baikal. Proc. Limnol. Inst., vol. 8, Nauka, Moscow, 495 pp.

Votintsev, K.K., Meshcheryakova, A.I., Popovskaya, G.I. (1975). ‘Cycling of organic matter in Lake Baikal.’ Nauka, Novosibirsk, Russia.

Wang, F., Liu, C., Wu, M., Yu, Y., Wu, F., Lü, S., Wei, Z., Xu, G. (2009). ‘Stable isotopes in sedimentary organic matter from Lake Dianchi and their indication of eutrophication history.’ *Water Air Soil Pollut.*, **1999**, 159-170.

Wang, H., Wang, H. (2009). ‘Mitigation of lake eutrophication: Loosen nitrogen control and focus on phosphorus abatement.’ *Progress in Natural Science*, **19**, (10), 1445-1451.

Wasmund, N., Nausch, G., Matthaus, W. (1998). ‘Phytoplankton spring blooms in the southern Baltic Sea – spatio-temporal development and long-term trend.’ *Journal of Plankton Research*, **20**, (6), 1099 – 1117.

Watanabe, I., Tanabe, S., Amano, M., Miyazaki, N., Petrov, E.A., Tatsukawa, R. (1998). ‘Age-dependent accumulation of heavy metals in Baikal seal (*Phoca sibirica*) from the Lake Baikal.’ *Arch. Environ. Contam. Toxicol.*, **35**, 518-526.

Watanabe, Y., Drucker, V.V. (1999). ‘Phytoplankton blooms in Lake Baikal, with reference to the lake’s present state of eutrophication.’ Ancient lakes. Their cultural and biological diversity, Kenobi Productions, Ghent (Belgium), 217 – 225.

Watanabe, T., Naraoka, H., Nishimura, M., Kawai, T. (2004). ‘Biological and environmental changes in Lake Baikal during the late Quaternary inferred from carbon, nitrogen and sulphur isotopes.’ *Earth and Planetary Science Letters*, **222**, 285-299.

Watanabe, T., Nakamura, T., Watanabe Nara, F., Kakegawa, T., Nishimura, M., Shimokawara, M., Matsunaka, T., Senda, R., Kawai, T. (2009). ‘A new age model for the sediment cores from Academician ridge (Lake Baikal) based on high-time-resolution AMS ¹⁴C data sets over the last 30 kyr: paleoclimatic and environmental implications.’ *Earth and Planetary Science Letters*, **286**, 347-354.

Watson, N.H.F., Thomson, K.P.B., Elder, F.C. (1975). ‘Sub-thermocline biomass concentration detected by transmissometer in Lake Superior.’ *Verh. Internat. Verein. Limnol.*, **19**, 682–688.

Wei, Z., Jibin, X., Jixiu, C., Yanming, Z., Qiaohong, M., Jun, O., Ying, C., Zhiguo, Z., Wei, L. (2010). 'Bulk organic carbon isotopic record of lacustrine sediments in Dahu Swamp, eastern Nanling Mountains in South China: Implications for catchment environmental and climatic changes in the last 16,000 years.' *Journal of Asian Earth Science*, **38**, 162-169

Weiss, R.F. (1991). 'Deep-water renewal and production in Lake Baikal.' *Nature*, **349**, 665 – 666.

Welschmeyer, N., Lorenzen, C. J. (1985a). 'Chlorophyll budgets: Zooplankton grazing and phytoplankton growth in a temperate fjord and the Central Pacific Gyres.' *Limnology and Oceanography*, **30**, (1), 1–21.

Wetzel, R.G. (1983). *Limnology*, 2nd Edition. Saunders College Publishing, Philadelphia, PA.

Wetzel R.G. (2001). 'Limnology: Lake and River Ecosystems.' Third Edition. N.Y., Academic Press.

Whalen, S. C., Cornwell, J.C. (1985). 'Nitrogen, phosphorus, and organic carbon cycling in an arctic Lake.' *Can. J. Fish. Aquat. Sci.*, **42**, 797-808.

White, D., Bush, A.B.G. (2010). Holocene climate, environmental variability and Neolithic biocultural discontinuity in the Lake Baikal region. In: Weber, A.W., Katzenberg, M.A., Schurr, T.G. (Eds.), *Prehistoric Hunter-gatherers of the Baikal Region, Siberia: Bioarchaeological Studies of Past Lifeways*. University of Pennsylvania Museum Press, Pennsylvania, p. 26.

White, B., Matsumoto, K. (2012). 'Casual mechanisms of the deep chlorophyll maximum in Lake Superior: A numerical modelling investigation.' *Journal of Great Lakes Research*, **38**, 504 – 513.

Whiteford, E.J., McGowan, S., Anderson, N.J. 'Regional and seasonal shifts in nutrient limitation of phytoplankton growth in lakes across SW Greenland in response to atmospheric N pollution.' (In prep).

Williamson, C.E., Stemberger, R.S., Morris, D.P., Frost, T.M. Paulsen, S.G. (1996). 'Ultraviolet radiation in North American lakes: Attenuation estimates from DOC

measurements and implications for plankton communities.' *Limnol. Oceanogr.*, **41**, (5), 1024 – 1034.

Williams, D.F., Peck, J., Karabanov, E.B., Prokopenko, A.A., Kravchinsky, V., King, J., Kuzmin, M.I. (1997). 'Lake Baikal record of continental climate response to orbital insolation during the past 5 million years.' *Science*, **278**, 1114-1117.

Williams, D.F., Kuzmin, M.I., Prokopenko, A.A., Karabanov, E.B., Khursevich, G.K., Bezrukova, E.V. (2001). 'The Lake Baikal drilling project in the context of a global lake drilling initiative.' *Quaternary International*, **80-81**, 3-18.

Wilhelm, S.W., Suttle, C.A. (1999). 'Viruses and nutrient cycles in the sea; viruses play critical roles in the structure and function of aquatic food webs.' *BioScience*, **49**, (10), 781 – 788.

Winder, M., Reuter, J.E., Schladow, S.G. (2009). 'Lake warming favours small-sized planktonic diatom species.' *Proc. R. Soc. B.*, **276**, 427 – 435.

Winslow LA, Read JS, Hanson PC, Stanley EH. (2014). 'Lake shoreline in the contiguous United States: quantity, distribution and sensitivity to observation resolution.' *Freshwater Biol.*, **59**, 213–223.

Wolfe, B.B, Edwards, T.W.D., Aravena, R. (1999). 'Changes in carbon and nitrogen cycling during tree-line retreat recorded in the isotopic content of lacustrine organic matter, western Taimyr Peninsula, Russia.' *The Holocene*, **9**, 2, 215-222.

Wrona, F.J., Prowse, T.D., Reist, J.D., Hobbie, J.E., Levesque, L.M.J., Vincent, W.F. (2006). 'Climate Change effects on aquatic biota, ecosystem structure and function.' *Climate Change Impacts on Arctic Freshwater Ecosystems and Fisheries*, **35**, (7), 359 – 369.

Wüest, A., T. M. Ravens, N. G. Granin, O. Kocsis, M. Schurter, and M. Sturm (2005), 'Cold intrusions in Lake Baikal: Direct observational evidence for deep-water renewal.' *Limnol. Oceanogr. Methods*, **50**, (1), 184–196.

Wu, B., Wang, J. (2002). 'Winter Arctic Oscillation, Siberian High and East Asian Winter Monsoon.' *Geophysical Research Letters*, **29**, 1-4.

Wulff, F., Stigebrandt, A., Rahm, L. (1990). ‘Nutrient dynamics of the Baltic Sea.’ *Ambio*, **19**, (3), 126 – 133.

Yang, X., Wu, X., Hao, H., He, Z. (2008). ‘Mechanisms and assessment of water eutrophication.’ *J Zhejiang Univ Sci B*, **9**, (3), 197 – 209.

Yang, H., Engstrom, D.R., Rose, N.L. (2010). ‘Recent changes in atmospheric mercury deposition recorded in the sediments of remote equatorial lakes in the Rwenzori mountains, Uganda.’ *Environ. Sci. Technol.*, **44**, 6570-6575.

Yang, H. (2015). ‘Lake sediments may not faithfully record decline of atmospheric pollutant deposition.’ *Environmental Science & Technology*, 12607-12608.

Yasnitsky, V.N. (1930). Results on observations of Baikal plankton in the region of Biological Station during 1926–1928. News of Biological Geographic Institute of Irkutsk State University 4 (3–4), 191–234.

Yoshii, K., Melnik, N.G., Timoshkin, O.A., Bondarenko, N.A., Anoshko, P.N., Yoshioka, T., Wada, E. (1999). ‘Stable isotope analyses of the pelagic food web in Lake Baikal.’ *Limnology and Oceanography*, **44**, (3), 502-511.

Yoshioka, T., Ueda, S., Khodzher, T., Bashenkhaeva, N., Korovyakova, I., Sorokovikova, L., Gorbunova, L. (2002). ‘Distribution of dissolved organic carbon in Lake Baikal and its watershed.’ *Limnology*, **3**, 159 – 168.

Yoshida, T., Sekino, T., Genkai-Kato, M., Logacheva, N.P., Bondarenko, N.A., Kawabata, Z., Khodzher, T.V., Melnik, N.G., Hino, S., Nozaki, K., Nishimura, Y., Nagata, T., Higashi, M., Nakanishi, M. (2003). ‘Seasonal dynamics of primary production in the pelagic zone of southern Lake Baikal.’ *Limnology*, **4**, 53-62.

Yoshioka, T., Mostofa, K.M.G., Konohira, E., Tanoue, E., Hayakawa, K., Takahashi, M., Ueda, S., Katsuyama, M., Khodzher, T., Bashenkhaeva, N., Korovyakova, I., Sorokovikova, L., Gorbunova, L. (2007). ‘Distribution and characteristics of molecular size fractions of freshwater – dissolved organic matter in watershed environments: its implication to degradation.’ *Limnology*, **8**, 29 – 44.

Zhamsueva, G.S., Zayakhanov, A.S., Starikov, A.V., Tsydypov, V.V., Ayurzhanayev, A.A., Golobokova, L.P., Filippova, U.G., Khodzher, T.V. (2012). ‘Chemical composition of aerosols in the atmosphere of Mongolia.’ *Russian Meteorology and Hydrology*, **37**, (8), 546-552.

Zhang, Z., He, X., Zhang, Z. (2012). ‘Eutrophication Status, Mechanism and Its Coupling Effect with Algae Blooming in Bohai.’ *Marine Environmental Science*, **4**, 465-468.

Zhao L, Wu Q, Marchenko SS, Sharkuu N (2010). ‘Thermal state of permafrost and active layer in central Asia during the International Polar Year.’ *Permafrost and Periglacial Processes*, **21**, 198-207.

Zhao, J., Bianchi, T.S., Li, X., Allison, M.A., Yao, P., Yu, Z. (2012). ‘Historical eutrophication in the Changjiang and Mississippi delta-front estuaries: Stable sedimentary chloropigments as biomarkers.’ *Continental Shelf Research*, **47**, 133 – 144.

Zhu, J., Lücke, A., Wissel, H., Müller, D., Mayr, C., Ohlendorf, C., Zolitschka, B., The PASADO Science Team. (2003). ‘The last Glacial-Interglacial transition in Patagonia, Argentina: the stable isotope record of bulk sedimentary organic matter from Laguna Potrok Aike.’ *Quaternary Science Reviews*, **71**, 205-218.

Appendix

Nutrients and DOC water profiles

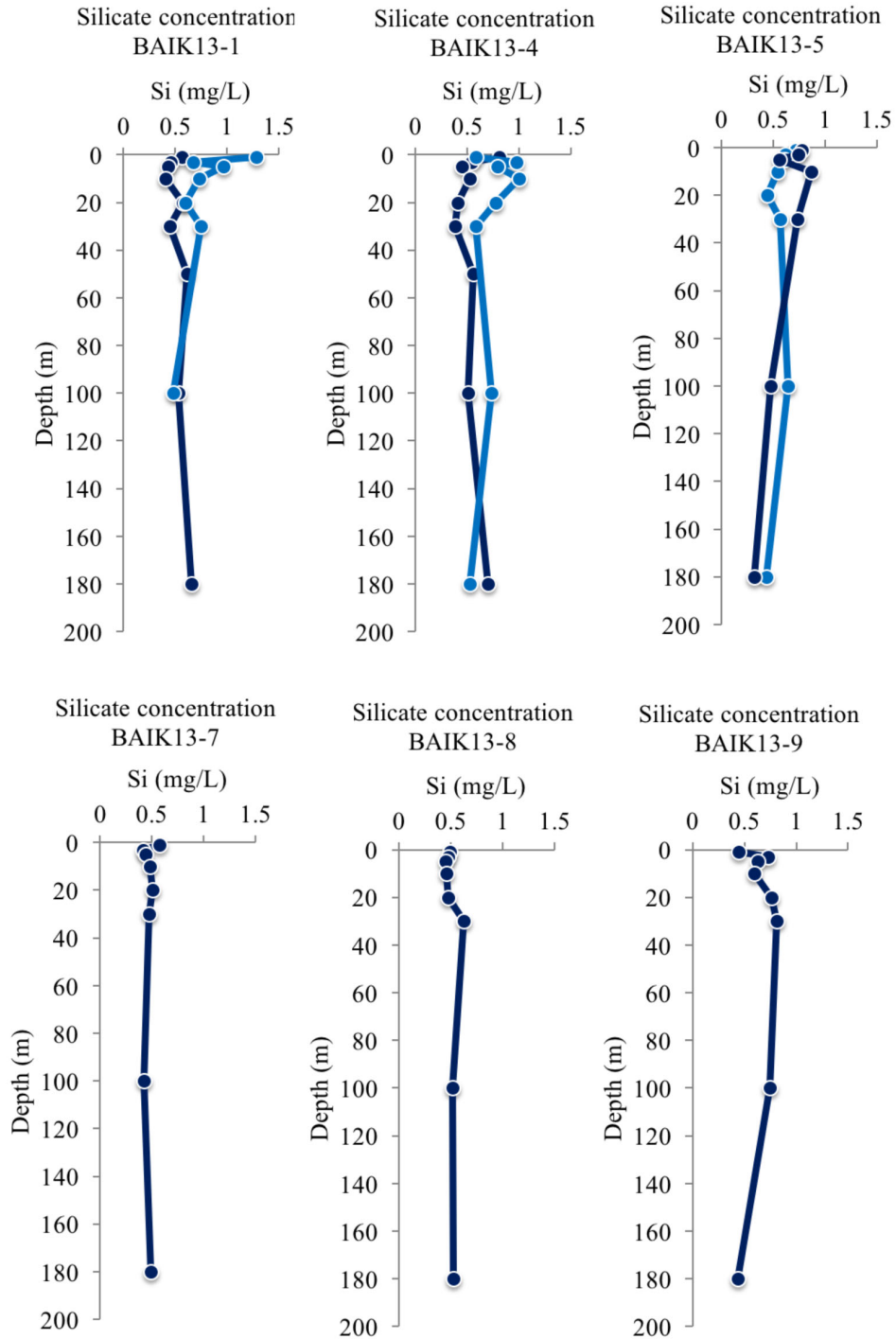


Figure 143: Water profiles of Silicate concentrations in the South basin sites. Light blue line represents March 2013 profiles and dark blue line represents August 2013 profiles.

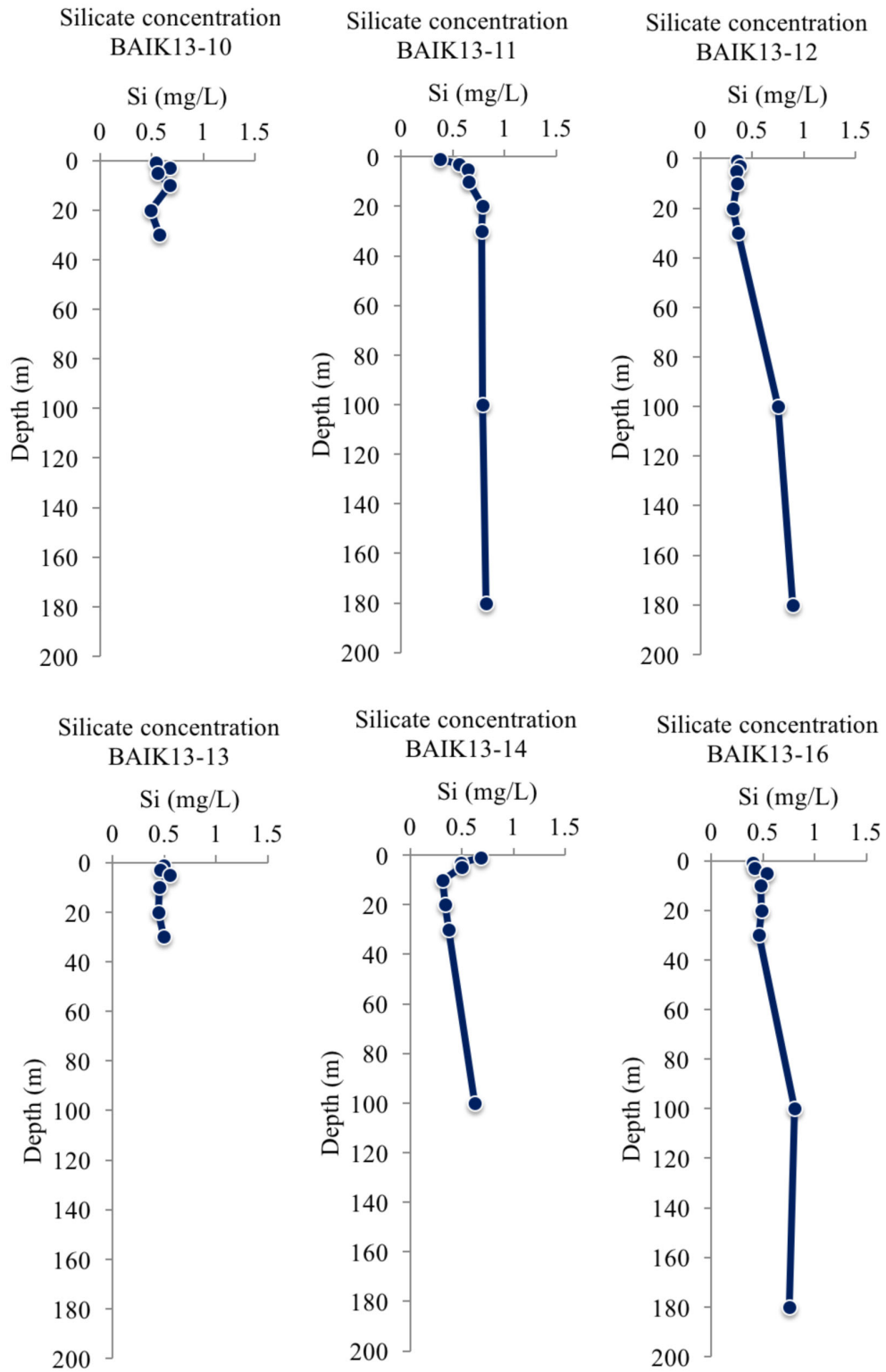


Figure 144: Water profiles of Silicate concentrations in the South basin/Selenga, Central Basin, Maloe More Bay and North basin/Chivsky Bay sites. Dark blue line represents August 2013 profiles.

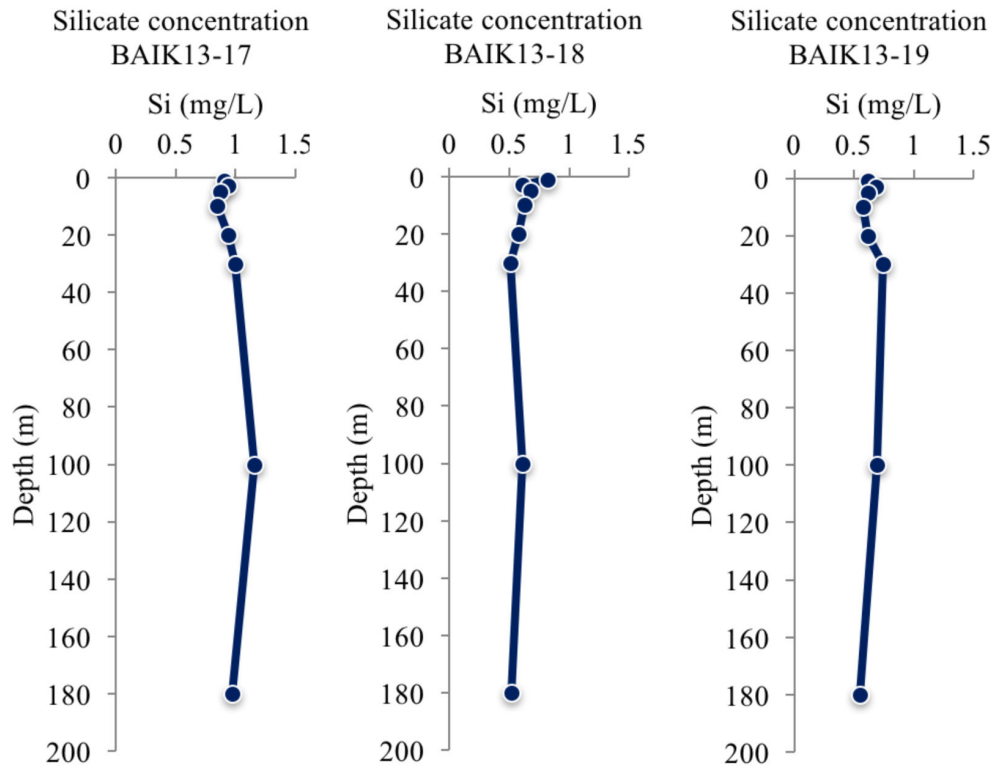


Figure 145: Water profiles of Silicate concentrations in the North basin sites. Dark blue line represents August 2013 profiles.

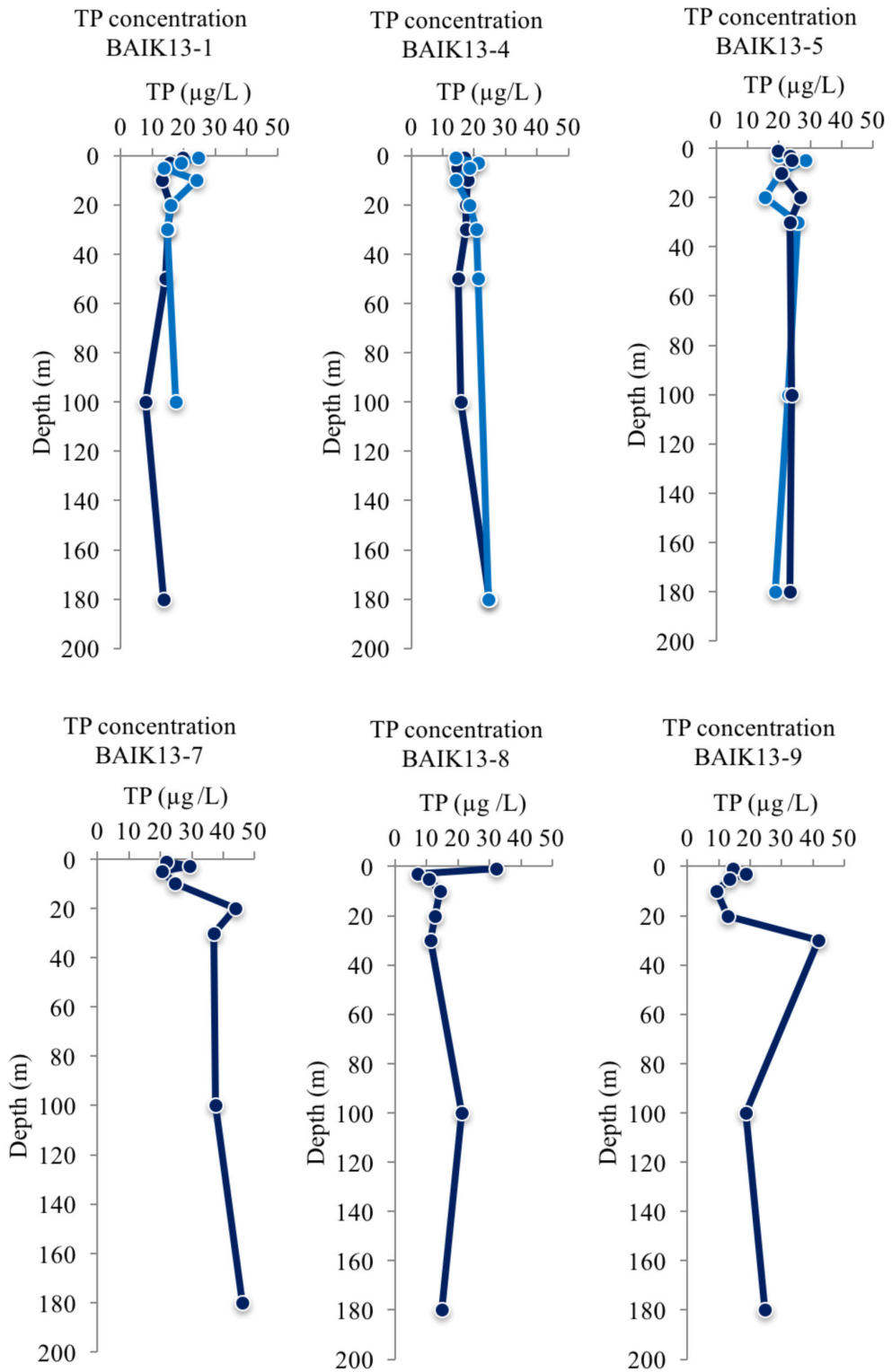


Figure 146: Water profiles of TP concentrations in the South basin sites. Light blue line represents March 2013 profiles and dark blue line represents August 2013 profiles.

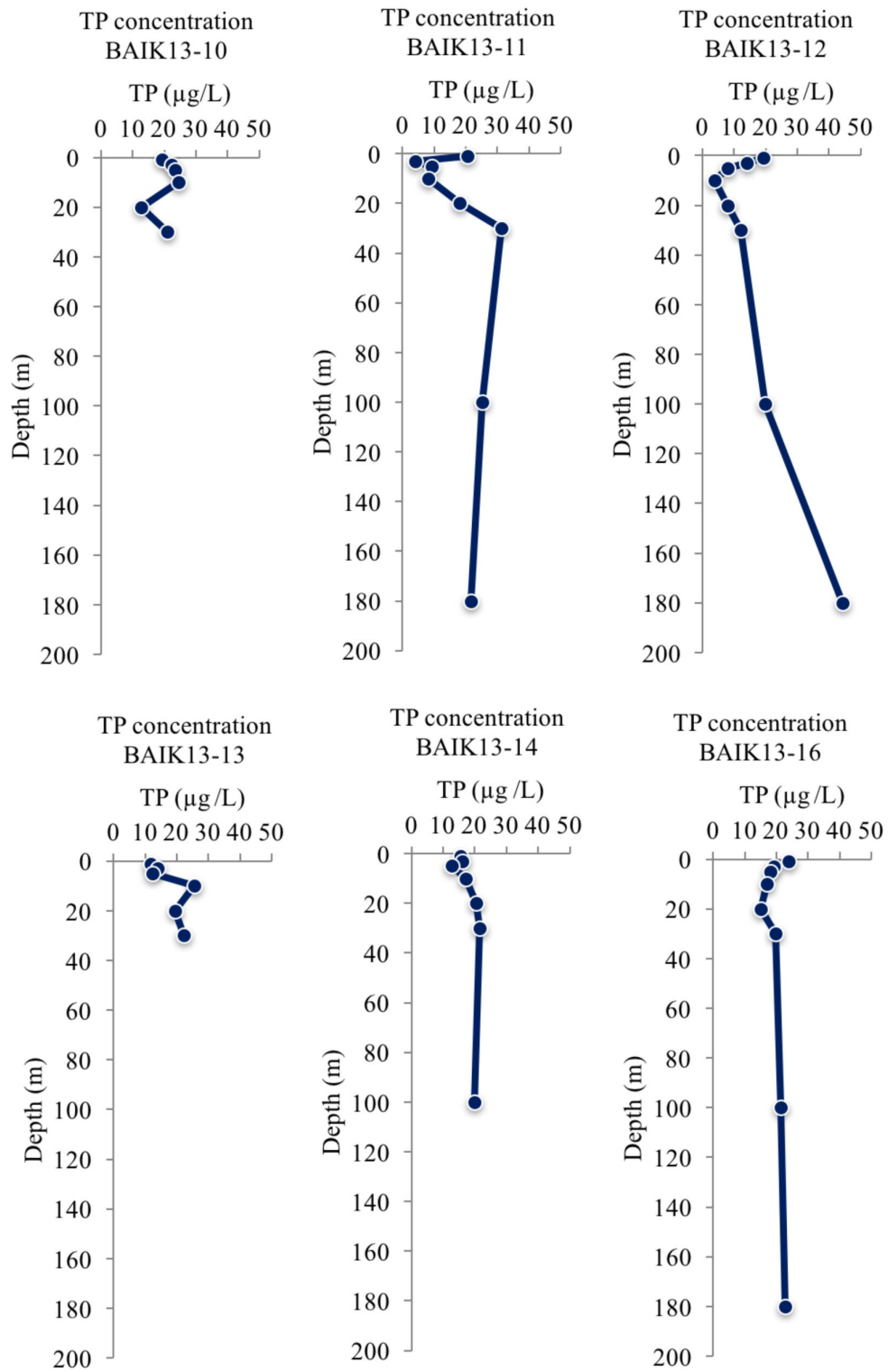


Figure 147: Water profiles of TP concentrations in the South basin/Selenga, Central Basin, Maloe More Bay and North basin/Chivsky Bay sites. Dark blue line represents August 2013 profiles.

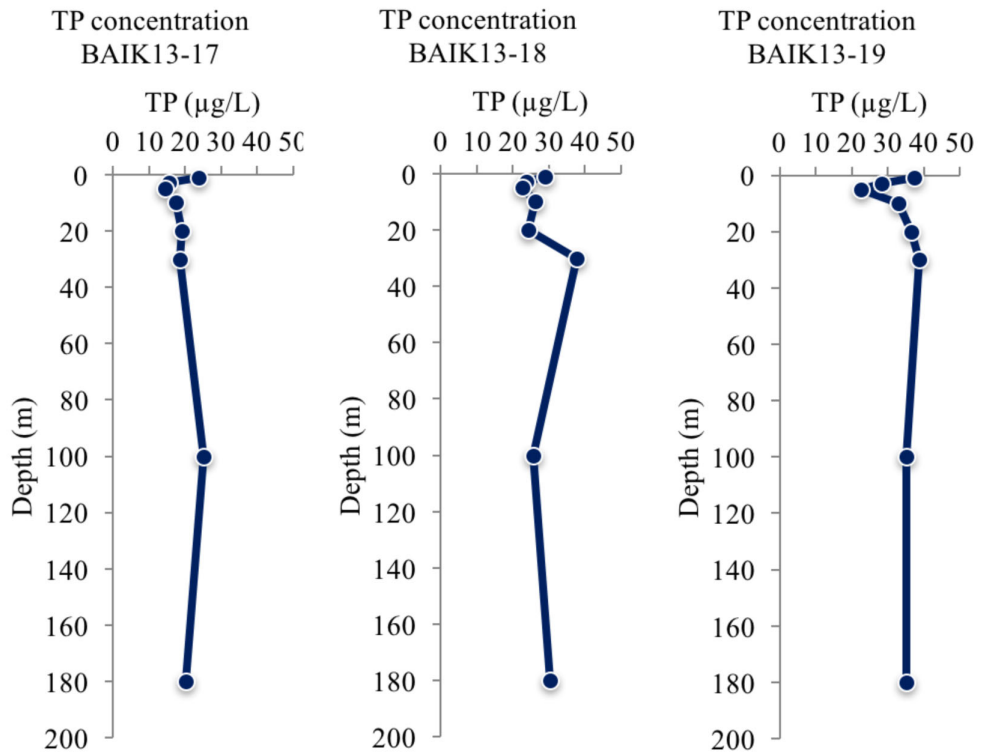


Figure 148: Water profiles of TP concentrations in the North basin sites. Dark blue line represents August 2013 profiles.

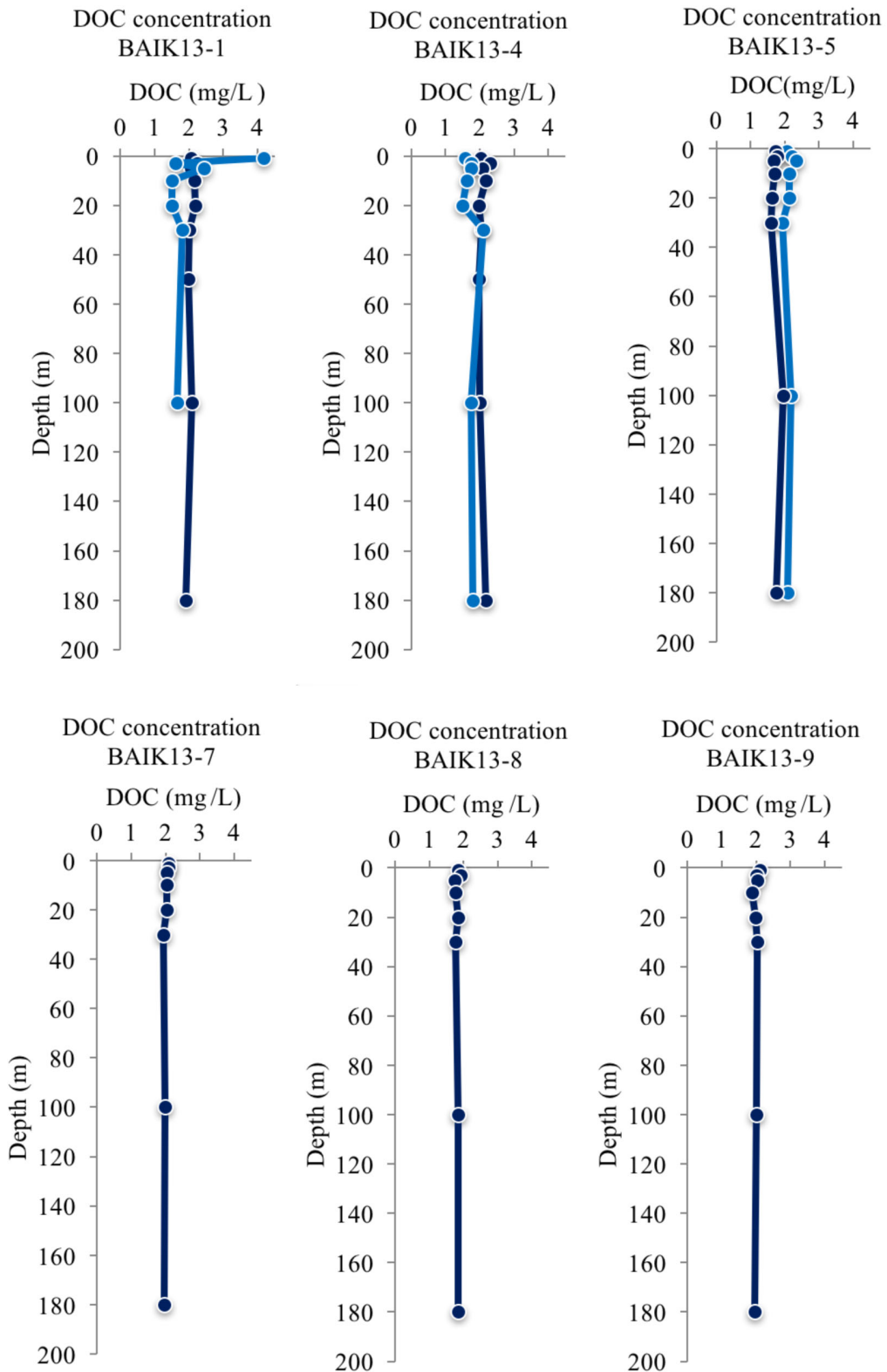


Figure 149: Water profiles of DOC concentrations in the South basin sites. Light blue line represents March 2013 profiles and dark blue line represents August 2013 profiles.

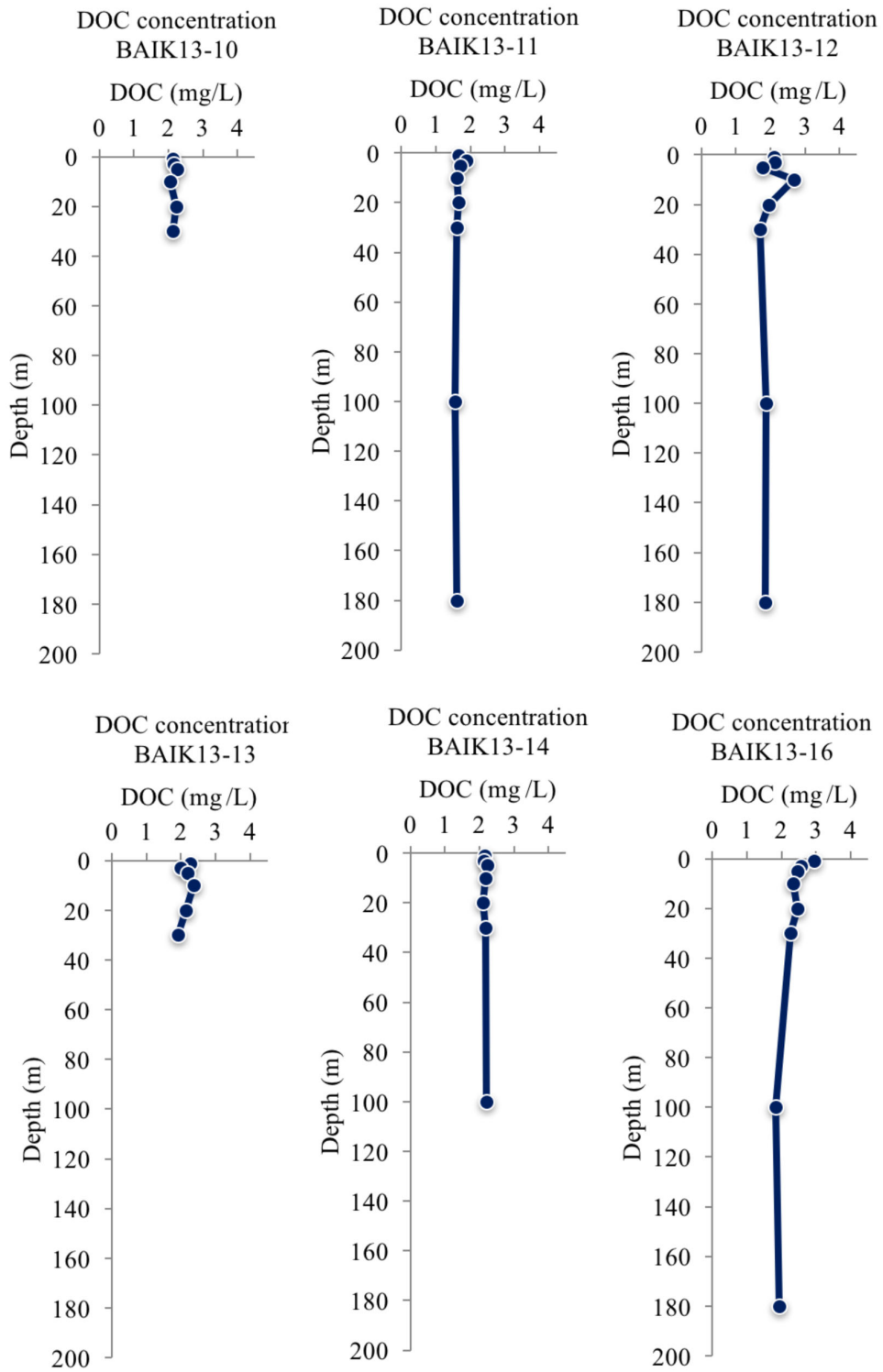


Figure 150: Water profiles of DOC concentrations in the South basin/Selenga, Central Basin, Maloe More Bay and North basin/Chivsky Bay sites. Dark blue line represents August 2013 profiles.

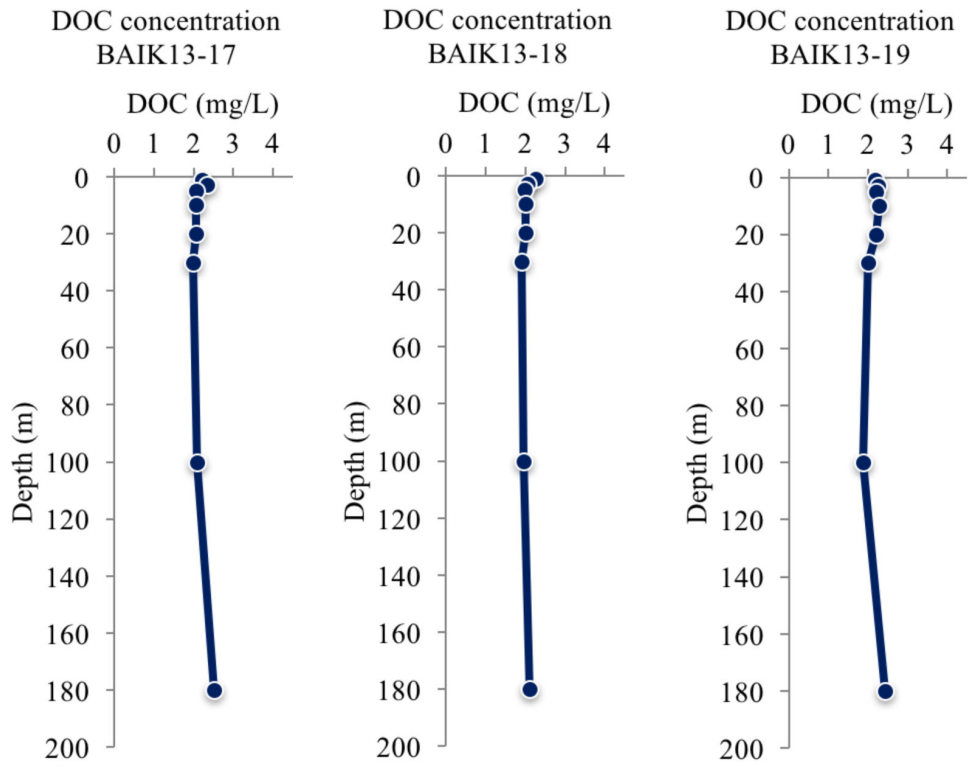


Figure 151: Water profiles of DOC concentrations in the North basin sites. Dark blue line represents August 2013 profiles.

Nutrient enrichment experiments datasets (results from day 0 and last day)

Table 56: Main pigment concentrations from each treatment (plus replicates) for nutrient enrichment experiment conducted underneath the South basin lake ice in March 2013.

Day	Treatment	Fucoxanthin (nmol/L)	Lutein (nmol/L)	Zeaxanthin (nmol/L)	Chl-<i>a</i> (nmol/L)
0	C	0.105	0.049	0.021	0.348
0	C	0.144	0.052	0.024	0.451
0	C	0.103	0.054	0.022	0.428
7	C	0.033	0.126	0.046	0.619
7	C	0.038	0.154	0.074	0.528
7	C	0.046	0.168	0.058	0.655
7	C	0.027	0.116	0.038	0.531
7	C	0.016	0.058	0.000	0.273
7	N+P	0.000	0.055	0.000	0.328
7	N+P	0.014	0.078	0.058	0.332
7	N+P	0.015	0.056	0.024	0.234
7	N+P	0.014	0.091	0.040	0.339
7	N+P	0.067	0.288	0.176	0.712
7	NPSi	0.033	0.128	0.043	0.538
7	NPSi	0.044	0.168	0.045	0.593
7	NPSi	0.030	0.123	0.040	0.580
7	NPSi	0.055	0.139	0.030	0.795

Table 57: Nutrient concentrations from each treatment (plus replicates) for nutrient enrichment experiment conducted underneath the South basin lake ice in March 2013.

Day	Treatment	Silicate (mg/L)	TP (µg/L)	Nitrate (mg/L)
0	C	0.030	33.601	0.492
0	C	0.018	29.512	0.472
0	C	0.014	25.422	0.748
0	N+P+S	0.176	63.982	2.438
0	N+P+S	0.114	61.645	2.602
0	N+P+S	0.096	75.667	2.069
7	C	0.004	27.175	0.584
7	C	0.028	29.512	0.441
7	C	0.026	30.680	0.451
7	C	0.033	34.770	0.441
7	C	0.028	42.949	0.554
7	N+P+S	0.106	82.677	2.182
7	N+P+S	0.123	100.205	2.448
7	N+P+S	0.097	90.273	2.245
7	N+P+S	0.101	56.971	1.701
7	N+P+S	0.126	73.330	2.472
7	N+P	0.083	54.050	0.613
7	N+P	0.094	63.397	0.803
7	N+P	0.105	66.903	0.613
7	N+P	0.100	58.139	0.694

Table 58: Main pigment concentrations from each treatment (plus replicates) for nutrient enrichment experiment conducted in a laboratory kunk on the South basin lake shore in March 2013.

Day	Treatment	Fucoxanthin (nmol/L)	Lutein (nmol/L)	Zeaxanthin (nmol/L)	Chl-a (nmol/L)
0	C	0.050	0.033	0.031	0.247
0	C	0.054	0.042	0.037	0.280
0	C	0.167	0.043	0.035	0.377
6	C	0.015	0.036	0.038	0.146
6	C	0.000	0.035	0.044	0.146
6	C	0.000	0.000	0.000	0.000
6	N+P	0.012	0.036	0.063	0.140
6	N+P	0.018	0.079	0.110	0.284
6	N+P	0.018	0.038	0.057	0.151
6	N+P+S	0.000	0.022	0.074	0.072
6	N+P+S	0.000	0.030	0.220	0.108

Table 59: Nutrient concentrations from each treatment (plus replicates) for nutrient enrichment experiment conducted in a laboratory kunk on the South basin lake shore in March 2013.

Day	Treatment	Silicate (mg/L)	TP (μ g/L)	Nitrate (mg/L)
Day 0	C	0.912	(-)	0.038
Day 0	C	0.549	(-)	0.018
Day 0	C	0.586	(-)	0.016
Day 0	N+P+S	1.864	20.065	0.000
Day 0	N+P+S	1.837	24.833	0.075
Day 0	N+P+S	1.918	19.469	0.077
Day 6	C	0.694	(-)	0.038
Day 6	C	0.740	(-)	0.028
Day 6	C	0.549	(-)	0.009
Day 6	N+P	0.731	16.488	0.016
Day 6	N+P	0.640	45.695	0.027
Day 6	N+P	0.740	20.661	0.020
Day 6	N+P+S	2.525	(-)	0.027
Day 6	N+P+S	2.476	13.508	0.033
Day 6	N+P+S	2.065	11.124	0.000

Table 60: Main pigment concentrations from each treatment (plus replicates) for nutrient enrichment experiment conducted in August 2013. Water was collected from BAIK13-12 and experimental in set-up in Maloe More Bay.

Day	Treatment	Fucoxanthin (nmol/L)	Lutein (nmol/L)	Zeaxanthin (nmol/L)	Chl-a (nmol/L)
0	C	0.310	0.000	0.000	0.604
0	C	3.342	0.033	0.021	5.442
0	C	0.372	0.025	0.029	0.764
0	N+P	1.679	0.038	0.026	2.545
0	N+P+S	0.710	0.020	0.000	1.110
11	C	0.341	0.013	0.010	0.174
11	C	0.200	0.018	0.021	0.274
11	N+P	0.795	0.040	0.076	0.071
11	N+P	0.114	0.039	0.021	0.022
11	N+P+S	0.269	0.000	0.376	0.187
11	N+P+S	0.234	0.000	0.257	0.109

Table 61: Nutrient and DOC concentrations from each treatment (plus replicates) for nutrient enrichment experiment conducted in August 2013. Water was collected from BAIK13-12 and experimental in set-up in Maloe More Bay. (-) indicated no sample measured.

Day	Treatment	Silicate (mg/L)	TP (µg/L)	Nitrate (mg/L)	DOC (mg/L)
0	C	0.07	17.54	0.05	2.21
0	C	0.00	9.84	0.00	1.95
0	C	0.03	11.03	0.00	1.99
0	N+P	0.04	435.47	0.17	2.22
0	N+P	0.01	(-)	0.20	2.12
0	N+P	0.00	(-)	0.16	2.18
0	N+P+S	0.13	410.01	0.06	8.25
0	N+P+S	0.05	(-)	0.05	8.35
0	N+P+S	0.28	(-)	0.05	8.30
11	C	0.00	21.57	0.00	4.00
11	C	0.00	20.88	0.01	4.40
11	N+P	0.11	500.37	0.00	4.79
11	N+P	0.04	496.24	0.04	6.31
11	N+P+S	0.28	545.84	0.02	6.53
11	N+P+S	0.08	514.84	0.04	7.42

Mercury

Table 62: Mercury (Hg) concentrations in the Baikal water samples.

Site	Water depth	Hg Concentration (ng L ⁻¹)
South basin/BAIK13-8	Surface	1.4
Selenga/BAIK13-10	Surface	1.6
Selenga Delta 1	Surface	6.0
Selenga Delta 2	Surface	4.5
Selenga Delta 3	Surface	5.53
Selenga Branch 1	Surface	0.34
Selenga Branch 2	Surface	1.92
Selenga River 1	Surface	8.1
Selenga River 2	Surface	6.1
Central basin	Surface	1.4
Central basin/BAIK13-12	Surface	0.02
North basin/BAIK13-19	Surface	3.2

Table 63: Mercury (Hg) concentrations in the sediments taken from Lake Baikal.

Site	Min depth (cm)	Max depth (cm)	Mid-depth (cm)	Hg concentrations (ng g ⁻¹)
Baik13-1C	2.0	2.2	2.1	67.3
Baik13-1C	12.6	12.8	12.7	55.2
Baik13-1C	22.6	22.8	22.7	29
Baik13-10A	0.2	0.6	0.4	47.7
Baik13-10A	2.2	2.6	2.4	50.6
Baik13-10A	4.2	4.4	4.3	46.1
Baik13-10A	6.0	6.2	6.1	48.2
Baik13-10A	8.0	8.4	8.2	48
Baik13-10A	10.0	10.2	10.1	47.5
Baik13-10A	12.0	12.2	12.1	39.2
Baik13-10A	19.8	20.0	19.9	31.1
Baik13-10A	33.0	33.2	33.1	25
Baik13-10A	49.4	50	49.7	26.4
Baik13-19B	0.6	0.8	0.7	51.1
Baik13-19B	2.8	3	2.9	52.6
Baik13-19B	4.6	4.8	4.7	42.8
Baik13-19B	6.4	6.6	6.5	41.1
Baik13-19B	8.6	8.8	8.7	46.1
Baik13-19B	10.2	10.4	10.3	41.3
Baik13-19B	12.0	12.2	12.1	35.5
Baik13-19B	22.4	22.6	22.5	37.3
Baik13-19B	32.0	32.2	32.1	28.6
Baik13-19B	42.6	42.8	42.7	30.2
Baik13-19B	64.8	65	64.9	29.5

²¹⁰Pb chronology profiles

Table 64: ²¹⁰Pb chronology of core BAIK13-1C taken from Baikal region, Russia.

Depth cm	Dry mass g cm ⁻²	Chronology			Sedimentation Rate		
		Date AD	Age yr	±	g cm ⁻² yr ⁻¹	cm yr ⁻¹	± %
0	0	2013	0				
0.3	0.0139	2011	2	2	0.009	0.091	7.5
1.1	0.1088	2003	10	2	0.0136	0.098	11.6
1.7	0.2081	1994	19	2	0.0087	0.045	12.4
2.5	0.3796	1976	37	3	0.0117	0.053	11.3
2.9	0.4714	1967	46	3	0.0079	0.035	14.7
3.1	0.5129	1962	51	4	0.0083	0.04	16.2
3.5	0.5958	1951	62	5	0.0068	0.029	18.6
3.9	0.6981	1933	80	7	0.005	0.02	27.5
4.1	0.7493	1924	89	9	0.0059	0.023	38.4
4.5	0.8506	1905	108	14	0.0046	0.018	68
4.7	0.9013	1883	130	26	0.0013	0.005	82.1

Table 65: ²¹⁰Pb concentrations for core BAIK13-1C taken from Baikal region, Russia

Depth cm	Dry Mass g cm ⁻²	Total		Pb-210 Supported		Unsupp		Cum Unsupported Pb-210	
		Bq Kg ⁻¹	±	Bq Kg ⁻¹	±	Bq Kg ⁻¹	±	Bq m ⁻²	±
0.3	0.0139	704.9	36.01	60.3	7.3	644.6	36.74	91.7	5.8
1.1	0.1088	373.87	32.13	51.04	6.98	322.83	32.88	533.3	34.6
1.7	0.2081	442.24	40.83	62.74	9.74	379.5	41.98	881.2	52.1
2.5	0.3796	206.37	13.77	40.82	3.02	165.55	14.1	1323.5	78.7
2.9	0.4714	227.58	20.19	44.31	4.86	183.27	20.77	1483.5	80.9
3.1	0.5129	193.25	17.6	45.51	4.41	147.74	18.14	1551.9	81.7
3.5	0.5958	176.45	15.35	48.29	3.63	128.16	15.77	1666.1	82.9
3.9	0.6981	156.91	16.11	54.96	3.99	101.95	16.6	1783.3	84.5
4.1	0.7493	117.91	16.26	53.38	4.24	64.53	16.8	1825.2	85.2
4.5	0.8506	106.73	23.15	61.28	6.59	45.45	24.07	1880.3	87
4.7	0.9013	128.79	14.75	44.24	3.63	84.55	15.19	1912.3	88.1
4.9	0.9453	95.14	14.62	45.39	3.95	49.75	15.14	1941.1	88.4
5.1	0.9894	41.57	9.54	57.28	3.08	-15.71	10.02	1944.2	88.6
5.3	1.0334	59.13	6.62	58.48	1.86	0.65	6.88		
5.9	1.1875	37.57	9.7	41.32	2.85	-3.75	10.11		
6.5	1.3725	44.67	10.59	44.89	2.87	-0.22	10.97		
8.9	2.0885	48.95	6.44	46.74	1.92	2.21	6.72		
12.5	3.6164	44.48	5.67	51.8	1.54	-7.32	5.88		

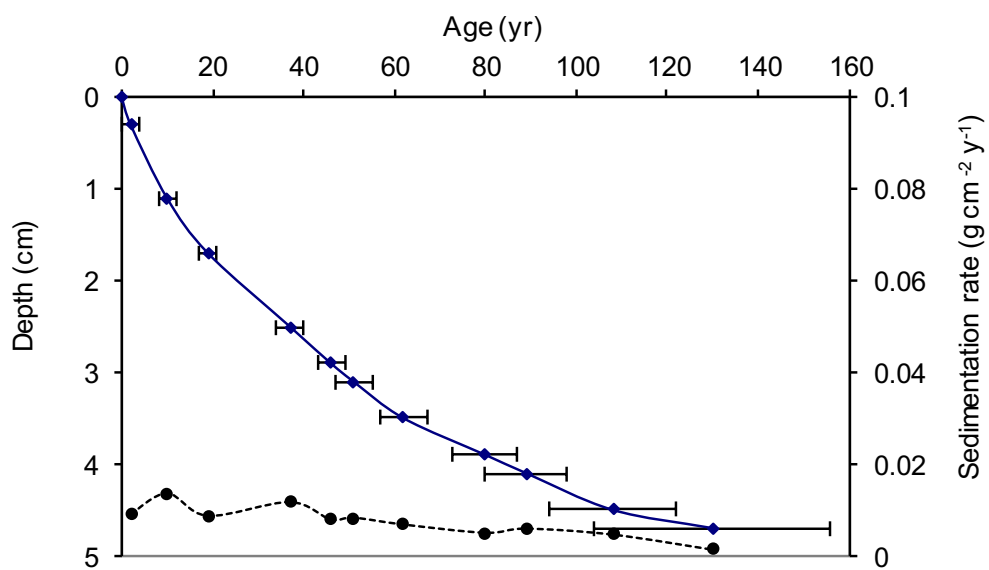


Figure 152: Radiometric chronology of core BAIK13-1C taken from Baikal region, Russia, showing the CRS model ^{210}Pb dates and sedimentation rates. The solid line shows age while the dashed line indicates sedimentation rate.

Table 66: ^{210}Pb chronology and sedimentation rates of core BAIK13-4F.

Depth	Dry mass	Chronology			Sedimentation Rate		
		Date	Age				
cm	g cm^{-2}	AD	yr	\pm	$\text{g cm}^{-2} \text{yr}^{-1}$	cm yr^{-1}	$\pm \%$
0	0	2013	0				
0.1	0.016	2013	0	7	0.0577	0.239	21.2
1.1	0.2656	2009	4	2	0.0849	0.327	25.1
2.1	0.5352	2006	7	2	0.0927	0.316	36.9
3.3	0.9107	2001	12	2	0.0668	0.173	24
4.1	1.3071	1998	15	2	0.3156	0.686	53.4
4.9	1.6474	1991	22	3	0.0146	0.035	18.6
5.5	1.8886	1970	43	4	0.0084	0.024	21.2
5.7	1.9267	1965	48	5	0.0062	0.032	17.4
6.1	2.003	1953	60	6	0.0071	0.037	27.4
6.5	2.0793	1940	73	8	0.0049	0.021	31.1
6.9	2.1886	1923	90	13	0.0094	0.033	52.6
7.7	2.4157	1901	112	23	0.0111	0.039	104.1
8.3	2.5882	1869	144	30	0.0025	0.009	137.6

Table 67: ^{210}Pb concentrations for core BAIK13-4F.

Depth	Dry Mass	Total		Pb-210 Supported		Unsupp		Cum Unsupported Pb-210	
		Bq Kg^{-1}	\pm	Bq Kg^{-1}	\pm	Bq Kg^{-1}	\pm	Bq m^{-2}	\pm
cm	g cm^{-2}								
0.1	0.016	168.54	23.85	43.03	5.55	125.51	24.49	20.2	2.9
1.1	0.2656	126.39	17.47	50.12	4.13	76.27	17.95	266.9	41.5
2.1	0.5352	126.62	22.13	63.06	5.46	63.56	22.79	454.9	66.5
3.3	0.9107	114.55	16.26	38.54	3.76	76.01	16.69	716.2	100.2
4.1	1.3071	57.7	7.42	43.07	1.94	14.63	7.67	863.9	116.3
4.9	1.6474	315.86	41.17	60.96	9.34	254.9	42.22	1150	140.6
5.5	1.8886	287.77	38.72	59.79	9.11	227.98	39.78	1731.7	181.2
5.7	1.9267	301.67	26.45	38.36	5.89	263.31	27.1	1825.3	183.5
6.1	2.003	203.94	31.05	43.81	7.65	160.13	31.98	1983.5	184.6
6.5	2.0793	207.74	24.77	51.94	5.97	155.8	25.48	2104	186.2
6.9	2.1886	91.17	15.17	43.54	3.44	47.63	15.56	2203.7	187.7
7.7	2.4157	74.04	15.06	54.11	3.77	19.93	15.52	2275.9	190.2
8.3	2.5882	80.65	10.46	47.56	2.69	33.09	10.8	2320.7	192.1
9.1	2.7999	46.7	12.83	54.08	3.24	-7.38	13.23	2347.9	193.5
11.1	3.7933	35.52	11.54	49.74	3.1	-14.22	11.95		

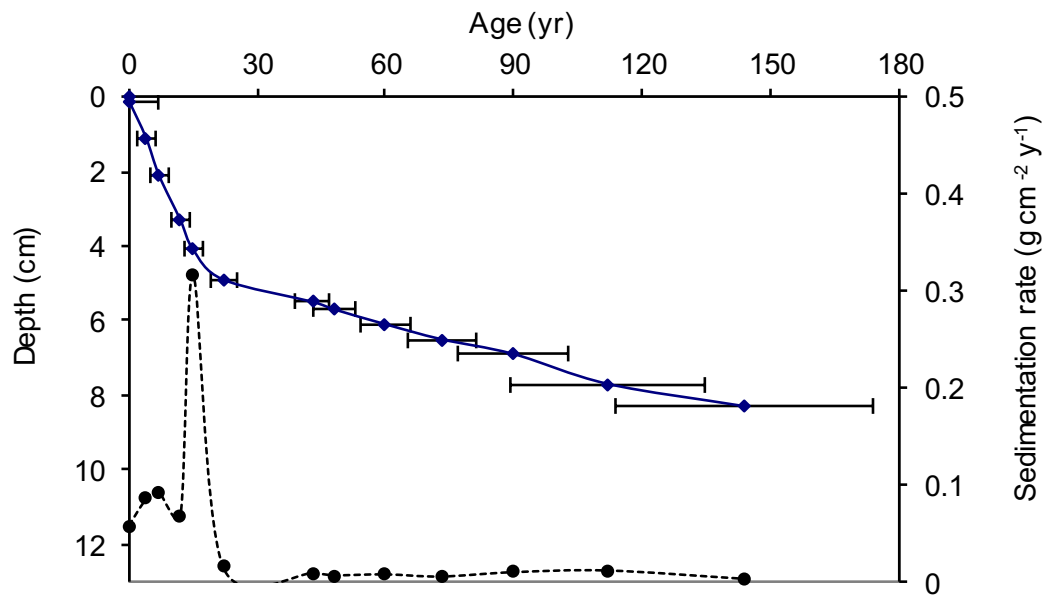


Figure 153: Radiometric chronology of core BAIK13-4F, showing the CRS model ^{210}Pb dates and sedimentation rates. The solid line shows age while the dashed line indicates sedimentation rate.

Table 68: ^{210}Pb chronology of core BAIK13-7A taken from BPPM.

Depth	Dry mass	Chronology			Sedimentation Rate		
		Date	Age				
cm	g cm^{-2}	AD	yr	\pm	$\text{g cm}^{-2} \text{ yr}^{-1}$	cm yr^{-1}	$\pm \%$
0	0	2013	0				
0.1	0.0153	2012	1	2	0.0199	0.122	23.3
0.5	0.0815	2008	5	2	0.0104	0.058	13.8
1.1	0.1946	1996	17	2	0.009	0.044	17
1.7	0.3268	1981	32	3	0.0089	0.04	20.7
2.3	0.4589	1963	50	4	0.0061	0.026	20.5
2.7	0.5609	1934	79	6	0.0019	0.007	20.2

Table 69: ^{210}Pb concentrations for core BAIK13-7A.

Depth	Dry Mass	Total		Pb-210 Supported		Unsupp		Cum Unsupported Pb-210	
		Bq Kg^{-1}	\pm	Bq Kg^{-1}	\pm	Bq Kg^{-1}	\pm	Bq m^{-2}	\pm
cm	g cm^{-2}								
0.1	0.0153	235.93	38.11	59.13	10.33	176.8	39.49	27.2	4.5
0.5	0.0815	357.77	33.49	63.92	8.92	293.85	34.66	179.8	21.5
1.1	0.1946	283.88	34.04	48.65	8.59	235.23	35.11	477.7	43.7
1.7	0.3268	213.17	27.15	62.52	7.82	150.65	28.25	728.6	62.3
2.3	0.4589	171.37	21.43	45.9	5.59	125.47	22.15	910.5	72.3
2.7	0.5609	204.56	14.62	40.51	3.07	164.05	14.94	1057.3	76.1
3.1	0.677	136.77	21.88	57.98	5.86	78.79	22.65	1192.3	78.9
3.7	0.8724	69.35	9.37	47.83	2.62	21.52	9.73	1278.5	86.1
4.1	1.014	35.52	9.14	53.62	2.52	-18.1	9.48	1280.9	87.4
5.1	1.3965	26.76	5.63	54.26	2.44	-27.5	6.14		
5.7	1.626	38.99	7.04	49.17	1.86	-10.18	7.28		
6.7	2.0131	37.34	7.07	53.46	2.04	-16.12	7.36		
7.3	2.2496	46.68	7.32	46.07	2.04	0.61	7.6		

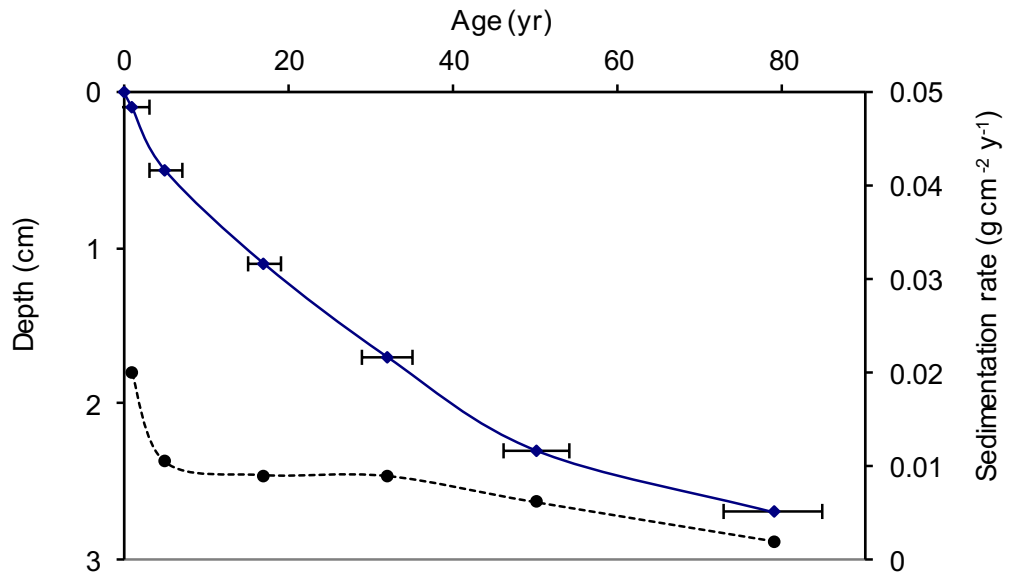


Figure 154: Radiometric chronology of core BAIK13-7A taken from BPPM, showing the CRS model ²¹⁰Pb dates and sedimentation rates. The solid line shows age while the dashed line indicates sedimentation rate.

Table 70: ^{210}Pb chronology of core BAIK13-10A.

Depth	Dry mass	Chronology			Sedimentation Rate		
		Date	Age	\pm	$\text{g cm}^{-2} \text{ yr}^{-1}$	cm yr^{-1}	$\pm \%$
cm	g cm^{-2}	AD	yr				
0	0	2013	0				
0.3	0.038	2013	0	2	0.1325	0.501	27.3
1.9	0.5028	2009	4	2	0.0929	0.297	18.2
3.7	1.1017	2000	13	2	0.0524	0.151	9.3
4.9	1.5416	1992	21	2	0.056	0.146	12.7
6.7	2.2556	1978	35	3	0.0444	0.113	15.4
7.3	2.4866	1971	42	4	0.0304	0.08	15.3
8.3	2.8653	1957	56	5	0.0223	0.058	20.2
8.5	2.9457	1953	60	6	0.023	0.056	28
9.3	3.2757	1938	75	9	0.0187	0.045	33.8
9.9	3.5296	1918	95	16	0.0084	0.02	50.3
10.3	3.6901	1894	119	18	0.0055	0.014	56.7
10.6	3.8104	1875	138	20	0.0077	0.019	61.6

Table 71: ^{210}Pb concentrations for core BAIK13-10A.

Depth	Dry Mass	Total		Pb-210 Supported		Unsupp		Cum Unsupported Pb-210	
		Bq Kg^{-1}	\pm	Bq Kg^{-1}	\pm	Bq Kg^{-1}	\pm	Bq m^{-2}	\pm
cm	g cm^{-2}								
0.3	0.038	187.1	30.08	71.48	7.87	115.62	31.09	43.8	8.6
1.9	0.5028	201.85	24.71	57.2	5.81	144.65	25.38	646.1	102.7
3.7	1.1017	241.13	13.54	44.7	2.84	196.43	13.83	1659.6	172.1
4.9	1.5416	187.4	14.91	44.79	3.08	142.61	15.22	2399	188.6
6.7	2.2556	162.42	13.74	47.05	2.94	115.37	14.05	3316.6	216.3
7.3	2.4866	178.22	14.26	39.58	2.98	138.64	14.57	3609.1	221.8
8.3	2.8653	167.18	13.44	46.66	2.87	120.52	13.74	4099	228.4
8.5	2.9457	171.88	21.91	67.33	5.5	104.55	22.59	4189.4	229.3
9.3	3.2757	124.88	15.67	46.16	3.69	78.72	16.1	4489.8	235.8
9.9	3.5296	141.24	8.25	47.02	1.76	94.22	8.44	4708.7	239.4
10.3	3.6901	120.44	8.78	50.23	2.04	70.21	9.01	4839.7	240
10.6	3.8104	91.53	17.85	63.72	4.46	27.81	18.4	4894.8	240.5
12.1	4.4122	64.52	14.11	61.53	3.69	2.99	14.58	4961.8	253.2
13.1	4.8134	45.47	8.87	62.23	2.45	-16.76	9.2		
14.5	5.3751	55.88	10.24	53.77	2.42	2.11	10.52		
17.5	6.5787	59.12	14.26	62.29	3.92	-3.17	14.79		
18.1	6.8194	68.6	13.46	61.14	3.64	7.46	13.94		

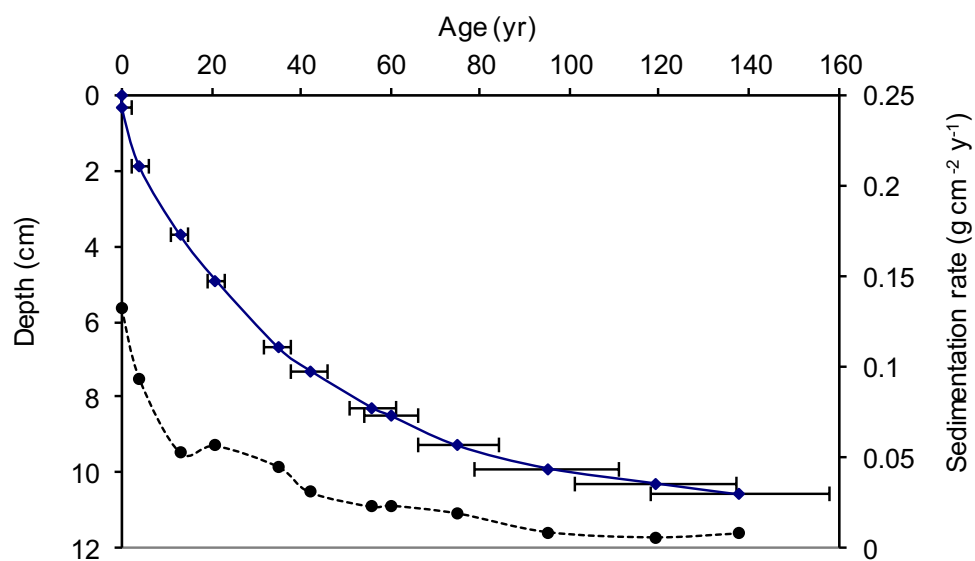


Figure 155: Radiometric chronology of core BAIK13-10A taken from Selenga Delta region, showing the CRS model ^{210}Pb dates and sedimentation rates. The solid line shows age while the dashed line indicates sedimentation rate.

Table 72: ^{210}Pb chronology of core BAIK13-11C.

Depth	Dry mass	Chronology			Sedimentation Rate		
		Date	Age				
cm	g cm^{-2}	AD	yr	\pm	$\text{g cm}^{-2} \text{yr}^{-1}$	cm yr^{-1}	$\pm \%$
0	0	2013	0				
0.2	0.0094	2012	1	2	0.0174	0.178	11.8
1.1	0.1074	2006	7	2	0.0137	0.104	10.7
2.1	0.2601	1995	18	2	0.0129	0.079	15.1
2.7	0.3685	1987	26	2	0.017	0.094	16.9
3.1	0.4408	1982	31	3	0.011	0.055	14.3
3.5	0.5304	1973	40	4	0.0091	0.04	18.6
3.9	0.6201	1962	51	5	0.0074	0.032	19.9
4.5	0.7591	1941	72	9	0.0054	0.023	34.6
4.9	0.8517	1929	84	13	0.0138	0.057	59.7
5.5	1.0008	1925	88	16	0.0324	0.131	78.3
6.1	1.1499	1919	94	17	0.0259	0.096	102.2
6.9	1.38	1907	106	22	0.013	0.044	88.6
7.5	1.5624	1901	112	30	0.0289	0.095	99.1
8.3	1.8057	1879	134	36	0.0109	0.035	104.5

Table 73: ^{210}Pb concentrations for core BAIK13-11C.

Depth	Dry Mass	Total		Pb-210 Supported		Unsupp		Cum Unsupported Pb-210	
		Bq Kg^{-1}	\pm	Bq Kg^{-1}	\pm	Bq Kg^{-1}	\pm	Bq m^{-2}	\pm
cm	g cm^{-2}								
0.2	0.0094	482.25	42.39	63.91	10.56	418.34	43.69	39.7	3.5
1.1	0.1074	497.22	37.35	61.16	9.14	436.06	38.45	458.3	36.8
2.1	0.2601	400.65	41.46	76.44	11.75	324.21	43.09	1034.6	72.4
2.7	0.3685	283.05	26.96	87.17	9.19	195.88	28.48	1310.7	88.1
3.1	0.4408	311.88	25.17	55.78	6.9	256.1	26.1	1473.1	91.3
3.5	0.5304	296.8	31.2	60.36	9.62	236.44	32.65	1693.7	95.1
3.9	0.6201	262.15	21.27	55.9	5.6	206.25	21.99	1891.9	99.4
4.5	0.7591	211.26	22.05	68.52	7.04	142.74	23.15	2131.6	104
4.9	0.8517	114.96	16.05	75.48	5.28	39.48	16.9	2206.1	106.6
5.5	1.0008	77.31	14.88	63.29	4.89	14.02	15.66	2242.7	108.9
6.1	1.1499	63.42	11.09	54.62	3.61	8.8	11.66	2259.4	111.1
6.9	1.38	70.54	11.49	49.22	3.61	21.32	12.04	2292	113.8
7.5	1.5624	66.77	11.17	55.27	4.19	11.5	11.93	2321	116.2
8.3	1.8057	62.83	10.94	53.57	3.8	9.26	11.58	2346.2	119.2
9.1	2.0633	54.57	8.22	45.55	2.75	9.02	8.67	2369.7	122.4
10.1	2.3997	59.49	9.82	62.62	3.32	-3.13	10.37	2379.6	125.8

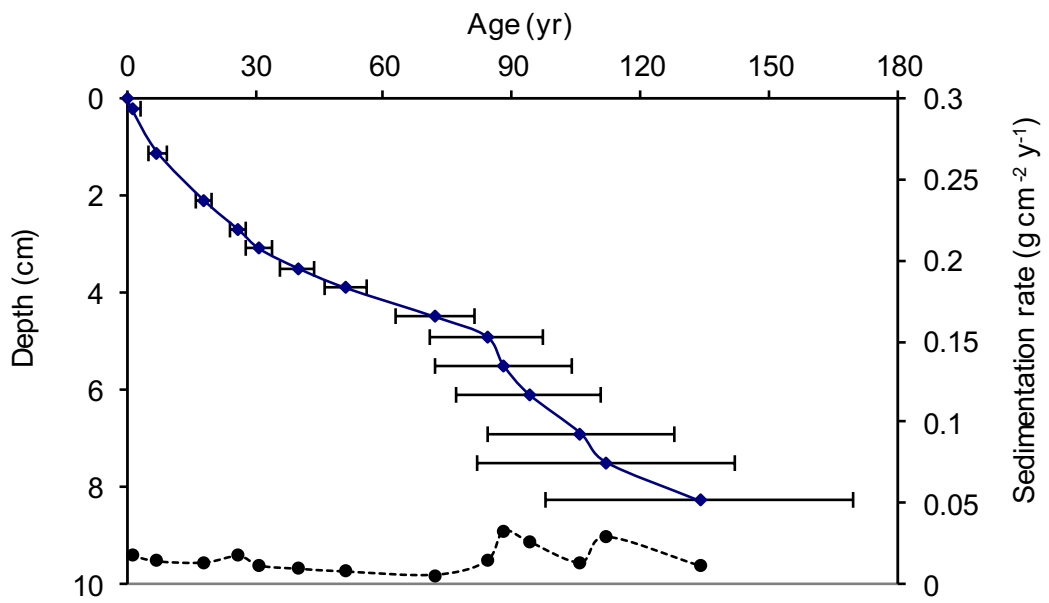


Figure 156: Radiometric chronology of core BAIK13-11C, showing the CRS model ^{210}Pb dates and sedimentation rates. The solid line shows age while the dashed line indicates sedimentation rate.

Table 74: ^{210}Pb chronology of core BAIK13-14C.

Depth	Dry mass	Chronology			Sedimentation Rate		
		Date	Age				
cm	g cm^{-2}	AD	yr	\pm	$\text{g cm}^{-2} \text{ yr}^{-1}$	cm yr^{-1}	$\pm \%$
0	0	2013	0				
0.2	0.0088	2013	0	2	0.03	0.234	11.1
1.3	0.1669	2007	6	2	0.025	0.149	9.6
2.5	0.3943	1997	16	2	0.0198	0.094	11.5
3.1	0.5439	1988	25	2	0.015	0.056	13.4
3.9	0.771	1968	45	3	0.0081	0.028	10.7
4.1	0.8301	1961	52	3	0.0092	0.031	16.8
4.3	0.8892	1954	59	3	0.0077	0.028	12.7
4.7	0.9934	1941	72	4	0.0086	0.033	17.6
5.1	1.0976	1927	86	6	0.0064	0.025	20.5
5.5	1.2012	1908	105	10	0.0045	0.017	34.6
6	1.3308	1884	129	19	0.0069	0.026	68.4
6.3	1.4128	1863	150	23	0.0023	0.008	80.9
6.5	1.4689	1841	172	26	0.0029	0.011	92.2

Table 75: ^{210}Pb concentrations for core BAIK13-14C.

Depth	Dry Mass	Total		Pb-210 Supported		Unsupp		Cum Unsupported Pb-210	
		Bq Kg^{-1}	\pm	Bq Kg^{-1}	\pm	Bq Kg^{-1}	\pm	Bq m^{-2}	\pm
cm	g cm^{-2}	Kg^{-1}		Kg^{-1}		Kg^{-1}			
0.2	0.0088	337.59	30.42	32.51	7.6	305.08	31.36	26.9	2.4
1.3	0.1669	336.35	25.22	30.08	5.68	306.27	25.85	510.1	41.1
2.5	0.3943	312.56	27.91	30.99	6.89	281.57	28.75	1178.1	77.1
3.1	0.5439	324.99	34.23	41.67	8.36	283.32	35.24	1600.7	94.6
3.9	0.771	309.82	22.82	29.85	4.84	279.97	23.33	2240.4	119.9
4.1	0.8301	241.39	29.14	42.27	7.01	199.12	29.97	2380.5	122.2
4.3	0.8892	216.6	16.79	26.49	3.6	190.11	17.17	2495.5	123.4
4.7	0.9934	145.75	14.03	31.29	3.99	114.46	14.59	2650.9	124.5
5.1	1.0976	131.71	9.39	32.24	2.42	99.47	9.7	2762.1	125.5
5.5	1.2012	102.52	13.61	24.72	3.47	77.8	14.05	2853.5	126.1
6	1.3308	51.96	8.27	27.87	2.27	24.09	8.58	2912.9	127.1
6.3	1.4128	65.06	7.4	27.09	1.95	37.97	7.65	2937.9	127.3
6.5	1.4689	42.34	11.46	27.35	2.93	14.99	11.83	2951.8	127.4
7.9	1.8576	28.14	7.52	27.98	2.26	0.16	7.85	2964.5	131
8.7	2.0718	23.35	6.5	26.36	1.88	-3.01	6.77		
10.1	2.4686	29.34	8.92	27.96	2.55	1.38	9.28		

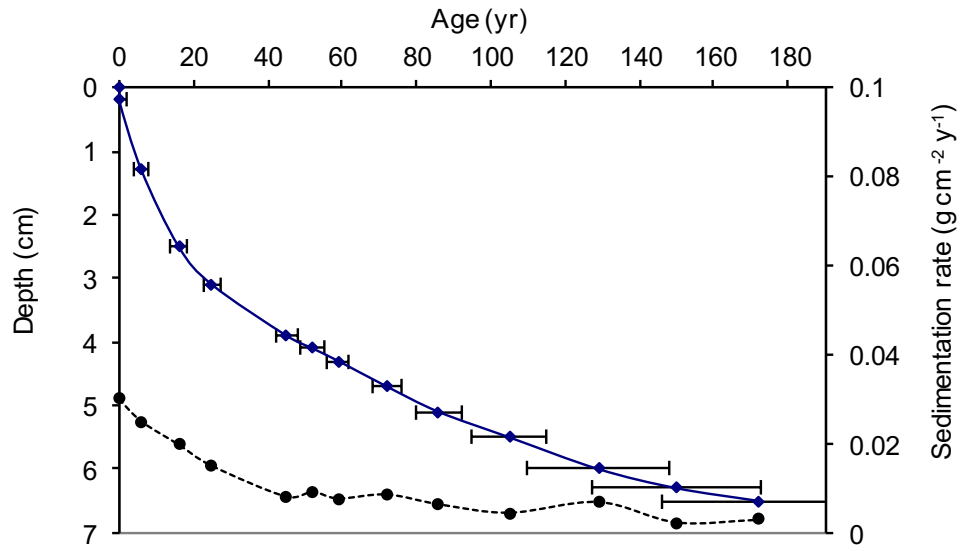


Figure 157: Radiometric chronology of coreBAIK13-14C, showing the CRS model ^{210}Pb dates and sedimentation rates. The solid line shows age while the dashed line indicates sedimentation rate.

Table 76: ^{210}Pb chronology and sedimentation rate of core BAIK13-18A.

Depth cm	Dry mass g cm^{-2}	Chronology			Sedimentation Rate		
		Date AD	Age yr	\pm	$\text{g cm}^{-2} \text{ yr}^{-1}$	cm yr^{-1}	$\pm \%$
0	0	2013	0				
0.5	0.1025	1999	14	2	0.0083	0.05	29.4
0.7	0.1354	1990	23	4	0.006	0.02	
1.1	0.1842	1985	28	4	0.0043	0.03	18.6
1.4	0.2278	1968	45	9	0.005	0.02	
1.9	0.3005	1948	65	9	0.0021	0.012	34.4
2.2	0.3574	1910	103	15	0.002	0.01	
2.7	0.4586	1869	144	15	0.002	0.01	39.7

Table 77: ^{210}Pb concentrations for core BAIK13-18A.

Depth cm	Dry Mass g cm^{-2}	Total		Pb-210 Supported		Unsupp		Cum Unsupported Pb-210	
		Bq Kg^{-1}	\pm	Bq Kg^{-1}	\pm	Bq Kg^{-1}	\pm	Bq m^{-2}	\pm
0.5	0.1025	450	77.77	153.96	23.75	296.04	81.32	425.6	62.9
0.7	0.1354	519.12	62.9	111.07	15.56	408.05	64.8	540.4	73.5
1.1	0.1842	444.54	44.8	66.87	9.85	377.67	45.87	732	78.8
1.4	0.2278	319.96	85.41	189.3	23.27	130.66	88.52	833.5	83.2
1.9	0.3005	315.97	38.33	74.62	9.88	241.35	39.58	964.6	97.3
2.2	0.3574	224.75	23.11	104.29	5.94	120.46	23.86	1063.5	99.9
2.7	0.4586	165.17	36.31	139.06	9.8	26.11	37.61	1126	103.3
2.9	0.4939	103.34	20.36	69.58	5.2	33.76	21.01	1136.5	104.8
3.4	0.5847	42.73	24.55	80.26	6.85	-37.53	25.49		
3.9	0.6793	68.46	16.21	63.23	4.35	5.23	16.78		
5.1	0.9247	50.9	23.3	76.08	7.29	-25.18	24.41		
9.1	1.7452	47.78	10.67	52.47	2.7	-4.69	11.01		

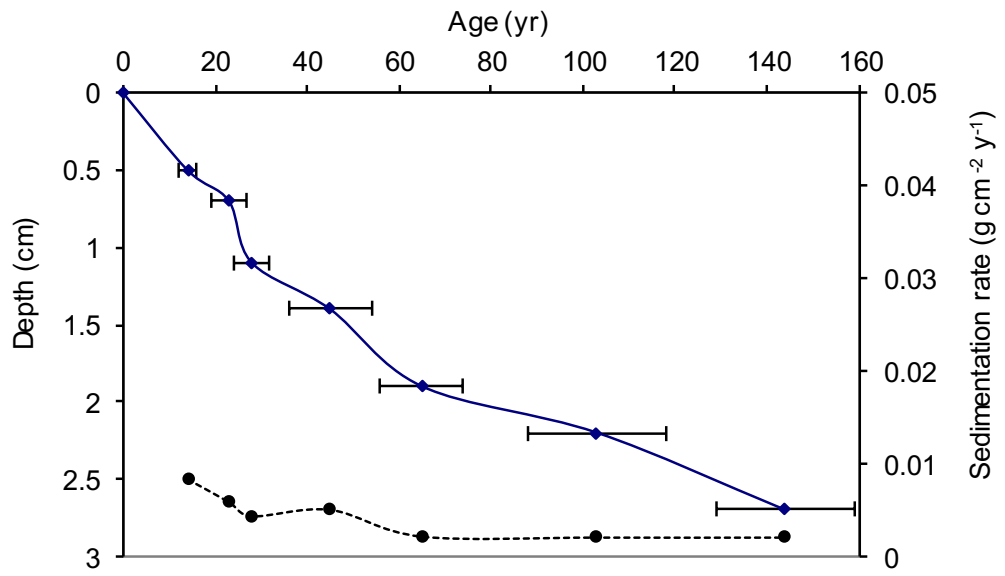


Figure 158: Radiometric chronology of core BAIK13-18A, showing the CRS model ^{210}Pb dates and sedimentation rates. The solid line shows age while the dashed line indicates sedimentation rate.

Table 78: ^{210}Pb chronology and sedimentation rates of core BAIK13-19B.

Depth cm	Dry mass g cm^{-2}	Chronology			Sedimentation Rate		
		Date AD	Age yr	\pm	$\text{g cm}^{-2} \text{ yr}^{-1}$	cm yr^{-1}	$\pm \%$
0	0	2013	0				
0.5	0.0601	2006	7	2	0.0084	0.06	26.6
1.1	0.1553	1998	15	4	0.0213	0.133	83.9
1.5	0.2209	1993	20	5	0.0071	0.043	33.3
2.1	0.3193	1982	31	8	0.0116	0.071	55.7
2.7	0.4177	1967	46	14	0.0041	0.023	57.7
3.3	0.5353	1954	59	20	0.009	0.041	52.1
4.1	0.727	1936	77	24	0.0055	0.023	104.9

Table 79: ^{210}Pb concentrations for core BAIK13-19B.

Depth cm	Dry Mass g cm^{-2}	Total		Pb-210 Supported		Unsupp		Cum Unsupported Pb-210	
		Bq Kg^{-1}	\pm	Bq Kg^{-1}	\pm	Bq Kg^{-1}	\pm	Bq m^{-2}	\pm
0.5	0.0601	250.87	29.93	77.35	7.16	173.52	30.77	114.5	14.3
1.1	0.1553	145.73	42.14	91.51	12.26	54.22	43.89	212.1	34
1.5	0.2209	200	27.05	62.4	6.54	137.6	27.83	270.8	45.3
2.1	0.3193	138.31	24.53	78.92	7.13	59.39	25.55	362.4	51.7
2.7	0.4177	175.5	24.58	67.87	6.16	107.63	25.34	442.2	57.6
3.3	0.5353	106.44	30.53	94.41	8.17	12.03	31.6	493.5	65.4
4.1	0.727	91.98	20.75	62.16	5.25	29.82	21.4	531.1	82.1
4.9	0.9186	78.74	13.58	61.3	3.46	17.44	14.01	575.3	90.5
5.1	0.9798	60.46	9.18	52.03	2.16	8.43	9.43	582.9	91.3
5.9	1.2421	42.53	16.46	65.89	4.66	-23.36	17.11		
6.9	1.5986	52.55	7.87	57.92	2.07	-5.37	8.14		

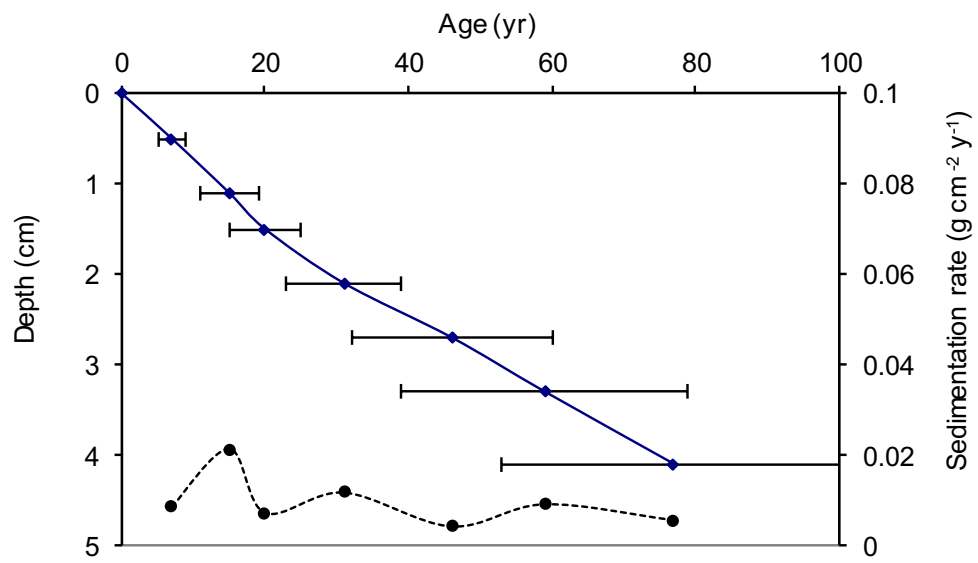


Figure 159: Radiometric chronology of core BAIK13-19B, showing the CRS model ²¹⁰Pb dates and sedimentation rates. The solid line shows age while the dashed line indicates sedimentation rate.

Sedimentary diatom profiles

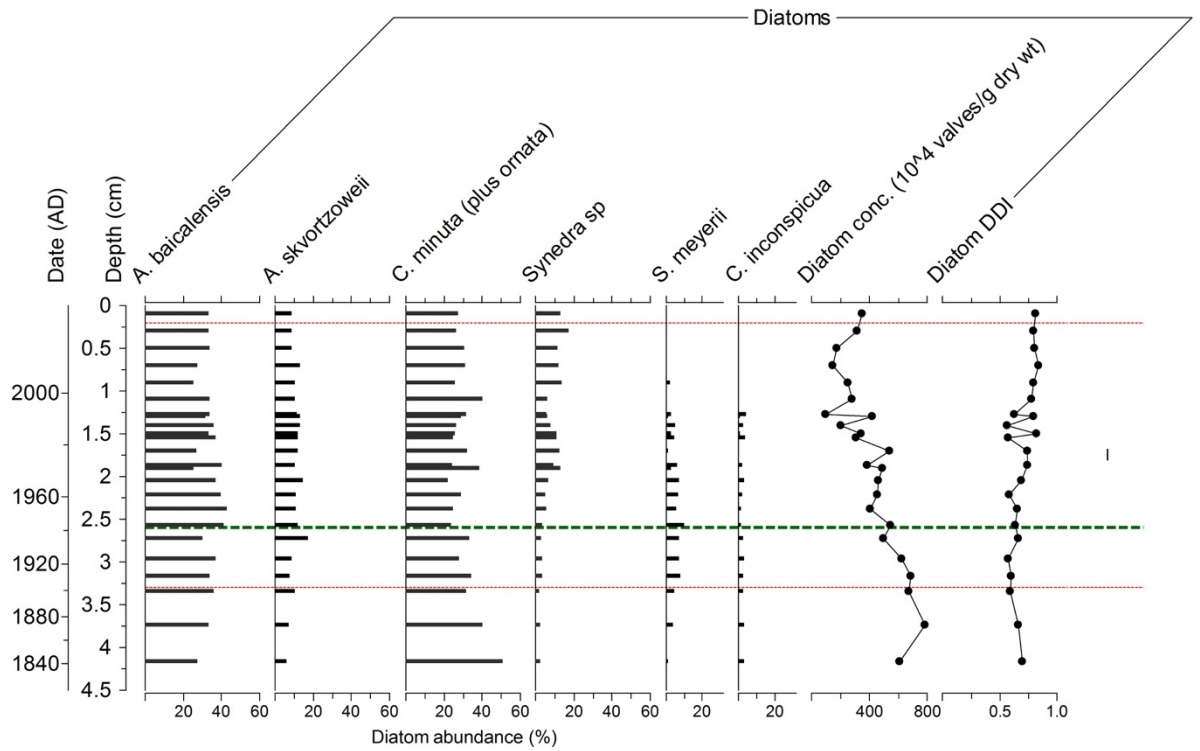


Figure 160: Diatom profile for BAIK13-7A in the South basin. Most abundant species are shown (abundance > 2%), with total diatom concentrations and diatom dissolution index (DDI) down-core. Dashed green line indicates onset of human influence in the Baikal region (Brunello et al., 2004).

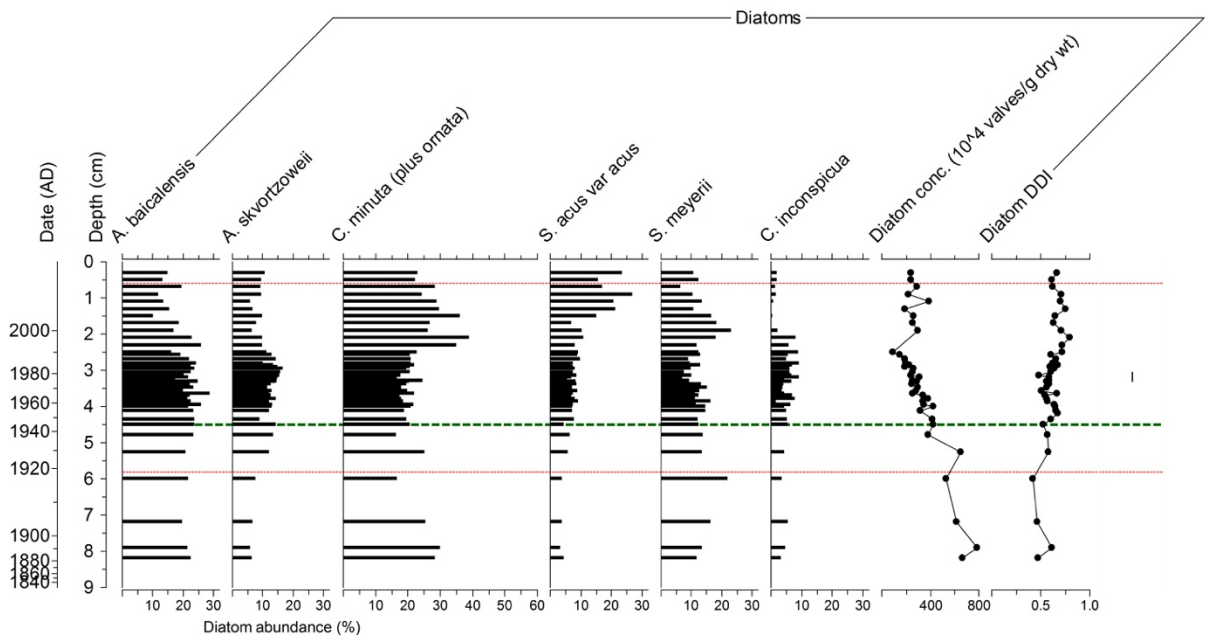


Figure 161: Diatom profile for BAIK13-11C in the South basin. Most abundant species are shown (abundance > 2%), with total diatom concentrations and diatom dissolution index (DDI) down-core. Dashed green line indicates onset of human influence in the Baikal region (Brunello et al., 2004).

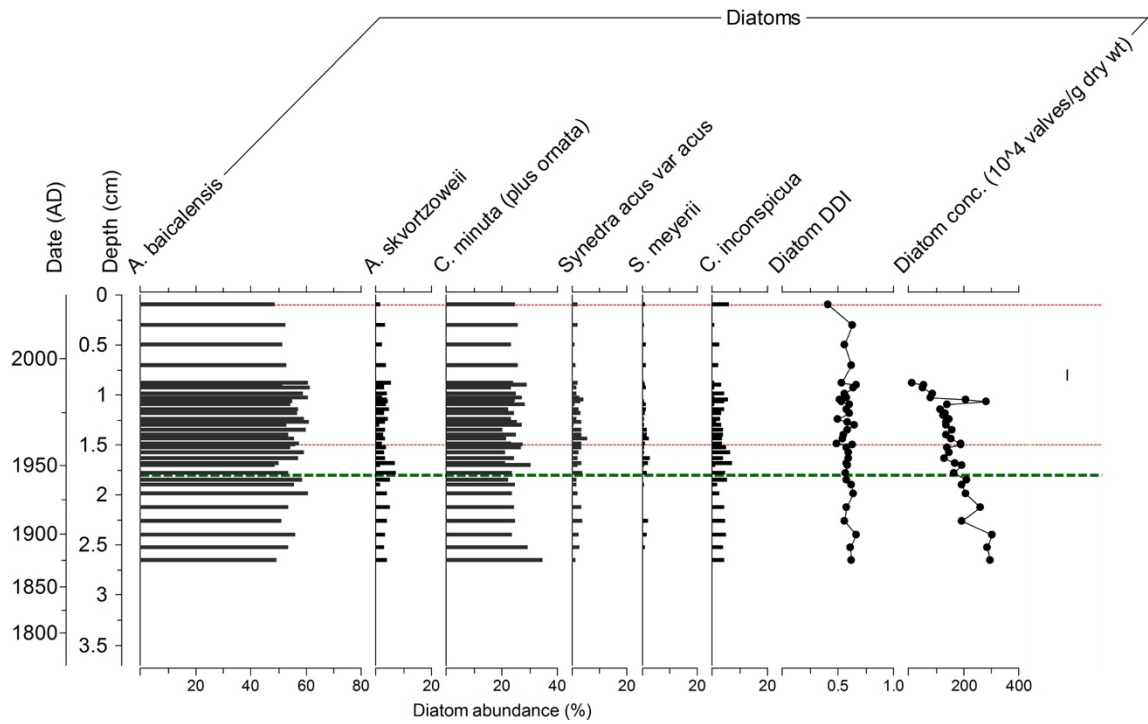


Figure 162: Diatom profile for BAIK13-18A in the North basin. Most abundance species are shown (abundance > 2%), with total diatom concentrations and diatom dissolution index (DDI) down-core. Dashed green line indicates onset of human influence in the Baikal region (Brunello et al., 2004).